UNSW SYDNEY

Tailored design of composite risers for deep water applications

Author:
Wang, Chunguang

Publication Date:
2013

DOI:
https://doi.org/10.26190/unsworks/16172

License:
https://creativecommons.org/licenses/by-nc-nd/3.0/au/
Link to license to see what you are allowed to do with this resource.

Downloaded from http://hdl.handle.net/1959.4/52672 in https://unsworks.unsw.edu.au on 2024-05-05

Tailored design of composite risers for deep water applications

Chunguang Wang

A thesis submitted in fulfilment of the requirements for the degree of

Doctor of Philosophy

UNSW

School of Engineering and Information Technology

The University of New South Wales

Canberra

March 2013

ORIGINALITY STATEMENT

'I hereby declare that this submission is my own work and to the best of my knowledge it contains no materials previously published or written by another person, or substantial proportions of material which have been accepted for the award of any other degree or diploma at UNSW or any other educational institution, except where due acknowledgement is made in the thesis. Any contribution made to the research by others, with whom I have worked at UNSW or elsewhere, is explicitly acknowledged in the thesis. I also declare that the intellectual content of this thesis is the product of my own work, except to the extent that assistance from others in the project's design and conception or in style, presentation and linguistic expression is acknowledged.'

Signed ……Chunguang Wang……………………………………

Date ……03/2013……………………………………

COPYRIGHT STATEMENT

‘I hereby grant the University of New South Wales or its agents the right to archive and to make available my thesis or dissertation in whole or part in the University libraries in all forms of media, now or here after known, subject to the provisions of the Copyright Act 1968. I retain all proprietary rights, such as patent rights. I also retain the right to use in future works (such as articles or books) all or part of this thesis or dissertation.
I also authorise University Microfilms to use the 350 word abstract of my thesis in Dissertation Abstract International (this is applicable to doctoral theses only).
I have either used no substantial portions of copyright material in my thesis or I have obtained permission to use copyright material; where permission has not been granted I have applied/will apply for a partial restriction of the digital copy of my thesis or dissertation.'

Signed ……………………………………………Chungguang Wang

Date ……………………………………………03/2013

AUTHENTICITY STATEMENT

‘I certify that the Library deposit digital copy is a direct equivalent of the final officially approved version of my thesis. No emendation of content has occurred and if there are any minor variations in formatting, they are the result of the conversion to digital format.’

Signed ……………………………………………Chungguang Wang

Date ……………………………………………03/2013

ABSTRACT

Currently offshore oil and gas industry uses production risers made of high grade steel. The weight of the steel risers has to be supported by tension from the floating platform at the top which limits the capacity of offshore operations. By reducing the weight of the risers, it is possible to exploit natural resources from deeper waters and to increase the production capacity, resulting in significant economic benefits.

Due to the desirable mechanical properties of advanced fibre reinforced polymer (FRP) composites, it has been recognised that offshore risers made of composite materials can lead to considerable weight savings. Previous projects investigating application of composite risers employed fibre reinforcements only in the hoop and axial directions in the design. The prototypes fabricated and tested in these projects confirm that FRP composites can indeed provide significant weight saving over steel risers. The main objective of this thesis is to demonstrate that by tailoring the design employing off-axis reinforcements the weight savings offered by advanced composite materials can be substantially increased.

Two different methodologies for the tailored design have been developed in this thesis to minimise the structural weight of the composite riser: one, using an iterative approach of manual inspection and selection and another employing the optimisation technique of Surrogate Assisted Evolutionary Algorithm. The tailored design approach has been applied to eight different material combinations including high strength and high modulus fibre reinforcements, thermoset and thermoplastic matrices and metallic and thermoplastic liner materials to optimise their laminate configurations for minimum structural weight. The designs are conducted in accordance with the Standards, considering both local load cases and global - functional as well as environmental - loads.

The results show that the tailored design including off-axis reinforcements provide significant weight advantage compared to the conventional approach using only axial and hoop reinforcements. Comparison of the structural weights of the risers with different material combinations shows that the combination of thermoplastic PEEK matrix reinforced with high strength AS4 fibres and PEEK liner offers the highest weight savings.

ACKNOWLEDGEMENTS

I would like to express my deepest thanks to my supervisor, Dr. Krishnakumar Shankar, for his guidance and enthusiastic encouragement throughout this research and I will always be grateful to him for improving my style and his support during difficult times. He has been an excellent supervisor and mentor and his infectious enthusiasm constant encouragement and valuable suggestions keep me motivated and provide the necessary direction for my research. Special thanks to my co-supervisor, Prof. Evgeny V. Morozov for his thoughtful critique of my work and support during the research.

Thanks to Denise Russell for her proof-reading which is a tremendous help in improving my writing skills. Many thanks to all my friends and colleagues at UNSW Canberra who made my stay and work in Canberra a memorable experience.

My deepest gratitude to my parents and girlfriend Liping; without their love, confidence, support and encouragement, I would not be able to complete my research work.

LIST OF PUBLICATIONS

[1] Chunguang Wang, Krishna Shankar and Evgeny V. Morozov. *Numerical analysis of deep sea steel risers under combined loads.* in *6th Australasian congress on applied mechanics*, 2010, Perth, Australia.

[2] Chunguang Wang, Krishna Shankar and Evgeny V. Morozov. *Local design of composite riser under burst, tension, and collapse cases.* in *18th International conference on composite materials*, 2011, Jeju Island, Korea.

[3] Chunguang Wang, Krishna Shankar and Evgeny V. Morozov. *Tailoring of composite reinforcements for weight reduction of offshore production risers.* Applied Mechanics and Materials, 2011. vol 66-68: p. 1416-1421.

[4] Chunguang Wang, Krishna Shankar and Evgeny V. Morozov. *Design of deep sea composite risers under combined environmental loads.* in *2012 Composites Australia & CRC-ACS conference*, 2012, Blue Mountain, Australia.

[5] Chunguang Wang, Krishna Shankar and Evgeny V. Morozov. *Design of composite risers for minimum weight*. World Academy of Science, Engineering and Technology, 2012. vol 72: p. 54-63.

[6] Chunguang Wang, Krishna Shankar and Evgeny V. Morozov. *Tailored local design of deep sea FRP composite risers.* submitted to: Materials and Structures (under revision).

[7] Chunguang Wang, Krishna Shankar and Evgeny V. Morozov. *Global design and analysis of deep sea composite risers under combined environmental loads.* submitted to: Ocean Engineering.

[8] Chunguang Wang, Krishna Shankar, Muhammad A. Ashraf, Evgeny V. Morozov and Tapabrata Ray. *Design of composite risers using surrogate assisted evolutionary optimisation.* submitted to: Composite Structures.

TABLE OF CONTENTS

Appendices

ABBREVIATIONS AND SYMBOLS

3D	Three-Dimensional
ABS	American Bureau of Shipping
API	American Petroleum Institute
ATP	Advanced Technology Programs
CFPR	Carbon Fibre Reinforced Polymer
CLT	Classical Laminate Theory
DACE	Design and Analysis of Computer Experiments
DNV	Det Norske Veritas
DOE	Design of Experiment
DWRRA	Deep Water Royalty Relief Act
EDP	Emergency Disconnect Package
FE	Finite Element
FEA	Finite Element Analysis
FPS	Floating Production System
FRP	Fibre Reinforced Polymer
FS	Factor of Safety
GOM	Gulf of Mexico
HM	High-Modulus
HS	High-Strength
ID	Internal Diameter
IFP	Institut Francais du Petrole
KOP	Kvaerner Oilfield Products
LC	Load Cases
LHS	Left-Hand Side
MCI	Metal-to-Composite Interface
MDO	Multidisciplinary Design Optimisation
MMS	Minerals Management Service
NCAS	Norske Conoco As
NIST	National Institute of Standards and Technology
OA	Orthogonal Array
OD	Outer Diameter

ORBF	Ordinary Radial Basis Function
ORSM	Operational Range Site Model
PEEK	Poly Ether Ether Ketone
RBF	Radial Basis Function
RHS	Right-Hand Side
ROM	Rule of Mixtures
RSM	Response Surface Methodology
SAEA	Surrogate Assisted Evolutionary Algorithm
SPP	Stress-Partitioning Parameter
TLP	Tension-Leg Platform
TTR	Top Tension Riser
VIV	Vortex-Induced Vibration
WD	Water Depth

A	Area of pipe section
A_i, A_o	Internal and external cross-section areas of riser (Eq.4-10)
C_D	Normal drag coefficient
C_M	Coefficient of inertia
D_m	Outside diameter (Eq. 3-5)
D_o , D_i	Outside and inside diameters
E	Young's modulus
G	Shear modulus
H	Wave high
H_m	Maximum wave height
H_s	Significant wave height
I	Area moment of inertia
L	Wave length
P_{axial}	Axial stress (Eq. 4-7)
P_b	Burst capacity (Eqs. 4-1, 4-5 and 4-6)
P_c	Collapse strength (Eqs. 4-3 and 4-11)
P_e	Elastic collapse pressure (Eq.4-11)
P_i, P_o	Internal and external pressures (Eq.4-10)
P_{ia}	Internal pressure_above sea leave

P_{ib}	Internal pressure_below sea leave
P_p	Propagating buckling strength (Eq. 4-4)
P_{st}	Shut-in pressure
P_y	Yield pressure at collapse (Eq.4-11)
R_i	Internal radius of the liner
R_{inter}	External radius of the liner/ internal radius of the composite body
R_o	External radius of the composite body
S_0	Mean displacement of platform (Eq. 3-1)
S_L	Mean displacement of the platform's low-frequency motion (Eq. 3-1)
S_n	Mean displacement of the platform's wave-frequency motion (Eq. 3-1)
T	Period of wave
T	True wall tension of different position (Eq. 4-7)
T_a	Axial tension force (Eq.4-10)
T_{eff}	Effective tension force (Eqs. 4-2 and 4-10)
T_y	Yield tension force (Eq. 4-2)
Tg	Glass transition temperature
T_L	Period of the platform's low-frequency motion (Eq. 3-1)
T_z	Period of low-frequency motion
U	Ultimate tensile strength (Eqs. 4-5 and 4-6)
V	Volume ration
Y	Yield strength (Eqs. 4-5, 4-6 and 4-12)
Yr	Reduced yield strength (Eqs. 4-7 and 4-11)
YS_m	Yield strength (Eq. 3-5)
d	Water depth
f_c	Collapse design factor (Eq. 4-3)
f_d	Burst design factor (Eq. 4-1)
f_e	Weld joint factor (Eq. 4-1)
f_{pc}	Propagating buckling design factor (Eq. 4-4)
f_t	Temperature de-rating factor (Eq. 4-1)
f_t	Tension design factor (Eq. 4-2)
k_n	Wave number (Eq. 3-1)
n	Stacking sequence
p_m	Hydrostatic test pressure (Eq. 3-5)

t	Riser wall thickness
t_{liner}	Thickness of the liner
t_0	Thicknesses of the 0° (axial) layers
t_θ	Thicknesses of the ±θ° (angular) layers
t_{90}	Thicknesses of the 90° (hoop) layers
t_m	Wall thickness (Eq. 3-5)
α_L	Phase angle between the low-frequency motion and wave (Eq. 3-1)
α_n	Phase angle between the wave-frequency motion and the wave (Eq. 3-1)
ε, γ	Strain of lamina
ω_n	Frequency of the wave (Eq. 3-1)
ϕ_n	Initial phase angle of the wave (Eq. 3-1)
γ_{FM}	Combined load effect and resistance factor
γ_{Rd}	Resistance model factor
γ_S	System factor
γ_{Sd}	Load model factor
ν	Poisson's ratio
θ	Reinforcement angle for the fibres
$\pm\theta$	Angles of the ±θ° (angular) layers
ρ	Density
ρ_i	Density of internal fluid
σ, γ	Stress of lamina
σ^C	Compressive strength
σ^T	Tension strength
Δ	Displacement

LIST OF FIGURES

LIST OF TABLES

CHAPTER 1

INTRODUCTION

1.1 Background

A riser is an indispensable component of an offshore oil and gas exploitation structure. It is used to transport extracted fluids from the sub-sea wellhead to the production platform on the sea surface (*production riser*) or guide a drilling stem and conduct the drilling fluid upwards (*drilling riser*). A typical offshore production platform may have up to 40 risers, each consisting of as many as 100 large diameter tubular segments (riser joints) which make up its length. For a top-tension riser (TTR), a tension is applied on its top to eliminate compressive stresses and maintain the riser's vertical position. Currently, the offshore oil and gas industry uses production risers made from high-grade steel, the weights of which limit the capacity of offshore operations to move into deeper waters. The weight of a riser and, consequently, the top tension required to keep it in the desired position increases with increasing depths of the sub-sea wellhead. At the same time, the top-tensioning capacity of the offshore platform limits the number of risers that can be attached to it. Therefore, if the weight of an individual riser can be reduced, it will become possible to exploit natural resources from deeper waters or install more risers on existing platforms, thereby increasing their production capacities.

Due to the desirable mechanical properties and low density of advanced fibre reinforced polymer (FRP) composites, it has been widely recognised that using them instead of steel in the manufacture of deep-sea riser systems will lead to considerable weight savings which will reduce the operational costs of existing platforms due to the low tension requirement for lighter risers and also facilitate extractions of oil and gas from greater depths [1-3], thereby providing significant economic benefits. Also, FRP composites have better thermal insulation properties, and corrosion and fatigue resistance than steel which provide additional benefits in terms of reducing maintenance costs. Another advantage of using FRP composites is that a design can be tailored to specific requirements and provide a wider range of possible configurations with different matrix and fibre reinforcement combinations, variations in fibre orientations, different stacking sequences and different liner materials. However, the use of composites for offshore risers also introduces challenges and added complexities to design and analysis.

Over the last three decades, several design studies and projects regarding the application of fibre reinforced composites in the manufacture of pipe segments for offshore risers have been conducted [4-8]. These designs and their fabricated prototypes confirm that FRP composites can, indeed, provide substantial weight savings over steel. However, most employed the simple approach of having fibre reinforcements in only the hoop and axial directions and made no attempt to optimise a laminate configuration to minimise structural weight. As one of the main advantages of fibre reinforced laminate construction is that the reinforcement orientations in an individual lamina can be tailored to maximise its load-carrying capacity, it appears reasonable that, by including composite layers reinforced in the off-axis directions and tailoring a composite's configuration, including its laminate sequence, fibre orientations and thicknesses of individual layers, greater weight savings and, thereby, economic benefits can be achieved.

1.2 Objective

The objective of this thesis is to demonstrate that the weight savings offered by the use of advanced fibre reinforced composites instead of steel for the construction of offshore risers can be significantly increased by including laminae with off-axis fibre reinforcements and tailoring the entire laminate configuration to minimise weight. This is achieved by comparing the weights of the tailored design (including fibre reinforcements in the off-axis directions) with those of the conventional design (with reinforcements in only the axial and hoop directions), using a steel riser as the benchmark. For both methods, the laminate configurations (including their inner liners) are optimised for minimum weight using iterative design procedures developed specifically for this purpose. The results from this manual optimisation procedure are further verified by a mathematical optimisation technique, the Surrogate Assisted Evolutionary Algorithm (SAEA), for the tailored design.

1.3 Scope

As this study is intended to demonstrate and quantify the weight savings that can be achieved by the proposed tailored design of laminated composite risers, its scope is limited to the design stage, with manufacturing processes not considered. Therefore, the following assumptions are made in this thesis.

- The manufacturing process is perfect and produces components that are flawless and true to their designs.

- The materials and structure are perfect, i.e., no effects of manufacturing flaws or defects that may occur in service are considered.
- All the metallic components, such as the metal-to-composite interface (MCI) and inner tube for fluid transportation, have standard geometries.
- Vortex-induced vibration (VIV) can be suppressed by the attached fairings.
- Requirements for the fatigue life and long-term durability of a composite riser are satisfied by employing long-term values for the strengths of its lamina.
- The designed riser is rigid (as opposed to flexible) and has a top-tension configuration.
- The effects of elevated temperatures of the transported fluids on material properties are ignored.

1.4 Methodology

In this study, a composite riser is designed based on the requirements in the Gulf of Mexico for the extraction of natural resources from a depth of about 2000m. Its configuration is that of a TTR with a metallic tension joint at its top and a metallic stress joint at its bottom.

Initially, a steel riser is designed for minimum weight by satisfying all the functional and environmental load requirements, both local and global, specified by the standards, for use as the benchmark. As the configuration of a composite riser is more complex and involves more variables than that of the steel riser, its design involves three stages, the first of which is the design of the local geometry of its composite tube (laminate configuration and thicknesses of liner and composite layers) under local loads. It is necessary to perform the local design first to obtain initial estimates of the laminate configuration and thicknesses of its liner and composite body since, as the forces and moments along the length of a riser under global loads are influenced by the large deformations to which it is subjected, they depend on the sectional geometry of the tube. The local design is performed using finite element analysis (FEA) with layered solid elements to accurately determine the stress distributions in each layer of the laminate. Once the local geometry is tentatively established, the design proceeds to the second stage which is an analysis of the entire riser under global loads to determine its critical locations and load combinations at these locations. One-dimensional pipe elements are employed in the FEA for global analysis, as using layered 3D elements over the full length of the riser (over 2000m) would be prohibitively expensive computationally. The third stage of the design is the structural verification of these critical sections under the combined forces, pressures and moments acting on them, as determined from the global analysis which is also conducted with layered 3D elements to accurately determine stress distributions. Obviously, if the factors of safety (FSs) do not meet the design specifications, these sections have to be redesigned and the entire design process repeated. Eight different material combinations, including high-modulus and high-strength carbon fibre reinforcements, thermoplastic and thermoset matrices, and thermoplastic and metallic liner materials, are studied in this thesis.

All eight composite material combinations are designed for minimum weight using both the conventional and tailored design procedures. The conventional design method, which has been employed in many previous projects [4-8], considers only fibre reinforcements in the axial and hoop directions whereas the tailored design also considers those in other intermediate angles which are optimised for minimum structural weight. The optimisation in both methods is performed using an iterative procedure which involves repetitive cycles of finite element stress analysis, evaluations of FSs and manual selections of laminate parameters. The results from the manual inspection and selection procedure are subsequently verified using the mathematical optimisation technique SAEA.

1.5 Outcomes

The outcomes achieved from this research are listed below.

- Methodologies using iterative cycles of manual inspection, evaluation and selection of parameters have been developed for the design of composite risers with minimum weight, using both the conventional and proposed tailored designs.
- For the first time, a composite riser has been designed for minimum weight using a tailored design which includes reinforcements in its off-axis as well as axial and hoop directions.
- A population-based evolutionary algorithm is successfully applied to perform optimisation of the design of the composite riser for minimum weight and verify the results for optimisation by manual inspection and selection.
- Using eight different material combinations, this thesis demonstrates that the weight savings offered by employing FRP composites instead of steel can be significantly increased by using the tailored design, which includes plies reinforced in off-axis orientations. The weight savings provided by the tailored design over that by conventional design are quantified using the steel riser as the benchmark.

1.6 Outline of Thesis

Chapter 1 is the introduction which provides the background to, objective and scope of, research methodology used and outcomes from, this research.

Chapter 2 presents a review of the literature on previous attempts to design and test deep-water risers using fibre reinforced composite materials which shows that composites can reduce structural weight and provides the motivation for this research.

This review finds that efforts to fully utilise the potential benefits of composite materials in the design of offshore risers is still incomplete. As a result, the research objective of achieving minimum weight by tailoring the laminate configuration comes out.

Chapter 3 provides an overview of the design approaches and material selections for both the steel and composite risers, and the configurations of the tension, stress, standard steel and composite joints. The local design load cases, environmental situation in the Gulf of Mexico and global design load cases prescribed by the standards, which specify the designs of both steel and composite risers, are presented.

Chapter 4 describes the design and analysis of the steel riser used as the benchmark, the detailed design procedure for satisfying all the local and global load cases and the FEA with Pipe59 elements employed for the design of the steel riser.

Chapter 5 presents the local design for a composite riser. The methodologies employed in the conventional and tailored approaches, both of which are optimised for minimum weight through iterative procedures of manual inspection and selection, and the finite element modelling used for stress and buckling analyses, are described. Finally, the results from the local designs for all eight composite material combinations are presented and compared.

Chapter 6 presents the global design for composite risers based on the local geometries optimised in *Chapter 5*. It includes an analysis of the entire composite risers under global loads and the structural verifications of the critical locations identified. Since the laminate configurations and thicknesses determined in *Chapter 5* do not consider global loads, at most, they can only be considered as tentative until the global design is performed and the adequacy of all sections to bear the forces and moments due to global loads is verified.

Chapter 7 presents an alternative procedure for conducting the tailored design in which SAEA is applied as the optimisation method to minimise the structural weight under specified load requirements. The purpose of the SAEA tailored design is to corroborate and authenticate the efficiency of the manually tailored design approach developed in *Chapter 5* and make any possible improvements.

Chapter 8 presents a summary of, and conclusions drawn from, this research, as well as recommendations for future research and development work which could be undertaken in collaboration with industry.

CHAPTER 2

LITERATURE REVIEW

2.1 Introduction

The consumption of energy, particularly in the form of oil and gas, is exponentially increasing throughout the world, a trend which is expected to continue in the future. However, as the crude resources of oil and gas on land are limited, those on the ocean floor become more and more attractive. During the past few decades, offshore exploration and production activities have moved significantly into deeper waters as the interest in deep-water reserves has grown significantly.

Using the Gulf of Mexico (GOM) as an example, its reserve amount of oil equivalents is estimated to be approximately 32 billion barrels (15 billion has been proven to exist) and annual production has been continually growing at an average rate of 38% rate from 1996 to 2003 [9]. Also, there are many times more reserves and production activities in its deep-water (deeper than 305m/1000ft) than shallow-water fields [10, 11]. More importantly, the average field size of added shallow-water reserves shows a declining trend while that of deep-water reserves has been increasing significantly since the beginning of the 1990s and, on average, has been more than ten times that of shallow-water reserves [10]. The ever-increasing discoveries of reserves in deep water has seen a reduction and increase in leasing activities in the shallow- and deep-water categories, respectively [11] (Fig. 2.1). This rapid increase in leasing activities in deep water demonstrates the fast growth in industrial interest in, and demand for, deep-water reserves.

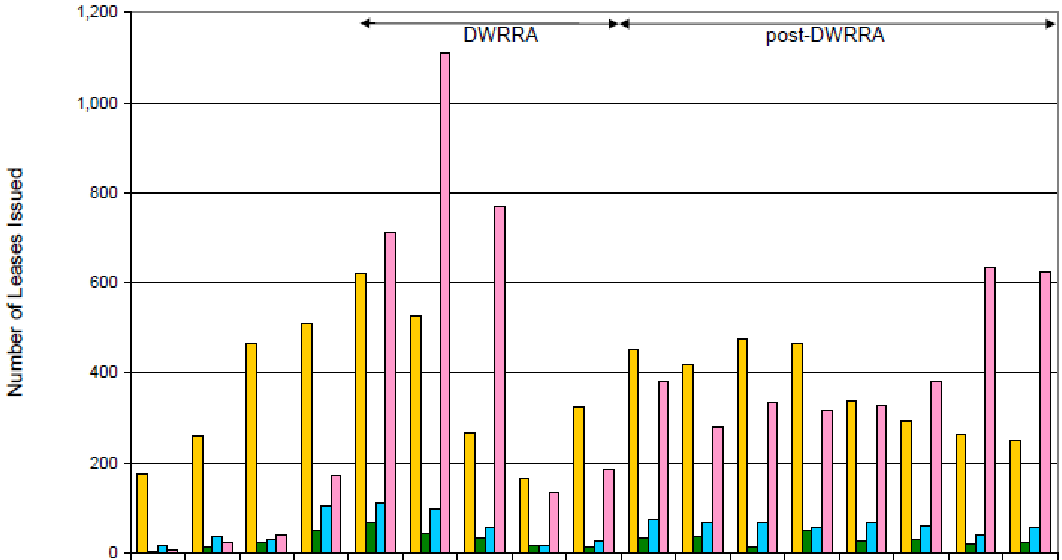

	1992	1993	1994	1995	1996	1997	1998	1999	2000	2001	2002	2003	2004	2005	2006	2007	2008
< 200 m	176	261	466	509	620	525	265	165	325	453	418	474	464	336	292	264	250
200 - 400 m	4	15	25	52	66	44	35	16	14	33	37	15	51	26	29	20	23
400 - 800 m	17	36	30	103	110	99	58	17	28	74	68	67	57	67	61	40	56
> 800 m	7	24	39	171	712	1,110	771	135	186	382	281	333	316	326	381	633	623

Lease Sale Year

Fig. 2.1. Number of leases issued each year subdivided by Deep Water Royalty Relief Act (DWRRA) water-depth categories [11]

Fig. 2.2 shows a number of different types of production system configurations employed in offshore oil and natural gas extraction, including conventional fixed platforms, compliant towers, different types of tension-leg platforms, semi-submersibles and floating production facilities. While these constructions vary mainly in the ways in which their platforms are positioned over sub-sea wells, as all require risers for the transportation of the extracted fluids from the wells to the production platform, the role of the riser is indispensible. For deep-water systems, tension-leg platforms (TLPs), spars and semi-submersibles (numbers 4 to 8 in Fig. 2.2) can be employed but the most common construction for long duration and high-level production facilities is the TLP.

(1) (2) (3) (4) (5) (6) (7) (8) (9) (10)

Fig. 2.2. Different types of production systems with risers: (1 and 2) conventional fixed platforms; (3) compliant tower; (4) vertically moored tension-leg platform; (5) mini-tension-leg platform; (6) spar; (7 and 8) semi-submersibles; (9) floating production, storage and offloading facilities; and (10) sub-sea completion and tie-back to host facility [12]

For the purposes of the investigation into the efficient design of composite risers undertaken in this study, the TLP is chosen as the production platform to which the risers are attached. The first working TLP (Hutton [13]) was deployed in the North Sea in the early 1980s and was followed by numerous other TLP systems. Their most frequently used working depth is approximately 305m to 1524m (1000ft to 5000ft) [11] but, using current technologies, this can be up to 2438m (8000ft) [14]. The vertical moorings in a TLP are called tendons or tethers. Tendons connect a platform to the sea floor and are always in tension, which is maintained by the excess buoyancy provided by the platform's hull, due to which the structure is vertically rigid but horizontally compliant. Oil and gas are then transferred from the wells to the platform through vertical production risers.

In offshore engineering, the materials usually employed for structural components are metals, with high-grade steel, titanium and aluminium alloys currently the most common materials for the construction of riser tubes. With the development of composite material technology, the utilisation of fibre reinforced polymer (FRP) composites is gradually increasing due to their superior mechanical properties, low density and other desirable properties, such as better thermal insulation, and corrosion and fatigue resistance.

2.2 Advantages of FRP Composites in Offshore Engineering

The introduction of composite materials for offshore applications began about six decades ago. They have attracted substantial attention from the offshore oil and gas industries primarily due to their high specific strengths and stiffnesses which contribute to weight reductions and cost savings. At present, composites are utilised in various topside components of platform, accumulator vessels, flow-lines, spoolable piping and tubing, flexible risers, composite tethers and buoyancy modules [5, 6, 15-28]. However, to date, their use in risers has been restricted to prototype production and drilling risers, although it is widely recognised that they can provide significant weight reductions for deep-water operating systems [4-8, 29].

Many previous studies have shown that, although the material costs of FRP composites are higher than those of steel, their total life-cycle costs will be less due to the add-on effects of their weight savings for other system components, such as decreased platform sizes, mooring pretensions and top-tension requirements, reduced total system weight, and stacked volume and buoyancy weights [1, 18], especially in deep-water applications [17, 30-32]. Specifically, an extended water depth means more severe load conditions and larger platform payloads which require significant increases in the fabricated steel required and additional mooring pretensions. It has been reported that a one-pound increase in platform payload translates to an additional four to seven dollars in cost [17, 31]. As a riser’s operational depth increases, the top tension required to be applied to it also increases for which more buoyancy in the hull and a larger platform are necessary. In addition, not only does the required length of the riser increase but also its thickness due to the higher hydrostatic pressures encountered.

Therefore, the effect of increased depth on a riser's weight and, thus, the top tension required is twofold. Research has found that sizes of TLPs increase at a much higher rate as their top tension are larger [18] which limits the number of risers that can be utilised or the depth to which they can be deployed. Based on the capacities of currently available platforms, the depth to which a steel riser can be economically deployed is between 1000 and 1500m [33] (and sometimes up to 1800m [34]) for production risers and over 3000m for drilling risers [34]. Therefore, the weight savings obtained from using FRP composite materials will allow more risers to be installed at existing depths, thereby increasing production, and the viable exploitation of petroleum resources greater depths [18, 35, 36]. In addition to a lower density, FRP composites have better thermal insulation properties, excellent damping, and corrosion and fatigue resistance [37, 38] which will provide more benefits by reducing maintenance costs.

In order to successfully apply composite materials in offshore risers, their durability in sea water also has to be considered. Venkatesan et al. [2] found that none of the long-term properties of carbon fibre reinforced polymer (CFRP) composites experienced any significant variations after exposure to pure water and sea water at different temperatures. On the other hand, many researchers, such as J.O. Jansons et al. [38], G.L.Balazs and A. Borosnyoi [37], and G.R. Ross and O.O. Ochoa [39, 40] found that the long-term tensile strength of a CFRP reduced to between 80% and 95% of its short-term values. When the thermoplastic composite carbon/PEEK was tested in boiling water [41], although its axial tensile strength was hardly affected, its transverse tensile strength decreased after exposure to the boiling water. It was concluded that, to avoid failure, the maximum service temperature of thermoplastic composites has to be well below the glass transition temperatures of their polymer matrices. Besides carbon fibres, other commonly used fibres in composites are glass, Aramid and some synthetic high-performance fibres such as M5, Zylon, Dyneema and Spectra. However, the performances of composites reinforced with these fibres significantly reduce under sub-sea conditions [37, 42-49].

Besides research into the mechanical properties of composite materials in sea water, the global responses and performances, including load distributions, fatigue, resonances and vortex-induced vibrations (VIVs) of entire composite risers (including their steel tension, stress and some standard joints) under global environmental and functional loads have also been investigated [18, 33, 50-54]. It has been found that, in general, the tension force decreases with an increasing water depth and the maximum bending moment is on the stress joint at the bottom, followed by the joints at the sea surface which have higher bending moments than those in the middle of the riser string [18, 50-52, 55, 56]. Compared with an all-steel riser, the axial tension and bending moment throughout an entire composite riser, including its tension, standard and stress joints, are reduced due to its lower overall weight [51, 52]. The excellent fatigue resistance of FRP, especially carbon fibre-reinforced, composites also adds to their durability, as confirmed by previous studies [50-52]. More specifically, the structural composite body of the composite’s riser joint is likely to have an infinite fatigue life [50-52] while those of the metal liner of the joint, its metal-to-composite interface (MCI), and steel tension and stress joints have also been found to be adequate [50, 52]. However, it may be noted that the fatigue properties of a FRP composite may vary depending on the choice of constituent materials and manufacturing process [51, 52], while the fatigue life of its steel liner welds can be significantly lower [52]. The resonant response study presented by Kim [51] demonstrated that the composite riser system in sea water did not show notable resonance due to the strong resistance of the drag force and vibration amplitudes in its bottom region which were relatively small compared with those in a steel riser [51]. In other words, the vibration waves descending from the top of the composite riser were damped much more than they were in a steel riser. Studies of VIV in composite risers found that the fundamental frequency of a composite riser was higher than that of a steel riser [54] because of its lower mass but that its value was relatively small [50, 51]. It was also found that VIV in a composite riser was sensitive to structural damping and tension variations [50] and, in general, increasing damping and tension could reduce VIV-induced fatigue [50, 53]. A. F. Omar et al. [54] found that the maximum VIV stresses induced in a composite riser were about half those in a comparable steel riser which indicated that composite risers would have considerably longer fatigue lives than steel risers. Another VIV study of composite risers conducted by K. Z. Huang [50] showed that VIV-induced fatigue damage caused by both long-term and extreme currents was moderate in a composite riser without VIV suppression and could be effectively suppressed by adding strakes. Therefore, strakes are normally cautiously used to provide an extra safety margin for VIV situations.

From the discussion above, it is clear that FRP composites offer several advantages over steel due to their excellent properties, such as high specific stiffness and strength, better thermal insulation, excellent damping, and corrosion and fatigue resistance which results in better global responses and performances, including smaller tension and bending distributions along the length of a riser and better fatigue and VIV responses. These characteristics provide an extended service life and require a lower platform size, mooring pretension and top tension which allows for a reduced total system weight, stacked volume and buoyancy weight, thereby making composite risers more cost efficient.

In addition, the design of a composite riser can be tailored to specific requirements by modifying some of its design variables, such as fibre and matrix combinations, fibre orientations, thicknesses of the liner and composite lamina, and stacking sequences. A tailored design which fully optimises these variables can enhance the benefits offered by FRP composites [55, 57, 58] and obtain greater weight savings.

2.3 History of FRP Composite Riser Development

FRP composites are relatively mature in the design and manufacturing arenas within aerospace, military and sports applications, while attempts to design and apply composite materials in offshore structures started about six decades ago, more specifically, for the fabrication of riser segments using FRP composites in the 1970s.

In 1973, Ahlstone [59] patented a drilling riser filament-wound structure made from glass fibres coated with an epoxy resin. The patented tubular geometry included an internal liner and protective sleeve on the exterior, and the weight of the composite riser joint was much less than that of an equivalent steel riser joint.

In the 1980s, the Institut Francais du Petrole (IFP) and Aerospatiale of France undertook a project to evaluate composite offshore tubular structures [5]. Their design consisted of orthogonal reinforcements with 9.6mm of glass fibre-reinforced circumferential layers and 7.3mm of carbon fibre-reinforced longitudinal layers, with a 1.1mm Buna inner liner and an internal diameter of 0.2286m. The static burst and tension, and fatigue and creep tests conducted, proved that this composite riser tube was capable of carrying the expected mechanical loads.

In the mid-1990s, the National Institute of Standards and Technology (NIST) Advanced Technology Programs (ATPs) developed and tested composite riser tubes for applications in water depths of between 1000m and 1500m [6]. The tube's body was a hybrid composite structure consisting of carbon and E-glass fibres in an epoxy matrix.

The low-angle off-axis and circumferential carbon fibre reinforcements provided axial and circumferential strengths and stiffnesses, respectively, with an E-glass fibre in the middle to increase the stability of the cross-section. A total of 40 layers of carbon and glass fibre-reinforced materials were used in the longitudinal and hoop directions. After a series of static and cyclic fatigue tests, it was found that these composite riser tubes met both performance and cost requirements.

In the joint industry project led by Norske Conoco AS (NCAS) and Kvaerner Oilfield Products (KOP), a demonstration composite drilling riser joint (a tube segment) was installed in the field on the Heidrun TLP in July 2001 [4]. The drilling riser joints had hydrogenated nitrile rubber and titanium as their internal liner materials and titanium was used for the connectors. The composite test segments were installed in three typical locations in the drilling riser string and operated successfully for about 45 days. This field testing clearly proved that composite riser joints could meet rigorous offshore requirements.

ConocoPhillips, Kvaerner Oilfield Products and ChevronTexaco jointly funded a composite riser project (Magnolia Project) in March 2003 [7]. The purpose was to replace a few steel joints with composite joints on the Magnolia TLP which operated at a depth of about 1425m, and the projected structural weight saving over steel for a 19.2m joint was around 48%. Unlike the NIST ATP projects, the Magnolia project used steel for the liner and connectors to make the composite riser joints more economical. However, these joints could not be installed on the Magnolia platform because there was a leak in the liner during the final field test which threw doubt on the steel liner's pressure integrity [8].

More recently, Doris Engineering, Freyssinet, Total and Soficar entered into a joint venture to develop carbon fibre-reinforced thermoplastic (PA11) tubes for 2000 to

3000m water depths [29]. In this project, for the first time, ±55^{o} reinforced angle layers were included to increase burst resistance. The burst, tension and collapse calculations and tests showed that the thermoplastic composite riser was technically feasible while more qualification tests are being conducted.

In July 2009, Airborne Composite Tubulars, MCS Advanced Sub-sea Engineering and OTM Consulting organised a joint industry programme [60] to prove the concept of a thermoplastic composite riser but no further details are currently available in the open literature.

While most previous designs of composite risers [4-8] employed the simple approach of having fibre reinforcements in the hoop and axial directions separately (in some previous projects, the axial reinforcements were replaced by low-angle composite layers due to manufacturing constraints on having lay fibres in the axial direction), the co-operative venture by Doris Engineering and others [29] mentioned above introduced fibre reinforcements at ±55^{o} angles in an attempt to improve efficiency and achieve further weight reduction based on the netting theory. According to the netting theory, ±54.7^{o} is the most efficient reinforcement angle for a filament-wound thin cylindrical pipe under internal pressure with an end effect (burst case for production riser design) which has a hoop stress to axial stress ratio of 2:1 and, with fibres laid at this optimum angle, reinforcements are not required in any other direction [61, 62]. While the same minimum weight can be achieved with reinforcements in multiple directions by appropriately choosing their thickness ratios, having a single fibre orientation also reduces the manufacturing effort [62]. The netting theory assumes that all loads are carried by the fibres located in each layer and no stresses are developed in the transverse direction. However, if the stiffness in the that direction is taken into account, stresses will develop in the transverse direction to the fibres which can cause matrix failure.

Also, as the optimum angle is calculated using thin shell assumptions, it is not valid for thick tubes. Therefore, for a thick laminated composite pipe, $\pm 54.7^{o}$ does not represent the most efficient direction for fibre reinforcement under internal pressure with an end effect. Further, the minimum laminate thickness also depends on the ratios of the transverse (and shear) stiffness and strength to those in the fibre direction. As, for a production riser with top tension, the ratio of the hoop stress to axial stress is not 2:1, even for thin tubes, $\pm 54.7^{o}$ is no longer the angle of optimum reinforcement orientation [57, 58]. For these reasons, we need to separately evaluate optimum reinforcement directions for thick laminated tubes for specific load cases (LCs) to achieve the maximum weight reduction.

Through the aforementioned industry projects and research studies, including lab tests, field tests and numerical simulations, the feasibility and effectiveness of using composite materials in a riser system have been proven and the current manufacturing technology is sufficiently mature to fabricate riser joints that can meet the requirements of ultra-deep-water usage. These projects also show that the industry is well aware of the weight and cost benefits that can result from the replacement of steel with FRP composites in the construction of offshore risers. However, no offshore riser currently being employed is made entirely of composites, except the demonstration composite drilling riser joint (a tube segment) installed in the field on the Heidrun TLP [4].

Previous designs used the simple approach of reinforcing in the axial and hoop directions separately and did not consider fibre reinforcements in other orientations. As research into the design of composite risers using off-axis fibre orientations in order to fully utilise their potential benefits in terms of weight savings appears to be lacking, the current study focuses on this aspect. Finite element modelling is employed to determine stress distributions in the different layers of composite risers under local and global design load conditions using various combinations of fibre orientations to investigate weight savings that can be achieved by the introduction of off-axis layers. Furthermore, an optimisation study is undertaken to fully ensure that the reinforcement orientations and lamination sequences selected provide the maximum weight savings and, thus, the greatest economic benefits.

CHAPTER 3

DESIGN SPECIFICATIONS AND MATERIAL SELECTION

3.1 Introduction

The literature survey in the previous chapter identified several studies which clearly showed that the use of fibre reinforced polymer composites for the construction of offshore risers can offer significant weight savings which translate to lower operational costs, higher production rates and the capability to extract fossil fuels from greater ocean depths. However, none of these studies considered the tailoring of the fibre reinforcement of composite layers to take full advantage of their directionally oriented mechanical properties. The aim of this thesis is to demonstrate that greater structural weight savings can be accomplished by an efficiently tailored design of the composite walls of offshore risers and to quantify the weight savings that can be achieved by different material combinations. This chapter provides an overview of the design conditions, specifications, load requirements and constraints, as well as the material combinations, selected for this study.

For designs of the steel riser used as the benchmark, composite risers using the conventional design of having reinforcements in only the hoop and axial directions, and the proposed tailored design having reinforcements in other directions as well, this thesis employs a general approach which follows the design codes and recommended practices for offshore risers (API (American Petroleum Institute), ABS (American Bureau of Shipping), DNV (Det Norske Veritas) and MMS (Minerals Management Service)) [63-72]. In particular, the load scenarios, load factors for the environmental and operational loads, usage factor and the factors of safety employed all comply with the following recommendations: API: Design of risers for floating production systems (FPSs) and tension-leg platforms (TLPs) [63]; API: Design, construction, operation and maintenance of offshore hydrocarbon pipelines [64]; ABS Design Code: Guide for building and classing subsea riser systems [66]; and DNV Design Code: Offshore standard (DNV-OS-C501) composite components [72]. However, it needs to be noted that these codes were developed mainly for steel risers and, although they provide recommendations for composite risers, the design procedure becomes highly complex when composite materials are employed; for instance, as discussed in *Chapter 4*, in the case of the steel riser, verification that the local load requirements are being met is quite simple and straightforward and the design, which mainly consists of determining the tube thickness, can be accomplished in one step considering both the local and global loads on the entire riser. However, when employing fibre reinforced laminate construction for the tube wall, firstly, the number of variables to be determined increases and includes the stacking sequence, various ply thicknesses and ply orientations (in the case of the tailored design) and, secondly, as the loads which influence the stresses in the different layers depend on the laminate configuration itself, an iterative procedure has to be adopted. Most importantly, as analysing such a long riser using 2D or 3D layered elements in a finite element (FE) software becomes computationally very expensive due to the large number of elements required to satisfy aspect ratio constraints, the design has to be conducted in three stages, the first for local loads using layered composite elements, the second for global loads using pipe elements with effective smeared material properties obtained from the local design and, after the global analysis, which provides the exact forces and moments acting on each segment of the riser, the third, a final verification stage, ensures that the local detailed configuration is sufficient to meet these loads. Further, noting that the hydrostatic pressure increases with increasing depth and the other loads vary along the length of the riser, the wall thicknesses in different segments along its length of the steel riser are minimised separately to obtain the minimum weight for it to be used as the benchmark against the composite risers. However, for the composite risers, the same geometry is maintained for all their standard riser joints along their full lengths as the purpose of this thesis is to demonstrate that the use of composites rather than steel can achieve significant weight savings and that by tailoring the orientation of their fibre reinforcements, even greater weight savings can be achieved. Although it is not attempted in this thesis, it may be possible to obtain even more weight reduction for an entire composite riser by minimising the weights of different sections along its length.

3.2 Riser Geometry Specifications

A tension leg platform (TLP) is a buoyant platform held in place by a mooring system which is a set of ‘tension legs’ or ‘tendons’ attached to the platform and connected to a foundation on the sea floor (Fig. 3.1). The hull is a buoyant structure that supports the deck section of this platform and the drilling and production equipments. The deck for the surface facilities rests on the hull. As the buoyancy of the hull exceeds the weight of the platform, taut moorings or ‘tension legs’ are required to secure the structure to the sea floor. A typical TLP would be installed with as many as 16 tendons.

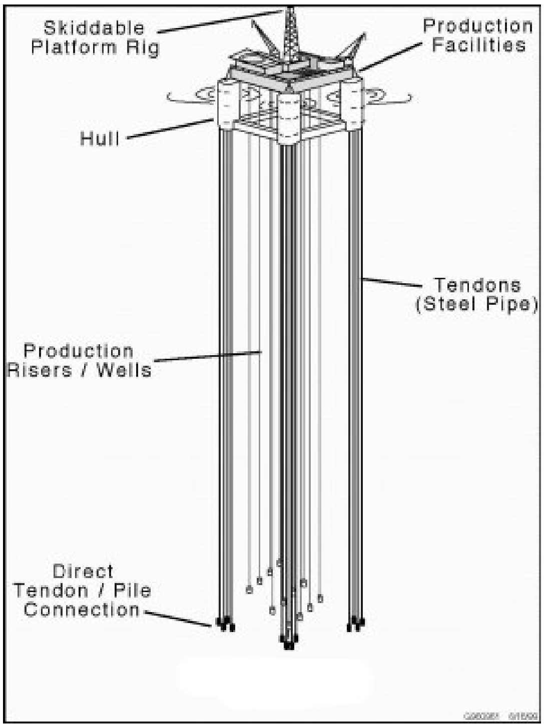

Fig. 3.1. Schematic of a typical tension leg platform [73]

Risers are long pipes that run from the seabed to the surface to guide a drilling stem or transport fluids from sub-sea wells to a floating platform or ship [34]. They are indispensable components of the oil and gas exploitation and production systems and their structural integrity is critical to safe field operations. According to their function, risers are classified as *drilling risers,* which are used to guide a drilling stem and conduct the drilling fluid upwards, and *production risers*, which raise the extracted oil or natural gas to a floating platform [34, 63]. Based on their design, there are *rigid top tension risers* (TTR), and *standard* and *alternative flexible risers* [34, 63, 74]. Drilling risers are mostly rigid TTRs (Fig. 3.2(a)) whereas production risers can be rigid or flexible, with the latter having various configurations, such as free hanging, steep S, steep wave, lazy wave, fixed S, tethered S and Chinese lantern, as shown in Figs. 3.2(b) and 3.2(c) [34]. Rigid production risers are used to connect a platform to the well directly beneath it while flexible risers connect a platform to wells further away. To the best of the authors' knowledge, almost invariably, all rigid production risers are configured as TTRs [18, 50, 52]. It should also be noted that all four previous design studies of composite riser joints [4-7, 29] included top tension in the load cases (LCs) they considered, even though only one was explicitly designed as a drilling riser joint. Therefore, this research focuses on a TTR, and the proposed tailored design implemented on it to demonstrate and quantify its weight savings can easily be adapted to other riser configurations by modifying load specifications.

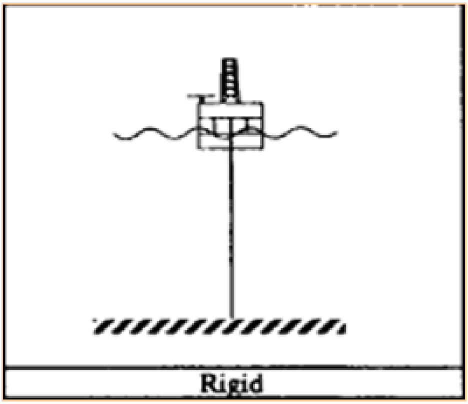

(a)

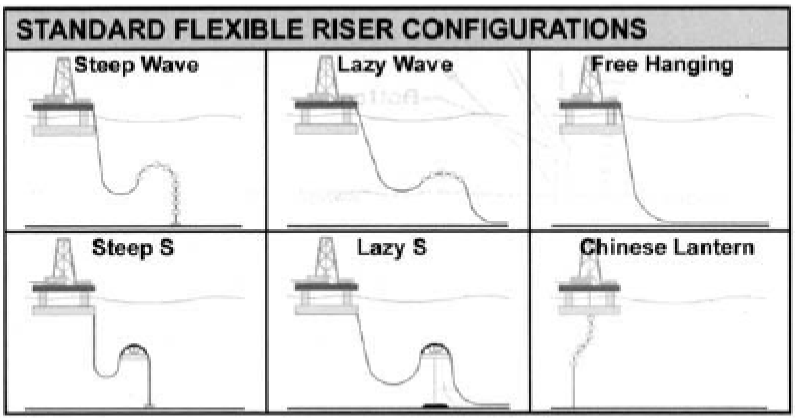

(b)

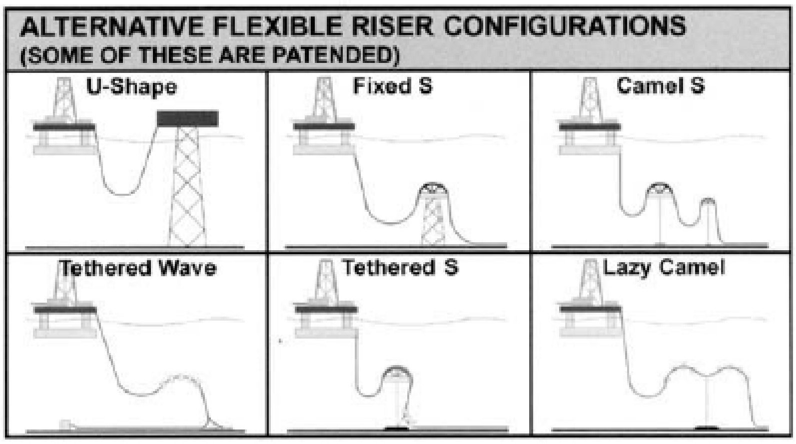

(c)

Fig. 3.2. Schematics of riser configurations (a) rigid risers; (b) standard flexible risers; and (c) alternative flexible risers [34]

In offshore engineering terminology, a rigid TTR normally consists of different segments (relatively short pipes with connectors at either end) called '*joints*'. Apart from standard riser joints (tubular segments which make up most of a riser's length) which may or may not have fairings, a TTR will have a tension joint at its top and a ball/flex connector or stress joint at its bottom, as shown in Figs. 3.3(a) and 3.3(b) respectively [75]. The flex joint [63] is constructed of alternating layers of metal and elastomeric materials which provides flexibility in the connection and allow large angular deflections in the riser without producing large bending moments near the end connector. The ball joint consists of a ball and socket housing that also provides for angular movement and minimal bending moments [63]. As the sliding friction and wear among its internal parts make the service life of a ball connector relatively short, it is not usually used for high-pressure and high-tension applications. On the other hand, the tapered stress joint [63] is designed as a transition member between the rigidly fixed or stiffer sections of the bottom of the riser at and its less stiff sections above which minimises angular movement and provides for large bending moments to be accommodated at the bottom of the riser. The stress joint is usually employed with an Emergency Disconnect Package (EDP) which disconnects the riser when the angular deformation/bending moment exceeds a certain specified value. For the design study in this thesis, a TTR system with a stress joint at the bottom (Fig. 3.3(b)) is considered. Since both these components occupy only a small portion of the length of the riser and their geometry is more involved due to the requirements for their connections to the rest of the system, standard configurations made of high strength steel are assumed for them. This research focuses only on the weight savings that can be achieved by employing fibre reinforced composites for the pipe segments of standard riser joints.

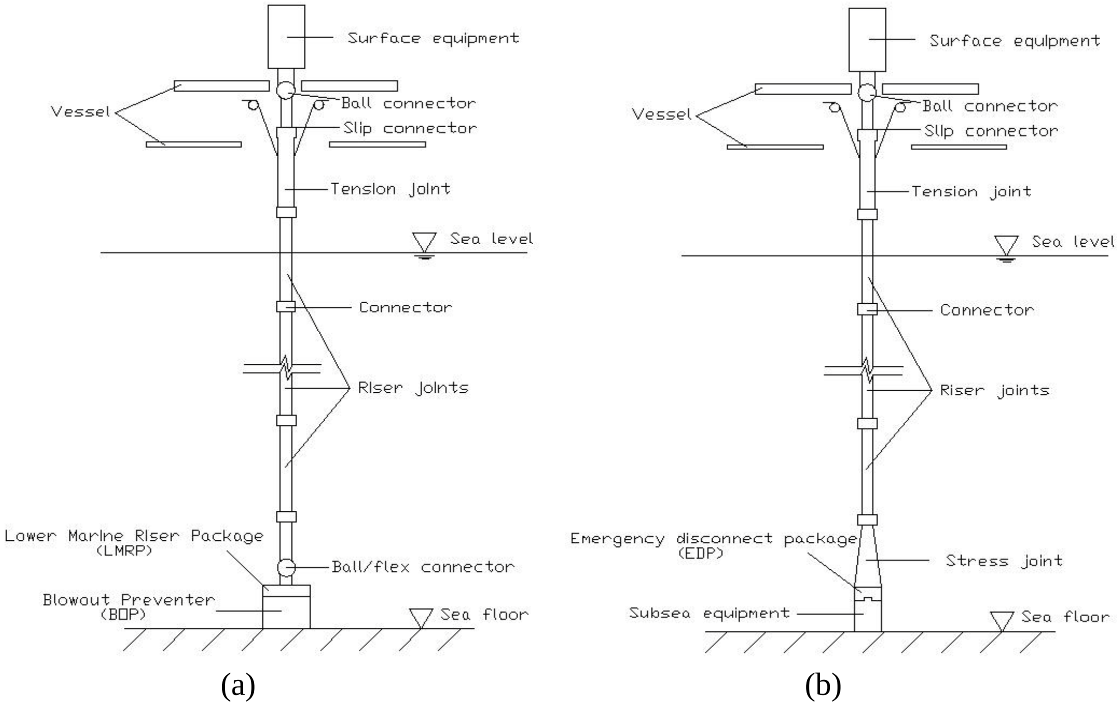

Fig. 3.3. Top tension risers with (a) flexible connector and (b) stress joint at bottom

Figs. 3.4(a) and 3.4(b) respectively show the cross-sections of the standard steel and standard composite riser joints employed in this study. The extracted fluids are transported by production tubings within the riser which are protected by the riser joints and the riser joints carry all the structural loads. The internal diameters (IDs) of both the steel and composite riser joints are fixed at 250mm while, as the thickness of each joint is determined by the design to accommodate all the loads considered, their outer diameters (ODs) depend on the design results. A standard production tubing with an ID of 118.6mm and an OD of 139.7mm is assumed to be situated inside the riser annulus and its weight is considered in the designs of both the steel and composite risers. If the production tubing fails, the internal pressure will act directly on the riser wall; otherwise, it is assumed that there is no internal pressure in the riser annulus. The steel riser joint is monolithic while the composite riser joint consists of an inner liner, a composite structural body and an external sacrificial layer.

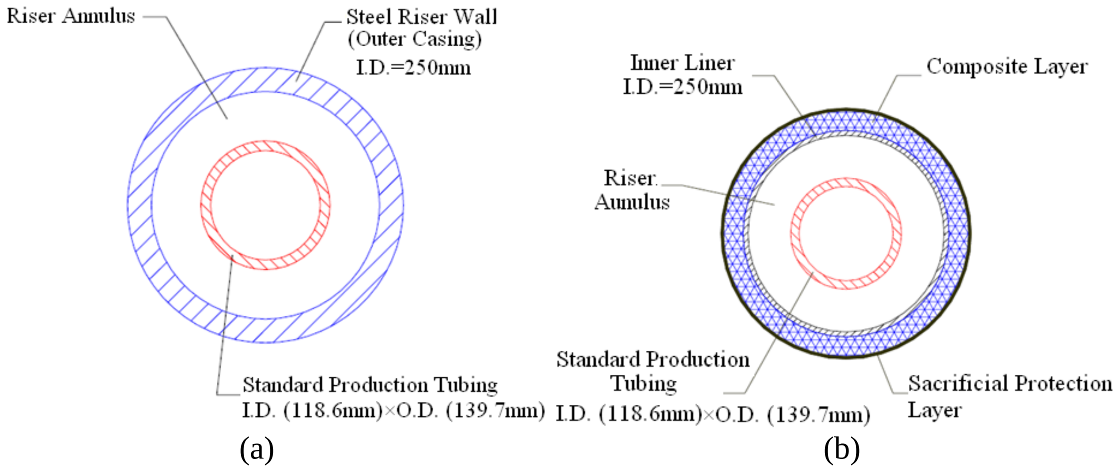

Fig. 3.4. Cross-section for (a) steel riser joint and (b) composite riser joint

As waves and currents induce drag loads on risers, devices for disrupting the coherence of a flow, such as helical strakes, are employed to reduce the vortex-induced vibration (VIV) effects. In the present study, as it is assumed that the VIV of risers are suppressed by fairings, fatigue damage due to VIV is not included. The fairings are employed on riser joints from the mean sea level to -624m below sea level and their additional weight is considered in determining the loads. A typical fairing segment used to mitigate VIV [63] is shown in Fig. 3.5.

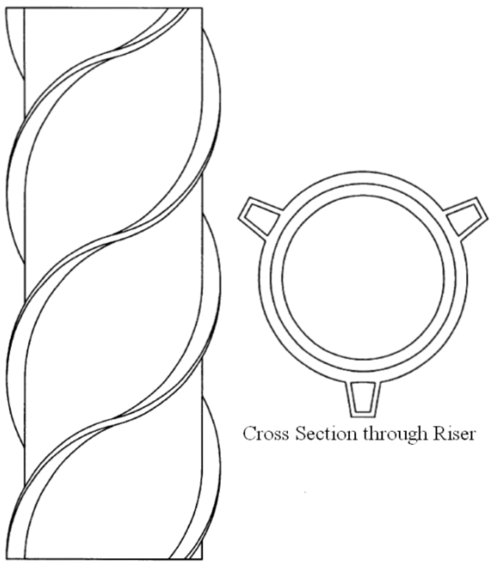

Fig. 3.5. Cross-section and span view of helical strakes used to mitigate VIV [63]

The general geometrical configurations of the tension joint, stress joint, typical composite riser joint and metal-to-composite interface (MCI), which are commonly employed and provide the basic geometry of the TTR in the present research, are shown in Figs. 3.6(a) to 3.6(d) respectively. In this thesis, the metallic tension joint at the top and metallic stress joint at the bottom are retained as the research focuses on improving the efficiency of the standard composite riser joints which form the bulk of the riser's structure and contribute to over 95% of its length. However, since the external liner and sacrificial layers of the composite riser joints have no contribution to load bearing, only their weights are taken into account in the analysis.

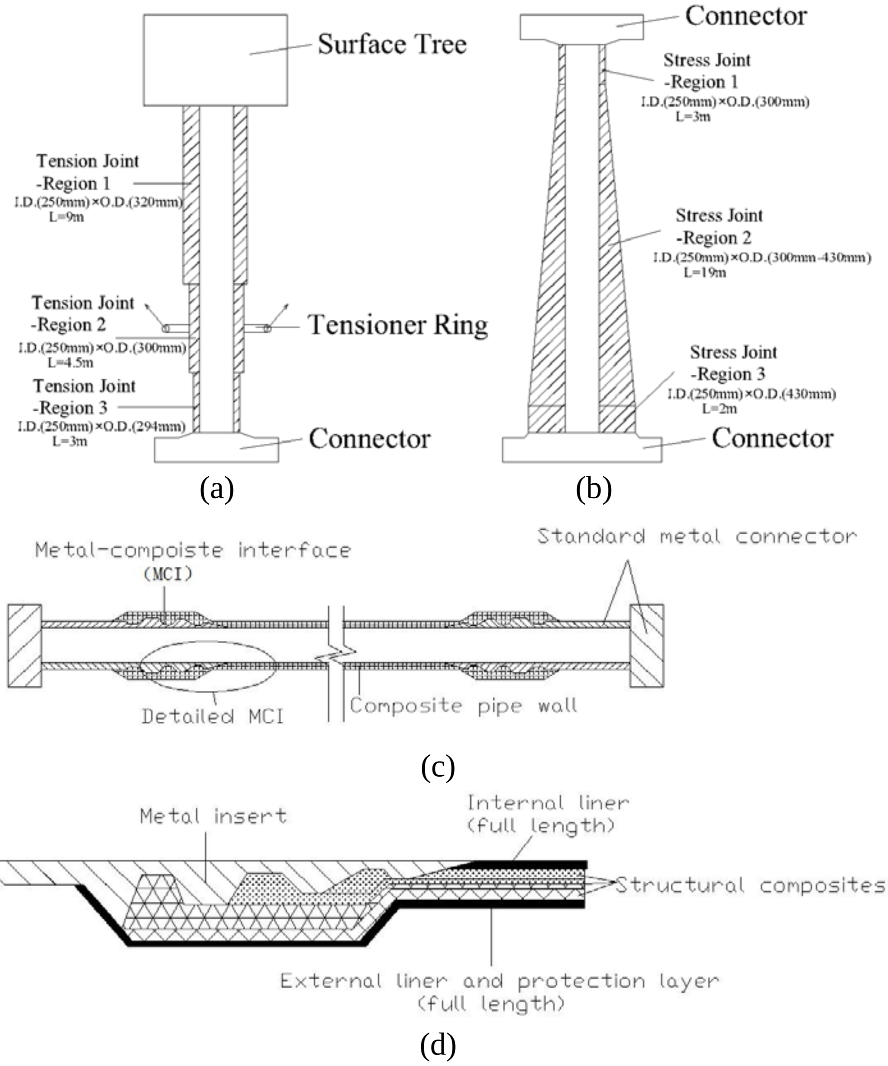

Fig. 3.6. General configurations of (a) tension joint; (b) stress joint; (c) typical composite riser joint and (d) details of metal to composite interface

As the depth from which oil or natural gas is extracted increases, longer risers have to be employed which dramatically increases the load on a production platform due not only to the greater power required for extraction but also the higher top tension required to support the weight of the risers. Thus, the benefits due to weight savings offered by composite materials are more apparent and significant for deep-sea applications. Hence, an ultra-deep-sea scenario with an extraction depth of about 2000m (depths over 305m are generally classified as deep-sea applications and those over 1524m as ultra-deep-sea applications [34]) is selected for the design study in this thesis. It should be noted that the proposed tailored design procedure can be easily adapted to risers of different lengths by considering the appropriate load requirements.

The foregoing paragraphs identify the configuration of the TTR, the overall geometry, i.e., length and ID of the riser and the configurations of the tension joint at the top and the stress joint at the bottom which are taken to be specified in the design. The focus of this study is to investigate the weight savings that can be achieved by tailoring the design of standard riser joints which comprise over 95% of the length of a riser and contribute to over 90% of its weight. Once the materials used in the design are also identified, the main parameter to be determined through the design study is the geometrical configuration of the composite tubular wall of the standard joints, i.e., the stacking sequence, number of plies, layer thicknesses and fibre orientations for the structural wall and thickness of the inner liner. To achieve this, firstly, the loading conditions and load parameters, which will be employed in an iterative design procedure to determine the tubular wall geometry, have to be identified. The following sections identify the load cases and materials selected for this research study.

3.3 Design Loads

The riser has to be designed to withstand local loads, such as internal and external pressures and tensions, as well as global loads, such as buoyancy, wave, current and platform displacement loads. To identify the load specifications for the design, it is assumed that the riser is to be installed on an offshore rig in the Gulf of Mexico as the environmental conditions and typical functional loads on a TTR riser with a length of about 2000m situated in the Gulf of Mexico have previously been used and are readily available in the literature [34, 51, 52, 63, 64, 66, 68, 69]. It may be noted that, in general, although the environmental and functional loads are the same for steel and composite risers, some of the loads such as the top tension depend on the riser's weight and geometry, while standards [63, 64, 66, 72] specify different load factors, usage factors and factors of safety for metallic and composite risers.

In general, the loads to be considered in this design can be divided into two categories: local loads, which govern the burst, tension, collapse and buckling capacities of the riser joints (tubular segments), and global loads which determine the overall structural capacity of the riser. For the steel riser used as the benchmark, the main parameter to be designed is the tube thickness which can be accomplished mainly by using a global analysis of the entire riser for both local and global loads. For the composite riser design, as both the local and global loads govern its parameters, the design has to be conducted iteratively by considering the local loads first to obtain an initial estimate of the laminate configuration, and then analysing the global loads to determine the actual forces and moments acting locally on the riser segments, and at last repeating the local analysis to ensure that the geometry is safe.

3.3.1 Local Load Cases

The local design situations considered for the steel riser are burst, tension, collapse and propagating buckles and, for the composite riser, burst, pure tension, tension with external pressure case, collapse and buckling under external pressure. It is important to note that, for the composite riser design, the stress and buckling analyses under local loads are conducted on a short pipe segment using 3D layered elements in order to separately determine the stresses in each layer as failure can occur in any layer. In contrast, the steel riser's capacities under local load cases can be obtained from analysing the entire length of the riser.

3.3.1.1 Local Load Cases for Steel Riser

The four local load cases considered for the steel riser design [63-65] are:

- Load Case 1 (burst): maximum internal pressure of 69.0MPa with end effect;
- Load Case 2 (tension with external and internal pressures): maximum tension force with and without internal and external pressures;
- Load Case 3 (collapse): maximum external pressure of 19.5MPa varying linearly along the depth of the riser; and
- Load Case 4 (propagating buckles): maximum external pressure of 19.5MPa varying linearly along the depth of the riser.

For the steel riser design, calculation of the effective tension force has to consider the five different combinations of pressure and tension listed in Table 3.1 which are based on different working situations for different global load cases, with the worst combination determining the effective tension capacity of the steel riser.

Table 3.1. Combinations to be considered for effective tension force calculation

Combination	Tension at top (kN)	Maximum internal pressure (MPa)	Maximum external pressure (MPa)
1	1.5 times effective weight with oil inside	0	19.5
2	1.5 times effective weight with oil inside	69.0	19.5
3	1.5 times effective weight with oil inside	58.6	19.5
4	1.2 times the effective weight with mud inside	35.7	19.5
5	1.5 times its effective weight with tubing inside without leakage	0	19.5

3.3.1.2 Local Load Cases for Composite Riser

The four local load cases considered for the composite riser design [66] are:

- Load Case 1 (burst): internal pressure of 155.25MPa with end effect (2.25 times the maximum internal pressure);
- Load Case 2 (tension): (a) pure maximum tension force with a load factor of 2.25; and (b) tension with external pressure: 2.25 times the maximum tension with an external pressure of 19.5 MPa;
- Load Case 3 (collapse): external pressure of 58.5MPa (maximum external pressure with a load factor of 3); and
- Load Case 4 (buckling): external pressure of 58.5MPa (maximum external pressure with a load factor of 3).

The tension force for the composite risers is the maximum of the three cases of (i) 1.5 times the effective weight of the riser with mud inside, (ii) 2.0 times its effective weight with oil inside, and (iii) 1.2 times its effective weight with tubing inside without leakage plus the tension due to the end effect of maximum external pressures [33, 67].

In this study, the tension is calculated based on a design length of 1970.1m for the riser and the effective weight is a function of the wall thickness (both liner and composite body) selected for the analysis.

3.3.2 Environmental Situations and Global Load Cases for both Steel and Composite Riser Designs in Gulf of Mexico

For a TTR, a tension is applied to its top to keep its vertical position and eliminate compressive stresses along its length. In addition, under operational conditions, risers are subjected to a variety of loads, such as hydrostatic pressure, internal fluid pressure, gravity, buoyancy, wave and current loads, and the motions of a floating platform or ship, as shown in Fig. 3.7. As many of these loads act simultaneously, an analysis is required to consider global design load cases which are combinations of different categories of environmental loading and riser conditions.

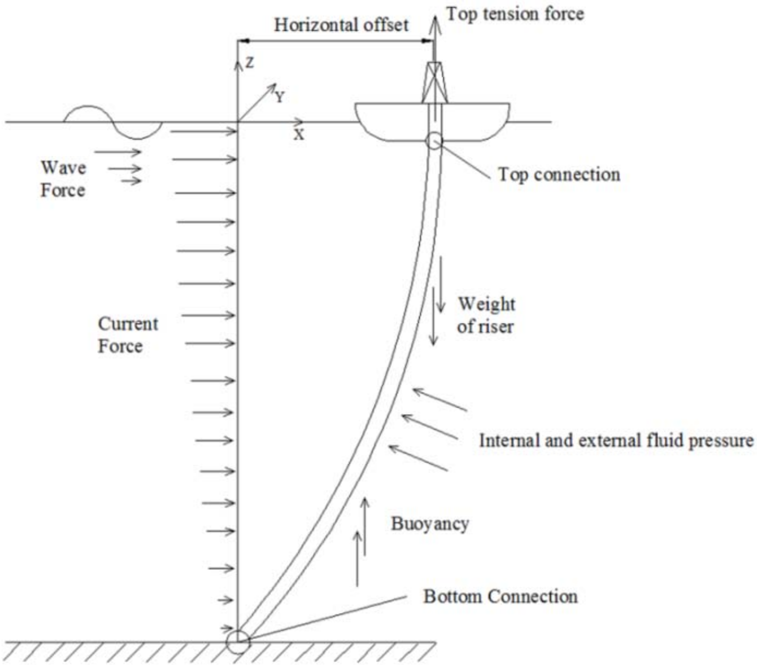

Fig. 3.7. Loads on a top-tension riser system

Environmental loads on a riser system consist of wave loading, which is determined from the statistical wave data for a specific location (usually in terms of significant wave height and peak period), current profiles and platform motions. Table 3.2 shows the environmental and platform movement data for the Gulf of Mexico [34, 51] which is used in the current design study.

Table 3.2. Environmental data for Gulf of Mexico [34, 51]

Type	H_s (m)	H_m (m)	T (sec)	Surface current velocity (m/s)	Mean TLP offset		Low freq. motion	
					% W.D.	Offset (m)	RMS (m)	T_z (sec)
1 year winter storm	4.88	9.08	9.0	0.36	2%	38.4	1.83	200
100 year Hurricane	12.50	23.25	14.0	1.22	6%	115.2	6.77	200
100 year loop current	2.74	5.10	8.0	2.13	9%	172.7	0.61	200

H_s - significant wave height
H_m - maximum wave height = 1.86Hs
T - period of wave
W.D. - water depth
T_z - period of low-frequency motion

In this study, the maximum wave height (1.86H_s) is used as the wave height in the single-wave time-domain analysis and variations in the current velocity with depth are determined according to the API Recommended Practice [68].

Fig. 3.8 illustrates the current profiles for 1-year winter storm, 100-year hurricane and 100-year loop current conditions. To model the wave and current loads, the normal drag coefficient (C_D) and coefficient of inertia (C_M) are required. In the present study, values of 1.0 and 0.7 are assigned to C_D for the bare riser joints and joints with fairings, respectively, and a value of 2.0 for C_M based on the recommendations of the API [63] and DNV [69].

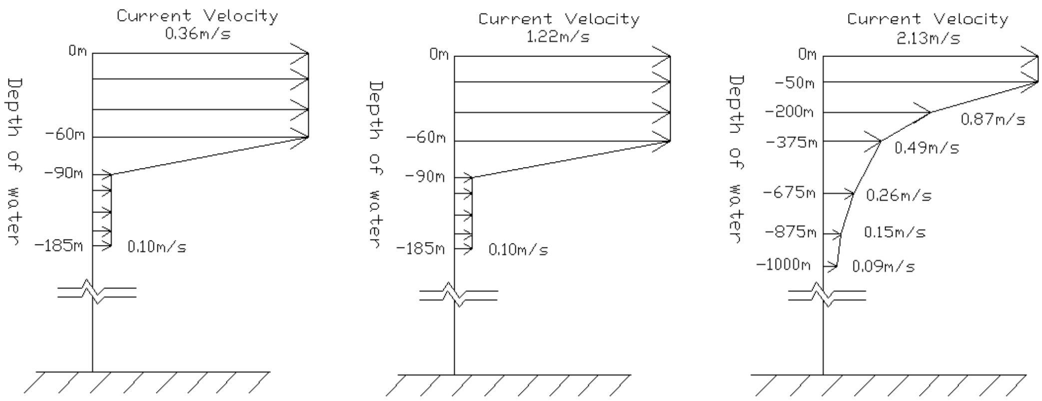

(a) (b) (c)

Fig. 3.8. Variations in current velocity with depth for (a) 1-year winter storm (b) 100-year hurricane and (c) 100-year loop [68]

The most commonly used wave theories are the Airy Wave, Stocks Wave, Cnoidal Wave and Solitary Wave, with each having its own scope for application and different assumptions and simplifications [68, 76-81]. Their applications in terms of appropriate water depths are summarised in Table 3.3 [78].

Table 3.3. Water depths for application of wave theories [78]

Water depth range	$\frac{d\,(\text{water depth})}{L\,(\text{wave length})}$	$\frac{H\,(\text{wave height})}{d\,(\text{water depth})}$	$\frac{H}{d}\left(\frac{L}{d}\right)^3$	Applicable wave theories
deep water	>0.5	<<1 <<1	<<1 <1	Airy Wave Stocks Wave
middle deep water	0.05—0.5	<<1 <<1	<<1 <1	Airy Wave Stocks Wave
shallow water	<0.05	<<1 <1	<<1 ≈1	Linear Wave Solitary wave /Cnoidal Wave
extreme-shallow water	<<0.05	<<1 <<1	<<1 >>1	Linear Wave Long Wave

Since the present research investigates the tailored design of production risers for deep-sea applications, the Airy Wave Theory is selected.

As a TLP can move laterally due to wave and current loads, this has to be taken into consideration in the load cases. This movement includes the mean displacement, and low-frequency and wave-frequency movements can be expressed as Eq. 3-1 [52, 82].

$$S(t) = S_0 + S_L \sin\left(\frac{2\pi t}{T_L} - \alpha_L\right) + \sum_{n=1}^{N} S_n \cos\left[k_n S(t) - \omega_n t + \emptyset_n + \alpha_n\right] \tag{3-1}$$

The first, second and third terms in Eq. 3-1, respectively represent the mean displacement of platform, low frequency motion and the wave frequency motion of platform, where

S_L : the mean displacement of the platform's low-frequency motion,

T_L : the period of the platform's low-frequency motion,

α_L: the phase angle between the low-frequency motion and wave (normally 0)，

S_n: the mean displacement of the platform's wave-frequency motion,

α_n: the phase angle between the wave-frequency motion and the wave，

ω_n: the frequency of the wave (rad/sec),

k_n: the wave number and

$\emptyset_n$: the initial phase angle of the wave.

Using Eq. 3-1, the TLP displacements for this study are calculated as follows.

1-year storm condition：

$$X = 38.4 + 1.83 \sin(0.0314t) + 0.656 \cos(-0.698t - 1.378) \tag{3-2}$$

100-year hurricane condition：

$$X = 115.2 + 6.77 \sin(0.0314t) + 14.77 \cos(-0.4486t - 1.694) \tag{3-3}$$

100-year loop current condition：

$$X = 172.7 + 0.61 \sin(0.0314t) + 0.557 \cos(0.785t) \tag{3-4}$$

In addition to the environmental loads and platform motions, there are also other functional and pressure loads on the riser. Major functional loads include the top tension and the combination of the gravity and buoyancy which provide the riser's effective weight. Pressure loads embrace both internal and external (hydrostatic) pressures and are often considered as part of the functional loads. The maximum internal pressure should be specified according to the application.

As a conservative way of considering the combination of all the environmental loads is to assume that waves, winds, currents and platform movements all act in the same direction (the environmental heading), this is used for all the events analysed in this study.

The global design load cases based on the environmental conditions up to a depth of about 2000m in the Gulf of Mexico employed in the global analyses of all the risers considered in this thesis, in accordance with the riser design codes and previous riser design projects [52, 63, 64, 66, 69], are tabulated in Table 3.4.

3.3.3 Summary of Load Cases

A summary of the local and global design load cases presented above is presented in Table 3.5. For both the steel and composite riser designs, all the local load cases have to be verified. Maintaining pressure and fluid tightness is a primary requirement for a riser. Also, as it is exposed to both internal and external pressures during its service life, the possibility of burst failure due to internal pressure and collapse and buckling due to external pressure should be considered in its design. The external hydrostatic pressure is highest at the sea floor, but it is still less than the internal pressure. In this study, the maximum shut-in internal pressure is 69.0MPa (at the bottom of the riser) while the maximum external hydrostatic pressure is 19.5MPa at the sea's bottom.

Table 3.4. Global design load cases for the riser system [64]

Global load cases	Riser condition	Fluid density (kg/m^3)		Internal pressure (MPa)[1]		Sea water density (kg/m^3)	Design environment	Mean TLP movement (m)	Tension ratio	
		Annulus	Tubing	Annulus	Tubing				Steel riser	Composite riser
LC1	external pressure test	0	NA[2]	0	NA	1030	1 year winter storm	38.4	1.5	
LC2	shut-in pressure test	800	NA	69.0	NA	1030	1 year winter storm	38.4	1.5	
LC3	shut-in with leak[3]	800	NA	58.6	NA	1030	1 year winter storm	38.4	1.5	
LC4	shut-in with leak[3] under hurricane	800	NA	58.6	NA[2]	1030	100 year hurricane	115.2	1.5	2
LC5	maximum production with leak[3]	800	NA	58.6	NA[2]	1030	100 year loop current	172.7	1.5	2
LC6	well killed[4] 1	1860	NA	35.7	NA[2]	1030	100 year hurricane	115.2	1.2	1.5
LC7	well killed[4] 2	1860	NA	35.7	NA[2]	1030	100 year loop current	172.7	1.2	1.5
LC8*	shut-in under hurricane	0	800	0	58.6	1030	100 year hurricane	115.2	1.5	1.2+end effect of external pressure
LC9*	maximum production	0	800	0	58.6	1030	100 year loop current	172.7	1.5	1.2+end effect of external pressure

1. The internal pressure at the bottom end of the riser is the maximum internal pressure.

2. NA stands for no tubing.

3. The load cases with leakage consider failure of the tubing and all pressures are applied to the riser wall.

4. For the well-killed situation, the production tubing is removed and mud inserted into the whole riser annulus.

* For load cases 8-9, the weight of the production tubing is considered.

Table 3.5. Summary of design load cases for both steel and composite risers

Local load cases		Global load cases	
No.	Name	No.	Name
1	burst case	1	external pressure test
2	tension case	2	shut-in pressure test
		3	shut-in with leak
		4	shut-in with leak[3] under hurricane
3	collapse under external pressure	5	maximum production with leak
		6	well killed 1
4	buckling under external pressure	7	well killed 2
		8	shut-in under hurricane
		9	maximum production

It has to be noted that, in terms of the tension case, five different combinations (Table 3.1) have to be considered for the steel riser and pure tension and tension with maximum external pressure for the composite riser. While the design and analyses under these local load cases can be conducted using the entire riser model for the steel riser, for the composite riser, they have to be performed at the short-length composite tubular level.

In terms of the global load cases, for the steel riser design are analysed under all the normal operating conditions (LC1-LC3) and design extreme conditions (LC4-LC9). On the other hand, for the composite riser design, only the extreme conditions (LC4-LC9) are considered since the factors of safety (FS) for the liner and composite layers that satisfy these will automatically satisfy the less severe global conditions (LC1-LC3).

3.4 Selection of Internal Production Tubing for Steel and Composite Risers

As can be seen in Fig. 3.4, it is assumed that, in riser design, a single standard production tubing is employed for transportation of the extracted fluids. Its weight is considered in the design for both steel and composite risers and, if it fails, the internal pressure will work directly on the riser wall; otherwise, it is assumed there is no internal pressure on the riser. In this study, the selection of the production tubing is based on its burst pressure-bearing capacity which is specified for different tube models in the API standard [70] in which the C95 pipe (118.6mm ID ×139.7mm OD) has the highest burst pressure allowance of 69.0MPa and meets the maximum internal pressure required in this study. This allowance also has to be examined using the pressure-bearing capacity equation (Eq. 3-5) and the lesser of its value and that specified in the standard (69.0MPa) is the final pressure capacity of the C95 pipe selected.

$$p_m = 2 \times f \times YS_m \times t_m / D_m \quad (3\text{-}5)$$

where

p_m is the hydrostatic test pressure; D_m is the outside diameter;

YS_m is the yield strength; t_m is the wall thickness;

f is a factor, based on the size and grade of the pipe (for C95 pipe, f=0.8)

Based on the geometry of the production tubing used in this study, as $p_m = 2 \times 0.8 \times 655 \times \frac{10.55}{139.7} = 79.1MPa$, the final pressure capacity of the C95 pipe is taken to be the value given by the API standard, i.e., 69.0MPa.

Thus, for both the steel and composite risers, C95 is employed as the production tubing and it is assumed that it does not make any contribution to load bearing. However, its weight is taken into consideration for loading of the riser and load cases with and without leakage from it are also analysed.

3.5 Design Approach for Steel Riser

In this thesis, the design of the steel riser employed as the benchmark to demonstrate and quantify the weight savings that can be achieved by the proposed tailored design of laminated composite risers is conducted according to API [63-65] and American Bureau of Shipping (ABS) [66] standards.

On the top of the riser, there are high axial stresses due to tension and the motion of the platform. To handle the high axial stresses, the tension joint has a larger wall thickness than that of standard riser joints. The stress joint at its bottom is also thicker than standard joints due to the high bending stresses there and it is tapered in order to withstand the varying bending moment distribution. Fairings are attached to the standard steel riser joints above -624m to mitigate VIV.

The design of the steel riser is based on the requirements for local burst, tension, collapse, propagating buckling capacities and structural capacity under different global load cases. All these cases can be analysed using the entire riser model, since steel is an isotropic material, and the stresses can be obtained directly from it without excessive utilisation of computer resources. The procedure adopted for the design of the steel riser is to first obtain an initial estimate of the minimum wall thickness required using the burst load capacity which is the most critical in most cases, followed by an analysis of the other local and global load cases to ensure that their requirements are met. The minimum wall thickness required to withstand the local and global loads is determined for every set of 10 joints (200m).

The procedure followed for the design of the steel riser is described in greater detail in the next chapter, *Design of Steel Riser*.

3.6 Design Approach for Composite Riser

For the composite riser design, the geometry of the standard riser joints, which make up over 95% of the total length of the riser, is determined with the aim of achieving the minimum structural weight in them. The tension joint at the top and stress joint at the bottom are still retained as steel while it is also assumed that fairings are attached to the standard composite riser joints above -624m to mitigate VIV. Unlike in the case of the steel riser, the same laminate geometry is retained for all the standard joints along the full length of the composite riser.

Unlike for the riser using isotropic steel, the stresses in the liner and every composite layer have to be determined for the composite riser design.

The geometry selected for the offshore riser is an ID of 250mm and a wall thickness anywhere between 30 and 100mm if it is made of FRP, depending on the materials employed and the depth for which it is designed, which makes it quite thick. Therefore, in numerical simulations using FE modelling, it is necessary to use 3D (solid) layered elements to accurately determine the stresses in each layer. Noting that a typical offshore riser has a length of about 2000m, this would involve the use of hundreds of thousands of 3D layered elements in order to maintain appropriate aspect ratios for them. However, a non-linear FE analysis (FEA) taking into account the large deformations of the riser under global loading and employing so many layered 3D elements would be prohibitively time consuming and resource intensive. Therefore, it is pragmatic to conduct the composite riser design in three stages: (1) a local design based on critical local load cases using layered 3D elements; (2) a global analysis of the entire composite riser under global load cases to determine the critical locations and critical load combinations at these locations using 1D pipe elements with smeared material properties; and (3) a structural verification of the critical local locations under the combined load cases obtained from the global analysis, again using layered 3D elements.

In both the conventional design with only axially and hoop reinforced piles and the tailored design including other ply orientations, the first stage of the design is conducted using 3D FEA with ANSYS13.0 under the four local load cases. The factors of safety (allowable strength/stress) in the liner and every composite lamina are calculated and employed to determine the local geometry, i.e., the inner liner thickness, stacking sequence, ply thicknesses and ply orientations, required to provide the minimum weight. First ply failure using the maximum stress failure criterion [83] is used as the design criterion. The distribution of only the in-plane stresses in every composite lamina is determined for each load case since the thickness of each individual layer is small and the stresses in the thickness direction are relatively small [51].

After obtaining the preliminary estimate of the geometry of the composite riser joint using the local loads, a global analysis of the entire composite riser under extreme global load cases (LC4-9) is conducted. In the FEA model, Pipe288, which is suitable for the pipe structure with a slenderness ratio ($\frac{GAL^2}{EI}$) greater than 30 [84], with effective composite tubular properties, is employed to perform a large displacement non-linear dynamic analysis in order to consider the dynamic effect of the environmental loads and platform motions and determine the forces and bending moments on each joint. The critical sections of the composite riser and critical load combinations are obtained in this second stage.

Finally, a structural verification of the critical locations under the combined load cases obtained from the global analysis is conducted to obtain the stresses in the liner and every composite layer from a local analysis of the critical pipe segments using short lengths of 4.5m, again using layered 3D elements. The critical load combination considered in this stage includes the internal pressure, external pressure, tension force, bending moment and shear force.

The design of the composite riser is much more involved than that of the steel riser and requires an iterative procedure due to the larger number of variables required to be determined. In the tailored design, which includes reinforcements at angles other than 0 and 90 degrees, as the fibre orientation of the off-axis laminae is an additional variable that has to be optimised to obtain the minimum weight of the structural joints, additional cycles in the iterative design procedure are required. The iterative procedures adopted for the conventional and proposed tailored designs, along with their results, are described in detail in *Chapters 5 and 6*.

3.7 Materials for Steel Riser

Several different kinds of steel alloys are generally used in mechanical engineering applications, depending on their ease of manufacture and cost, and the requirements of the application. Among the main criteria for the selection of alloys for underwater applications are durability and resistance to corrosion because, once a riser is installed, it will be difficult and expensive to repair or replace its steel segments. It is also desirable to use a high-strength alloy in order to minimise a riser's weight and, thus, the top tension required. As a steel alloy with a higher strength requires thinner pipe walls which makes it lighter, it incurs lower pipe procurement, transport-to-site and welding costs [85]. The steel commonly used for the manufacture of production risers is X80 and that for inner production tubing C95 [52, 86-88]. Today, although it is possible to produce higher grades of steel, such as X100, as their large-scale industrial application appears to be premature [86], in this study, X80 is employed for the steel riser wall and C95 for the production tubing and, since the material of the steel riser is not allowed to yield, a linear elastic material model of X80 is considered. The mechanical properties of these two grades of steel are listed in Table 3.6.

Table 3.6. Properties of steel X80 [71] and C95 [70]

Name	Density (kg/m^3)	Modulus of elasticity (GPa)	Damping ratio	Poisson's ratio	Yield stress (MPa)	Ultimate stress (MPa)
X80	7850	207	0.03	0.3	555	625
C95	7850	207	0.03	0.3	655	724

3.8 Selection of Materials for Composite Riser

3.8.1 Materials for Structural Composite Layers

It is important to ensure that the matrix and fibre reinforcements selected can satisfy the long-term environmental and mechanical load requirements [67]. For those used in deep-sea composite risers, many of their properties, such as the Young's modulus, Poisson's ratio and stress and strain at failure, as well as the influence of seawater on them, have to be considered.

It should be noted that, as the properties of each layer in the composite laminate is a combination of the properties of the constituent materials, the matrix and reinforcement fibres have to be carefully selected while consideration also needs to be given to the overall properties of the 'composite' material.

3.8.1.1 Selection of Reinforcement Fibres

The reinforcement fibres determine the main mechanical properties required in a structural composite, such as the longitudinal tensile modulus and strength. Fibres commonly used for the reinforcement of polymer composites are carbon fibre, glass fibre, Aramid fibre and synthetic high-performance fibres, such as M5, Zylon, Dyneema and Spectra. In general, the mechanical properties of glass, Aramid and high-performance fibres reinforced composites significantly deteriorate due to moisture ingression, especially in sub-sea conditions [37, 45-49], whereas carbon fibre-reinforced composites retain their mechanical properties to a greater extent in seawater [2, 37-40]. Moreover, carbon fibres normally have much higher specific stiffness and specific strength than most other fibres (except for the new synthetic high-performance ones) and provide better fatigue characteristics to the composite by reducing the strain in the polymer matrix for a given load [89]. The low coefficient of thermal expansion and high stress corrosion resistance also make carbon fibres more attractive for the reinforcement of a composite [83, 89]. However, as the impact resistance of carbon fibre composites is not as good as that of glass fibre-reinforced ones, external protection layers are normally applied to risers made of them to overcome this problem.

From the variety of carbon fibres available, two are selected for this study: a high-strength (HS) carbon fibre, AS4, and a high-modulus (HM) carbon fibre, P75, since longitudinal stiffness and strength are the main contributions of the fibre reinforcement to a structural composite. As it was not clear at the beginning of this study which of these properties would dominate and provide a higher weight saving for the riser, both are chosen.

The mechanical properties of the AS4 (HS) and P75 (HM) carbon fibres are given in Table 3.7 [61, 90-92]. As can be seen, the tension modulus in the fibre direction of the P75 (HM) carbon fibre is more than double that of the AS4 (HS) fibre (although the transverse modulus is 35% smaller) whereas the AS4 is about 90% stronger than the P75. It should also be noted that the density of the P75 carbon fibre is about 20% higher than that of the AS4 carbon fibre.

Table 3.7. Mechanical properties of reinforcing fibres chosen for the composite riser design

Fibre	Density (kg/m^3) ρ	Elastic modulus E_1 (GPa)	Transverse modulus E_2 (GPa)	Shear modulus G_{12}(GPa)	Poisson's ratio ν_{12}	Poisson's ratio ν_{23}	Shear modulus G_{23} (GPa)*	Ultimate strength (MPa)
AS4(HS)[92]	1750	235.0	14.00	28.0	0.20	0.25	5.6	3590
P75(HM)[90]	2160	517.0	9.00	13.0	0.23	0.74	2.59	1900

* $G_{23} = \dfrac{E_2}{2(1+\upsilon_{23})}$

3.8.1.2 Selection of Matrices

The matrix material holds the fibres together and transfers the load among them. Moreover, it governs the transverse modulus, transverse strength and in-plane and inter-laminar shear properties of the composite.

The selection of the matrix for the design of a deep-sea composite riser should consider the following aspects [67]:

(1) Resistance to the ingress of moisture from seawater, crude oil, gas and other fluids;

(2) Satisfaction of the matrix-cracking allowance during manufacturing and in operational situations; and

(3) Suitability of the glass transition temperature (Tg) for the service conditions and cure cycles.

Two main types of matrices are applied in structural composites, thermosets and thermoplastics. Thermoset matrices [83, 89] are insoluble and infusible after cure because their chains are rigidly joined with strong covalent bonds, and are the most common resin systems used due to their ease of processing and low cost. On the other hand, thermoplastic matrices [83, 89] do not undergo any chemical transformation as they are softened from a solid state during processing and then returned to a solid after processing is completed. Compared with thermosets, thermoplastics are more difficult and slower to process but have virtually unlimited shelf and pot lives and can be repaired since the transition to the softened stage can be accomplished at any time by the application of heat [89].

Of the thermoset matrices, both epoxy and vinyl ester have good water resistance. However, as epoxy [67, 83] has much better mechanical properties and is well-suited for filament winding, it is used in most structural applications, including in the aerospace and offshore engineering.

Of the thermoplastic matrices, poly ether ether ketone (PEEK) has a high damage tolerance and low water absorption [89] and its Tg is 143°C [90], which is higher than the temperature of the oil/gas being transported in a production riser. Hence, it is the most popular thermoplastic used for offshore composite tubulars. It is also common to use the same thermoplastic for the inner liner and composite structural tubular wall in order to avoid debonding between the liner and composite body. Therefore, for the investigation in this thesis, PEEK is chosen as the thermoplastic matrix with PEEK liner, and epoxy as the thermoset matrix with liners of different materials.

The mechanical properties of epoxy [61] and PEEK [91] are shown in Table 3.8. Their moduli are much smaller than those of carbon fibres but that of epoxy is 20% higher than that of PEEK, and they have similar densities and strengths. However, PEEK's elongation at the break is more than 10 times that of epoxy.

Table 3.8. Mechanical properties of matrices chosen for the composite riser design

Matrix	Density (kg/m^3) ρ	Elastic modulus E (GPa)	Shear modulus G (GPa)	Poisson's ratio ν	Ultimate strength (MPa)	Elongation at break (%)
epoxy[61]	1200	4.50	1.6	0.40	130	2-6
PEEK[91]	1300	3.64	1.3	0.40	120	50

3.8.2 Liner Materials

A production riser used in offshore engineering must ensure fluid tightness. However as, in general, fibre-reinforced composite materials are not expected to possess perfect fluid tightness because of the possibility of microcracking [93], additional liner(s) are usually used as barriers against fluids and should be made of materials which can resist corrosion and abrasion. Typical internal liner materials include synthetic rubbers, thermoplastic polymers and structural metals, and multi-layered liners may be made of different materials, such as steel and rubber. When a liner is used, bonding between it and the structural composite laminate is critical since the load capacity can reduce significantly in debonded areas [51, 94, 95]. As the purpose of the liner is to maintain fluid tightness, the loads directed to the liner should be minimised [67] and, when a thermoplastic polymeric liner is used, the same material should be used as the matrix for the fibre-reinforced structural tubular wall to avoid debonding [29] while, when metal liners are used, the manufacturing process should be carefully monitored.

In general, an external liner and sacrificial glass fibre layers may be added to resist environmental effects and corrosion resulting from direct contact with seawater, temperature, UV radiation, etc [67].

According to previous design studies [51, 52, 67], the inner liner and reinforced composite body are the main structural segments of a composite riser wall which means that both are considered to bear loads together while, as the external liner and sacrificial layers are the protection segments, no load-bearing capacity is considered in composite riser designs. The inner liner materials considered in this study include steel, titanium and aluminium alloys and the thermoplastic PEEK. In the FEA, a bilinear kinematic hardening material model is used for the metal liners and an elastic material model for the PEEK liner.

3.8.2.1 PEEK Liner

As mentioned above, in order to avoid debonding, the same thermoplastic polymeric is used for both the liner and composite matrix [29], the elastic properties of which are the same as those listed in Table 3.8 while the ultimate strength of PEEK is 120MPa [91].

3.8.2.2 Steel Liner

The same alloy used for the steel riser is applied as the steel liner in the composite riser. The elastic properties of the steel (X80) used for the inner liner are the same as those used for the steel structural tube listed in Table 3.6. A bilinear kinematic hardening model with values of 207GPa for the elastic modulus and 1.25GPa for the tangent modulus after yield is used for the X80 steel liner (Fig. 3.9), as listed in Table 3.9.

Table 3.9. Parameters for bilinear constitutive model of steel X80[71]

Density (kg/m^3)	Modulus of elasticity (GPa)	Damping ratio	Poisson's ratio	Yield stress (MPa)	Ultimate stress (MPa)	Elongation at break [92] (%)
7850	207	0.03	0.3	555	625	5.868

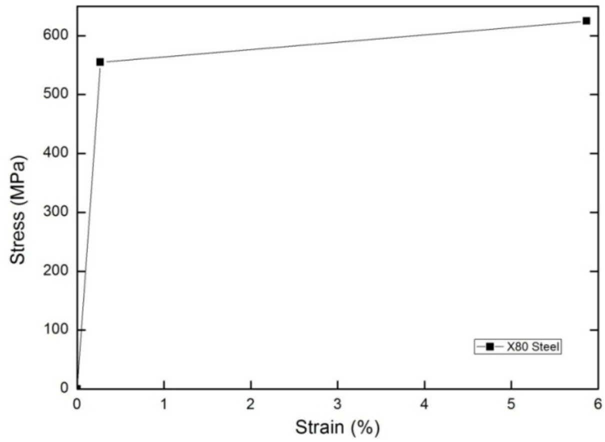

Fig. 3.9. Bilinear kinematic hardening model of X80 steel

3.8.2.3 Titanium Alloy Liner

The titanium alloy has high compressive and tensile strengths, low density, inherent flexibility, high fatigue resistance in air and seawater, exceptional resistance to well fluids, seawater and erosion due to high-velocity flowing fluids, and high durability/damage tolerance [96]. More specifically, Ti-6Al-4V-based alpha-beta titanium alloys have been modified to combine several desirable traits, including high strength, excellent fabricability, high milling capability and low alloy formulation cost for drilling and offshore component applications [96, 97]. Therefore, in this thesis, the titanium alloy Ti-6Al-4V is applied as one of the metal liners for composite riser design. Its properties used are taken from the literature [96-98] and listed in Table 3.10. The bilinear kinematic hardening model of titanium (Fig. 3.10) has an elastic modulus of 113.8GPa and a tangent modulus of 0.53GPa after yield.

Table 3.10. Parameters for bilinear constitutive model of titanium alloy Ti-6Al-4V [98]

Density (kg/m^3)	Modulus of elasticity (GPa)	Poisson's ratio	Yield stress (MPa)	Ultimate stress (MPa)	Elongation at break (%)
4430	113.8	0.342	880	950	14

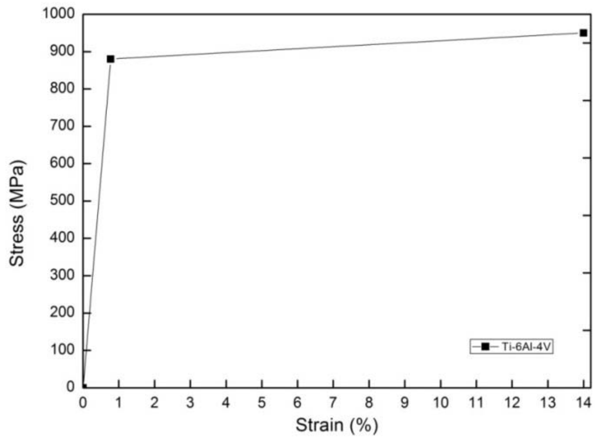

Fig. 3.10. Bilinear kinematic hardening model of Ti-6Al-4V titanium

3.8.2.4 Aluminium Alloy Liner

The most important feature of using aluminium alloys as materials for tubular manufacturing is that they provide exceptional strength-to-weight ratio. D16T, AK4-T1 and 1953T1 are the most commonly used aluminium tube materials in offshore projects [99, 100] and meet not only the requirements of offshore operations but are also easy to produce commercially as pipes with variable diameters [99]. Of these three aluminium alloys, 1953T1 has the highest strength and, since the purpose of the composite riser design is to achieve weight reduction, it is used in this study [99]. Its properties are taken from the literature [99] and are listed in Table 3.11 while its bilinear kinematic hardening model (Fig. 3.11) has an elastic modulus of 71GPa and a tangent modulus of 0.88GPa after yield.

Table 3.11. Parameters for bilinear constitutive model of aluminium alloy 1953T1[99]

Density (kg/m^3)	Modulus of elasticity (GPa)	Poisson's ratio	Yield stress (MPa)	Ultimate stress (MPa)	Elongation at break (%)
2780	71	0.3	480	540	7.5

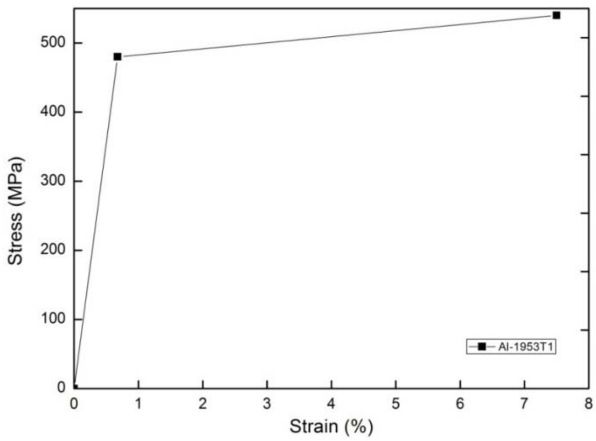

Fig. 3.11. Bilinear kinematic hardening model of Al-1953T1 aluminium

3.9. Determination of Composite Lamina Properties

Although the material properties of fibre-reinforced unidirectional laminae can be determined experimentally by mechanical tests on unidirectional laminate samples, this is very resource intensive. In the present study, in the FEA of composite tubulars for local design, 3D solid elements, which require their strength and stiffness properties in all directions to be specified, are employed. However, determining all these properties experimentally would be prohibitively time consuming and detract from the main purpose of this thesis which is to demonstrate and quantify the weight savings that can be achieved by the proposed tailored design of laminated composite risers. Therefore, it is considered expedient and sufficient to employ the laminae properties obtained from manufacturers' specifications or research publications. However, as it is difficult to find all the 3D mechanical properties of composite laminae from the available literature, it is necessary to determine them analytically from the values of the constituent materials, fibres and matrices obtained from the literature using micromechanics. As the nine elastic constants of the 3D unidirectional lamina estimated using different theoretical models yield slightly different values, wherever possible, these values are compared with previously published results in order to select the most accurate ones.

3.9.1 Lamina Elastic Constants

A unidirectional composite lamina is orthotropic and its stiffness can be defined by nine elastic constants, E_1, E_2, E_3, G_{12}, G_{13}, G_{23}, ν_{12}, ν_{13} and ν_{23}. In a case in which its fibres are packed regularly in a hexagonal array, it can be considered transversely isotropic [67], for which 2 and 3 directions are interchangeable, and the number of elastic constants required to characterise it is reduced to five: E_1, E_2, G_{12}, ν_{12} and either G_{23} or ν_{23}. In other words, for a transversely isotropic material, $E_2 = E_3$, $G_{12} = G_{13}$ and $\nu_{12}=\nu_{13}$.

Based on the properties of the AS4 and P75 carbon fibres, and the epoxy and PEEK matrices listed in Table 3.7 and Table 3.8, respectively, the effective material modulus properties of the unidirectional laminae are predicted using three theoretical models: the rule of mixtures (ROM) [101], the semi-empirical model (Halpin-Tsai Model [83, 102] and stress-partitioning parameter (SPP) [89]) and the elasticity approach [83]. The equations for these theoretical/semi-empirical models are Eqs. 3-7 to

3-12 for the ROM, Eqs. 3-13 to 3-18 for the semi-empirical model and Eqs.3-19 to 3-24 for the elasticity approach. Eq. 3-6 gives the expression for the density of the lamina obtained by the ROM from the densities of the fibre and matrix. In Eqs. 3-6 to 3-24, the subscripts m, f, 1, 2 and 3 stand for the matrix, fibre, fibre direction, in-plane transverse direction and through thickness direction of the lamina, respectively. The lamina co-ordinate system is shown in Fig. 3.12 in which it should be noted that the lamina properties are highly dependent on the fibre volume ration (V_f) which has to be chosen judiciously.

$$\rho = \rho_f V_f + \rho_m V_m \tag{3-6}$$

Equations for ROM [101]:

$$E_1 = E_{f1} V_f + E_m V_m \tag{3-7}$$

$$E_2 = \frac{E_{f2} E_m}{E_m V_f + E_{f2} V_m} \tag{3-8}$$

$$G_{12} = \frac{G_{f12} G_m}{G_m V_f + G_{f12} V_m} \tag{3-9}$$

$$\nu_{12} = \nu_{f12} V_f + \nu_m V_m \tag{3-10}$$

$$\nu_{23} = \frac{\nu_{f23} \nu_m}{\nu_m V_f + \nu_{f23} V_m} \tag{3-11}$$

$$G_{23} = G_{f23} V_f + G_m V_m \tag{3-12}$$

Equations for semi-empirical model [83, 89, 102, 103]:

$$E_1 = E_{f1} V_f + E_m V_m \tag{3-13}$$

$$\frac{E_2}{E_m} = \frac{1+\xi\eta V_f}{1-\eta V_f} \tag{3-14}$$

where $\eta = \frac{(E_{f2}/E_m)-1}{(E_{f2}/E_m)+\xi}$ and, for circular fibres, $\xi = 2$ [104].

$$\frac{G_{12}}{G_m} = \frac{1+\xi\eta V_f}{1-\eta V_f} \tag{3-15}$$

where $\eta = \frac{(G_{f12}/G_m)-1}{(G_{f12}/G_m)+\xi}$ and $\xi = 1 + 40V_f^{10}$[103].

$$\nu_{12} = \nu_{f12}V_f + \nu_m V_m \tag{3-16}$$

$$G_{23} = G_m \left[\frac{V_f+\eta_{23}(1-V_f)}{\eta_{23}(1-V_f)+\frac{G_m}{G_{f23}}V_f}\right] \tag{3-17}$$

where $\eta_{23} = \frac{3-4\nu_m+G_m/G_{f23}}{4(1-\nu_m)}$

$$\nu_{23} = \frac{E_2}{2G_{23}} - 1 \tag{3-18}$$

Equations for the elasticity approach [83, 105]:

$$E_1 = E_{f1}V_f + E_m V_m - \frac{2E_m E_{f1} V_f (\nu_{f12}-\nu_m)^2(1-V_f)}{E_{f1}(2\nu_m^2 V_f-\nu_m+V_f\nu_m-V_f-1)+E_m(-1-2V_f\nu_{f12}^2+\nu_{f12}-V_f\nu_{f12}+2\nu_{f12}^2+V_f)} \tag{3-19}$$

$$\nu_{12} = \nu_{f12}V_f + \nu_m V_m + \frac{V_m V_f(\nu_{f12}-\nu_m)(2\nu_m^2 E_{f1}-\nu_m E_{f1}-E_{f1}+E_m-E_m\nu_{f12}-2\nu_{f12}^2 E_m)}{E_{f1}(2\nu_m^2 V_f-\nu_m+V_f\nu_m-V_f-1)+E_m(2\nu_{f12}^2-V_f\nu_{f12}-2V_f\nu_{f12}^2+\nu_{f12}+V_f-1)} \tag{3-20}$$

$$\nu_{23} = \frac{K^*-mG_{23}}{K^*+mG_{23}} \tag{3-21}$$

where $m = 1 + 4K^* \frac{\nu_{12}^2}{E_1}$

$$K^* = \frac{K_m(K_f+G_m)V_m+K_f(K_m+G_m)V_f}{(K_f+G_m)V_m+(K_m+G_m)V_f}$$

$$K_f = -\frac{1}{2}\frac{E_{f1}E_{f2}}{-E_{f1}+E_{f1}\nu_{f23}+2\nu_{f12}^2 E_{f2}} \text{ [105]}$$

$$K_m = \frac{E_m}{2(1+\nu_m)(1-2\nu_m)}$$

$$A\left(\frac{G_{23}}{G_m}\right)^2 + 2B\left(\frac{G_{23}}{G_m}\right) + C = 0 \tag{3-22}$$

where

$$A = 3V_f(1-V_f)^2\left(\frac{G_{f23}}{G_m}-1\right)\left(\frac{G_{f23}}{G_m}+\eta_f\right) + \left[\frac{G_{f23}}{G_m}\eta_m + \eta_f\eta_m - \left(\frac{G_{f23}}{G_m}\eta_m - \eta_f\right)V_f^3\right]\left[V_f\eta_m\left(\frac{G_{f23}}{G_m}-1\right) - \left(\frac{G_{f23}}{G_m}\eta_m + 1\right)\right]$$

$$B = -3V_f(1-V_f)^2\left(\frac{G_{f23}}{G_m}-1\right)\left(\frac{G_{f23}}{G_m}+\eta_f\right) + \frac{1}{2}\left[\frac{G_{f23}}{G_m}\eta_m + \left(\frac{G_{f23}}{G_m}\eta_m - 1\right)V_f + 1\right]\left[(\eta_m-1)\left(\frac{G_{f23}}{G_m}\eta_m+\eta_f\right) - 2\left(\frac{G_{f23}}{G_m}\eta_m-\eta_f\right)V_f^3\right] + \frac{V_f}{2}(\eta_m+1)\left(\frac{G_{f23}}{G_m}\eta_m - 1\right)\left[\frac{G_{f23}}{G_m} + \eta_f + \left(\frac{G_{f23}}{G_m}\eta_m - \eta_f\right)V_f^3\right]$$

$C = -3V_f(1-V_f)^2\left(\frac{G_{f23}}{G_m}-1\right)\left(\frac{G_{f23}}{G_m}+\eta_f\right)+\left[\frac{G_{f23}}{G_m}\eta_m+\left(\frac{G_{f23}}{G_m}-1\right)V_f+1\right]\left[\frac{G_{f23}}{G_m}+\eta_f+\left(\frac{G_{f23}}{G_m}\eta_m-\eta_f\right)V_f^3\right]$

$\eta_f = 3-\nu_{f23}$

$\eta_m = 3-\nu_m$

$$E_2 = 2(1+\nu_{23})G_{23} \qquad (3\text{-}23)$$

$$G_{12} = G_m\frac{G_f(1+V_f)+G_m(1-V_f)}{G_f(1-V_f)+G_m(1+V_f)} \qquad (3\text{-}24)$$

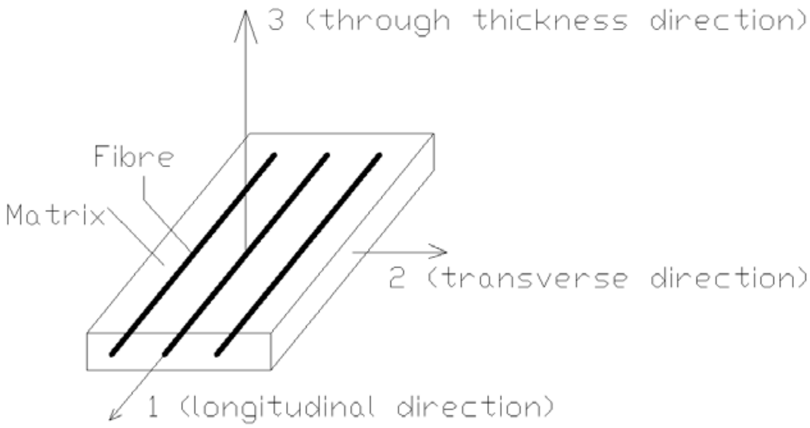

Fig. 3.12. Lamina co-ordinate system

Table 3.12 lists the 2D elastic properties of the four material systems obtained from previously published experimental studies [90, 106-108] and the fibre volume fractions for which the unidirectional properties are given.

Table 3.12. Elastic properties of unidirectional lamina from literature

Name	Fibre volume	Density ρ (kg/m3)	E_1 (GPa)	E_2=E_3 (GPa)	G_{12}= G_{13} (GPa)	ν_{12}=ν_{13}
AS4–epoxy [106]	0.6	1530	135.4	9.37	4.96	0.32
P75-epxoy [90]	0.6	1776	310	6.6	4.1	0.29
AS4-PEEK [107]	0.58	1561	131.0	8.70	5.00	0.28
P75-PEEK [108]	0.55	1773	280.0	6.7		

The elastic constants E_1, E_2 (=E_3), G_{12} (=G_{13}) and ν_{12} (=ν_{13}) estimated from the above three theoretical models using the fibre volume fractions listed in Table 3.12 are compared with each other and those available from the literature in Figs. 3.13(a) to 3.13 (d), respectively. It can be seen in Fig. 3.13(a) that all three models predict the longitudinal stiffness (E_1) very well because this is based on the simple ROM. Also, agreement between the in-plane Poisson's ratio (ν_{12}) values predicted by the models and the measured values is also reasonably good. The ROM seems to perform worst at predicting the transverse modulus and in-plane stiffness, with an error of about 20% in E_2 and about 30% in G_{12}. In all cases, the elasticity approach yields values that are closest to the measured values, followed by the semi-empirical approach.

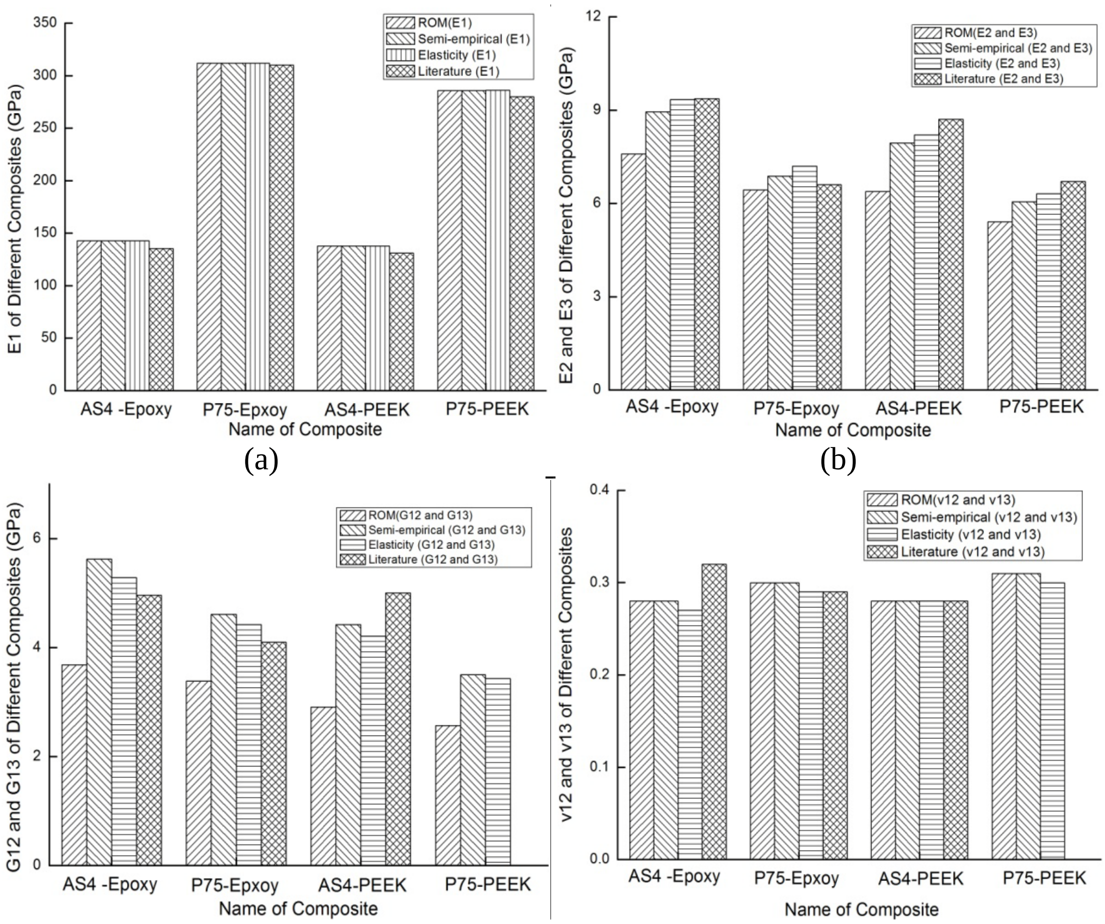

(a) (b)

(c) (d)

Fig. 3.13. Comparisons of elastic constants estimated from theoretical models and published values for (a) E_1, (b) E_2 and E_3, (c) G_{12} and G_{13}, and (d) ν_{12} and ν_{13}

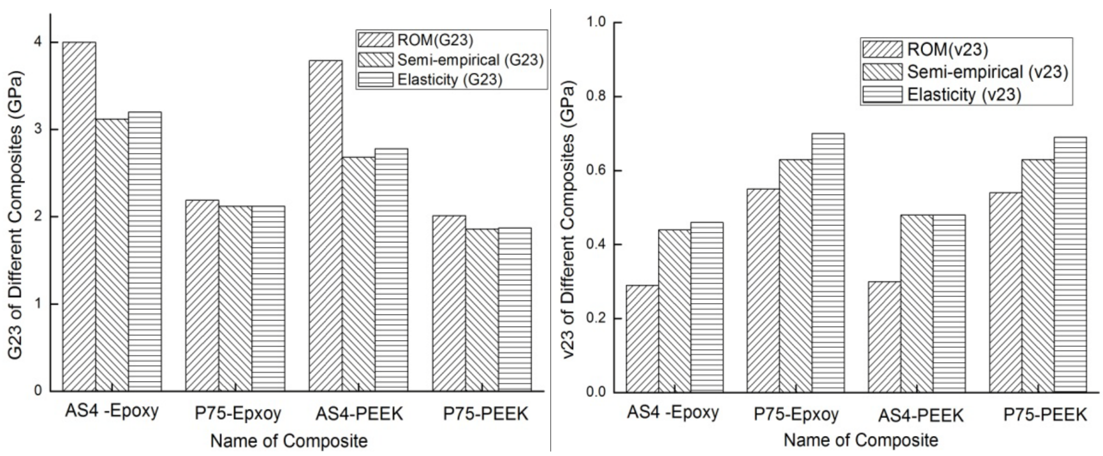

(a) (b)

Fig. 3.14. Comparisons of predictions by theoretical models for (a) G_{23} and (b) ν_{23}

Figs. 3.14(a) and 3.14(b) show comparisons of the values of G_{23} and ν_{23} predicted by the three theoretical models. No published values are available for these parameters as their through thickness values are quite difficult to measure. The difference between the values obtained from the semi-empirical model and elasticity approach is less than 10% while the ROM values differ from them by about 20% to 40%.

In summary, the above analysis shows that the semi-empirical model and elasticity approach provide good agreement in predicting the elastic constants of the unidirectional lamina, with those obtained from the latter being more accurate when compared with the experimental values. However, it is important to note that, as all the theoretical models have their own assumptions and simplifications, the experimental data is considered more reliable. Therefore, in the present work, the values of E_1, E_2, E_3, G_{12}, G_{13}, ν_{12} and ν_{13} are taken from the published literature (Table 3.12). The values of G_{23} and ν_{23}, which are not available in the literature, are calculated using the elasticity approach which appears to be the most accurate model. The nine elastic constants finally selected for use in the FEA in this thesis are listed in Table 3.13.

Table 3.13. Elastic constants of unidirectional lamina used in FE model

Name	Fibre volume	Density ρ (kg/m3)	E_1 (GPa)	E_2=E_3 (GPa)	G_{12}= G_{13} (GPa)	ν_{12}= ν_{13}	G_{23} (MPa)	ν_{23}
AS4 –epoxy	0.60	1530	135.4	9.37	4.96	0.32	3.20	0.46
AS4-PEEK	0.58	1561	131.0	8.70	5.00	0.28	2.78	0.48
P75-epxoy	0.60	1776	310.0	6.60	4.10	0.29	2.12	0.70
P75-PEEK	0.55	1773	280.0	6.70	3.43	0.30	1.87	0.69

3.9.2 Lamina Strength Properties

Although it is recommended that the long-term strengths under seawater should be used as the failure strengths [6, 31, 67] for composite riser design, for carbon fibre reinforced composites, different studies have reported different values; for example, J.O.

Jansons et al. [38] found that the tensile strengths of carbon/epoxy composite rods decreased from their short-term values to 92.9 % in pure water and 85.5% in seawater. The work of G.L. Balazs and A. Borosnyoi [37] showed that the long-term tensile strength of CFRP reduced to 80%-95% of its short-term values. In contrast, the study by R. Venkatesan, E.S. Dwarakadasa and M. Ravindran [2] indicated that the properties of carbon fibre reinforced composites do not vary significantly after a six month exposure to the actual sea environment at various water depths.

In the present study, 80% of the short-term strengths from the literature are used as the long-term strengths to achieve a conservative design, and are listed in Table 3.14.

Table 3.14. Long-term strength of unidirectional lamina used in FE model

Name	Fibre volume	σ_1^T[MPa]	σ_1^C[MPa]	σ_2^T[MPa]	σ_2^C[MPa]	τ_{12}[MPa]
AS4 –epoxy [109]	0.60	1732	1256	49.4	167.2	71.2
AS4-PEEK [107]	0.58	1648	864	62.4	156.8	125.6
P75-epxoy [90]	0.60	720	328	22.4	55.2	176.0
P75-PEEK [108]	0.55	668	364	24.8	136.0	68.0

Comparing Tables 3.13 and 3.14, it can be seen that the Young's moduli in the fibre direction of the high modulus P75 reinforced composites are more than twice those of the composites with AS4 reinforcement while those of the P75 laminae in the transverse direction are 20% to 40% lower. On the other hand, the laminae reinforced with the HS AS4 fibres have higher strengths in both the fibre and transverse directions, with their tensile strengths being more than double those of the P75 laminae in both cases.

3.10 Material Combinations for Composite Riser Design Study

Overall, two different fibre reinforcements, HS carbon fibre AS4 and HM carbon fibre P75, and two different matrix materials, epoxy (thermoset) and PEEK (thermoplastic), are selected. The fibre reinforced polymer composites studied in the present riser design include four different fibre and polymer matrix combinations, AS4/epoxy, AS4/PEEK, P75/epoxy and P75/PEEK, while thermoplastic PEEK, steel, and titanium and aluminium alloys are considered for the inner liner. The above composite body and liner materials give rise to eight practical material system combinations which are considered for the present design study and presented in Table 3.15. It may be noted that, to avoid debonding between the matrix and liner material, only the PEEK liner is used with the AS4/PEEK and P75/PEEK composite bodies. With the fibre reinforced epoxy materials, AS4/epoxy and P75/epoxy, three metallic materials, aluminium alloy, steel and titanium alloy, respectively, are considered.

Table 3.15. Material combinations considered in the design

Configuration	Fibre	Matrix	Liner Material
1	AS4	PEEK	PEEK
2	P75	PEEK	PEEK
3	AS4	epoxy	steel
4	P75	epoxy	steel
5	AS4	epoxy	titanium
6	P75	epoxy	titanium
7	AS4	epoxy	aluminium
8	P75	epoxy	aluminium

3.11 Summary

This chapter begins with descriptions of the design specifications, in terms of the given geometrical parameters, environmental and functional loads, and the load cases to be considered in the designs of the steel and composite risers undertaken in this thesis. The rationale for the selection of the materials – a X80 alloy for the steel riser, and AS4 (HS) and P75 (HM) fibres, and epoxy and PEEK matrices for the composite body and liner materials – are presented. The mechanical properties of the constituent materials obtained from the literature are given, followed by the methods used to estimate their lamina elastic properties. Finally, the mechanical properties, elastic constants and strength values used in the 3D FE models employed in the design studies are presented, along with a list of the eight material combinations chosen for investigation. *Chapter 4* presents the design of the steel riser which is used as the benchmark against which the composite risers designed in subsequent chapters using both the conventional design and proposed tailored design for maximising weight savings are compared.

CHAPTER 4

DESIGN OF STEEL RISER

4.1 Introduction

An overview of the design conditions, specifications, load requirements and constraints, and design approaches and material combinations selected for this study were presented in the previous chapter. The main purpose of this thesis is to demonstrate and quantify the weight savings that can be achieved by the proposed tailored design of laminated composite risers compared with the conventional design process. For this purpose, the design and analysis of the steel riser used as the benchmark, which is used to estimate the weight savings of the conventional and tailored designs of composite risers, are presented in this chapter. The design is based on the requirements of both local load cases (the burst, tension, collapse and propagating buckling cases listed in Section 3.3.1, *Chapter 3*) and global load cases (listed as cases 1-9 in Section 3.3.2, *Chapter 3*). It is noted that the design and analysis of all these cases can be performed using the entire model of the steel riser. Unlike the traditional steel riser, in which all its standard joints are the same thickness along their lengths, in this study, since the forces, pressures and moments vary along this riser's length, every ten standard steel riser joints are designed separately for minimum weight in order to achieve the minimum possible weight for the entire steel riser and, thereby, a more conservative benchmark. For all the local load cases, the design factor (the ratio of the applied force to the allowable force) has to be smaller than the value specified by steel riser design codes [63-65]. For the global load cases, the usage factor (defined as the ratio of the Von Mises stress to the allowable strength) [66] is utilised to verify the design and is maintained below 1.0. The local load capacities of the steel riser are calculated using equations from the API standards [63-65] while the design under the global load cases is conducted using the finite element analysis (FEA) software ANSYS 13.0.

In the following sections, firstly, the finite element model of the steel riser is presented and then the design procedure employed and geometry of the steel riser are described. Finally, the results from the detailed analysis of the designed riser geometry for both the local and global load cases are presented.

4.2 Finite Element Model and Boundary Conditions

The finite element model of the entire steel riser for analysis of the global load cases is created using the FEA software ANSYS version 13.0 which has a pipe element, Pipe59, specifically designed to model submerged pipe segments. The global coordinate system of this model and the element coordinate system of Pipe59 are shown in Fig. 4.1.

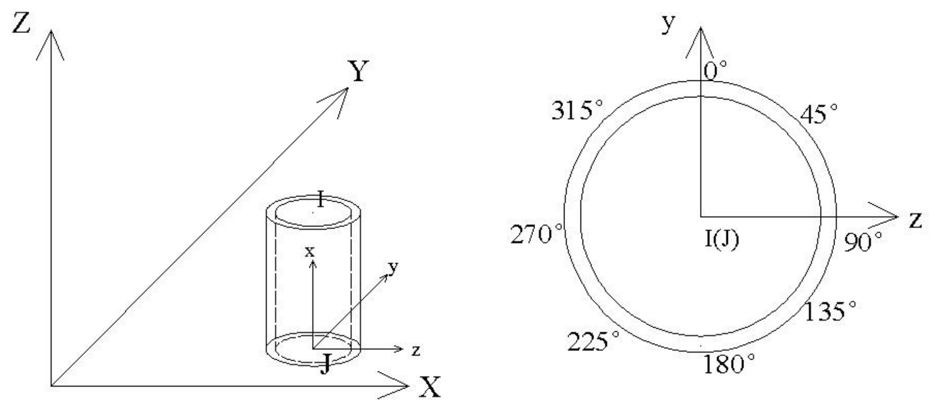

Fig. 4.1. Global coordinate and element coordinate systems

A total of 2117 elements are used over the full length of the steel riser (1970.1m), including the tension joint at the top and stress joint at the bottom, and its configuration is illustrated in Fig. 4.2. The tension joint at the top is 16.5m long, the standard steel riser joints are from 16.0m to -1904m the length of the riser (the origin of the length co-ordinate axis is at sea level and is positive upwards) and the stress joint at the bottom is 24.0m long, with the wellhead and casing making up another 9.6m to complete the full 1970.1 length of the riser. It is assumed that fairings are attached to the standard steel riser joints above -624m to mitigate vortex-induced vibration (VIV). As mentioned in Section 3.2, *Chapter 3*, and shown in Fig. 4.2, the internal diameter of the riser is 250mm and a standard production tubing made of C95 steel is employed inside. The purpose of this design is to determine the minimum wall thicknesses of the steel riser joints to provide design and usage factors below specified values for all load cases.

In order to consider the dynamic effect of the environmental loads and platform motion, the large displacement non-linear dynamic analysis option is chosen. Ball and slip support conditions are applied at the top of the riser to allow rotations and displacements so that the top tension force and displacements of the platform can be employed there, and a fixed support condition at the bottom which is achieved by applying fixed constraints (zero displacements and zero rotations) to the nodes of the elements representing the wellhead under the mudline (Fig. 4.2). For the steel riser under local load cases, its design factors are determined using equations given by steel riser standards [63-65] and, under the global load cases, the Von Mises stresses are checked at 90°and 270°, which are diametrically opposite points in the wave direction in the element coordinate system, on both the upper and lower nodes of each element (Fig. 4.1).

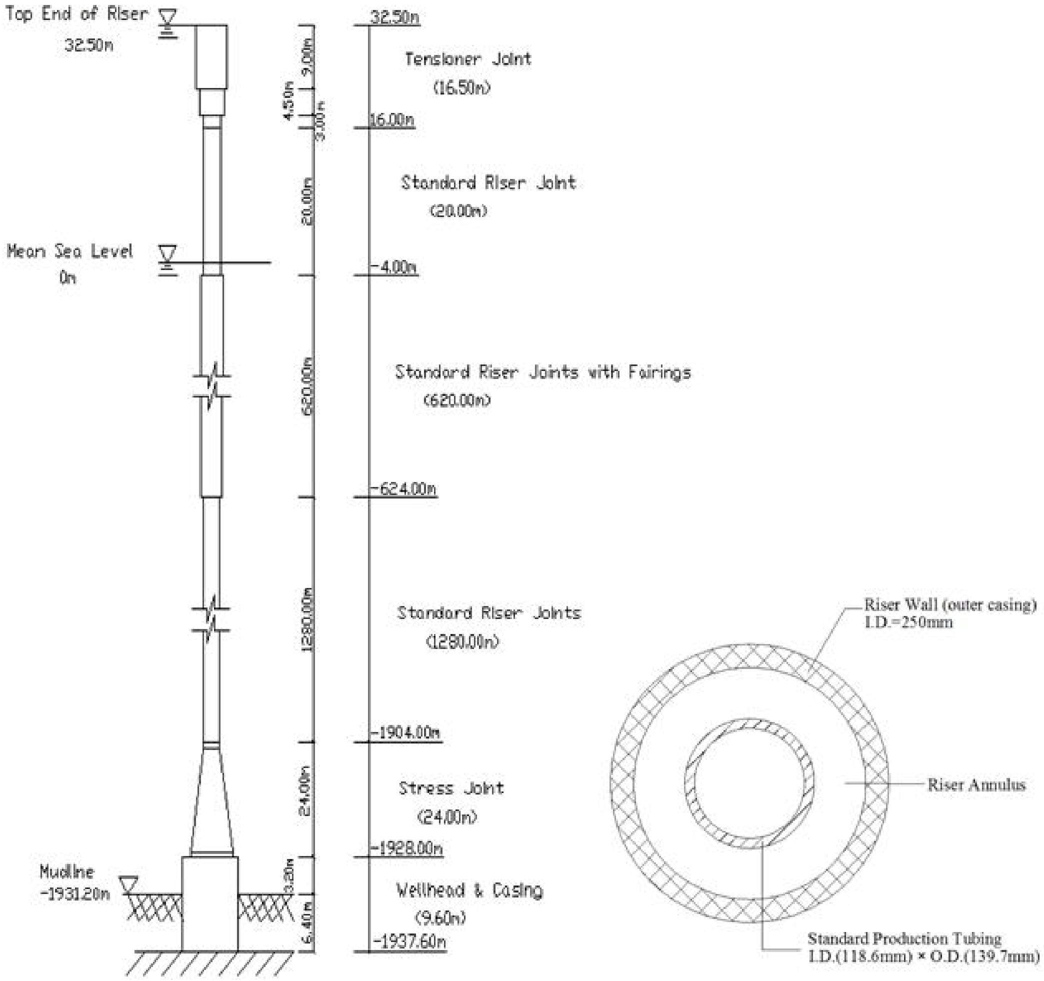

Fig. 4.2. Specified geometry and cross section of steel riser

4.3 Design Procedure for Steel Riser

The design procedure for the steel riser consists of determining local load capacities for burst, tension, collapse and propagating buckling cases using the equations given by API standards [63-65] and structural capacities under different global load cases using FEA. The burst, tension, collapse and propagating buckling design factors have to be smaller than 0.75, 0.60, 0.70 and 0.72, respectively [63-65]. The allowance strengths are 0.67 and 0.80 times the yield stress of the steel material for global design cases under normal operating conditions and extreme or temporary conditions, respectively [66].

The design of the steel riser is conducted using the following steps.

- *Step 1:* This is based on the burst capacity of the riser. The maximum design shut-in (internal) pressure is 69.0MPa and the burst design factor, $f_{\mathrm{d}} = \frac{\text{Net internal pressure}}{\text{Burst strength}}$, has to be smaller than 0.75 [64] under this load case while the design burst pressure has to satisfy Eq. 4-1 given by API RP 1111 [64].

$$P_{net\ internal\ pressure} \leq f_d f_e f_t P_b \tag{4-1}$$

where:

f_d: burst design factor

f_e: weld joint factor (1.0)

f_t: temperature de-rating factor (1.0)

P_b: burst capacity

Therefore, we can obtain an initial estimate of the required wall thickness of the riser tube to ensure that the design burst capacity (right-hand side (RHS) of Eq. 4-1) is just greater than the net internal pressure applied (left-hand side (LHS) of Eq. 4-1).

- *Step 2:* In this, the effective tension forces at different elevations of the riser are calculated to ensure that the tension design factor (f_t) is smaller than 0.6, as defined by Eq. 4-2 [64].

$$f_{\mathrm{t}} = \frac{\text{Effective tension force}}{\text{Yield tension force}} = \frac{\mathrm{T_{eff}}}{\mathrm{T_y}} \leq 0.6 \tag{4-2}$$

- *Step 3*: This involves calculating the collapse strengths at different elevations of the riser to ensure that the collapse design factor (f_c) is smaller than 0.7, while the maximum external pressure is 19.5MPa.

$$f_{\mathrm{c}} = \frac{\text{Net external pressure}}{\text{Collpase strength}} = \frac{\mathrm{P_{net\ external\ pressure}}}{\mathrm{P_c}} \leq 0.7 \tag{4-3}$$

- *Step 4:* This involves calculating the propagating buckling capacities at different elevations of the riser to ensure that the propagating buckling design factor (f_{pc}) is smaller than 0.72, as given by Eq. 4-4 [63, 64].

$$f_{\mathrm{pc}} = \frac{\text{Net external pressure}}{\text{Propagating buckling strength}} = \frac{\mathrm{P_{net\ external\ pressure}}}{\mathrm{P_p}} \leq 0.72 \tag{4-4}$$

- *Step 5:* This final step ensures that the requirements of all the global load cases (LC1-9) listed in Table 3.4 in *Chapter 3* are satisfied. In it, a FEA of the entire riser is conducted using the Pipe59 element. Each usage factor, defined as the percentage ratio of the actual maximum Von Mises stress to the allowable strength, is determined and maintained below 1.0.

Although the initial wall thickness estimated in the burst case (*Step 1*) is employed in subsequent steps, if the specified design or usage factor is not achieved in any of these steps, the wall thickness is increased to meet the required factor. Since the forces, pressures and moments vary along the length of the riser, the above steps are repeated for every ten standard steel riser joints (200m) to determine the minimum thickness of each set of ten joints required to obtain the minimum structural weight for the steel riser.

4.4 Geometry of Steel Riser Designed for Minimum Weight

The minimum thicknesses required for the different sections of the steel riser are determined using the design procedure presented in the above section. The design results, in terms of the minimum thicknesses required, along with details of the cross-sections and positions of the joints along the length of the riser, are presented in Table 4.1. The tension joint at the top has three regions from the top to bottom of 35mm (9m), 25mm (4.5m) and 22mm (3m) in thickness, respectively. The stress joint at the bottom is also divided into 3 regions: the top has a uniform thickness of 25mm for 3m, the middle a tapered thickness of from 25mm to 90mm for 19m and the bottom a uniform thickness of 90mm for 2m. Standard riser joints are designed for every 200m and have thicknesses of 22mm from 16m to -424m, 23mm from -424m to -1024m, 24mm from -1024m to -1624m and 25mm from -1624m to -1904m.

Table 4.1. Geometry and weights of steel riser joints designed for minimum weight

Region	O.D. (m)	I.D. (m)	Thickness (m)	Region extremities (m)		No. of joints	Length (m)	Air weight		Effective weight (global LC1-LC5)		Effective weight (global LC6-LC7)		Effective weight (global LC8-LC9)	
				Top	Bottom			Total weight (kg)	Weight per unit length (kg/m)	Total weight (kg)	Weight per unit length (kg/m)	Total weight (kg)	Weight per unit length (kg/m)	Total weight (kg)	Weight per unit length (kg/m)
tension joint-region 1	0.32	0.25	0.035	32.5	23.5	1	9	2323	258	2676	297	3145	349	2711	301
tension joint-region 2	0.3	0.25	0.025	23.5	19	1	4.5	763	169	939	209	1174	261	957	213
tension joint-region 3	0.294	0.25	0.022	19	16	1	3	552	184	670	223	826	275	681	227
bare standard joint	0.294	0.25	0.022	16	-4	1	20	3170	158	3675	184	4716	236	3751	188
standard joints with fairings (1-21)	0.294	0.25	0.022	-4	-424	21	420	71610	170	58742	140	80604	192	60347	144
standard joints with fairings (21-31)	0.296	0.25	0.023	-424	-624	10	200	35554	178	29236	146	39647	198	30000	150
bare standard joints (1-20)	0.296	0.25	0.023	-624	-1024	20	400	66308	166	53672	134	74493	186	55200	138
bare standard joints (21-50)	0.298	0.25	0.024	-1024	-1624	30	600	103854	173	84324	141	115556	193	86617	144
bare standard joints (51-64)	0.3	0.25	0.025	-1624	-1904	14	280	50529	180	41143	147	55719	199	42214	151
stress joint (min) stress joint (max)	0.3 0.43	0.25 0.25	0.025 0.09	-1904	-1928	1	24	15258	636	12986	541	14235	593	13078	545
wellhead & casing	0.92	0.80	0.06	-1928	-1937.6	1	9.60	12210	1270	9500	990	9500	990	9500	990

As well as the thicknesses and locations of the different riser joints, their weights in the air and effective weights are listed in Table 4.1. The weight in air consists of the structural weight of the riser tube and added mass of parts such as the connector and fairings. The effective weights for the different global load cases are combinations of their weights in the air, the fluid inside them and their buoyancy.

The structural weights and thicknesses of the standard steel riser joints extracted from Table 4.1 are summarised in Table 4.2. As their thicknesses vary from 22mm to 25mm, their structural weights are range from 148kg/m to 170kg/m. The structural weight of the designed steel riser is used as the benchmark. Compared with the traditional steel riser, which has the same thickness throughout its length, this new steel riser configuration provides an approximately 10% weight saving.

Table 4.2. Structural weights and thicknesses of standard steel riser joints

Location (m)	Structural weight (kg/m)	Thickness (mm)
16m to -424m	148	22
-424m to -1024m	155	23
-1024m to -1624m	162	24
-1624m to 1904m	170	25

4.5 Analysis of Designed Steel Riser under Local and Global Load Cases

The analysis results under both the local and global load cases of the steel riser with the geometry determined in Section 4.4 are presented in the following sections.

4.5.1 Burst Capacity

The design maximum shut-in (internal) pressure of the riser is 69.0MPa and its internal pressures at different elevations are obtained from the relationships shown in Table 4.3.

Table 4.3. Internal pressure at different locations of riser

Position of riser (m)	X=(+32.5— -1928.0)
Shut-in pressure (MPa)	P_{st} =69.0
Density of internal fluid (kg/m^3)	ρ_i =800
Internal pressure_below sea leave (MPa)	$P_{ib}= P_{st}-\rho_i g\left\|depth - X\right\|$
Internal pressure_above sea leave (MPa)	$P_{ia} =P_{ib(X=0)}-\rho_i gX$

The minimum burst capacity of the riser is determined by the minimum of the values given by Eq. 4-5 and Eq. 4-6, as per API RP 1111 [64], based on its geometry at different locations.

$$P_b = 0.45(Y + U)\ln\left({}^{D_o}/_{D_i}\right) \tag{4-5}$$

$$P_b = 0.9(Y + U)\frac{\mathrm{t}}{D_o - \mathrm{t}} \tag{4-6}$$

where:

P_b: burst capacity; Y: yield strength;

U: ultimate tensile strength; D_o and D_i: outside and inside diameters;

t: riser wall thickness.

In API Bulletin 5C3 [65], it is mentioned that the reduced yield strength (Yr), which takes axial stresses into account, should be used to calculate the reduction in material strength as

$$Y_r = [\sqrt{1 - 0.75\left({}^{P_{axial}}/_{Y}\right)^2} - 0.5\,{}^{P_{axial}}/_{Y}]Y \tag{4-7}$$

where

P_{axial}: axial stress =T/A; T: true wall tension of different position;

A: area of pipe section

Therefore, Eq. 4-5 and Eq. 4-6 are modified to Eq. 4-8 and Eq. 4-9, respectively.

$$P_b = 0.45(Y_r + U)\ln\left({}^{D_o}/_{D_i}\right) \tag{4-8}$$

$$P_b = 0.9(Y_r + U)\frac{\mathrm{t}}{D_o - \mathrm{t}} \tag{4-9}$$

Using Eqs. 4-8 and 4-9, the burst strengths and net internal pressure of the riser are shown in Fig. 4.3 in which it can be seen that the latter increases from 53.6MPa at the top to 69.0MPa at the bottom and the burst strengths of the standard riser joints trend in the same way but are much higher for the tension and stress joints. The shape changes in the burst strengths along the length of the riser are due to changes in thickness of the riser wall. The burst strengths calculated from Eqs. 4-8 and 4-9 are close to each other. The thickness is determined every ten riser joints (every 200m) to make the burst design factor (f_d) slightly smaller than the required value of 0.75 [64].

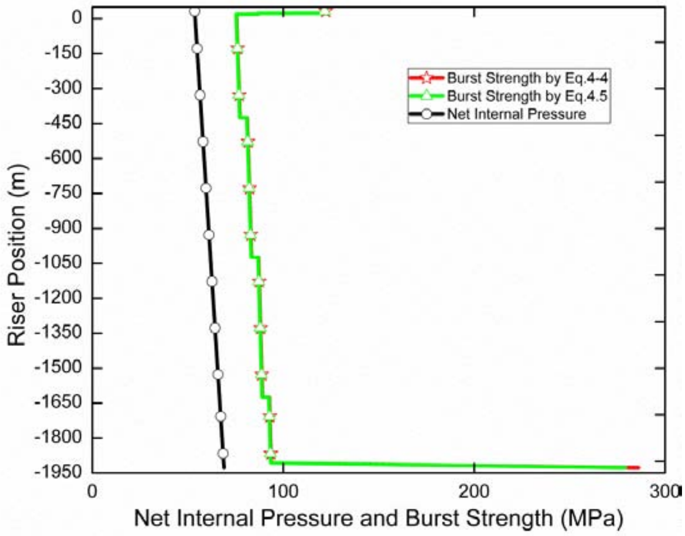

Fig. 4.3. Net internal pressure and burst strength

Based on the net internal pressure and burst strengths illustrated in Fig. 4.3, the distribution of the burst design factor, $f_{\mathrm{d}} = \frac{\text{Net internal pressure}}{\text{Burst Strength}}$, along the length of the riser, is shown in Fig. 4.4. The maximum burst design factor is 0.749 at -1624m of the riser and, for all the other standard riser joints, the burst design factors are between 0.71 and 0.75 which indicates that the burst capacity initially determines the minimum thickness of the standard riser joints.

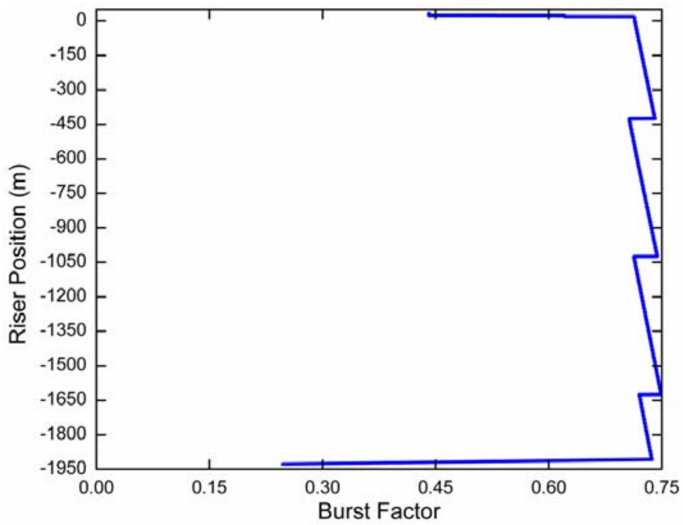

Fig. 4.4. Burst design factor along length of riser

4.5.2 Tension Capacity

The effective tension force is calculated by Eq. 4-10 [64] in which the effects of internal and external pressures on it are considered.

$$T_{eff} = T_a - P_i A_i + P_o A_o \quad (4\text{-}10)$$

where:

T_{eff}: effective tension force; P_i, P_o: internal and external pressures, respectively;

T_a: axial tension force; A_i, A_o : internal and external cross-section areas of riser.

The effective tension force has to consider different combinations of axial tension and internal and external pressures according to the local load cases for the steel riser presented in Table 3.1, *Chapter 3*. The values of these combinations are listed in Table 4.4.

Table 4.4. Combinations of axial tension and internal and external pressures for effective tension force calculation

Combination	Tension at top (kN)	Maximum internal pressure (MPa)	Maximum external pressure (MPa)
1	4200	0	19.5
2	4200	69.0	19.5
3	4200	58.6	19.5
4	4500	35.7	19.5
5	4350	0	19.5

The effective tension forces based on these five combinations are illustrated in Fig. 4.5. The yield tension force of the riser is T_y=SA, where S is the yield strength of the material and A the cross-sectional area of the pipe, as also plotted in Fig. 4.5. As can be seen in this figure, the effective tension force generally decreases with the increasing depth of the riser. Combinations 1 and 5, which are without internal pressure, provide the largest effective tension forces while the yield tension force increases with the increasing thickness of the riser wall. Since the tension and stress joints have higher thicknesses than the standard riser joints, the yield tension forces there are higher.

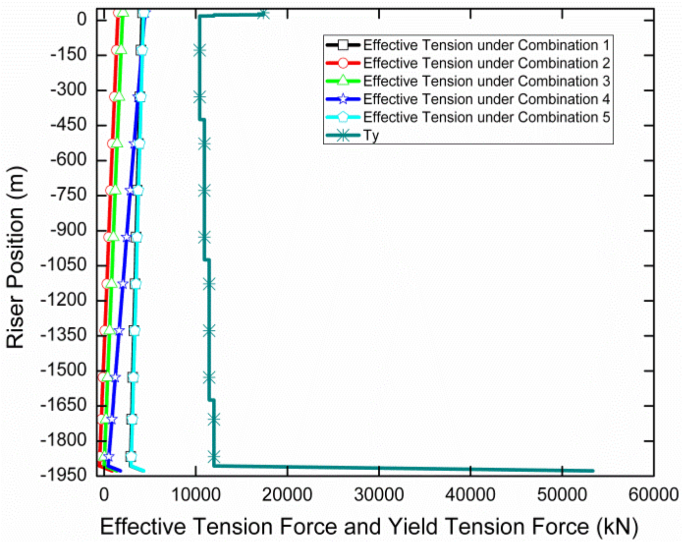

Fig. 4.5. Effective and yield tension forces

Based on the effective and yield tension forces illustrated in Fig. 4.5, the tension design factor, $f_{\mathrm{t}} = \frac{\text{Effective tension force}}{\text{Yield tension force}}$, along the length of the riser, is shown in Fig. 4.6.

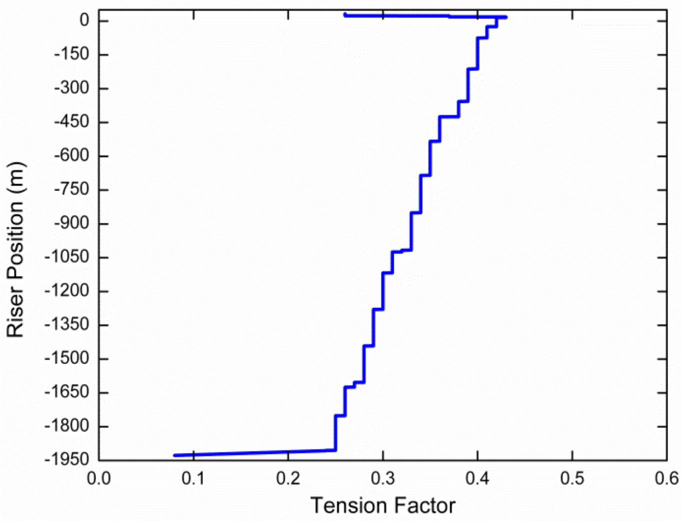

Fig. 4.6. Tension design factor along length of riser

As the maximum tension factor is 0.43 at 19m-16m at the tension joint of the riser, the riser wall thickness determined by load case 1 (the burst case) satisfies the tension capacity requirement.

4.5.3 Collapse Capacity

When the external pressure is higher than the internal pressure, a riser can collapse which happens mainly during installation conditions when there is no fluid inside it and, thus, no internal pressure, and is based on the riser's collapse strength which is the maximum net external pressure it can withstand without failure; the maximum external pressure is 19.5MPa and variations in it are based on depth. The collapse strength of a riser is calculated by Eq. 4-11 [63, 64] based on its geometry at different locations.

$$P_c = \frac{P_y P_e}{\sqrt{P_y^2 + P_e^2}} \tag{4-11}$$

where

P_y: yield pressure at collapse= $\frac{2Y_r t}{D_o}$; P_e: elastic collapse pressure=$2E\frac{(\frac{t}{D_o})^3}{(1-\nu^2)}$

Y_r: reduced yield strength due to axial stress=$[\sqrt{1-0.75\left({P_{axial}}/{Y}\right)^2} - 0.5\,{P_{axial}}/{Y}]Y$;

ν: Poisson's ratio (0.3 for steel); E : modulus of elasticity

The collapse strengths of the riser using Eq. 4-11 and net external pressures are plotted in Fig. 4.7 in which it can be seen that the latter increases from 0MPa at the top to 19.5MPa at the bottom while the collapse strengths of the standard riser joints follow the same trend but are much higher at the tension and stress joints. The shape change in the collapse strength along the length of the riser is due to the change in thickness of the riser wall.

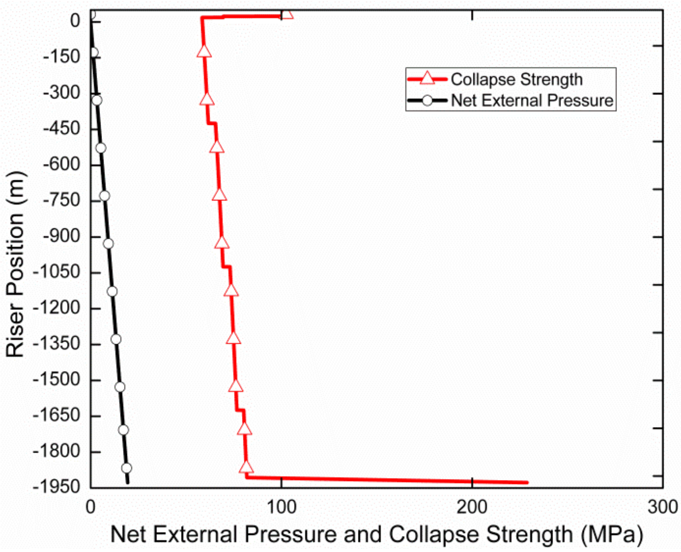

Fig. 4.7. Net external pressure and collapse strength

Based on the net external pressures and collapse strengths illustrated in Fig. 4.7, the plot of the collapse design factor, $f_c = \frac{\text{Net external pressure}}{\text{Collapse strength}}$, along the length of the riser is shown in Fig. 4.8.

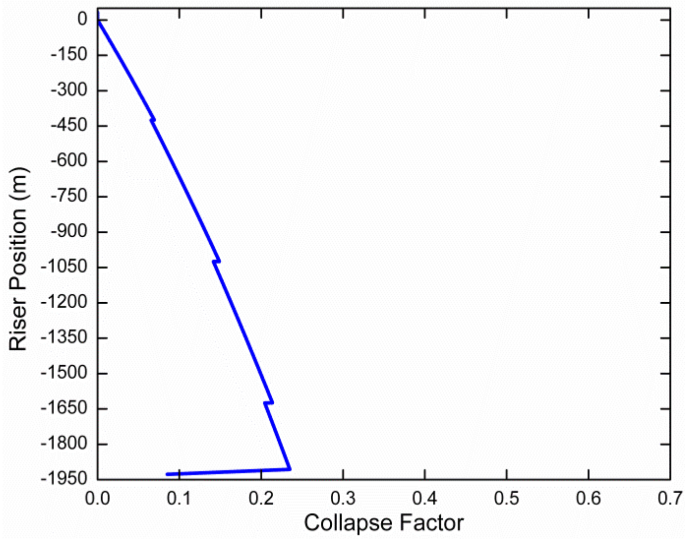

Fig. 4.8. Collapse factor along length of riser

As the maximum collapse factor is 0.235 at -1907m at the stress joint of the riser, the riser wall thickness determined by the burst case satisfies the collapse capacity requirement.

4.5.4 Propagating Buckling Capacity

The impacts of foreign objects, excessive bending during installation or under operational off-design conditions, as well as wear and corrosion, lead to dents, local buckles and reductions in the thickness of a riser wall. As all these defects might locally reduce the buckling capacity of a riser pipe, the propagating buckling pressure (P_p) should be checked for riser design and is calculated by Eq. 4-12 given by API [63, 64].

$$P_p = 24Y\left(\frac{t}{D_o}\right)^{2.4} \qquad (4\text{-}12)$$

where Y_r (the reduced yield stress) is used instead of Y (the yield stress).

The propagating buckling pressure of the riser using Eq. 4-12 and the net external pressure are illustrated in Fig. 4.9 in which it can be seen that the latter increases from 0MPa at the top to 19.5MPa at the bottom while the former of the standard riser joints follows the same trend but is much higher at the tension and stress joints. The shape change in the propagating buckling capacity along the length of the riser is due to the change in thickness of the riser wall.

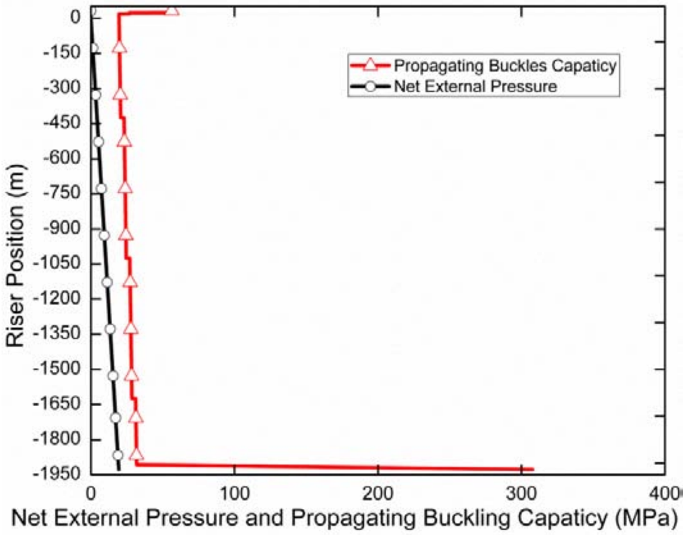

Fig. 4.9. Net external pressure and propagating buckling capacity

Based on the net external pressure and propagating buckling pressure illustrated in Fig. 4.9, the plot of the propagating buckling design factor, $f_{\mathrm{pc}} = \frac{\text{Net external pressure}}{\text{Propagating buckling strength}}$, along the length of the riser is shown in Fig. 4.10.

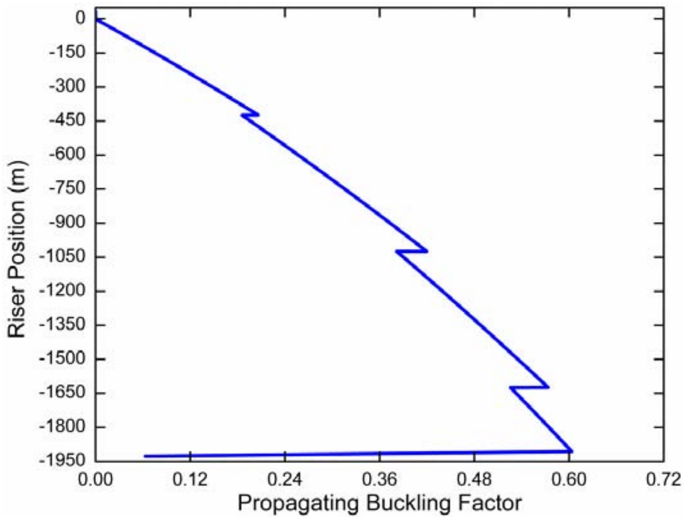

Fig. 4.10. Propagating buckling factor along length of riser

The maximum propagating buckling factor is 0.603 at -1907m at the stress joint of the riser which shows that the riser wall thickness determined by the burst case satisfies the propagating buckling capacity requirement.

4.5.5 Stresses under Different Global Load Cases

The global load cases used for the working stress design are described in *Chapter 3* (Table 3.4) and the maximum values of the Von Mises stresses at diametrically opposite points in the wave direction along the riser for each load case are shown in Fig. 4.11. The green vertical lines on the right of these figures indicate the allowable strength of steel for the different load cases. More specifically, according to ABS standard [10], 67% and 80% of the yield stress of the material are identified as the allowable stresses for global design under normal operating conditions (371Mpa for LC1-LC3), and global design under extreme or temporary conditions (444MPa for LC4-LC9), respectively.

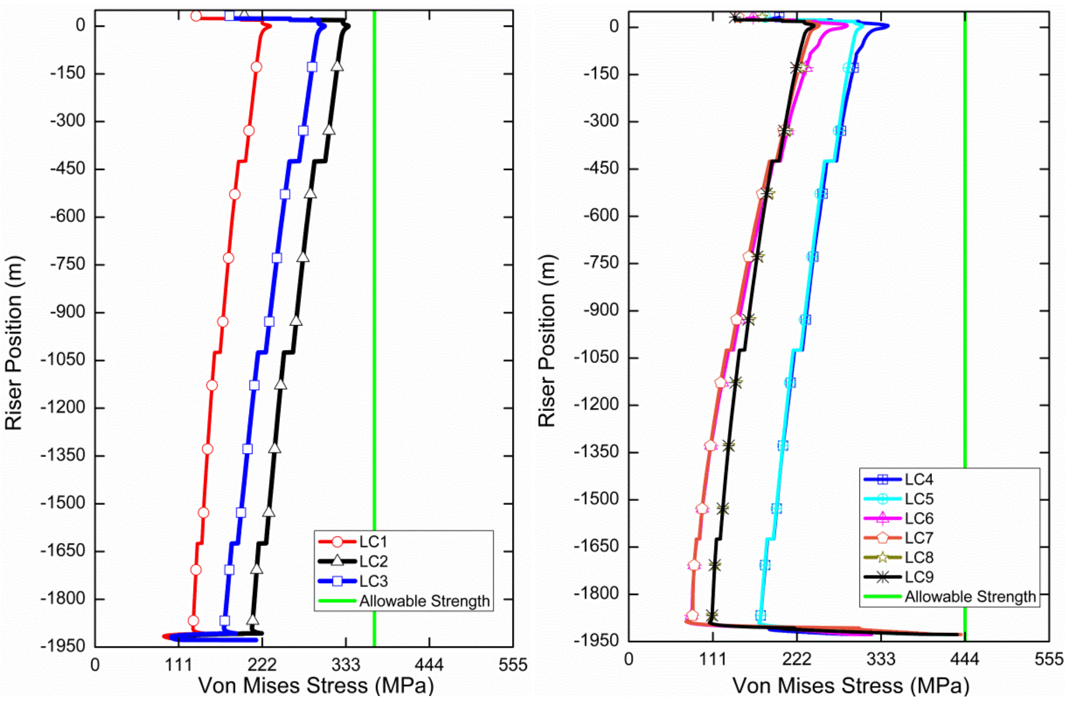

(a) (b)

Fig. 4.11. Von Mises stress distributions along length of steel riser for (a) normal operating conditions (LC1-LC3) and (b) extreme conditions (LC4-LC9)

From Fig. 4.11, it is clear that Von Mises stresses under all the design global load cases are smaller than the allowable strength. Based on the Von Mises stress distributions and allowance strength illustrated, the usage factors, defined as the percentage ratio of the actual maximum Von Mises stress to the allowable stress, are shown in Fig. 4.12 in which it can be seen that those of the entire riser do not exceed the allowance (100%). Generally, the usage factors of standard riser joints decrease with increasing depth and those at the tension and stress joints are relatively higher since the load conditions at these locations are more severe.

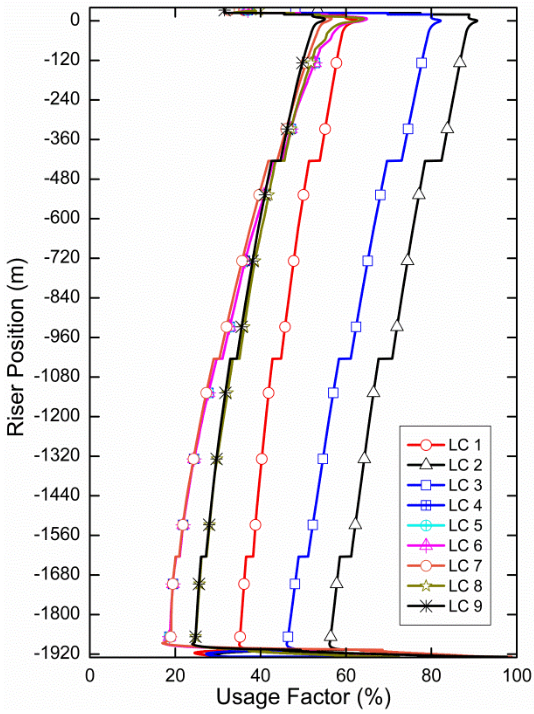

Fig. 4.12. Usage factors under different global load cases

The comparison of the capacities under both the local and global load cases shows that the thicknesses of standard riser joints are determined by their burst capacities while that of the stress joint is determined by global load case 7.

4.6 Summary

This chapter describes the design of the steel riser used as the benchmark in this study to demonstrate and quantify the weight savings that can be achieved by composite risers. Its entire configuration and the FEA model using element Pipe59 are presented. The thicknesses of the steel riser tubes are determined every ten riser joints and the design results provide about a 10% weight saving over the traditional steel riser which has the same thickness throughout its length. The structural weight of the designed riser is 170kg/m, and its burst, tension, collapse, propagating buckling and structural capacities under different global load cases are evaluated. Using its structural weight and thickness as benchmarks, the weight reductions that can be achieved by the composite riser designed using the conventional and proposed tailored procedures are estimated in the following chapters. *Chapter 5* and *Chapter 6* present the local and global designs of the composite risers, respectively, using both conventional and tailored design approaches, with the local designs optimised for a minimum structural weight using an iterative approach of manual inspection and selection. *Chapter 7* presents the application of the optimisation technique for minimum structural weight, the Surrogate-Assisted Evolutionary Algorithm (SAEA) to corroborate the results from the manual approach employed for the tailored designs in *Chapter 5*.

CHAPTER 5

LOCAL DESIGN OF COMPOSITE RISER

5.1 Introduction

In the previous chapter, a steel riser with a minimum weight was designed to be used as the benchmark for determining the weight savings that can be achieved by employing fibre-reinforced polymer composites in designs of risers. This chapter presents a local design of composite risers using the conventional design approach (with reinforcements in only the axial and hoop directions) and the proposed tailored design which also has reinforcements in the off-axis directions. A global design of the composite risers required to complete the design process is described in *Chapter 6*. The local design stage ensures the local load capacities of the composite riser under the four local load cases and, in it, it is necessary to obtain the first estimate of the composite riser's tubular geometry on which its deformations and, thus, forces and bending moments due to global loads, depend. The local design, i.e., determinations of the stacking sequence, layer thickness, fibre orientation, etc., is conducted for four load cases: burst, tension (pure tension and tension with external pressure), maximum external pressure and buckling under external pressure (local load cases 1 to 4 listed in *Chapter 3*), as prescribed by the ABS standard [66]. It is to be noted that, in the local design study in this chapter, only the static load capacities of the riser are checked and the long-term durability of a structure is taken into consideration by employing long-term instead of short-term strength values. For a complete analysis of long-term durability, it would be necessary to test for resistance against long-term stress rupture by establishing a stress rupture curve with test results up to 10,000 hours. However, since our objective is mainly to demonstrate the weight savings that can be achieved by employing a tailored as opposed to a conventional design for the construction of a composite riser, this is considered beyond the scope of this thesis.

A three-dimensional (3D) finite element analysis (FEA) of a local riser joint is conducted to determine its stress distributions and buckling capacity under the local load cases. In this stage, geometric configurations of each of the eight different composite body and liner combinations (Table 3.15 in *Chapter 3*) are optimised to yield minimum margins of safety (factor of safety (FS) of just above 1.0) and, thereby, provide minimum structural weights. These designs for minimum weight of the eight material combinations in this chapter is performed using two different approaches: the conventional approach with only axial and hoop reinforcements in the composite layers; and the proposed tailored design in which fibre reinforcements in off-axis directions are also considered, both of which use an iterative procedure of manual inspection and selection of the optimum parameters. The application of mathematical optimisation tools to confirm this manual approach for the tailored design is presented in *Chapter 7*.

There are three main reasons for attempting to optimise a riser's ply orientations and stacking sequences to obtain its minimum thickness under local loads: (1) the optimum ply orientation of $\pm 54.7^{o}$ is valid only if the presence of the matrix is ignored, for a thin shell under internal pressure; (2) when a tube with end caps is subjected to axial tension in addition to internal pressure, as the ratio of the axial stress resultant to the circumferential stress resultant is no longer 0.5, the angle of ±54.7^o predicted by the netting theory no longer holds; and (3) the composite tubes used for deep sea risers are quite thick and neither the netting nor thin shell theories can adequately predict the stress distribution in their laminates. The inadequacy of the netting theory in terms of correctly predicting the optimum ply orientation for the minimum thickness of a thin composite tube under internal pressure is first illustrated using classical laminate theory (CLT) to analyse 4-ply and 8-ply laminates. Then, determinations of optimum ply orientations and stacking sequences to obtain the minimum thicknesses required for the laminate tubes of composite risers subjected to the four local load cases prescribed by the standards is undertaken, first using the conventional orthogonal design and then the proposed tailored design, both of which use an iterative procedure of manual inspection and selection.

5.2 Minimum Thickness for Composite Tube under Internal Pressure using Classical Laminate Theory

For the local design of composite riser tubes, of the four load cases, the burst case is predominant. Its axial force due to the end effects of internal pressure is much higher than that of the top tension case alone; for example, for the composite tube made from AS4/PEEK with PEEK liner, the design top tension force is about 5500kN (with a tension factor of 2.25) while the end effects due to the design internal pressure of 155.25MPa (with a pressure factor of 2.25) produce a tension of over 7600kN. Therefore, the burst load case, i.e., a cylindrical tube with closed ends under internal pressure, is employed to study the effect of various fibre reinforcement angles on the minimum laminate thickness. As noted in the introduction, the optimum angle for the reinforcement of a filament-wound thin cylindrical pipe under internal pressure with end effects is given by the netting theory as ±54.7^o and the corresponding minimum thickness as $1.5\frac{pr}{\sigma_1}$, where p is the internal pressure, r the mean radius and σ_1 the ply strength in the fibre direction [62]. However, for a composite with fibres embedded in a matrix, transverse and shear stresses appear and failure of the matrix because of these stresses also has to be considered. More significantly, for some combinations of fibre and matrix strengths and stiffnesses, the effect of the stresses carried by the matrix is to reduce the overall thickness of the laminate below that required by the netting theory. In this section, CLT [83] is used to determine the minimum thickness required for a pipe under the burst load (internal pressure with end effects), as a function of the fibre reinforcement angles for different values of the transverse and shear stiffnesses and strengths in comparison with those in the fibre direction. First ply failure using the maximum stress failure criterion [83] is applied to normal the stresses in the fibre and transverse directions and in-plane shear stress to determine the minimum ply thickness required and, thus, the minimum laminate thickness.

5.2.1 Minimum Thickness for Four-ply Symmetrically Balanced Ply Laminate

Initially, a four-ply laminate with a lay-up of $[\pm\theta]_s$, for which all four plies have the same thicknesses and stress magnitudes, is considered. A MATLAB code is written to calculate the minimum laminate thickness for the burst case with this lay-up using CLT [83]. The basic equation of CLT relating the strains and curvatures to the stress and moment resultants is given in Eq. 5-1 and the global coordinate system (x, y) and principal material coordinate system (1 and 2 for the fibre and transverse directions, respectively) are illustrated in Fig. 5.1.

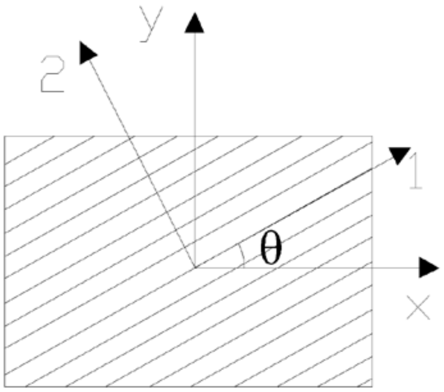

Fig. 5.1. Global coordinate and principal material coordinate systems

$$\begin{bmatrix} A_{xx} & A_{xy} & A_{xs} & B_{xx} & B_{xy} & B_{xs} \\ A_{xy} & A_{yy} & A_{ys} & B_{xy} & B_{yy} & B_{ys} \\ A_{xs} & A_{ys} & A_{ss} & B_{xs} & B_{ys} & B_{ss} \\ B_{xx} & B_{xy} & B_{xs} & D_{xx} & D_{xy} & D_{xs} \\ B_{xy} & B_{yy} & B_{ys} & D_{xy} & D_{yy} & D_{ys} \\ B_{xs} & B_{ys} & B_{ss} & D_{xs} & D_{ys} & D_{ss} \end{bmatrix} \begin{bmatrix} \varepsilon_x^0 \\ \varepsilon_y^0 \\ \gamma_{xy}^0 \\ \kappa_x^0 \\ \kappa_y^0 \\ \kappa_s^0 \end{bmatrix} = \begin{bmatrix} N_x \\ N_y \\ N_s \\ M_x \\ M_y \\ M_s \end{bmatrix} \tag{5-1}$$

In Eq. 5-1, the full ABD matrix consists of three parts: (1) an extensional matrix [A] which relates the resultant in-plane forces to the in-plane strains; (2) a bending stiffness matrix [D] which relates the resultant bending moments to the plate curvatures; and (3) a coupling stiffness matrix [B] which couples the force and moment terms to the mid-plane strains and mid-plane curvatures, respectively. For the burst case, N_x is equal to *pr/2* and N_y to *pr* (where *p* and *r* are the internal pressure and mean radius of the pipe, respectively). All the other stress and moment resultants are zero while the subscripts x, y and xy refer to the axial and hoop directions and in-plane shear of the laminate, respectively.

Using the values of N_x and N_y from Eq. 5-1, $\begin{bmatrix} \varepsilon_x^0 \\ \varepsilon_y^0 \\ \gamma_{xy}^0 \end{bmatrix}$, is obtained which is the same for every layer, and then the stresses $\begin{bmatrix} \sigma_x \\ \sigma_y \\ \tau_{xy} \end{bmatrix}$ in each layer is obtained from Eq. 5-2.

$$
\begin{bmatrix} \sigma_x \\ \sigma_y \\ \tau_{xy} \end{bmatrix} = \begin{bmatrix} Q_{xx}(\theta) & Q_{xy}(\theta) & Q_{xs}(\theta) \\ Q_{xy}(\theta) & Q_{yy}(\theta) & Q_{ys}(\theta) \\ Q_{xs}(\theta) & Q_{ys}(\theta) & Q_{ss}(\theta) \end{bmatrix} \begin{bmatrix} \varepsilon_x \\ \varepsilon_y \\ \gamma_{xy} \end{bmatrix} \tag{5-2}
$$

The stresses in the fibre and transverse directions and in-plane shear are obtained by coordinate transformations using Eq. 5-3.

$$
\begin{bmatrix} \sigma_1 \\ \sigma_2 \\ \tau_{12} \end{bmatrix} = \begin{bmatrix} c^2 & s^2 & 2cs \\ s^2 & c^2 & -2cs \\ -cs & cs & c^2 - s^2 \end{bmatrix} \begin{bmatrix} \sigma_x \\ \sigma_y \\ \sigma_{xy} \end{bmatrix} \tag{5-3}
$$

where

c= cos θ and s=sin θ.

Applying the maximum stress failure criterion in the MATLAB code, the stresses in the fibre and transverse directions and in-plane shear are normalised to the strengths in those directions. For every material property given in the code, the minimum thicknesses required to make the laminate safe are calculated for all fibre orientations from 0^o to 90^o using CLT, after obtaining which they are normalised to the minimum thickness obtained by the netting theory ($1.5\frac{pr}{\sigma_1}$).

Figs. 5.2(a) to 5.2(d) show variations in the minimum laminate thickness for each case, normalised by the value given by the netting theory ($1.5\frac{pr}{\sigma_1}$), for a four-ply $[\pm\theta]_s$ laminate as a function of the fibre reinforcement angle for different values of the modulus ratio (E_2/E_1), strength ratio (S_2/S_1), normalised shear stiffness (G_{12}/E_1) and normalised shear strength (S_{12}/S_1) with the other ratios held constant. It may be noted that the thicknesses required for all plies are the same since the stresses are the same in all layers. The lowest values of the stiffness and strength ratios used in these plots, i.e., E_2/E_1=0.07, G_{12}/E_1=0.04, S_2/S_1=0.03 and S_{12}/S_1=0.04, are those corresponding to the carbon fibre AS4-reinforced epoxy with a fibre volume fraction of 0.6, the mechanical properties of which are listed in Table 3.13 and Table 3.14 in *Chapter 3*.

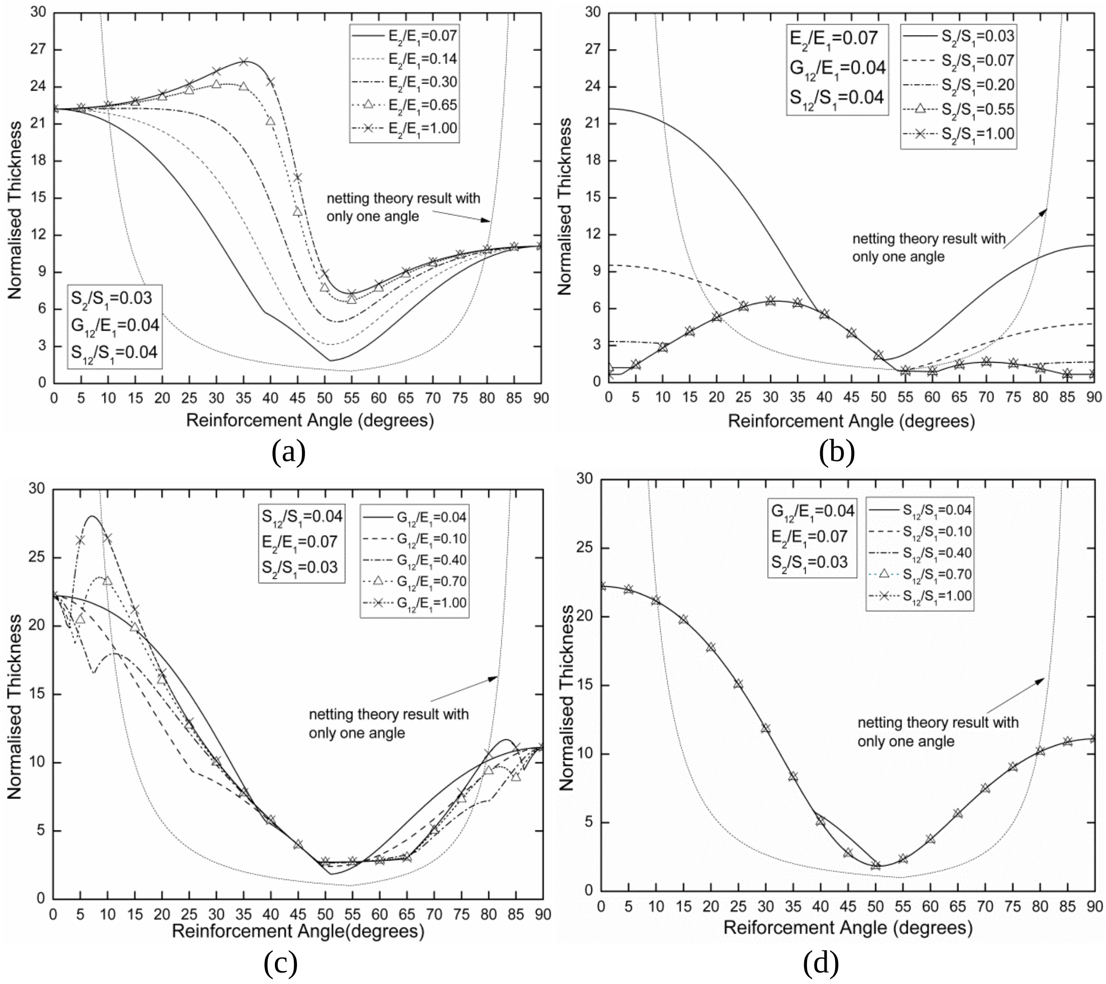

Fig. 5.2. Variations in normalised thickness of 4-ply $[\pm\theta]_s$ laminate with fibre reinforcement angle with normalised (a) modulus ratio E_2/E_1, (b) strength ratio S_2/S_1, (c) shear stiffness G_{12}/E_1 and (d) shear stiffness S_{12}/S_1

The reason for the sharp changes in the gradients of some of the curves in Fig. 5.2 is the shift in the failure mode from that caused by transverse direction stress to that caused by in-plane shear; for example, for all the curves in Fig. 5.2(a), except that of E_2/E_1=0.07, the failure occurs under transverse stress and the curves are smooth whereas, in the case of E_2/E_1=0.07, the cause of failure shifts from the transverse to shear stress at an angle of about 39^o and back to the transverse stress at about 51^o which produces sharp changes in the gradient of the curve at these locations. Variations in the tube thickness using the fibre orientation given by the netting theory ($\max\left(\frac{pr}{2\sigma_1\cos^2\theta}, \frac{pr}{\sigma_1\sin^2\theta}\right)$) are also plotted in Fig. 5.2 for comparison. It may be noted that, as the netting theory curve is independent of the transverse and shear stiffness and strength values, it is the same in all figures. The minimum thickness in this curve occurs at $\theta=\pm54.7^o$ which has a normalised value of 1.0. For all the properties considered in Fig. 5.2(a), the minimum thicknesses predicted by the laminate theory are higher than those given by the netting theory and rise with increasing values of the transverse stiffness ratio (E_2/E_1). Fig. 5.2(b) shows that the minimum required thickness decreases with increasing values of the transverse strength ratio (S_2/S_1) and drops below that given by the netting theory for values of S_2/S_1 equal to and greater than 0.07. It is also seen that the regions dominated by shear failure (the central portions of the curves defined by the sharp gradient changes) become larger as the transverse strength ratio increases. It can be seen that the minimum required thickness increases marginally when G_{12}/E_1 rises (Fig. 5.2(c)), while increases in S_{12}/S_1 have virtually no effect (Fig. 5.2(d)).

The minimum normalised thicknesses and optimum angles of reinforcement for the different combinations of stiffness and strength ratios investigated for the four-ply symmetrical angle ply laminates are listed in Table 5.1.

Table 5.1. Optimum reinforcement angles and minimum thicknesses for 4-ply symmetrically balanced $[\pm\theta]_s$ laminates

Stiffness and strength ratios			Optimum reinforcement angle	Normalised thickness ($t*\sigma_1/1.5pR$)
AS4-epoxy: $E_2/E_1=0.07$; $S_2/S_1=0.03$ $G_{12}/E_1=0.04$; $S_{12}/S_1=0.04$			51.0^o	1.84
$S_2/S_1=0.03$ $G_{12}/E_1=0.04$ $S_{12}/S_1=0.04$	$\frac{E_2}{E_1}$	0.14	51.0^o	3.16
		0.30	52.5^o	5.00
		0.65	54.0^o	6.65
		1.00	54.5^o	7.28
$E_2/E_1=0.07$ $G_{12}/E_1=0.04$ $S_{12}/S_1=0.04$	$\frac{S_2}{S_1}$	0.07	54.0^o	0.94
		0.20	60.5^o	0.88
		0.55	90.0^o	0.67
		1.00	0.00^o	0.67
$E_2/E_1=0.07$ $S_2/S_1=0.03$ $S_{12}/S_1=0.04$	$\frac{G_{12}}{E_1}$	0.10	51.0^o	2.41
		0.40	51.0^o	2.67
		0.70	51.0^o	2.71
		1.00	51.0^o	2.73
$E_2/E_1=0.07$ $S_2/S_1=0.03$ $G_{12}/E_1=0.04$	$\frac{S_{12}}{S_1}$	0.10	50.5^o	1.84
		0.40	50.5^o	1.84
		0.70	50.5^o	1.84
		1.00	50.5^o	1.84

The optimum angle of reinforcement for the minimum thickness of the four-ply lay-up with stiffness and strength ratios corresponding to those of AS4/epoxy is obtained as 51^{o} using CLT, with the minimum thickness being 1.84 times that given by the netting theory, as shown in the first row in Table 5.1. The minimum thickness according to the netting theory, $1.5\frac{pr}{\sigma_1}$, is independent of the transverse and shear stiffnesses and strengths of the composites while the values in Table 5.1 clearly show that, if the ratio of the transverse stiffness to longitudinal stiffness (E_2/E_1) is increased, the optimum angle increases from 51^{o} and the minimum thickness required rises significantly to up to 7 times the value predicted by the netting theory. This is because more loads are borne by the matrix due to the higher stiffness in the transverse direction while the transverse strength remains unchanged whereas, when the transverse strength ratio (S_2/S_1) increases, the optimum angle increases but the minimum required thickness reduces to values well below that predicted by the netting theory. An increase in the shear stiffness ratio (G_{12}/E_1) causes only a marginal rise in the required thickness while a change in the shear strength ratio (S_{12}/S_1) has virtually no effect on it, and neither affect the optimum angle of reinforcement.

5.2.2 Minimum Thickness for Eight-ply Symmetrically Balanced Laminate

Using CLT [83], the analysis performed for the four-ply laminates is extended to eight-ply balanced symmetrical laminates with a $[\pm\theta/\pm(90-\theta)]_s$ lay-up to determine the minimum thickness under internal pressure with end effects. A MATLAB code for these calculations is created and the process is similar to that for the four-ply laminate, with the only difference being that the thicknesses of some layers may be zero in which case their stiffness are not considered. It may be noted that, since the stresses are in-plane, the stacking sequence has no effect. The thicknesses of the ±θ layers and ±(90-θ) layers are, in general, different and a total laminate thickness is the sum of all these thicknesses. As in the case of the four-ply symmetrically balanced laminate, the maximum stresses in the fibre and transverse directions and in-plane shear are compared with their strength values to determine the minimum thickness required for each ply.

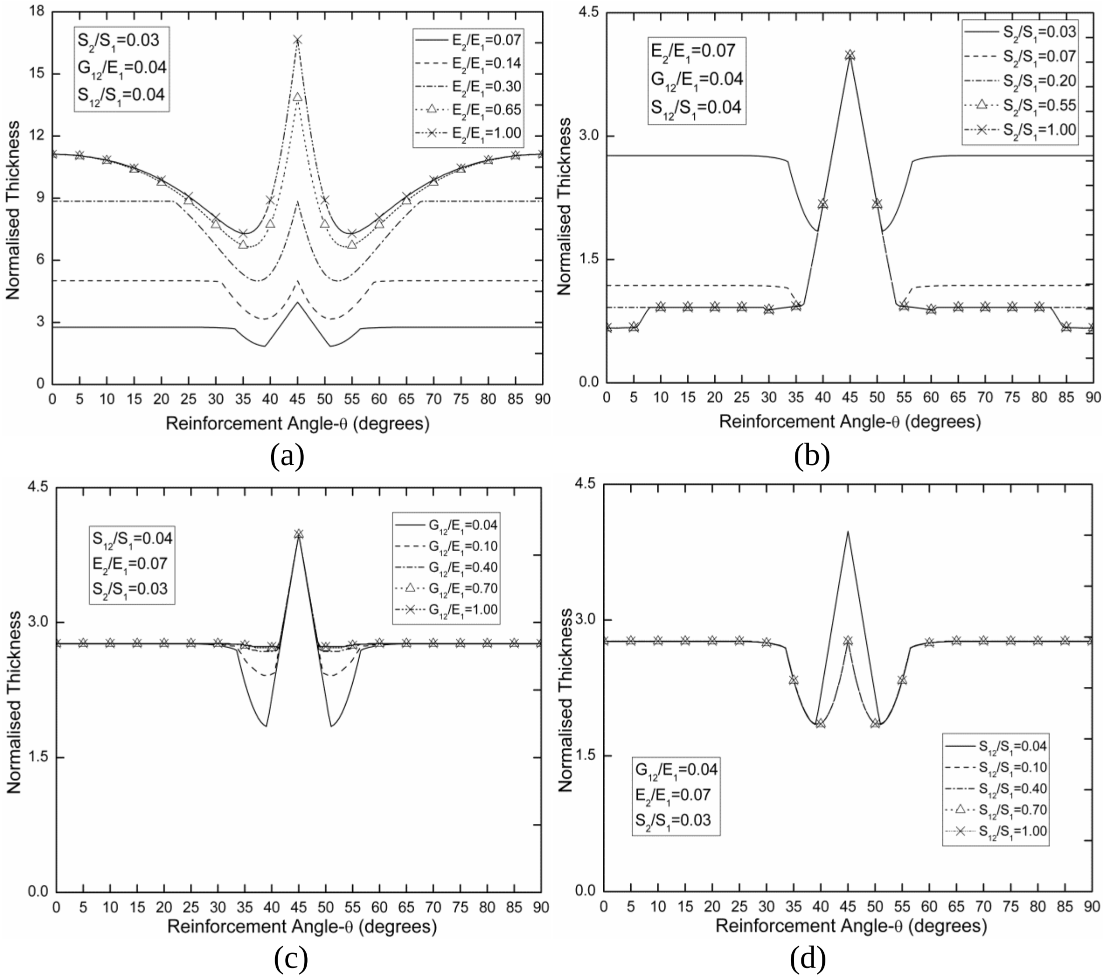

Fig. 5.3. Variations in normalised thickness of 8-ply $[\pm\theta, \pm(90\text{-}\theta)]_s$ laminate with fibre reinforcement angle with normalised (a) modulus ratio E_2/E_1, (b) strength ratio S_2/S_1, (c) shear stiffness G_{12}/E_1 and (d) shear stiffness S_{12}/S_1

Figs. 5.3(a), 5.3(b), 5.3(c) and 5.3(d) show variations in the minimum laminate thickness with a reinforcement angle for the eight-ply laminate with a $[\pm\theta/ \pm(90\text{-}\theta)]_s$ lay-up for different values of E_2/E_1, S_2/S_1, G_{12}/E_1 and S_{12}/S_1, with the other strength and stiffness ratios held constant.

The trends seen in these figures are similar to those for the four-ply laminate, with the minimum required laminate thickness increasing with rising values of the stiffness ratios (E_2/E_1 and G_{12}/E_1) (Figs. 5.3(a) and 5.3(c)) and decreasing with increasing values of the transverse strength ratio (S_2/S_1) (Fig. 5.3(b)) while the shear strength ratio (S_{12}/S_1) seems to have little effect (Fig. 5.3(d)). However, surprisingly, it is found that the optimum angle of reinforcement and minimum laminate thickness for the eight-ply laminate are exactly the same as those obtained for the four-ply laminate for all the stiffness and strength combinations investigated. This is illustrated in Fig. 5.4(a) in which variations in laminate thickness for the four-ply and eight-ply laminates with reinforcement angles (θ) are plotted together for three values of E_2/E_1. It can be seen that their curves are separate for small and large values of θ but overlap for intermediate values, with their optimum reinforcement angles and minimum laminate thicknesses coinciding. The reason for this is that, when one of the plies has an orientation in the mid-range, the thicknesses of the layers perpendicular to it become zero for the required laminate thickness, as illustrated in Fig. 5.4(b) in which the normalised thickness values for the ±θ and ±(90-θ) layers and total thickness are plotted for the symmetrical eight-ply AS4/epoxy laminate (E_2/E_1=0.07, G_{12}/E_1=0.04, S_2/S_1=0.03 and S_{12}/S_1=0.04).

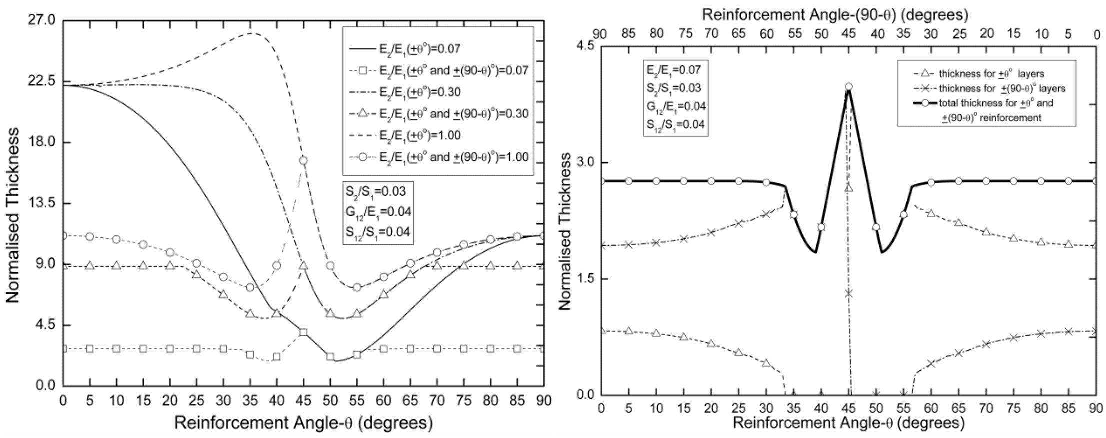

(a) (b)

Fig. 5.4. (a) Comparison of normalised thicknesses of 4-ply and 8-ply laminates with different transverse stiffness ratios E_2/E_1 and (b) thicknesses of orthogonal plies and total thickness variations for typical case

This observed behaviour is typical of all the stiffness and strength ratios investigated, with one layer’s thickness becoming zero while the others have reinforcements in the mid-range. The reason for this is that, when half the layers are oriented with values of $\pm\theta$ in the mid-range, their transverse strains become relatively small, thereby causing low transverse stresses. When the thicknesses of these plies are adjusted to prevent failure in the fibre direction, they become sufficient to carry all the loads and require no plies in the orthogonal direction. It can also be observed in Fig. 5.4(a) that, while the curves for the four-ply $[\pm\theta]_s$ and eight-ply $[\pm\theta/\pm(90-\theta)]_s$ laminates overlap in the mid-region for values of θ, away from this region, the total laminate thickness for the eight-ply laminate is much lower. This is because, when the fibres are oriented close to the axial or hoop direction of the pipe in a four-ply laminate, their thicknesses have to be significantly increased to accommodate their transverse stresses whereas, in an eight-ply laminate with orthogonal fibre reinforcement, both the hoop and axial stresses are mainly resisted by the fibres.

5.2.3 Summary and Discussion

The foregoing 2D analysis clearly shows that, even for thin laminates, the optimum angle of reinforcement and minimum thickness required for a composite tube with internal pressure are different from those predicted by the netting theory due to the finite stiffness and strength of the matrix. It may be noted that results from the netting would be valid for only one ratio of the circumferential to axial stress resultants (provided it was thin-walled) and, if this ratio changed from that for which the reinforcement angle was chosen, the fibres would no longer be able to bear the load; for instance, if the reinforcement angle was chosen as 54.7^o to minimise the tube thickness for only the internal pressure, any additional tension, such as that due to top tension in the riser, would have to be borne by the liner. Therefore, if the laminate reinforcement was chosen as 54.7^o based on the netting theory, it would make the liner much thicker and the overall weight of the tube greater; for example, for an AS4/PEEK composite tube designed using the netting theory (a $\pm 54.7^{o}$ reinforced fibre with liner), the required thickness of its PEEK liner to carry the maximum design tensile and burst loads would be 12 times higher than if the laminate was designed using the 3D FEA result, resulting in a tube that was three times heavier.

Further, the netting theory is based on thin-shell assumptions which no longer hold good for thick tubes in which variations in the circumferential lengths of their layers causes further variations in the stress distribution across their laminates. For accurate estimations of stresses in thick-walled tubes, it is necessary to conduct a 3D analysis, as in this study which uses 3D solid elements in ANSYS.

5.3. Finite Element (FE) Model

This section describes the FEA model employed for the local design of composite riser tubes to achieve a minimum weight using both the conventional design (only axial and hoop reinforcements) and manually tailored design proposed in this thesis which uses additional fibre reinforcements in other orientations.

For both design procedures, the stresses in the composite tubes are determined using 3D FE modelling with ANSYS 13.0. Since a composite cylinder wall is quite thick, the radii of its different layers vary considerably and, therefore, the ratio of its applied hoop stress to axial stress also varies appreciably from its inner to outer layers [110]. Because of the coupling between different layers and the thickness of the composite wall, 3D solid elements (Solid 186) are employed for both its liner and composite laminate in the FEA (see Fig. 5.5). More specifically, the composite laminate is modelled with layered solid elements and the liner with homogeneous isotropic solid elements, both Solid186 but with different material properties. The cylindrical tube is constrained in the axial direction at one end but free at the other while its rigid body motions are also constrained. In the fabrication of metal liners, often autofrettage is employed, a technique in which the tube is subjected to an enormous internal pressure which causes its internal portions to yield and results in internal compressive residual stresses in the inner layers which increase the durability of the metallic liner as well as its resistance to stress corrosion cracking. However, the effect of autofretting is not considered in this thesis.

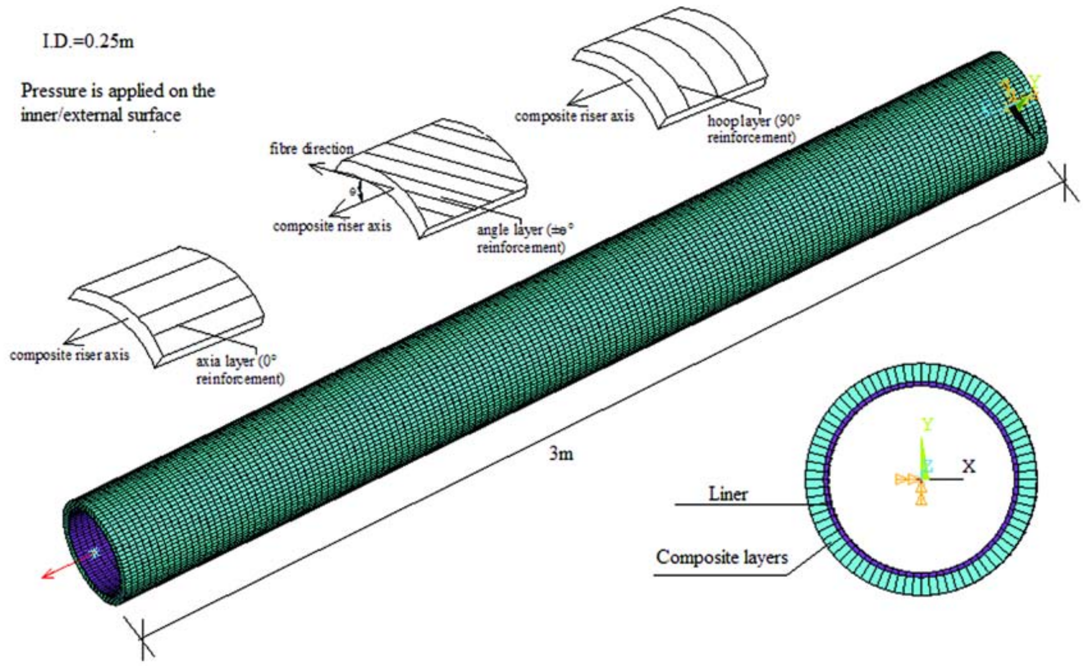

Fig. 5.5. FEA model of composite tube and coordinate system

Based on convergence studies, eighty elements are employed in the circumferential direction and fifty elements per metre in the axial direction. The length (3m for stress analysis and 5m for buckling analysis) and inner diameter (0.25m) of the tube are fixed with its outer diameter dependent on the thickness selected. Essentially, the design process consists of conducting stress and buckling analyses in ANSYS for the four local load cases, which have different thicknesses of their composite laminates and liners, and determining their factors of safety (FSs). In cases in which the design is determined in terms of stresses so is the FS, except in the buckling case where it is defined in terms of the buckling pressure. The two definitions of the FS employed in the analysis are

$$Factor\ of\ Safety\ (local\ load\ cases\ 1\ to\ 3) = \frac{allowance\ strength}{actural\ stress} \quad (5\text{-}4)$$

$$Factor\ of\ Safety\ (local\ load\ case\ 4 - bukcling) = \frac{allowable\ buckling\ pressure}{design\ buckling\ pressure} \quad (5\text{-}5)$$

The iterative procedure for selecting the thickness and fibre orientation values in order to arrive at a minimum weight by bringing the minimum FS to 1.0 or just above is described in the next section.

First ply failure using the maximum stress failure criterion is employed in the local design procedure to ensure that the FSs for the stresses in all the plies remain above 1.0.

In the linear value buckling analysis under external pressure, it is found that, while short cylinders have higher critical pressures, as the length of the cylinder increases, the critical pressure asymptotes to a constant value [111, 112]. The length of the FEA model of the tube for an eigenvalue buckling analysis is determined by convergence analysis to this asymptotic value. The geometries of risers made from AS4/PEEK with PEEK liner with [0/90] and [0/±52/90] reinforcements are used (see Fig. 5.6) to examine the influence of length on the critical buckling pressure (B.P.) and a length of 5m, which is sufficient to estimate the minimum buckling pressure, is obtained.

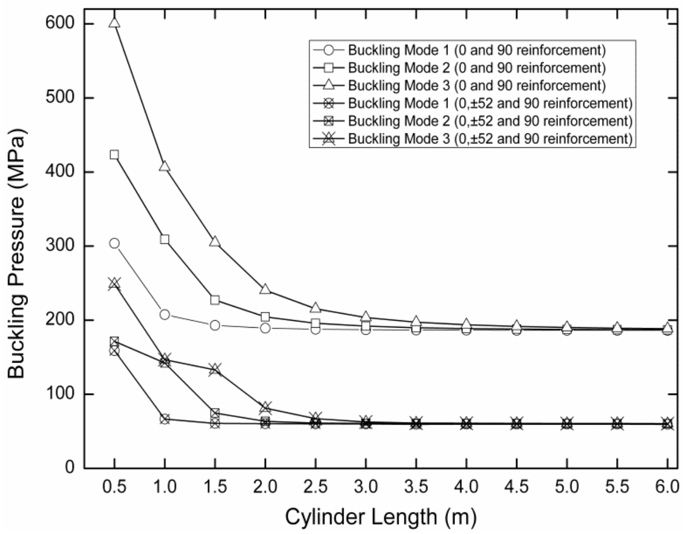

Fig. 5.6 Variations in buckling pressure with cylinder length

The stresses in the different composite layers and liner under the burst case for an AS4/PEEK body with PEEK liner are also determined using the exact elastic solution given by M. Xia et al. [110] based on 3D anisotropic elasticity, the theoretical equations for which are provided in *Appendix A*. The stresses from the FEA simulation are compared with those from the exact elastic solution [110] for the geometries obtained from the conventional and tailored design procedures and illustrated in Fig. 5.7 and Fig. 5.8, respectively.

For the conventional design geometry, under a 155.25MPa internal pressure, the Von Mises stress in the PEEK liner is 99.7MPa using FEA simulation and 98.9MPa using the analytical method, a 0.8% difference. As can be seen in Fig. 5.7, the FEA simulation usually offers slightly higher stress distributions in the composite laminate but differences in their stresses in the fibre and transverse directions are less than 5% and less than 10%, respectively.

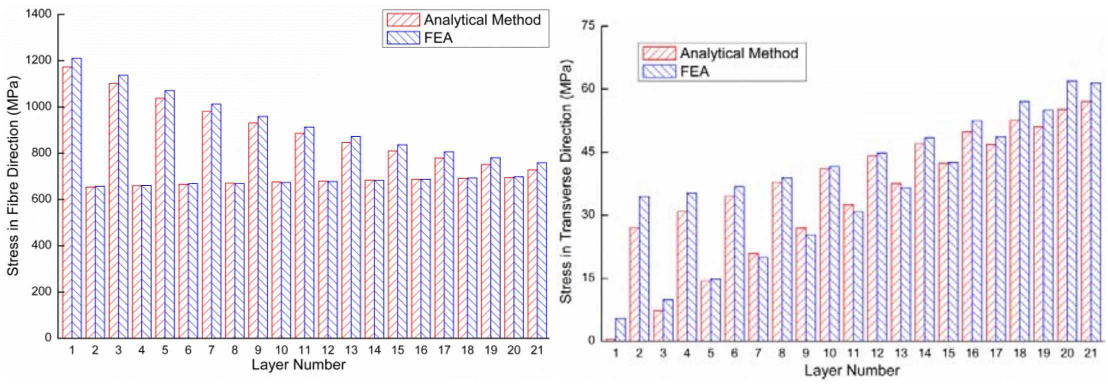

(a) (b)

Fig. 5.7. Stress comparisons of composite layers with 0° and 90° reinforcements under burst case for AS4/PEEK with PEEK liner in (a) fibre direction and (b) transverse direction

For the tailored design geometry, under a 155.25MPa internal pressure, the Von Mises stress in the PEEK liner is 115.9MPa using FEA simulation and 115.8MPa using the analytical method, a 0.1% difference. As can be seen in Fig. 5.8, differences in the composite laminate's stresses in their fibre and transverse directions are less than 1% and less than 8%, respectively, and in their in-plane shears less than 0.5%.

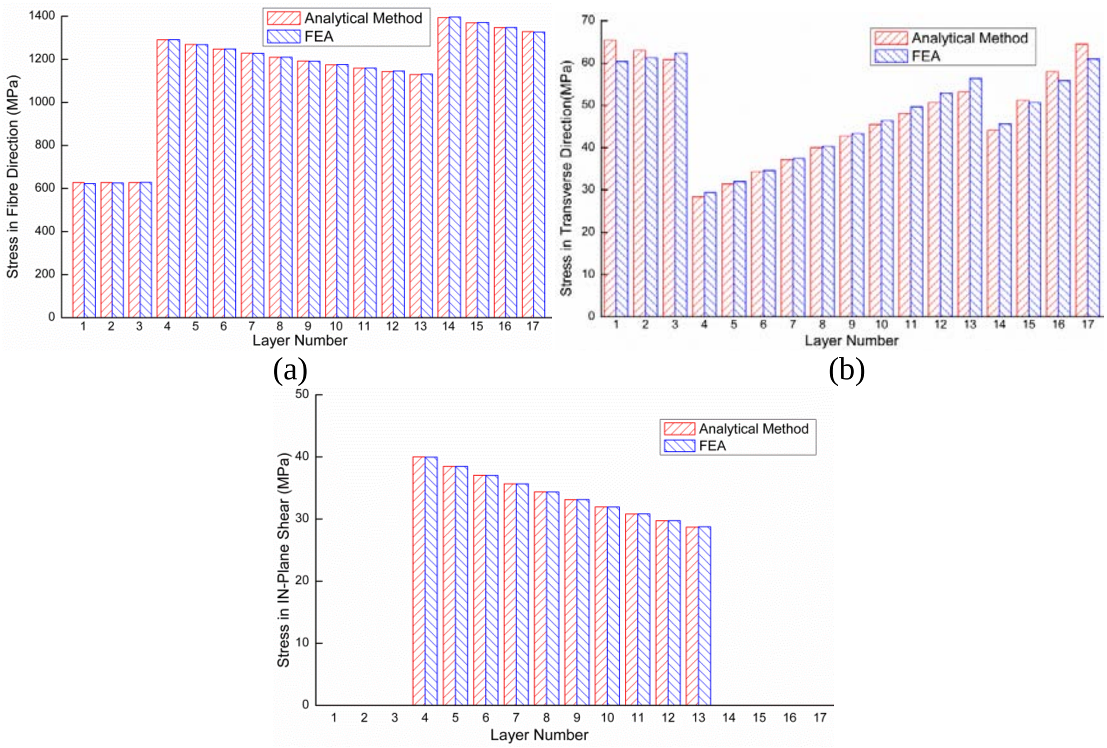

(a) (b) (c)

Fig. 5.8. Stress comparisons of composite layers with 0°, ±52° and 90° reinforcements under burst case for AS4/PEEK with PEEK liner in (a) fibre direction, (b) transverse direction and (c) in-plane shear

This comparison evidences agreement between the exact elastic solution [110] and FE simulation which confirms the accuracy of the stress analysis using FEA simulation.

5.4 Procedures for Local Design

Two design procedures are developed for the local design of the tubes of a composite riser: the conventional ‘orthogonal’ design in which the laminate has reinforcements in only the axial and hoop directions; and the tailored design in which reinforcements in the axial, hoop and other orientations are considered. In this study, all eight different material system combinations (Table 3.15 in *Chapter 3*) are designed using both procedures to determine the optimum geometries for achieving minimum weight. In the case of the tailored design, the geometry consists of the ply orientations, stacking sequences and composite layer and liner thicknesses. For the conventional design, the same parameters are determined, except that the ply orientations (0 and 90 degrees) are already known.

In both procedures, first ply failure using the maximum stress failure criterion [83] is applied to determine the minimum ply thickness required and, thus, the minimum laminate thickness, for which the normal stresses in the fibre and transverse directions and in-plane shear stress are compared with the longitudinal, transverse and shear strengths of the lamina. An eigenvalue buckling analysis is also conducted using the FE model to determine the buckling pressure for the configuration under investigation. An iterative procedure is employed to vary the liner and composite layer thicknesses, fibre orientations and stacking sequences until a minimum FS of just above 1.0 is achieved for all layers of the composite for load cases 1 to 3, and for buckling of the cylinder under external pressure (load case 4), which gives the minimum weight required for each configuration considered for each type of design.

5.4.1 Conventional Design Procedure

In the conventional 'orthogonal' design, the fibre reinforcements are in only the axial and hoop directions. A flowchart of the conventional design is shown in Fig. 5.9.

- *Step 1:* The design conditions and combinations of materials (for the reinforcement fibres, matrix and liner) are selected.
- *Step 2:* Initial estimates of the thicknesses required for the layers reinforced in the axial and hoop directions are made based on the membrane theory for the design burst pressure with end effects, assuming that the axial stress is carried by the axially reinforced layers and the hoop stress by the circumferentially reinforced ones, as in the netting theory.
- *Step 3:* Using the initial estimates of the thicknesses of the composite layers and a guessed value for the liner thickness, a 3D FEA of the model is conducted for only

the burst case to obtain the FS in each layer to determine whether the thicknesses of the layers – in the axial or hoop direction – should be increased (if the FS is less than 1) or reduced (if the safety margin is too high). At the end of this step, the thicknesses of the axial and hoop layers are optimised for the burst condition for the liner thickness chosen.

- *Step 4:* The process in *Step 3* is repeated for different values of the liner thickness and that which gives the minimum overall structural weight is selected.
- *Step 5:* A similar process to that in *Step 4* is repeated but all four load cases are considered. At the end of this process, the minimum thicknesses of the axial and hoop-reinforced layers and liner required to satisfy all load cases are obtained.

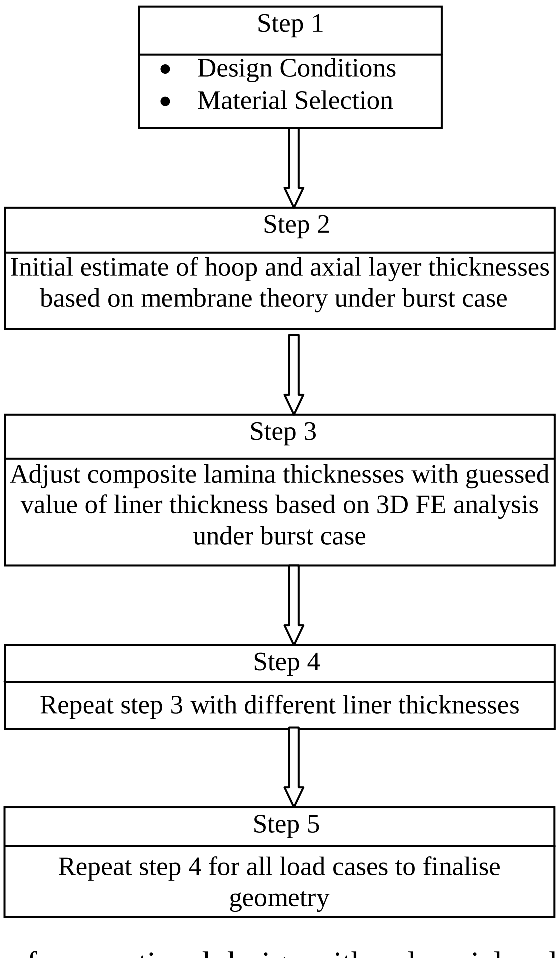

Fig. 5.9. Flowchart of conventional design with only axial and hoop reinforcements

5.4.2 Tailored Design Procedure

The design variables for the tailored design include the thicknesses of the liner and composite layers, and the fibre orientations and stacking sequences of the composite laminate. A flowchart of the tailored design is shown schematically in Fig. 5.10.

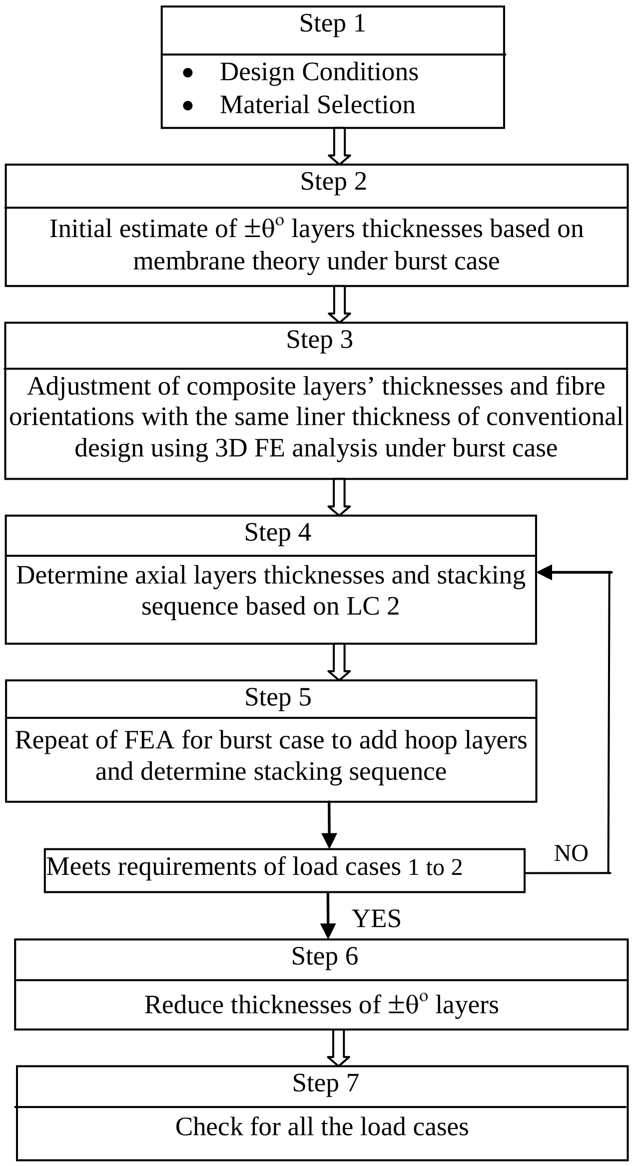

Fig. 5.10. Flowchart of proposed tailored design including angle reinforcements

- *Step 1:* The design conditions and combinations of materials (for the fibre reinforcement, matrix and liner) are selected.
- *Step 2:* The initial optimum angle of reinforcement $\pm\theta^o$ and the layer thicknesses are estimated based on the burst capacity using the membrane theory.
- *Step 3:* This step is similar to that of the conventional design except that the stresses from the FEA are employed to re-estimate the thicknesses and fibre orientations of the layers in the $\pm\theta^o$ directions required to avoid failure using the same liner thickness as determined by the conventional design.
- *Step 4*: The tension load cases are employed to add axially reinforced layers to the angle ply laminate designed in *Step 3* to withstand axial loads.
- *Step 5:* The burst case is analysed again to determine the thicknesses of the hoop-reinforced layers required to reduce the in-plane transverse stresses in the axial-reinforced layers which are susceptible to transverse failure under burst pressure due to their low transverse strengths.

It is necessary to perform several iterations of *Steps 4* and *5* to converge on the minimum thicknesses of the 0^o and 90^o layers to be added.

- *Step 6:* The additional layers with hoop and axially reinforcements permit reductions in the number of angle plies.

Several iterations of *Steps 3* to *6* are conducted to home in on the optimum thicknesses of the axial, hoop and angle plies required to withstand both the design burst and design tension loads. In this iterative loop, variations in the stacking sequence of the laminate are also examined to determine the best combination of it and thicknesses of the plies to provide the least weight under these load cases.

- *Step 7:* The design is checked for all load cases and the thicknesses of the plies increased if required.

5.5 Results for AS4/PEEK with PEEK Liner using Conventional Design

Table 5.2 gives the geometry of the composite riser tube optimised for minimum thickness using the conventional design under the local load cases, which yields a 21-ply composite laminate [90/(0/90)$_{10}$] with alternating hoop and axially reinforced layers of 1.85 and 1.165mm thicknesses, respectively, which results in a total laminate thickness of 32mm, with a 6mm PEEK liner and structural weight of 52.4kg/m.

Table 5.2. Geometry of AS4/PEEK with PEEK liner riser with orthogonal reinforcements

Layer no.	Ply orientation (degrees)	Thickness (mm)	Layer no.	Ply orientation (degrees)	Thickness (mm)
liner		6	11	90	1.850
1	90 (hoop)	1.850	12	0	1.165
2	0 (axial)	1.165	13	90	1.850
3	90	1.850	14	0	1.165
4	0	1.165	15	90	1.850
5	90	1.850	16	0	1.165
6	0	1.165	17	90	1.850
7	90	1.850	18	0	1.165
8	0	1.165	19	90	1.850
9	90	1.850	20	0	1.165
10	0	1.165	21	90	1.850
Total thickness: 38mm and structural weight: 52.4kg/m					

5.5.1 Results for AS4/PEEK with PEEK Liner [90/(0/90)$_{10}$] under Burst Case

The design internal burst pressure for the composite riser is 155.25MPa under which the Von Mises stress in the PEEK liner is 99.7MPa and FS=1.20. Figs. 5.11(a) and 5.11(b), respectively, show the FSs in the fibre and transverse directions under load case 1 (burst load) for all the layers in the conventional design geometry. The minimum FS in the fibre direction is 1.36 (layer 1 in Fig. 5.11(a)) while that in the transverse direction is 1.00 (layers 20 and 21 in Fig. 5.11(b)). It is evident that, under the burst case, the in-plane transverse stresses are the most critical stresses and determine the minimum thickness of the composite AS4/PEEK body with only 0^o and 90^o reinforcements.

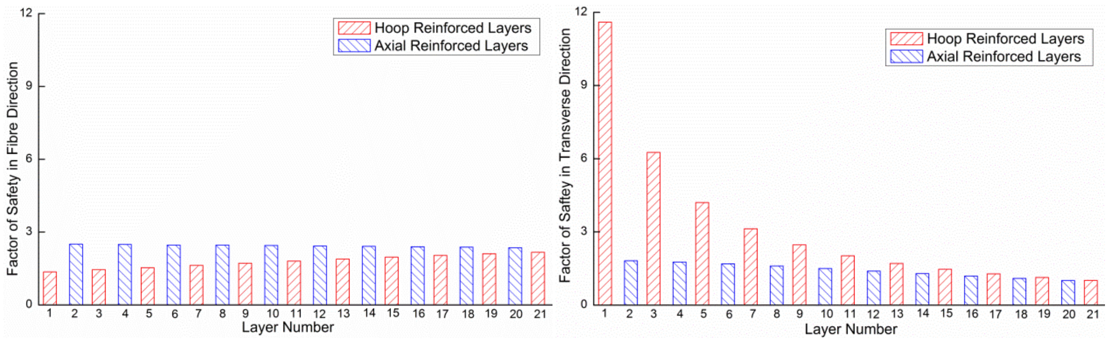

(a) (b)

Fig. 5.11. FSs for composite layers with 0° and 90^{o} reinforcements for load case 1 for AS4/PEEK with PEEK liner in (a) fibre direction and (b) transverse direction

5.5.2 Results for AS4/PEEK with PEEK Liner [90/(0/90)$_{10}$] under Pure Tension Case

As described in *Chapter 3*, the tension force has to be calculated using three different cases which yield values of 2450kN, 1270kN and 2455kN, respectively. Therefore, the design tension force is taken to be 2455×2.25=5525kN.

Under a 5525kN pure tension, the Von Mises stress in the PEEK liner is 13.0MPa, providing FS=9.23. Figs. 5.12(a) and 5.12(b) show the FSs in every layer under load case 2(a) (pure tension) for the conventional design. As can be seen, they are quite large which indicates that this load case is not as critical as the burst case for this material combination (the FSs for stresses in the fibre direction of the hoop-reinforced layers in Fig. 5.12(a) are well above 30 since loading is mainly in the axial direction).

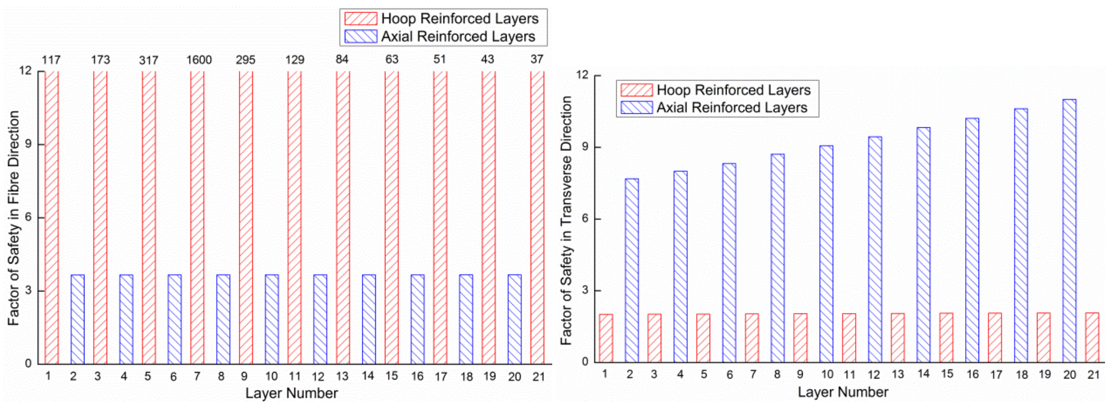

(a) (b)

Fig. 5.12. FSs for composite layers with 0° and 90° reinforcements for load case 2(a) for AS4/PEEK with PEEK liner in (a) fibre direction and (b) transverse direction

5.5.3 Results for AS4/PEEK with PEEK Liner [90/(0/90)$_{10}$] under Tension with External Pressure Case

The tension force for load case 2(b) (tension with an external pressure of 19.5MPa) is also 5525kN and the Von Mises stress in the PEEK liner is 12.9MPa, providing FS=9.30. Fig. 5.13 shows its FSs under load case 2(b) for the conventional design with the minimum being 2.2 in the transverse direction in layer 1 (Fig. 5.13(b)).

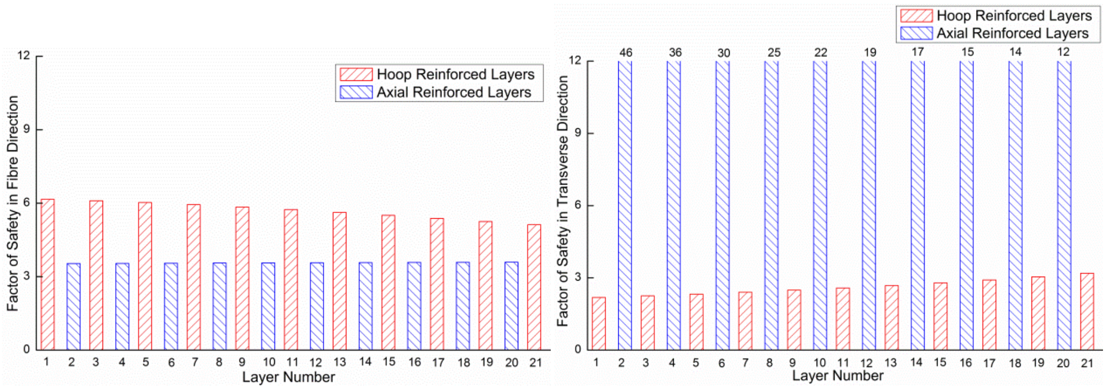

(a) (b)

Fig. 5.13. FSs for composite layers with 0° and 90° reinforcements for load case 2(b) for AS4/PEEK with PEEK liner in (a) fibre direction and (b) transverse direction

5.5.4 Results for AS4/PEEK with PEEK Liner [90/(0/90)$_{10}$] under Collapse Case

The design collapse pressure for the composite riser is 58.5MPa under which the Von Mises stress in the PEEK liner is 13.4MPa, providing FS=8.95. Fig. 5.14 shows the FSs under load case 3 (collapse load) for the conventional design, with the minimum being 1.9 in the fibre direction in layer 1 (Fig. 5.14(a)).

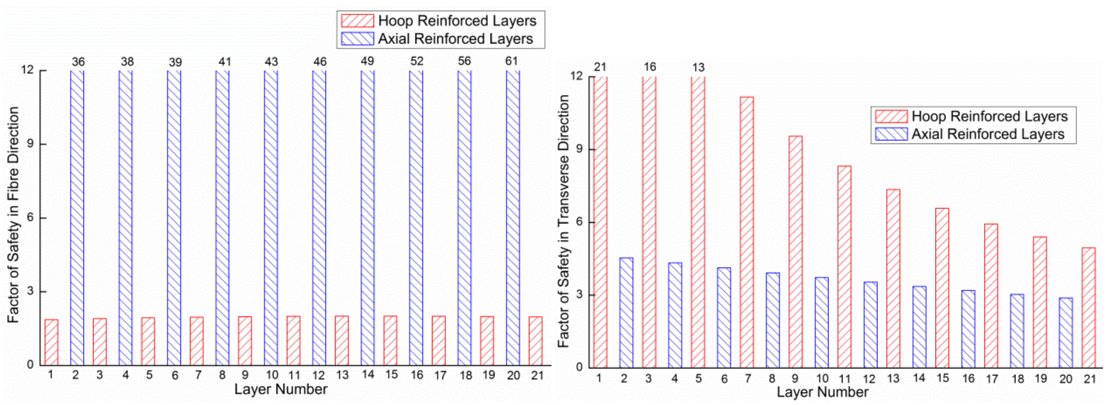

(a) (b)

Fig. 5.14. FSs for composite layers with 0° and 90° reinforcements for load case 3 for AS4/PEEK with PEEK liner in (a) fibre direction and (b) transverse direction

5.5.5 Results for AS4/PEEK with PEEK Liner [90/(0/90)$_{10}$] under Buckling Case

The geometry of the AS4/PEEK with PEEK liner riser using the conventional design is also checked for buckling under external pressure (load case 4) and the critical buckling pressure obtained is 186.4MPa (mode 1) which is much higher than the design buckling pressure of 58.5MPa. The first three mode shapes can be seen in Fig. 5.15 in which the number of circumferential waves is 2 for all three modes and the number of half-waves along the axial direction 1, 2 and 3 for modes 1, 2 and 3, respectively.

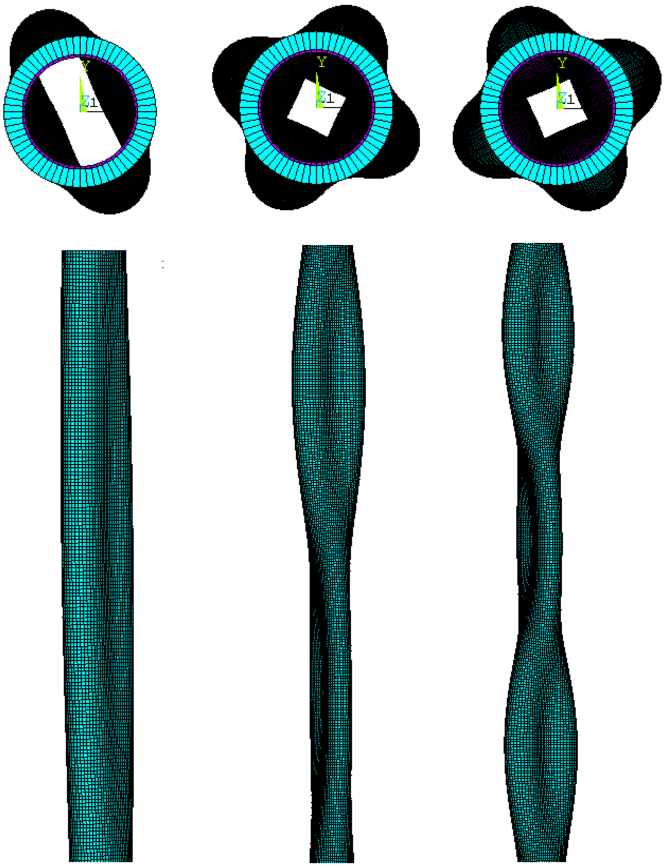

(a) B.P.=186.4MPa (b) B.P.=187.5MPa (c) B.P.=190.1MPa

Fig. 5.15. Mode shapes of composite riser with 0° and 90° reinforcements for AS4/PEEK with PEEK liner (5m): (a) mode 1 (b) mode 2 and (c) mode 3

5.6 Results for AS4/PEEK with PEEK Liner using Tailored Design

Following the tailored design procedure, the effects of fibre orientations and stacking sequences on the structural weight are determined and presented in Figs. 5.16 and 5.17, respectively. In step 2 of the manually tailored local design of the composite riser, for the burst case (without a liner), the best fibre orientation is 54.7° and the minimum thickness 17.7mm according to the netting theory and 51° and 24.2mm according to the CLT theory. These best reinforcement angles have to be verified in step 3 of the design procedure using 3D FEA simulation under the burst case with the same liner thickness obtained by the conventional design results (6mm) and, in the FEA model, the geometry of $[\pm\theta]_5$ with 24.2mm of laminate and 6mm of liner is employed. Variations in the minimum FSs in the fibre direction, in-plane transverse direction and in-plane shear of the composite laminate are illustrated in Fig. 5.16.

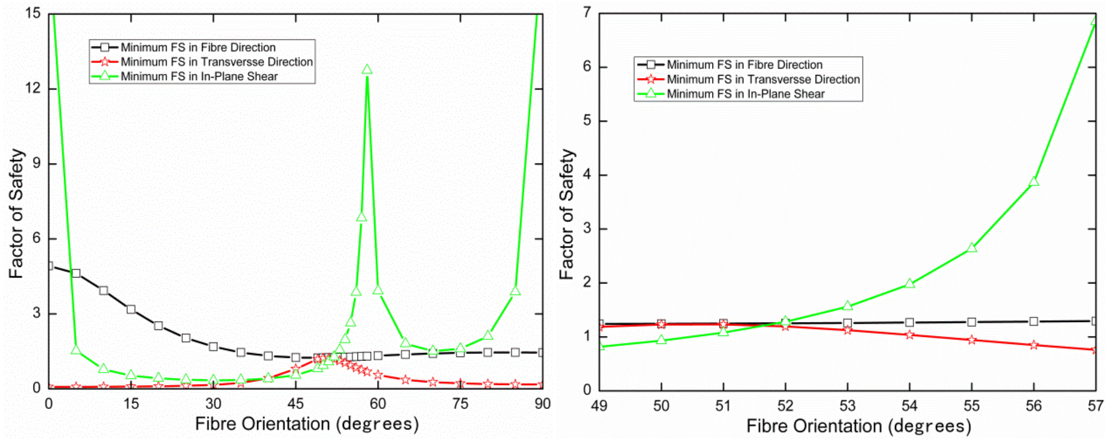

Fig. 5.16. Variations in FS with fibre orientation for burst capacity: (a) full range of angles and (b) magnified view

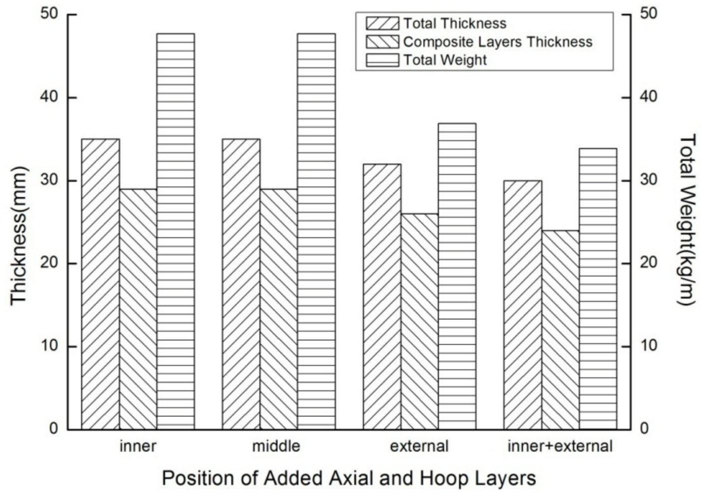

Fig. 5.17. Influence of stacking sequences on thickness and weight

Similarly, the effect of the stacking sequences on the weight and thickness is illustrated in Fig. 5.17. The four typical locations at which additional axial and hoop reinforcements are provided to the ±θ layers are: (1) innermost layer, (2) middle of the $\pm\theta^o$ layers, (3) outermost layer and (4) axial reinforcements in the innermost layer with hoop reinforcements added in the outermost layer.

It can be seen in Figs. 5.16 and 5.17 that $\pm52^o$ is the most efficient angle for taking full advantage of the reinforcement strengths in every direction under the burst case. The stacking sequence with $\pm52^o$ reinforced layers between its axial (innermost) and hoop (outermost) layers provides the lowest total thickness and, therefore, the lowest structural weight.

Table 5.3 gives the geometry of the composite riser tube optimised for minimum thickness using the manually tailored design.

Table 5.3. Geometry of AS4/PEEK with PEEK liner riser, including angle reinforcements

Layer no.	Ply orientation (degrees)	Thickness(mm)	Layer no.	Ply orientation (degrees)	Thickness(mm)
liner		6	9	-52	1.30
1	0 (axial)	1.48	10	52	1.30
2	0	1.48	11	-52	1.30
3	0	1.48	12	52	1.30
4	52	1.30	13	-52	1.30
5	-52	1.30	14	90 (hoop)	1.64
6	52	1.30	15	90	1.64
7	-52	1.30	16	90	1.64
8	52	1.30	17	90	1.64
Total thickness: 30mm and structural weight: 39.9kg/m					

The tailored design, including the angle plies, provides a 17-layer composite laminate $[0_3/(+52,-52)_5/90_4]$ with the 0^o, $\pm52^o$ and 90^o having thicknesses of 1.48, 1.30 and 1.64mm, respectively. The total laminate thickness for the design, including the angle plies, is only 24mm, with same 6mm thickness of the PEEK liner. It is also to be noted that the optimum angle of reinforcement for the angle plies is obtained as $\pm52^o$ using the 3D FEA, not $\pm54.7^o$ as predicted by the netting theory. If a $\pm54.7^o$ reinforcement is employed, the required thickness of each of the 10 angle plies would be 1.5mm instead of 1.3mm and result in a total laminate thickness of 26mm instead of the 24mm obtained with ±52°.

5.6.1 Results for AS4/PEEK with PEEK Liner $[0_3/(\pm 52)_5/90_4]$ under Burst Case

The design internal burst pressure for this composite riser is 155.25MPa under which the Von Mises stress in the PEEK liner is 115.9MPa, providing FS=1.03. Figs. 5.18(a), 5.18(b) and 5.18(c), respectively, show the FSs in the fibre and transverse directions and in-plane shear for all the layers under load case 1 (burst load) for the manually tailored design with additional angle plies and considering different stacking sequences. The minimum FSs are 1.18 in the fibre direction (layer 14 in Fig. 5.18(a)), 1.00 in the transverse direction (layer 3 in Fig. 5.18(b)) and about 3.00 in in-plane shear (layer 4 in Fig. 5.18(c)). In this case, the in-plane transverse stresses are the most critical stresses and determine the thicknesses of the composite layers.

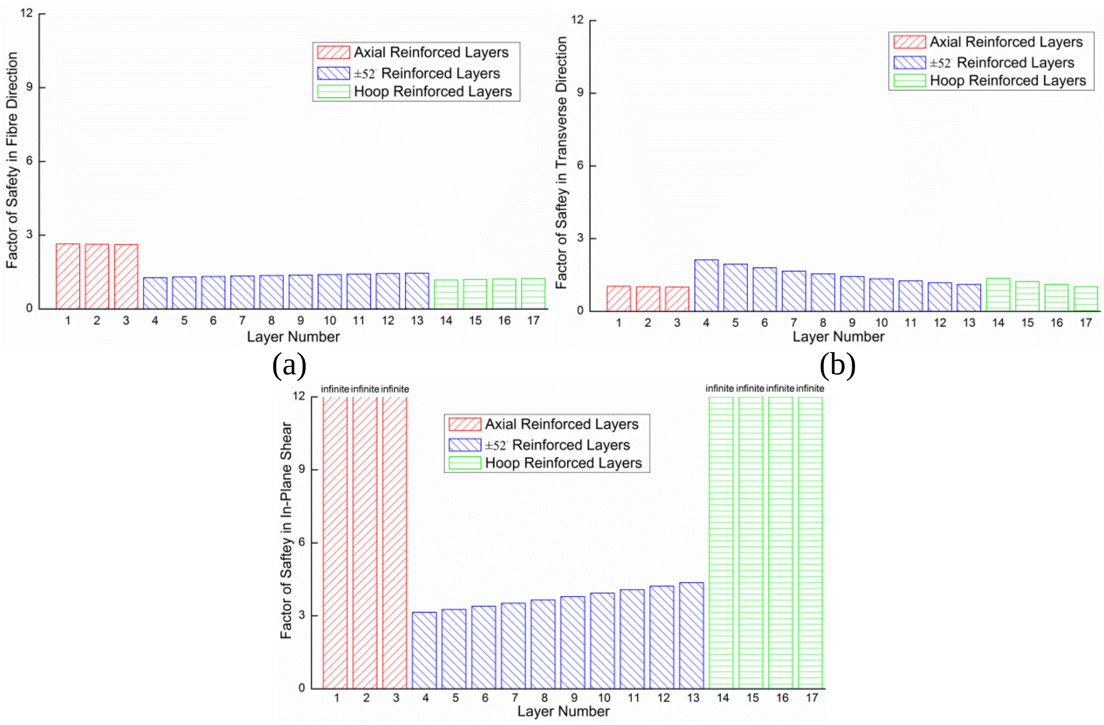

Fig. 5.18. FSs for composite layers with 0°, ±52° and 90° reinforcements for load case 1 for AS4/PEEK with PEEK liner in (a) fibre direction, (b) transverse direction and (c) in-plane shear

5.6.2 Results for AS4/PEEK with PEEK Liner $[0_3/(\pm 52)_5/90_4]$ under Pure Tension Case

As described in *Chapter 3*, the tension force has to be calculated using three different cases which yield values of 2340kN, 1100kN and 2200kN, respectively. Therefore, the design tension force is taken to be 2340×2.25=5265kN.

Under a pure tension (5265kN), the Von Mises stress in the PEEK liner is 23.5MPa, providing FS=5.11. Figs. 5.19(a), 5.19(b) and 5.19(c) show the FSs in all the layers under load case 2(a) (pure tension) for the manually tailored design. In this case, while the other FSs are relatively high, the minimum FS is about 1.1 in the transverse direction of the hoop layers (layer 14, Fig. 5.19(b)).

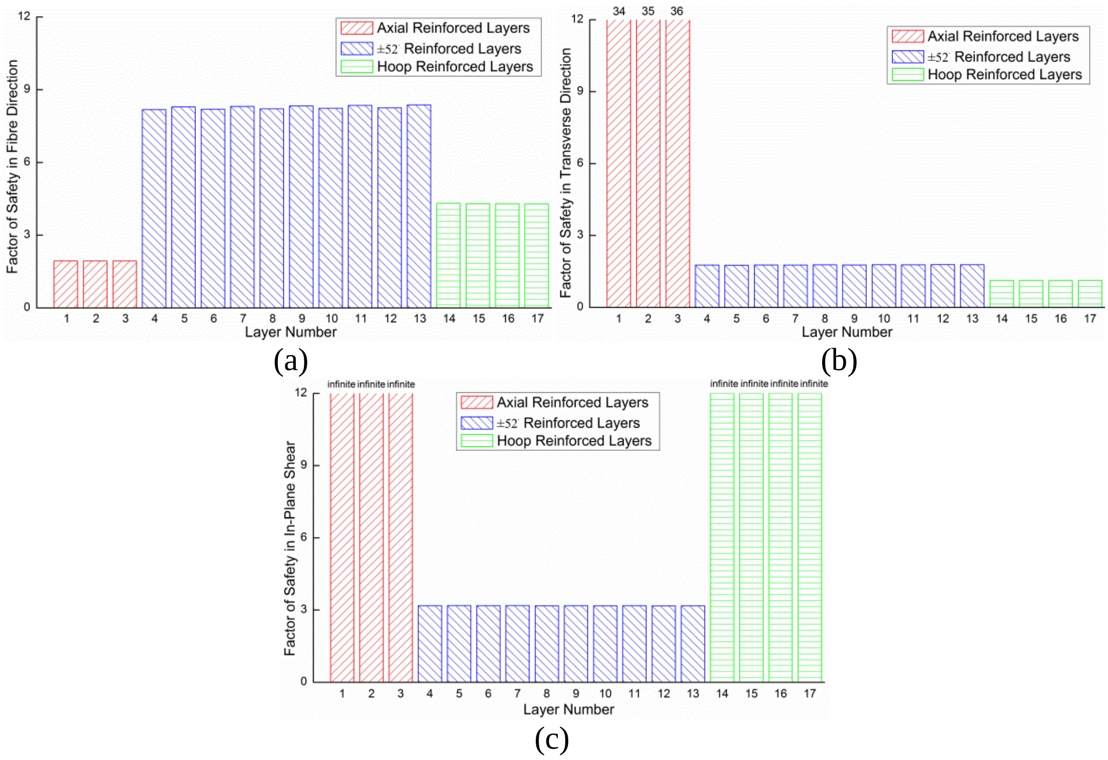

Fig. 5.19. FSs for composite layers with 0°, ±52° and 90° reinforcements for load case 2(a) for AS4/PEEK with PEEK liner in (a) fibre direction, (b) transverse direction and (c) in-plane shear

5.6.3 Results for AS4/PEEK with PEEK Liner [0_3/($\pm$52)$_5$/90_4] under Tension with External Pressure Case

The tension force under load case 2(b) (tension with an external pressure of 19.5MPa) is the same as that for load case 2(a), that is, 5265kN, and the Von Mises stress in the PEEK liner is 27.7MPa, providing FS=4.33. Fig. 5.20 shows the FSs under load case 2(b) for the manually tailored design with the minimum being 1.16 in the transverse direction in layer 14 (Fig. 5.20(b)).

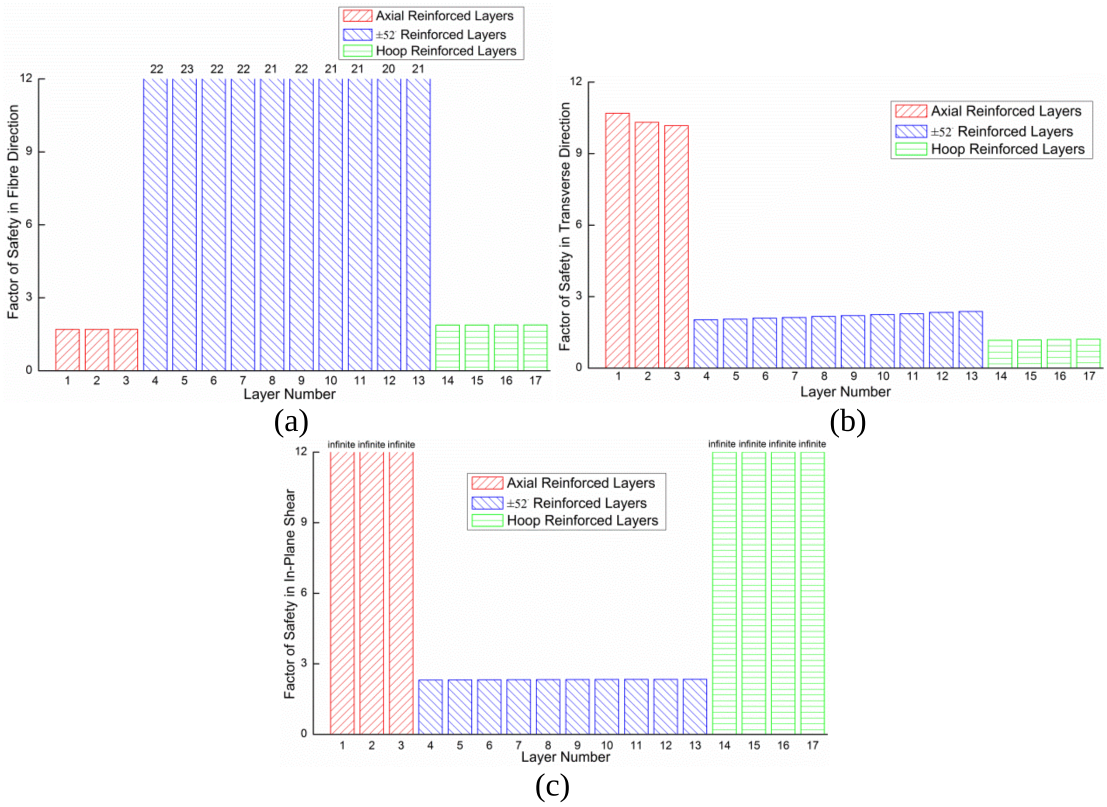

Fig. 5.20. FSs for composite layers with 0°, ±52° and 90° reinforcements for load case 2(b) for AS4/PEEK with PEEK liner in (a) fibre direction, (b) transverse direction and (c) in-plane shear

5.6.4 Results for AS4/PEEK with PEEK Liner [0_3/($\pm$52)$_5$/90_4] under Collapse Case

The design collapse pressure for the composite riser is 58.5MPa and, under this external over-pressure, the Von Mises stress in the PEEK liner is 25.2MPa, providing FS=4.76. Fig. 5.21 shows the FSs under load case 3 (collapse load) for the manually tailored design with the minimum being 1.1 in the fibre direction in layer 14 (Fig. 5.21(a)).

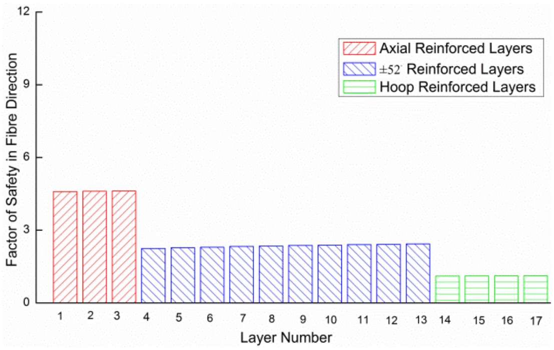

(a)

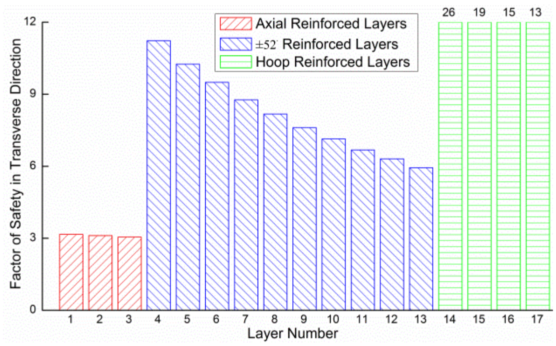

(b)

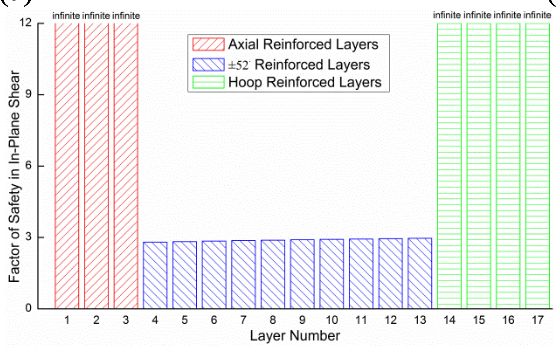

(c)

Fig. 5.21. FSs for composite layers with 0°, ±52° and 90° reinforcements for load case 3 for AS4/PEEK with PEEK liner in (a) fibre direction, (b) transverse direction and (c) in-plane shear

5.6.5 Results for AS4/PEEK with PEEK Liner $[0_3/(\pm 52)_5/90_4]$ under Buckling Case

The geometry of the AS4/PEEK with PEEK liner riser using the tailored design is also checked for buckling under external pressure (load case 4). The critical buckling pressure obtained is 59.6MPa (mode 1) which is only slightly higher than the design buckling pressure of 58.5MPa. The first three mode shapes are shown in Fig. 5.22 in which it can be seen that the number of circumferential waves is 2 for all three modes and the number of half-waves along the axial direction 2, 3 and 2 for modes 1, 2 and 3, respectively.

(a) B.P.=59.6MPa (b) B.P.=60.3MPa (c) B.P.=60.6MPa
Fig. 5.22. Mode shapes of composite riser with 0°, ±52° and 90° reinforcements for AS4/PEEK with PEEK liner (5m): (a) mode 1, (b) mode 2 and (c) mode 3

5.7 Comparison of Conventional and Tailored Designs for AS4/PEEK with PEEK Liner Riser

The conventional design yields a 21-ply composite laminate $[90/(0/90)_{10}]$ with alternating hoop and axially reinforced layers which results in a total thickness of 38mm and structural weight of 52.4kg/m. The tailored design, including the angle plies, provides a 17-layer composite laminate $[0_3\ /(+52,-52)_5\ /90_4]$ with a total thickness of 30mm and structural weight of 39.9kg/m. The manually tailored design provides a total thickness saving of 21% and structural weight reduction of 24%.

It may be noted that, for the burst case, the minimum FS in the transverse direction is close to 1.0 for both the conventional and tailored designs, while their FSs in the fibre direction are well above 1.0. Thus, for the AS4/PEEK with PEEK liner, matrix cracking is the most critical failure mode and dictates the design. However, for other material combinations, such as the P75/PEEK with PEEK liner discussed in the next section, fibre failure can be the most critical failure mode.

5.8 Tailored Design Results for P75/PEEK with PEEK Liner for Burst Case

In the case of the AS4/PEEK composite body with PEEK liner described in the foregoing section, the critical factor in design is matrix cracking in the transverse direction. However, with a high-modulus (and low-strength) P75 fibre reinforcement, fibre failure becomes the critical factor. To illustrate this, the results for the tailored design of the P75/PEEK composite body with PEEK liner under load case 1 (the burst case) are presented here. According to the tailored design process presented in Fig. 5.10, the P75/PEEK with PEEK liner offers the geometry of a composite riser tube with a 43-layer composite laminate with $[0_9\ /(+55.5,-55.5)_2\ /90_{10}\ /(+55.5,-55.5)_{10}]$. Its total laminate thickness is 86mm with a 6mm thick liner which provides a 26.1% structural weight saving over the conventional design. Here, only the FSs under load case 1 (burst load) for the manually tailored design are presented (the results under other load cases are presented in *Appendix B*). Under a 155.25MPa design internal pressure, the FS of the PEEK liner is 1.59, and Figs. 5.23(a), (b) and (c) show those of the P75/PEEK composite body with PEEK liner in the fibre and transverse directions and in-plane shear, respectively, for all its layers. The minimum FS is 1.00 in the fibre direction (layer 10 in Fig. 5.23(a)) while the minimum in the transverse direction (layer 10 in Fig. 5.23(b)) is 1.85 and in in-plane shear (layer 10 in Fig. 5.23(c)) about 9.1. In this case, the stresses in the fibre direction are the most critical for defining the failure mode and determining the thickness of the composite layers. Detailed results for the other load cases for the P75/PEEK body with PEEK liner using the tailored design and all load cases using the conventional design are presented in *Appendix B.*

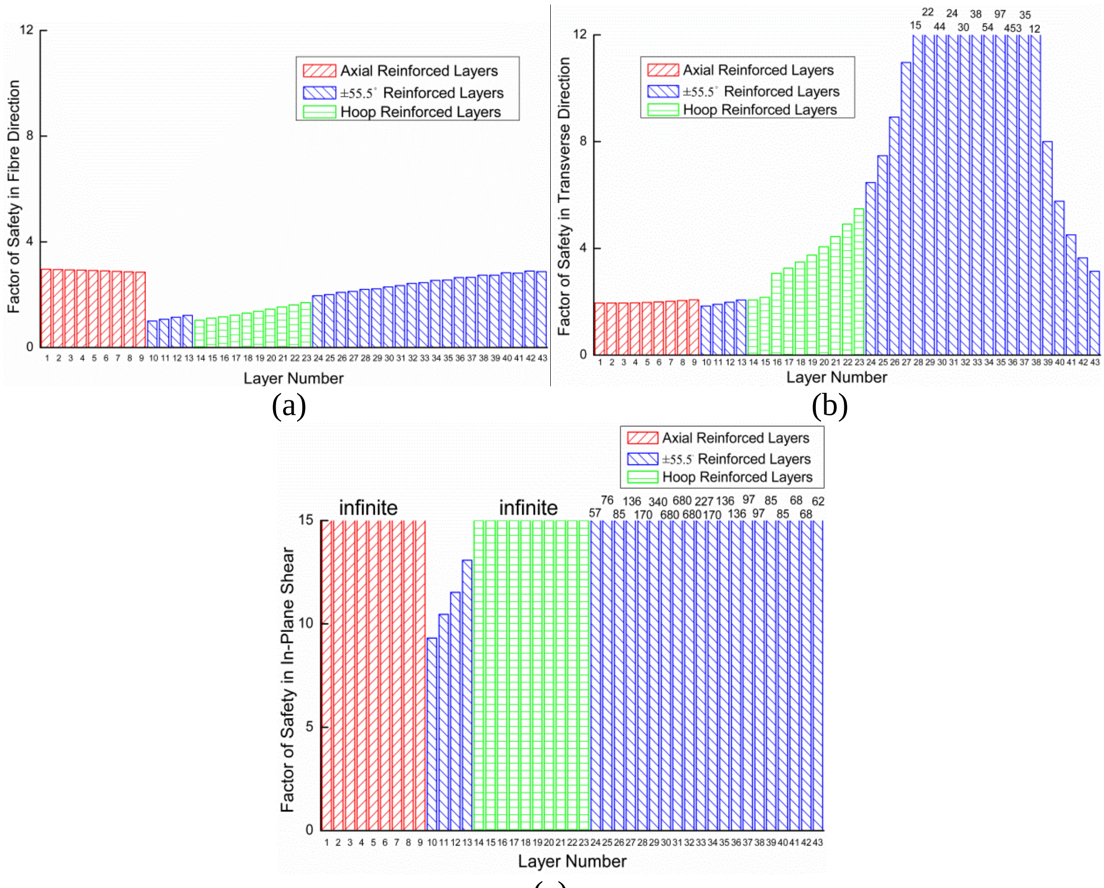

Fig. 5.23. FSs for composite layers with 0°, ±55.5° and 90° reinforcements for load case 1 for P75/PEEK with PEEK liner in (a) fibre direction, (b) transverse direction and (c) in-plane shear

5.9 Conventional and Tailored Design Results for Remaining Material Combinations

Detailed results for all the conventional and manually tailored designs under all the local load cases for the remaining six material combinations listed in Table 3.15 in *Chapter 3* are presented in *Appendix B.*

5.10 Comparisons and Discussion

5.10.1 Comparison of Structural Weights and Thicknesses

A comparison of the optimised structural weights for all the material combinations considered in this thesis (Table 3.15 in *Chapter 3*), normalised with the structural weight of a steel pipe with the same inner diameter as required to meet the same design requirements which is found to be 170kg/m in *Chapter 4*, is presented in Fig. 5.24.

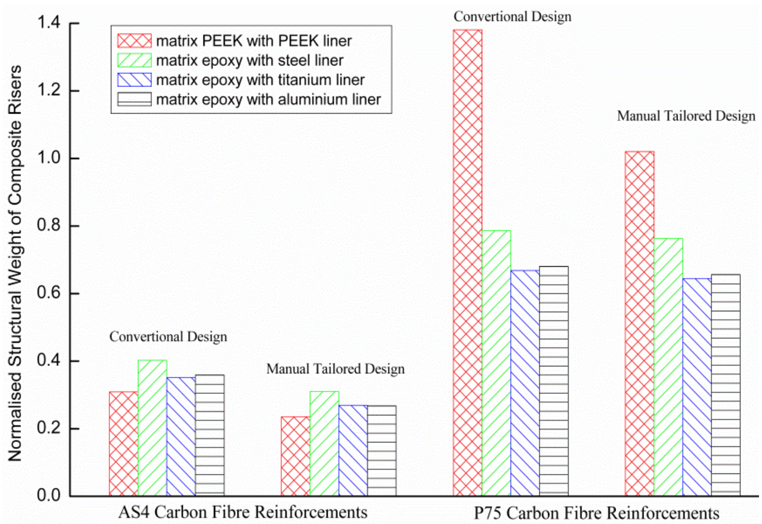

Fig. 5.24. Comparison of normalised structural weights

The first eight bars in Fig. 5.24 are for composite tubes reinforced with AS4 fibres while the last eight are for tubes reinforced with P75 carbon fibres. The first four in each group are the minimum structural weights obtained using the conventional design with only axial and circumferential reinforcements and the last four those obtained using the manually tailored design which includes angle ply reinforcements. The first bar in each group of four is for the composites with a PEEK matrix and PEEK liner while the other three are for the epoxy-based composites with liners of steel, titanium and aluminium alloy, respectively. From Fig. 5.24, it is apparent that all the composite risers, except the P75/PEEK composite with PEEK liner, offer substantial structural weight savings compared with the steel riser. In general, reinforcements with high-strength AS4 fibres are found to be much more beneficial than those with high-stiffness P75 fibres. While the P75/PEEK composites with PEEK liners are heavier than steel, the same composite pipes with metallic liners have structural weights lower than that of steel. On the other hand, when reinforced with AS4 fibres, the pipe with a thermoplastic liner has a lower weight than those with metallic liners. In fact, the AS4/PEEK composite pipe with PEEK liner has the least structural weight of all material combinations. It is also clear that, in every case, the manually tailored design with angle reinforcements included offers greater weight savings than the conventional design with only axial and circumferential reinforcements.

To complete the picture, Fig. 5.25 presents a comparison of the normalised effective weights of the composite riser tubes designed using both approaches for the eight material combinations.

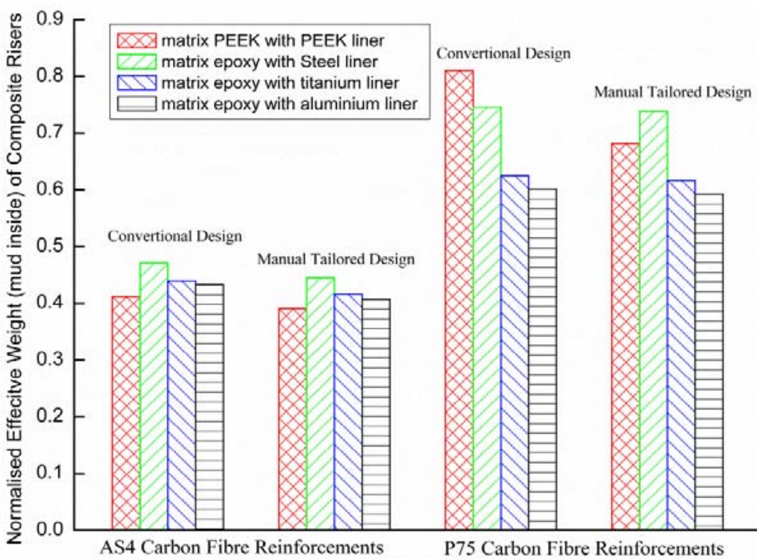

Fig. 5.25. Comparison of normalised effective weights

The effective weight considers the effect of the structural weight, buoyancy, weight of the internal fluids (mud inside) and added mass, such as connectors and fairings. It is seen that all the designs offer some effective weight savings compared with the steel riser, including the P75/PEEK with PEEK liner. When the effective weight is considered, the performances of conventionally designed composite tubes are comparable with those of manually tailored designed composite tubes with angle plies. The effect of improvements due to the introduction of angle plies on the effective weight becomes small because of the relatively high magnitudes of the weights of the mud inside, connectors and fairings compared with the structural weight of only the riser tube.

The penalty for savings in weight using a composite construction is an increase in the overall tubular thickness. Fig. 5.26 shows a comparison of the overall wall thicknesses of the eight material combinations designed using both procedures which are normalised with that of the steel riser.

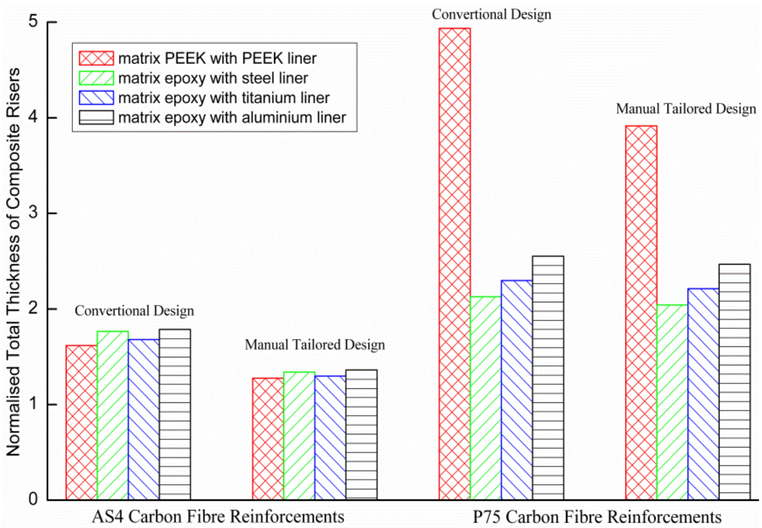

Fig. 5.26. Comparison of normalised thicknesses

As is evident in Fig. 5.26, the total wall thickness of each composite riser is higher than that of steel. Once again, the laminates reinforced with HM P75 carbon fibres fare much worse, with the P75/PEEK pipes with PEEK liners having thicknesses of four to five times that of steel. It is clear that the P75/PEEK composite with PEEK liner is the least desirable material combination as it has higher structural weights and significantly higher thicknesses than steel. Fig. 5.26 also shows that the manually tailored design with angle plies provides lower thickness in every case (which accounts for their lower weights in Fig. 5.24) compared with the conventional design. The AS4/PEEK with PEEK liner is once again the best performer, with the least thickness of all the configurations considered. The AS4/PEEK composite with angle reinforcements and PEEK liner has only a 20% greater overall thickness than steel and would be quite acceptable considering that it offers a 76% structural weight saving compared with a steel construction. The thickness of the tube with angle plies is about 21% lower than that obtained using the conventional design. A detailed comparison of the structural weights and thicknesses using different design procedures is presented in Table 5.4.

Table 5.4. Comparison of structural weights and thicknesses of optimised configurations with and without angle ply reinforcements

Material combination	Lay-up	Structural weight (kg/m)	Weight saving (%)	Thickness (mm)	Thickness saving (%)
AS4/PEEK with PEEK liner	$[90/(0/90)_{10}]$	52.4	23.9	38	21.1
	$[0_3/(\pm52)_5/90_4]$	39.9		30	
AS4/epoxy with steel liner	$[90/(0/90)_{10}]$	68.2	22.9	41.5	24.1
	$[0_3/(\pm53.5)_5/90_4]$	52.6		31.5	
AS4/epoxy with titanium liner	$[90/(0/90)_{10}]$	59.6	23.3	39.5	22.8
	$[0_3/(\pm53)_5/90_4]$	45.7		30.5	
AS4/epoxy with aluminium liner	$[90/(0/90)_{10}]$	60.9	25.5	42	23.8
	$[0_4/(\pm53.5)_5/90_4]$	45.4		32	
P75/PEEK with PEEK liner	$[0_{15}/90_{22}]$	234.2	26.1	116	20.7
	$[0_9/(\pm55.5)_2/90_{10}/(\pm55.5)_{10}]$	173.0		92	
P75/PEEK with steel liner	$[90_{16}/0_3]$	133.3	2.9	50	4.0
	$[\pm69/69/90_8/-69/(\pm69)_2/0_3]$	129.4		48	
P75/PEEK with titanium liner	$[90_{18}/0_3]$	113.3	3.5	54	3.7
	$[\pm66/90_8/(\pm66)_4/0_3]$	109.3		52	
P75/PEEK with aluminium liner	$[90_{14}/0_3]$	115.4	3.6	60	3.3
	$[65/90_5/-65/(\pm65)_3/0_3]$	111.3		58	

In the case of the AS4/PEEK composite body with PEEK liner, the conventional design gives a structural weight of 52.4kg/m while the manually tailored design including angle plies results in a normalised weight of only 39.9kg/m, that is, a weight saving of 24% over the conventional design using the same composite materials. For the AS4 composite riser with steel, titanium and aluminium liners, the structural weight savings using the manually tailored design are 23%, 23% and 25% over the conventional design, respectively.

5.10.2 Effect of Reinforcement Fibres

The detailed analysis results also show that, for the HS fibre (AS4)-reinforced riser, as the stresses in the transverse direction determine its minimum thickness in order to satisfy the local load cases, the thinnest liner is used to achieve the minimum weight of the riser. On the contrary, when the HM fibre (P75) is used, the composite lamina is likely to fail in the fibre direction and the thicknesses of the liner required to achieve the minimum weight are different for the various material combinations.

The AS4 fibres are high strength, with more than two times the strength of the high-modulus P75 fibres, but only about half their stiffness (elastic modulus). Also, both the AS4 and P75 reinforced riser bodies are much stronger than the PEEK liner. The AS4-reinforced composite body can carry a much higher load, or in other words, requires a much lower thickness than the P75 riser. In addition, due to the higher stiffness of the P75 riser, the composite body reinforced with P75 carries a larger fraction of the load than the liner when compared to the AS4-reinforced composite riser. Hence the P75 composite body needs to be much thicker than the AS4-reinforced composite body; for instance, in the manually tailored design, the P75/PEEK composite body is about 3.6 times thicker than the AS4/PEEK composite body (86mm compared with 24mm), with both using PEEK liners of 6mm thickness, which results in the P75/PEEK riser with PEEK liner having a structural weight over 4 times higher (173kg/m as opposed to 40kg/m). It is to be noted that, for the AS4/PEEK riser with PEEK liner, the liner contributes about 16% to its total structural weight whereas, for the P75/PEEK riser with PEEK liner, the liner’s contribution is only about 4% with the remaining 96% of its structural weight due to its composite body.

When AS4-reinforced epoxy is employed for the composite body with metallic liners, the liner thickness reduces to about one-third that of the PEEK liner but does not significantly change its weight. However, the thickness of its composite body increases appreciably, resulting in 10 to 30% higher overall structural weights for the AS4/epoxy risers with metallic liners. On the other hand, when the high-modulus P75-reinforced epoxy risers are used with metallic liners, the thickness of the composite body reduces by about 50% compared with that of the P75/PEEK body, while the liner thickness nearly doubles. It is noted that, for the P75/PEEK-reinforced risers, the contribution of the PEEK liner to the overall weight is very small as the 50% reduction in the thickness of the composite body due to using metallic liners reduces the overall weight by 25% to 35% compared with the structural weight of the P75/PEEK body with PEEK liner. Therefore, when the high-strength AS4 is used for reinforcement, the AS4/PEEK with PEEK liner has the least weight whereas, when the high-modulus P75 is used, the P75/PEEK with PEEK liner has a higher structural weight than the P75/epoxy with metallic liners.

5.10.3 Role of Liner in Load Bearing

Considering the effect of liner materials, the use of metallic liners shows a consistent trend of decreasing weight with decreasing specific stiffness (E/ρ) (steel, Ti and Al, in that order). Employing a PEEK rather than metallic liner appears to further reduce the weight only when a high-strength carbon fibre (AS4), not high-modulus fibre (P75), reinforcement is used. Moreover, when a metal liner is employed, loads are carried jointly by the liner and composite body before the liner yields, after which loads are carried mainly by the composite body. In contrast, when a PEEK liner is employed, loads are carried mainly by the composite body since the stiffness of the liner is much less than that of the fibre-reinforced composite body.

5.11 Examination of Last Ply Failure

The designs in the foregoing sections are conducted on the first ply failure criterion, i.e., as soon as one ply fails, the laminate is considered to have failed. Some laminate designs employ last ply failure criterion (where failure is considered to occur only after every ply in the laminate fails), and, although it is too radical to be employed in the design of underwater risers, this section considers employing it as an alternative. In the progressive failure process for identifying last ply failure, the following steps are undertaken.

(1) Use the designed loads to verify feasibility.

(2) Check the lamina stresses against the given failure criterion (maximum stress failure criterion in my study). If no damage is identified, increase the loads with the initial stiffness matrix. If damage is detected, reduce the stiffnesses of the failed layers to zero and recalculate the stress distribution using the discounted stiffness matrix.

(3) Repeat the preceding steps until the last ply fails.

In this section, the AS4/PEEK with PEEK liner composite riser is presented as an example of design results using the last ply failure criterion while the results for the other three material combinations with AS4 fibre reinforcements are presented in *Appendix C*.

5.11.1 Last Ply Failure Analysis of AS4/PEEK with PEEK Liner [90/(0/90)$_{10}$]

5.11.1.1 Last Ply Failure under Burst Case

Fig. 5.27 illustrates the progressive failure process for identifying last ply failure for the AS4/PEEK with PEEK liner composite cylinder with 0° and 90˚ reinforcements under burst case.

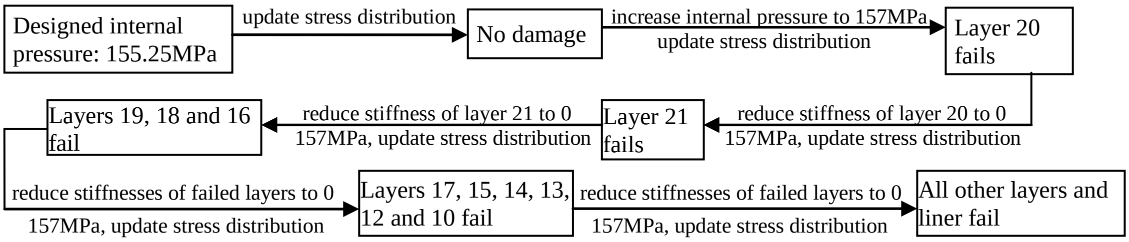

Fig. 5.27. Progressive failure process for AS4/PEEK with PEEK liner composite cylinder with 0° and 90° reinforcements for burst case

The progressive failure results demonstrate that, when some layers fail, stresses in other layers increase since the stiffnesses of the failed layers are reduced to zero. Both the first and last layer failure pressures are 157MPa under the burst load case for the AS4/PEEK with PEEK liner composite cylinder with 0° and 90˚ reinforcements.

5.11.1.2 Last Ply Failure under Pure Tension Case

Fig. 5.28 shows the progressive failure process for identifying last ply failure for the AS4/PEEK with PEEK liner composite cylinder with 0° and 90° reinforcements under pure tension case.

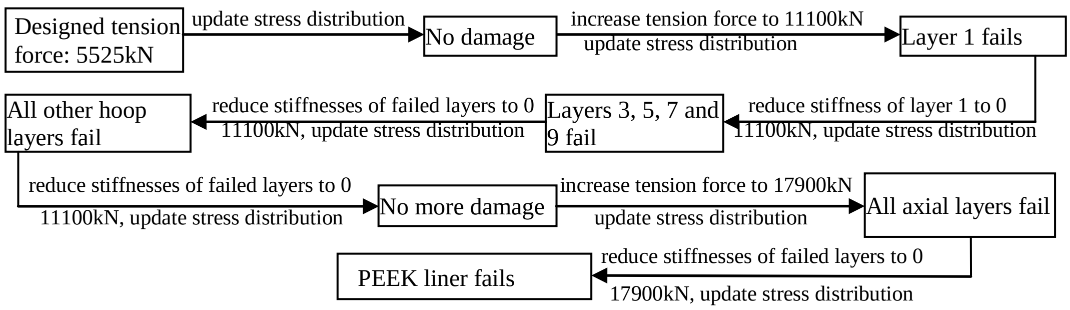

Fig. 5.28. Progressive failure process for AS4/PEEK with PEEK liner composite cylinder with 0° and 90° reinforcements for pure tension case

In the pure tension case, the tension forces for the first and last layer failures are 11100kN and 17900kN, respectively, for the AS4/PEEK with PEEK liner composite cylinder with 0° and 90° reinforcements.

5.11.1.3 Last Ply Failure under Tension with External Pressure Case

Fig. 5.29 shows the progressive failure process for identifying last ply failure for the AS4/PEEK with PEEK liner composite cylinder with 0° and 90° reinforcements under axial tension with external pressure.

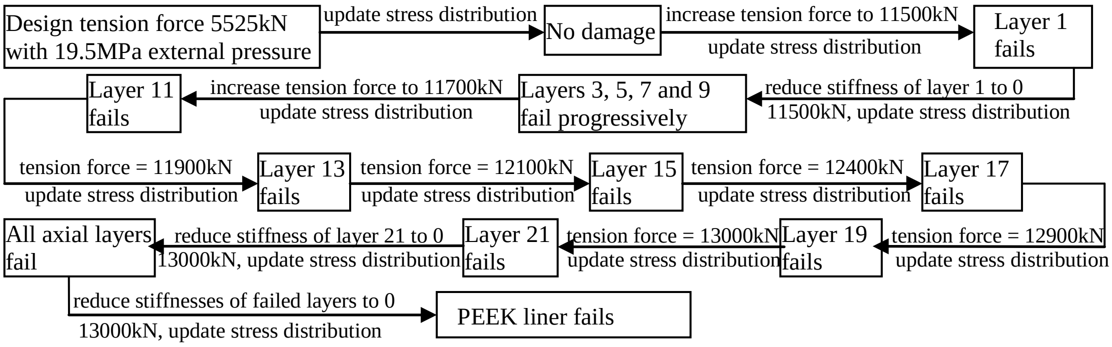

Fig. 5.29. Progressive failure process for AS4/PEEK with PEEK liner composite cylinder with 0° and 90° reinforcements for tension with external pressure case

In the tension with external pressure (19.5MPa) case, the tension forces for the first and last layer failures are 11500kN and 13000kN, respectively, for the AS4/PEEK with PEEK liner composite cylinder with 0° and 90° reinforcements.

5.11.1.4 Last Ply Failure under Collapse Case

Fig. 5.30 shows the progressive failure process for identifying last ply failure for the AS4/PEEK with PEEK liner composite cylinder with 0° and 90° reinforcements under external pressure.

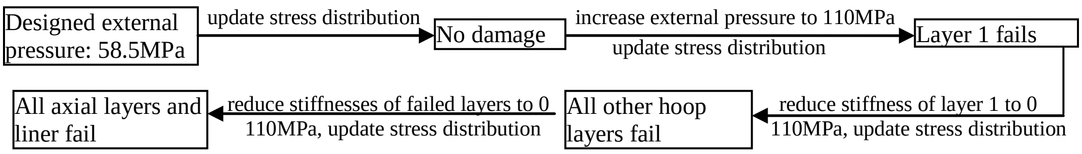

Fig. 5.30. Progressive failure process for AS4/PEEK with PEEK liner composite cylinder with 0° and 90° reinforcements for collapse case

Both the first and last layer failure pressures are 110MPa under the collapse case for the AS4/PEEK with PEEK liner composite cylinder with 0° and 90° reinforcements.

5.11.2 Last Ply Failure Analysis of AS4/PEEK with PEEK Liner $[0_3/(\pm 52)_5/90_4]$

5.11.2.1 Last Ply Failure under Burst Case

Fig. 5.31 shows the progressive failure process for identifying last ply failure for the AS4/PEEK with PEEK liner composite cylinder with 0°, ±52° and 90° reinforcements under the burst case.

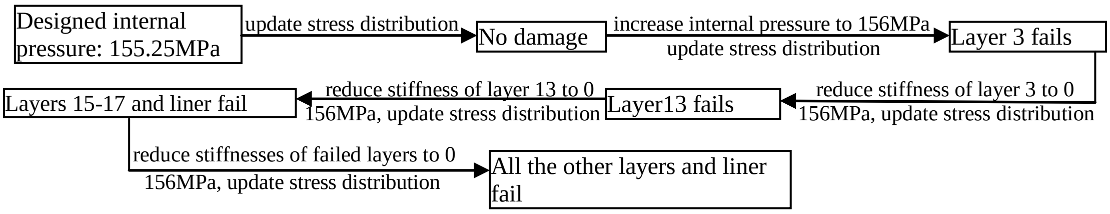

Fig. 5.31. Progressive failure process for AS4/PEEK with PEEK liner composite cylinder with 0°, ±52° and 90° reinforcements for burst case

Both the first and last layer failure pressures are 156MPa under the burst case for the AS4/PEEK with PEEK liner composite cylinder with 0°, ±52° and 90° reinforcements.

5.11.2.2 Last Ply Failure under Pure Tension Case

Fig. 5.32 shows the progressive failure process for identifying last ply failure for the AS4/PEEK with PEEK liner composite cylinder with 0°, ±52° and 90° reinforcements under the pure tension case.

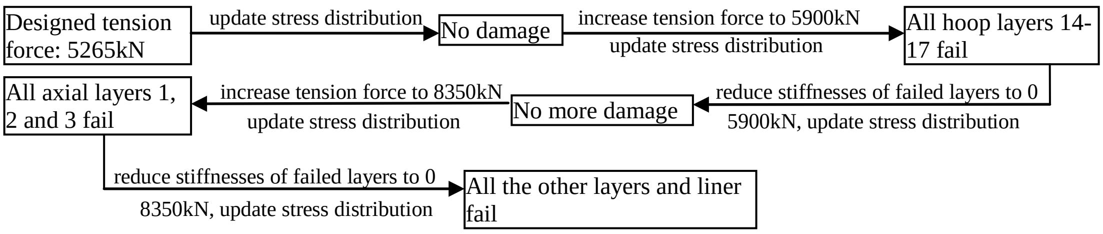

Fig. 5.32. Progressive failure process for AS4/PEEK with PEEK liner composite cylinder with 0°, ±52° and 90° reinforcements for pure tension case

In the pure tension case, the tension forces for the first and last layer failures are 5900kN and 8350kN, respectively, for the AS4/PEEK with PEEK liner composite cylinder with 0˚, ±52˚ and 90˚ reinforcements.

5.11.2.3 Last Ply Failure under Tension with External Pressure Case

Fig. 5.33 shows the progressive failure process for identifying last ply failure for the AS4/PEEK with PEEK liner composite cylinder with 0°, ±52° and 90° reinforcements under axial tension with external pressure.

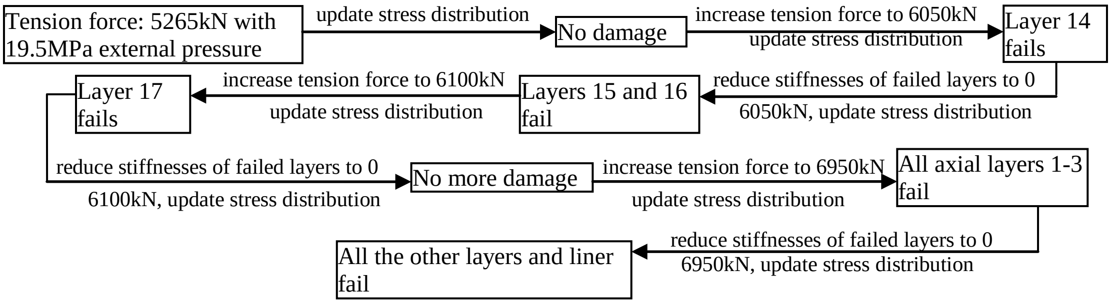

Fig. 5.33. Progressive failure process for AS4/PEEK with PEEK liner composite cylinder with 0°, ±52° and 90° reinforcements for tension with external pressure case

In the tension with external pressure (19.5MPa) case, the tension forces for the first and last layer failures are 6050kN and 6950kN, respectively, for the AS4/PEEK with PEEK liner composite cylinder with 0°, ±52° and 90° reinforcements.

5.11.2.4 Last Ply Failure under Collapse Case

Fig. 5.34 shows the progressive failure process for identifying last ply failure for the AS4/PEEK with PEEK liner composite cylinder with 0°, ±52˚ and 90˚ reinforcements under external pressure.

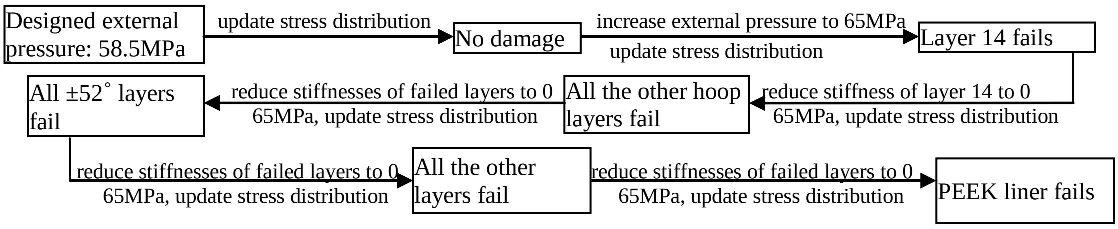

Fig. 5.34. Progressive failure process for AS4/PEEK with PEEK liner composite cylinder with 0°, ±52° and 90° reinforcements for collapse case

Both the first and last layer pressures are 65MPa under the collapse case for the AS4/PEEK with PEEK liner composite cylinder with 0°, ±52˚ and 90° reinforcements.

5.11.3 First and Last Ply Failure Loads

Table 5.5 shows the local load capacities of the composite riser with AS4 reinforcements using the two different design procedures.

Table 5.5. Local load factors of composite riser with AS4 fibre reinforcements with different design geometries

Material combination	Lay-up	Load factors under burst case		Load factors under pure tension case		Load factors under tension with external pressure case		Load factors under collapse case		Eigenvalue buckling case
		First ply failure	Last ply failure	First ply failure	Last ply failure	First ply failure	Last ply failure	First ply failure	Last ply failure	
AS4/PEEK with PEEK liner	$[90/(0/90)_{10}]$	1.01	1.01	2.02	3.26	2.09	2.37	1.88	1.88	3.19
	$[0_3/(\pm 52)_5/90_4]$	1.00	1.00	1.13	1.60	1.16	1.33	1.11	1.11	1.02
AS4/epoxy with steel liner	$[90/(0/90)_{10}]$	1.01	1.01	1.83	3.90	1.93	3.76	3.40	3.40	6.63
	$[0_3/(\pm 53.5)_5/90_4]$	1.01	1.01	1.03	1.53	1.08	1.09	2.02	2.02	3.52
AS4/epoxy with Ti liner	$[90/(0/90)_{10}]$	1.01	1.01	1.85	4.00	1.96	4.07	3.37	3.37	5.60
	$[0_3/(\pm 53)_5/90_4]$	1.01	1.01	1.06	1.62	1.14	1.23	2.05	2.05	2.76
AS4/epoxy with Al liner	$[90/(0/90)_{10}]$	1.01	1.01	1.99	4.37	2.11	4.25	3.36	3.36	5.97
	$[0_4/(\pm 53.5)_5/90_4]$	1.00	1.00	1.18	1.84	1.27	1.37	2.07	2.07	2.53

The load factor is defined as the ratio of the failure load to the designed load and, when it is larger than 1.0, the structure is safe. It is obvious from the table that, for some local load cases, the safety margin is much higher than the allowance, especially for the riser with only 0° and 90° reinforcements. However, in order to satisfy all the local load cases, the worst situation determines the design geometry. More importantly, the smaller safety margin of the riser with [0/±θ/90] reinforcements indicates the better efficiency of the tailored design with angle reinforcement layers.

5.12 Consideration of Design allowing Matrix Cracking

The maximum stress failure criterion used in this thesis considers failures in the fibre and transverse directions and in-plane shear separately. As the latter two are associated with matrix cracking which is included as one of the failure modes to be considered. For some material combinations, matrix cracking is the most critical failure mode, such as in the case of the AS4/PEEK with PEEK liner described in Sections 5.5 and 5.6 whereas for other cases, such as that of the P75/PEEK with PEEK liner (Section 5.8), fibre failure is the most critical. It is to be noted that, as design standards require a composite riser to be capable of withstanding the burst case conditions without leakage (assuming that the liner may have cracked) which means without any matrix cracking in the composite body, the design criteria used in this study do not allow matrix cracking.

However, in order to investigate whether the tailored design offers any weight advantage if matrix cracking is permitted, an analysis is conducted on the AS4/PEEK with PEEK liner allowing matrix cracking, i.e., considering that only fibre failure constitutes failure. The results show that, if matrix cracking is permitted, the composite body can be thinner and, therefore, have a lower weight. However, the tailored design with angle reinforcements still yields a configuration with lower weight than the conventional design if matrix cracking is not included as a failure criterion. The conventional design with matrix cracking provides a 21-ply composite laminate $[90/(0/90)_{10}]$ with alternating hoop- and axially reinforced layers with thicknesses of 1.42 and 0.57mm, respectively, resulting in a total laminate thickness of 21.32mm and a PEEK liner 6mm thick. The tailored design including the angle plies provides a 17-layer composite laminate $[90_2/(\pm 55)_4/90_2/0_3/90_2]$ with thicknesses of 1.8, 1.0, 1.2, 1.25 and 1.0mm, respectively, which has a total laminate thickness of only 19.75mm with the same 6mm thick PEEK liner.

Fig. 5.35 compares the structural weights obtained for the AS4/PEEK riser with PEEK liner using the conventional and tailored design approaches both when matrix cracking is allowed and when it is not. It can be seen that, with matrix cracking, both designs provide lower weights, about 69% and 84% of the designs with no matrix cracking for the conventional design and the tailored design, respectively. If matrix cracking is permitted, the manually tailored design still provides a weight saving but only of about 7% compared with the conventional design with matrix cracking.

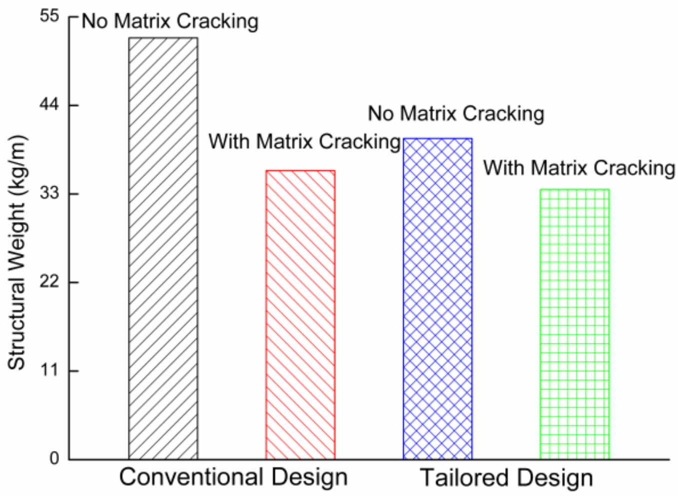

Fig. 5.35. Comparison of structural weights of designs with and without matrix cracking permitted (AS4/PEEK with PEEK liner)

The tailored design with matrix cracking presented in this section is based on local load cases as the performances of the geometry for the global load cases have to be verified. The global design of the geometry with matrix cracking is conducted in

Section 6.7, *Chapter 6*, and includes global analyses of different global load cases followed by structural verification.

5.13 Summary and Conclusions

This chapter begins with the calculation of the minimum thickness of a composite tube under internal pressure with end effects using CLT for different material properties which provide basic information on how the material properties influence the design. The far more accurate FEA model using 3D elements to conduct the local design is presented, followed by local design procedures for the conventional design with axial and hoop reinforcements and the tailored design which includes inclined reinforcements. The local designs for all the eight material combinations listed in Table 3.15 in *Chapter 3* are performed using both the conventional and tailored approaches. In this chapter, the results for the AS4/PEEK with PEEK liner composite riser are presented in detail as an illustration while the results for the other seven material combinations are provided in *Appendix B.*

The comparisons of the conventional and tailored designs conducted in this chapter reveal that the latter offers additional structural weight savings of up to 26% over the former and not only reduces the necessary tension force but also the raw materials required for construction as well as operational costs.

The local design stage ensures the load capacities of the composite riser under the four local load cases. As the deformations and, thus, the forces and bending moments due to global loads depend on the geometric configuration of the riser, it is necessary to obtain a fairly accurate estimate of the riser geometry using the local design before a global analysis can be performed. The laminate geometries designed for minimum structural weight in this local design stage are employed in the global analysis and structural verification of the composite riser, taking into consideration of the global mechanical and environmental loads, in *Chapter 6*.

CHAPTER 6

GLOBAL DESIGN OF COMPOSITE RISER

6.1 Introduction

The local design of the composite riser conducted in *Chapter 5* is necessary: (1) to ensure that the composite riser tube satisfies the local load cases (LC); and (2) because the forces and bending moments in the global analysis, which include large deformations, depend on its geometric configuration. This chapter presents the global analysis and structural verification of composite risers based on the geometries of the composite tubes obtained in the local design stage. The two stages in global design are the analysis of the entire riser under global loads and structural verifications of its critical sections identified from the global analysis.

The local design conducted in *Chapter 5* shows that using high-strength carbon fibres (AS4) for the composite riser segments is much more efficient in terms of reducing weight than using high-modulus carbon fibre (P75). It is also found that using steel as the liner material for the AS4-reinforced composite tubes results in a higher weight than using PEEK, titanium and aluminium materials. Therefore, only the three most promising material systems (Fig. 5.24 in *Chapter 5* and Table 3.15 in *Chapter 3*) are selected for the global design in this study, namely, (i) the AS4/PEEK body with

PEEK liner (ii) AS4/epoxy body with titanium liner and (iii) AS4/epoxy body with aluminium liner.

In this chapter, a global analysis of the entire riser for different global load cases is performed to determine the moments and forces that occur along it due to global functional and environmental loads. It considers different combinations of the operational and environmental loads applied to the entire riser, including platform motion, top tension force, internal pressure, hydrostatic pressure, gravity, buoyancy, and wave and current loads, which are illustrated schematically in Fig. 3.7 and listed in Table 3.4 in *Chapter 3*. In this chapter, only the extreme conditions (LC4-LC9) are considered since the factors of safety (FS) for the liner and composite layers that satisfy them will automatically satisfy the less severe global conditions (LC1-LC3). The critical sections of the riser and the forces and moments acting on them are identified in this stage, as presented in Sections 6.2 and 6.3. Then, a final structural verification of the critical sections of the riser under the forces and moments determined in the global analysis is conducted and discussed in Sections 6.4 and 6.5.

6.2 Finite Element Model and Load Cases for Global Analysis of Composite Risers

In *Chapter 5*, the standard composite riser joints are designed for minimum weights under the local design loads. As the tension joint at the top, three standard riser joints (60m) next to it at sea level and stress joint at the bottom of a riser are subjected to very high stresses, they are the same as the steel riser, that is, made from high-grade steel (X80) and with the same geometries, including lengths, diameters and thicknesses (Table 4.1 in *Chapter 4*). For the global analysis, the geometries of all the other (composite) standard riser joints (laminate sequences, ply thicknesses and orientations) are taken to be the same as those obtained from the manually tailored design in *Chapter 5*. This entire riser configuration is shown in Fig. 6.1.

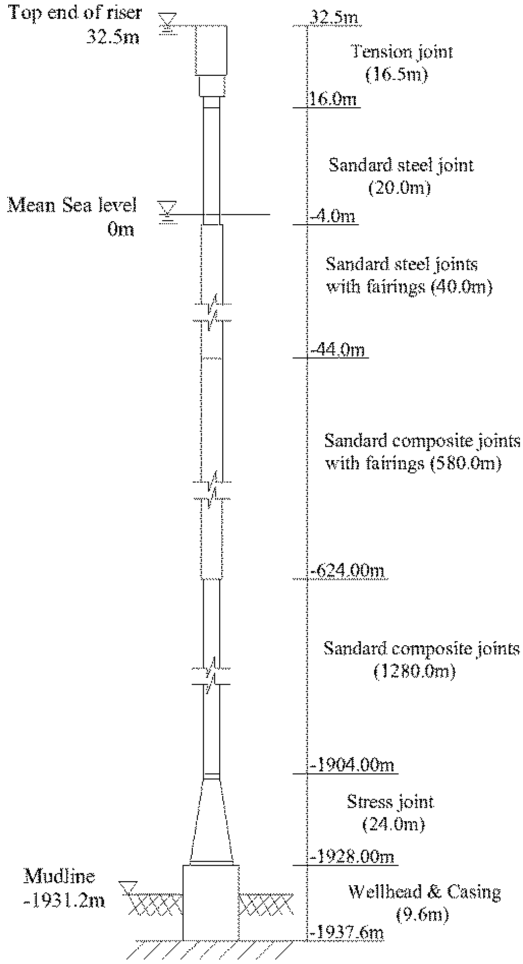

Fig. 6.1 Composite riser configuration for global analysis

The tension joint at the top is 16.5m long, the standard steel riser joints from 16.0m to -44m the length of the riser (the origin of the length co-ordinate axis is at sea level and positive upwards), the standard composite riser joints from -44m to -1904m along the length of the riser (a total of 93 composite joints) and the stress joint at the bottom 24.0m long, with the wellhead and casing making up another 9.6m to complete the full 1970.1 length of the riser. Again, it is assumed that fairings are attached to the standard steel riser joints above -624m to mitigate vortex-induced vibration (VIV). As mentioned in Section 3.2, *Chapter 3*, and shown in Fig. 4.2, *Chapter 4*, the internal diameter of the riser is 250mm with a standard production C95 steel tubing inside. It may be noted that the global analysis and structural verification are performed for only the tailored design configurations of the three most promising material combinations. The rationale for not conducting global designs of the conventional geometries is that, since they are of much higher thicknesses for the same material combinations than the tailored geometries, they would either pass the global design or, if not, their thicknesses (and weights) would have to be further increased which would make them worse in comparison to the tailored design geometries. Therefore, the estimated weight savings achieved using the tailored design in this thesis are conservative.

6.2.1 Finite Element Model of Composite Riser for Global Analysis

In the design stage for global analysis, the entire composite riser is modelled in ANSYS13.0 using pipe element 288. The wave and current loadings are applied by selecting the option 'ocean loads' and providing inputs of the water depth, water density, wave period, wave height, wave length, wave theory, current velocity, current location, drag coefficient, coefficient of inertia, etc. As Pipe288, being a one-dimensional element, does not have restrictions on its aspect ratio, each element can be quite long and the 1970.1m length of the riser can be covered by a relatively small number of elements. Furthermore, although Pipe288 supports anisotropic material properties, it requires the homogenised material properties of the whole cross-section in three dimensions rather than the properties of individual layers, the stresses from which cannot be extracted. A total of 2127 elements are used for the entire composite riser in the global analysis. In order to consider the dynamic effects of environmental loads and platform motions, a large-displacement non-linear dynamic analysis option is chosen. Ball and slip support conditions are applied at the top and the fixed support condition at the bottom of the riser. As the ball and slip supports allow rotations and displacements, the top tension forces and displacements of the platform can be used. The fixed support condition at the bottom is achieved by applying fixed constraints to the elements which simulates a wellhead under the mud-line (Fig. 6.1).

6.2.2 Effective Material Properties of Composite Riser Tube

The geometric parameters, i.e., laminate layer thicknesses, fibre orientations, stacking sequences and liner thickness employed in the global analysis of the composite riser are those determined from its local design (*Chapter 5*).

In order to model the composite riser using pipe elements, the 3D homogenous effective properties of the layered composite geometries obtained from the local design are calculated for the composite pipe elements used in the global analysis.

The classical laminated plate theory (CLT) [83] provides an effective way of analysing thin composite laminates while higher-order plate theories can be applied to moderately thick laminates to improve accuracy. However, the CLT and higher-order plate theories are limited by their 2D natures and cannot be used to calculate 3D properties [113]. The theory and equations [113, 114] of the 3D effective properties of the composite tube employed in this study for the global analysis are given in Eqs. 6-1 to 6-8, and the global coordinate of the composite laminate and material principal coordinate system are illustrated in Fig. 6.2.

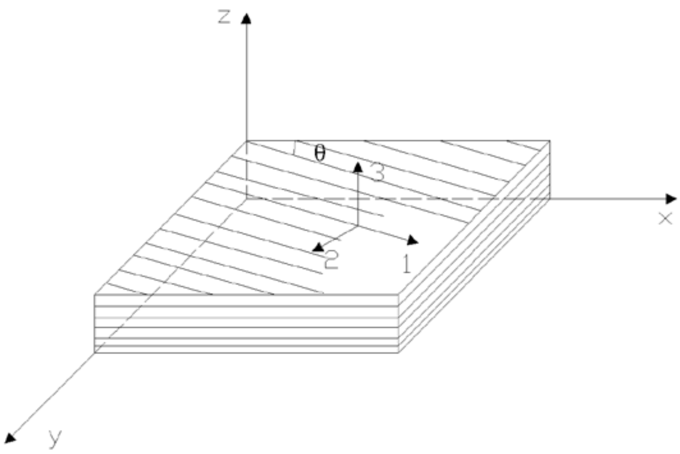

(1, 2, 3): material principal coordinate system
(x, y, z): global coordinate of composite laminate
Fig. 6.2. Global coordinate of composite laminate and material principal coordinate

The principal compliance matrix $\left[S_{ij}^{'}\right]^{(k)}$ for transversely isotropic composite lamina is calculated by

$$\left[S_{ij}^{'}\right]^{(k)} = \begin{bmatrix} 1/E_1 & -\nu_{12}/E_1 & -\nu_{13}/E_1 & 0 & 0 & 0 \\ -\nu_{21}/E_2 & 1/E_2 & -\nu_{23}/E_2 & 0 & 0 & 0 \\ -\nu_{31}/E_3 & -\nu_{32}/E_3 & 1/E_3 & 0 & 0 & 0 \\ 0 & 0 & 0 & 1/G_{23} & 0 & 0 \\ 0 & 0 & 0 & 0 & 1/G_{13} & 0 \\ 0 & 0 & 0 & 0 & 0 & 1/G_{12} \end{bmatrix}^{(k)} \tag{6-1}$$

Then, the principle elasticity matrix of each composite lamina is $\left[C_{ij}^{'}\right]^{(k)} = \left[S_{ij}^{'}\right]^{-1(k)}$ and the lamina elasticity matrix $\left[C_{ij}\right]$ can be expressed in terms of $\left[C_{ij}^{'}\right]$ and the ply orientation angle θ by

$$\left[C_{ij}\right] = \begin{bmatrix} c^2 & s^2 & 0 & 0 & 0 & 2cs \\ s^2 & c^2 & 0 & 0 & 0 & -2cs \\ 0 & 0 & 1 & 0 & 0 & 0 \\ 0 & 0 & 0 & c & -s & 0 \\ 0 & 0 & 0 & s & c & 0 \\ -cs & cs & 0 & 0 & 0 & c^2-s^2 \end{bmatrix} \left[C_{ij}^{'}\right] \begin{bmatrix} c^2 & s^2 & 0 & 0 & 0 & cs \\ s^2 & c^2 & 0 & 0 & 0 & -cs \\ 0 & 0 & 1 & 0 & 0 & 0 \\ 0 & 0 & 0 & c & -s & 0 \\ 0 & 0 & 0 & s & c & 0 \\ -2cs & 2cs & 0 & 0 & 0 & c^2-s^2 \end{bmatrix} \tag{6-2}$$

where

θ is the ply angle, c= cos θ and s=sin θ.

For N layers of transversely isotropic composite laminate, the laminate stiffness is calculated by

$$\left[\overline{C}\right] = \begin{bmatrix} \overline{C}_{11} & \overline{C}_{12} & \overline{C}_{13} & 0 & 0 & \overline{C}_{16} \\ \overline{C}_{12} & \overline{C}_{22} & \overline{C}_{23} & 0 & 0 & \overline{C}_{26} \\ \overline{C}_{13} & \overline{C}_{23} & \overline{C}_{33} & 0 & 0 & \overline{C}_{36} \\ 0 & 0 & 0 & \overline{C}_{44} & \overline{C}_{45} & 0 \\ 0 & 0 & 0 & \overline{C}_{45} & \overline{C}_{55} & 0 \\ \overline{C}_{16} & \overline{C}_{26} & \overline{C}_{36} & 0 & 0 & \overline{C}_{66} \end{bmatrix} \tag{6-3}$$

The $\overline{C}_{ij}$ in Eq. 6-3 are given by Eqs. 6-4 to 6-7 in which $v_k = \frac{t_k}{h}$, where t_k is the thickness of the kth lamina and h the total thickness of the laminate.

$$\overline{C}_{\mathrm{ij}} = \sum_{\mathrm{k=1}}^{\mathrm{N}} \mathrm{v_k} \left[C_{ij}^{k} - \frac{C_{i3}^{k} C_{3j}^{k}}{C_{33}^{k}} + \frac{C_{i3}^{k} \sum_{l=1}^{N} \frac{\mathrm{v}_l C_{3j}^{k}}{C_{33}^{k}}}{C_{33}^{k} \sum_{l=1}^{N} \frac{\mathrm{v}_l}{C_{33}^{k}}} \right] \text{ for (i, j=1, 2, 3, 6)} \tag{6-4}$$

$$\overline{C}_{\mathrm{ij}} = \overline{C}_{\mathrm{ji}} = 0 \text{ for (i=1, 2, 3, 6 and j=4, 5)} \tag{6-5}$$

$$\overline{C}_{\mathrm{ij}} = \frac{\sum_{k=1}^{N} \frac{\mathrm{v}_k}{\Delta_k} C_{ij}^{k}}{\sum_{k=1}^{N} \sum_{l=1}^{N} \frac{\mathrm{v}_k \mathrm{v}_l}{\Delta_k \Delta_l} (C_{44}^{k} C_{55}^{l} - C_{45}^{k} C_{54}^{l})} \text{ for (i, j =4, 5)} \tag{6-6}$$

$$\Delta_k = (C_{44}^{k} C_{55}^{k} - C_{45}^{k} C_{54}^{k}) \tag{6-7}$$

The effective elastic compliance matrix of the composite laminate is $[\overline{S}]=[\overline{C}]^{-1}$. Finally, the effective engineering moduli are obtained as

$$\overline{E}_{\mathrm{x}} = \frac{1}{\overline{S}_{11}}; \quad \overline{E}_{\mathrm{y}} = \frac{1}{\overline{S}_{22}}; \quad \overline{E}_{\mathrm{z}} = \frac{1}{\overline{S}_{33}}; \quad \overline{\nu}_{\mathrm{yz}} = -\frac{\overline{S}_{23}}{\overline{S}_{22}}; \quad \overline{\nu}_{\mathrm{xz}} = -\frac{\overline{S}_{31}}{\overline{S}_{11}};$$

$$\overline{\nu}_{\mathrm{xy}} = -\frac{\overline{S}_{21}}{\overline{S}_{11}}; \quad \overline{G}_{\mathrm{yz}} = -\frac{1}{\overline{S}_{44}}; \quad \overline{G}_{\mathrm{xz}} = -\frac{1}{\overline{S}_{55}}; \quad \overline{G}_{\mathrm{xy}} = -\frac{1}{\overline{S}_{66}}; \tag{6-8}$$

A MATLAB code is created for calculating the 3D effective properties of the composite tube using the 3D laminate property theory [113, 114]. The tension modulus obtained by the 3D laminate property theory is verified by the FEA results using Solid186 with real composite lay-ups.

Table 6.1. 3D effective properties of composite tubes used in global analysis

Name	$\rho_{effective}$ (kg/m^3)	$E_{x\_tension}$ (GPa)	$E_{x\_bending}$* (GPa)	E_y (Gpa)	E_z (Gpa)	G_{xy} (Gpa)	G_{xz} (Gpa)	G_{yz} (Gpa)	ν_{xy}	ν_{xz}	ν_{yz}
AS4/PEEK-PEEK liner (0/±52/90)	1513.3	30.40	29.00	50.28	9.59	16.44	2.46	2.75	0.251	0.378	0.284
AS4/epoxy-Ti liner (0/±53/90)	1700.8	40.50	36.50	66.25	12.01	22.84	4.10	4.35	0.275	0.344	0.272
AS4/epoxy-Al liner(0/±53.5/90)	1599.8	41.40	37.20	64.12	11.92	20.57	4.07	4.28	0.254	0.349	0.293

*from static FEA

The effective 3D elastic constants used in the global analysis of the composite riser design are listed in Table 6.1, where the subscripts x, y and z refer to the axial, hoop and radial directions, respectively. These homogenous constants are based on the

3D lamina and liner material properties presented in *Chapter 3* (Sections 3.8 and 3.9) and composite tubular geometries obtained from the local design stage in *Chapter 5.*

We have to note that, for a composite laminate, there can be a significant difference between its effective moduli in tension and bending ($E_{x\_tension}$ and $E_{x\_bending}$). To check whether the difference between the two moduli is significant for the laminates considered in the design, the effective bending modulus is evaluated using static analyses of the FEA models of the selected lay-ups with Solid186 (layered brick) and Elbow290 (composite pipe) under bending situations and compared with the results for the FEA models using Pipe288 with effective bending engineering constants. The three FEA models for calculating $E_{x\_bending}$, a cantilever pipe under a transverse force of 1000N, a simple support pipe with an evenly distributed force of 500N/m and a cantilever pipe under a transverse displacement of 3m, are illustrated in Figs. 6.3(a), (b) and (c), respectively.

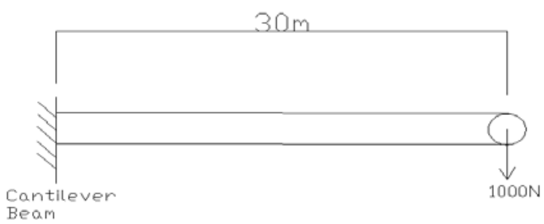

(a) LC1

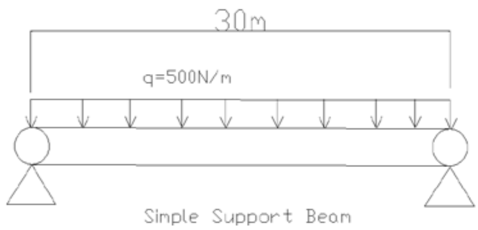

(b) LC2

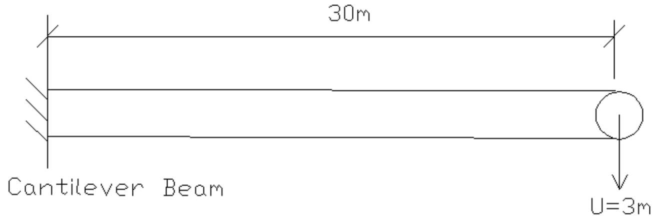

(c) LC3

Fig. 6.3. FEA models for calculating $E_{x\_bending}$: (a) cantilever pipe under transverse force, (b) simple support pipe with evenly distributed force and (c) cantilever pipe under transverse displacement

The maximum displacements in Figs. 6.3(a) and 6.3(b), and maximum bending moments in Fig. 6.3(c) are compared. The effective $E_{x\_bending}$ can be obtained from LC1 and LC2 using $E_{x\_bending}(FEA) \approx \frac{PL^3}{3I\Delta}$ and $E_{x\_bending}(FEA) = \frac{5qL^4}{384I\Delta}$, respectively.

As in the case of the AS4/PEEK with PEEK liner, the difference between $E_{x\_tension}$ and $E_{x\_bending}$ is less than 5%, an average value of 29.7GPa is used for the effective Young's modulus in bending and the in-plane modes. For the other two material combinations, AS4/epoxy with titanium and aluminium liners, since the difference between their $E_{x\_tension}$ and $E_{x\_bending}$ moduli is greater than 5%, both are used in the global analysis to determine the worst-case scenario.

6.2.3 Global Load Cases for Composite Riser

The global design load cases are combinations of different categories of environmental loading and riser conditions. For analysis, the extreme global load cases 4 to 9 listed in Table 3.4 in *Chapter 3* are used for analysis since the FSs of their liners and composite layers which satisfy these extreme conditions will satisfy the less severe conditions of the global design.

The environmental situation and platform movement data in the Gulf of Mexico used for the composite riser design are exactly the same as those for steel riser design [34, 51]. The coefficient of inertia (C_M) is set to 2.0 for all the joints and the value for C_D (normal drag coefficient) is taken as 1.0 for the bare riser joints and 0.7 for the joints with fairings, respectively, as recommended by design standards [63, 69].

For the different global load cases, the tension forces applied on each of the three risers using the tailored design, AS4/PEEK with PEEK liner and AS4/epoxy with titanium and aluminium liners, are given in Table 6.2. The top tensions applied in different global load cases are based on the effective weights of the composite risers. A riser's effective weight is a function of the density of its different material combinations, wall thicknesses and different contents in the riser. The top tension ratios for the different global load cases are given in Table 3.4 in *Chapter 3*.

Table 6.2. Tension forces applied for different material combinations for different global load cases

Material Combination	Tension Force for Global Analysis (kN)		
	LCs 4-5	LCs 6-7	LCs 8-9
AS4/PEEK with PEEK liner $[0_3/(\pm 52)_5/90_4]$	1100	2340	2200
AS4/epoxy with titanium liner $[0_3/(\pm 53)_5/90_4]$	1300	2500	2330
AS4/epoxy with aluminium liner $[0_4/(\pm 53.5)_5/90_4]$	1250	2430	2320

The global analysis is performed to examine the responses of the composite riser over its entire length and identify critical locations and the force, pressure and moment components at these locations.

6.3 Results from Global Analysis for AS4/PEEK Riser with PEEK Liner $[0_3/(\pm 52)_5/90_4]$

This section presents detailed results for the riser with the AS4/PEEK composite body and PEEK liner analysed using its effective 3D properties with pipe elements for the laminate configuration and thickness combinations which provide the least structural weight, as determined by the local analysis performed in *Chapter 5*. The global analysis results for various combinations of tension, bending, shear force and pressure of the different global design load cases are presented.

The variations in internal and external pressures as functions of depth along the length of the riser are shown in Figs. 6.4(a) and 6.4(b) for global load cases LC4 to LC9. It may be noted that, as pressure variations are independent of the materials used, they are the same for all material combinations considered.

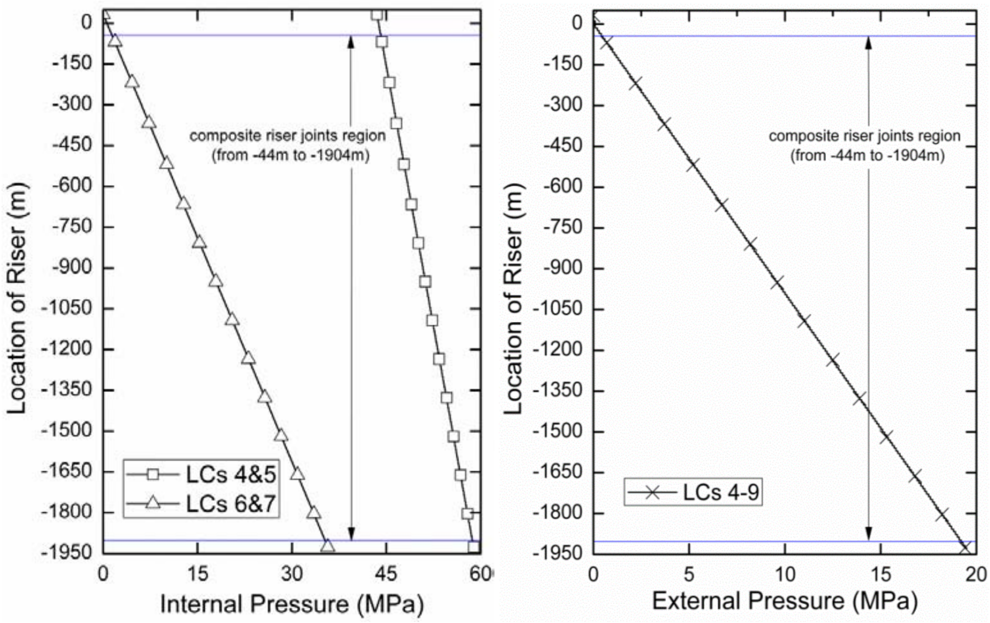

(a) (b)

Fig. 6.4. (a) Internal pressure for global load cases LC4 to LC7 and (b) external pressure for global load cases LC4 to LC9

The tension force, bending moment and shear force distributions estimated from the global analysis conducted using FE modelling for global load cases LC4 to LC9 are presented in Figs. 6.5 to 6.7, respectively. The blue horizontal lines in these figures indicate the top and bottom of the composite riser section at depths of -44m and -1904m, respectively. It should be noted that, in designing the composite riser, we are only concerned with the tension, bending moment and shear force magnitudes within this region.

Fig. 6.5 shows the effective tension force distributions along the entire riser. It is clear that the maximum tension force is 3156.7kN in the composite section of the riser which occurs under load case LC4 at the top. The maximum effective tension force includes the top tension, end-effect of internal and external pressures, and bending of the riser. For load cases LC4 and LC5, as the internal pressures are much higher than the external pressures, the tension forces due to their end-effects are positive values. For load cases LC6 and LC7, the magnitudes of the internal pressure are similar to those of the external pressure while, for load cases LC8 and LC9, they are zero. Therefore, the end-effect of the pressures is to provide a negative tension due to the large wall thickness of the stress joint which provides a much larger outer surface on which the external pressure can act. Overall, the tension force in the entire riser is positive and sufficiently large to maintain the vertical position of the riser.

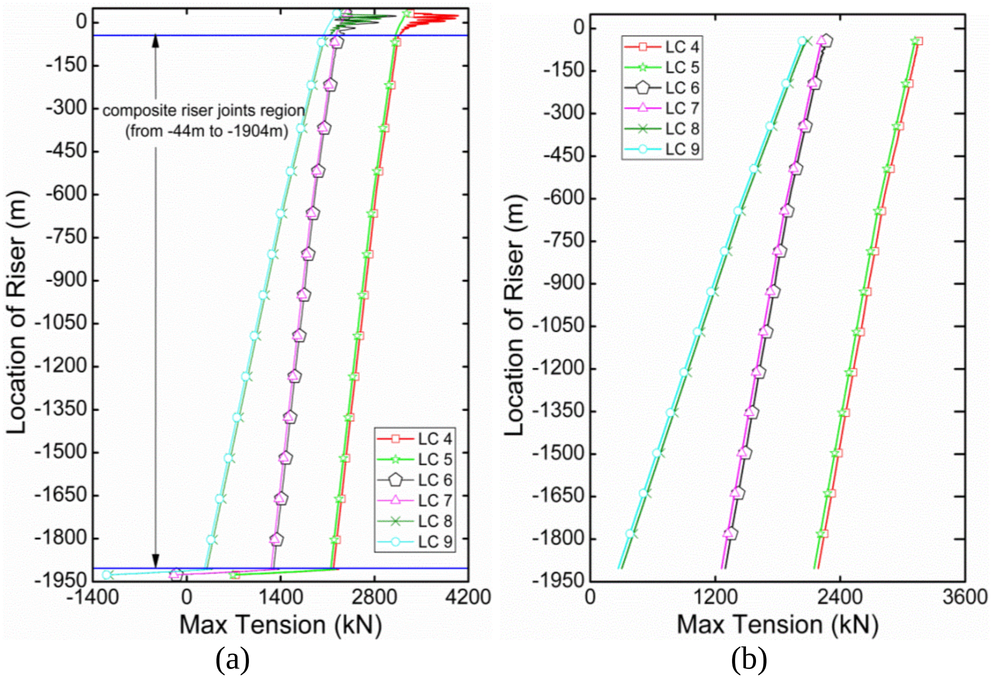

Fig. 6.5. Tension forces for different load cases: (a) full-length riser; and (b) composite riser region

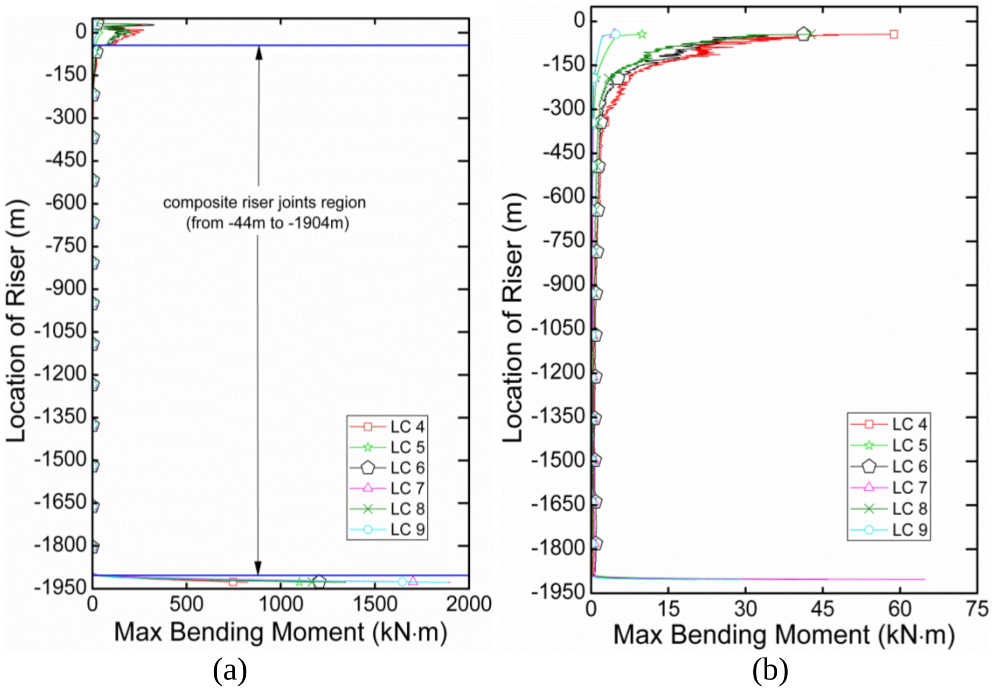

Fig. 6.6. Bending moments for different load cases: (a) full-length riser; and (b) composite riser region

Fig. 6.6 shows the bending moment distributions along the entire riser. The maximum bending moments in the composite section of the riser occur at the top and bottom, with values of 58.8kN·m under LC4 at the top and 64.9kN·m under LC7 at the bottom. It may be noted that the bending moments are much higher in the metallic stress joints at the bottom, reaching up to around 2000kN·m for load cases LC7 and LC9.

Fig. 6.7 shows the shear force distributions along the entire riser. The maximum shear force (171.7kN) in the composite region occurs under LC9 at the bottom.

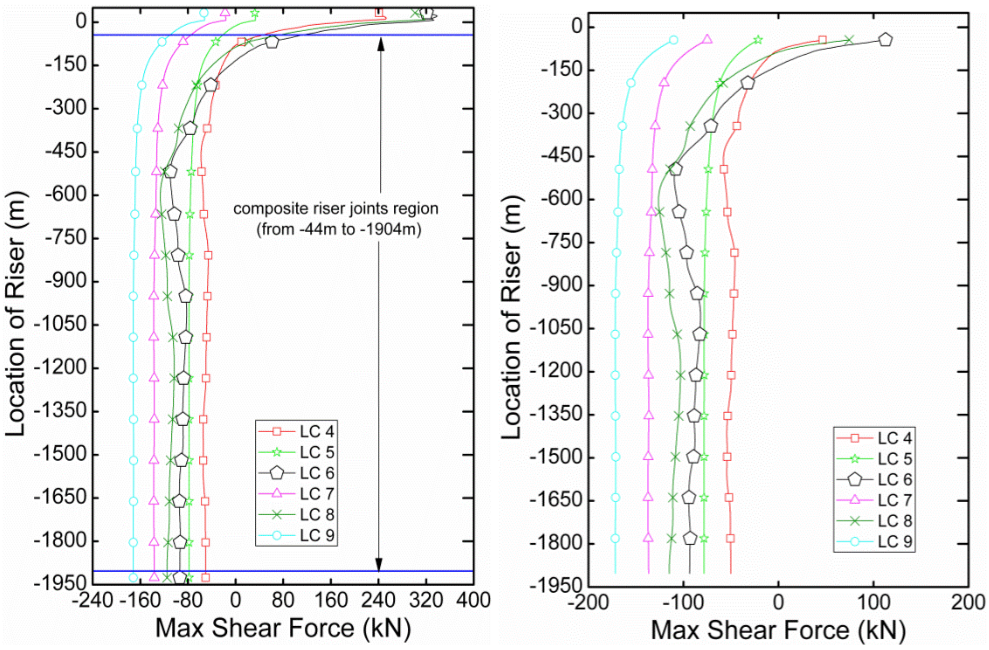

Fig. 6.7. Shear forces for different load cases: (a) full-length riser; and (b) composite riser region

In Figs. 6.4 to 6.7, it can be seen that, in the composite riser joints region, the internal and external pressures increase from top to bottom, the tension forces decrease from top to bottom, and the maximum bending moments and shear forces occur at the top or bottom joint under different load cases. Therefore, it can be said that the top and bottom joints are the most critical locations.

The critical load combinations at the critical top and bottom joints are given in Table 6.3 for the different load cases. From them, the following most critical cases (highlighted in red) are selected for structural integrity verification by local stress analysis: LC4_top, LC4_bottom, LC5_bottom, LC6_top, LC6_bottom, LC7_bottom, LC9_top and LC9_bottom.

Table 6.3. Critical load combinations for AS4/PEEK with PEEK liner riser from global analysis

Load Case	Location	Tension (kN)	Internal Pressure (MPa)	External Pressure (MPa)	Shear Force (kN)	Bending Moment (kN·m)
4	Top	3156.7	44.3	0.7	46.4	58.8
	Bottom	2197.3	58.7	19.2	50.3	41.6
5	Top	3117.7	44.3	0.7	31	9.9
	Bottom	2159.0	58.7	19.2	78.3	61.0
6	Top	2265.2	1.8	0.7	112.7	41.3
	Bottom	1305.6	35.3	19.2	93.5	46.0
7	Top	2219.3	1.8	0.7	85.6	4.5
	Bottom	1269.3	35.3	19.2	136.7	64.9
8	Top	2089.4	0	0.7	74.4	42.7
	Bottom	319.9	0	19.2	115	20.6
9	Top	2032.8	0	0.7	120.8	4.8
	Bottom	285.6	0	19.2	171.8	29.2

6.4 Finite Element Model for Structural Verifications of Composite Risers

Once the critical locations are identified from the global analysis, structural verifications of the critical composite riser sections under the actual forces and moments at these locations is performed using 3D solid elements to verify structural integrity, i.e., to ensure that the stresses are still within the specified allowable limits.

In the structural verification stage, the stress analysis is again conducted using the 3D FEA model of the local pipe section with 4.5m long (Fig. 5.5 in *Chapter 5* and Fig. 6.8 in this chapter) for the most critical load combinations (Table 6.3). The same FEA model (3D solid layered elements, Fig. 5.5 in *Chapter 5*) used in the local design process is applied, again with a 4.5m length.

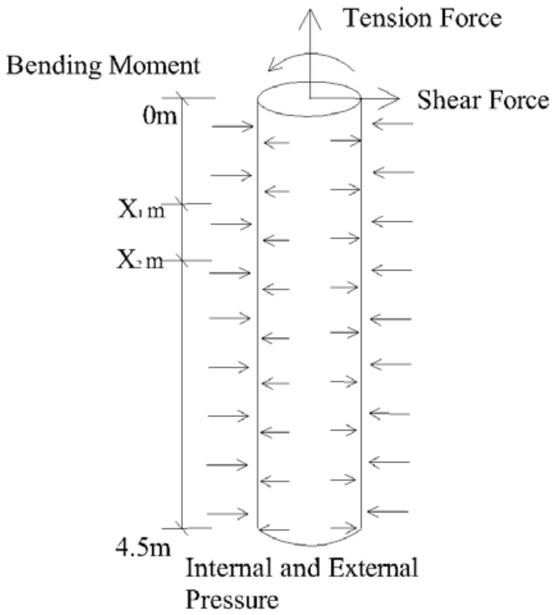

Fig. 6.8. Loads on pipe section for structural verification

Although the local design in *Chapter 5* does not take into account the forces and moments caused by the global environmental and functional loads considered in the global analysis, they are included here. Further, the structural capacities for the larger FSs required by the standards [72] are verified while the minimum FSs required are 1.53 for the composite laminae, 1.74 for the PEEK liner and 1.68 for the titanium and aluminium liners [72] under all the force combinations obtained from the global analysis. The FS in the current stage is equal to $\gamma_{FM} \times \gamma_{Sd} \times \gamma_{Rd} \times \gamma_S$, where γ_{FM} =1.15 for the composite layers and PEEK liner, and 1.11 for the titanium and aluminium liners (combined load effect and resistance factor), γ_{Sd} =1.10 (load model factor), γ_{Rd} =1.10 for the composite lamina and 1.25 for all the liners (resistance model factor) and γ_S=1.10 (system factor). It is important to note that the shear force at the end will algebraically add to the bending moment distribution along the length of the model. The stresses generated using both clockwise and anti-clockwise moments and the pressure, shear and tension loads are compared at one common location, X_1 (1m from the top of the pipe section modelled) and another, X_2. As the position of X_2 has to be determined to achieve the same bending moment at this location as determined by the global analysis, it depends on the load combination and has to be determined separately for each load case.

6.5 Results from Final Structural Verification for AS4/PEEK Riser with PEEK Liner $[0_3/(\pm 52)_5/90_4]$

Results from the stress analysis of the AS4/PEEK riser with PEEK liner for the eight most important load combinations in Table 6.3 are presented below for illustration.

(1) FSs for the AS4/PEEK with PEEK liner $[0_3/(\pm 52)_5/90_4]$ under global load case LC4 at the top of the composite region where, as X_1=1m and the bending moment applied at the top=105.2kN·m, X_2=3.535m

The FSs obtained under load case LC4_top for the in-plane longitudinal, in-plane transverse and in-plane shear stresses in all layers are presented in Figs. 6.9(a), 6.9(b) and 6.9(c), respectively, where layer 1 is the innermost composite layer. The minimum FS obtained for the liner is 3.11 and the minimum FSs for the stresses in the fibre direction are 3.42 in the axially reinforced layers (0°) (layer 3), 3.76 in the plies reinforced at ±52° (layer 4) and 4.29 in the circumferentially reinforced layers (90°) (layer 14) (Fig. 6.9(a)), for the transverse stresses, 3.49 in the axially reinforced layers (layer 3), 2.17 in the ±52° layers (layer 13) and 1.64 in the 90° layers (layer 17) (Fig. 6.9(b)) and, for the shear stresses in all layers, over 12.0 (Fig. 6.9(c)). Therefore, the minimum FS under load case LC4_top is 1.64 which is due to the stresses in the transverse direction in layer 17 (reinforced in the hoop direction) in the composite body.

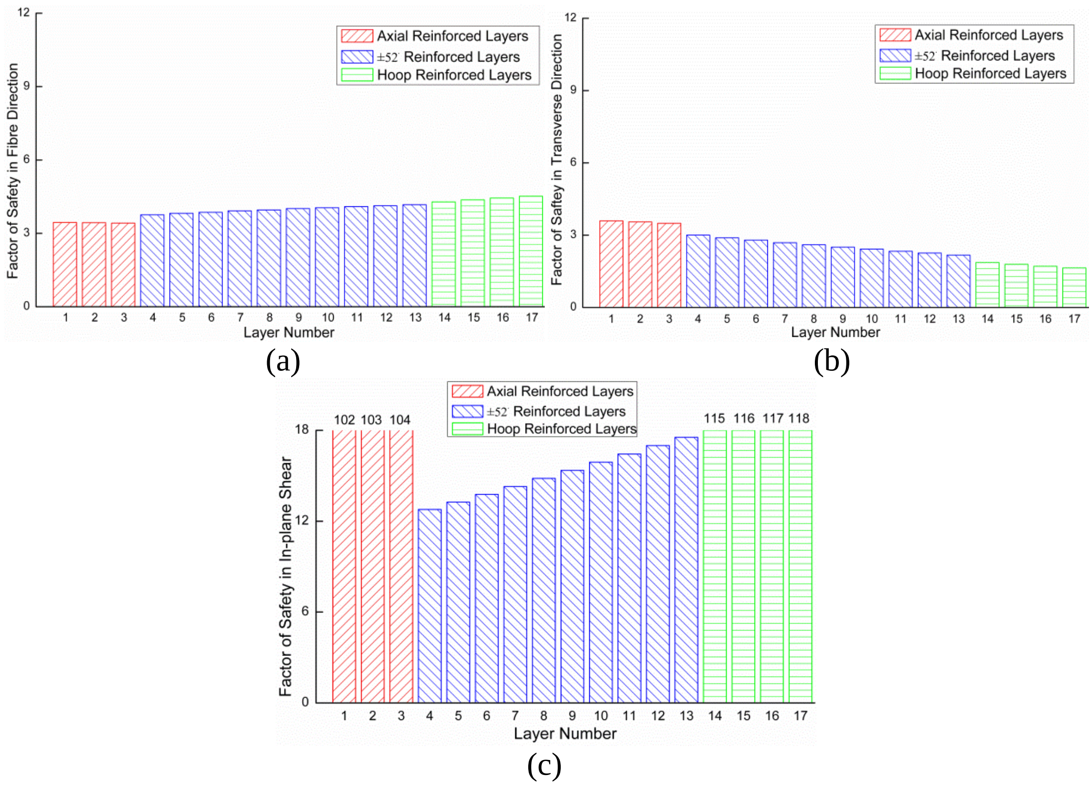

Fig. 6.9. FSs of composite layers with 0°, ±52° and 90° reinforcements under LC4_top for AS4/PEEK with PEEK liner in (a) fibre direction, (b) transverse direction and (c) in-plane shear

(2) FSs for the AS4/PEEK with PEEK liner $[0_3/(\pm52)_5/90_4]$ under global load case LC4 at the bottom of the composite region where, as X_1=1m and the bending moment applied at the top=91.9kN·m, X_2=2.655m

The FSs obtained under load case LC4_bottom for the in-plane longitudinal, in-plane transverse and in-plane shear stresses in all layers are presented in Figs. 6.10(a), 6.10(b) and 6.10(c), respectively. The minimum FS obtained for the liner is 3.00, and the minimum FSs for the stresses in the fibre direction are 4.83 in the axially reinforced layers (0°) (layer 3), 4.52 in the plies reinforced at ±52° (layer 4) and 5.11 in the circumferentially reinforced layers (90°) (layer 14) (Fig. 6.10(a)), for the transverse stresses, 9.26 in the axially reinforced layers (layer 3), 4.97 in the ±52° layers (layer 13) and 3.27 in the 90° layers (layer 17) (Fig. 6.10(b)), and, for the shear stresses in all layers, over 12.0 (Fig. 6.10(c)). Therefore, the minimum FS under load case LC4_bottom is 3.00 which is due to the Von Mises stress in the liner.

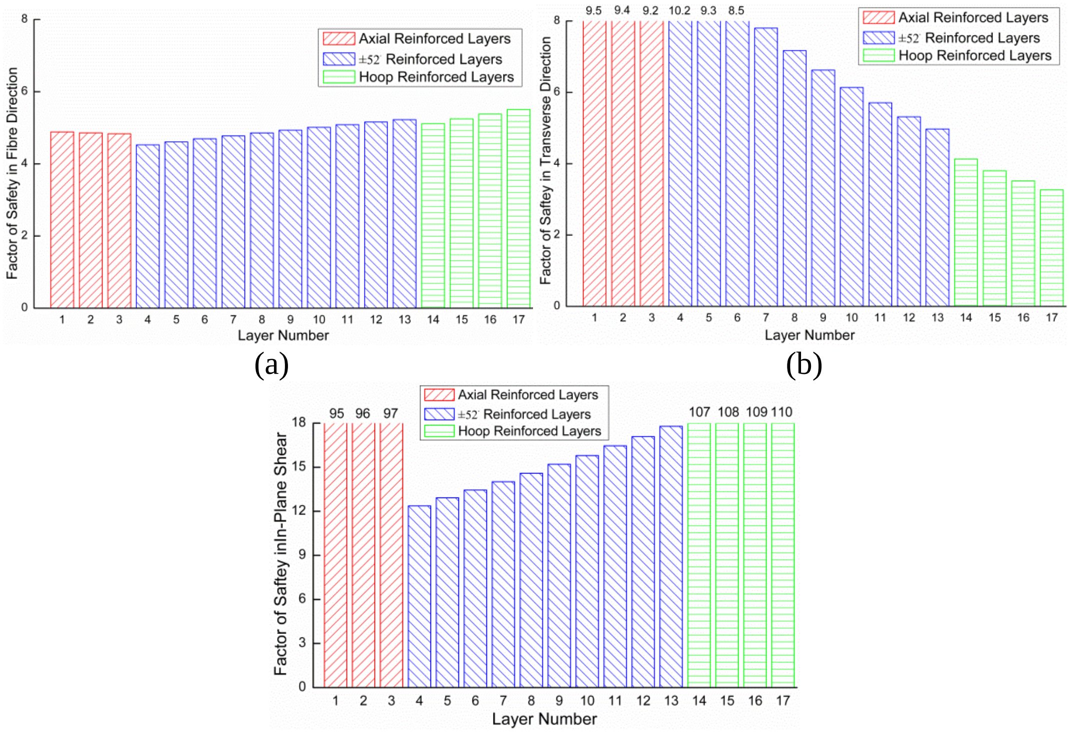

(a) (b)

(c)

Fig. 6.10. FSs of composite layers with 0°, ±52° and 90° reinforcements under LC4_ bottom for AS4/PEEK with PEEK liner in (a) fibre direction, (b) transverse direction, and (c) in-plane shear

(3) FSs for the AS4/PEEK with PEEK liner $[0_3/(\pm52)_5/90_4]$ under global load case LC5 at the bottom of the composite region where, as X_1=1m and the bending moment applied at the top=139.3kN·m, X_2=2.559m

The FSs obtained under load case LC5_ bottom for the in-plane longitudinal, in-plane transverse and in-plane shear stresses in all layers are presented in Figs. 6.11(a), 6.11(b) and 6.11(c), respectively. The minimum FS obtained for the liner is 2.96 and the minimum FSs for the stresses in the fibre direction are 4.33 in the axially reinforced layers (0°) (layer 3), 4.37 in the plies reinforced at ±52° (layer 4) and 4.92 in the circumferentially reinforced layers (90°) (layer 14) (Fig. 6.11(a)), for the transverse stresses, 9.12 in the axially reinforced layers (layer 3), 4.33 in the ±52° layers (layer 13) and 2.82 in the 90° layers (layer 17) (Fig. 6.11(b)) and, for the shear stresses in all layers, over 10.0 (Fig. 6.11(c)). Therefore, the minimum FS under load case

LC5_bottom is 2.82 which is due to the stresses in the transverse direction in layer 17 (reinforced in the hoop direction) in the composite body.

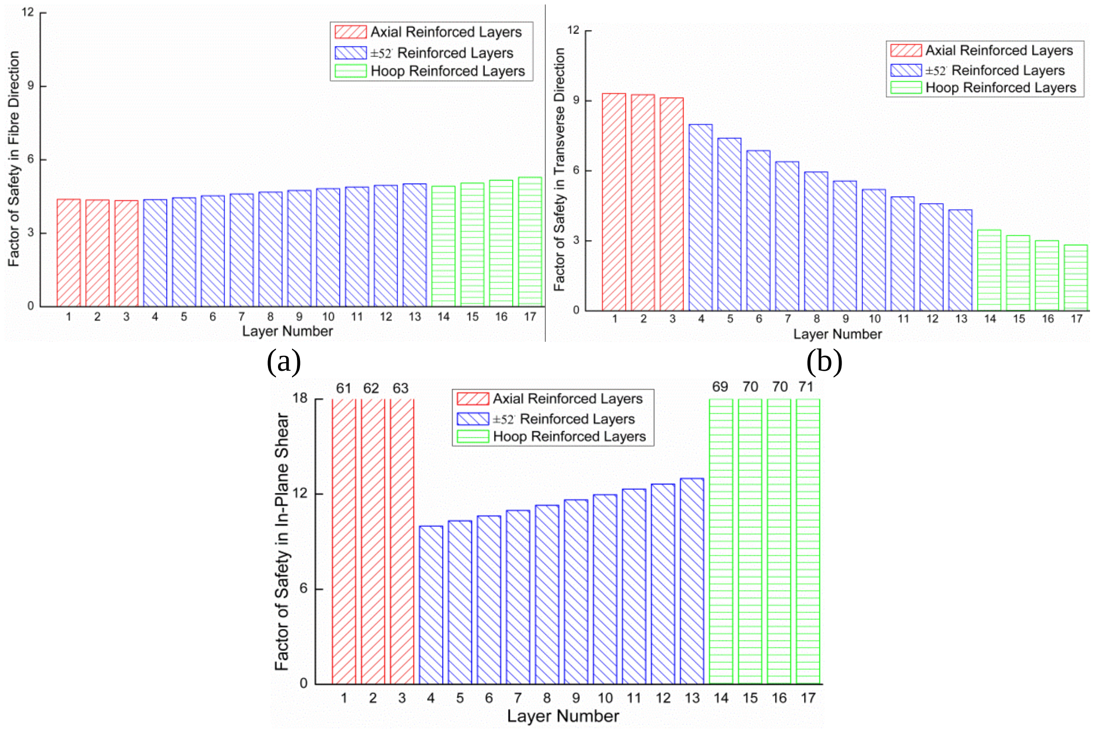

(c)

Fig. 6.11. FSs of composite layers with 0°, ±52° and 90° reinforcements under LC5_bottom for AS4/PEEK with PEEK liner in (a) fibre direction, (b) transverse direction and (c) in-plane shear

(4) FSs for the AS4/PEEK with PEEK liner $[0_3/(\pm52)_5/90_4]$ under global load case LC6 at the top of the composite region where, as X_1=1m and the bending moment applied at top=154.0kN·m, X_2=1.733m

The FSs obtained under load case LC6_top for the in-plane longitudinal, in-plane transverse and in-plane shear stresses in all layers are presented in Figs. 6.12(a), 6.12(b) and 6.12(c), respectively. The minimum FS obtained for the liner is 8.81 and the minimum FSs for the stresses in the fibre direction are 3.54 in the axially reinforced layers (0°) (layer 3), 12.00 in the plies reinforced at ±52° (layer 4) and 8.44 in the circumferentially reinforced layers (90°) (layer 17) (Fig. 6.12(a)), for the transverse stresses, 54.74 in the axially reinforced layers (layer 1), 3.14 in the ±52° layers (layer 13) and 2.00 in the 90° layers (layer 17) (Fig. 6.12(b)) and, for the shear stresses in all layers, 5.79 in layer 13 (Fig. 6.12(c)). Therefore, the minimum FS under load case LC6_top is 2.0 which is due to the transverse stresses in layer 17 (reinforced in the hoop direction) in the composite body.

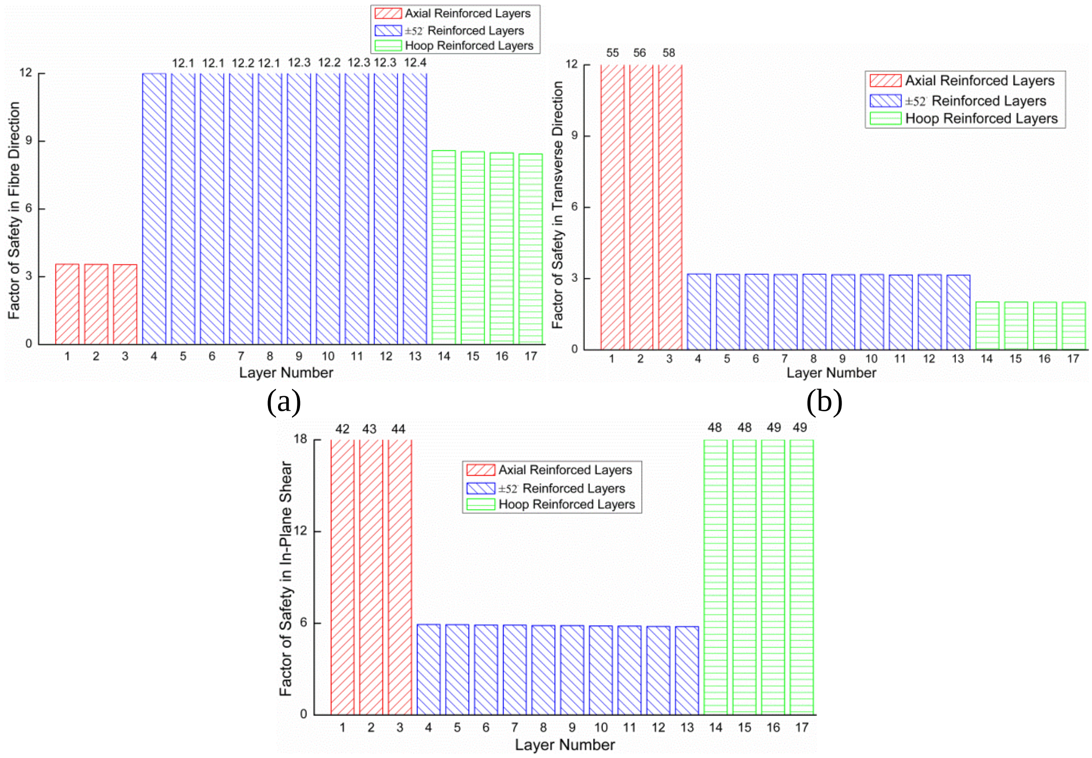

(c)

Fig. 6.12. FSs of composite layers with 0°, ±52° and 90° reinforcements under LC6_top for AS4/PEEK with PEEK liner in (a) fibre direction, (b) transverse direction and (c) in-plane shear

(5) FSs for the AS4/PEEK with PEEK liner $[0_3/(\pm 52)_5/90_4]$ under global load case LC6 at the bottom of the composite region where, as X_1=1m and the bending moment applied at the top=139.5kN·m, X_2=1.984m

The FSs obtained under load case LC6_bottom for the in-plane longitudinal, in-plane transverse and in-plane shear stresses in all layers are presented in Figs. 6.13(a), 6.13(b) and 6.13(c), respectively. The minimum FS obtained for the liner is 5.16 and the minimum FSs for the stresses in the fibre direction are 5.51 in the axially reinforced layers (0°) (layer 3), 8.66 in the plies reinforced at ±52° (layer 4) and 15.74 in the circumferentially reinforced layers (90°) (layer 14) (Fig. 6.13(a)), for the transverse stresses, 50.42 in the axially reinforced layers (layer 3), 9.69 in the ±52° layers (layer 13) and 4.63 in the 90° layers (layer 17) (Fig. 6.13(b)) and, for the shear stresses in all layers, 13.01 in layer 13 (Fig. 6.13(c)). Therefore, the minimum FS under load case LC6_bottom is 4.63 which is due to the transverse stresses in layer 17 (reinforced in the hoop direction) in the composite body.

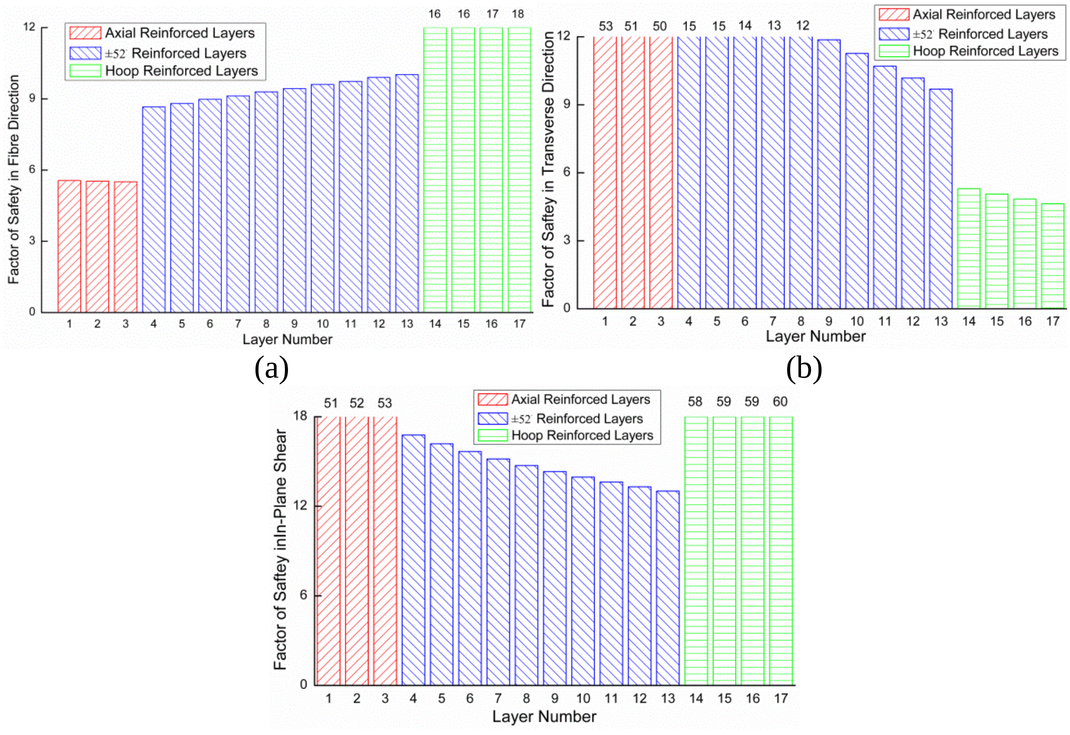

Fig. 6.13. FSs of composite layers with 0°, ±52° and 90° reinforcements under LC6_bottom for AS4/PEEK with PEEK liner in (a) fibre direction, (b) transverse direction and (c) in-plane shear

(6) FSs for the AS4/PEEK with PEEK liner $[0_3/(\pm52)_5/90_4]$ under global load case LC7 at the bottom of the composite region where, as X_1=1m and the bending moment applied at the top=201.6kN·m, X_2=1.950m

The FSs obtained for load case LC7_bottom for the in-plane longitudinal, in-plane transverse and in-plane shear stresses in all layers are presented in Figs. 6.14(a), 6.14(b) and 6.14(c), respectively. The minimum FS obtained for the liner is 4.99 and the minimum FSs for the stresses in the fibre direction are 4.87 in the axially reinforced layers (0°) (layer 3), 7.99 in the plies reinforced at ±52° (layer 4) and 14.10 in the circumferentially reinforced layers (90°) (layer 14) (Fig. 6.14(a)), for the transverse stresses, 48.40 in the axially reinforced layers (layer 3), 7.46 in the ±52° layers (layer 13) and 3.79 in the 90° layers (layer 17) (Fig. 6.14(b)) and, for the shear stresses in all layers, 10.78, in layer 13 (Fig. 6.14(c)). Therefore, the minimum FS under load case LC7_bottom is 3.79 which is due to the transverse stresses in layer 17 (reinforced in the hoop direction) in the composite body.

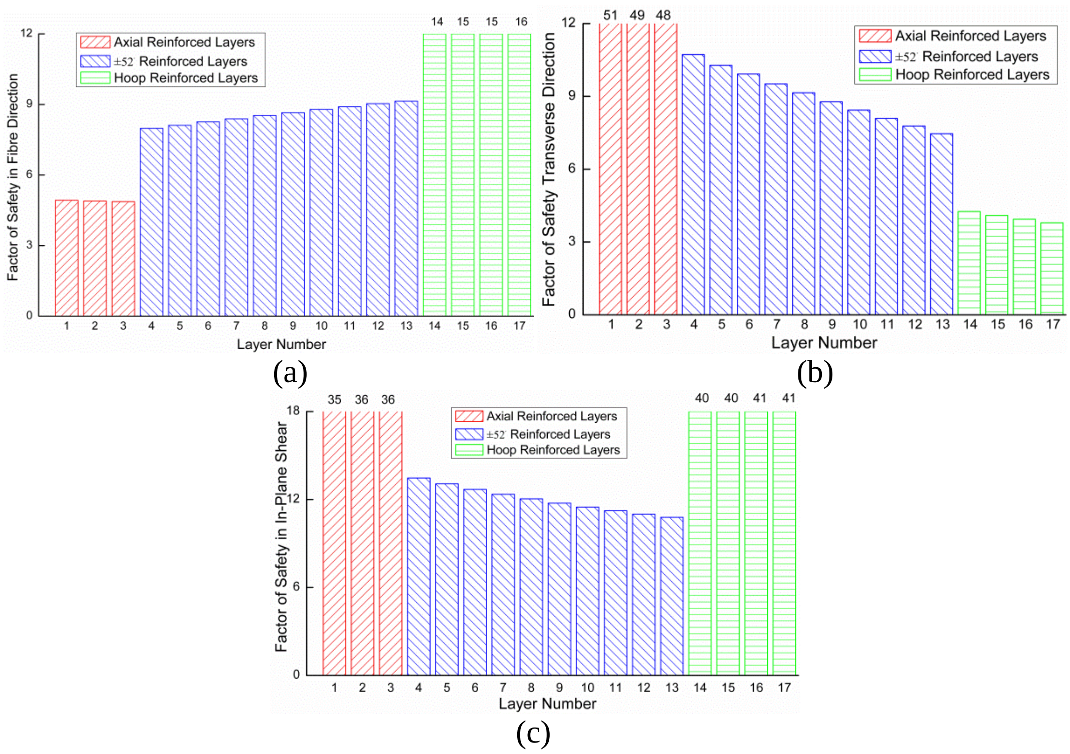

Fig. 6.14. FSs for composite layers with 0°, ±52° and 90° reinforcements under LC7_bottom for AS4/PEEK with PEEK liner in (a) fibre direction, (b) transverse direction and (c) in-plane shear

(7) FSs for the AS4/PEEK with PEEK liner $[0_3/(\pm 52)_5/90_4]$ under global load case LC9 at the top of the composite region where, as X_1=1m and the bending moment applied at the top=125.6kN·m, X_2=1.08m

The FSs obtained under load case LC9_top for the in-plane longitudinal, in-plane transverse and in-plane shear stresses in all layers are presented in Figs. 6.15(a), 6.15(b) and 6.15(c), respectively. The minimum FS obtained for the liner is 12.02 and the minimum FSs for the stresses in the fibre direction are 4.70 in the axially reinforced layers (0°) (layer 3), 14.71 in the plies reinforced at ±52° (layer 4) and 9.45 in the circumferentially reinforced layers (90°) (layer 17) (Fig. 6.15(a)), for the transverse stresses, 346.67 in the axially reinforced layers (layer 1), 3.97 in the ±52° layers (layer 5) and 2.75 in the 90° layers (layer 14) (Fig. 6.15(b)) and, for the shear stresses in all layers, 7.41 in layer 4 (Fig. 6.15(c)). Therefore, the minimum FS under load case LC9_top is 2.75 which is due to the transverse stresses in layer 17 (reinforced in the hoop direction) in the composite body.

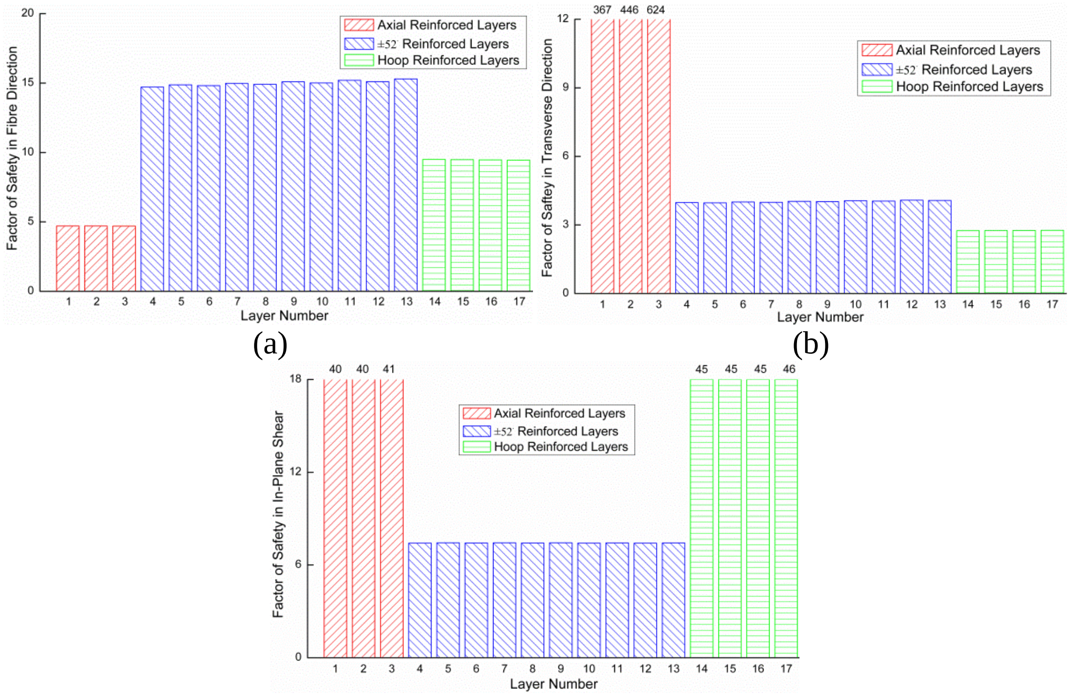

(c)

Fig. 6.15. FSs of composite layers with 0°, ±52° and 90° reinforcements under LC9_top for AS4/PEEK with PEEK liner in (a) fibre direction, (b) transverse direction and (c) in-plane shear

(8) FSs for AS4/PEEK with PEEK liner $[0_3/(\pm 52)_5/90_4]$ under global load case LC9 at the bottom of the composite region where, as X_1=1m and the bending moment applied at the top=201kN·m, X_2=1.340m

The FSs obtained under load case LC9_bottom for the in-plane longitudinal, in-plane transverse and in-plane shear stresses in all layers are presented in Figs. 6.16(a), 6.16(b) and 6.16(c), respectively. The minimum FS obtained for the liner is 11.73 and the minimum FSs for the stresses in the fibre direction are 7.00 in the axially reinforced layers (0°) (layer 3), 5.03 in the plies reinforced at ±52° (layer 4) and 3.04 in the circumferentially reinforced layers (90°) (layer 14) (Fig. 6.16(a)), for the transverse stresses, 9.24 in the axially reinforced layers (layer 3), 14.33 in the ±52° layers (layer 13) and 9.90 in the 90° layers (layer 14) (Fig. 6.16(b)) and, for the shear stresses in all layers, 6.16 in layer 4 (Fig. 6.16(c)). Therefore, the minimum FS for load case LC9_bottom is 3.04 which is due to the stresses in the fibre direction in layer 14 (reinforced in the hoop direction) in the composite body.

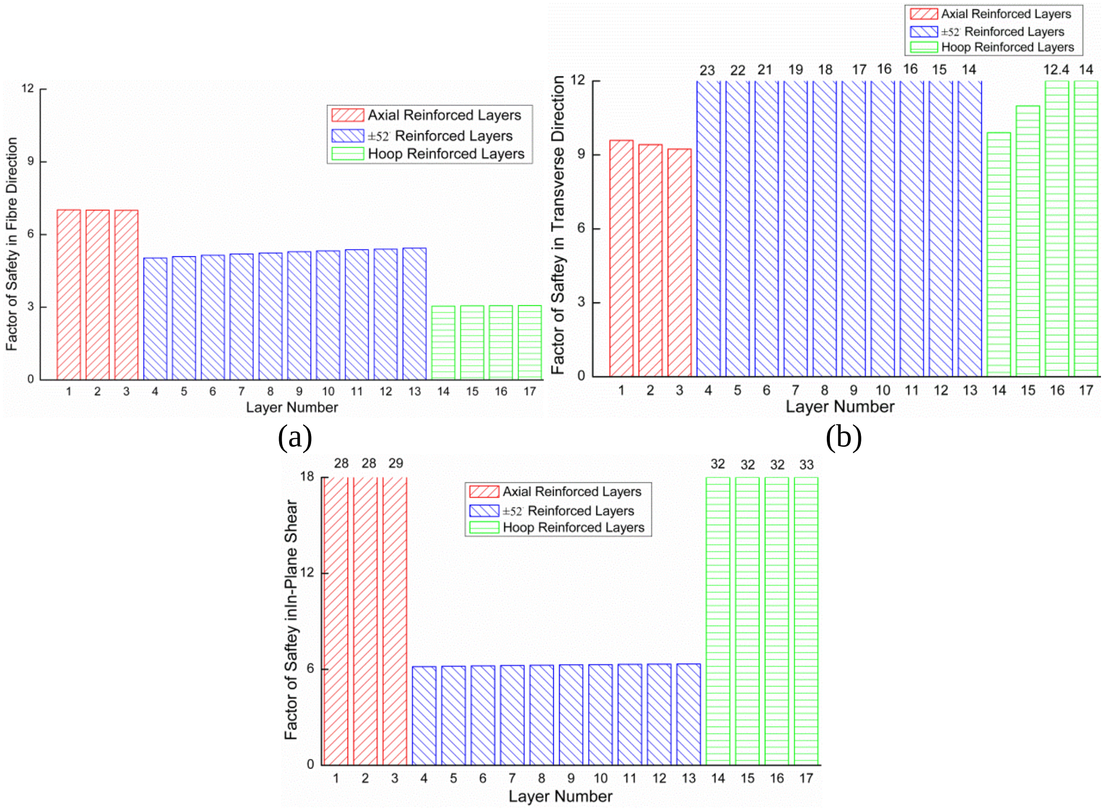

Fig. 6.16. FSs of composite layers with 0°, ±52° and 90° reinforcements under LC9_bottom for AS4/PEEK with PEEK liner in (a) fibre direction, (b) transverse direction and (c) in-plane shear

6.6 Global Design of AS4/Epoxy Bodies with Titanium and Aluminium Liners

Similar detailed results for the AS4/epoxy composite bodies with titanium and aluminium liners using the manually tailored design are presented in *Appendix D* and a summary of the design results for all three material combinations for the global design is presented in Table 6.7.

6.7 Consideration of Design allowing Matrix Cracking

In Section 5.12 *Chapter 5*, the tailored design of the AS4/PEEK composite body with PEEK liner is conducted with matrix cracking in order to investigate whether weight savings could still be achieved. In this section, a global analysis under different global load cases followed by structural verification using geometry with matrix cracking is conducted. The global design load cases employed in the global FEA are the same as those used for the tailored design geometries in Section 6.2 and the effective 3D composite tubular properties employed are listed in Table 6.4.

Table 6.4. Effective 3D properties of composite tube used in global analysis

Name (with matrix cracking)	$\rho_{effective}$ (kg/m^3)	$E_{x\_tension}$ (GPa)	$E_{x\_bending}$ (GPa)	E_y (GPa)	E_z (GPa)	G_{xy} (GPa)	G_{xz} (GPa)	G_{yz} (GPa)	ν_{xy}	ν_{xz}	ν_{yz}
AS4/PEEK-PEEK liner [0/±55/90]	1504.5	29.7	32.5	60.18	9.34	12.38	2.22	2.69	0.160	0.433	0.320

By conducting a global analysis of the entire riser using pipe elements (Pipe288), the critical locations and force, moment and pressure combinations at these locations are identified, and the magnitudes of the loads at these critical locations are listed in Table 6.5. The critical load combinations for the worst cases shown in Table 6.5 are taken to be those which are the most severe of those estimated using the tension modulus and those calculated using the bending modulus.

Table 6.5. Worst cases of critical load combinations for composite riser from global analysis

Load Case	Location	Tension (kN)	Internal Pressure (MPa)	External Pressure (MPa)	Shear Force (kN)	Bending Moment (kN·m)
4	Top	3123.5	44.3	0.7	42.8	53.4
	Bottom	2268.0	58.7	19.2	49.6	38.8
5	Top	3070	44.3	0.7	29.3	9.8
	Bottom	2226.2	58.7	19.2	75.6	57.3
6	Top	2251.0	1.8	0.7	97.5	37.2
	Bottom	1370.3	35.3	19.2	93.0	43.7
7	Top	2170.9	1.8	0.7	85.7	4.2
	Bottom	1337	35.3	19.2	134.4	61.7
8	Top	1988.6	0	0.7	77.6	39.9
	Bottom	341.7	0	19.2	114.2	20.2
9	Top	1934.7	0	0.7	118.1	4.6
	Bottom	301.2	0	19.2	164.9	28.6

In the final stage, a local analysis of the identified critical sections with their corresponding load combinations is again conducted using 3D layered solid elements. The minimum FSs in the PEEK liner and various layers of the composite body of the AS4/PEEK riser with the geometry allowing matrix cracking are given in Table 6.6.

Table 6.6. Minimum FSs for liner and composite layers of AS4/PEEK with PEEK liner with matrix cracking

Material Combination	Liner		Composite Layer- Fibre Direction		
	FS	LC	FS	Layer	LC
AS4-PEEK [0/±55/90]	2.88	LC5-B	2.47	15	LC4-T

Minimum FS required: 1.53 for composite layers, 1.74 for PEEK liner [72]

The results presented in Table 6.6 show that the composite tubular geometry optimised for minimum weight in the local design stage with matrix cracking is able to withstand the global loads successfully, providing FSs of just above the values required by the standards [72].

6.8 Summary and Discussions

Table 6.7 shows the minimum FSs for the liners and composite bodies of all three material combinations, and the critical global load cases in which they occur, from the global design of the composite riser.

Table 6.7. FSs for liners and composite layers of riser configurations studied

Material Combination	Liner		Composite Layer- Fibre Direction			Composite Layer- Transverse Direction			Composite Layer– In-Plane Shear		
	FS	LC	FS	Layer	LC	FS	Layer	LC	FS	Layer	LC
AS4-PEEK [0/±52/90]	2.96	LC5_B	3.04	14	LC9_B	1.64	17	LC4_T	5.79	13	LC6_T
AS4-Titanium [0/±53/90]	1.97	LC4_T	4.37	3	LC6_T	1.57	17	LC4_T	3.94	13	LC6_T
AS4-Aluminium [0/±53.5/90]	1.79	LC4_T	4.82	4	LC4_T	1.62	18	LC4_T	4.56	14	LC6_T

Minimum FS required: 1.53 for composite layers, 1.74 for PEEK liner and 1.68 for metallic liners [72]

The results presented in Table 6.7 show that all the composite tubular geometries developed for minimum weight under the local load conditions in *Chapter 5* successfully withstand the global loads for the configuration of the entire riser developed in this chapter, providing their FSs are just above the values required by the standards. As mentioned in Section 6.2, not only the tension and stress joints but also the three standard riser joints at around sea level are retained as X80 steel because their forces and moments are much higher at the end regions of the composite riser (Figs. 6.5, 6.6 and 6.7) where the composite joints designed for local loadings would fail. In order to ensure that the entire composite riser is safe, we could either redesign the composite riser joints, at least in the upper section, with higher thicknesses which would require repeating the iterative design process in *Chapter 5*, again optimising the orientations and lamination sequences for minimum weight and repeating the global design process to ensure that the newly optimised geometry is safe under global loads. This would mean going through the cycles between the local and global design a few times before the composite joints could withstand the concentrated forces and moments at their ends. On the other hand, the simpler approach adopted in this thesis is to use steel (X80) for the three end joints which experience concentrated loads, with the rationale being that any increase in weight due to using three steel joints compared with redesigning the entire composite riser will be negligible in terms of the structural weight of the entire riser.

In the detailed results from the structural verification, it is seen that, although the most vulnerable layer of the riser geometry is different for different load cases, the minimum FSs are obtained in the outermost composite lamina for the stresses in the transverse direction for all three material combinations, and are 1.64, 1.57 and 1.62, respectively, for the AS4/PEEK with PEEK liner and AS4/epoxy with titanium and aluminium liners. For the AS4/epoxy with titanium liner, its minimum FS is only 2.5% over the specified requirement of 1.53 for its composite body. It may also be noted that the top joint (segment) of the composite riser is the most critical region and that, of all the cases, the minimum FS occurs under global load case 4, the shut-in condition with a 100-year hurricane, which has the highest effective top tension and a large bending moment. Together, *Chapters 5* and *6* contain the complete process for the design of a composite riser using both the conventional and manually tailored approaches. In the next chapter, a mathematical optimisation technique is employed to corroborate and authenticate the efficiency of the manual iterative approach employed for the tailored design in *Chapter 5* and check whether further improvements are possible.

CHAPTER 7

SAEA OPTIMISATION OF COMPOSITE RISER

7.1 Introduction

From the analysis in previous chapters, it is evident that the benefits of applying FRP composite materials in riser design become more significant when different design variables are tailored to specific requirements using the tailored design approach. In the local design in *Chapter 5*, the geometric configuration of the composite tube is selected to provide the minimum structural weight using a manual iterative design process, wherein the thicknesses, fibre orientations and stacking sequence of its composite layers are progressively adjusted to provide the minimum required factor of safety (FS) for each of the four local design load cases. The iterative design procedure developed using a common-sense engineering approach for both the conventional and proposed manually tailored designs yields good results in terms of proving that substantial weight savings can be achieved using laminated composite materials for the manufacture of a riser, particularly from the tailored design with fibre reinforcements at appropriate off-axis angles. Although the geometries obtained using the manually tailored design procedure provide an approximate 25% weight saving over the conventional composite riser design (with only axial and hoop reinforcements), they require many evaluations (FEA verifications) as well as expertise in making design decisions.

In this chapter, a mathematical optimisation technique is employed to corroborate and authenticate the efficiency of the manually tailored design approach employed in *Chapter 5* and incorporate any possible improvements. This design optimisation is performed using the population-based Surrogate Assisted Evolutionary Algorithm (SAEA). The objective is minimisation of the structural weight and satisfaction of the critical local as well as global load cases which provide the constraints. Its optimal design results are verified by employing the optimum geometry in a finite element analysis (FEA) model to ensure that the local and global design requirements are satisfied.

For each material combination selected, the design parameters of the composite riser joint comprise: (1) the thicknesses of different composite layers; (2) the thickness of the liner; (3) the reinforcement angles of the composite layers; (4) the numbers of composite layers; and (5) the stacking sequence. For every design parameter, there are almost unlimited possibilities which cannot be optimised without simplification. The design optimisation of such a complex system represents a formidable challenge for conventional gradient-based optimisation approaches because of their high likelihood of converging at non-global optima and their sensitivity to the starting design point due to the natures of their local searches [115-117]. Evolutionary algorithms are particularly suitable for non-linear optimisation problems with non-smooth design spaces by virtue of their global searches [117]. However, as the application of population-based optimisation approaches to complex systems commonly entails prohibitive computational cost, surrogate models can effectively mitigate the computational load by replacing expensive function evaluations with approximations [116, 118]. In this chapter, the structural weight of the tailored geometry, i.e., with off-axis reinforcements of the standard riser joint, is minimised using the optimisation technique SAEA and the results compared with those obtained from the conventional design method (with only axial and hoop reinforcements) and manually tailored design developed in *Chapter 5*.

The following sections in this chapter describe the generation and modification processes of the training database, the optimisation procedure and comparisons of the results from the SAEA optimisation and manual iterative design methods for minimum structural weight conducted in the earlier chapters for the selected composite risers, namely, the AS4/PEEK with PEEK liner, and AS4/epoxy with titanium and aluminium liners. Also, the optimised geometries are verified using a detailed FEA.

7.2 Optimisation Approach

The Surrogate Assisted Evolutionary Algorithm (SAEA) [119] used in this study was developed by the Multidisciplinary Design Optimisation (MDO) group at the UNSW campus in Canberra. It is an elitist real-coded genetic algorithm with simulated binary crossover and polynomial mutation [117, 120], and the database for training and verification of its optimisation code are generated using the FEA software ANSYS13.0.

7.2.1 Design Requirements and Conditions

The composite riser joints considered in the study are based on the same design requirements for a 2000m water depth in the Gulf of Mexico (see Section 3.3, *Chapter 3*) used earlier. The design variables are simplified into six geometric parameters for each material combination: (1) the thickness of the liner, t_{liner}; (2) the thicknesses of the 0° (axial) layers, t_0, (3) ±θ° (angular) layers, t_θ, (4) and 90° (hoop) layers, t_{90}; (5) the angles of the ±θ° (angular) layers, ±θ°; and (6) the variable indicating the stacking sequence, *n* (Fig. 7.1). The numbers of layers of the 0^o, ±θ° and 90° plies are taken to be the same as those determined by the manually tailored design in *Chapter 5*, i.e., 3 plies of 0^o, 10 of $\pm\theta°$ and 4 of 90^o for the AS4/PEEK and AS4/titanium, and 4 of 0^o, 10 of $\pm\theta°$ and 4 of 90^o for the AS4/aluminium. The lamina thicknesses of layers with the same orientations are assumed to be equal and, by keeping the numbers of layers fixed, the design optimises them, i.e., the total thickness of all layers with each fibre orientation.

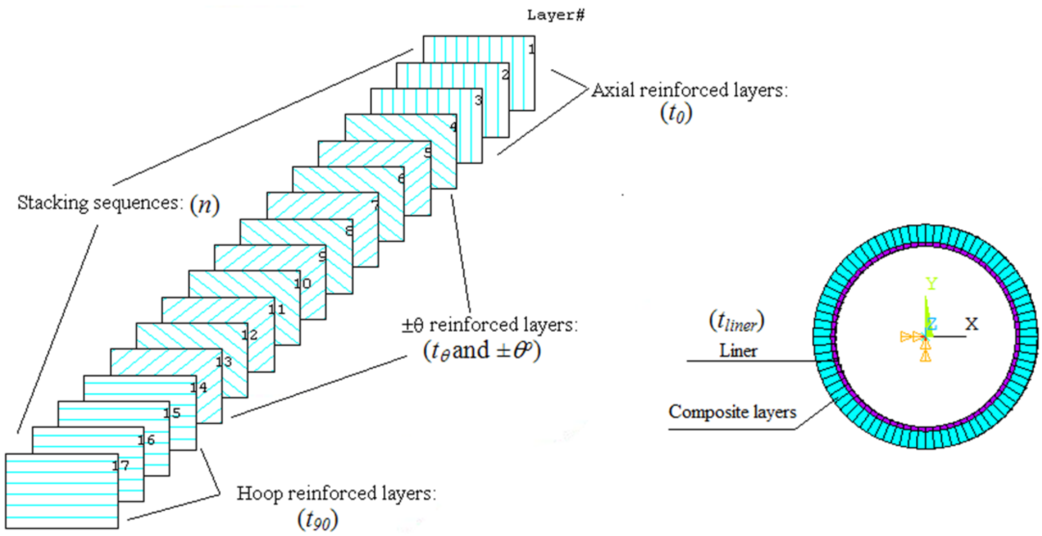

Fig. 7.1. Parametric representation of composite riser tube

The ranges given for the design variables are: (1) 6-12mm for t_{liner} for the PEEK liner and 2-8mm for the metal liners; (2) 0-2.5mm for t_0; (3) 0-2.5mm for t_θ; (4) 0-2.5mm for t_{90}; (5) 0-90° for the reinforcement angle, θ; and (6) n_1,.., n_6 for the stacking sequence variable, n, where n_1=[0/±θ/90], n_2=[0/90/±θ], n_3=[±θ/0/90], n_4=[±θ/90/0]; n_5=[90/0/±θ] and n_6=[90/±θ/0]. The stacking sequence proceeds from the inside to outside of the riser wall. Normally, the database for optimisation is created by a design of experiment (DOE) using different sampling methods, such as the random, Latin Hypercube, Orthogonal Array (OA) and Hammersley Sequence [121]. In this study, OA sampling, which could provide a uniform coverage of the design space [121-123], is selected. An OA is a matrix of n rows and k columns with every element being one of the q symbols 0, . . . , q-1 and its notation is OA (n, k, q, t), where n is the row number of the array which depends on both the distinct level number, q, which means that q points are included for each design variable, and strength level number, t, and k the number of design variables. More specifically, in this study, the OA program is employed as OA ($2q^2$, k, q, 2) [124] which, for a problem with 6 design variables using 5 distinct levels, requires only 50 samples. In contrast, a full-factor sampling method for the same problem would require 7776 (6^5) samples.

The design constraints are the requirements of the local load cases (see *Chapter 3*) 1 (burst), 2(a) (pure tension), 2(b) (tension with external pressure), 3 (collapse) and 4 (buckling).

For load cases 1, 3 and 4, their requirements for pressure are taken as 155.25MPa, 58.5 MPa and 58.5MPa, respectively. The tension force requirements for load cases 2(a) and 2(b) depend on the geometry of the riser joint and have to be calculated in the optimisation iterative cycle.

7.2.2. Objective Function

The objective function of the optimised design to be minimised is the structural weight, as defined by

$$W_{structural} = \rho_{liner} \times \pi \times (R_{inter}^2 - R_i^2) + \rho_{composite} \times \pi \times (R_o^2 - R_{inter}^2) \tag{7-1}$$

where R_i is the internal radius of the liner, R_{inter} the external radius of the liner (internal radius of the composite body), R_o the external radius of the composite body, ρ_{liner} the density of the liner and $\rho_{composite}$ the density of the composite body. The optimised geometry must also satisfy the requirements of both the local and global loads.

7.2.3. Material Combinations

The material combinations considered in the optimisation design are the AS4/PEEK with PEEK liner, and AS4/epoxy with titanium and aluminium liners which are selected based on the promising results presented in *Chapters 5 and 6*. The elastic constants and long-term strengths of the unidirectional composite lamina used in the study are shown in Table 3.13 and Table 3.14 (*Chapter 3*), respectively, and the material properties of the liners listed in Tables 3.8, 3.10 and 3.11 (*Chapter 3*), respectively.

7.2.4. FEA Model

The full design process for the composite riser consists of the local design, global analysis and structural verification stages. The FEA models used in the optimisation process are the same as those used in *Chapters 5* and *6* for the local and global designs, respectively, as are the entire riser configuration and FS requirements.

7.2.5. Design Optimisation

In order to optimise the geometry of the composite riser joint, its structural weight has to be minimised for the given load requirements which make up the optimisation constraints.

The optimisation problem is stated as:

Minimise: structural weight

Subject to: local design requirements, namely, burst, pure tension, tension with external pressure, external pressure and buckling; and

Design variables: $x_{Li} \leq x_i \leq x_{Ui}$ ($i = 1, \ldots, 6$).

Design optimisation is performed in an iterative manner through a sequential process. Fig. 7.2 schematically shows the optimisation chain which consists of the following six steps.

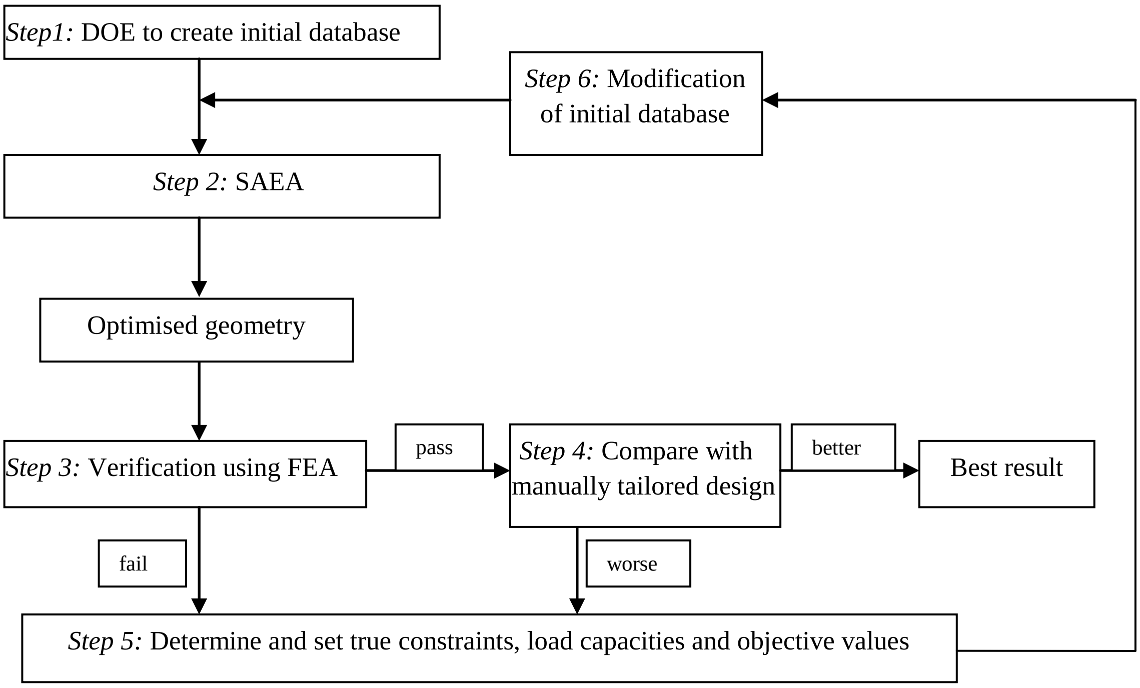

Fig. 7.2. Optimisation chain

- *Step 1:* Create the initial training database through the DOE using OA for each selected material combination.
- *Step 2:* Employ the SAEA to determine an 'optimised' result based on the training database.
- *Step 3:* Verify the predicted 'optimised' solution using a FEA simulation and, if it passes, go to *Step 4*; otherwise, go to *Step 5*.
- *Step 4:* Compare the results from the 'optimised' solution and manually tailored design approach developed in *Chapter 5*. If the former is better than the latter, it is considered the best result; otherwise, go to *Step 5*.
- *Step 5:* Determine the true values of the constraints, load capacities and objective functions from the FEA results for the geometry optimised in *Step 2* and go to *Step 6*.
- *Step 6:* Modify the training database to include the additional points consisting of the true constraints and objective values obtained in *Step 5*. (Note: in *Step 6* of the

first iteration, the results from the manually tailored design conducted in *Chapter 5* are also added to the training database).

At the beginning of the iteration steps (creation of the initial training database), the constraints and objective functions are estimated from the initial trial geometry of the riser using FEA. At the end of *Step 2*, along with the 'optimised' geometry, the values of the constraints, load capacities and objective functions corresponding to it are also estimated. However, as these values are only approximate as they are taken from the surrogate model and may differ from the 'true' values, in *Step 5,* they are recalculated using the FEA results for the 'optimised' geometry determined in *Step 2*.

In every design optimisation cycle, optimisation is performed over 200 generations, each with a population size of 200, and simulated binary crossover and polynomial mutation are used as recombination operators with probabilities of 0.9 and 0.1, respectively. To reduce computational effort, the optimisation process is efficiently assisted by predictions from various surrogate models [116, 125], including the operational range site model (ORSM), response surface methodology (RSM), ordinary radial basis function (ORBF), radial basis function (RBF) and design and analysis of computer experiments (DACE). Then, the approximation given by the surrogate model with the best prediction accuracy replaces that of the actual FEA evaluation when the solid diagonal distance of the solution to the closest point in the archive is within a given threshold (5%). Surrogate models are trained using the solutions initially obtained by OA [124] sampling, 80% of which are used to train the surrogate models and the other 20% to check accuracy.

The structural weight is employed as the objective function for minimisation (Eq.7-1) and the feasibility of each individual is verified by the true constraint functions through FEA solutions. Six design parameters are used as the design variables with respective limits (their upper and lower bounds are given in Section 7.2.1).

7.3 Optimisation Results for AS4/PEEK Composite Body with PEEK Liner

The geometry of the composite riser is optimised following the optimisation chain given in Section 7.2.5 for the three selected material combinations, noting that the optimisation SAEA is applied to the tailored design, i.e., the geometry including off-axis reinforcements. The results for the AS4/PEEK composite body with PEEK liner obtained by SAEA after verification of its optimised geometry are detailed below for illustration.

7.3.1 Iteration Cycles of Optimisation

As shown in the optimisation chain in Fig. 7.2, in the first cycle of optimisation, the initial DOE database (for the AS4/PEEK with PEEK liner riser consisting of the design variables, load capacities and structural weight listed in Table E.1 in *Appendix E*) is employed. The progressive result for the objective function value (structural weight) using the initial DOE database in the first SAEA optimisation cycle is plotted in Fig. 7.3. This optimisation, performed for up to 200 generations based on the initial DOE database, provides a reduction in structural weight from 63.1kg/m to 45.3kg/m (the true value is 44.91kg/m). It may be noted that this optimisation result approaches its asymptotic value within about 60 generations.

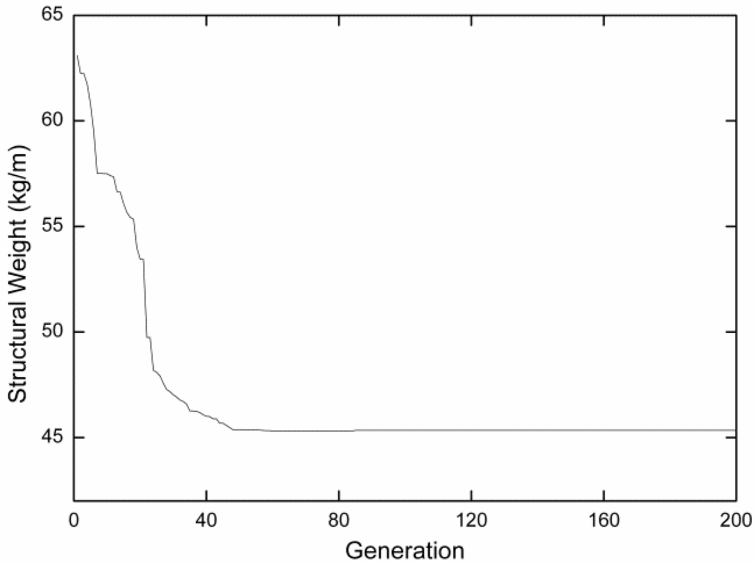

Fig. 7.3. Progress of optimisation in first cycle

Although the 'optimised' structural weight of 44.91kg/m obtained from the first optimisation cycle is about 12% higher than the minimum weight of 39.93kg/m obtained from the manually tailored design in *Chapter 5*, it is still lower than the minimum weight from the conventional design of 52.41kg/m. Therefore, it is obvious that more iterative cycles are needed to generate a more accurate 'optimised' geometry. In the iterative optimisation process, the ranges of the variables, training database and constraint functions are modified after each cycle to converge towards the final geometry. It is found that the predicted load capacities are somewhat larger than their true values while the predicted minimum structural weight is correct. Although the errors in load capacities predicted by the surrogate models in the optimisation are quite small, they can cause many predicted 'feasible' points to violate the constraint functions in the verification using the FEA simulation. A detailed analysis shows that, for the AS4/PEEK with PEEK liner riser, the constraints of load cases 1 (burst), 3 (collapse) and 4 (buckling) are quite sensitive to the design.

The true structural weights obtained after every optimum design cycle are plotted against the cycle numbers in Fig. 7.4, where the dashed-dotted green line represents the structural weight obtained by the manually tailored design developed in

Chapter 5 (39.93kg/m). The blocks in the figure show the true structural weights after each optimisation cycle and a cross inside any of them indicates that the 'optimised' geometry in the given cycle number satisfies all the constraint requirements (local load cases 1-4), as determined from the results using the FEA simulation.

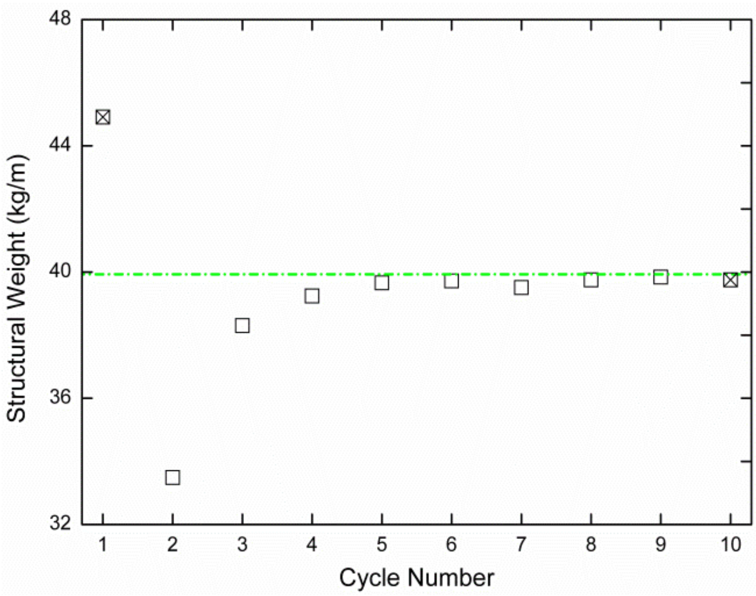

Fig. 7.4. True structural weight results for every optimisation design cycle

In Fig. 7.4, it is evident that, after three or four cycles, the optimised structural weight asymptotes to the value of the minimum weight from the manually tailored design but that a fully feasible optimised geometry which satisfies all the constraints and provides less structural weight than that of the manually tailored design is obtained only in the tenth cycle, after which the optimised structural weight is 39.75kg/m.

The final values obtained after the 10^{th} cycle for the six design parameters, t_{liner}, t_0, t_θ, t_{90}, $\pm\theta^o$ and n, are 6.0mm, 1.24mm, 1.36mm, 1.64mm, 51.0^o and 1, respectively, for the AS4/PEEK with PEEK liner riser. This optimised geometry providing the least weight is verified by the FEA simulation during the optimisation process.

The values of the design variables of the optimum design (SAEA) of the AS4/PEEK with PEEK liner are plotted in Fig. 7.5 for comparison with those of the conventional and tailored designs using the iterative approach of manual inspection and selection. It should be noted that, for the conventional design, as there is no off-axis angle of reinforcement, θ, there is no t_θ and no stacking sequence variable, *n*. In this figure, the values of the design variables in the Y axis are normalised with the values shown at the top of the figure in order to facilitate the display of all the values in the same graph. It can be seen that the thicknesses of the axial and off-axis layers from the tailored designs using the manual approach and mathematical optimisation (SAEA) yield different results, while the thicknesses of the hoop layers and liner are the same as are the stacking sequences. The optimum angles of the off-axis layers are also different, being 52^o for the manually tailored design and 51^o for the SAEA tailored design. However, the overall thicknesses of the configurations of both tailored designs are quite close, being 30mm and 29.88mm, respectively as are the structural weights, being 39.93kg/m and 39.75kg/m, respectively.

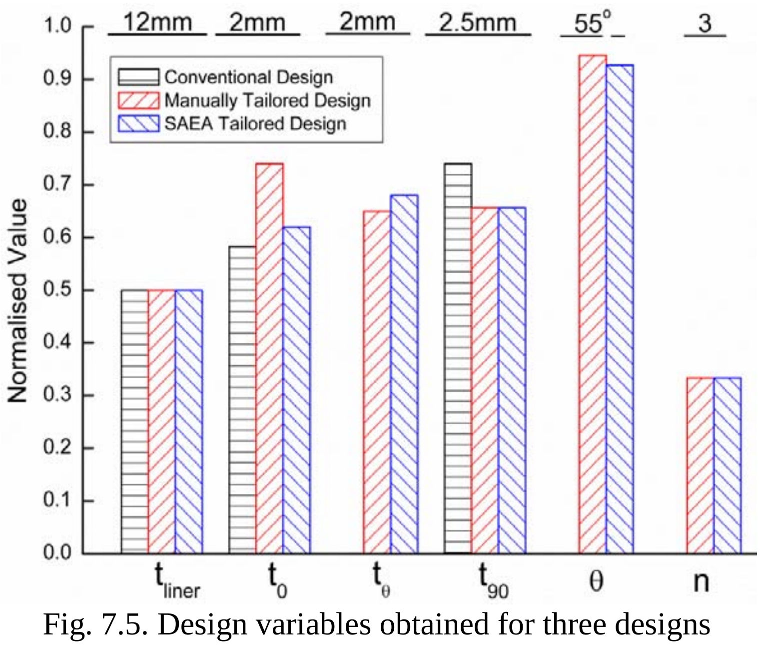

Fig. 7.5. Design variables obtained for three designs

7.3.2 Verification for Local Load Cases

The local load capacities of the optimum geometry using SAEA for the AS4/PEEK with PEEK liner are presented in Fig. 7.6, normalised with respect to the magnitudes of the corresponding load requirements, and the normalised load capacities of the manually optimised geometry (manually tailored design). It can be seen that, although there are some differences in the load capacities provided by the two tailored design approaches, their structural weights are very close. The green dashed line with the ordinate value of 1.0 represents the normalised load requirement for each case.

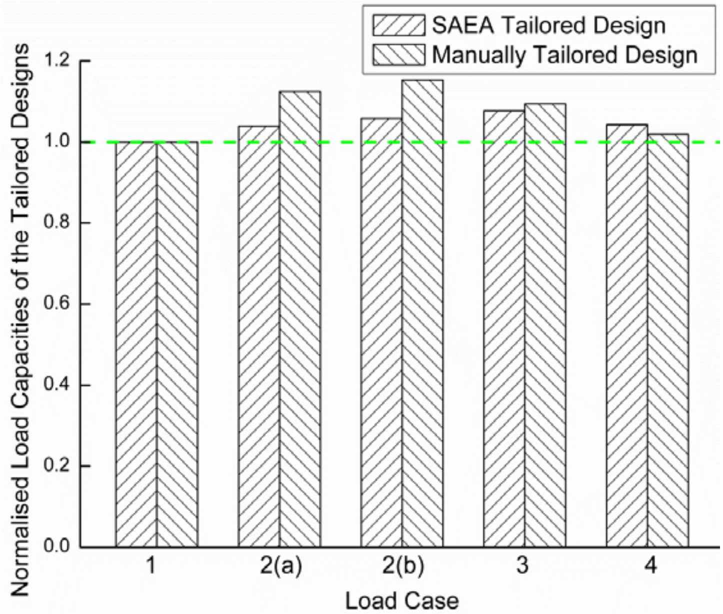

Fig. 7.6. Comparison of load capacities of tailored designs

7.3.3 Verification for Global Load Cases

As the optimisation process using SAEA is based on local load constraints, the performance of the optimum geometry for global load cases has to be verified. Both the global design procedure for all the material combinations selected, and the global design load cases used for the global FE analysis are the same as those in *Chapter 6*. The effective 3D composite tubular properties employed in the global FE analysis are listed in Table 7.1 using the same calculation process as in *Chapter 6*.

Table 7.1. Effective 3D properties of composite tube used in global analysis

Name	$\rho_{effective}$ (kg/m^3)	$E_{x\_tension}$= $E_{x\_bending}$ (GPa)	E_y (GPa)	E_z (GPa)	G_{xy} (GPa)	G_{xz} (GPa)	G_{yz} (GPa)	ν_{xy}	ν_{xz}	ν_{yz}
AS4/PEEK-PEEK liner [0/±51.0/90]	1513.1	27.8	49.3	9.57	17.24	2.49	2.75	0.265	0.372	0.26

Conducting a global analysis of the entire riser using pipe elements (Pipe288), as in *Chapter 6,* the critical locations and force, moment and pressure combinations at these locations are identified (the magnitudes of the loads at the critical locations are listed in Table F.1 in *Appendix F*). In the final stage, a local analysis of the identified critical sections with the corresponding load combinations is conducted again using layered solid elements, as in *Chapter 6*. The minimum FSs in the PEEK liner and various layers of the composite body of the AS4/PEEK riser with the geometry optimised using the optimisation technique SAEA are given in Table 7.2.

Table 7.2. Minimum FSs for liner and composite layers of AS4/PEEK with PEEK liner with SAEA optimised geometry

Material Combination	Liner		Composite Layers-Fibre Direction			Composite Layers-Transverse Direction			Composite Layers–In-plane Shear		
	FS	LC	FS	Layer	LC	FS	Layer	LC	FS	Layer	LC
AS4-PEEK [0/±51.0/90]	2.96	LC5-B	2.94	14	LC9-B	1.64	17	LC4-T	5.13	13	LC6-T

Minimum FS required: 1.53 for composite layers, 1.74 for PEEK liner and 1.68 for metallic liners [72]

The results presented in Table 7.2 show that the composite tubular geometry optimised for minimum weight in the local design stage using SAEA is able to successfully withstand the global loads providing their FSs are just above the values required by the standards [72].

7.4 Optimisation Results for AS4/Epoxy Composite Bodies with Titanium and Aluminium Liners

The similar results obtained for the AS4/epoxy composite bodies with titanium and aluminium liners using SAEA are presented in *Appendix F* and the design results for all three material combinations listed in Table 7.3.

7.5 Comparison of Results from Optimisation

The results from the optimisation for minimum structural weight using the mathematical approach of SAEA are compared with those obtained using the manual iteration procedure for the three selected material combinations, namely, the AS4/PEEK composite body with PEEK liner, and AS4/epoxy composite bodies with titanium and aluminium liners in Table 7.3 and Figs. 7.7 and 7.8. For each material combination, the table lists the stacking sequence, thicknesses of the liner and composite layers and structural weight obtained using the conventional design (with only hoop and axial reinforcements) and tailored design using the manual iterative approaches in *Chapter 5* and optimised geometry using the SAEA in this chapter.

Table 7.3. Comparison of optimisation results with previous designs

Material Combination	Design Method	Configuration	Thickness(mm)					Structural Weight(kg/m)
			liner	0^o	θ^o	90^o	total	
AS4/PEEK - PEEK liner	Conventional design	[liner/90/$(0/90)_{10}$]	6.00	1.165	0.00	1.85	38.00	52.41
	Manual tailored design	[liner/0_3/$(+52.0,-52.0)_5$/90_4]	6.00	1.48	1.30	1.64	30.00	39.93
	SAEA Tailored design	[liner/0_3/$(+51.0,-51.0)_5$/0_4]	6.00	1.24	1.36	1.64	29.88	39.75
AS4/epoxy - titanium liner	Conventional Design	[liner/90/$(0/90)_{10}$]	2.00	1.385	0.00	2.15	39.50	59.56
	Manual tailored design	[liner/0_3/$(+53.0,-53.0)_5$/90_4]	2.00	1.70	1.64	1.75	30.50	45.71
	SAEA tailored design	[liner/0_3/$(+53.4,-53.4)_5$/90_4]	2.00	1.77	1.61	1.73	30.33	45.46
AS4/epoxy - aluminium liner	Conventional Design	[liner/90/$(0/90)_{10}$]	2.00	1.525	0.00	2.25	42.00	60.93
	Manual tailored design	[liner/0_4/$(+53.5,-53.5)_5$/0_4]	2.00	1.62	1.60	1.88	32.00	45.35
	SAEA tailored design	[liner/0_4/$(+53.4,-53.4)_5$/90_4]	2.00	1.62	1.57	1.93	31.90	45.20

As can be seen in Table 7.3 and Fig. 7.7, the difference in structural weight between the manually tailored design and the design optimised with SAEA is minimal (both being significantly lower than the weight obtained using the conventional design) and their stacking sequences are exactly the same for all three material combinations. It is also clear that, in every case, the mathematical optimisation (SAEA tailored design) gives marginally better weight savings (about 0.5%) than the manually iterated tailored design. The main reason for this is that adding the manually tailored design results to the training database provides more accurate approximations but allows the optimisation procedure to converge to these points using surrogate models.

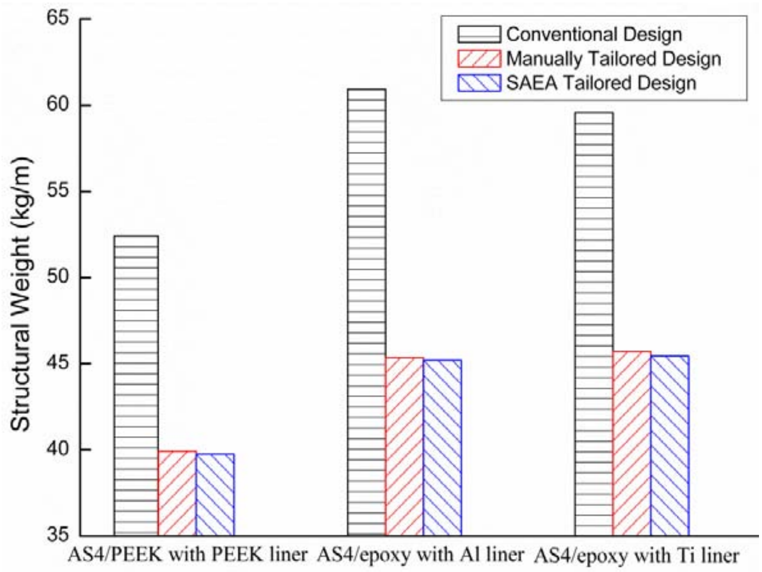

Fig. 7.7. Comparison of structural weights obtained for three designs

The improved structural weight obtained from the SAEA tailored design comes from small reductions in the overall thicknesses of the composite bodies compared with those from the manually tailored design, as seen in column 8 in Table 7.3. However, both these designs provide significant improvements in structural weight and thickness (over 20%) over the conventional design, as seen in Figs. 7.7 and 7.8.

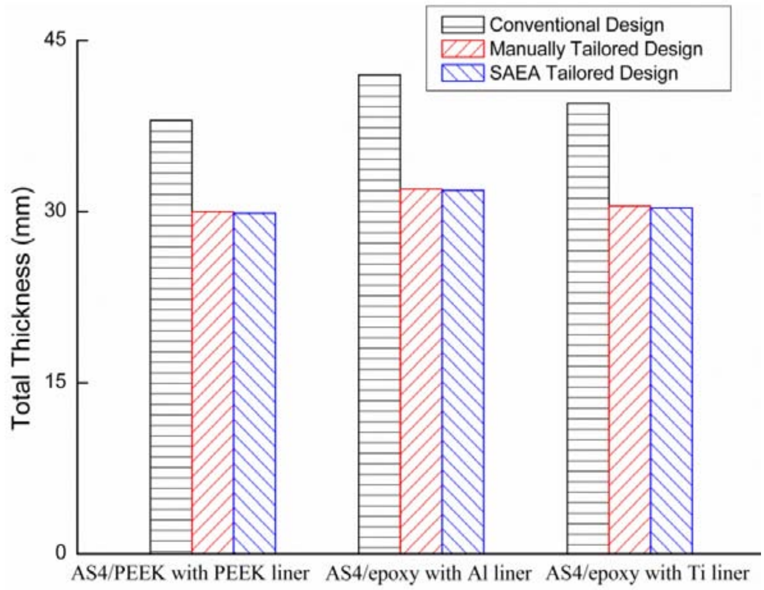

Fig. 7.8. Comparison of total thicknesses obtained for three designs

7.6 Summary

The results discussed in this chapter demonstrate the successful application of population-based optimisation using the SAEA for the design of a composite riser joint. The main advantage of employing surrogate-based optimisation is its capability to tackle the effect of multiple variables with fewer FEA simulations and reduce the need for design experience. In this chapter, the SAEA tailored design offers slightly lower minimum structural weights and marginally lower thicknesses than those of the manually optimised tailored design in *Chapter 5*, and its results corroborate and authenticate the efficiency of the iterative approach of the manually tailored design employed in *Chapters 5* and *6.*

CHAPTER 8

SUMMARY AND CONCLUSIONS

The aim of this study is to demonstrate and quantify the weight savings that can be achieved by tailoring the design of composite risers for deep-water offshore applications. In this thesis, composite risers are designed using eight different material combinations and their performances investigated, primarily through computational simulations. This research focuses on tailoring a design to take full advantage of the benefits offered by the orthotropic natures of fibre-reinforced composites in order to maximise weight savings and, thereby, cost savings, and developing its methodology. In the tailored design, not only the ply thicknesses, but also the fibre orientations and stacking sequence of the composite layers are optimised for minimum weight. Its results are compared with those obtained using the conventional design approach optimised for minimum weight in which fibre reinforcements are employed in only the axial and hoop directions. Employing steel risers designed for the same loading conditions as the benchmark, it is demonstrated that the tailored design offers significantly greater weight savings than the conventional design in all cases. The optimisations for minimum weight of both the tailored and conventional designs are initially performed using an iterative procedure of manual inspection and selection of the design parameters for all eight material combinations. Subsequently, the mathematical optimisation technique used for the tailored designs of the three most promising material combinations, the Surrogate Assisted Evolutionary Algorithm (SAEA), yields minimum weights very close to those obtained from the manual selection procedure which verifies the proposed approach.

It is evident from this study that, although all the composite material combinations considered offer weight savings over the steel riser, it is much more beneficial to use high-strength (HS) rather than high-modulus (HM) carbon fibre reinforcements as their failure modes are different. For HS (AS4) fibre reinforcements, failure is dominated by transverse stresses due to matrix cracking whereas, for HM (P75) fibre reinforcements, it generally occurs in the fibre direction. Also, of the eight different combinations of fibre reinforcements with PEEK and epoxy matrices (with PEEK and metallic liners for the two matrices, respectively), the best weight savings are offered when PEEK is used as the material for both the laminate matrix and liner. Compared with the steel riser, the structural weight saving in riser tubes per unit length offered by the conventional design using the HS AS4 reinforcement in the PEEK matrix with PEEK liner is 69% while, for the same material combination using the proposed tailored approach, it is 76%, a 7% greater weight reduction (24% weight saving with respect to the weight obtained by the conventional design).

Some findings from the designs of composite risers in this study are:

- HS carbon fibre reinforcements are much more efficient than HM carbon fibre reinforcements;
- The best laminate stacking sequence for a composite riser is [0/±θ/90] and, for a HS carbon fibre-reinforced pipe in which its innermost layers are axially reinforced, the fibre orientations, θ, of its angle plies have different values of between 51^{o} and 54^{o}

when optimised for minimum weight for different matrix and liner materials whereas, for a composite riser reinforced with HM carbon fibres, the optimum values of θ range between 55^o and 69^o;

- When a metal liner is employed, it participates in the load bearing until it yields, after which the load is carried mainly by the composite body;
- The thinnest liner provides the greatest structural weight saving for a HS carbon fibre-reinforced composite; and
- The minimum weights of the tailored designs optimised by the mathematical approach SAEA and iterative manual inspection and selection processes are within 1% of each other which confirms that either optimisation approach can be employed to tailor the design.

It may be noted that, although this study specifically considers the top-tension riser, the same tailored design approach could easily be applied to other types of composite risers and pipes.

Some of the areas in which further research and development work involving collaboration between industry and academia needs to be undertaken to enable FRP composites to be used for critical deep-water applications in the offshore oil and gas industry include:

(1) Assessing long-term characteristics of composite materials in deep-sea environments;

(2) Determining the dynamic responses of composite pipelines and riser structures, such as the fluid-structure interactions of rigid and flexible composite risers/pipelines due to VIV;

(3) Updating existing manufacturing technology to develop faster and more cost-effective manufacturing processes; and

(4) Developing detailed designs of the connectors and metal-to-composite interfaces (MCI) of composite riser joints.

References

[1] Salama, M.M., et al. *Composite risers are ready for field applications-status oftechnology, field demonstration and life cycle economics*. in *13th annual deep offshore technology conference*, 2001. Brazil.

[2] Venkatesan, R., E.S. Dwarakadasa, and M. Ravindran. *Study on behavior of carbon fiber-reinforced composite for deep sea applications*. in *Offshore technology conference*, 2002. Houston, Texas: OTC 14325.

[3] Ochoa, O.O. and M.M. Salama, *Offshore composites: transition barriers to an enabling technology.* Composites Science and Technology, 2005. **65**(15-16): p. 2588-2596.

[4] Salama, M.M., et al. *The first offshore field installation for a composite riser joint*. in *Offshore technology conference*, 2002. Houston, Texas: OTC 14018.

[5] Sparks, C.P., et al. *Mechanical testing of high-performance composite tubes for TLP production risers*. in *Offshore technology conference*, 1988. Houston, Texas: OTC 5797.

[6] Salama, M.M., D.B. Johnson, and J.R. Long, *Composite production riser-testing and qualification.* SPE Production & Facilities, 1998: p. 170-177.

[7] Smith, K.L. and M.E. Leveque, *Ultra-deepwater production systems technical-progress report*, 2003, ConocoPhillips Company: USA.

[8] Smith, K.L. and M.E. Leveque, *Ultra-deepwater production systems-final report*, 2005, ConocoPhillips Company: USA.

[9] Pelsoci, T.M., *Composites manufacturing technologies: applications in automotive, petroleum, and civil infrastructure industries*, 2004, National Institute of Standards and Technology: USA.

[10] Richardson, G.E., et al., *Deepwater Gulf of Mexico 2008: America's offshore energy future*, 2008, U.S. Department of the Interior Minerals Management Service, Gulf of Mexico OCS Region.

[11] Nixon, L.D., et al., *Deepwater Gulf of Mexico 2009: interim report of 2008 highlights*, 2009, U.S. Department of the Interior Minerals Management Service, Gulf of Mexico OCS Region.

[12] *Types of offshore oil and gas structures*, National Oceanic and Atmospheric Administration. [cited 2012]; Available from: http://oceanexplorer.noaa.gov/explorations/06mexico/background/oil/media/types_600.html.

[13] Demirbilek, Z., *Tension leg platform: a state of the art review*, 1989, USA: American Society of Civil Engineerings.

[14] Bian, X., S.J. Leverette, and O.R. Rijken. *A TLP solution for 8000 ft water depth*. in *Proceedings of the ASME 2010: 29th international conference on ocean, offshore and arctic engineering*, 2010. Shanghai, China: p. 255-262.

[15] Lo, K.H., et al., *Progress challenges and opportunities in the application of composites offshore*. Composite materials for offshore operations-3, S.S. Wang, J.G. Williams, and K.H. Lo, 2001, Houston, TX, USA: University of Houston-CEAC.

[16] Saad, P., M.M. Salama, and O. Jahnsen. *Application of composites to deepwater top tensioned riser systems*. in *21st international conference on offshore mechanics and arctic engineering*, 2002. Oslo, Norway: p. 255-261.

[17] Salama, M.M. *Lightweight materials for deepwater offshore structures*. in *Offshore technology conference*, 1986. Houston, Texas: OTC 5185.

[18] Karayaka, M., et al. *Composite production riser dynamics and its effects on tensioners, stress joints, and size of deep water tension leg platform*. in *Offshore technology conference*, 1998. Houston, Texas: OTC 8666.

[19] Andersen, W.F., et al. *The application of advanced composite technology to marine drilling riser systems: design, manufacturing and test*. in *Offshore technology conference*, 1997. Houston, Texas: OTC 8433.

[20] Andersen, W.F., J. O. Burgdorf, and T.F. Sweeney. *Comparative analysis of 12,500 ft. water depth steel and advanced composite drilling risers*. in *Offshore technology conference*, 1998. Houston, Texas: OTC 8732.

[21] Andersen, W.F., J.J. Anderson, and L.S. Landriault. *Full-scale testing of prototype composite drilling riser joints-interim report*. in *Offshore technology conference*, 1998. Houston, Texas: OTC 8668.

[22] Baldwin, D.D., et al. *Composite production riser design*. in *Offshore technology conference*, 1997. Houston, Texas: OTC 8431.

[23] Baldwin, D.D., K.H. Lo, and J.R. Long. *Design verification of a composite production riser*. in *Offshore technology conference*, 1998. Houston, Texas: OTC 8664.

[24] Johnson, D.B., et al. *Composite production riser-manufacturing development and qualification testing*. in *Offshore technology conference*, 1998. Houston, Texas: OTC 8665.

[25] Johnson, D.B., D.D. Baldwin, and J.R. Long. *Mechanical performance of composite production risers*. in *Offshore technology conference*, 1999. Houston, Texas: OTC 11008.

[26] Karayaka, M. *Integration of advanced material components to deepwater platforms*. in *Offshore technology conference*, 2000. Houston, Texas: OTC 12027.

[27] Sparks, C.P. *Lightweight composite production risers for a deep water tension leg platform*. in *Proceedings of the fifth international offshore mechanics and arctic engineering (OMAE) symposium*, 1986. p. 86-93.

[28] Salama, M.M., *Lightweight materials for mooring lines of deepwater tension leg platforms.* Marine Technology, 1984. **21**(3): p. 234-241.

[29] Picard, D., et al. *Composite carbon thermoplastic tubes for deepwater application*. in *Offshore technology conference*, 2007. Houston, Texas: OTC 19111.

[30] Tamarelle, P.J.C. and C.P. Sparks. *High-performance composite tubes for offshore applications*. in *Offshore technology conference*, 1987. Houston, Texas: OTC 5384.

[31] Salama, M.M. *Some challenges and innovations for deepwater developments*. in *Offshore technology conference*, 1997. Houston, Texas: OTC 8455.

[32] Chianis, J.W. and P.B. Poll, *New concepts extend dry-tree production into deep water.* Oil & Gas Journal, 1999: p. 89-94.

[33] Beyle, A.I., et al., *Composite risers for deep-water offshore technology: problems and prospects. 1. metal-composite riser.* Mechanics of Composite Materials, 1997. **33**(5): p. 403-414.

[34] Chakrabarti, S.K., *Handbook of offshore engineering*. 1st ed. Vol. 1. 2005, Great Britain: Elsevier.

[35] *Different riser materials compete for acceptance*, 2003, Drilling Contractor. p. 30-31.

[36] Hanna, S.Y., M.M. Salama, and H. Hannus. *New tendon and riser technologies improve TLP competitiveness in ultra-deepwater*. in *Offshore technology conference*, 2001. Houston, Texas: OTC 12963.

[37] Balazs, G.L. and A. Borosnyoi. *Long-term behavior of FRP*. in *Proceedings of the international workshop on composites in construction: a reality*, 2001. American Society of Civil Engineers. p. 84-91.

[38] Jansons, J.O., et al., *Effect of water absoption, elevated temperatures and fatigue on the mechanical properties of carbon-fiber-reinforced epoxy composites for flexible risers.* Mechanics of Composite Materials, 2002. **38**(4): p. 299-310.

[39] Ochoa, O.O. and G.R. Ross, *Hybrid composites: models and tests for environmental aging.* Journal of Reinforced Plastics and Composites, 1998. **17**(9): p. 787-799.

[40] Ross, G.R. and O.O. Ochoa, *Environmental effects on unsymmetric composite laminates.* Journal of Thermoplastic Composite Materials, 1991. **4**(3): p. 266-284.

[41] Bismarck, A., M. Hofmeier, and G. Dörner, *Effect of hot water immersion on the performance of carbon reinforced unidirectional poly(ether ether ketone) (PEEK) composites: stress rupture under end-loaded bending.* Composites Part A: Applied Science and Manufacturing, 2007. **38**(2): p. 407-426.

[42] d'Almeida, J.R.M., R.C. de Almeida, and W.R. de Lima, *Effect of water absorption of the mechanical behavior of fiberglass pipes used for offshore service waters.* Composite Structures, 2008. **83**(2): p. 221-225.

[43] Ellyin, F. and R. Maser, *Environmental effects on the mechanical properties of glass-fiber epoxy composite tubular specimens.* Composites Science and Technology, 2004. **64**(12): p. 1863-1874.

[44] d'Almeida, J.R.M., *Effects of distilled water and saline solution on the interlaminar shear strength of an aramid/epoxy composite.* Composites, 1991. **22**(6): p. 448-450.

[45] Aktas, A. and I. Uzun, *Sea water effect on pinned-joint glass fibre composite materials.* Composite Structures, 2008. **85**(1): p. 59-63.

[46] Huang, G. and H. Sun, *Effect of water absorption on the mechanical properties of glass/polyester composites.* Materials & Design, 2007. **28**(5): p. 1647-1650.

[47] Machida, A., *Recommendation for design and construction of concrete structrues using continuous fibre reinforcing materials*, 1997, Japan Socitey of Civil Engineers: Tokyo.

[48] Kotek, R., *Recent advances in polymer fibers.* Polymer Reviews, 2008. **45**(2): p. 221-229.

[49] Afshari, M., et al., *High performance fibers based on rigid and flexible polymers.* Polymer Reviews, 2008. **48**(2): p. 230-274.

[50] Huang, K.Z. *Composite TTR design for an ultradeepwater TLP*. in *Offshore technology conference*, 2005. Houston, Texas: OTC 17159.

[51] KIM, W.K., *Composite production riser assessment*, in *Mechanical Engineering (PhD)*, 2007, Texas A&M University: Texas, U.S.A.

[52] Ward, E.G., et al., *A comparative risk analysis of composite and steel production risers*, 2007, Texas A&M University: USA.

[53] Rakshit, T., S. Atluri, and C. Dalton, *VIV of a composite riser at moderate reynolds number using CFD.* Journal of Offshore Mechanics and Arctic Engineering, 2008. **130**: p. 011009-1-10.

[54] Omar, A.F., et al. *A comparative study of the performance of top-tensioned composite and steel risers under vertex-induced loading*. in *Offshore technology conference*, 1999. Houston, Texas: OTC 11009.

[55] Wang, C., K. Shankar, and E.V. Morozov. *Design of deep sea composite risers under combined environmental loads*. in *2012 composites Australia & CRC-ACS conference*, 2012. Leura, NSW, Australia.

[56] Wang, C., K. Shankar, and E.V. Morozov, *Design of composite risers for minimum weight.* World Academy of Science, Engineering and Technology, 2012. **72**: p. 54-63.

[57] Wang, C., K. Shankar, and E.V. Morozov, *Tailoring of composite reinforcements for weight reduction of offshore production risers.* Applied Mechanics and Materials, 2011. **66-68**: p. 1416-1421.

[58] Wang, C., K. Shankar, and E.V. Morozov. *Local design of composite riser under burst, tension, and collapse cases*. in *18th internaltional conference on composite materials*, 2011. Jeju, Korea.

[59] Ahlstone, A.G., *Light weiht marine riser pipe*, U.S. Patent:3768842. 1973: USA.

[60] *Thermoplastic composite riser* 2009, Airborne. [cited 2009]; Available from: http://www.airbornecompositetubulars.com/attachments/118_White_Paper_Thermoplastic_Composite_Riser.pdf.

[61] Gay, D., S.V. Hoa, and S.W. Tsai, *Composite materials:design and application*. 4th ed, 2003, USA: CRC Press LLC.

[62] Vasiliev, V.V. and E.V. Morozov, *Advanced mechanics of composite materials*. 2nd ed, 2007, Great Britain: Elsevier.

[63] API, *Design of risers for floating production systems (FPSs) and tension-leg platforms (TLPs)*, 1998, American Petroleum Institute.

[64] API, *Design, construction, operation and maintenance of offshore hydrocarbon pipelines*, 1999, American Petroleum Institute.

[65] API, *Bulletin on formulas and calculations for casing, tubing, drill pipe, and line pipe properties (API Bulletin 5C3)*, 1994, American Petroleum Institute.

[66] ABS, *Guide for buliding and classing subsea riser systems*, in *Design requirements and loads*, 2008, American Bureau of Shipping.

[67] Ochoa, O.O., *Composite riser experience and design guildance*, 2006, Texas A&M University: USA.

[68] API, *Recommended practice for planning, designing and constructing fixed offshore platforms-working stress design*, 2000, American Petroleum Institute.

[69] DNV, *Enviromental conditions and enviromental loads (DNV-RP-C205)*, 2009, Det Norske Veritas.

[70] API, *Specification for casing and tubing (API Specification 5CT)*, 2005, American Petroleum Institute.

[71] API, *Specification for line pipe (ANSI/API Specification 5L)*, 2007, American Petroleum Institute.

[72] DNV, *Offshore standard for composite components (DNV-OS-C501)*, 2009, Det Norske Veritas.

[73] *Tension Leg Platform*, [cited 2010]; Available from: http://www.globalsecurity.org/military/systems/ship/platform-tension-leg.htm.

[74] Clausen, T., *Dynamic risers key component for deepwater drilling, floating production.* Offshore Magazine, 2001. **61**(5): p. 89-93.

[75] DNV, *Offshore standard for dynamic risers (DNV-OS-F201)*, 2001, Det Norske Veritas.

[76] Dean, R.G., *Relative validities of water wave theories.* Journal of the Waterways, Harbors and Coastal Engineering Division, 1970. **96**(1): p. 105-119.

[77] LeMéhauté, B., *An introduction to hydrodynamics and water waves*, 1976, New York: Springer-Verlag.

[78] Fang, H., *Fundamental theory of offshore drilling and exploitation equipments*. 1st ed, 1984, Beijing: Petroleum Industry Press.

[79] Zhu, Y., *Analyses of the ranges of validity for several wave theories.* Coastal engineering, 1983. **2**(2): p. 11-27.

[80] Komar, P.D., *Beach processes and sedimentation*, 1976: Prentice-Hall, Inc.

[81] Zhu, Y., *Wave mechanics for ocean engineering*. 1st ed, 1991, Tianjin: Tianjin University Press.

[82] Sexton, R.M. and L.K. Agbezuge. *Random wave and vessel motion effects on drilling riser dynamics*. in *Offshore technology conference*, 1976. Houston,Texas: p. OTC 2650.

[83] Kaw, A.K., *Mechanics of composite materials*. 2nd ed, 2006, USA: CSC Press.

[84] *ANSYS Element Reference*, ANSYS Inc.

[85] Williams, J.G., *Advances in steels for high strength ERW linepipe application in Australia.* Material Forum, 2007. **31**: p. 1-10.

[86] Spinelli, C.M. and L.Prandi. *High grade steel pipeline for long distance projects at intermediate pressure*. in *7th Pipeline technology conference*, 2012. Hannover, Germany.

[87] Hillenbrand, H.G., et al., *Technological solutions for high strength gas pipelines*, 2008, EUROPIPE Technical Report.

[88] Hillenbrand, H.G., C.J. Heckmann, and K.A. Niederhoff, *X80 line pipe for large-diameter high strength pipelines*, 2002, EUROPIPE Technical Report.

[89] Barbero, E.J., *Introduction to composite materials design*, 1998, Philadelphia: Taylor and Francis.

[90] Pilato, L.A. and M.J. Michno, *Advanced composite materials*, 1994, Germany: Springer-Verlag.

[91] *Overview of materials for Polyetheretherketone (unreinforced)*, Matweb. [cited 2010]; Available from:

http://www.matweb.com/search/DataSheet.aspx?MatGUID=2164cacabcde4391a596640d553b2ebe.

[92] King, T.R., et al., *Micromechanics prediction of the shear strength of carbon fiber/epoxy matrix composites: the influence of the matrix and interface strengths.* Journal of Composite Materials, 1992. **26**(4): p. 558-573.

[93] Kong, Q. and F. Kong, *Applocation of fiber-wound composites on offshore oil and gas industry.* Fiber Composites, 2008. **4**: p. 24-27,39.

[94] Theotokoglou, E.E., *Behaviour of thick composite tubes considering of delamination.* Theoretical and Applied Fracture Mechanics, 2006. **46**(3): p. 276-285.

[95] Ramirez, G. and M.D. Engelhardt, *Experimental investigation of a large-scale composite riser tube under external pressure.* Journal of Pressure Vessel Technology, 2009. **131**: p. 051205-1-8.

[96] Schutz, R.W., C.F. Baxter, and P.L. Boster, *Applying titanium alloys in drilling and offshore production systems.* JOM Journal of the Minerals, Metals and Materials Society, 2001. **53**(4): p. 33-35.

[97] DNV, *Recommended practice for design of titanium risers (DNV-RP-F201)*, 2002, Det Norske Veritas.

[98] *ASM material data sheet-titanium (Ti-6Al-4V)* 2011, ASM Aerospace Specificaiton Metal Inc. [cited 2011]; Available from:
http://asm.matweb.com/search/SpecificMaterial.asp?bassnum=MTP641.

[99] Gelfgat, M.Y., et al. *Drillstring with aluminum alloy pipes design and practices*. in *SPE/IADC drilling conference*, 2003. Amsterdam, Netherlands.

[100] Gelfgat, M.Y. and V.S. Basovich. *Aluminium alloy tubulars for oil and gas industry*. in *SPE annual technical conference and exhibition*, 2005. Dallas, Texas, USA.

[101] Altenbach, H., J. Altenbach, and W. Kissing, *Mechanics of Composite Structural Elements*, 2004, New York: Springer.

[102] Tsai, S.W. and H.T. Hahn, *Introduction to composite materials*, 1980, Western Hemisphere: Technomic Publishing AG.

[103] Hewitt, R.L. and M.C.D. Malherbe, *An approximation for the longitudinal shear modulus of continuous fibre composites.* Journal of Composite Materials, 1970. **4**: p. 280-282.

[104] Halpin, J.C., *Effects of environmental factors on composite materials*, 1969, Air Force Materials Laboratory.

[105] Kriz, R.D. and W.W. Stinchcomb, *Elastic moduli of transversely isotropic graphite fibers and their composites.* Experimental Mechanics, 1978. **19**(2): p. 41-49.

[106] Mak, Y.P., *Strain rate effects on tensile fracture and damage tolerance of composite laminates*, in *Department of Aeronautics and Astronautics (Master of Science)*, 1992, Massachusetts Institute of Technology: USA.

[107] *AS4/PEEK unidirectional prepreg database*, [cited 2010]; Available from: http://composite.about.com/library/data/blc-as4apc2-1.htm.

[108] Blair, C. and G.A. Jensen. *Processs development and characterization fo ultra high modulus, drapable graphite/thermoplastic composites for space applictions*. in *37th international SAMPLE symposium*, 1992. Anaheim, California: p. 115-127.

[109] *Composite materials handbook*. Polymer matrix composites materials properties. Vol. 2. 2002.

[110] Xia, M., H. Takayanagi, and K. Kemmochi, *Analysis of multi-layered filament-wound composite pipes under internal pressure.* Composite Structures, 2001. **53**(4): p. 483-491.

[111] Vodenitcharova, T. and P. Ansourian, *Buckling of circular cylindrical shells subject to uniform lateral pressure.* Engineering Structures, 1996. **18**(8): p. 604-614.

[112] Mirfakhraei, P. and D. Redekop, *Buckling of circular cylindrical shells by the differential quadrature method.* International Journal of Pressure Vessels and Piping, 1998. **75**(4): p. 347-353.

[113] Sun, C.T. and S. Li, *Three-dimensional effective elastic constant for thick laminates.* Journal of Composite Materials, 1988. **22**: p. 629-639.

[114] Bogetti, T.A., C.P.R. Hoppel, and W.H. Drysdale, *Three-dimensional effective property and strength prediction of thick laminated composite media*, 1995, U.S. Army Research Laboratory: USA.

[115] Ogawa, H., et al. *Full flow-path optimization of axisymmetric scramjet engines* in *International space planes and hypersonic systems and technologies conference*, 2011. San Francisco, CA: American Institute of Aeronautics and Astronautics p. 1762-1775.

[116] Forrester, A.I.J., A. Sobester, and J. Keane, *Engineering design via surrogate modelling - a practical guide*, 2008, United Kingdom: John Wiley & Sons.

[117] Deb, K., *Multi-objective optimization using evolutionary algorithms* 1st ed, 2001, New York: John Wiley & Sons

[118] Queipo, N.V., et al., *Surrogate-based analysis and optimization.* Progress in Aerospace Sciences, 2005. **41**(1): p. 1-28.

[119] Ray, T. and W. Smith, *A surrogate assisted parallel multiobjective evolutionary algorithm for robust engineering design.* Engineering Optimization, 2006. **38**(8): p. 997-1011.

[120] Deb, K., et al., *A fast and elitist multiobjective genetic algorithm: NSGA-II.* IEEE Transactions on Evolutionary Computation, 2002. **6**(2): p. 182-197.

[121] Simpson, T.W., D.K.J. Lin, and W. Chen, *Sampling strategies for computer experiments: design and analysis.* International journal of Reliability and Applications, 2001. **2**(3): p. 209-240.

[122] Kodiyalam, S. and J. Sobieszczanski-Sobieski. *Alternate sampling methods for use with multidisciplinary design optimization in a high performance computing environment*. in *ASME DETC/IEC conference*, 2001. p. DETC2001/DAC-21081.

[123] Montgomery, D.C., *Design and analysis of experiments*, 5th, 2001, U.S.A: John Wiley & Sons.

[124] Owen, A., *Programs constrct and manipulate orthogonal arrays*.

[125] Sacks, J., et al., *Design and analysis of computer experiments.* Statistical Science, 1989. **4**(4): p. 409-423.

APPENDIX A

THEORY FOR EXACT ELASTIC SOLUTION OF STRESSES IN COMPOSITE TUBE

In this Appendix, the three dimensional elastic solution for filament wound composite pipes under internal pressure published by M. Xia, et al. [110] is presented. The shear twist coupling characteristic and effect of Poisson's Ratio of the material are considered and each lamina is regarded as an anisotropic material. For an n-layered composite cylinder, there are 2n+2 unknown constants to be determined. After all the constants are solved for, the stresses in each layer can be calculated based on the boundary conditions, strain-displacement relations and the stress-strain relations.

The basic equations of the 3D elastic solution from Xia, et al [110] employed are given below. The cylindrical coordinate system and the material principal coordinate system are illustrated in Fig. A.1.

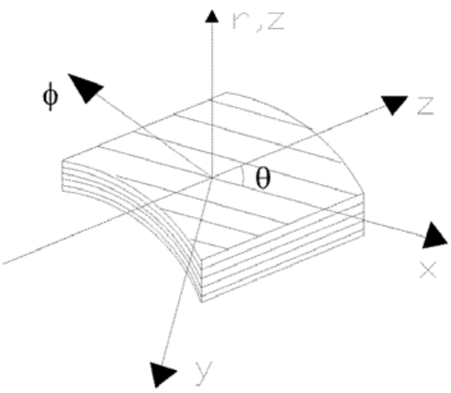

(x, y, z): material principal coordinate system
(r, ϕ, z): cylindrical coordinate system
Fig. A.1. Cylindrical coordinate system and material principal coordinate system

The flexibility matrix of a transversely isotropic lamina is given by

$$\begin{bmatrix} C_{xx} & C_{xy} & C_{xz} \\ C_{xy} & C_{yy} & C_{yz} \\ C_{xz} & C_{yz} & C_{zz} \end{bmatrix} = \begin{bmatrix} 1/E_x & -\nu_{xy}/E_x & -\nu_{xz}/E_x \\ -\nu_{xy}/E_x & 1/E_y & -\nu_{yz}/E_y \\ -\nu_{xz}/E_x & -\nu_{yz}/E_y & 1/E_z \end{bmatrix} \tag{A-1}$$

The off-axis stiffness constants can be calculated from

$$\left\{\overline{C}_{ij}^{(k)}\right\} = [A_{kl}]\left\{C_{ij}^{(k)}\right\} \tag{A-2}$$

Where,

$$\left\{\overline{C}_{ij}^{(k)}\right\} = \left\{\overline{C}_{11}^{(k)}, \overline{C}_{12}^{(k)}, \overline{C}_{13}^{(k)}, \overline{C}_{16}^{(k)}, \overline{C}_{22}^{(k)}, \overline{C}_{23}^{(k)}, \overline{C}_{26}^{(k)}, \overline{C}_{33}^{(k)}, \overline{C}_{36}^{(k)}, \overline{C}_{44}^{(k)}, \overline{C}_{45}^{(k)}, \overline{C}_{55}^{(k)}, \overline{C}_{66}^{(k)}\right\}^T;$$

$$\left\{C_{ij}^{(k)}\right\} = \left\{C_{xx}^{(k)}, C_{yy}^{(k)}, C_{zz}^{(k)}, C_{xy}^{(k)}, C_{xz}^{(k)}, C_{yz}^{(k)}, G_{yz}^{(k)}, G_{xz}^{(k)}, G_{xy}^{(k)}\right\}^T;$$

$$[A_{kl}] = \begin{bmatrix} c^4 & s^4 & 0 & 2c^2s^2 & 0 & 0 & 0 & 0 & 4c^2s^2 \\ c^2s^2 & c^2s^2 & 0 & c^4+s^4 & 0 & 0 & 0 & 0 & -4c^2s^2 \\ 0 & 0 & 0 & 0 & c^2 & s^2 & 0 & 0 & 0 \\ c^3s & -cs^3 & 0 & cs^3-c^3s & 0 & 0 & 0 & 0 & 2cs^3-2c^3s \\ s^4 & c^4 & 0 & 2c^2s^2 & 0 & 0 & 0 & 0 & 4c^2s^2 \\ 0 & 0 & 0 & 0 & s^2 & c^2 & 0 & 0 & 0 \\ cs^3 & -c^3s & 0 & c^3s-cs^3 & 0 & 0 & 0 & 0 & 2c^3s-2cs^3 \\ 0 & 0 & 1 & 0 & 0 & 0 & 0 & 0 & 0 \\ 0 & 0 & 0 & 0 & cs & -cs & 0 & 0 & 0 \\ 0 & 0 & 0 & 0 & 0 & 0 & c^2 & s^2 & 0 \\ 0 & 0 & 0 & 0 & 0 & 0 & -cs & cs & 0 \\ 0 & 0 & 0 & 0 & 0 & 0 & s^2 & c^2 & 0 \\ c^2s^2 & c^2s^2 & 0 & -2c^2s^2 & 0 & 0 & 0 & 0 & (c^2-s^2)^2 \end{bmatrix}$$

θ is the cylindrical angle of the fibres form the pipe axis, c= cos θ, s=sin θ.

For a composite pipe under internal pressure with *n* layers, there are 2*n*+2 unknown constants of integration ($E^{(n)}$, $D^{(n)}$, ε_0 and γ_0) which can be determined by solving Eq. A-3. The elements a, d and e in Eq. A-3 are functions of $\overline{C}_{ij}^{(k)}$.

$$
\begin{Bmatrix} D^{(1)} \\ \bullet \\ \bullet \\ \bullet \\ D^{(n)} \\ E^{(1)} \\ \bullet \\ \bullet \\ \bullet \\ E^{(n)} \\ \varepsilon_0 \\ \gamma_0 \end{Bmatrix} =
$$

$$
\begin{bmatrix}
d_{11} & 0 & \bullet & \bullet & \bullet & 0 & e_{11} & 0 & \bullet & \bullet & \bullet & 0 & a_{11} & a_{12} \\
d_{12} & d_{22} & & & & 0 & e_{12} & e_{12} & & & & 0 & a_{21} & a_{22} \\
\bullet & & \bullet & & & \bullet & \bullet & & \bullet & & & \bullet & \bullet & \bullet \\
\bullet & & & \bullet & & \bullet & \bullet & & & \bullet & & \bullet & \bullet & \bullet \\
\bullet & & & & \bullet & \bullet & \bullet & & & & \bullet & \bullet & \bullet & \bullet \\
0 & \bullet & \bullet & \bullet & d_{n,n-1} & d_{nn} & 0 & \bullet & \bullet & \bullet & e_{n,n-1} & e_{nn} & a_{n1} & a_{n2} \\
d_{n+1,1} & d_{n+1,2} & \bullet & \bullet & \bullet & 0 & e_{n+1,1} & e_{n+1,2} & \bullet & \bullet & \bullet & 0 & a_{n+1,1} & a_{n+1,2} \\
0 & d_{n+2,2} & d_{n+2,3} & & & \bullet & 0 & d_{n+2,2} & d_{n+2,3} & & & \bullet & \bullet & \bullet \\
\bullet & & \bullet & & & \bullet & \bullet & \bullet & \bullet & & & \bullet & \bullet & \bullet \\
\bullet & & & \bullet & & \bullet & \bullet & \bullet & & \bullet & & \bullet & \bullet & \bullet \\
\bullet & & & & d_{2n-1,n-1} & d_{2n-1,n} & \bullet & \bullet & & & e_{2n-1,n-1} & e_{2n-1,n} & \bullet & \bullet \\
0 & 0 & \bullet & \bullet & \bullet & d_{2n,n} & 0 & 0 & \bullet & \bullet & \bullet & e_{2n,n} & a_{2n,1} & a_{2n,2} \\
d_{2n+1,1} & \bullet & \bullet & \bullet & \bullet & d_{2n+1,n} & e_{2n+1,1} & \bullet & \bullet & \bullet & \bullet & e_{2n+1,n} & a_{2n+1,1} & a_{2n+1,2} \\
d_{2n+2,1} & \bullet & \bullet & \bullet & \bullet & d_{2n+2,n} & e_{2n+2,1} & \bullet & \bullet & \bullet & \bullet & e_{2n+2,n} & a_{2n+2,1} & a_{2n+2,1}
\end{bmatrix}^{-1}
\begin{Bmatrix} -p_0 \\ 0 \\ \bullet \\ \bullet \\ \bullet \\ \bullet \\ \bullet \\ \bullet \\ \bullet \\ 0 \\ \dfrac{r_0^2 p_0}{2} \\ 0 \end{Bmatrix}
\tag{A-3}
$$

After determining ($E^{(n)}$, $D^{(n)}$, ε_0 and γ_0), the solutions for the strains $\left\{\varepsilon_z^{(k)}, \varepsilon_\theta^{(k)}, \varepsilon_r^{(k)}, \gamma_{\theta r}^{(k)}, \gamma_{zr}^{(k)}, \gamma_{z\theta}^{(k)}\right\}^T$ can be determined from the Eqs. A-4 to A-11:

$$u_r^{(k)} = D^{(k)} r^{\beta^{(k)}} + E^{(k)} r^{-\beta^{(k)}} + \alpha_1^{(k)} \varepsilon_0 r + \alpha_2^{(k)} \gamma_0 r^2 \tag{A-4}$$

where $\alpha_1^{(k)} = \frac{\overline{C}_{12}^{(k)} - \overline{C}_{13}^{(k)}}{\overline{C}_{33}^{(k)} - \overline{C}_{22}^{(k)}}$, $\alpha_2^{(k)} = \frac{\overline{C}_{26}^{(k)} - 2\overline{C}_{36}^{(k)}}{4\overline{C}_{33}^{(k)} - \overline{C}_{22}^{(k)}}$ and $\beta^{(k)} = \sqrt{\overline{C}_{22}^{(k)} / \overline{C}_{33}^{(k)}}$.

$$u_\theta^{(k)} = \gamma_0 r z \tag{A-5}$$

$$\varepsilon_z^{(k)} = \varepsilon_0 \tag{A-6}$$

$$\varepsilon_\theta^{(k)} = \frac{u_r^{(k)}}{r} \tag{A-7}$$

$$\varepsilon_r^{(k)} = \frac{\mathrm{d}u_r^{(k)}}{\mathrm{d}r} \tag{A-8}$$

$$\gamma_{\theta r}^{(k)} = \frac{\mathrm{d}u_\theta^{(k)}}{\mathrm{d}r} - \frac{u_\theta^{(k)}}{r} \tag{A-9}$$

$$\gamma_{zr}^{(k)} = 0 \tag{A-10}$$

$$\gamma_{z\theta}^{(k)} = \gamma_0 r \tag{A-11}$$

From the strains, the stresses in each layer and the liner can be obtained by

$$\begin{Bmatrix} \sigma_z \\ \sigma_\theta \\ \sigma_r \\ \tau_{\theta r} \\ \tau_{zr} \\ \tau_{z\theta} \end{Bmatrix}^{(k)} = \begin{bmatrix} \overline{C}_{11} & \overline{C}_{12} & \overline{C}_{13} & 0 & 0 & \overline{C}_{16} \\ \overline{C}_{12} & \overline{C}_{22} & \overline{C}_{23} & 0 & 0 & \overline{C}_{26} \\ \overline{C}_{13} & \overline{C}_{23} & \overline{C}_{33} & 0 & 0 & \overline{C}_{36} \\ 0 & 0 & 0 & \overline{C}_{44} & \overline{C}_{45} & 0 \\ 0 & 0 & 0 & \overline{C}_{45} & \overline{C}_{55} & 0 \\ \overline{C}_{16} & \overline{C}_{26} & \overline{C}_{36} & 0 & 0 & \overline{C}_{66} \end{bmatrix}^{(k)} \begin{Bmatrix} \varepsilon_{\mathrm{z}} \\ \varepsilon_\theta \\ \varepsilon_{\mathrm{r}} \\ \gamma_{\theta r} \\ \gamma_{\mathrm{zr}} \\ \gamma_{z\theta} \end{Bmatrix}^{(k)} \tag{A-12}$$

The stresses under the burst case from the FEA simulation are compared to the 3D solutions obtained from the above equations for the geometries optimised with the conventional and the tailored design procedures in Section 5.3 Chapter 5. The agreement between the theory and FEA simulation is very good, which confirms the accuracy of the stress analysis using FEA simulation.

APPENDIX B

LOCAL DESIGN RESULTS FOR THE OTHER MATERIAL COMBINATIONS

Content Table of Local Design Results Presented in Appendix B

Material combination		Design approach	Appendix no.
Composite	Liner		
P75/PEEK	PEEK	conventional design	Appendix B.1
		manually tailored design	Appendix B.2
AS4/epoxy	steel	conventional design	Appendix B.3
		manually tailored design	Appendix B.4
	titanium	conventional design	Appendix B.5
		manually tailored design	Appendix B.6
	aluminium	conventional design	Appendix B.7
		manually tailored design	Appendix B.8
P75/epoxy	steel	conventional design	Appendix B.9
		manually tailored design	Appendix B.10
	titanium	conventional design	Appendix B.11
		manually tailored design	Appendix B.12
	aluminium	conventional design	Appendix B.13
		manually tailored design	Appendix B.14

B.1 Results for P75/PEEK with PEEK Liner Using Conventional Design

Table B.1 gives the geometry of the composite riser tube optimised for minimum thickness using the conventional design under the local load cases. The conventional design yields a 37-ply composite laminate [$0_{15}/90_{22}$] with all reinforced layers having thicknesses of 3mm except the hoop layer 37 is 2mm, which results in a total laminate thickness of 110mm, with a 6mm PEEK liner and the structural weight of 234.2kg/m. Here, if the alternate hoop and axial reinforcements stacking sequence is applied, the total thickness of the composite cylinder would be twice than that given in Table B.1.

Table B.1. Geometry of P75/PEEK with PEEK liner riser with orthogonal reinforcements

Layer	Orientation (degree)	Thickness(mm)	Layer	Orientation (degree)	Thickness(mm)
liner		6	19	90	3
1	0 (axial)	3	20	90	3
2	0	3	21	90	3
3	0	3	22	90	3
4	0	3	23	90	3
5	0	3	24	90	3
6	0	3	25	90	3
7	0	3	26	90	3
8	0	3	27	90	3
9	0	3	28	90	3
10	0	3	29	90	3
11	0	3	30	90	3
12	0	3	31	90	3
13	0	3	32	90	3
14	0	3	33	90	3
15	0	3	34	90	3
16	90 (hoop)	3	35	90	3
17	90	3	36	90	3
18	90	3	37	90	2
Total thickness: 116mm and structural weight: 234.2kg/m					

B.1.1 Results for P75/PEEK with PEEK Liner [$0_{15}/90_{22}$] under Burst Case

The design internal burst pressure for the composite riser is 155.25MPa for which the Von Mises stress in the PEEK liner is 85.0MPa and FS=1.41. Figs. B.1(a) and B.1(b), respectively, show the factors of safety (FSs) in the fibre and transverse directions under load case 1 (burst load) for all the layers in the conventional design geometry. The minimum FS in the fibre direction is 1.01 (layer 16 in Fig. B.1(a)), while that in the transverse direction is 1.98 (layers 16 in Fig. B.1(b)). It is evident that, under burst case, the stresses in fibre direction are the most critical stresses and determine the minimum thickness of the composite P75/PEEK with PEEK liner with only 0^{o} and 90^{o} reinforcements.

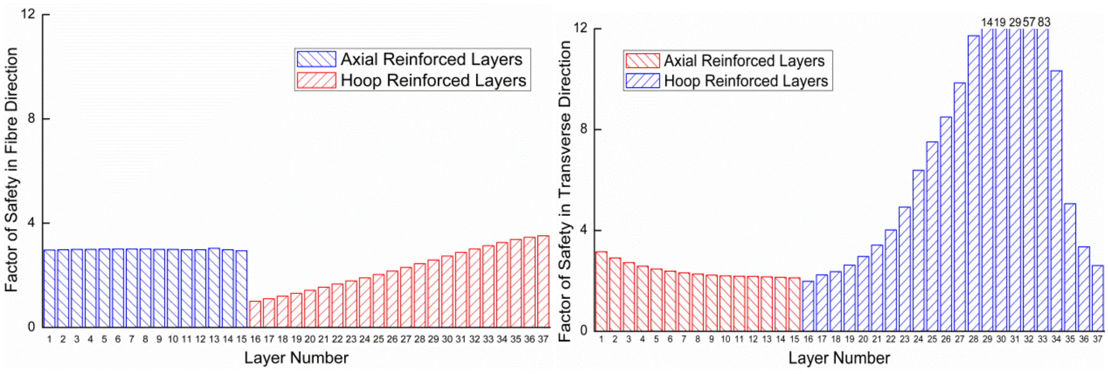

(a) (b)

Fig. B.1. FSs for composite layers with 0° and 90˚ reinforcements for load case 1 for P75/PEEK with PEEK liner in (a) fibre direction, and (b) transverse direction

B.1.2 Results for P75/PEEK with PEEK Liner [$0_{15}/90_{22}$] under Pure Tension Case

As described in *Chapter 3*, the tension force has to be calculated using three different cases, which yield values of 4635kN, 4180kN and 6130kN, respectively. Therefore, the design tension force is 6130×2.25=13800kN.

Under a 13800kN pure tension, the Von Mises stress in the PEEK liner is 4.6MPa, providing FS=26.09. Figs. B.2(a) and B.2(b) show the FSs in every layer under load case 2(a) (pure tension) for the conventional design. As can be seen, the minimum FS in the fibre direction is 2.21 (axial layer 1 in Fig. B.2(a)), while the minimum FS in the transverse direction is 2.72 (hoop layer 16 in Fig. B.2(b)).

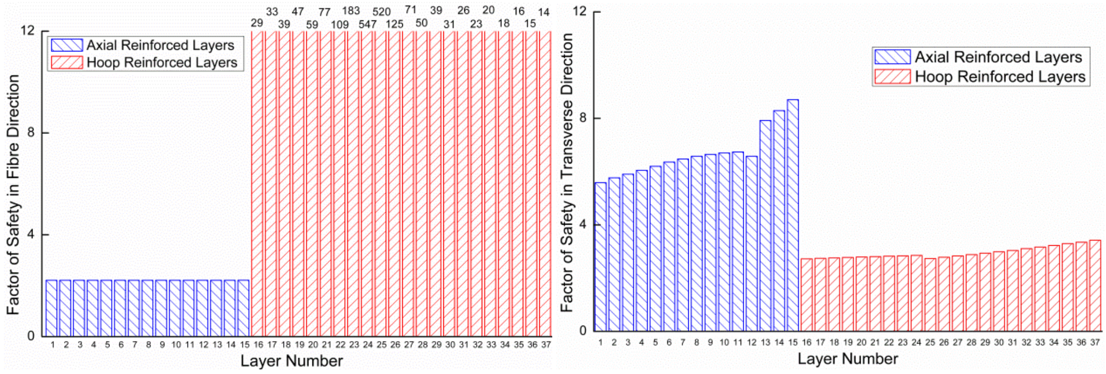

(a) (b)

Fig. B.2. FSs for composite layers with 0° and 90˚ reinforcements for load case 2(a) for P75/PEEK with PEEK liner in (a) fibre direction, and (b) transverse direction

B.1.3 Results for P75/PEEK with PEEK Liner [$0_{15}/90_{22}$] under Tension with External Pressure Case

The tension force under load case 2(b) (tension with an external pressure of 19.5MPa) is also 13800kN and the Von Mises stress in the PEEK liner is 4.3MPa, providing FS=27.91. Fig. B.3 shows its FSs under load case 2(b) for the conventional design with the minimum being 2.1 in fibre direction in layer 1 (Fig. B.3(a)).

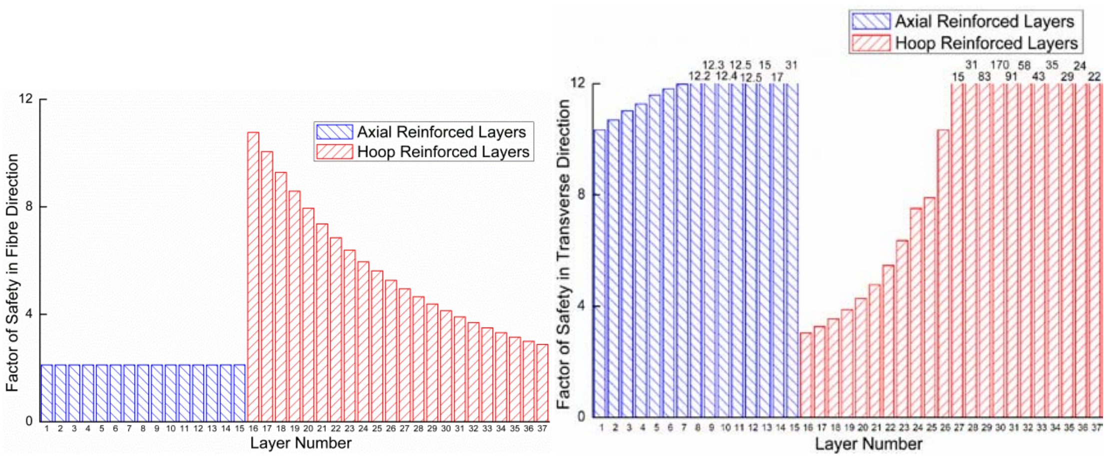

(a) (b)

Fig. B.3. FSs for composite layers with 0° and 90˚ reinforcements for load case 2(b) for P75/PEEK with PEEK liner in (a) fibre direction, and (b) transverse direction

B.1.4 Results for P75/PEEK with PEEK Liner [$0_{15}/90_{22}$] under Collapse Case

The design collapse pressure for the composite riser is 58.5MPa under which the Von Mises stress in the PEEK liner is 3.5MPa, providing FS=34.28. Fig. B.4 shows the FSs under load case 3 (collapse load) for the conventional design, with the minimum being 1.2 in fibre direction in layer 37 (Fig. B.4(a)).

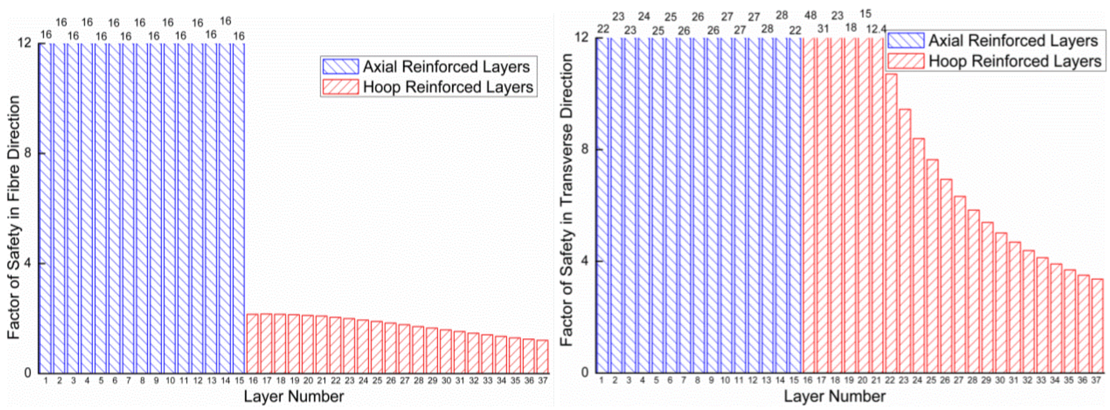

(a) (b)

Fig. B.4. FSs for composite layers with 0° and 90˚ reinforcements for load case 3 for P75/PEEK with PEEK liner in (a) fibre direction, and (b) transverse direction

B.1.5 Results for P75/PEEK with PEEK Liner [$0_{15}/90_{22}$] under Buckling Case

The geometry of P75/PEEK with PEEK liner riser using the conventional design is also checked for buckling under external pressure (load case 4) and the critical buckling pressure obtained is 857.1MPa (mode 1), which is much higher than the design buckling pressure of 58.5MPa. The first three mode shapes can be seen in the Fig. B.5 in which the number of circumferential waves is 2 for all three modes and the number of half-waves along the axial direction 1, 2 and 3 for modes 1, 2 and 3, respectively.

(a) B.P.=857.1MPa (b) B.P.=865.8MPa (c) B.P.=885.807MPa
Fig. B.5. Mode shapes of composite riser with 0° and 90^{o} reinforcements for P75/PEEK with PEEK liner (5m): (a) mode 1 (b) mode 2 and (c) mode 3

B.2 Results for P75/PEEK with PEEK Liner Using Tailored Design

Table B.2 gives the geometry of the composite riser tube optimised for minimum thickness using the tailored design under the local load cases, which yields a 43-ply composite laminate $[0_9/(+55.5,-55.5)_2/90_{10}/(+55.5,-55.5)_{10}]$. The total laminate thickness for the design including the angle plies is only 86mm with same 6mm thickness of the PEEK liner, providing a 26.1% structural weight saving over the conventional design. It is again to be noted that the optimum angle of reinforcement for the angle plies is obtained as ±55.5^{o} using the 3D FEA, not ±54.7^{o} as predicted by the netting theory.

Table B.2. Geometry of P75/PEEK with PEEK liner riser including angle reinforcements

Layer	Orientation (degree)	Thickness (mm)	Layer	Orientation (degree)	Thickness(mm)
liner		6	22	90	2
1	0 (axial)	2	23	90	2
2	0	2	24	-55.5	2
3	0	2	25	55.5	2
4	0	2	26	-55.5	2
5	0	2	27	55.5	2
6	0	1.8	28	-55.5	2
7	0	1.8	29	55.5	2
8	0	1.8	30	-55.5	2
9	0	1.8	31	55.5	2
10	-55.5	2.2	32	-55.5	2
11	55.5	2.2	33	55.5	2
12	-55.5	2.2	34	-55.5	2
13	55.5	2.2	35	55.5	2
14	90 (hoop)	2	36	-55.5	2
15	90	2	37	55.5	2
16	90	2	38	-55.5	2
17	90	2	39	55.5	2
18	90	2	40	-55.5	2
19	90	2	41	55.5	2
20	90	2	42	-55.5	2
21	90	2	43	55.5	2
Total thickness: 92mm and structural weight: 173.0kg/m					

B.2.1 Results for P75/PEEK with PEEK Liner $[0_9\ /(\pm 55.5)_2\ /90_{10}\ /(\pm 55.5)_{10}]$ under Burst Case

The design results under burst case are presented in Section 5.8 in *Chapter 5*.

B.2.2 Results for P75/PEEK with PEEK Liner $[0_9\ /(\pm 55.5)_2\ /90_{10}\ /(\pm 55.5)_{10}]$ under Pure Tension Case

As described in *Chapter 3*, the tensions force has to be calculated using three different cases which yield values of 3930kN, 3240kN and 4900kN, respectively. Therefore, the design tension force is 4900×2.25=11000kN.

Under a pure tension (11000kN), the Von Mises stress in the PEEK liner is 7.41MPa, providing FS=16.19. Figs. B.6(a), B.6(b) and B.6(c) show the FSs in all the layers under load case 2(a) (pure tension) for the manually tailored design. In this case, the minimum FS in the fibre direction is about 1.17 (layer 1, Fig. B.7(a)) and that in the transverse direction is about 1.59 (layer 14, Fig. B.7(b)) while the FS in every layer in in-plane shear is relatively high.

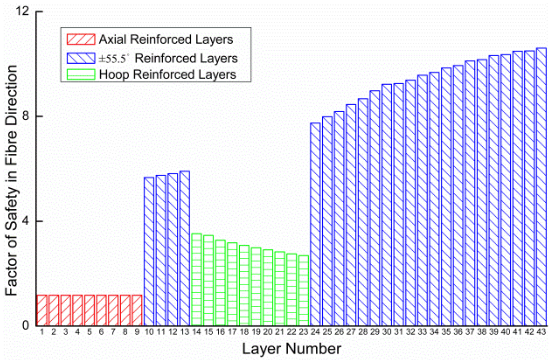

(a)

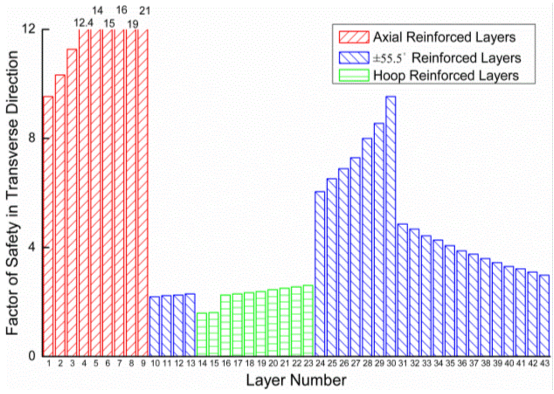

(b)

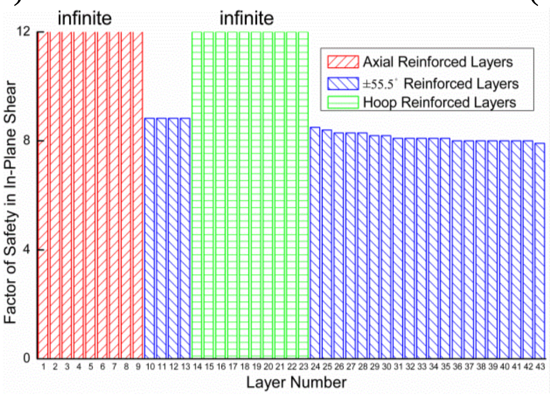

(c)

Fig. B.6. FSs for composite layers with 0°, ±55.5˚ and 90˚ reinforcements for load case 2(a) for P75/PEEK with PEEK liner in (a) fibre direction, (b) transverse direction and (c) in-plane shear

B.2.3 Results for P75/PEEK with PEEK Liner $[0_9 /(\pm 55.5)_2 /90_{10} /(\pm 55.5)_{10}]$ under Tension with External Pressure Case

The tension force under load case 2(b) (tension with external pressure of 19.5MPa) is the same as that for load case 2(a), that is, 11000kN, and the Von Mises stress in the PEEK liner is 8.55MPa, providing FS=14.03. Fig. B.7 shows the FSs under load case 2(b) for the manually tailored design with the minimum being 1.00 in fibre direction in layer 1 (Fig. B.7(a)).

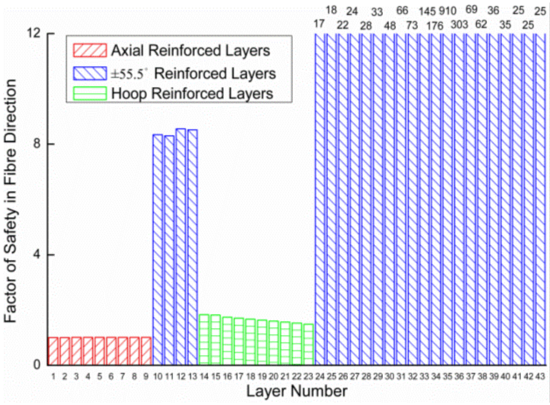

(a)

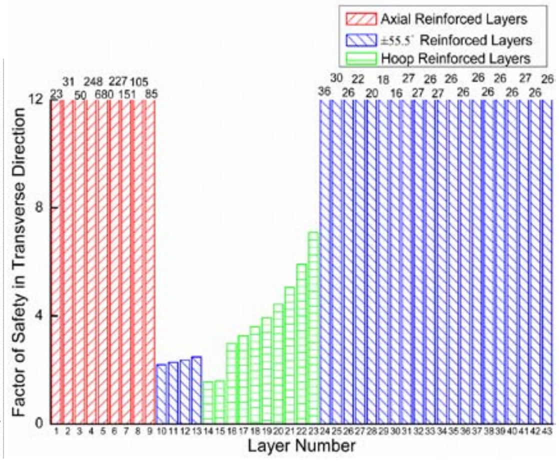

(b)

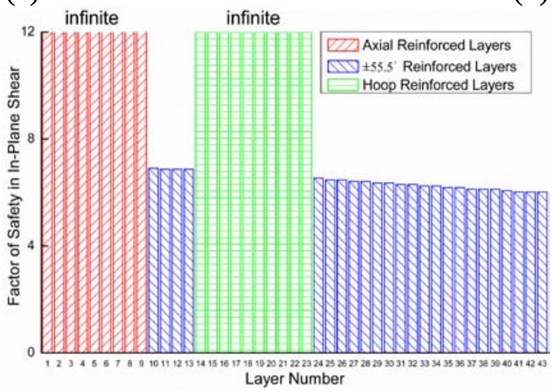

(c)

Fig. B.7. FSs for composite layers with 0°, ±55.5° and 90° reinforcements for load case 2(b) for P75/PEEK with PEEK liner in (a) fibre direction, (b) transverse direction and (c) in-plane shear

B.2.4 Results for P75/PEEK with PEEK Liner $[0_9 /(\pm 55.5)_2 /90_{10} /(\pm 55.5)_{10}]$ under Collapse Case

The design collapse pressure for the composite riser is 58.5MPa and, under this external over-pressure, the Von Mises stress in the PEEK liner is 5.2MPa, providing FS=23.08. Fig. B.8 shows the FSs under load case 3 (collapse load) for manually tailored design with the minimum being 1.12 in fibre direction in layer 23 (Fig. B.8(a)).

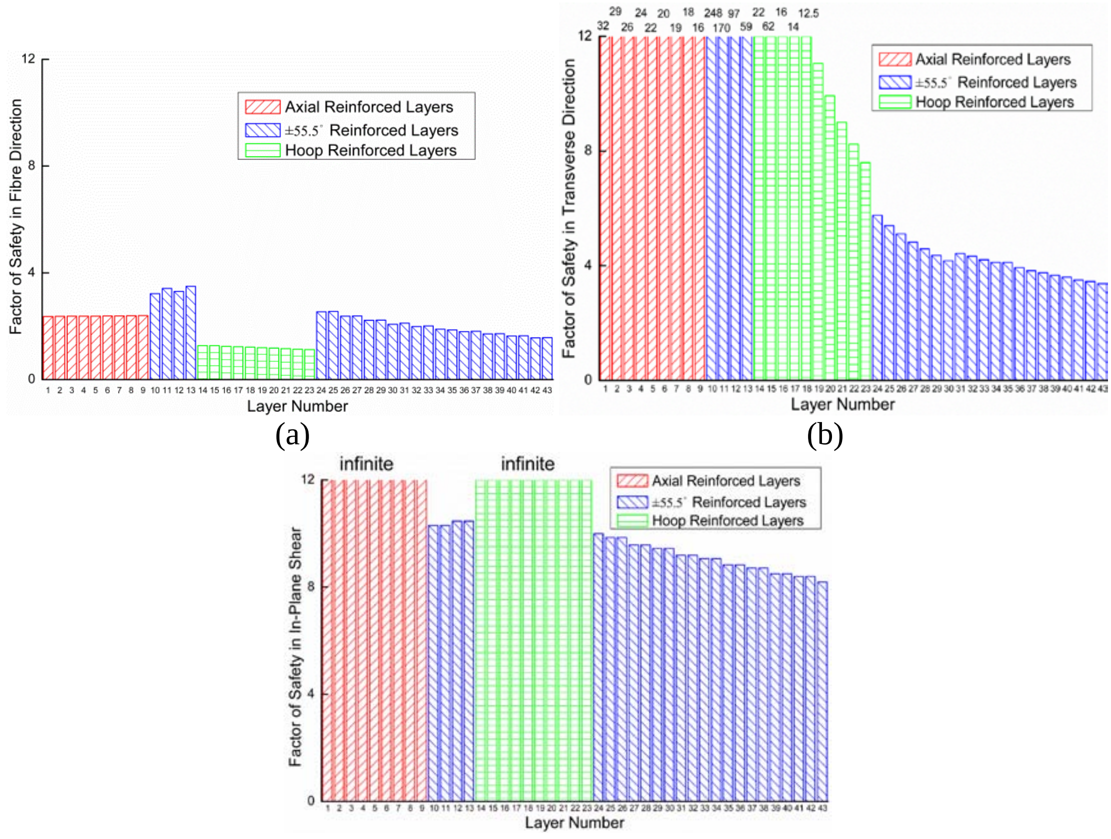

Fig. B.8. FSs for composite layers with 0°, ±55.5˚ and 90˚ reinforcements for load case 3 for P75/PEEK with PEEK liner in (a) fibre direction, (b) transverse direction and (c) in-plane shear

B.2.5 Results for P75/PEEK with PEEK Liner [0_9 /$(\pm55.5)_2$ /90_{10} /$(\pm55.5)_{10}$] under Buckling Case

The geometry of P75/PEEK with PEEK liner riser using the tailored design is also checked for buckling under external pressure (load case 4). The critical buckling pressure obtained is 702.0MPa (mode 1), which is much higher than the design buckling pressure of 58.5MPa. The first three mode shapes are shown in the Fig. B.9 in which it can be seen that the number of circumferential waves is 2 for all three modes and the number of half-waves along the axial direction 1, 2 and 3 for modes 1, 2 and 3, respectively.

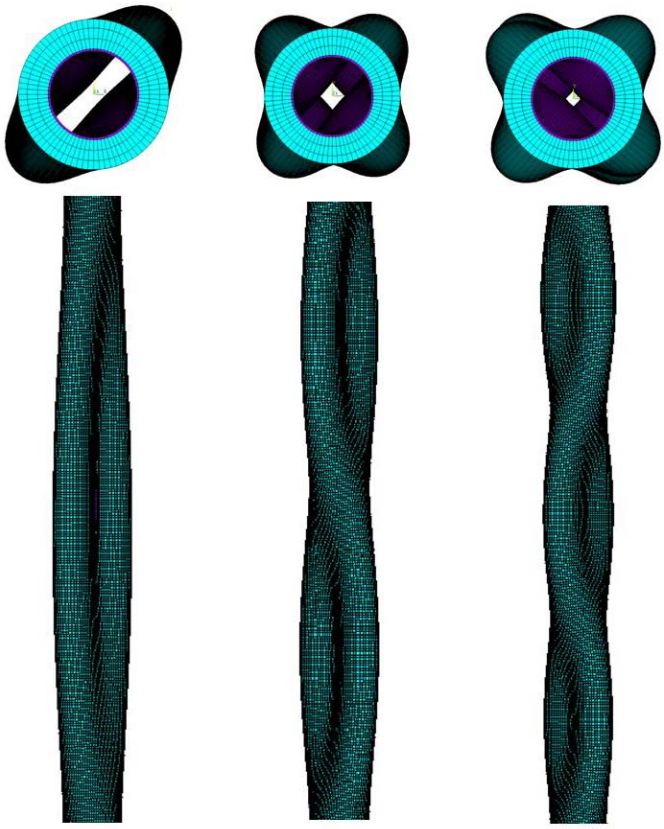

(a) B.P.=702.0MPa (b) B.P.=721.4MPa (c) B.P.=756.1MPa
Fig. B.9. Mode shapes of composite riser with 0°, ±55.5˚ and 90˚ reinforcements for P75/PEEK with PEEK liner (5m): (a) mode 1 (b) mode 2 and (c) mode 3

B.3 Results for AS4/Epoxy with Steel Liner Using Conventional Design

Table B.3 gives the geometry of the composite riser tube optimised for minimum thickness using the conventional design under the local load cases, which yields a 21-ply composite laminate $[90/(0/90)_{10}]$ with alternating hoop and axially reinforced layers of 2.25mm and 1.475mm thicknesses, respectively, which results in a total laminate thickness of 39.5mm, with a 2mm steel liner and structural weight of 68.2kg/m. Unlike PEEK liner riser, the thickness of steel liner would affect total weight significantly, thus, the first step is the determination of the thickness of steel liner. The variations of thickness and weight according to the different thicknesses of steel liner are shown in Fig. B.10 in which it can be seen that when the steel liner is 2mm, the total weight is the minimum. Hence for the following analysis, 2mm steel liner is used.

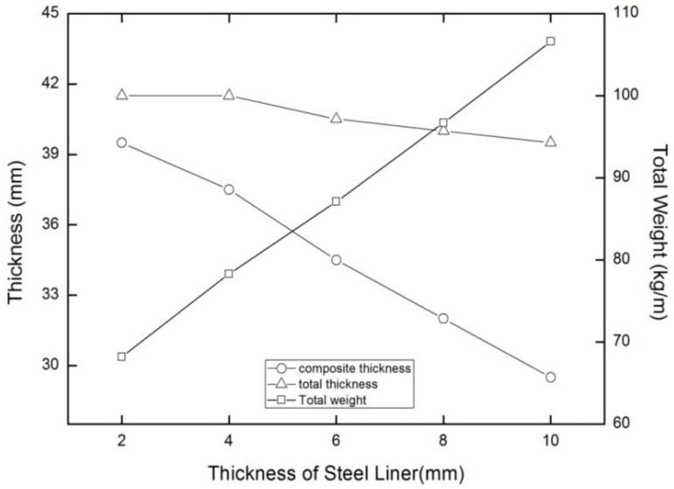

Fig. B.10. Thickness and weight of composite cylinder according to different thicknesses of steel liner

Table B.3. Geometry of AS4/epoxy with steel liner riser with orthogonal reinforcements

Layer	Orientation (degree)	Thickness(mm)	Layer	Orientation (degree)	Thickness(mm)
liner		2	11	90	2.25
1	90 (hoop)	2.25	12	0	1.475
2	0 (axial)	1.475	13	90	2.25
3	90	2.25	14	0	1.475
4	0	1.475	15	90	2.25
5	90	2.25	16	0	1.475
6	0	1.475	17	90	2.25
7	90	2.25	18	0	1.475
8	0	1.475	19	90	2.25
9	90	2.25	20	0	1.475
10	0	1.475	21	90	2.25
Total thickness: 41.5mm and structural weight: 68.2kg/m					

B.3.1 Results for AS4/Epoxy with Steel Liner [90/(0/90)$_{10}$] under Burst Case

The design burst pressure for the composite riser is 155.25MPa for which the Von Mises stress in the steel liner is 566.03MPa and FS=1.10. Figs. B.11(a) and B.11(b), respectively, show the FSs in the fibre and transverse directions under load case 1 (burst load) for all the layers in the conventional design geometry. The minimum FS in the fibre direction is 1.72 (layer 1 in Fig. B.11(a)), while that in the transverse direction is 1.00 (layers 20 and 21 in Fig. B.11(b)). It is evident that, under burst case, the in-plane transverse stresses are the most critical stresses and determine the minimum thickness of the composite AS4/epoxy with steel liner with only 0^o and 90^o reinforcements.

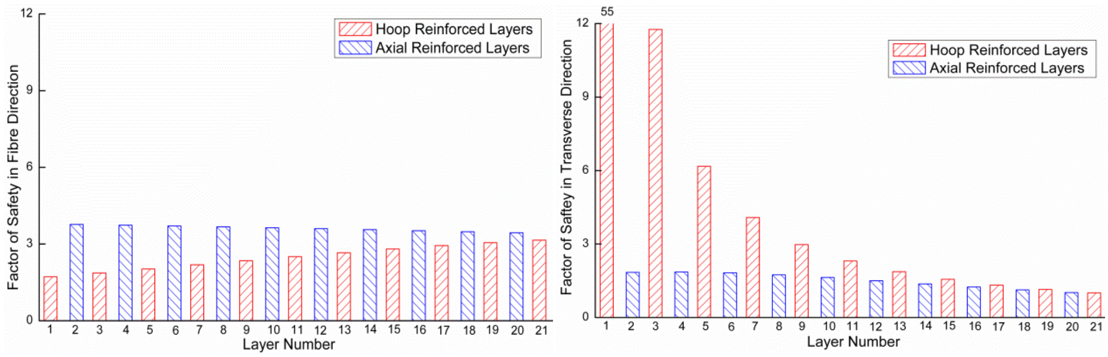

(a) (b)

Fig. B.11. FSs for composite layers with 0° and 90˚ reinforcements for load case 1 for AS4/epoxy with steel liner in (a) fibre direction and (b) transverse direction

B.3.2 Results for AS4/Epoxy with Steel Liner [90/(0/90)$_{10}$] under Pure Tension Case

As described in *Chapter 3*, the tension force has to be calculated using three different cases which yield values of 2790kN, 1710kN and 2790kN, respectively. Therefore, the design tension force is 2790×2.25=6280kN.

Under a 6280kN pure tension, the Von Mises stress in the steel liner is 521.2MPa, providing FS=1.20. Figs. B.12(a) and B.12(b) show the FSs in every layer under load case 2(a) (pure tension) for the conventional design. As can be seen, they are quite large which indicates that this load case is not as critical as the burst case for this material combination (the FSs for stresses in the fibre direction for the hoop reinforced layers in Fig. B.12(a) are well above 40 since the loading is mainly in the axial direction).

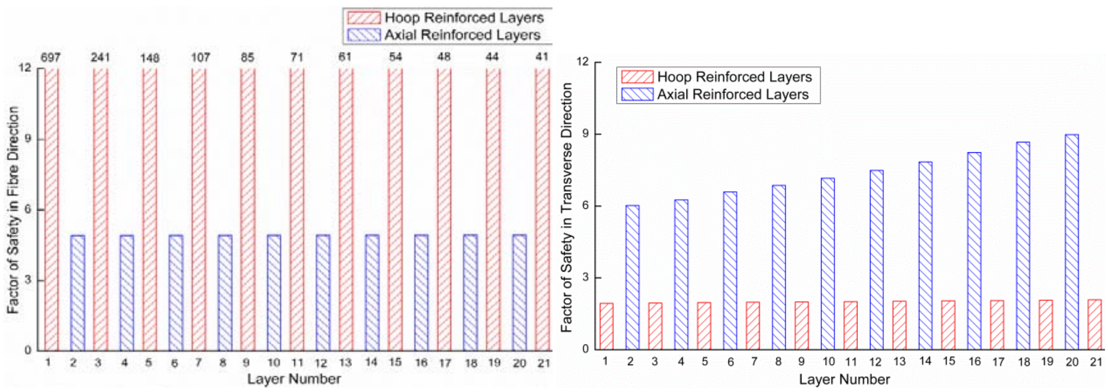

(a) (b)

Fig. B.12. FSs for composite layers with 0° and 90˚ reinforcements for load case 2(a) for AS4/epoxy with steel liner in (a) fibre direction and (b) transverse direction

B.3.3 Results for AS4/Epoxy with Steel Liner [90/(0/90)$_{10}$] under Tension with External Pressure Case

The tension force under load case 2(b) (tension with external pressure of 19.5MPa) is also 6280kN and the Von Mises stress in the steel liner is 555.1MPa, providing FS=1.12. Fig. B.13 shows its FSs under load case 2(b) for the conventional design with the minimum being 2.19 in transverse direction in layer 1 (Fig. B.13(b)).

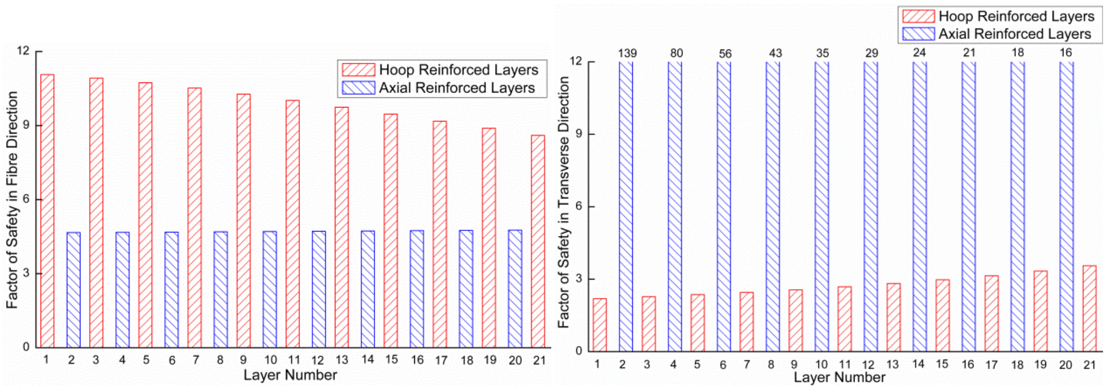

(a) (b)

Fig. B.13. FSs for composite layers with 0° and 90˚ reinforcements for load case 2(b) for AS4/epoxy with steel liner in (a) fibre direction and (b) transverse direction

B.3.4 Results for AS4/Epoxy with Steel Liner [90/(0/90)$_{10}$] under Collapse Case

The design collapse pressure for the composite riser is 58.5MPa under which the Von Mises stress in the steel liner is 498.30MPa, providing FS=1.25. Fig. B.14 shows the FSs under load case 3 (collapse load) for the conventional design, with the minimum being 3.58 in transverse direction in layer 20 (Fig. B.14(b)).

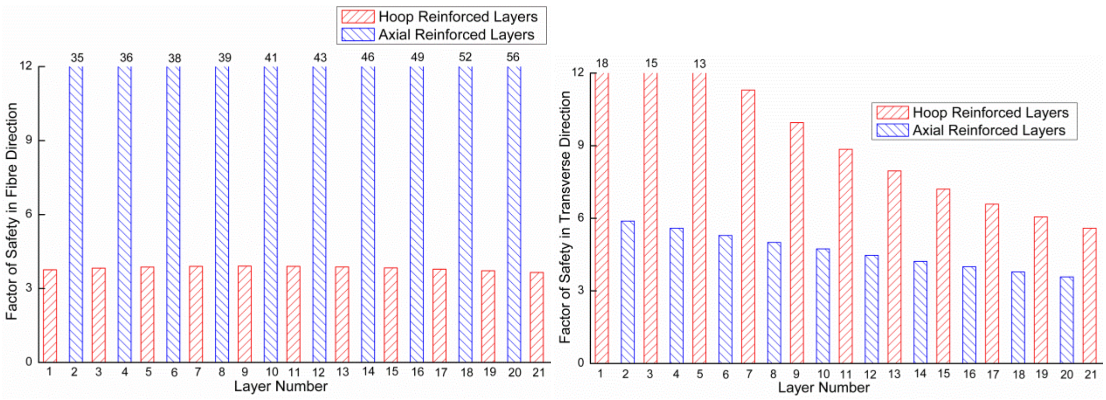

(a) (b)

Fig. B.14. FSs for composite layers with 0° and 90˚ reinforcements for load case 3 for AS4/epoxy with steel liner in (a) fibre direction and (b) transverse direction

B.3.5 Results for AS4/Epoxy with Steel Liner [90/(0/90)$_{10}$] under Buckling Case

The geometry of AS4/epoxy with steel liner riser using the conventional design is also checked for buckling under external pressure (load case 4) and the critical buckling pressure obtained is 387.6MPa (mode 1), which is much higher than the design buckling pressure of 58.5MPa. The first three mode shapes can be seen in the Fig. B.15 in which the number of circumferential waves is 2 for all three modes and the number of half-waves along the axial direction 1, 2 and 3 for modes 1, 2 and 3, respectively.

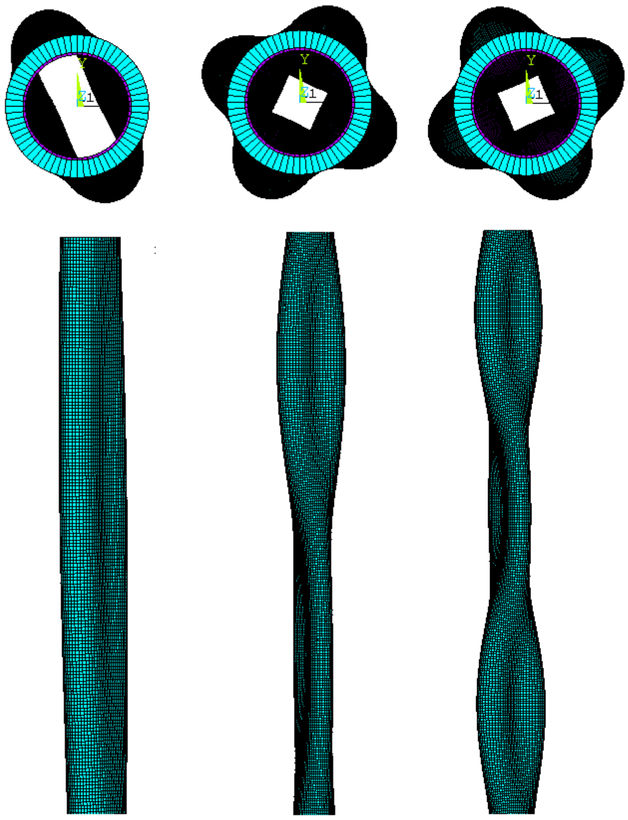

(a) B.P.=387.6MPa (b) B.P.=389.8MPa (c) B.P.=395.3MPa

Fig. B.15. Mode shapes of composite riser with 0° and 90° reinforcements for AS4/epoxy with steel liner (5m): (a) mode 1 (b) mode 2 and (c) mode 3

B.4 Results for AS4/Epoxy with Steel Liner Using Tailored Design

Following the tailored design procedure, the effects of fibre orientations and stacking sequences on the structural weight are determined and presented in Figs. B.16 and B.17, respectively. In the step 2 of the manually tailored local design of composite riser, for the burst case (without a liner), the best fibre orientation is 54.7° and the minimum thickness is 16.8mm according to the netting theory and 51° and 32.4mm according to CLT theory. These best reinforcement angles have to be verified in step 3 of the design procedure using 3D FEA simulation under burst case with the same liner thickness obtained by conventional design results (2mm) and, in the FEA model, the geometry of $[\pm\theta]_5$ with 32.4mm of laminate and 2mm of liner is employed. Variations in the minimum FSs in fibre direction, in-plane transverse direction and in in-plane shear of composite laminate are illustrated in Fig. B.16.

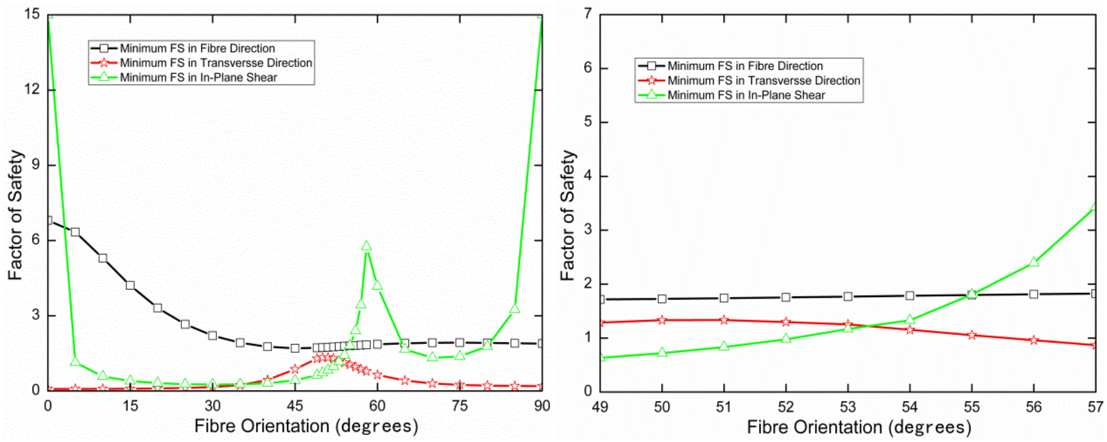

(a) (b)

Fig. B.16. Variations of FS with fibre orientation for burst capacity (a) full range of angles (b) magnified view

Similarly, the effect of the stacking sequences on the weight and thickness is illustrated in Fig. B.17. The four typical locations at which additional axial and hoop reinforcements are provided to the ±θ layers are: (1) innermost layer, (2) middle of the ±θ° layers, (3) outermost layer and (4) axial reinforcements in the innermost layer with hoop reinforcements added in the outermost layer.

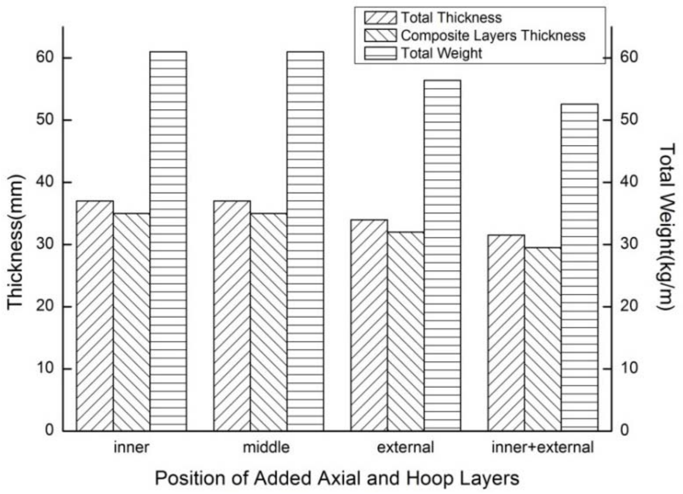

Fig. B.17. Influence of stacking sequences on the thickness and weight

It can be seen in Fig. B.16 and Fig. B.17 that ±53.5° is the most efficient angle for taking full advantage of the reinforcement strengths in every direction under burst case. The stacking sequence with the ±53.5° reinforced layers between its axial (innermost) and hoop (outermost) layers provides the lowest total thickness and, therefore, the lowest structural weight.

Table B.4 gives the geometry of the composite riser tube optimised for minimum thickness using the manually tailored design.

Table B.4. Geometry of AS4/epoxy with steel liner riser including angle reinforcements

Layer	Orientation (degree)	Thickness(mm)	Layer	Orientation (degree)	Thickness(mm)
liner		2	9	-53.5	1.72
1	0 (axial)	1.8	10	53.5	1.72
2	0	1.9	11	-53.5	1.72
3	0	1.8	12	53.5	1.72
4	53.5	1.72	13	-53.5	1.72
5	-53.5	1.72	14	90 (hoop)	1.7
6	53.5	1.72	15	90	1.7
7	-53.5	1.72	16	90	1.7
8	53.5	1.72	17	90	1.7
Total thickness: 31.5mm and structural weight: 52.6kg/m					

The tailored design, including the angle plies provides a 17-layer composite laminate $[0_3/(+53.5,-53.5)_5/90_4]$ with the 0^o, $\pm53.5^o$ and 90^o having thicknesses of 1.8(1.9), 1.72 and 1.70mm respectively. The total laminate thickness for the design, including the angle plies, is only 29.5mm with same 2mm thickness of the steel liner. It is again to be noted that the optimum angle of reinforcement for the angle plies is obtained as $\pm53.5^o$ using the 3D FEA, not $\pm54.7^o$ as predicted by netting theory.

B.4.1 Results for AS4/Epoxy with Steel Liner $[0_3/(\pm53.5)_5/90_4]$ under Burst Case

The design burst pressure for the composite riser is 155.25MPa under which the Von Mises stress in the steel liner is 571.51MPa, providing FS=1.09. Figs. B.18(a), B.18(b) and B.18(c), respectively, show the FSs in the fibre, transverse directions and in-plane shear for all the layers under load case 1 (burst load) for the manually tailored design with additional angle plies and considering different stacking sequences. The minimum FSs are 1.63 in the fibre direction (layer 14 in Fig. B.18(a)), 1.00 in the transverse direction (layer 3 in Fig. B.18(b)) and about 2.10 in shear (layer 4 in Fig. B.18(c)). In this case, the in-plane transverse stresses are the most critical stresses and determine the thickness of the composite layers.

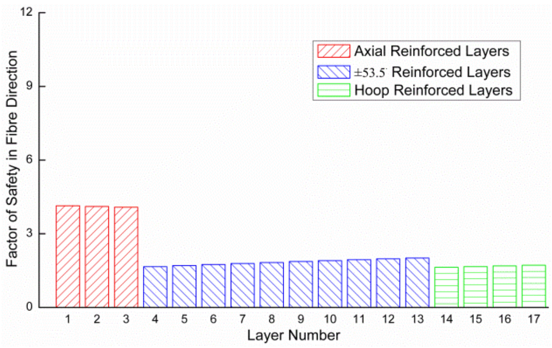

(a)

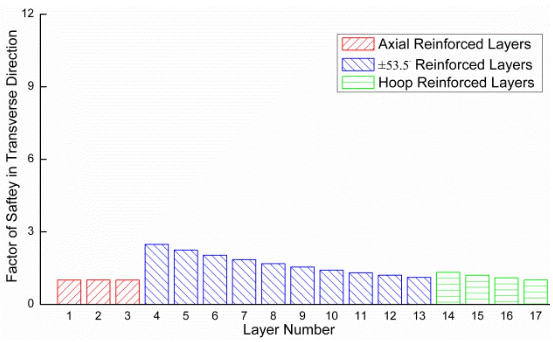

(b)

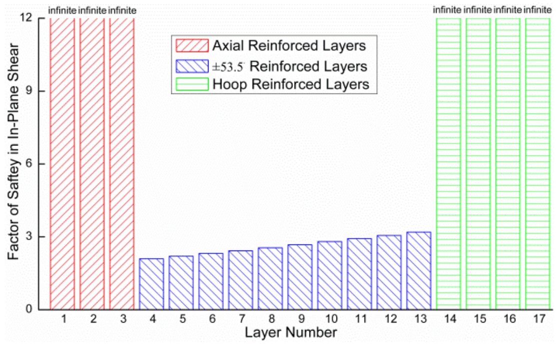

(c)

Fig. B.18. FSs for composite layers with 0°, ±53.5˚ and 90˚ reinforcements for load case 1 for AS4/epoxy with steel liner in (a) fibre direction (b) transverse direction, and (c) in-plane shear

B.4.2 Results for AS4/Epoxy with Steel Liner [0_3 /($\pm$53.5)$_5$ /90_4] under Pure Tension Case

As described in *Chapter 3*, the tension force has to be calculated using three different cases which yield values of 2640kN, 1520kN and 2480kN, respectively. Therefore, the design tension force is 2640×2.25=5940kN.

Under a pure tension (5940kN), the Von Mises stress in the steel liner is 558.2MPa, providing FS=1.12. Figs. B.19(a), B.19(b) and B.19(c) show the FSs in all the layers under load case 2(a) (pure tension) for the manually tailored design. In this case, while the other FSs are relatively high, the minimum FS in the transverse direction of the hoop layers is about 1.03 (layer 17, Fig. B.19(b)).

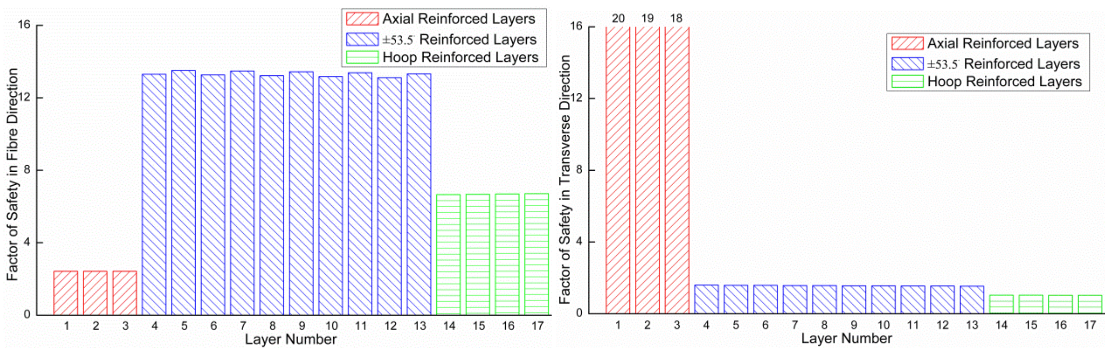

(a) (b)

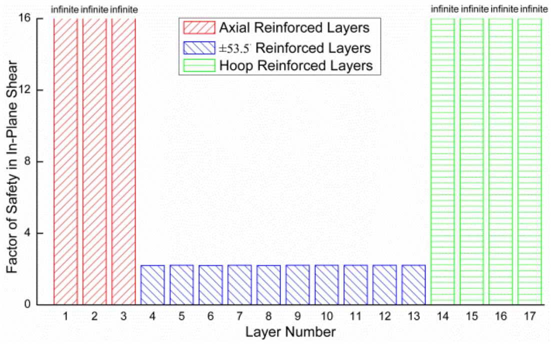

(c)

Fig. B.19. FSs for composite layers with 0°, ±53.5˚ and 90˚ reinforcements under load case 2(a) for AS4/epoxy with steel liner in (a) fibre direction, (b) transverse direction and (c) in-plane shear

B.4.3 Results for AS4/Epoxy with Steel Liner [0_3 /(±53.5)$_5$ /90_4] under Tension with External Pressure Case

The tension force under load case 2(b) (tension with external pressure of 19.5MPa) is the same as that for load case 2(a), that is 5940kN, and the Von Mises stress in the steel liner is 559.5MPa, providing FS=1.12. Fig. B.20 shows the FSs under load case 2(b) for the manually tailored design with the minimum being 1.08 in transverse direction in layer 14 (Fig. B.20(b)).

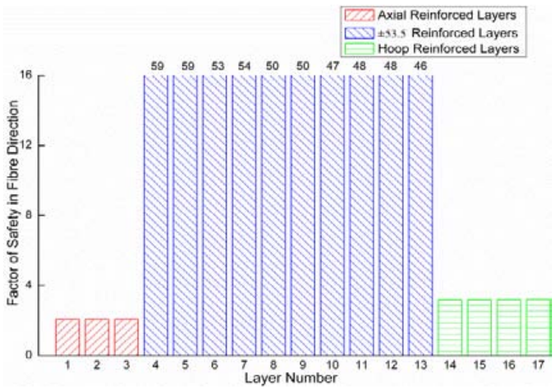

(a)

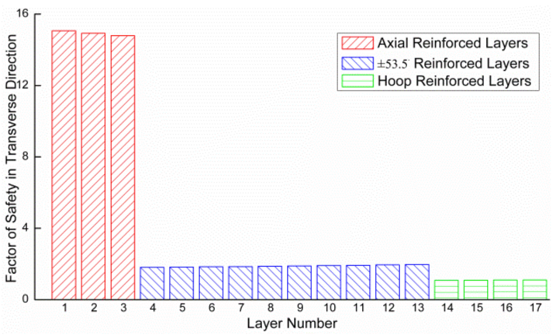

(b)

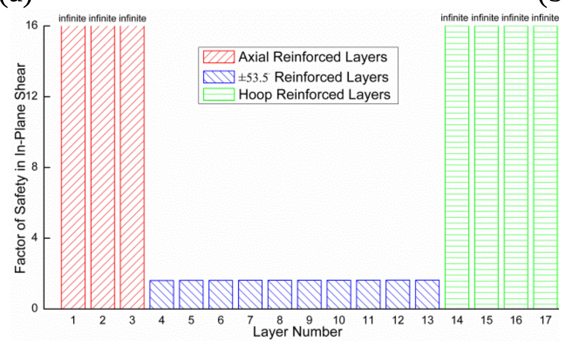

(c)

Fig. B.20. FSs for composite layers with 0°, ±53.5˚ and 90˚ reinforcements for load case 2(b) for AS4/epoxy with steel liner in (a) fibre direction, (b) transverse direction and (c) in-plane shear

B.4.4 Results for AS4/Epoxy with Steel Liner [0_3 /($\pm$53.5)$_5$ /90_4] under Collapse Case

The design collapse pressure for the composite riser is 58.5MPa and under this external over-pressure, the Von Mises stress in the steel liner is 557.81MPa, providing FS=1.12. Fig. B.21 shows the FSs under load case 3 (collapse load) for the manually tailored design with the minimum being 2.14 in fibre direction in layer 14 (Fig. B.21(a)).

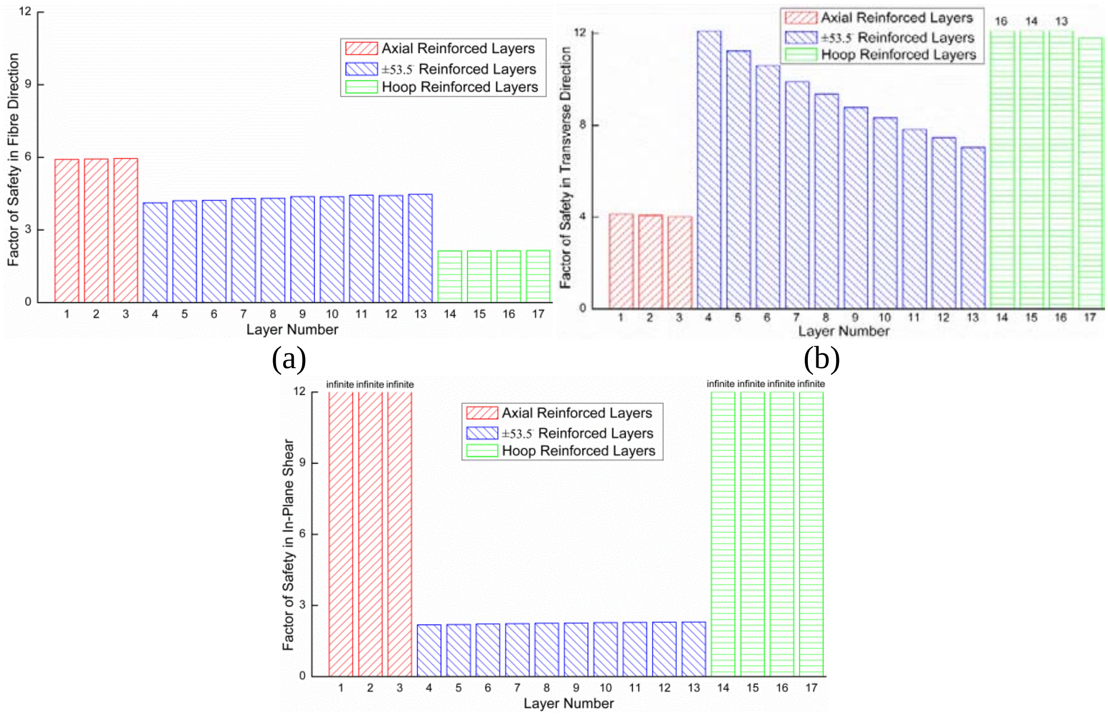

(c)

Fig. B.21. FSs for composite layers with 0°, ±53.5˚ and 90˚ reinforcements for load case 3 for AS4/epoxy with steel liner in (a) fibre direction, (b) transverse direction and (c) in-plane shear

B.4.5 Results for AS4/Epoxy with Steel Liner [0_3 /($\pm$53.5)$_5$ /90_4] under Buckling Case

The geometry of AS4/epoxy with steel liner riser using the tailored design is also checked for buckling under external pressure (load case 4). The critical buckling pressure obtained is 206.2MPa (mode 1), which is much higher than the design buckling pressure of 58.5MPa. The first three mode shapes are shown in the Fig. B.22 in which it can be seen that the number of circumferential waves is 2 for all three modes and the number of half-waves along the axial direction 1, 2 and 3 for modes 1, 2 and 3, respectively.

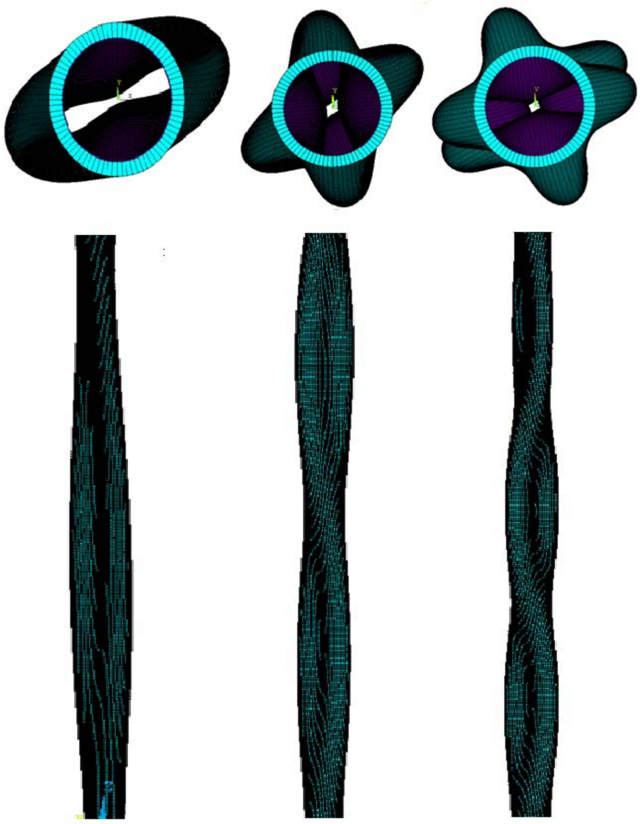

(a) B.P.= 206.2MPa (b) B.P.=206.8MPa (c) B.P.=208.4MPa
Fig. B.22. Mode shapes of composite riser with 0°, ±53.5˚ and 90˚ reinforcements for AS4/epoxy with steel liner (5m): (a) mode 1, (b) mode 2 and (c) mode 3

B.5 Results for AS4/Epoxy with Titanium Liner Using Conventional Design

Table B.5 gives the geometry of the composite riser tube optimised for minimum thickness using the conventional design under the local load cases which yields a 21-ply composite laminate $[90/(0/90)_{10}]$ with alternating hoop and axially reinforced layers having thicknesses of 2.15mm and 1.385mm, respectively, which results in a total laminate thickness of 37.5mm, with a 2mm titanium liner and structural weight of 59.6kg/m. Unlike PEEK liner riser, the thickness of titanium liner would affect total weight significantly, thus, the first step is the determination of the thickness of titanium liner. The variations of thickness and weight according to the different thicknesses of titanium liner are shown in Fig. B.23 in which it can be seen that when the titanium liner is 2mm, the total weight is the minimum. Hence for the following analysis, 2mm titanium liner is used.

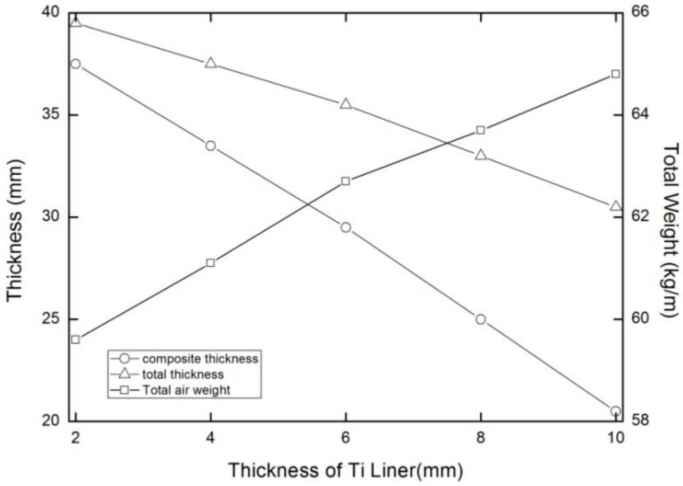

Fig. B.23. Thickness and weight of composite cylinder according to different thickness of titanium liner

Table B.5. Geometry of AS4/epoxy with titanium liner riser with orthogonal reinforcements

Layer	Orientation (degree)	Thickness(mm)	Layer	Orientation (degree)	Thickness(mm)
liner		2	11	90	2.15
1	90 (hoop)	2.15	12	0	1.385
2	0 (axial)	1.385	13	90	2.15
3	90	2.15	14	0	1.385
4	0	1.385	15	90	2.15
5	90	2.15	16	0	1.385
6	0	1.385	17	90	2.15
7	90	2.15	18	0	1.385
8	0	1.385	19	90	2.15
9	90	2.15	20	0	1.385
10	0	1.385	21	90	2.15
Total thickness: 39.5mm and structural weight: 59.6kg/m					

B.5.1 Results for AS4/Epoxy with Titanium Liner [90/(0/90)$_{10}$] under Burst Case

The design internal burst pressure for the composite riser is 155.25MPa for which the Von Mises stress in the titanium liner is 881.4MPa, providing FS=1.08. Figs. B.24(a) and B.24(b), respectively, show the FSs in the fibre and transverse directions under load case 1 (burst load) for all the layers in the conventional design geometry. The minimum FS in the fibre direction is 1.74 (layer 1 in Fig. B.24(a)), while that in the transverse direction is 1.00 (layers 20 and 21 in Fig. B.24(b)). It is evident, that under burst case, the in-plane transverse stresses are the most critical stresses and determine the minimum thickness of the composite AS4/epoxy with titanium liner with only 0^{o} and 90^{o} reinforcements.

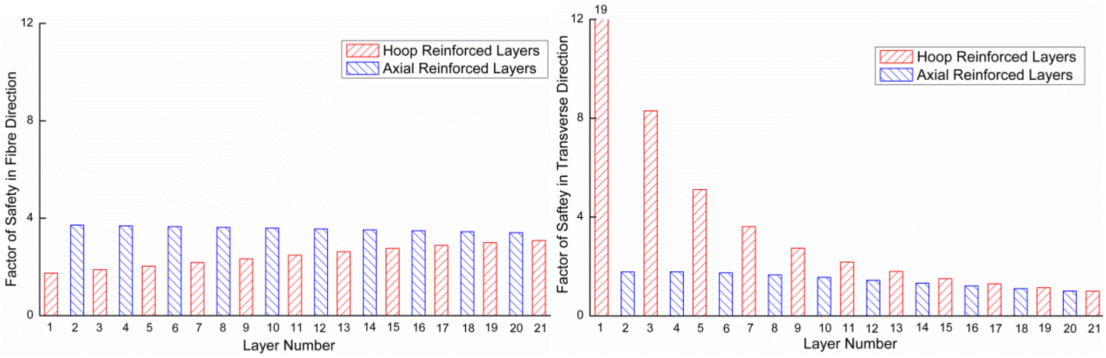

(a) (b)

Fig. B.24. FSs for composite layers with 0° and 90˚ reinforcements for load case 1 for AS4/epoxy with titanium liner in (a) fibre direction, and (b) transverse direction

B.5.2 Results for AS4/Epoxy with Titanium Liner [90/(0/90)$_{10}$] under Pure Tension Case

As described in *Chapter 3*, the tension force has to be calculated using three different cases which yield values of 2600kN, 1470kN and 2600kN, respectively. Therefore the design tension force is 2600×2.25=5850kN.

Under a 5850kN pure tension, the Von Mises stress in the titanium liner is 309.47MPa, providing FS=3.07. Figs. B.25(a) and B.25(b) show the FSs in every layer under load case 2(a) (pure tension) for the conventional design. As can be seen, they are quite large which indicates that this load case is not as critical as the burst case for this material combination (the FSs for stresses in the fibre direction for the hoop-reinforced layers in Fig. B.25(a) are well above 40 since the loading is mainly in the axial direction).

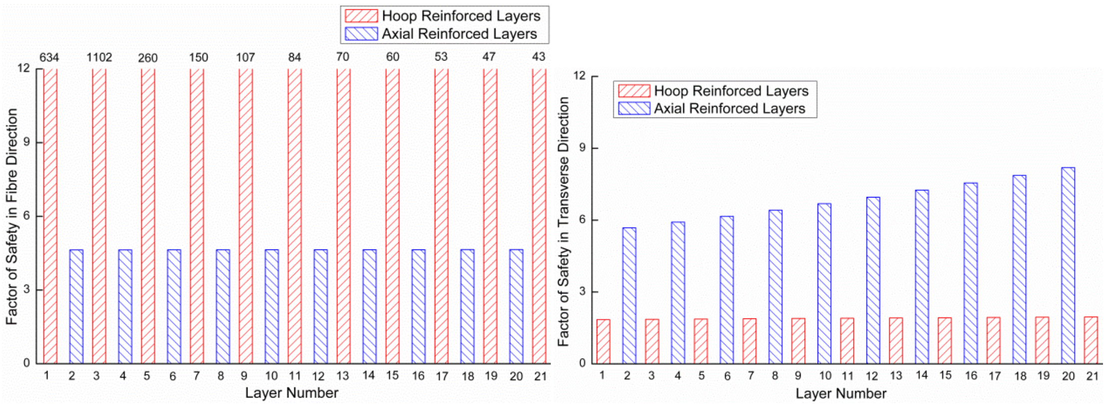

(a) (b)

Fig. B.25. FSs for composite layers with 0° and 90˚ reinforcements for load case 2(a) for AS4/epoxy with titanium liner in (a) fibre direction, and (b) transverse direction

B.5.3 Results for AS4/Epoxy with Titanium Liner [90/(0/90)$_{10}$] under Tension with External Pressure Case

The tension force under load case 2(b) (tension with external pressure of 19.5MPa) is also 5850kN and the Von Mises stress in the titanium liner is 328.47MPa, providing FS=2.89. Fig. B.26 shows the FSs under load case 2(b) for the conventional design with the minimum being 2.07 in transverse direction in layer 1 (Fig. B.26(b)).

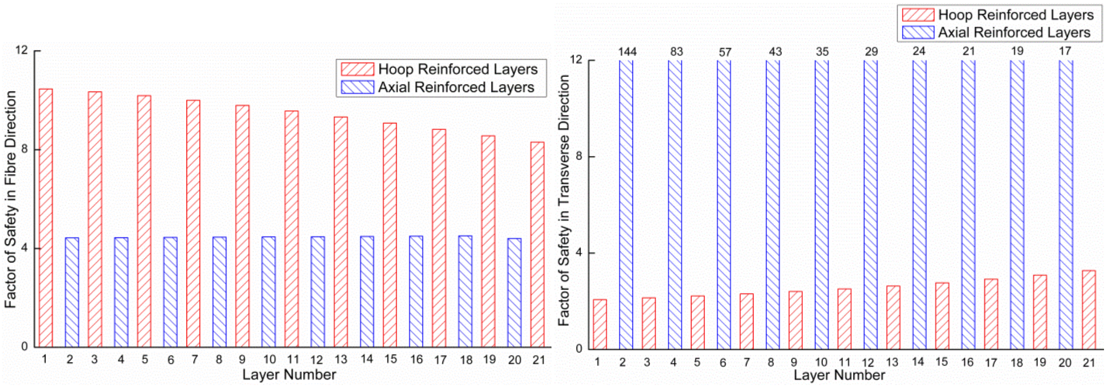

(a) (b)

Fig. B.26. FSs for composite layers with 0° and 90° reinforcements for load case 2(b) for AS4/epoxy with titanium liner in (a) fibre direction, and (b) transverse direction

B.5.4 Results for AS4/Epoxy with Titanium Liner [90/(0/90)$_{10}$] under Collapse Case

The design collapse pressure for the composite riser is 58.5MPa under which the Von Mises stress in the titanium liner is 304.79MPa, providing FS=3.12. Fig. B.27 shows the FSs under load case 3 (collapse load) for the conventional design, with the minimum being 3.41 in fibre direction in layer 1 (Fig. B.27(a)).

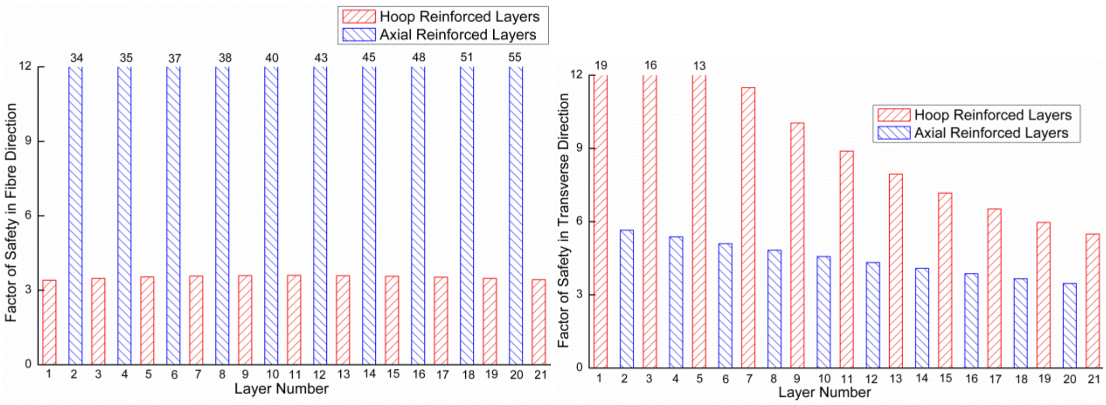

(a) (b)

Fig. B.27. FSs for composite layers with 0° and 90° reinforcements for load case 3 for AS4/epoxy with titanium liner in (a) fibre direction, and (b) transverse direction

B.5.5 Results for AS4/Epoxy with Titanium Liner [90/(0/90)$_{10}$] under Buckling Case

The geometry of AS4/epoxy with titanium liner riser using the conventional design is also checked for buckling under external pressure (load case 4) and the critical buckling pressure obtained is 327.6MPa (mode 1), which is much higher than the design buckling pressure of 58.5MPa. The first three mode shapes can be seen in the Fig. B.28 in which the number of circumferential waves is 2 for all three modes and the number of half-waves along the axial direction 1, 2 and 3 for modes 1, 2 and 3, respectively.

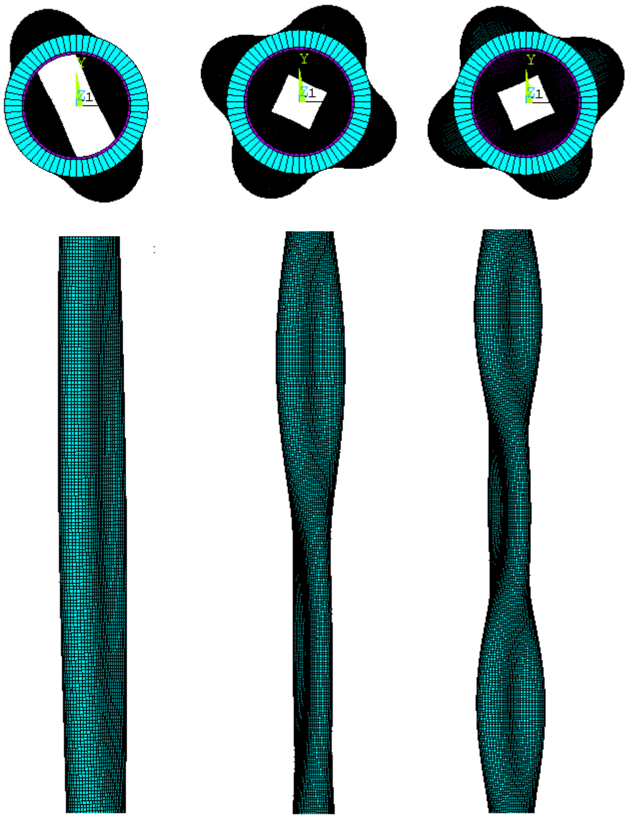

(a) B.P.=327.6MPa (b) B.P.=329.4MPa (c) B.P.=334.0MPa

Fig. B.28. Mode shapes of composite riser with 0° and 90° reinforcements for AS4/epoxy with titanium liner (5m): (a) mode 1 (b) mode 2 and (c) mode 3

B.6 Results for AS4/Epoxy with Titanium Liner Using Tailored Design

Following the tailored design procedure, the effects of fibre orientations and stacking sequences on the structural weight are determined and presented in Figs. B.29 and B.30, respectively. In the step 2 of the tailored local design of composite riser, for the burst case (without liner), the best fibre orientation is 54.7° and the minimum thickness is 16.8mm according to the netting theory and 51° and 32.4mm according to CLT theory. These best reinforcement angles have to be verified in step 3 of the design procedure using 3D FEA simulation under burst case with the same liner thickness obtained by conventional design results (2mm). In the FEA model, the geometry of

$[\pm\theta]_5$ with 32.4mm of laminate and 2mm of liner is employed. Variations in the minimum FSs in fibre direction, in-plane transverse direction and in in-plane shear of composite laminate are illustrated in Fig. B.29.

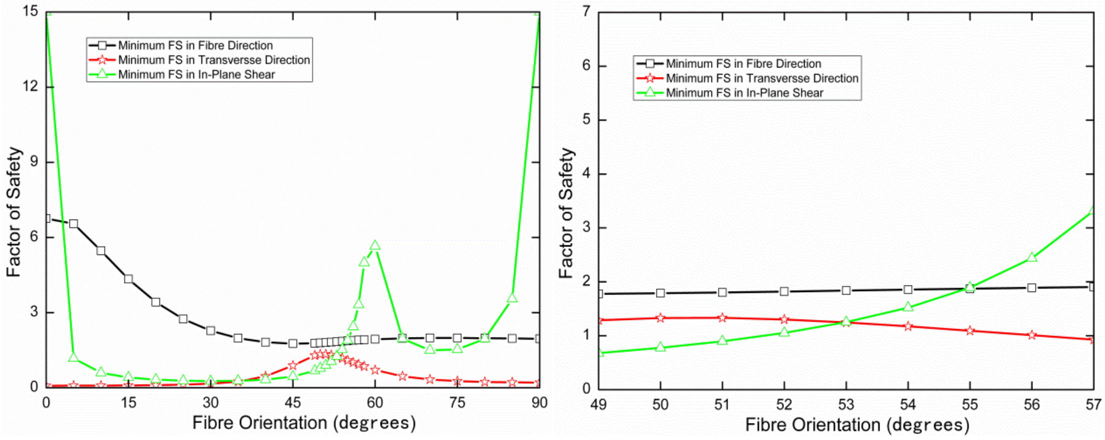

(a) (b)

Fig. B.29. Variations in FS with fibre orientation for burst capacity (a) full range of angles (b) magnified view

Similarly, the effect of the stacking sequences on the weight and thickness is illustrated in Fig. B.30. The four typical locations at which additional axial and hoop reinforcements are provided to the $\pm\theta$ layers are: (1) innermost layer, (2) middle of the $\pm\theta^{o}$ layers, (3) outermost layer and (4) axial reinforcements in the innermost layer with hoop reinforcements added in the outermost layer.

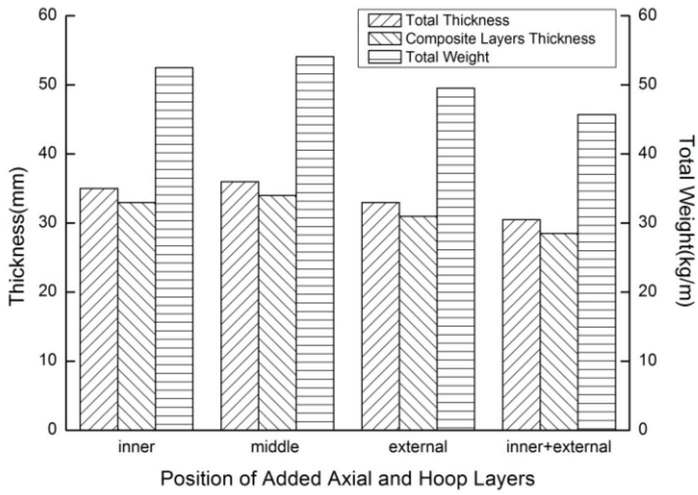

Fig. B.30. Influence of stacking sequences on the thickness and weight

It can be seen in Fig. B.29 and Fig. B.30 that $\pm 53^{o}$ is the most efficient angle for taking full advantage of their reinforcement strengths in every direction under the burst case. The stacking sequence with the $\pm 53^{o}$ reinforced layers between its axial (innermost) and hoop (outermost) layers provides the lowest total thickness and, therefore, the lowest structural weight.

Table B.6 gives the geometry of the composite riser tube optimised for minimum thickness using the tailored design.

Table B.6. Geometry of AS4/epoxy with titanium liner riser including angle reinforcements

Layer	Orientation (degree)	Thickness (mm)	Layer	Orientation (degree)	Thickness(mm)
liner		2	9	-53	1.64
1	0 (axial)	1.70	10	53	1.64
2	0	1.70	11	-53	1.64
3	0	1.70	12	53	1.64
4	53	1.64	13	-53	1.64
5	-53	1.64	14	90 (hoop)	1.75
6	53	1.64	15	90	1.75
7	-53	1.64	16	90	1.75
8	53	1.64	17	90	1.75
Total thickness: 30.5mm and structural weight: 45.7kg/m					

The tailored design, including the angle plies, provides a 17-layer composite laminate $[0_3/(+53,-53)_5/90_4]$ with the 0^o, $\pm 53^o$ and 90^o having thicknesses of 1.70, 1.64 and 1.75mm, respectively. The total laminate thickness for the design, including the angle plies is only 28.5mm with the same 2mm thickness of the titanium liner. It is again to be noted that the optimum angle of reinforcement for the angle plies is obtained as $\pm 53^o$ using the 3D FEA, not $\pm 54.7^o$ as predicted by netting theory.

B.6.1 Results for AS4/Epoxy with Titanium Liner $[0_3/(\pm 53)_5/90_4]$ under Burst Case

The design burst pressure for the composite riser is 155.25MPa under which the Von Mises stress in the titanium liner is 883.63MPa, providing FS=1.07. Figs. B.31(a), B.31(b) and B.31(c) respectively show the FSs in the fibre, transverse directions and in-plane shear for all the layers under load case 1 (burst load) for the manually tailored design with additional angle plies and considering different stacking sequences. The minimum FSs are 1.65 in the fibre direction (layer 14 in Fig. B.31(a)), 1.01 in the transverse direction (layer 3 and layer 17 in Fig. B.31(b)) and about 2.16 in shear (layer 4 in Fig. B.31(c)). In this case, the in-plane transverse stresses are most critical stresses and determine the thickness of the composite layers.

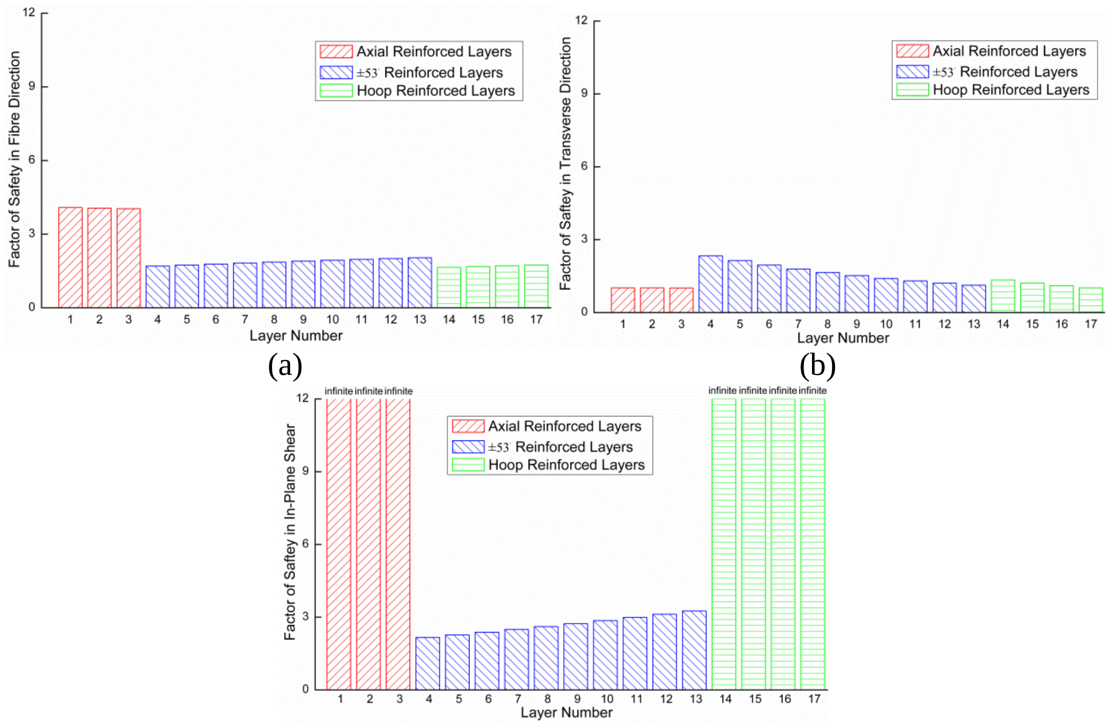

(a) (b)

(c)

Fig. B.31. FSs for composite layers with 0°, ±53˚ and 90˚ reinforcements for load case 1 for AS4/epoxy with titanium liner in (a) fibre direction, (b) transverse direction and (c) in-plane shear

B.6.2 Results for AS4/Epoxy with Titanium Liner [0_3 /$(\pm53)_5$ /90_4] under Pure Tension Case

As described in *Chapter 3*, the tension force has to be calculated using three different cases, which yield values of 2500kN, 1300kN and 2330kN, respectively. Therefore the design tension force is 2500×2.25=5625kN.

Under a pure tension (5625kN), Von Mises stress in the titanium liner is 573.74MPa, providing FS=1.65. Figs. B.32(a), B.32(b) and B.32(c) show the FSs in all the layers under load case 2(a) (pure tension) for the manually tailored design. In this case, while the other FSs are relatively high, the minimum FS is about 1.06 in the transverse direction of the hoop layers in layer 17 (Fig. B.32(b)).

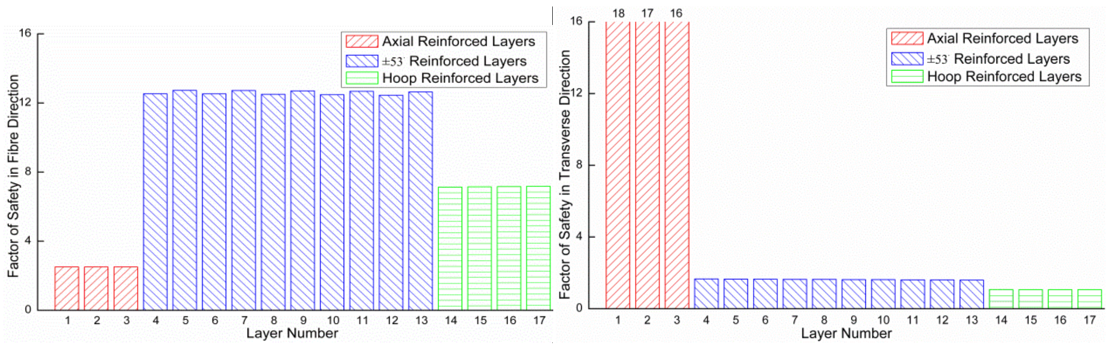

(a) (b)

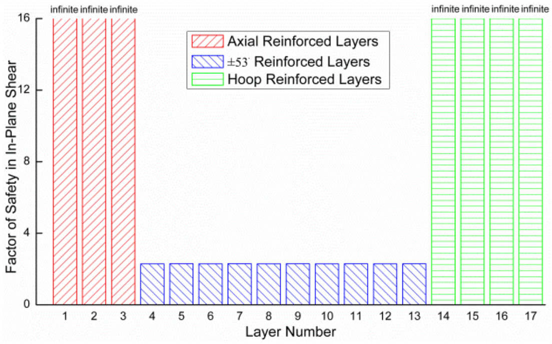

(c)

Fig. B.32. FSs for composite layers with 0°, ±53˚ and 90˚ reinforcements for load case 2(a) for AS4/epoxy with titanium liner in (a) fibre direction, (b) transverse direction and (c) in-plane shear

B.6.3 Results for AS4/Epoxy with Titanium Liner $[0_3 /(\pm 53)_5 /90_4]$ under Tension with External Pressure Case

The tension force under load case 2(b) (tension with external pressure of 19.5MPa) is the same as that for load case 2(a), that is 5625kN, and the Von Mises stress in the titanium liner is 697.69MPa, providing FS=1.36. Fig. B.33 shows the FSs under load case 2(b) for the manually tailored design with the minimum being 1.15 in the transverse direction in layer 14 (Fig. B.33(b)).

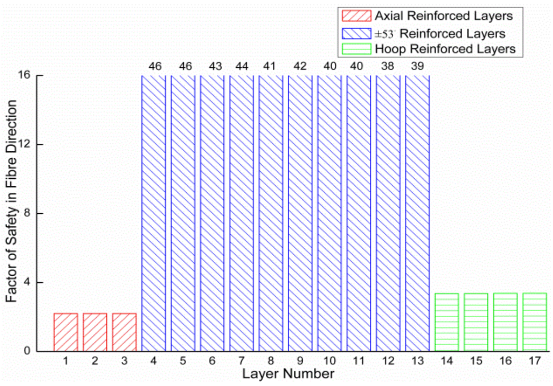

(a)

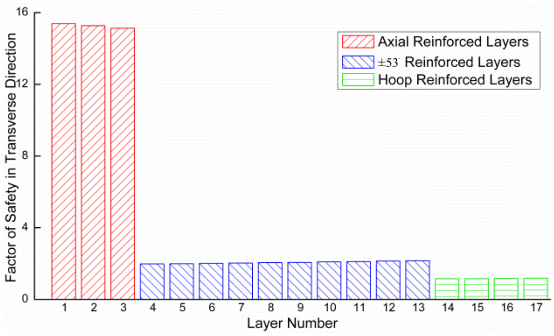

(b)

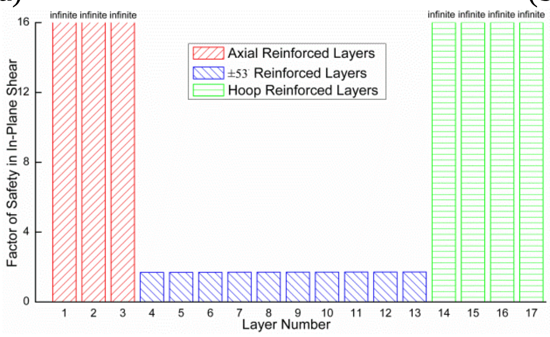

(c)

Fig. B.33. FSs for composite layers with 0°, ±53˚ and 90˚ reinforcements for load case 2(b) for AS4/epoxy with titanium liner in (a) fibre direction, (b) transverse direction and (c) in-plane shear

B.6.4 Results for AS4/Epoxy with Titanium Liner $[0_3 /(\pm 53)_5 /90_4]$ under Collapse Case

The design collapse pressure for the composite riser is 58.5MPa under which the Von Mises stress in the titanium liner is 580.56MPa, providing FS=1.64. Fig. B.34 shows the FSs under load case 3 (collapse load) for manually tailored design with the minimum being 2.11 in fibre direction in layer 14 (Fig. B.34(a)).

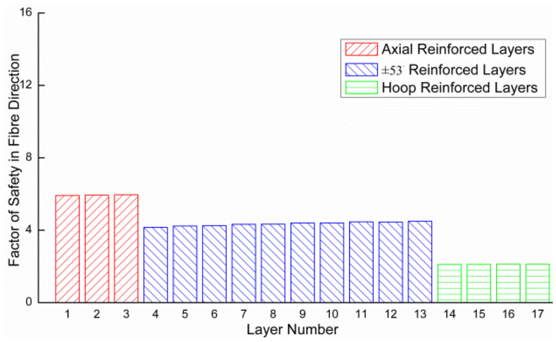

(a)

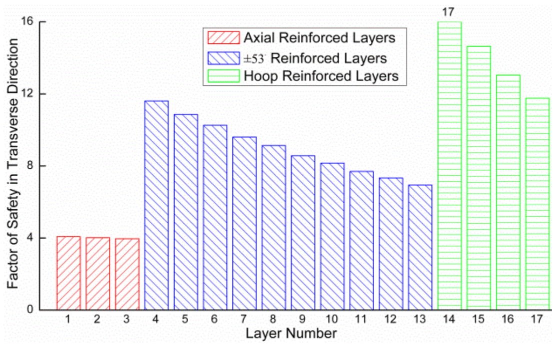

(b)

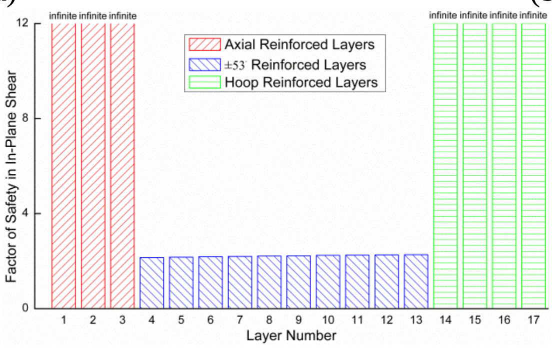

(c)

Fig. B.34. FSs for composite layers with 0°, ±53˚ and 90˚ reinforcements for load case 3 for AS4/epoxy with titanium liner in (a) fibre direction, (b) transverse direction and (c) in-plane shear

B.6.5 Results for AS4/Epoxy with Titanium Liner $[0_3/(\pm 53)_5/90_4]$ under Buckling Case

The geometry of AS4/epoxy with titanium liner riser using the tailored design is also checked for buckling under external pressure (load case 4). The critical buckling pressure obtained is 161.2MPa (mode 1), which is much higher than the design buckling pressure of 58.5MPa. The first three mode shapes are shown in the Fig. B.35 in which the number of circumferential waves is 2 for all three modes and the number of half-waves along the axial direction 2, 2 and 3 for modes 1, 2 and 3, respectively.

(a) B.P.= 161.2MPa (b) B.P.= 161.4MPa (c) B.P.= 161.9MPa

Fig. B.35. Mode shapes of composite riser with 0°, ±53˚ and 90˚ reinforcements for AS4/epoxy with titanium liner (5m): (a) mode 1, (b) mode 2 and (c) mode 3

B.7 Results for AS4/Epoxy with Aluminium Liner Using Conventional Design

Table B.7 gives the geometry of the composite riser tube optimised for minimum thickness using the conventional design under the local load cases. The conventional design yields a 21-ply composite laminate $[90/(0/90)_{10}]$ with alternating hoop and axially reinforced layers having thicknesses of 2.25mm and 1.525mm, respectively, which results in a total laminate thickness of 40mm and with a 2mm aluminium liner and the structural weight of 60.9kg/m. Unlike PEEK liner riser, the thickness of aluminium liner would affect total weight significantly, thus, the first step is the determination of the thickness of aluminium liner. The variations of thickness and weight according to the different thicknesses of aluminium liner are shown in Fig. B.36 in which it can be seen that when the aluminium liner is 2mm, the total weight is the minimum. Hence for the following analysis, 2mm aluminium liner is used.

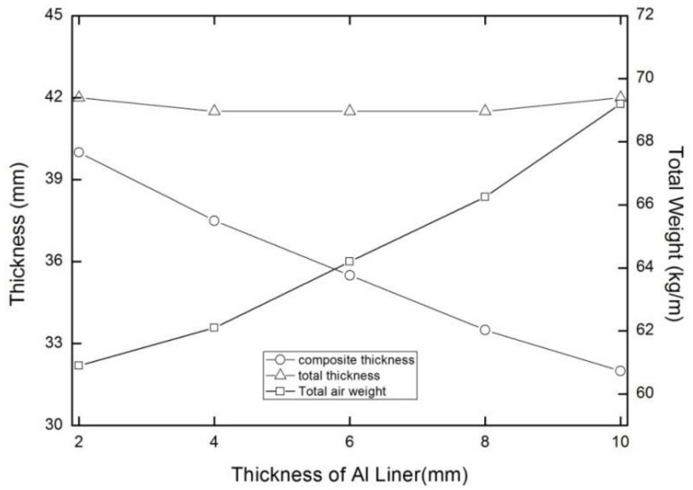

Fig. B.36. Thickness and weight of composite cylinder according to different thickness of aluminium liner

Table B.7. Geometry of AS4/epoxy with aluminium liner riser with orthogonal reinforcements

Layer	Orientation (degree)	Thickness (mm)	Layer	Orientation (degree)	Thickness (mm)
liner		2	11	90	2.25
1	90 (hoop)	2.25	12	0	1.525
2	0 (axial)	1.525	13	90	2.25
3	90	2.25	14	0	1.525
4	0	1.525	15	90	2.25
5	90	2.25	16	0	1.525
6	0	1.525	17	90	2.25
7	90	2.25	18	0	1.525
8	0	1.525	19	90	2.25
9	90	2.25	20	0	1.525
10	0	1.525	21	90	2.25
Total thickness: 42mm and structural weight: 60.9kg/m					

B.7.1 Results for AS4/Epoxy with Aluminium Liner $[90/(0/90)_{10}]$ under Burst Case

The design burst pressure for the composite riser is 155.25MPa under which the Von Mises stress in the aluminium liner is 483.87MPa, providing FS=1.12. Figs. B.37(a) and B.37(b), respectively, show the FSs in the fibre and transverse directions under load case 1 (burst load) for all the layers in the conventional design geometry. The minimum FS in the fibre direction is 1.70 (layer 1 in Fig. B.37(a)), while that in the transverse direction is 1.01 (layers 20 and 21 in Fig. B.37(b)). It is evident that, under burst case, the in-plane transverse stresses are the most critical stresses and determine the minimum thickness of the composite AS4/epoxy with aluminium liner with only 0^o and 90^o reinforcements.

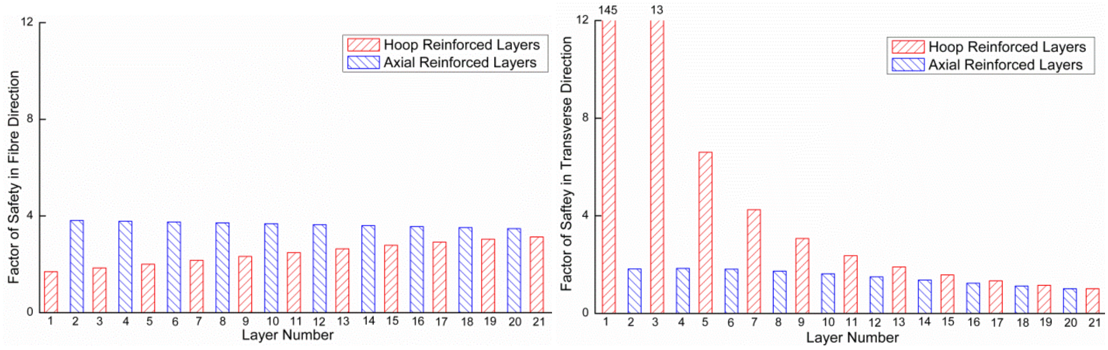

(a) (b)

Fig. B.37. FSs for composite layers with 0° and 90˚ reinforcements for load case 1 for AS4/epoxy with aluminium liner in (a) fibre direction and (b) transverse direction

B.7.2 Results for AS4/Epoxy with Aluminium Liner [90/(0/90)$_{10}$] under Pure Tension Case

As described in *Chapter 3*, the tension force has to be calculated using three different cases, which yield values of 2570kN, 1425kN and 2625kN, respectively. Therefore, the design tension force is 2625×2.25=5905kN.

Under a 5905kN pure tension, the Von Mises stress in the aluminium liner is 176.86MPa, providing FS=3.05. Figs. B.38(a) and B.38(b) show the FSs in every layer under load case 2(a) (pure tension) for the conventional design. As can be seen, they are quite large which indicates that this load case is not as critical as the burst case for this material combination (the FSs for stresses in the fibre direction for the hoop-reinforced layers in Fig. B.38(a) are well above 50, since the loading is mainly in the axial direction).

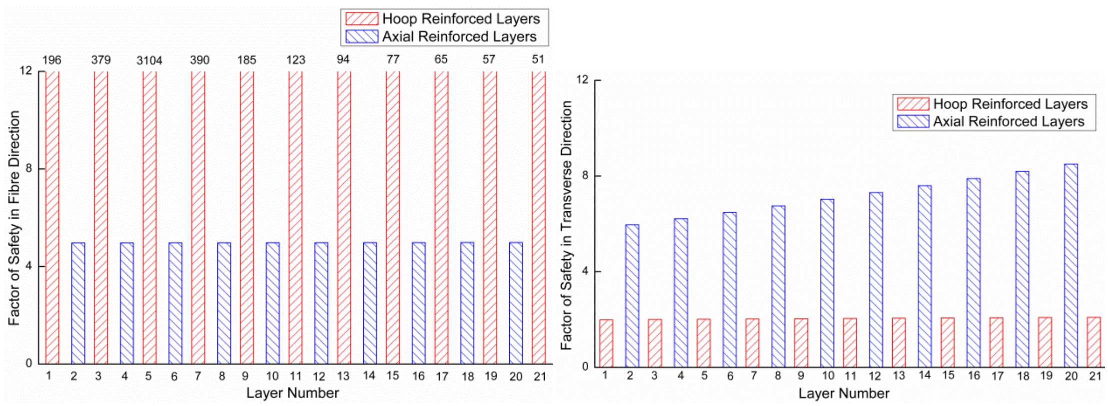

(a) (b)

Fig. B.38. FSs for composite layers with 0° and 90˚ reinforcements for load case 2(a) for AS4/epoxy with aluminium liner in (a) fibre direction and (b) transverse direction

B.7.3 Results for AS4/Epoxy with Aluminium Liner [90/(0/90)$_{10}$] under Tension with External Pressure Case

The tension force under load case 2(b) (tension with external pressure of 19.5MPa) is also 5905kN and the Von Mises stress in the aluminium liner is 192.86MPa, providing FS=2.80. Fig. B.39 shows its FSs under load case 2(b) for the conventional design with the minimum being 2.24 in transverse direction in layer 1 (Fig. B.39(b)).

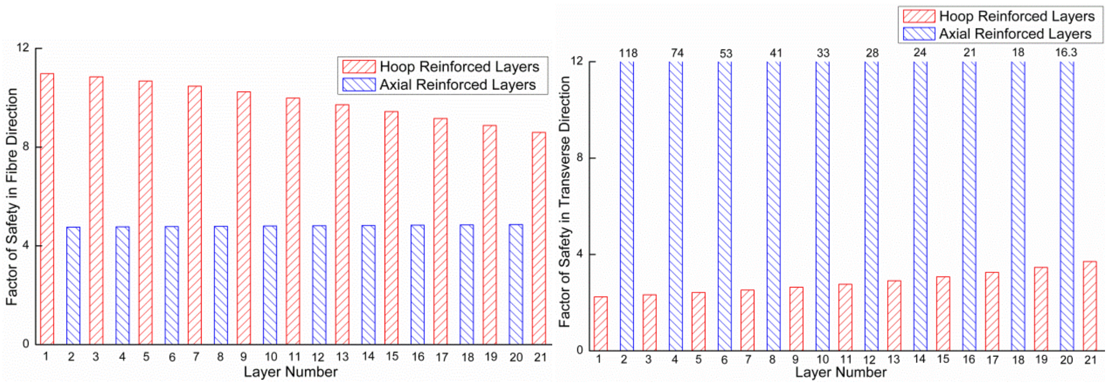

(a) (b)

Fig. B.39. FSs for composite layers with 0° and 90˚ reinforcements for load case 2(b) for AS4/epoxy with aluminium liner in (a) fibre direction and (b) transverse direction

B.7.4 Results for AS4/Epoxy with Aluminium Liner [90/(0/90)$_{10}$] under Collapse Case

The design collapse pressure for the composite riser is 58.5MPa under which the Von Mises stress in the aluminium liner is 190.02MPa, providing FS=2.84. Fig. B.40 shows the FSs under load case 3 (collapse load) for the conventional design, with the minimum being 3.40 in fibre direction in layer 1 (Fig. B.40(a)).

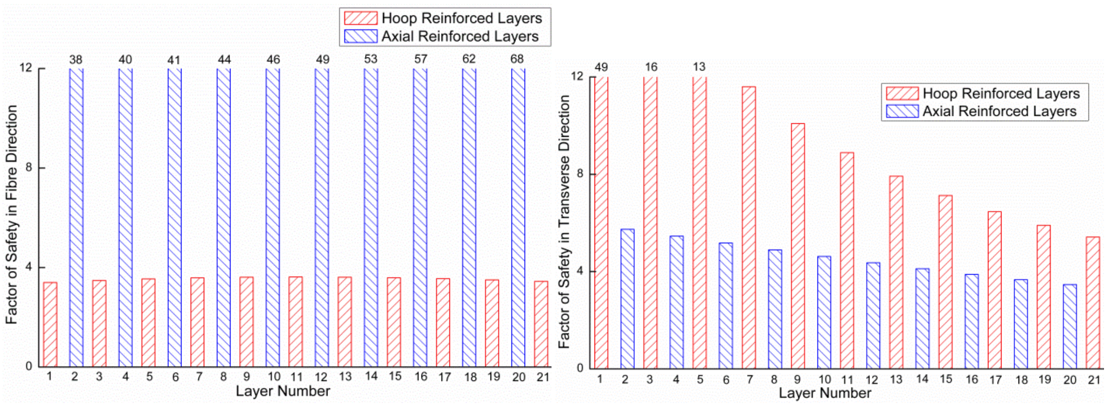

(a) (b)

Fig. B.40. FSs for composite layers with 0° and 90˚ reinforcements for load case 3 for AS4/epoxy with aluminium liner in (a) fibre direction and (b) transverse direction

B.7.5 Results for AS4/Epoxy with Aluminium Liner [90/(0/90)$_{10}$] under Buckling Case

The geometry of AS4/epoxy with aluminium liner riser using the conventional design is also checked for buckling under external pressure (load case 4) and the critical buckling pressure obtained is 349.3MPa (mode 1), which is much higher than the design buckling pressure of 58.5MPa. The first three mode shapes can be seen in the Fig. B.41 in which the number of circumferential waves is 2 for all three modes and the number of half wave along the axial direction 1, 2 and 3 for modes 1, 2 and 3, respectively.

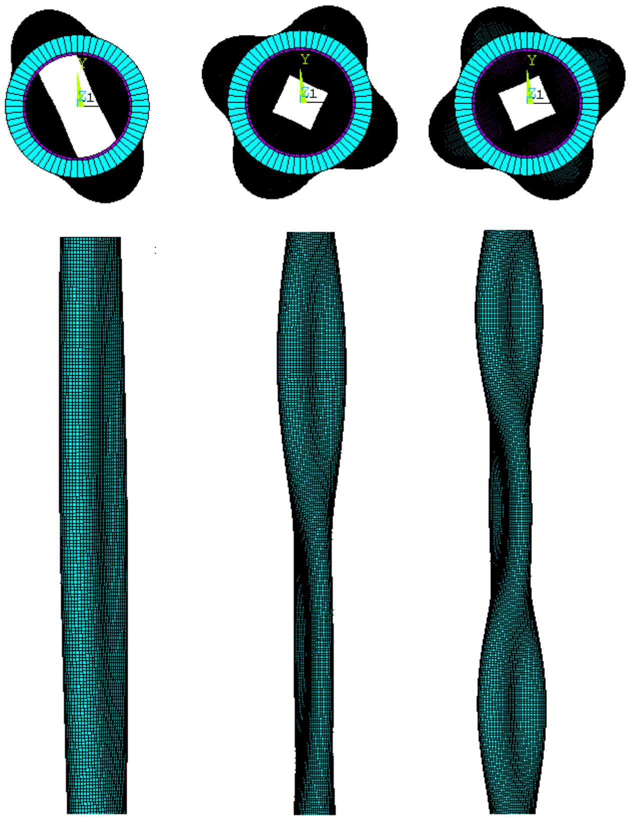

(a) B.P.=349.3MPa (b) B.P.=351.5MPa (c) B.P.=356.6MPa

Fig. B.41. Mode shapes of composite riser with 0° and 90° reinforcements for AS4/epoxy with aluminium liner (5m): (a) mode 1 (b) mode 2 and (c) mode 3

B.8 Results for AS4/Epoxy with Aluminium Liner Using Tailored Design

Following the tailored design procedure, the effects of fibre orientations and stacking sequences on the structural weight are determined and presented in Figs. B.42 and B.43, respectively. In the step 2 of the manually tailored local design of composite riser, for the burst case (without a liner), the best fibre orientation is 54.7° and the minimum thickness is 16.8mm according to the netting theory and 51° and 32.4mm according to CLT theory. These best reinforcement angles have to be verified in step 3 of the design procedure using 3D FEA simulation under the burst case with the same liner thickness obtained by conventional design results (2mm) and, in the FEA model, the geometry of $[\pm\theta]_5$ with 32.4mm of laminate and 2mm of liner is employed. Variations in minimum FSs in fibre direction, in-plane transverse direction and in-plane shear of composite laminate are illustrated in Fig. B.42.

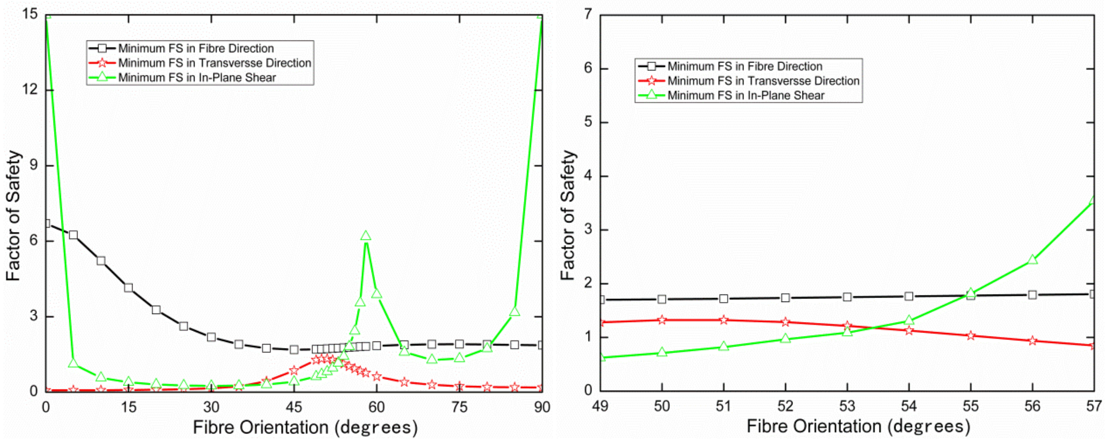

(a) (b)

Fig. B.42. Variations of FS with fibre orientation for burst capacity (a) full range of angles (b) magnified view

Similarly, the effect of the stacking sequences on the weight and thickness is illustrated in Fig. B.43. The four typical locations at which additional axial and hoop reinforcements are provided to the ±θ layers are: (1) innermost layer, (2) middle of the $\pm\theta^o$ layers, (3) outermost layer and (4) axial reinforcements in the innermost layer with hoop reinforcements added in the outermost layer.

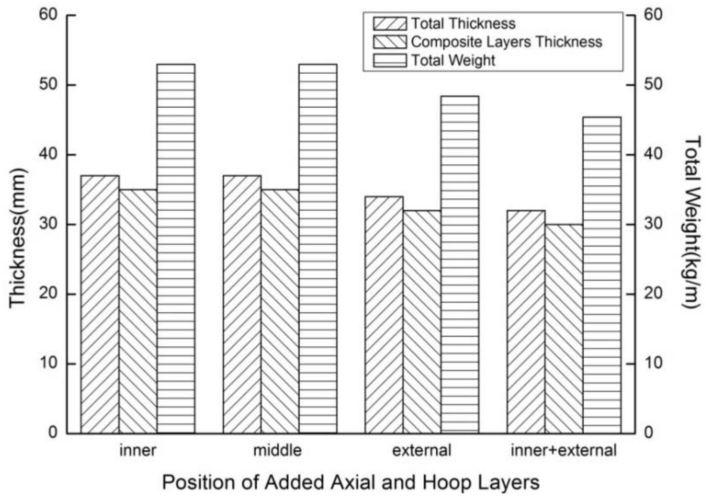

Fig. B.43. Influence of stacking sequences on the thickness and weight

It can be seen in Fig. B.42 and Fig. B.43 that the $\pm53.5^o$ is the most efficient angle for taking full advantage of their reinforcement strengths in every direction under burst case. The stacking sequence with the $\pm53.5^o$ reinforced layers its axial (innermost) and hoop (outermost) layers provides the lowest total thickness and, therefore, the lowest structural weight.

Table B.8. Geometry of AS4/epoxy with aluminium liner riser including angle reinforcements

Layer	Orientation (degree)	Thickness (mm)	Layer	Orientation (degree)	Thickness (mm)
liner		2	10	-53.5	1.60
1	0	1.62	11	53.5	1.60
2	0	1.62	12	-53.5	1.60
3	0	1.62	13	53.5	1.60
4	0	1.62	14	-53.5	1.60
5	53.5	1.60	15	90 (hoop)	1.88
6	-53.5	1.60	16	90	1.88
7	53.5	1.60	17	90	1.88
8	-53.5	1.60	18	90	1.88
9	53.5	1.60			
Total thickness: 32mm and structural weight: 45.4kg/m					

Table B.8 gives the geometry of the composite riser tube optimised for minimum thickness using the manually tailored design. The tailored design, including the angle plies, provides an 18 layer composite laminate $[0_4/(+53.5,-53.5)_5/90_4]$ with the 0^o, $\pm53.5^o$ and 90^o having thicknesses of 1.62, 1.60 and 1.88mm respectively. The total laminate thickness for the design, including the angle plies, is only 30mm, with the same 2mm thickness of the aluminium liner. It is again to be noted that the optimum angle of reinforcement for the angle plies is obtained as $\pm53.5^o$ using the 3D FEA, not $\pm54.7^o$ as predicted by netting theory.

B.8.1 Results for AS4/Epoxy with Aluminium Liner $[0_4/(\pm53.5)_5/90_4]$ under Burst Case

The design burst pressure for the composite riser is 155.25MPa under which the Von Mises stress in the aluminium liner is 487.99MPa, providing FS=1.11. Figs. B.44(a), B.44(b) and B.44(c), respectively, show the FSs in the fibre and transverse directions and in-plane shear for all the layers under load case 1 (burst load) for the manually tailored design with additional angle plies and considering different stacking sequences. The minimum FSs are 1.61 in the fibre direction (layer 15 in Fig. B.44(a)), 1.00 in the transverse direction (layer 4 and layer 18 in Fig. B.44(b)) and about 2.13 in shear (layer 5 in Fig. B.44(c)). In this case, the in-plane transverse stresses are most critical stresses and determine the thickness of the composite layers.

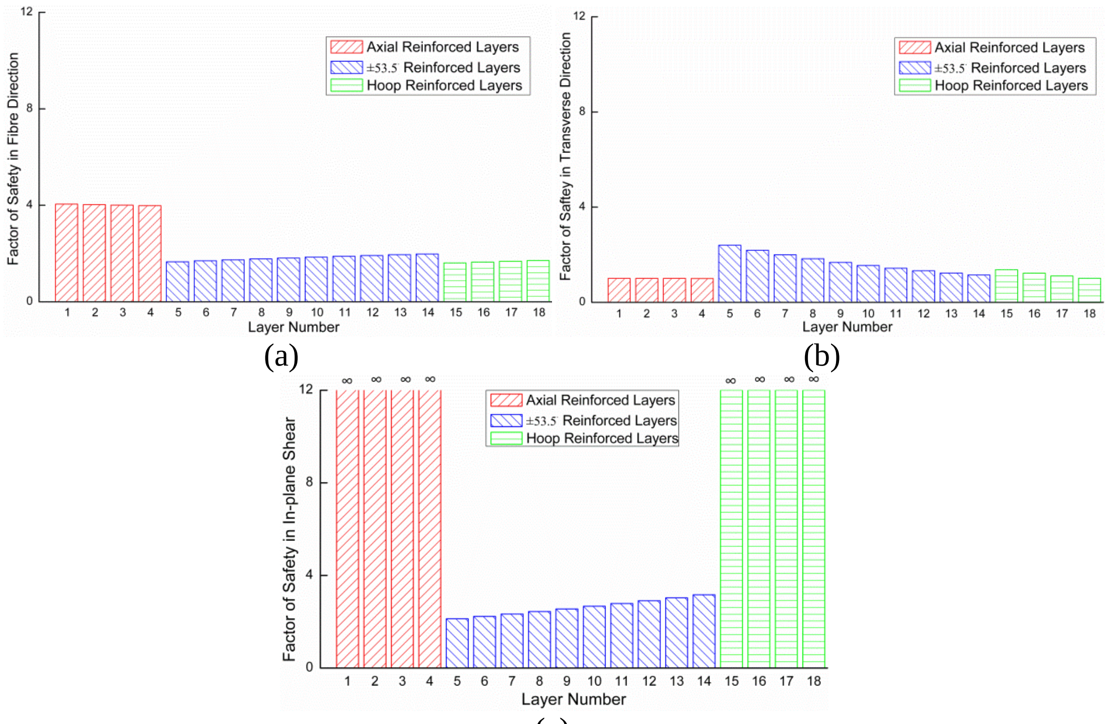

(c)

Fig. B.44. FSs for composite layers with 0°, ±53.5° and 90° reinforcements for load case 1 for AS4/epoxy with aluminium liner in (a) fibre direction, (b) transverse direction and (c) in-plane shear

B.8.2 Results for AS4/Epoxy with Aluminium Liner [0_4 /($\pm$53.5)$_5$ /90_4] under Pure Tension Case

As described in *Chapter 3*, the tension force has to be calculated using three different cases, which yield values of 2430kN, 1250kN and 2430kN, respectively. Therefore, the design tension force is 2430×2.25=5470kN.

Under a pure tension (5470kN), the Von Mises stress in the aluminium liner is 324.47MPa, providing FS=1.66. Figs. B.45(a), B.45(b) and B.45(c) show the FSs in all the layers under load case 2(a) (pure tension) for the manually tailored design. In this case, while the other FSs are relatively high, the minimum FS is about 1.16 in the transverse direction of the hoop layers in layer 18 (Fig. B.45(b)).

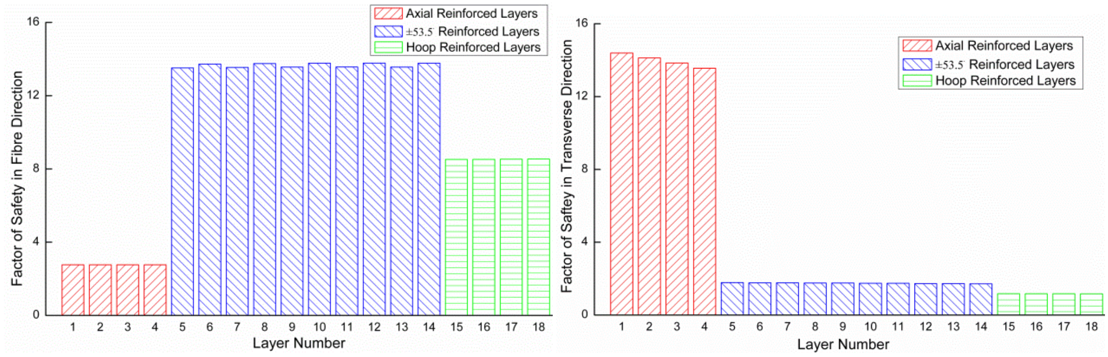

(a) (b)

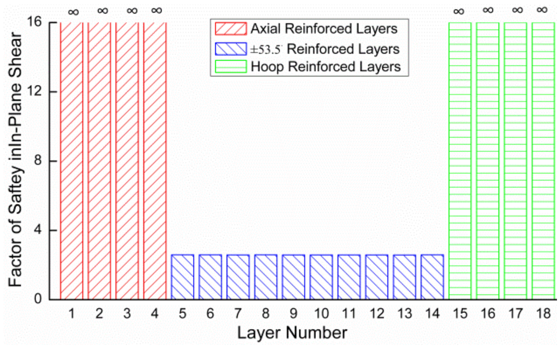

(c)

Fig. B.45. FSs for composite layers with 0°, ±53.5˚ and 90˚ reinforcements for load case 2(a) for AS4/epoxy with aluminium liner in (a) fibre direction (b) transverse direction, and (c) in-plane shear

B.8.3 Results for AS4/Epoxy with Aluminium Liner [0_4 /(±53.5)$_5$ /90_4] under Tension with External Pressure Case

The tension force under load case 2(b) (tension with external pressure of 19.5MPa) is the same as that for load case 2(a), that is, 5470kN, and the Von Mises stress in the aluminium liner is 403.96MPa, providing FS=1.34. Fig. B.46 shows the FSs under load case 2(b) for the manually tailored design with the minimum being 1.30 in transverse direction in layer 15 (Fig. B.46(b)).

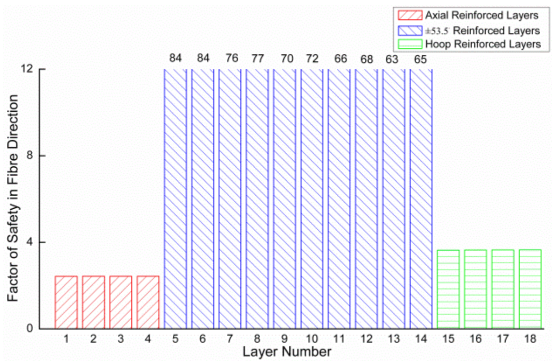

(a)

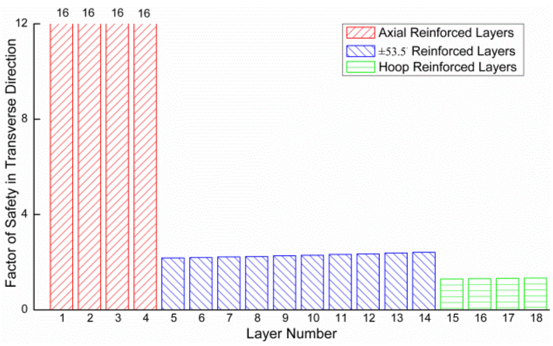

(b)

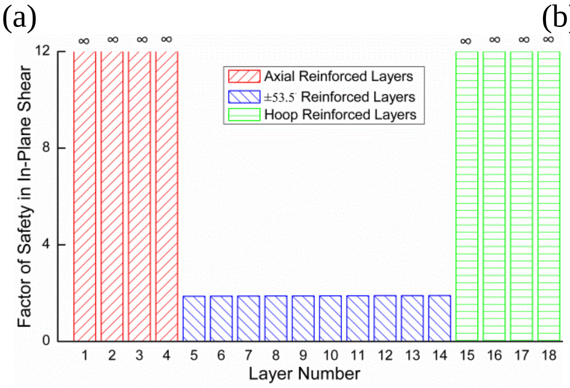

(c)

Fig. B.46. FSs for composite layers with 0°, ±53.5˚ and 90˚ reinforcements for load case 2(b) for AS4/epoxy with aluminium liner in (a) fibre direction (b) transverse direction, and (c) in-plane shear

B.8.4 Results for AS4/Epoxy with Aluminium Liner $[0_4 /(\pm 53.5)_5 /90_4]$ under Collapse Case

The design collapse pressure for the composite riser is 58.5MPa and under this external over-pressure, the Von Mises stress in the aluminium liner is 367.48MPa, providing FS=1.47. Fig. B.47 shows the FSs under load case 3 (collapse load) for the manually tailored design with the minimum being 2.11 in fibre direction in layer 15 (Fig. B.47(a)).

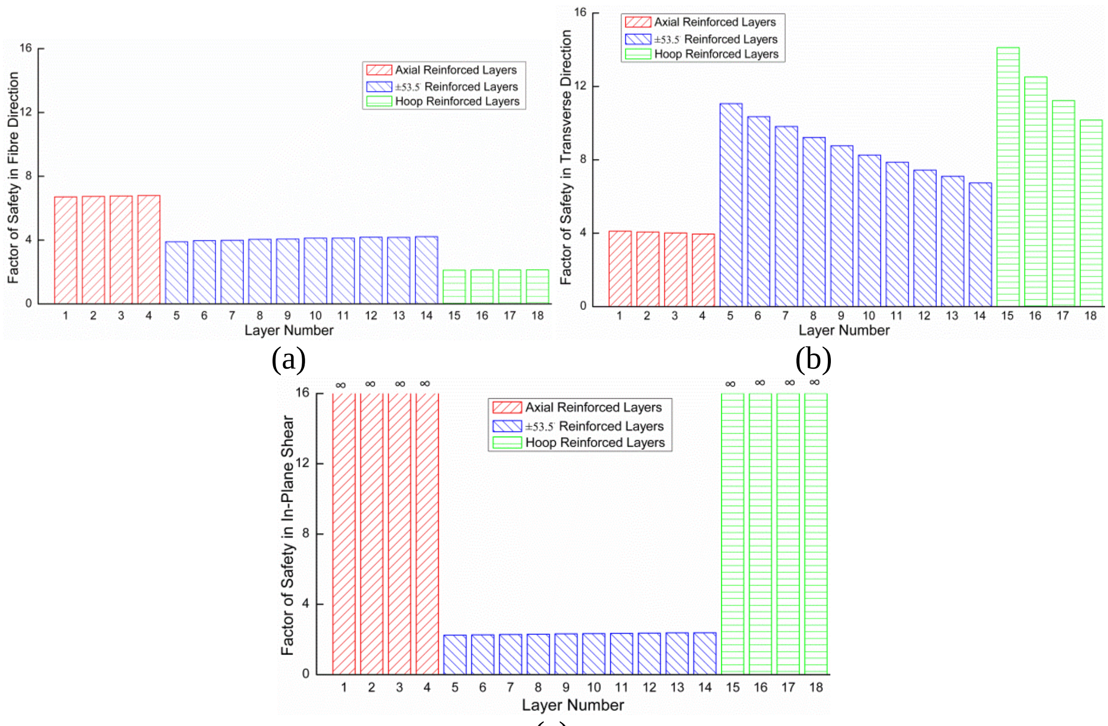

Fig. B.47. FSs for composite layers with 0°, ±53.5˚ and 90˚ reinforcements for load case 3 for AS4/epoxy with aluminium liner in (a) fibre direction, (b) transverse direction and (c) in-plane shear

B.8.5 Results for AS4/Epoxy with Aluminium Liner $[0_4 /(\pm 53.5)_5 /90_4]$ under Buckling Case

The geometry of AS4/epoxy with aluminium liner riser using the tailored design is also checked for buckling under external pressure (load case 4). The critical buckling pressure obtained is 148.10MPa (mode 1), which is much higher than the design buckling pressure of 58.5MPa. The first three mode shapes are shown in the Fig. B.48 in which it can be seen the number of circumferential waves is 2 for all three modes and the number of half-waves along the axial direction 2, 1 and 3 for modes 1, 2 and 3, respectively.

(a) B.P.= 148.10MPa (b) B.P.=148.2MPa (c) B.P.=148.6MPa
Fig. B.48. Mode shapes of composite riser with 0°, ±53.5˚ and 90˚ reinforcements for AS4/epoxy with aluminium liner (5m): (a) mode 1, (b) mode 2 and (c) mode 3

B.9 Results for P75/Epoxy with Steel Liner Using Conventional Design

Table B.9 gives the geometry of the composite riser tube optimised for minimum thickness using the conventional design under the local load cases which yields a 19-ply composite laminate [$90_{16}/0_3$] with hoop (2.00/3.00mm) and axially reinforced layers (2.00/3.00mm), respectively, which results in a total laminate thickness of 40mm, with a 10mm steel liner and structural weight of 133.3kg/m. Unlike PEEK liner riser, the thickness of steel liner would affect total weight significantly, thus, the first step is the determination of the thickness of steel liner. The variations of thickness and weight according to the different thicknesses of steel liner are shown in Fig. B.49 in which it can be seen that when the steel liner is 10mm, the total weight is the minimum. Hence for the following analysis, 10mm steel liner is used.

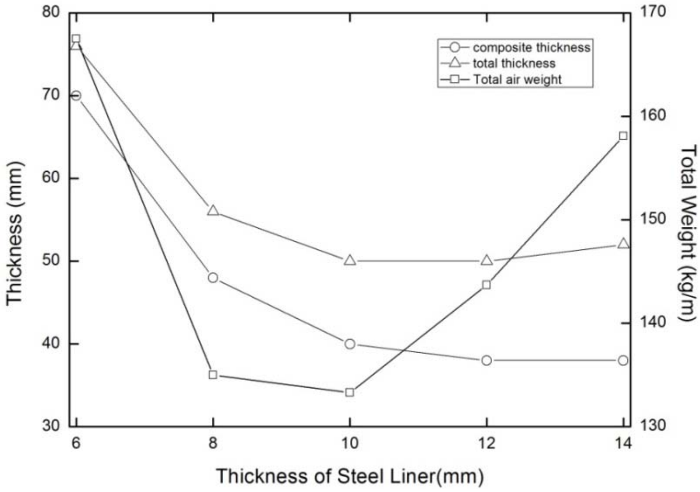

Fig. B.49. Thickness and weight of composite cylinder according to different thicknesses of steel liner

Table B.9. Geometry of P75/epoxy with steel liner riser with orthogonal reinforcements

Layer	Orientation (degree)	Thickness (mm)	Layer	Orientation (degree)	Thickness(mm)
liner		10	10	90	2
1	90(hoop)	2	11	90	2
2	90	2	12	90	2
3	90	2	13	90	2
4	90	2	14	90	2
5	90	2	15	90	2
6	90	2	16	90	3
7	90	2	17	0 (axial)	2
8	90	2	18	0	3
9	90	2	19	0	2
Total thickness: 50mm and structural weight: 133.3kg/m					

B.9.1 Results for P75/Epoxy with Steel Liner [$90_{16}/0_3$] under Burst Case

The design internal burst pressure for the composite riser is 155.25MPa under which the Von Mises stress in the steel liner is 556.84MPa, providing FS=1.12. Figs. B.50(a) and B.50(b), respectively, show the FSs in the fibre and transverse directions under load case 1 (burst load) for all the layers in the conventional design geometry. The minimum FS in the fibre direction is 1.01 (layer 1 in Fig. B.50(a)), while that in the transverse direction is 1.12 (layer 19 in Fig. B.50(b)). It is evident that, under the burst case, the stresses in fibre direction are the most critical stresses and determine the minimum thickness of the composite P75/epoxy with steel liner with only 0^o and 90^o reinforcements.

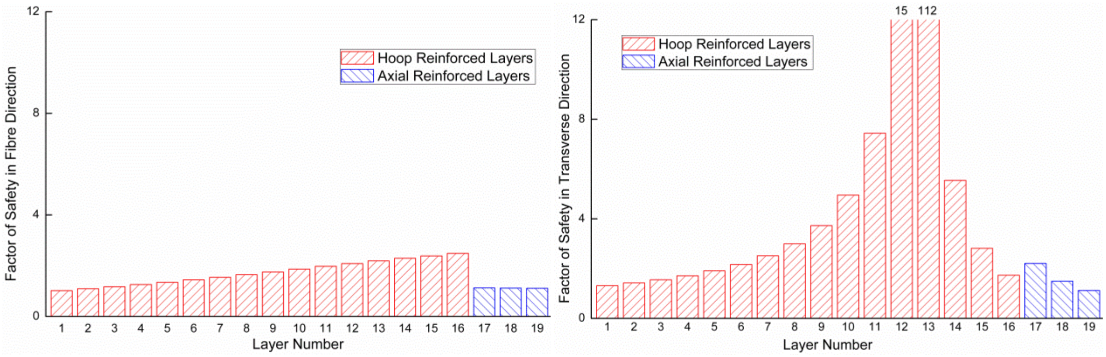

(a) (b)

Fig. B.50. FSs for composite layers with 0° and 90˚ reinforcements for load case 1 for P75/epoxy with steel liner in (a) fibre direction and (b) transverse direction

B.9.2 Results for P75/Epoxy with Steel Liner [$90_{16}/0_3$] under Pure Tension Case

As described in *Chapter 3*, the tension force has to be calculated using three different cases, which yield values of 4350kN, 3740kN and 4185kN, respectively. Therefore, the design tension force is 4350×2.25=9800kN.

Under a 9800kN pure tension, the Von Mises stress in the steel liner is 447.84MPa, providing FS=1.39. Figs. B.51(a) and B.51(b) show the FSs in every layer under load case 2(a) (pure tension) for the conventional design. As can be seen, the minimum FSs for stresses in the fibre direction and transverse direction are 1.04 (layer 17) and 1.07 (layer 1), respectively.

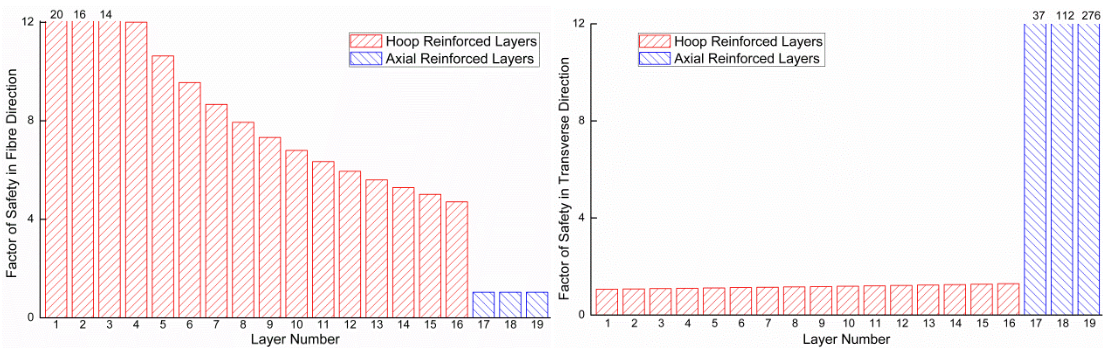

(a) (b)

Fig. B.51. FSs for composite layers with 0° and 90˚ reinforcements for load case 2(a) for P75/epoxy with steel liner in (a) fibre direction and (b) transverse direction

B.9.3 Results for P75/Epoxy with Steel Liner [$90_{16}/0_3$] under Tension with External Pressure Case

The tension force under load case 2(b) (tension with external pressure of 19.5MPa) is also 9800kN and the Von Mises stress in the steel liner is 470.7MPa, providing FS=1.33. Fig. B.52 shows the FSs under load case 2(b) for the conventional design with the minimum FSs being 1.01 (layer 17) in the fibre direction and 1.24 (layer 1) in transverse direction, respectively.

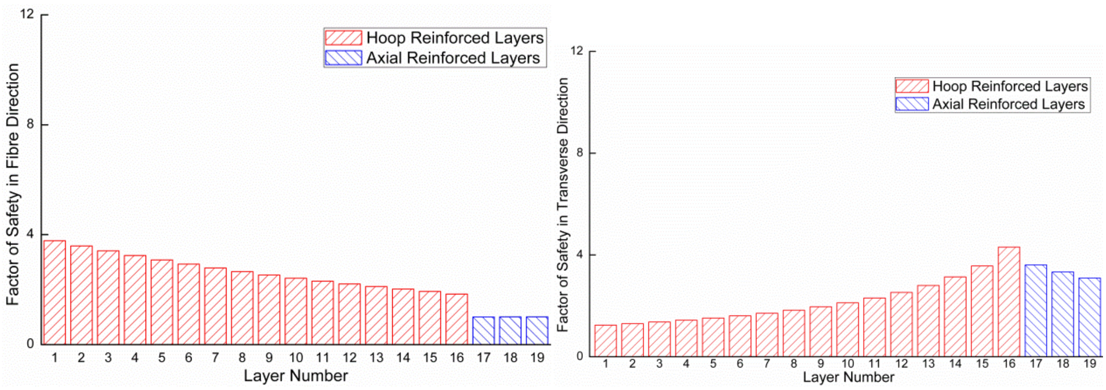

(a) (b)

Fig. B.52. FSs for composite layers with 0° and 90˚ reinforcements for load case 2(b) for P75/epoxy with steel liner in (a) fibre direction and (b) transverse direction

B.9.4 Results for P75/Epoxy with Steel Liner [$90_{16}/0_3$] under Collapse Case

The design collapse pressure for the composite riser is 58.5MPa under which the Von Mises stress in the steel liner is 148.3MPa, providing FS=4.21. Fig. B.53 shows the FSs under load case 3 (collapse load) for the conventional design, with the minimum FSs being 1.01 (layer 16) in fibre direction and 1.04 (layer 19) in transverse direction, respectively.

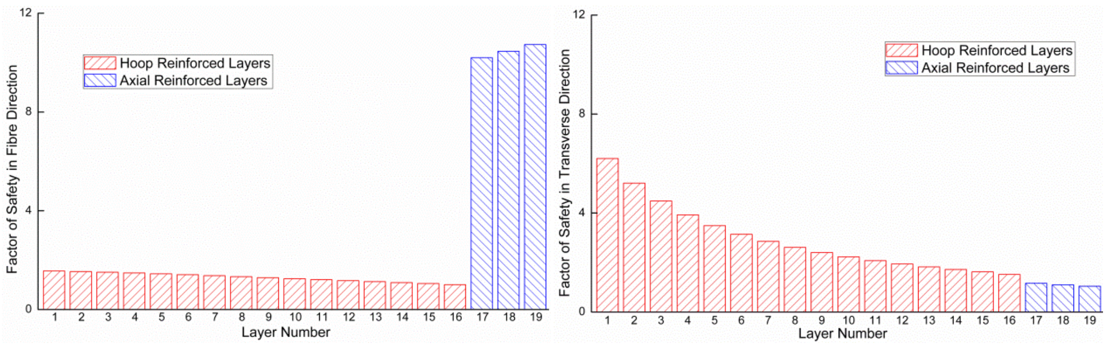

(a) (b)

Fig. B.53. FSs for composite layers with 0° and 90˚ reinforcements for load case 3 for P75/epoxy with steel liner in (a) fibre direction and (b) transverse direction

B.9.5 Results for P75/Epoxy with Steel Liner [$90_{16}/0_3$] under Buckling Case

The geometry of P75/epoxy with steel liner riser using the conventional design is also checked for buckling under external pressure (load case 4). The critical buckling pressure for the conventional design obtained is 673.2MPa (mode 1), which is much higher than the design buckling pressure of 58.5MPa. The first three mode shapes can be seen in the Fig. B.54 in which the number of circumferential waves is 2 for all three modes and the number of half-waves along the axial direction 1, 2 and 3 for modes 1, 2 and 3, respectively.

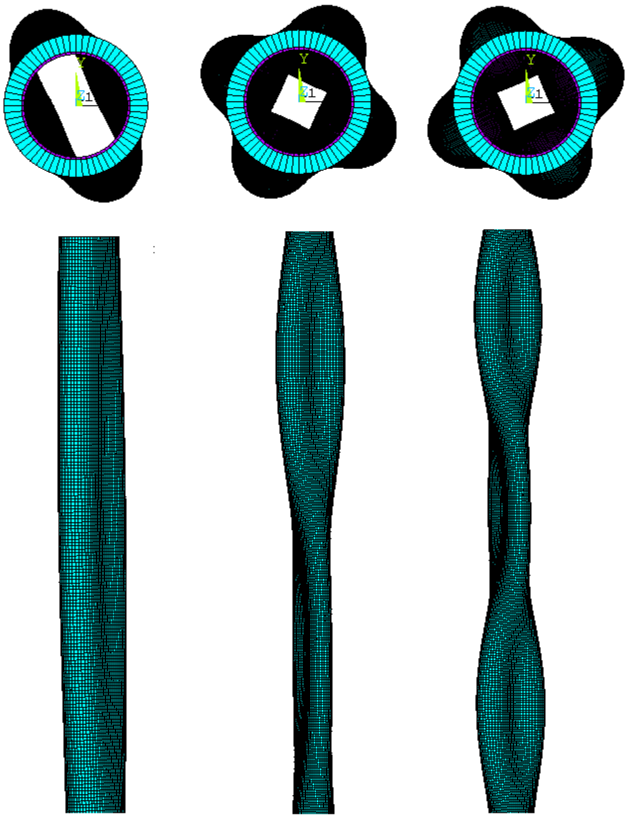

(a) B.P.= 673.2MPa (b) B.P.=675.2MPa (c) B.P.=684.1MPa
Fig. B.54. Mode shapes of composite riser with 0° and 90° reinforcements for P75/epoxy with steel liner (5m): (a) mode 1 (b) mode 2 and (c) mode 3

B.10 Results for P75/Epoxy with Steel Liner Using Tailored Design

Table B.10 gives the geometry of the composite riser tube optimised for minimum thickness using the tailored design under the local load cases, which provides a 19-layer composite laminate [(+69,-69,+69) $/90_8$, $/(-69, +69)_2$ /-69 $/0_3$] with the 0°, 90° and ±69° having thicknesses of 2.40, 2.05 and 1.80mm, respectively. The total laminate thickness, including the angle plies, is only 38mm with same 10mm thickness for the steel liner, providing a 3% structural weight saving over the conventional design. It is again to be noted that the optimum angle of reinforcement for the angle plies is obtained as ±69° using the 3D FEA, not ±54.7° as predicted by netting theory.

Table B.10. Geometry of P75/epoxy with steel liner riser including angle reinforcements

Layer	Orientation (degree)	Thickness (mm)	Layer	Orientation (degree)	Thickness (mm)
Liner		10	10	90	2.05
1	69	1.80	11	90	2.05
2	-69	1.80	12	-69	1.80
3	69	1.80	13	69	1.80
4	90(hoop)	2.05	14	-69	1.80
5	90	2.05	15	69	1.80
6	90	2.05	16	-69	1.80
7	90	2.05	17	0 (axial)	2.40
8	90	2.05	18	0	2.40
9	90	2.05	19	0	2.40
Total thickness: 48mm and structural weight: 129.4kg/m					

B.10.1 Results for P75/Epoxy with Steel Liner [±69 /69 /90$_8$/ -69/ (±69)$_2$ /0$_3$] under Burst Case

The design internal burst pressure for the composite riser is 155.25MPa under which the Von Mises stress in the steel liner is 556.78MPa, providing FS=1.12. Figs. B.55(a), B.55(b) and B.55(c), respectively, show the FSs in the fibre, transverse directions and in-plane shear for all the layers under load case 1 (burst load) for the manually tailored design with additional angle plies and considering different stacking sequences. The minimum FSs are 1.01 in the fibre direction (layer 1 in Fig. B.55(a)), 1.06 in the transverse direction (layer 19 in Fig. B.55(b)) and about 73.33 in in-plane shear (layer 1 in Fig. B.55(c)). In this case, both the stresses in transverse and fibre directions are the most critical stresses and determine the thickness of the composite layers.

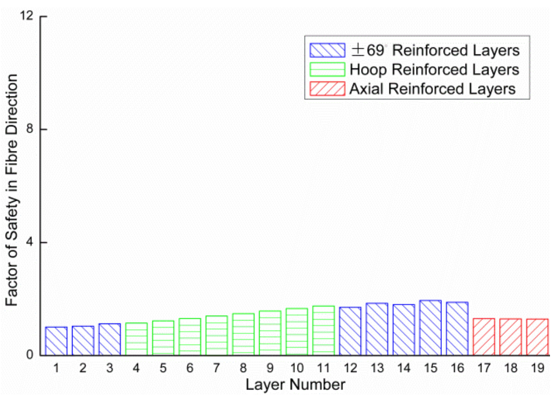

(a)

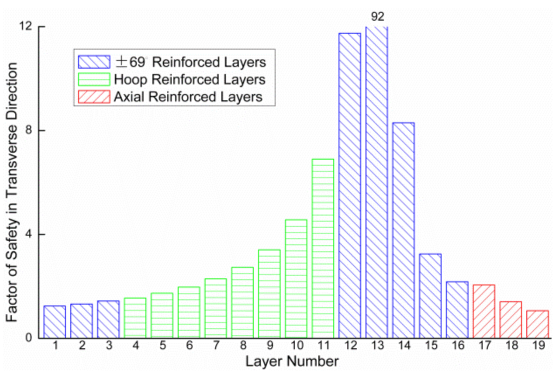

(b)

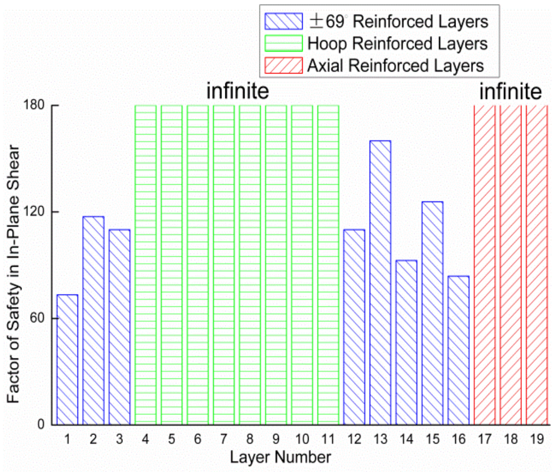

(c)

Fig. B.55. FSs for composite layers with 0°, ±69˚ and 90˚ reinforcements for load case 1 for P75/epoxy with steel liner in (a) fibre direction, (b) transverse direction and (c) in-plane shear

B.10.2 Results for P75/Epoxy with Steel Liner [±69 /69 /90$_8$/ -69/ (±69)$_2$ /0$_3$] under Pure Tension Case

As described in *Chapter 3*, the tension force has to be calculated using three different cases, which yield values of 4300kN, 3680kN and 4110kN, respectively. Therefore, the design tension force is 4300×2.25=9700kN.

Under a pure tension (9700kN), the Von Mises stress in the steel liner is 445.2MPa, providing FS=1.40. Figs. B.56(a), B.56(b) and B.56(c) show the FSs in all the layers under load case 2(a) (pure tension) for the manually tailored design. In this case, the minimum FS is about 1.05 in the fibre direction of the axial layers (layer 17, Fig. B.56(a)).

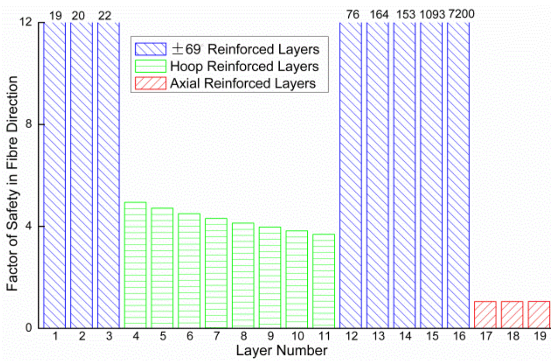

(a)

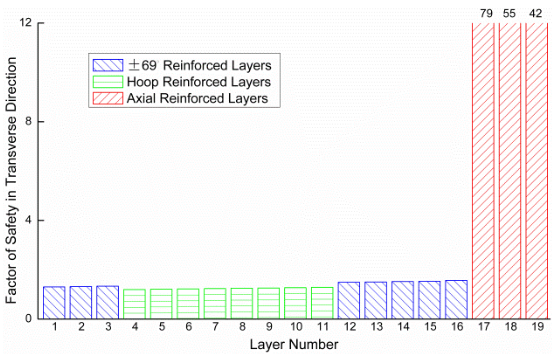

(b)

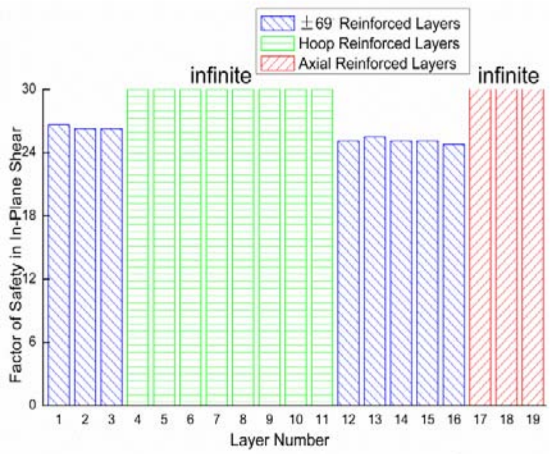

(c)

Fig. B.56. FSs for composite layers with 0°, ±69° and 90° reinforcements for load case 2(a) for P75/epoxy with steel liner in (a) fibre direction, (b) transverse direction and (c) in-plane shear

B.10.3 Results for P75/Epoxy with Steel Liner [±69 /69 /90_8/ -69/ $(\pm69)_2$ /0_3] under Tension with External Pressure Case

The tension force under load case 2(b) (tension load with external pressure) is the same as that for load case 2(a), that is, 9700kN, and the Von Mises stress in the steel liner is 478.88MPa, providing FS=1.30. Fig. B.57 shows the FSs under load case 2(b) for the manually tailored design with the minimum being 1.00 in fibre direction in layer 17 (Fig. B.57(a)).

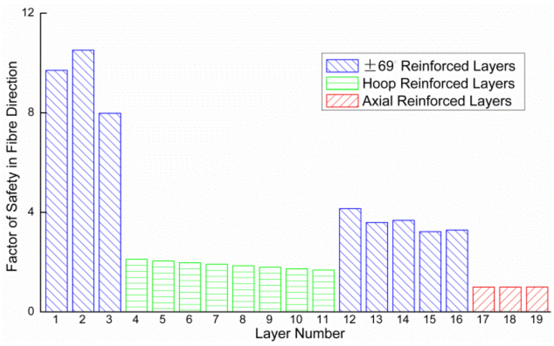

(a)

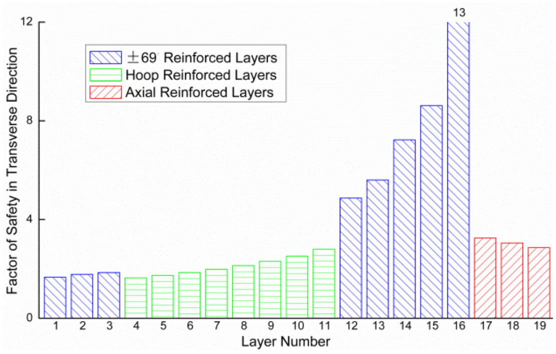

(b)

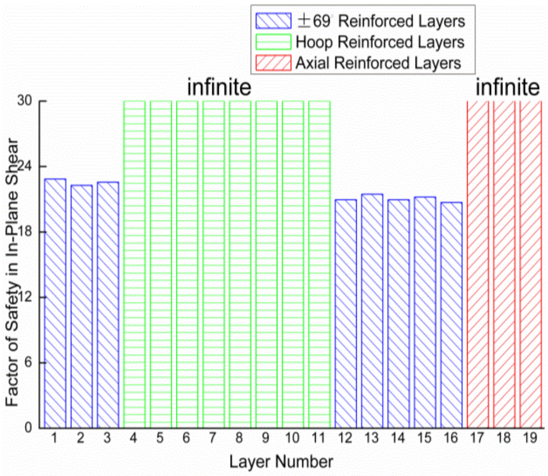

(c)

Fig. B.57. FSs for composite layers with 0°, ±69˚ and 90˚ reinforcements for load case 2(b) for P75/epoxy with steel liner in (a) fibre direction, (b) transverse direction and (c) in-plane shear

B.10.4 Results for P75/Epoxy with Steel Liner [±69 /69 /90_8/ -69/ $(\pm69)_2$ /0_3] under Collapse Case

The design collapse pressure for the composite riser is 58.5MPa and under this external over-pressure, the Von Mises stress in the steel liner is 184.1MPa, providing FS=3.39. Fig. B.58 shows the FSs under load case 3 (collapse load) for the manually tailored design with the minimum FSs being 1.03 (layer 11) in fibre direction and 1.02 (layer 19) in transverse direction, respectively.

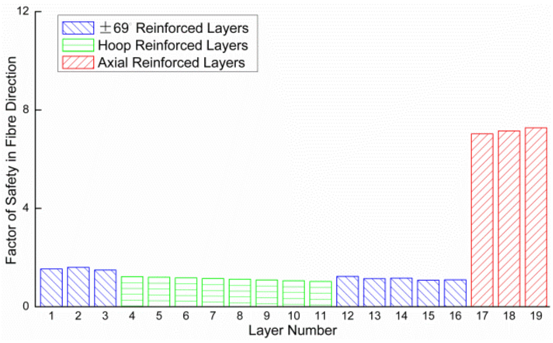

(a)

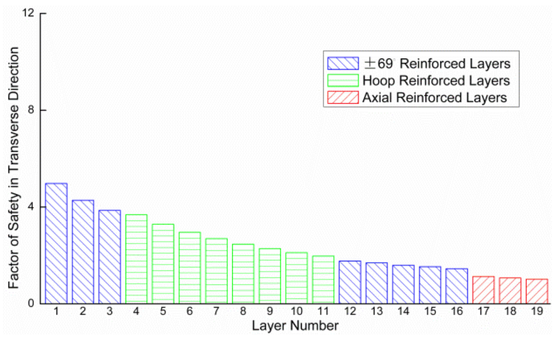

(b)

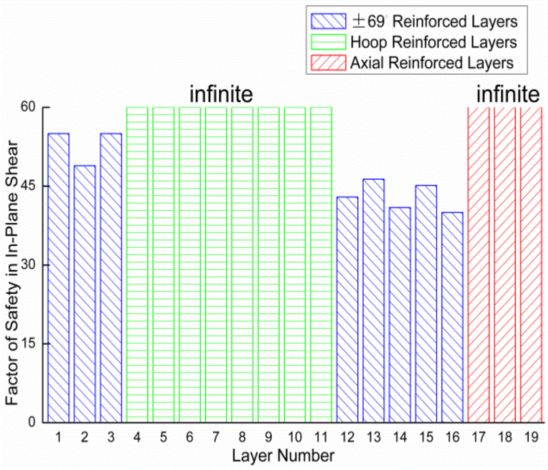

(c)

Fig. B.58. FSs for composite layers with 0°, ±69˚ and 90˚ reinforcements for load case 3 for P75/epoxy with steel liner in (a) fibre direction, (b) transverse direction and (c) in-plane shear

B.10.5 Results for P75/Epoxy with Steel Liner [±69 /69 /90_8/ -69/ $(\pm69)_2$ /0_3] under Buckling Case

The geometry of P75/epoxy with steel liner riser using the tailored design is also checked for buckling under external pressure (load case 4). The critical buckling pressure obtained is 582.9MPa (mode 1), which is much higher than the design buckling pressure of 58.5MPa. The first three mode shapes are shown in the Fig. B.59 in which it can be seen that the number of circumferential waves is 2 for all three modes and the number of half wave along the axial direction 1, 2 and 3 for modes 1, 2 and 3, respectively.

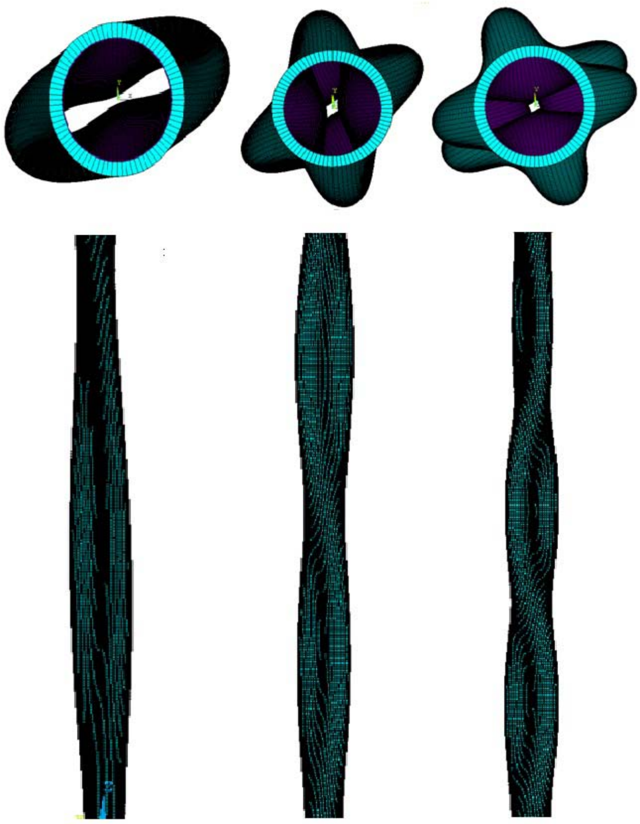

(a) B.P.= 582.9MPa (b) B.P.=588.4MPa (c) B.P.=600.7MPa
Fig. B.59. Mode shapes of composite riser with 0°, ±69˚ and 90˚ reinforcements for P75/epoxy with steel liner (5m): (a) mode 1, (b) mode 2 and (c) mode 3

B.11 Results for P75/Epoxy with Titanium Liner Using Conventional Design

Table B.11 gives the geometry of the composite riser tube optimised for minimum thickness using the conventional design under the local load cases, which yields a 21-ply composite laminate [$90_{18}/0_3$] with hoop (2.00/3.00mm) and axially reinforced layers (2.00/3.00mm), resulting in a total laminate thickness of 44mm, with a 10mm titanium liner and structural weight of 113.3kg/m. Unlike PEEK liner riser, the thickness of titanium liner would affect total weight significantly, thus, the first step is the determination of the thickness of titanium liner. The variations of thickness and weight according to the different thicknesses of titanium liner are shown in Fig. B.60 in which it can be seen that when the titanium liner is 10mm, the total weight is the minimum. Hence for the following analysis, 10mm titanium liner is used.

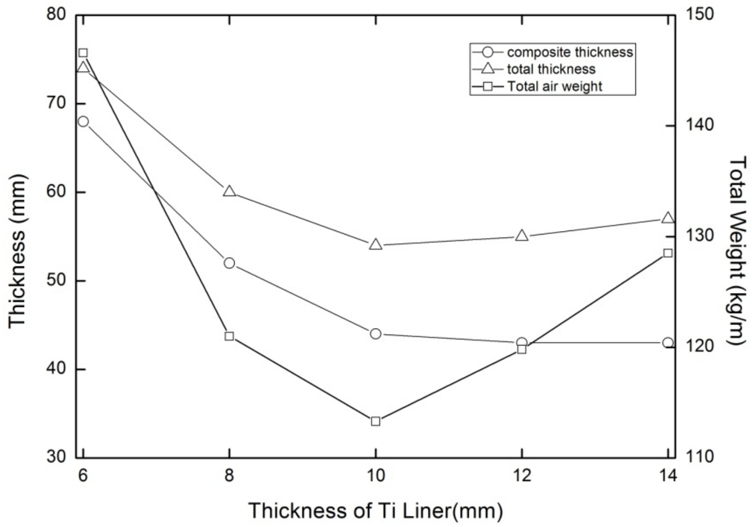

Fig. B.60. Thickness and weight of composite cylinder according to different thicknesses of titanium liner

Table B.11. Geometry of P75/epoxy with titanium liner riser with orthogonal reinforcements

Layer	Orientation (degree)	Thickness(mm)	Layer	Orientation (degree)	Thickness(mm)
liner		10	11	90	2
1	90(hoop)	2	12	90	2
2	90	2	13	90	2
3	90	2	14	90	2
4	90	2	15	90	2
5	90	2	16	90	2
6	90	2	17	90	2
7	90	2	18	90	3
8	90	2	19	0 (axial)	2
9	90	2	20	0	3
10	90	2	21	0	2
Total thickness: 54mm and structural weight: 113.3kg/m					

B.11.1 Results for P75/Epoxy with Titanium Liner [$90_{18}/0_3$] under Burst Case

The design internal burst pressure for the composite riser is 155.25MPa under which the Von Mises stress in the titanium liner is 495.11MPa and FS=1.92. Figs. B.61(a) and B.61(b), respectively, show the FSs in the fibre and transverse directions under load case 1 (burst load) for all the layers in the conventional design geometry. The minimum FS in the fibre direction is 1.00 (layer 1 in Fig. B.61(a)), while that in the transverse direction is 1.13 (layers 21 in Fig. B.61(b)). It is evident that, under burst case, the stresses in fibre direction are the most critical stresses and determine the minimum thickness of the composite P75/epoxy with titanium liner with only 0^o and 90^o reinforcements.

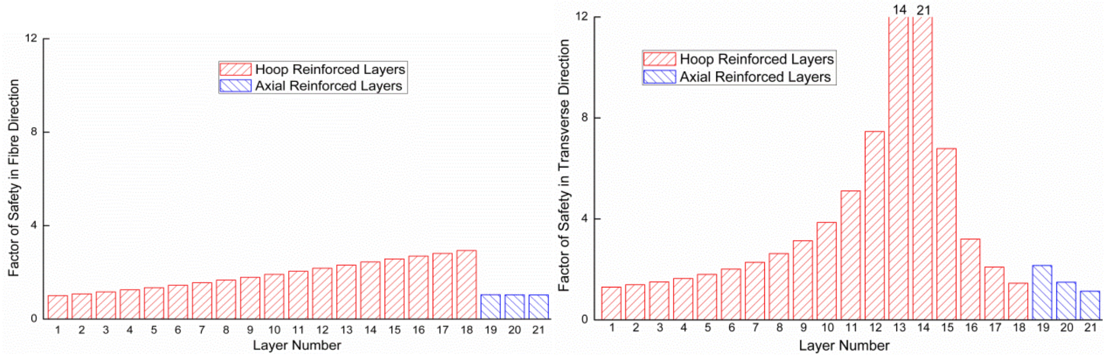

(a) (b)

Fig. B.61. FSs for composite layers with 0° and 90˚ reinforcements for load case 1 for P75/epoxy with titanium liner in (a) fibre direction and (b) transverse direction

B.11.2 Results for P75/Epoxy with Titanium Liner [$90_{18}/0_3$] under Pure Tension Case

As described in *Chapter 3*, the tension force has to be calculated using three different cases, which yield values of 3645kN, 2850kN and 3732kN, respectively. Therefore, the design tension force is 3732×2.25=8400kN.

Under an 8400kN pure tension, the Von Mises stress in the titanium liner is 251.2MPa, providing FS=3.78. Figs. B.62(a) and B.62(b) show the FSs in every layer under load case 2(a) (pure tension) for the conventional design. As can be seen, the minimum FSs for stresses in the fibre direction and transverse direction are 1.05 (layer 19) and 1.12 (layer 1), respectively.

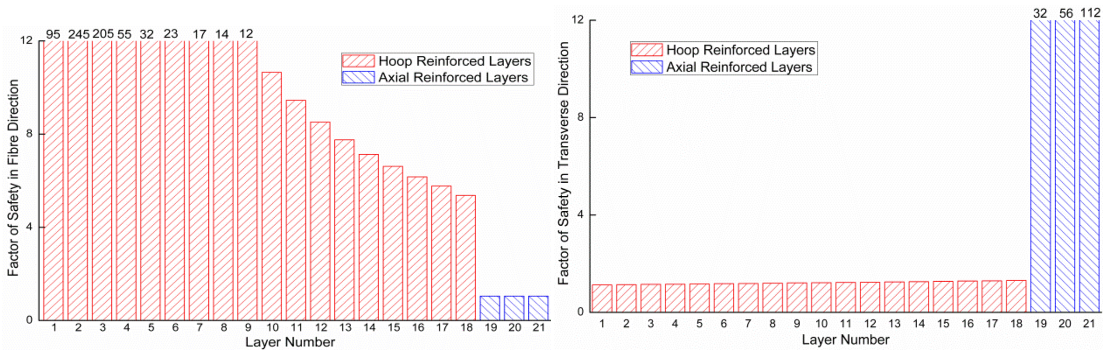

(a) (b)

Fig. B.62. FSs for composite layers with 0° and 90˚ reinforcements for load case 2(a) for P75/epoxy with titanium liner in (a) fibre direction and (b) transverse direction

B.11.3 Results for P75/Epoxy with Titanium Liner [$90_{18}/0_3$] under Tension with External Pressure Case

The tension force under load case 2(b) (tension with external pressure of 19.5MPa) is also 8400kN and the Von Mises stress in the titanium liner is 262.1MPa, providing FS=3.62. Fig. B.63 shows its FSs under load case 2(b) for the conventional design with the minimum being 1.0 in fibre direction in layer 21 (Fig. B.63(a)).

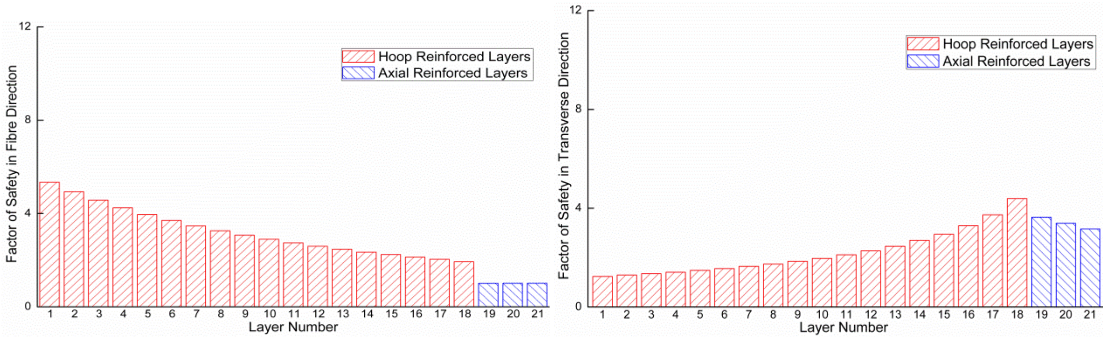

(a) (b)

Fig. B.63. FSs for composite layers with 0° and 90˚ reinforcements for load case 2(b) for P75/epoxy with titanium liner in (a) fibre direction and (b) transverse direction

B.11.4 Results for P75/Epoxy with Titanium Liner $[90_{18}/0_3]$ under Collapse Case

The design collapse pressure for the composite riser is 58.5MPa under which the Von Mises stress in the titanium liner is 81.59MPa, providing FS=11.64. Fig. B.64 shows the FSs under load case 3 (collapse load) for the conventional design, with the minimum FSs being 1.00 (layer 18) in fibre direction and 1.04 (layer 21) in transverse direction, respectively.

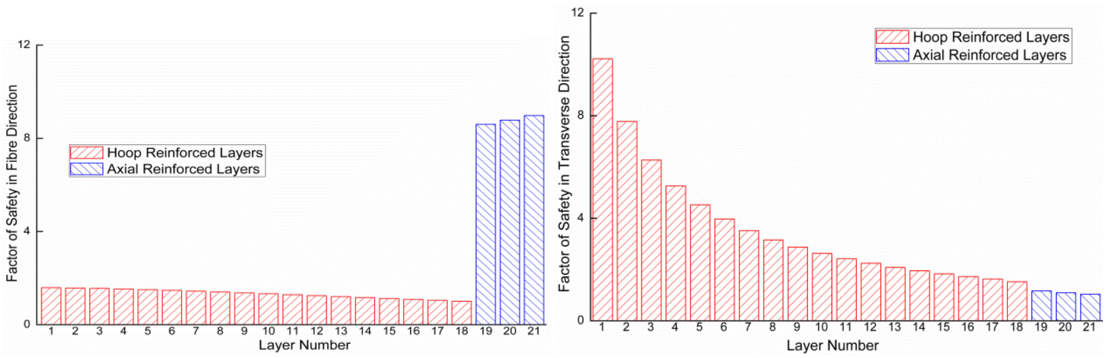

(a) (b)

Fig. B.64. FSs for composite layers with 0° and 90˚ reinforcements for load case 3 for P75/epoxy with titanium liner in (a) fibre direction and (b) transverse direction

B.11.5 Results for P75/Epoxy with Titanium Liner $[90_{18}/0_3]$ under Buckling Case

The geometry of P75/epoxy with titanium liner riser using the conventional design is also checked for buckling under external pressure (load case 4) and the critical buckling pressure obtained is 683.1MPa (mode 1) which is much higher than the design buckling pressure of 58.5MPa. The first three mode shapes can be seen in the Fig. B.65

in which the number of circumferential waves is 2 for all three modes and the number of half-waves along the axial direction 1, 2 and 3 for modes 1, 2 and 3, respectively.

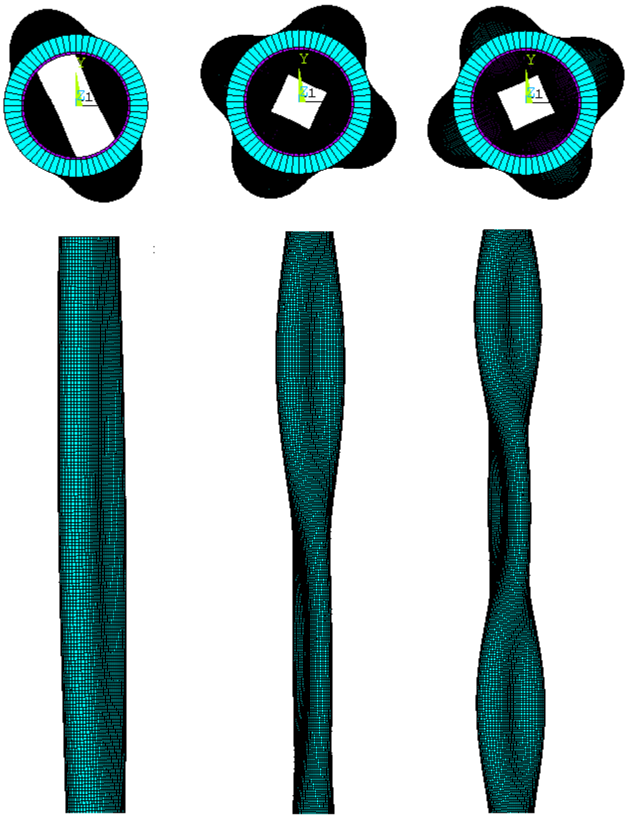

(a) B.P.= 683.1MPa (b) B.P.=685.7MPa (c) B.P.=695.5MPa
Fig. B.65. Mode shapes of composite riser with 0° and 90° reinforcements for P75/epoxy with titanium liner (5m): (a) mode 1 (b) mode 2 and (c) mode 3

B.12 Results for P75/Epoxy with Titanium Liner Using Tailored Design

Table B.12 gives the geometry of the composite riser tube optimised for minimum thickness using the tailored design under the local load cases, which yields a 21-layer composite laminate $[(+66,-66)/90_8/(+66,-66)_4/0_3]$ with the 0^o, 90^o and $\pm66^o$ having thicknesses of 2.50, 2.175 and 1.71mm, respectively, which results in a total laminate thickness of 42mm, with a 10mm titanium liner and structural weight of 109.3kg/m, providing a 3.5% structural weight saving over the conventional design. It is again to be noted that the optimum angle of reinforcement for the angle plies is obtained as $\pm66^o$ using the 3D FEA, not $\pm54.7^o$ as predicted by netting theory.

Table B.12. Geometry of P75/epoxy with titanium liner riser including angle reinforcements

Layer	Orientation (degree)	Thickness(mm)	Layer	Orientation (degree)	Thickness(mm)
liner		10	11	66	1.71
1	66	1.71	12	-66	1.71
2	-66	1.71	13	66	1.71
3	90 (hoop)	2.175	14	-66	1.71
4	90	2.175	15	66	1.71
5	90	2.175	16	-66	1.71
6	90	2.175	17	66	1.71
7	90	2.175	18	-66	1.71
8	90	2.175	19	0 (axial)	2.50
9	90	2.175	20	0	2.50
10	90	2.175	21	0	2.50
Total thickness: 52mm and structural weight: 109.3kg/m					

B.12.1 Results for P75/Epoxy with Titanium Liner [±66 /90_8 /$(\pm66)_4$ /0_3] under Burst Case

The design internal burst pressure for the composite riser is 155.25MPa under which the Von Mises stress in the titanium liner is 476.53MPa, providing FS=1.99. Figs. B.66(a), B.66(b) and B.66(c), respectively, show the FSs in the fibre and transverse directions and in-plane shear for all the layers under load case 1 (burst load) for the manually tailored design with additional angle plies and considering different stacking sequences. The minimum FSs are 1.00 in the fibre direction (layer 1 in Fig. B.66(a)), 1.07 in the transverse direction (layer 21 in Fig. B.66(b)) and about 70.40 in shear (layer 1 and layer 18 in Fig. B.66(c)). In this case, both the stresses in transverse and in fibre directions are the most critical stresses and determine the thickness of the composite layers.

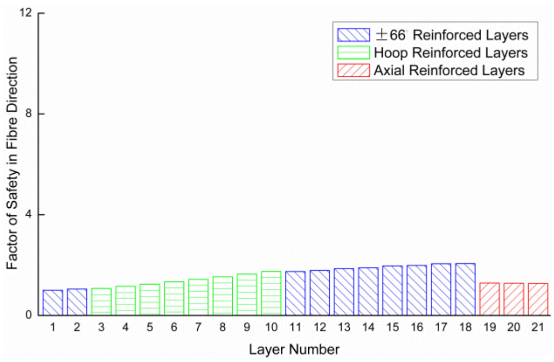

(a)

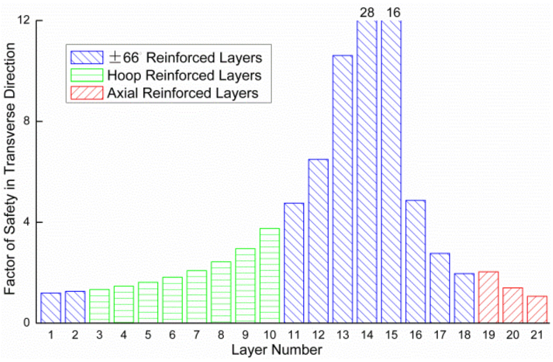

(b)

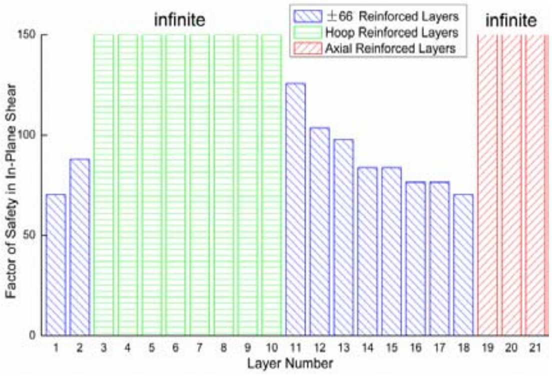

(c)

Fig. B.66. FSs for composite layers with 0°, ±66˚ and 90˚ reinforcements for load case 1 for P75/epoxy with titanium liner in (a) fibre direction, (b) transverse direction and (c) in-plane shear

B.12.2 Results for P75/Epoxy with Titanium Liner [±66 /90_8 /$(\pm66)_4$ /0_3] under Pure Tension Case

As described in *Chapter 3*, the tension force has to be calculated using three different cases, which yield values of 3600kN, 2800kN and 3660kN, respectively. Therefore, the design tension force is 3660×2.25=8235kN.

Under an 8235kN pure tension, the Von Mises stress in the titanium liner is 238.75MPa, providing FS=3.98. Figs. B.67(a), B.67(b) and B.67(c) show the FSs in all the layers under load case 2(a) (pure tension) for the manually tailored design with the minimum being 1.09 in the fibre direction of the axial layers (layer 19, Fig. B.67(a)).

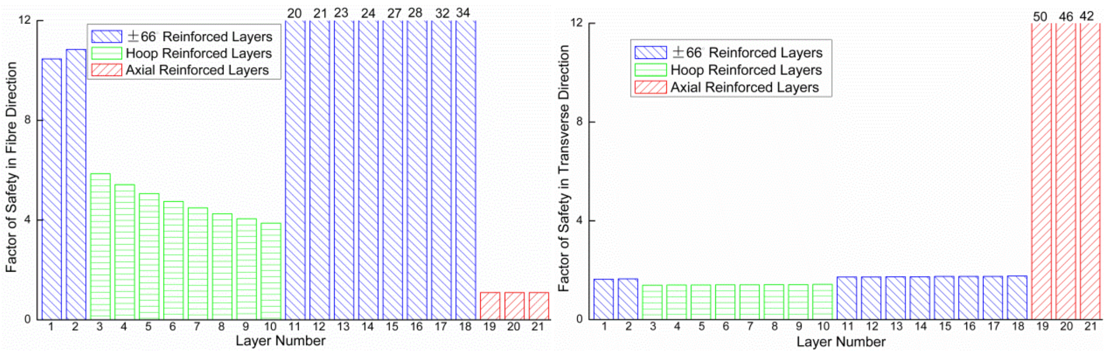

(a) (b)

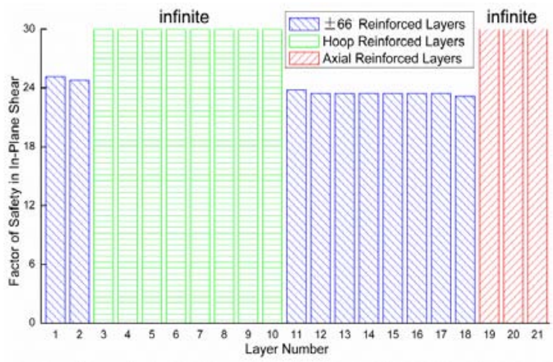

(c)

Fig. B.67. FSs for composite layers with 0°, ±66˚ and 90˚ reinforcements for load case 2(a) for P75/epoxy with titanium liner in (a) fibre direction, (b) transverse direction and (c) in-plane shear

B.12.3 Results for P75/Epoxy with Titanium Liner [±66 /90_8 /$(\pm66)_4$ /0_3] under Tension with External Pressure Case

The tension force under load case 2(b) (tension with external pressure of 19.5MPa) is the same as that for load case 2(a), that is, 8235kN, and the Von Mises stress in the titanium liner is 258.7MPa, providing FS=3.67. Fig. B.68 shows the FSs under load case 2(b) for the manually tailored design with the minimum being 1.02 in fibre direction in layer 19 (Fig. B.68(a)).

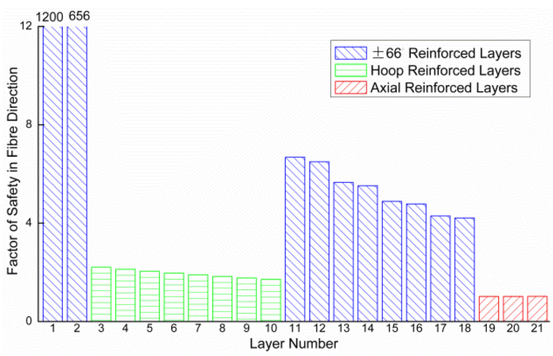

(a)

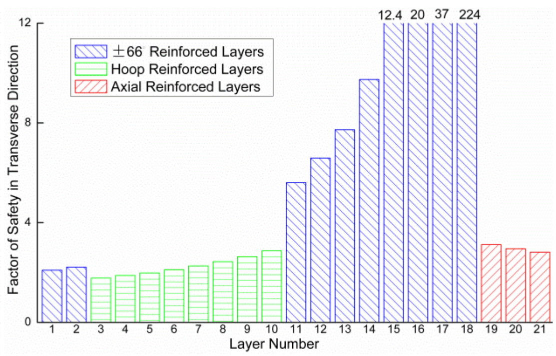

(b)

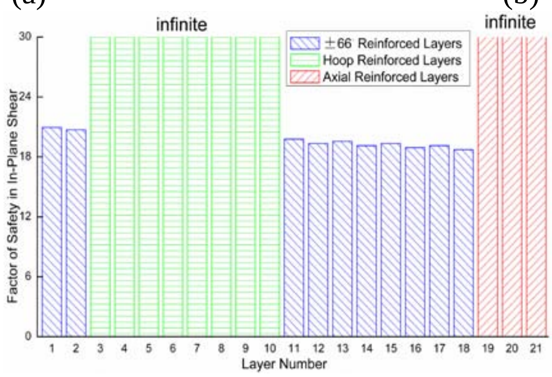

(c)

Fig. B.68. FSs for composite layers with 0°, ±66˚ and 90˚ reinforcements for load case 2(b) for P75/epoxy with titanium liner in (a) fibre direction, (b) transverse direction and (c) in-plane shear

B.12.4 Results for P75/Epoxy with Titanium Liner [±66 /90_8 /$(\pm 66)_4$ /0_3] under Collapse Case

The design collapse pressure for the composite riser is 58.5MPa and, under this external over-pressure, the Von Mises stress in the titanium liner is 110.5MPa, providing FS=8.60. Fig. B.69 shows the FSs under load case 3 (collapse load) for manually tailored design with the minimum FSs being 1.02 (layer 10) in fibre direction and 1.00 (layer 21) in transverse direction, respectively.

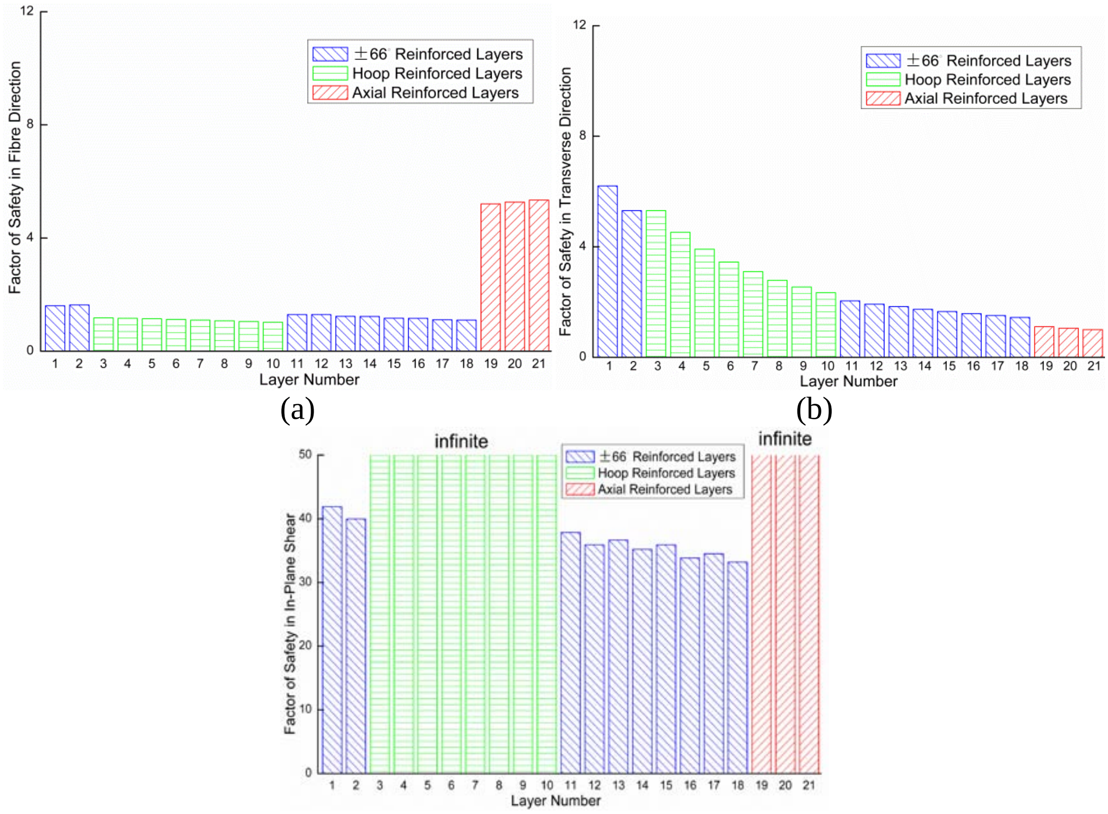

(a) (b)

(c)

Fig. B.69. FSs for composite layers with 0°, ±66˚ and 90˚ reinforcements for load case 3 for P75/epoxy with titanium liner in (a) fibre direction, (b) transverse direction and (c) in-plane shear

B.12.5 Results for P75/Epoxy with Titanium Liner [±66 /90_8 /$(\pm 66)_4$ /0_3] under Buckling Case

The geometry of the P75/epoxy with titanium liner riser using the tailored design is also checked for buckling under external pressure (load case 4). The critical buckling pressure obtained is 573.8MPa (mode 1), which is much higher than the design buckling pressure of 58.5MPa. The first three mode shapes are shown in Fig. B.70 in which it can be seen that the number of circumferential waves is 2 for all three modes and the number of half-waves along the axial direction 1, 2 and 3 for modes 1, 2 and 3, respectively.

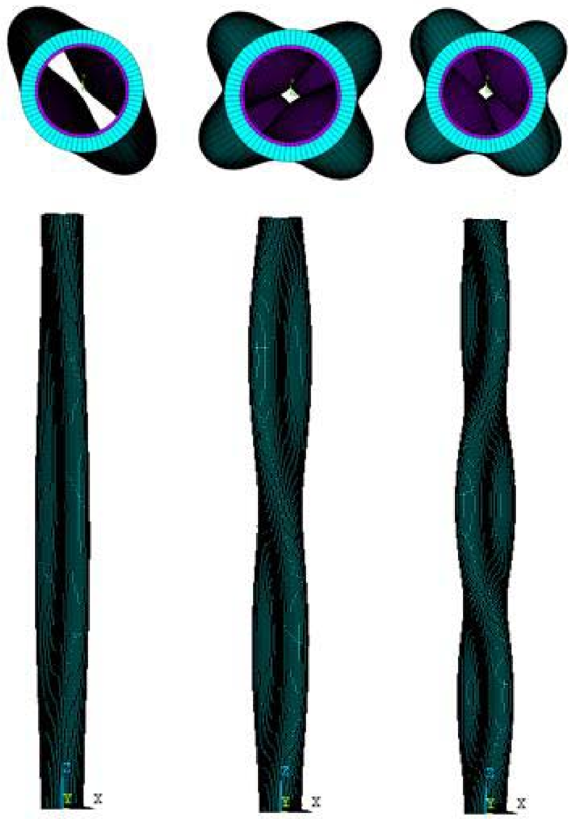

(a) B.P.= 573.8MPa (b) B.P.=580.9MPa (c) B.P.=595.7MPa
Fig. B.70. Mode shapes of composite riser with 0°, ±66˚ and 90˚ reinforcements for P75/epoxy with titanium liner (5m): (a) mode 1, (b) mode 2 and (c) mode 3

B.13 Results for P75/Epoxy with Aluminium Liner Using Conventional Design

Table B.13 gives the geometry of the composite riser tube optimised for minimum thickness using the conventional design under the local load cases, which yields a 17-ply composite laminate [$90_{14}/0_3$] with hoop and axially reinforced layers having thicknesses of 2.75mm and 2.50mm, respectively, which results in a total laminate thickness of 46mm, with a 14mm aluminium liner and structural weight of 115.4kg/m. Unlike PEEK liner riser, the thickness of aluminium liner would affect total weight significantly, thus, the first step is the determination of the thickness of aluminium liner. The variations of thickness and weight according to the different thicknesses of aluminium liner are shown in Fig. B.71 in which it can be seen that when the aluminium liner is 14mm, the total weight is the minimum. Hence for the following analysis, 14mm aluminium liner is used.

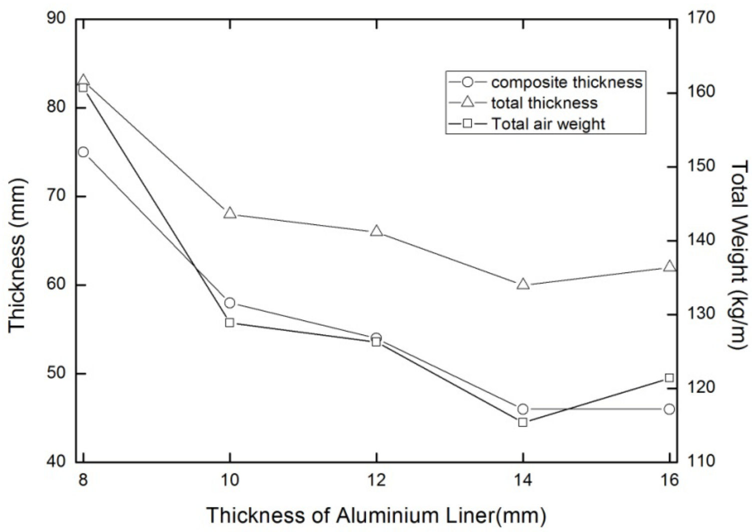

Fig. B.71. Thickness and weight of composite cylinder according to different thicknesses of aluminium liner

Table B.13. Geometry of P75/epoxy with aluminium liner riser with orthogonal reinforcements

Layer	Orientation (degree)	Thickness (mm)	Layer	Orientation (degree)	Thickness (mm)
liner		14	9	90	2.75
1	90 (hoop)	2.75	10	90	2.75
2	90	2.75	11	90	2.75
3	90	2.75	12	90	2.75
4	90	2.75	13	90	2.75
5	90	2.75	14	90	2.75
6	90	2.75	15	0 (axial)	2.50
7	90	2.75	16	0	2.50
8	90	2.75	17	0	2.50
Total thickness: 60mm and structural weight: 115.4kg/m					

B.13.1 Results for P75/Epoxy with Aluminium Liner [$90_{14}/0_3$] under Burst Case

The design internal burst pressure for the composite riser is 155.25MPa under which the Von Mises stress in the aluminium liner is 338.79MPa and FS=1.59. Figs. B.72(a) and B.72(b), respectively, show the FSs in the fibre and transverse directions under load case 1 (burst load) for all the layers in the conventional design geometry. The minimum FS in the fibre direction is 1.00 (layer 1 in Fig. B.72(a)), while that in the transverse direction is 1.14 (layers 17 in Fig. B.72(b)). It is evident, that under burst case, the stresses in fibre direction are the most critical stresses and determine the minimum thickness of the composite P75/epoxy with aluminium liner with only 0^o and 90^o reinforcements.

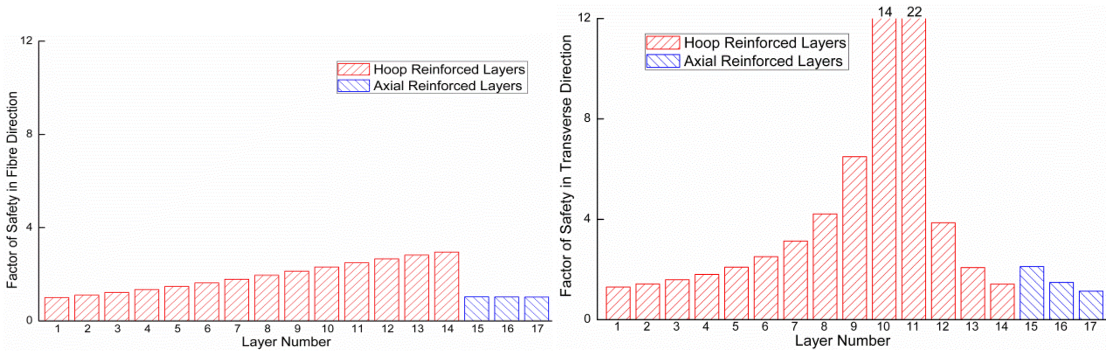

(a) (b)

Fig. B.72. FSs for composite layers with 0° and 90˚ reinforcements for load case 1 for P75/epoxy with aluminium liner in (a) fibre direction and (b) transverse direction

B.13.2 Results for P75/Epoxy with Aluminium Liner [$90_{14}/0_3$] under Pure Tension Case

As described in *Chapter 3*, the tension force has to be calculated using three different cases, which yield values of 3500kN, 2670kN and 3757kN, respectively. Therefore, the design tension force is 3757kN ×2.25=8450kN.

Under an 8450kN pure tension, the Von Mises stress in the aluminium liner is 149.1MPa and FS=3.62. Figs. B.73 shows the FSs in every layer under load case 2(a) (pure tension) for the conventional design with the minimum FSs being 1.07 (layer 15) in the fibre direction and 1.21 (layer 1) in transverse direction, respectively.

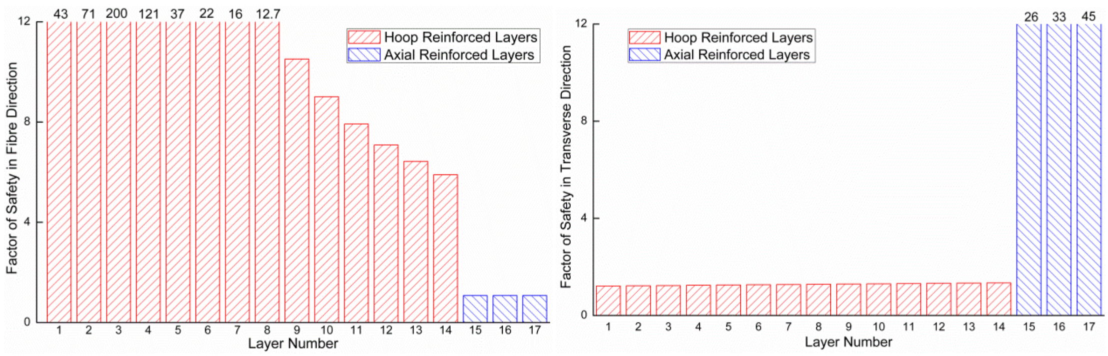

(a) (b)

Fig. B.73. FSs for composite layers with 0° and 90˚ reinforcements for load case 2(a) for P75/Epoxy with aluminium liner in (a) fibre direction and (b) transverse direction

B.13.3 Results for P75/Epoxy with Aluminium Liner [$90_{14}/0_3$] under Tension with External Pressure Case

The tension force under load case 2(b) (tension with external pressure of 19.5MPa) is also 8450kN and the Von Mises stress in the aluminium liner is 157.0MPa, providing FS=3.44. Fig. B.74 shows the FSs under load case 2(b) for the conventional design with the minimum being 1.03 in fibre direction in layer 15 (Fig. B.74(a)).

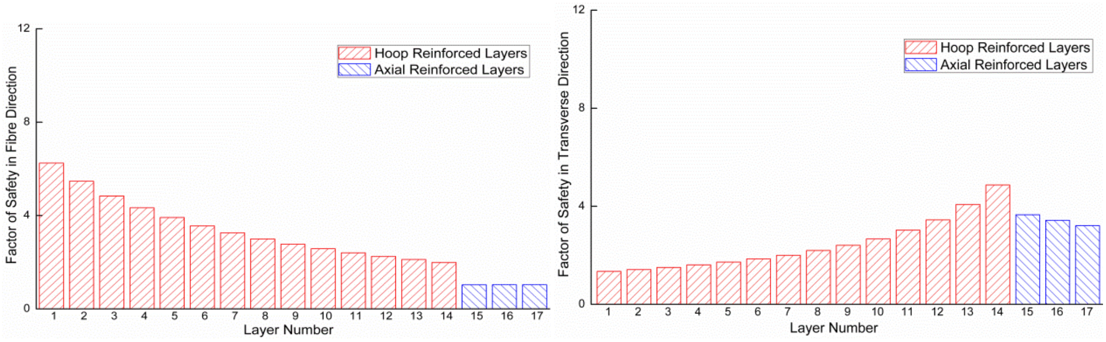

(a) (b)

Fig. B.74. FSs for composite layers with 0° and 90˚ reinforcements for load case 2(b) for P75/epoxy with aluminium liner in (a) fibre direction, and (b) transverse direction

B.13.4 Results for P75/Epoxy with Aluminium Liner [$90_{14}/0_3$] under Collapse Case

The design collapse pressure for the composite riser is 58.5MPa under which the Von Mises stress in the aluminium liner is 52.73MPa, providing FS=10.24. Fig. B.75 shows the FSs under load case 3 (collapse load) for the conventional design, with the minimum FSs being 1.00 (layer 14) in fibre direction and 1.04 (layer 17) in transverse direction, respectively.

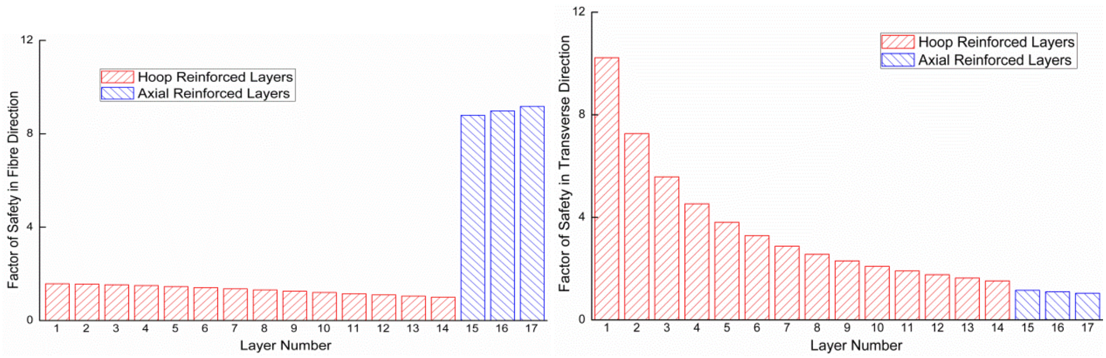

(a) (b)

Fig. B.75. FSs for composite layers with 0° and 90˚ reinforcements for load case 3 for P75/epoxy with aluminium liner in (a) fibre direction, and (b) transverse direction

B.13.5 Results for P75/Epoxy with Aluminium Liner [$90_{14}/0_3$] under Buckling Case

The geometry of P75/epoxy with aluminium liner riser using the conventional design is also checked for buckling under external pressure (load case 4) and the critical buckling pressure obtained is 732.4MPa (mode 1), which is much higher than the design buckling pressure of 58.5MPa. The first three mode shapes can be seen in Fig. B.76 in which the number of circumferential waves is 2 for all three modes and the number of half-waves along the axial direction 1, 2 and 3 for modes 1, 2 and 3, respectively.

(a) B.P.= 732.4MPa (b) B.P.=736.4MPa (c) B.P.=749.3MPa
Fig. B.76. Mode shapes of composite riser with 0° and 90^{o} reinforcements for P75/epoxy with aluminium liner (5m): (a) mode 1 (b) mode 2 and (c) mode 3

B.14 Results for P75/Epoxy with Aluminium Liner Using Tailored Design

Table B.14 gives the geometry of the composite riser tube optimised for minimum thickness using the tailored design under the local load cases, which yields a 16-ply composite laminate [+65/90$_5$/(-65, +65)$_3$/-65/0$_3$] with the 0^{o}, 90^{o} and ±65^{o} of 2.50, 2.77 and 2.85(2.80)mm thickness, respectively, which results in a total laminate thickness of 44mm, with a 14mm aluminium liner and structural weight of 111.3kg/m, providing a 3.5% structural weight saving over the conventional design. It is again to be noted that the optimum angle of reinforcement for the angle plies is obtained as ±65^{o} using the 3D FEA, not ±54.7^{o} as predicted by the netting theory.

Table B.14. Geometry of P75/epoxy with aluminium liner riser including angle reinforcements

Layer	Orientation (degree)	Thickness (mm)	Layer	Orientation (degree)	Thickness (mm)
liner		14	9	-65	2.85
1	65	2.85	10	65	2.85
2	90 (hoop)	2.77	11	-65	2.80
3	90	2.77	12	65	2.80
4	90	2.77	13	-65	2.80
5	90	2.77	14	0 (axial)	2.50
6	90	2.77	15	0	2.50
7	-65	2.85	16	0	2.50
8	65	2.85			
Total thickness: 58mm and structural weight: 111.3kg/m					

B.14.1 Results for P75/Epoxy with Aluminium Liner [65 /90$_5$ /-65 /(±65)$_3$ /0$_3$] under Burst Case

The design internal burst pressure for the composite riser is 155.25MPa under which the Von Mises stress in the aluminium liner is 326.72MPa, providing FS=1.65. Figs. B.77(a), B.77(b) and B.77(c), respectively, show the FSs in the fibre and transverse directions and in-plane shear for all the layers under load case 1 (burst load) for the manually tailored design with additional angle plies and considering different stacking sequences. The minimum FSs are 1.02 in the fibre direction (layer 1 in Fig. B.77(a)), 1.07 in the transverse direction (layer 16 in Fig. B.77(b)) and about 60.69 in shear (layer 1 in Fig. B.77(c)). In this case, both the stresses in transverse and in fibre directions are most critical stresses and determine the thickness of the composite layers.

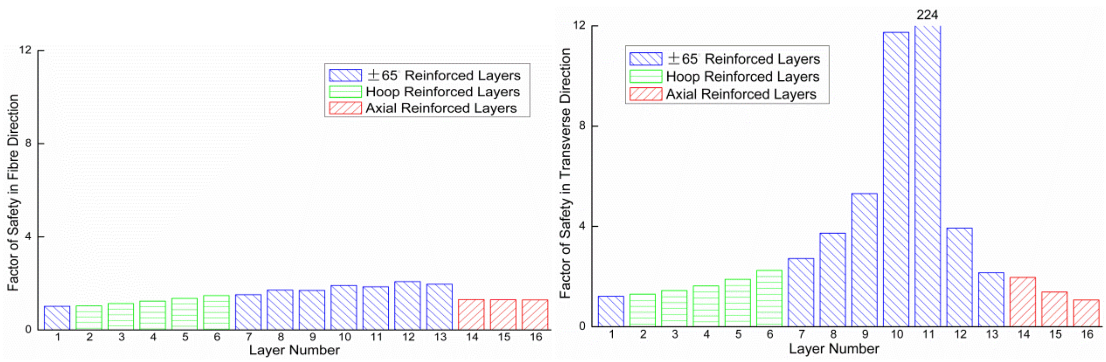

(a) (b)

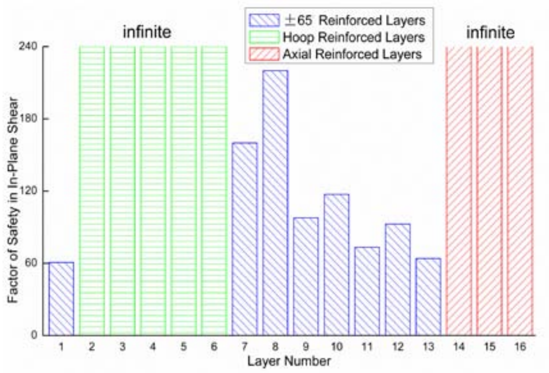

(c)

Fig. B.77. FSs for composite layers with 0°, ±65˚ and 90˚ reinforcements for load case 1 for P75/epoxy with aluminium liner in (a) fibre direction, (b) transverse direction and (c) in-plane shear

B.14.2 Results for P75/Epoxy with Aluminium Liner [$65/90_5/-65/(\pm65)_3\ /0_3$] under Pure Tension Case

As described in *Chapter 3*, the tension force has to be calculated using three different cases, which yield values of 3450kN, 2600kN and 3676kN, respectively. Therefore, the design tension force is 3676×2.25=8270kN.

Under a pure tension (8270kN), the Von Mises stress in the aluminium liner is 147.3MPa, providing FS=3.66. Figs. B.78(a), B.78(b) and B.78(c) show the FSs in all the layers under load case 2(a) (pure tension) for the manually tailored design. In this case, while the other FSs are relatively high, the minimum FS is about 1.09 in the fibre direction of the axial layers (layer 16, Fig. B.78(a)).

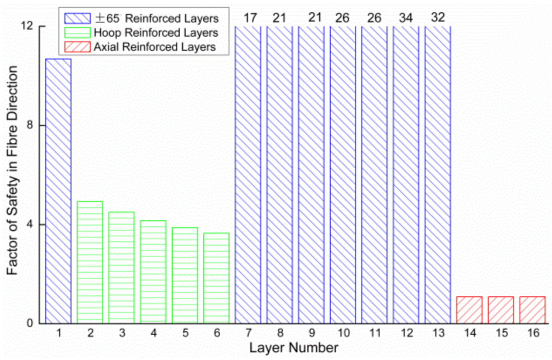

(a)

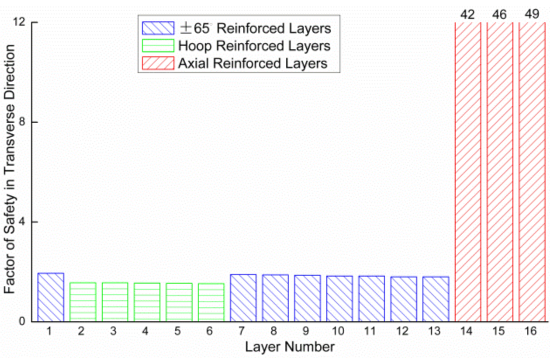

(b)

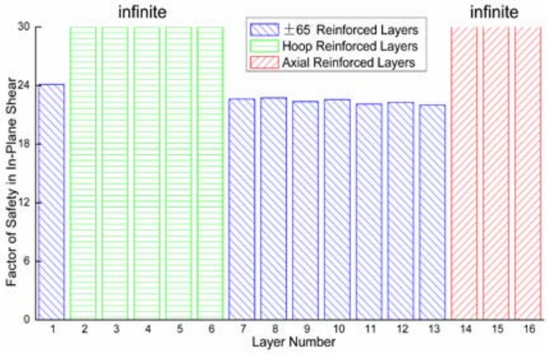

(c)

Fig. B.78. FSs for composite layers with 0°, ±65˚ and 90˚ reinforcements for load case 2(a) for P75/epoxy with aluminium liner in (a) fibre direction, (b) transverse direction and (c) in-plane shear

B.14.3 Results for P75/Epoxy with Aluminium Liner [65 /90$_5$ /-65 /(±65)$_3$ /0$_3$] under Tension with External Pressure Case

The tension force under load case 2(b) (tension with external pressure of 19.5MPa) is the same as that for load case 2(a), that is, 8270kN, and the Von Mises stress in the aluminium liner is 164.36MPa, providing FS=3.28. Fig. B.79 shows the FSs under load case 2(b) for the manually tailored design with the minimum being 1.00 in fibre direction in layer 14 (Fig. B.79(a)).

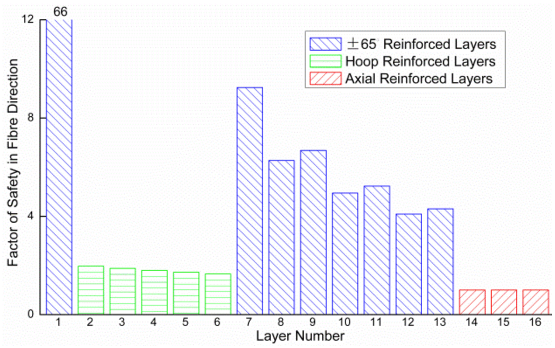

(a)

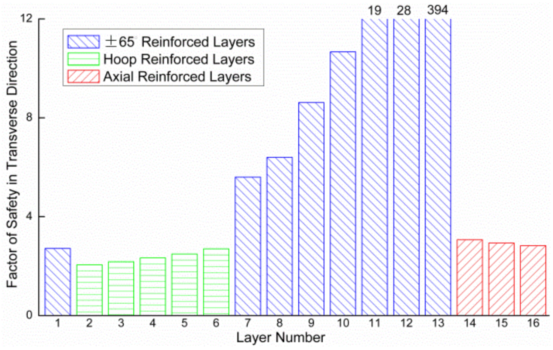

(b)

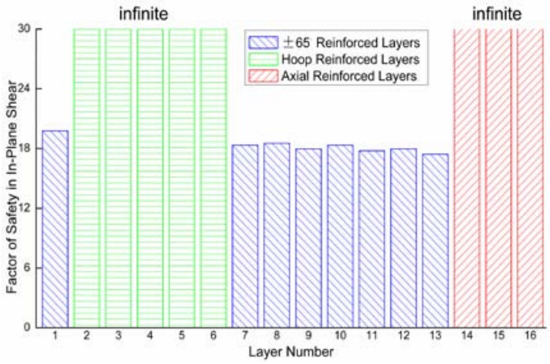

(c)

Fig. B.79. FSs for composite layers with 0°, ±65˚ and 90˚ reinforcements for load case 2(b) for P75/epoxy with aluminium liner in (a) fibre direction (b) transverse direction, and (c) in-plane shear

B.14.4 Results for P75/Epoxy with Aluminium Liner [65 $/90_5$ /-65 $/(\pm65)_3$ $/0_3$] under Collapse Case

The design collapse pressure for the composite riser is 58.5MPa and, under this external over-pressure, the Von Mises stress in the aluminium liner is 79.0MPa, providing FS=6.83. Fig. B.80 shows the FSs under load case 3 (collapse load) for the manually tailored design with the minimum FSs being 1.01 (layer 6) in fibre direction and 1.00 (layer 16) in transverse direction, respectively.

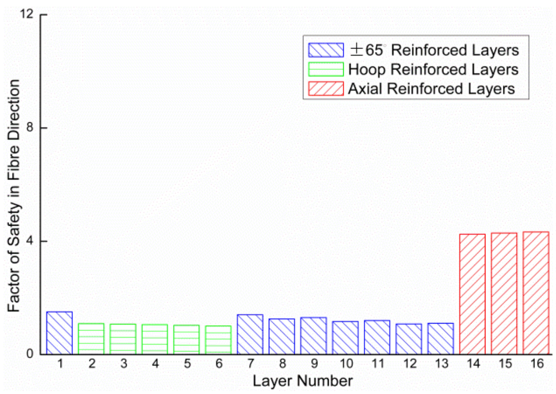

(a)

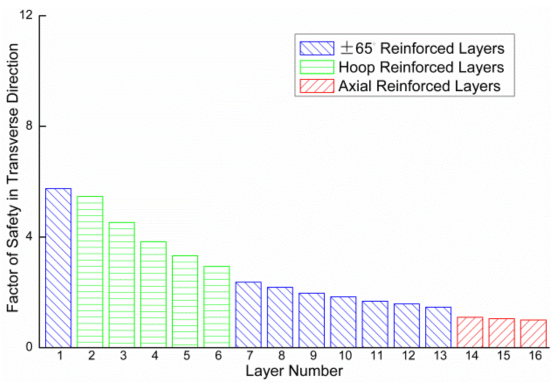

(b)

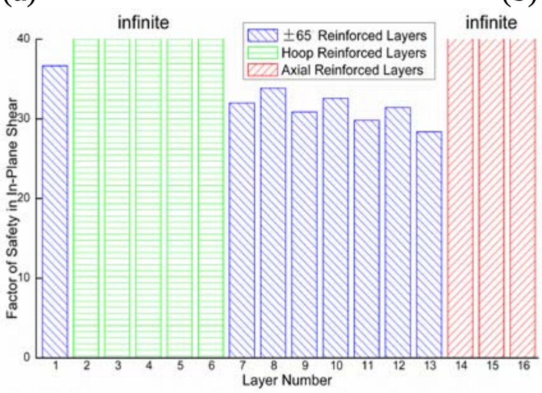

(c)

Fig. B.80. FSs for composite layers with 0°, ±65˚ and 90˚ reinforcements for load case 3 for P75/epoxy with aluminium liner in (a) fibre direction (b) transverse direction, and (c) in-plane shear

B.14.5 Results for P75/Epoxy with Aluminium Liner [65 $/90_5$ /-65 $/(\pm65)_3$ $/0_3$] under Buckling Case

The geometry of P75/epoxy with aluminium liner riser using the tailored design is also checked for buckling under external pressure (load case 4). The critical buckling pressure obtained is 622.5MPa (mode 1), which is much higher than the design buckling pressure of 58.5MPa. The first three mode shapes are shown in the Fig. B.81 in which it can be seen that the number of circumferential waves is 2 for all three modes and the number of half-waves along the axial direction 1, 2 and 3 for modes 1, 2 and 3, respectively.

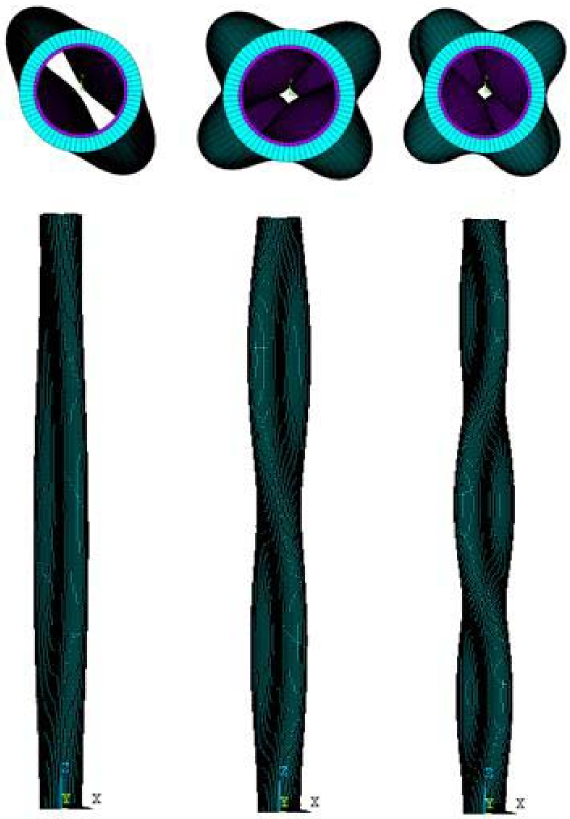

(a) B.P.= 622.5MPa (b) B.P.=632.0MPa   (c) B.P.=651.0MPa
Fig. B.81. Mode shapes of composite riser with 0°, ±65˚ and 90˚ reinforcements for P75/epoxy with aluminium liner (5m): (a) mode 1, (b) mode 2 and (c) mode 3

APPENDIX C

LAST PLY FAILURE ANALYSIS FOR THE OTHER MATERIAL COMBINATIONS

C.1 Last Ply Failure Analysis of AS4/Epoxy with Steel Liner $[90/(0/90)_{10}]$

C.1.1 Last Ply Failure under Burst Case

Fig. C.1 shows the progressive failure process for identifying last ply failure for AS4/epoxy with steel liner composite cylinder with 0° and 90° reinforcements under burst case.

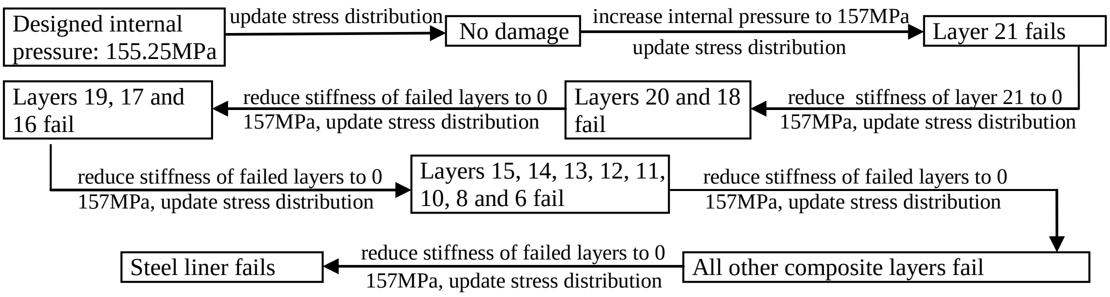

Fig. C.1. Progressive failure process for AS4/epoxy with steel liner composite cylinder with 0° and 90° reinforcements for burst case

Both the first and last layer failure pressures are 157MPa under the burst load case for AS4/epoxy with steel liner composite cylinder with 0° and 90° reinforcements.

C.1.2 Last Ply Failure under Pure Tension Case

Fig. C.2 shows the progressive failure process for identifying last ply failure for AS4/epoxy with steel liner composite cylinder with 0° and 90° reinforcements under pure tension case.

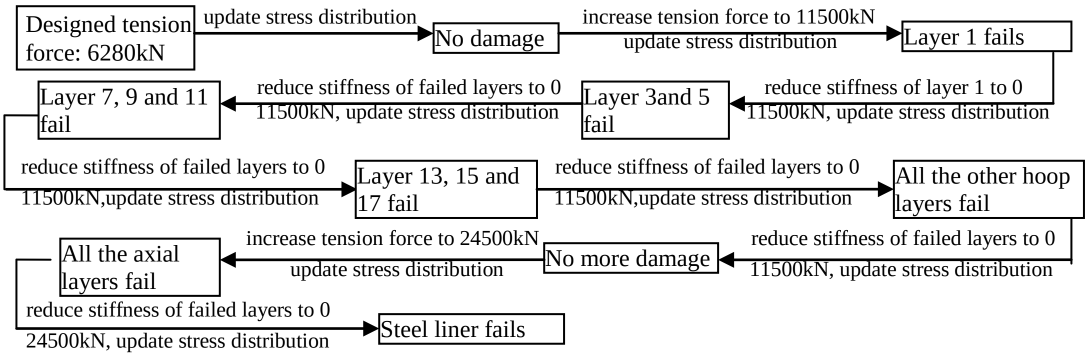

Fig. C.2. Progressive failure process for AS4/epoxy with steel liner composite cylinder with 0° and 90° reinforcements for pure tension case

In the pure tension case, the tension forces for the first and last layer failures are 11500kN and 24500kN, respectively, for AS4/epoxy with steel liner composite cylinder with 0° and 90° reinforcements.

C.1.3 Last Ply Failure under Tension with External Pressure Case

Fig. C.3 shows the progressive failure process for identifying last ply failure for AS4/epoxy with steel liner composite cylinder with 0° and 90° reinforcements under axial tension with external pressure.

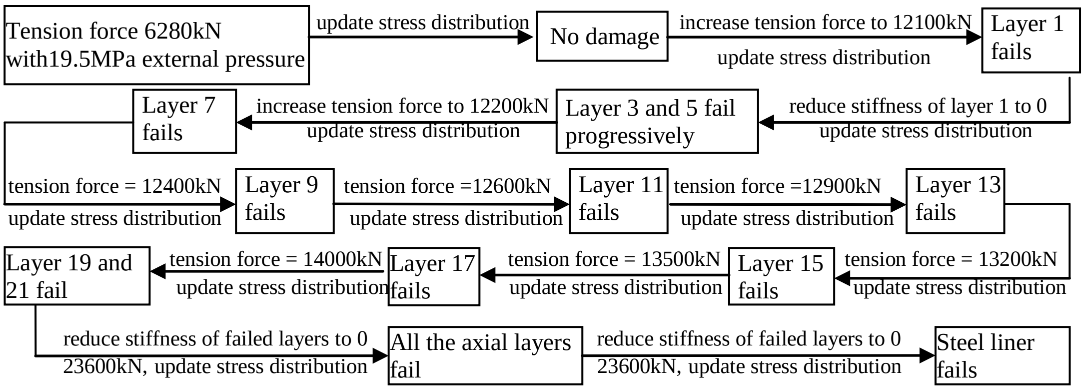

Fig. C.3. Progressive failure process for AS4/epoxy with steel liner composite cylinder with 0° and 90° reinforcements for tension with external pressure case

In the tension with external pressure (19.5MPa) case, the tension forces for the first and last layer failures are 12100kN and 23600kN, respectively, for AS4/epoxy with steel liner composite cylinder with 0° and 90° reinforcements.

C.1.4 Last Ply Failure under Collapse Case

Fig. C.4 shows the progressive failure process for identifying last ply failure for AS4/epoxy with steel liner composite cylinder with 0° and 90° reinforcements under external pressure.

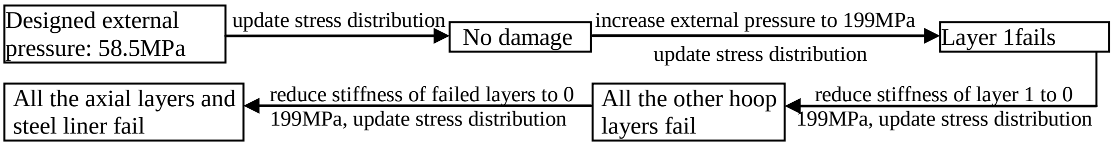

Fig. C.4. Progressive failure process for AS4/epoxy with steel liner composite cylinder with 0° and 90° reinforcements under collapse case

Both the first and last layer failure pressures are 199MPa under the collapse case for the AS4/epoxy with steel liner composite cylinder with 0° and 90° reinforcements.

C.2 Last Ply Failure Analysis of AS4/Epoxy with Steel Liner [0_3 /$(\pm 53.5)_5$ /90_4]

C.2.1 Last Ply Failure under Burst Case

Fig. C.5 shows the progressive failure process for identifying last ply failure for the AS4/epoxy with steel liner composite cylinder with 0°, ±53.5° and 90° reinforcements under burst case.

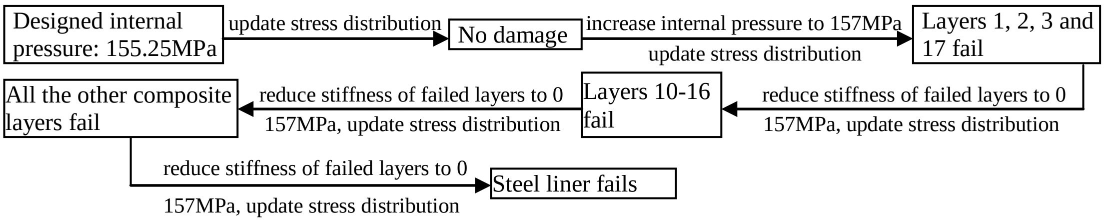

Fig. C.5. Progressive failure process for AS4/epoxy with steel liner composite cylinder with 0°, ±53.5° and 90° reinforcements under burst case

Both the first and last layer failure pressures are 157MPa under burst case for AS4/epoxy with steel liner composite cylinder with 0°, ±53.5° and 90° reinforcements.

C.2.2 Last Ply Failure under Pure Tension Case

Fig. C.6 shows the progressive failure process for identifying last ply failure for AS4/epoxy with steel liner composite cylinder with 0°, ±53.5° and 90° reinforcements under pure the tension case.

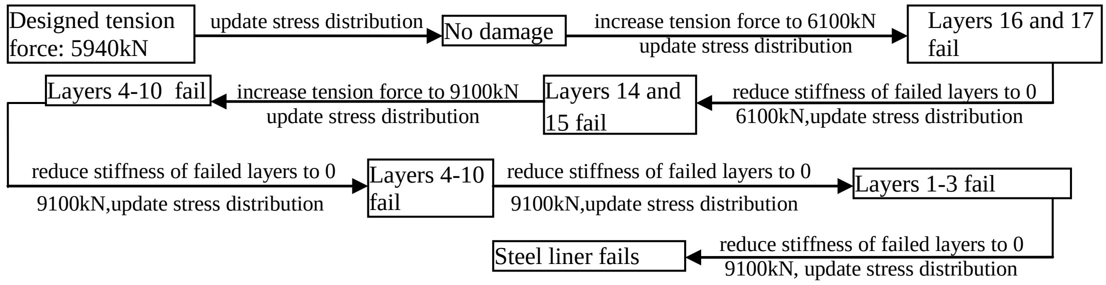

Fig. C.6. Progressive failure process for AS4/epoxy with steel liner composite cylinder with 0°, ±53.5° and 90° reinforcements under pure tension case

In the pure tension case, the tension forces for the first and last layer failures are 6100kN and 9100kN, respectively, for AS4/epoxy with steel liner composite cylinder with 0°, ±53.5° and 90° reinforcements.

C.2.3 Last Ply Failure under Tension with External Pressure Case

Fig. C.7 shows the progressive failure process for identifying last ply failure for AS4/epoxy with steel liner composite cylinder with 0°, ±53.5° and 90° reinforcements under axial tension with external pressure.

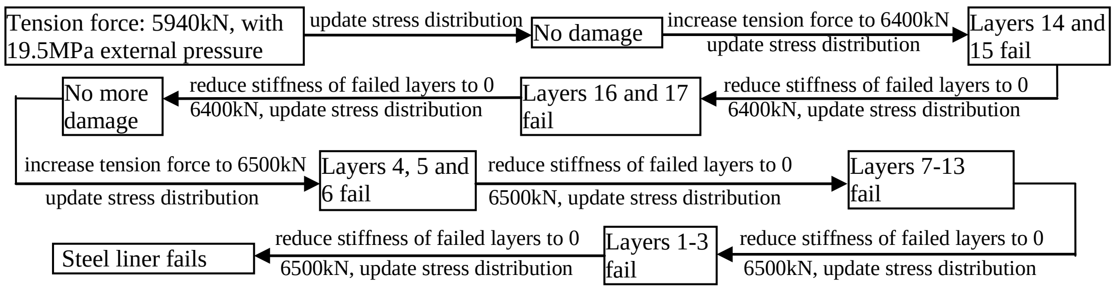

Fig. C.7. Progressive failure process for AS4/epoxy with steel liner composite cylinder with 0°, ±53.5° and 90° reinforcements under tension with external pressure case

In the tension with external pressure (19.5MPa) case, the tension forces for the first and last layer failures are 6400kN and 6500kN, respectively, for AS4/epoxy with steel liner composite cylinder with 0°, ±53.5° and 90° reinforcements.

C.2.4 Last Ply Failure under Collapse Case

Fig. C.8 shows the progressive failure process for identifying last ply failure for the AS4/epoxy with steel liner composite cylinder with 0°, ±53.5° and 90° reinforcements under external pressure.

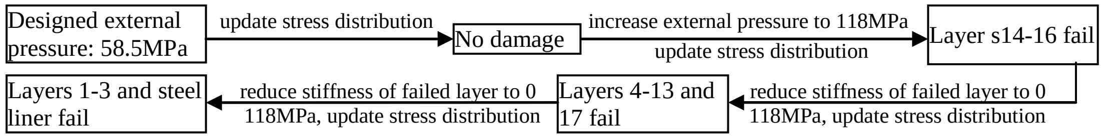

Fig. C.8. Progressive failure process for AS4/epoxy with steel liner composite cylinder with 0°, ±53.5° and 90° reinforcements under collapse case

Both the first and last layer failure pressures are 118MPa under collapse case for AS4/epoxy with steel liner composite cylinder with 0°, ±53.5° and 90° reinforcements.

C.3 Last Ply Failure Analysis of AS4/Epoxy with Titanium Liner [90/(0/90)$_{10}$]

C.3.1 Last Ply Failure under Burst Case

Fig. C.9 shows the progressive failure process for identifying last ply failure for AS4/epoxy with titanium liner composite cylinder with 0° and 90° reinforcements under burst case.

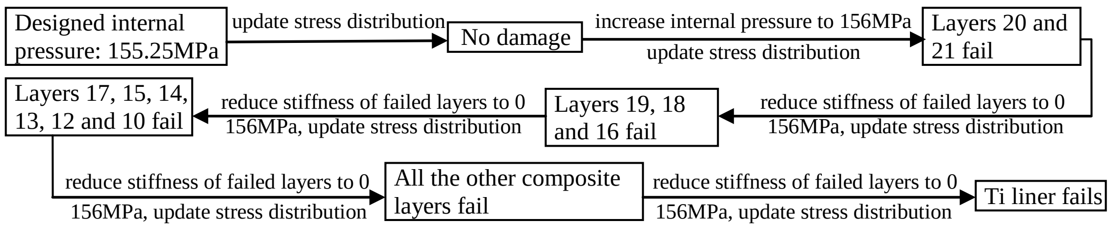

Fig. C.9. Progressive failure process for AS4/epoxy with titanium liner composite cylinder with 0° and 90° reinforcements under burst case

Both the first and last layer failure pressures are 156MPa under burst case for AS4/epoxy with titanium liner composite cylinder with 0° and 90° reinforcements.

C.3.2 Last Ply Failure under Pure Tension Case

Fig. C.10 shows the progressive failure process for identifying last ply failure for the AS4/epoxy with titanium liner composite cylinder with 0° and 90° reinforcements under pure tension case.

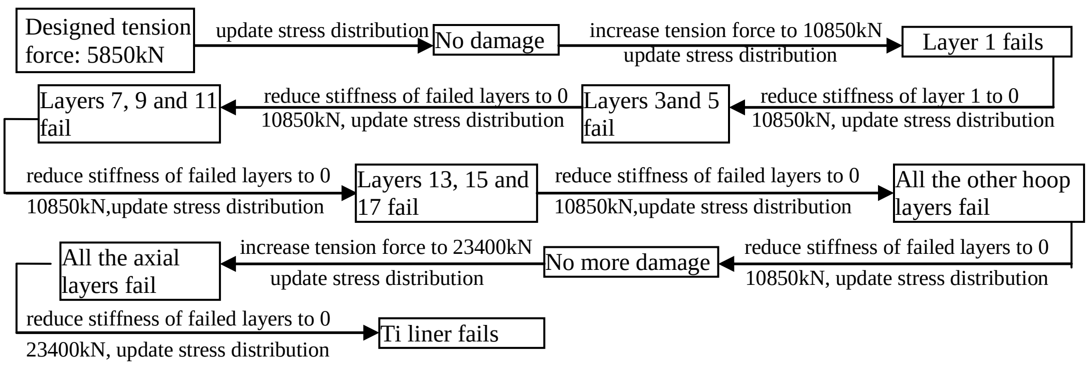

Fig. C.10. Progressive failure process for AS4/epoxy with titanium liner composite cylinder with 0° and 90° reinforcements under pure tension case

In the pure tension case, the tension forces for the first and last layer failures are 10850kN and 23400kN, respectively, for AS4/epoxy with titanium liner composite cylinder with 0° and 90° reinforcements.

C.3.3 Last Ply Failure under Tension with External Pressure Case

Fig. C.11 shows the progressive failure process for identifying last ply failure for the AS4/epoxy with titanium liner composite cylinder with 0° and 90° reinforcements under axial tension with external pressure.

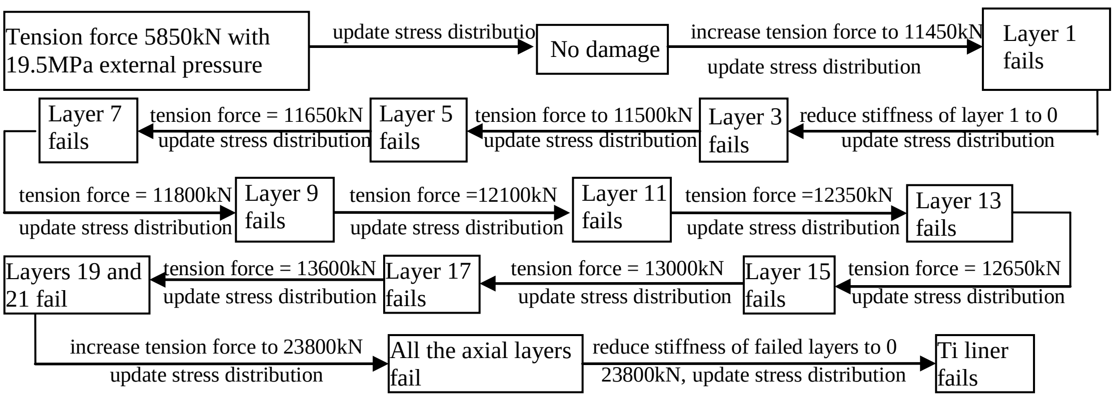

Fig. C.11. Progressive failure process for AS4/epoxy with titanium liner composite cylinder with 0° and 90° reinforcements under tension with external pressure case

In the tension with external pressure (19.5MPa) case, the tension forces for the first and last layer failures are 11450kN and 23800kN, respectively, for AS4/epoxy with titanium liner composite cylinder with 0° and 90° reinforcements.

C.3.4 Last Ply Failure under Collapse Case

Fig. C.12 shows the progressive failure process for identifying last ply failure for AS4/epoxy with titanium liner composite cylinder with 0° and 90° reinforcements under external pressure.

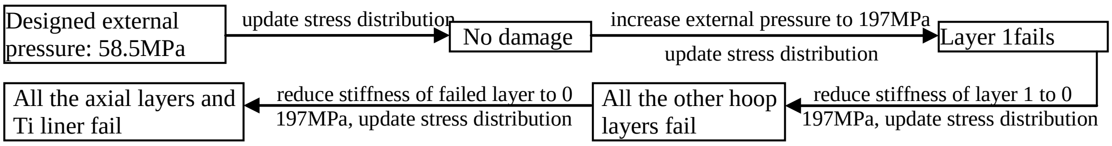

Fig. C.12. Progressive failure process for AS4/epoxy with titanium liner composite cylinder with 0° and 90° reinforcements under collapse case

Both the first and last layer failure pressures are 197MPa under collapse case for AS4/epoxy with titanium liner composite cylinder with 0° and 90° reinforcements.

C.4 Last Ply Failure Analysis of AS4/Epoxy with Titanium Liner $[0_3/(\pm 53)_5/90_4]$

C.4.1 Last Ply Failure under Burst Case

Fig. C.13 shows the progressive failure process for identifying last ply failure for AS4/epoxy with titanium liner composite cylinder with 0°, ±53° and 90° reinforcements under burst case.

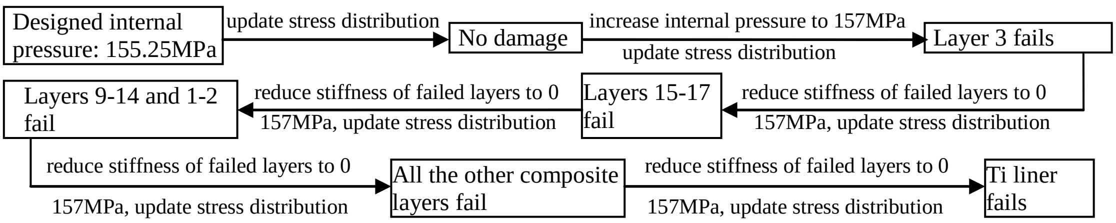

Fig. C.13. Progressive failure process for AS4/epoxy with titanium liner composite cylinder with 0°, ±53° and 90° reinforcements under burst case

Both the first and last layer failure pressures are 157MPa under the burst case for AS4/epoxy with titanium liner composite cylinder with 0°, ±53° and 90° reinforcements.

C.4.2 Last Ply Failure under Pure Tension Case

Fig. C.14 shows the progressive failure process for identifying last ply failure for the AS4/epoxy with titanium liner composite cylinder with 0°, ±53° and 90° reinforcements under pure tension case.

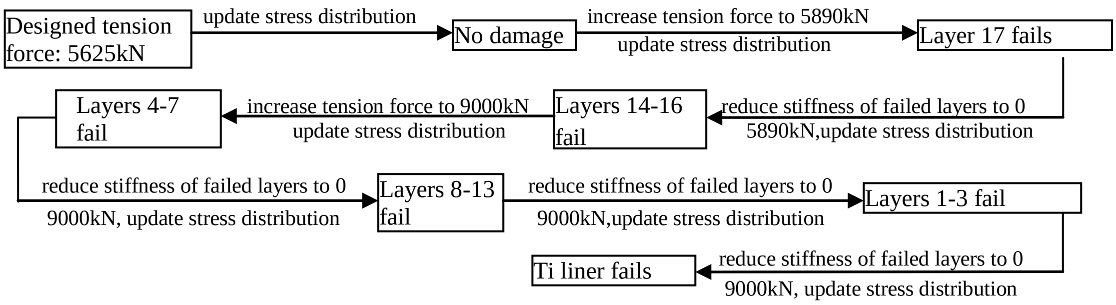

Fig. C.14. Progressive failure process for AS4/epoxy with titanium liner composite cylinder with 0°, ±53° and 90° reinforcements under pure tension case

In the pure tension case, the tension forces for the first and last layer failures are 5890kN and 9000kN, respectively, for AS4/epoxy with titanium liner composite cylinder with 0°, ±53° and 90° reinforcements.

C.4.3 Last Ply Failure under Tension with External Pressure Case

Fig. C.15 shows the progressive failure process for identifying last ply failure for AS4/epoxy with titanium liner composite cylinder with 0°, ±53° and 90° reinforcements under axial tension with external pressure case.

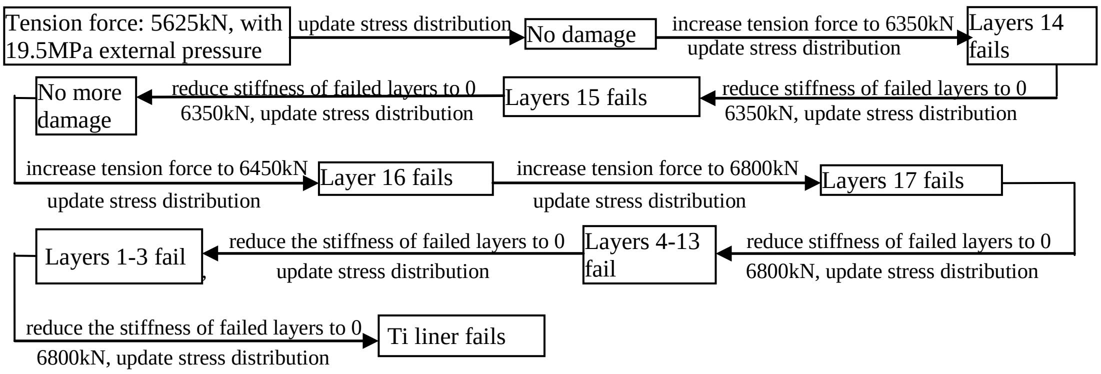

Fig. C.15. Progressive failure process for AS4/epoxy with titanium liner composite cylinder with 0°, ±53° and 90° reinforcements under tension with external pressure case

In the tension with external pressure (19.5MPa) case, the tension forces for the first and last layer failures are 6350kN and 6800kN, respectively, for AS4/epoxy with titanium liner composite cylinder with 0°, ±53° and 90° reinforcements.

C.4.4 Last Ply Failure under Collapse Case

Fig. C.16 shows the progressive failure process for identifying last ply failure for the AS4/epoxy with titanium liner composite cylinder with 0°, ±53° and 90° reinforcements under external pressure.

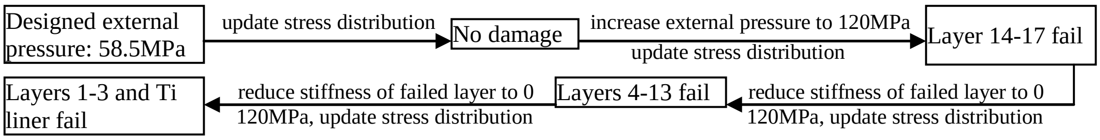

Fig. C.16. Progressive failure process for AS4/epoxy with titanium liner composite cylinder with 0°, ±53° and 90° reinforcements under collapse case

Both the first and last layer failure pressures are 120MPa under collapse case for AS4/epoxy with titanium liner composite cylinder with 0°, ±53° and 90° reinforcements.

C.5 Last Ply Failure Analysis of AS4/Epoxy with Aluminium Liner [90/(0/90)$_{10}$]

C.5.1 Last Ply Failure under Burst Case

Fig. C.17 shows the progressive failure process for identifying last ply failure for AS4/epoxy with aluminium liner composite cylinder with 0° and 90° reinforcements under burst case.

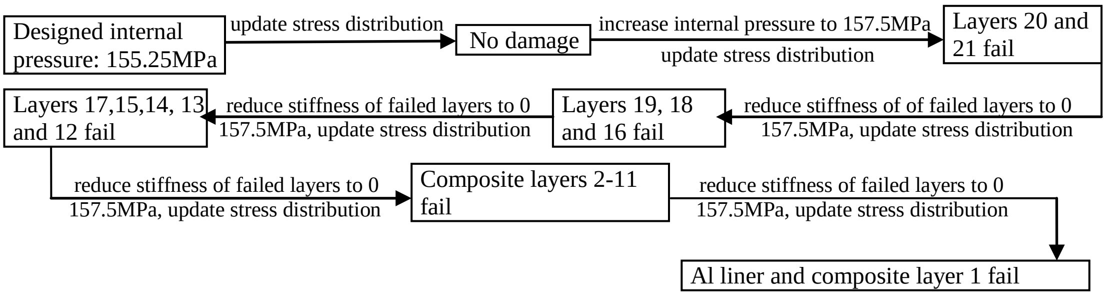

Fig. 17. Progressive failure process for AS4/epoxy with aluminium liner composite cylinder with 0° and 90° reinforcements under burst case

Both the first and last layer failure pressures are 157.5MPa under burst case for the AS4/epoxy with aluminium liner composite cylinder with 0° and 90° reinforcements.

C.5.2 Last Ply Failure under Pure Tension Case

Fig. C.18 shows the progressive failure process for identifying last ply failure for the AS4/epoxy with aluminium liner composite cylinder with 0° and 90° reinforcements under pure tension case.

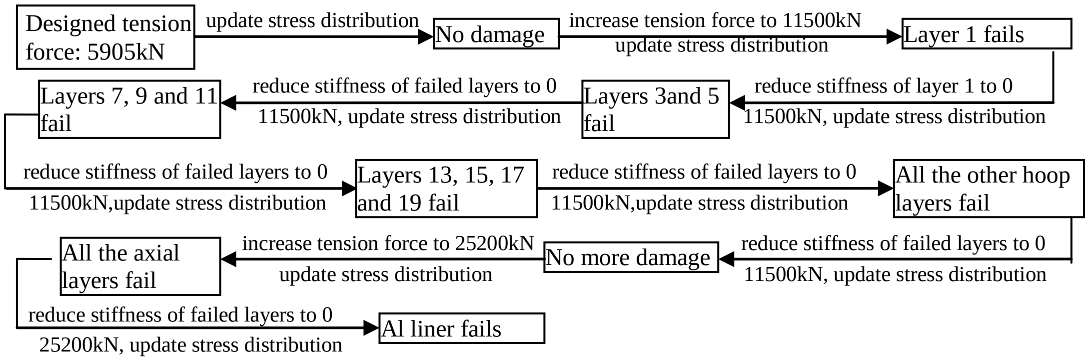

Fig. C.18. Progressive failure process for AS4/epoxy with aluminium liner composite cylinder with 0° and 90° reinforcements under pure tension case

In the pure tension case, the tension forces for the first and last layer failures are 11500kN and 25200kN, respectively, for AS4/epoxy with aluminium liner composite cylinder with 0° and 90° reinforcements.

C.5.3 Last Ply Failure under Tension with External Pressure Case

Fig. C.19 shows the progressive failure process for identifying last ply failure for AS4/epoxy with aluminium liner composite cylinder with 0° and 90° reinforcements under axial tension with external pressure.

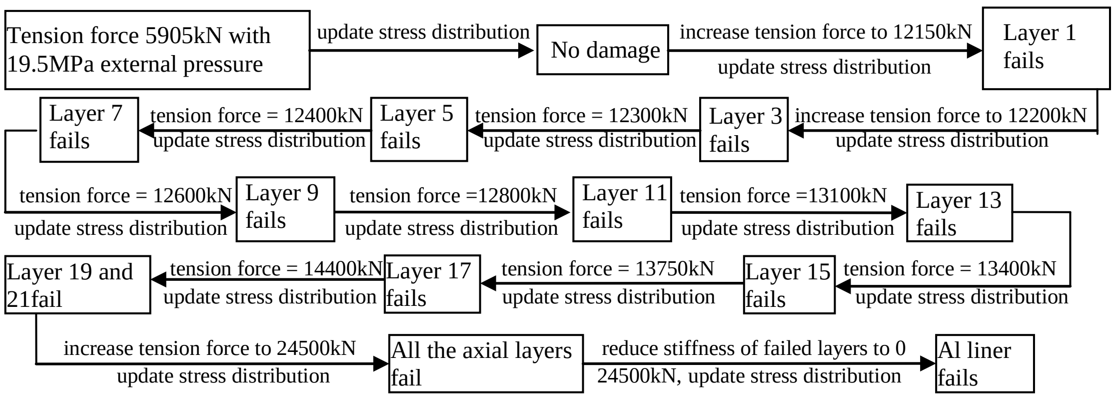

Fig. C.19. Progressive failure process for AS4/epoxy with aluminium liner composite cylinder with 0° and 90° reinforcements under tension with external pressure case

In the tension with external pressure (19.5MPa) case, the tension forces for the first and last layer failures are 12150kN and 24500kN, respectively, for AS4/epoxy with aluminium liner composite cylinder with 0° and 90° reinforcements.

C.5.4 Last Ply Failure under Collapse Case

Fig. C.20 shows the progressive failure process for identifying last ply failure for the AS4/epoxy with aluminium liner composite cylinder with 0° and 90° reinforcements under external pressure.

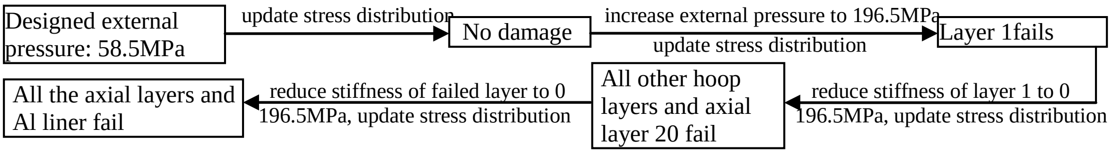

Fig. C.20. Progressive failure process of AS4/epoxy with aluminium liner composite cylinder with 0° and 90° reinforcements under collapse case

Both the first and last layer failure pressures are 196.5MPa under collapse case for AS4/epoxy with aluminium liner composite cylinder with 0° and 90° reinforcements.

C.6 Last Ply Failure Analysis of AS4/Epoxy with Aluminium Liner [0_4 /$(\pm 53.5)_5$ /90_4]

C.6.1 Last Ply Failure under Burst Case

Fig. C.21 shows the progressive failure process for identifying last ply failure for the AS4/epoxy with aluminium liner composite cylinder with 0°, ±53.5° and 90° reinforcements under burst case.

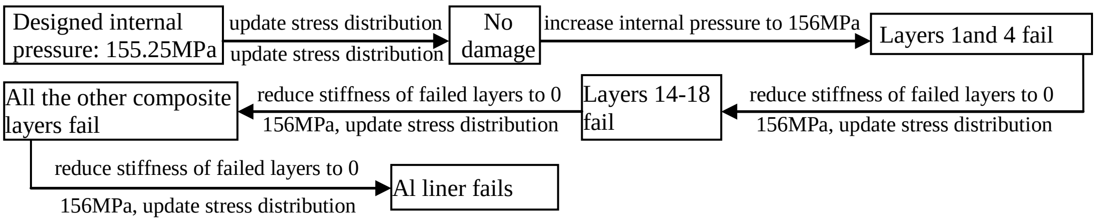

Fig. C.21. Progressive failure process for AS4/epoxy with aluminium liner composite cylinder with 0°, ±53.5° and 90° reinforcements under burst case

Both the first and last layer failure pressures are 156MPa under burst case for the AS4/epoxy with aluminium liner composite cylinder with 0°, ±53.5° and 90° reinforcements.

C.6.2 Last Ply Failure under Pure Tension Case

Fig. C.22 shows the progressive failure process for identifying last ply failure for the AS4/epoxy with aluminium liner composite cylinder with 0°, ±53.5° and 90° reinforcements under pure tension case.

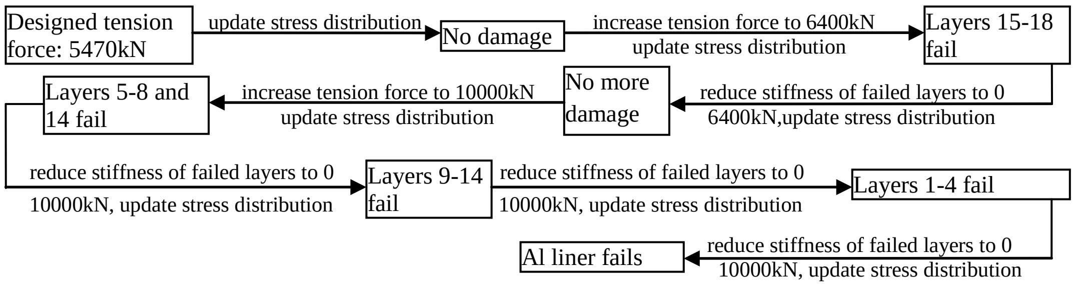

Fig. C.22. Progressive failure process for AS4/epoxy with aluminium liner composite cylinder with 0°, ±53.5° and 90° reinforcements under pure tension case

In the pure tension case, the tension forces for the first and last layer failures are 6400kN and 10000kN, respectively, for AS4/epoxy with aluminium liner composite cylinder with 0°, ±53.5° and 90° reinforcements.

C.6.3 Last Ply Failure under Tension with External Pressure Case

Fig. C.23 shows the progressive failure process for identifying last ply failure for AS4/epoxy with aluminium liner composite cylinder with 0°, ±53.5° and 90° reinforcements under axial tension with external pressure.

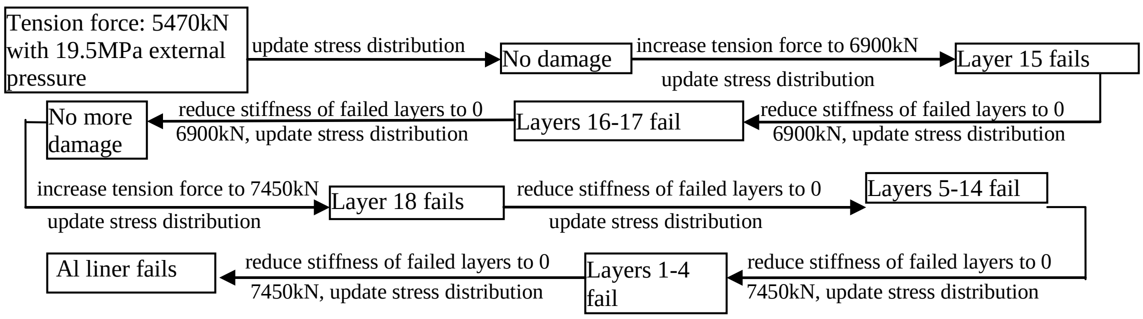

Fig. C.23. Progressive failure process for AS4/epoxy with aluminium liner composite cylinder with 0°, ±53.5° and 90° reinforcements under tension with external pressure case

In the tension with external pressure (19.5MPa) case, the tension forces for the first and last layer failures are 6900kN and 7450kN, respectively, for the AS4/epoxy with aluminium liner composite cylinder with 0°, ±53.5° and 90° reinforcements.

C.6.4 Last Ply Failure under Collapse Case

Fig. C.24 shows the progressive failure process for identifying last ply failure for AS4/epoxy with aluminium liner composite cylinder with 0°, ±53.5° and 90° reinforcements under external pressure.

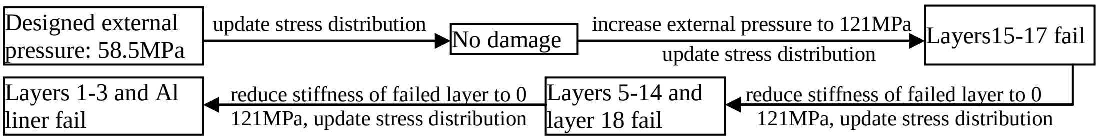

Fig. C.24. Progressive failure process for AS4/epoxy with aluminium liner composite cylinder with 0°, ±53.5° and 90° reinforcements under collapse case

Both the first and last layer failure pressures are 121MPa under collapse case for AS4/epoxy with aluminium liner composite cylinder with 0°, ±53.5° and 90° reinforcements.

APPENDIX D

RESULTS OF GLOBAL DESIGN FOR THE OTHER MATERIAL COMBINATIONS

D.1 Global Design Results of AS4/Epoxy with Titanium Liner $[0_3/(\pm53)_5/90_4]$ Riser

D.1.1 Results from Global Analysis for AS4/Epoxy Riser with Titanium Liner $[0_3/(\pm53)_5/90_4]$

This section presents the detailed results of the riser with the AS4/epoxy composite body and titanium liner analysed using its effective 3D properties with pipe elements for the laminate configuration and thickness combinations which provide the least structural weight, as determined by the local analysis performed in *Chapter 5*. The global analysis results for various combinations of tension, bending, shear force and pressure of the different global design load cases are presented. The difference between bending and tension moduli is larger than 5%, hence, both of them are analysed for AS4/epoxy with titanium liner riser. The results under different global load cases are illustrated below.

The tension force, bending moment and shear force distributions estimated from the global analysis conducted using FE modelling for global load cases LC4 to LC9 are presented in Figs. D.1-D.3, respectively. The blue horizontal lines in these figures indicate the top and bottom of the composite riser section, at depths of -44m and -1904m, respectively. It should be noted that, in designing the composite riser, we are only concerned about the tension, bending moment and shear force magnitudes within this region.

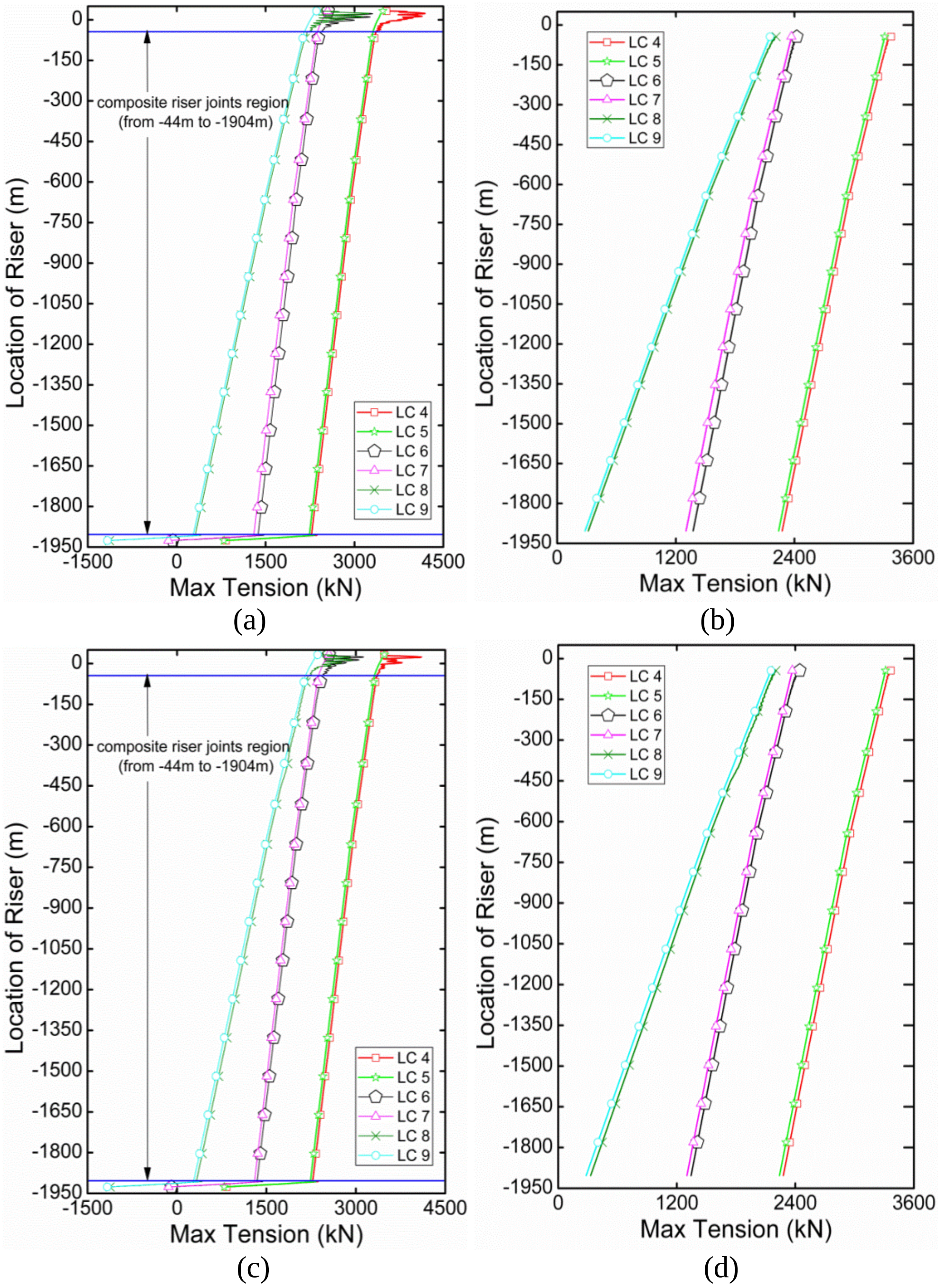

Fig. D.1. Tension forces for different load cases: (a) full-length riser, (b) composite riser region with bending modulus and (c) full-length riser, (d) composite riser region with tension modulus

Fig. D.1 shows the effective tension force distribution along the entire riser. It is clear that the maximum tension force is 3378.1kN in the composite section of the riser which occurs under load case LC4 at the top end with bending modulus.

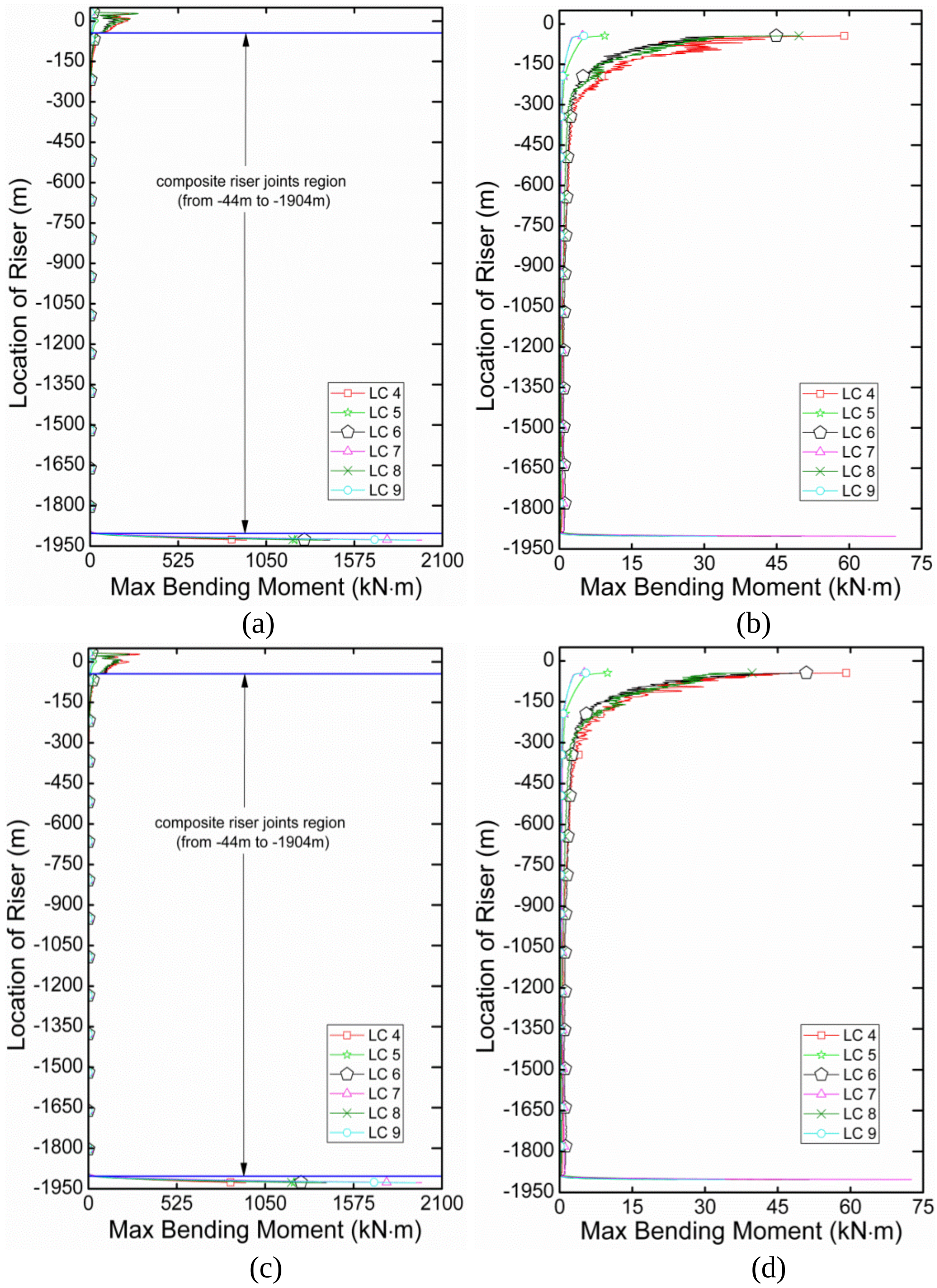

Fig. D.2. Bending moments for different load cases: (a) full-length riser, (b) composite riser region with bending modulus and (c) full-length riser, (d) composite riser region with tension modulus

Fig. D.2 shows the bending moment distribution along the entire riser. The maximum bending moments in the composite section of the riser occur at both the top and bottom, with tension modulus, with values of 59.1kN·m under LC4 at the top and 72.6kN·m under LC7 at the bottom. It may be noted that the bending moments are much higher in the metallic stress joints at the bottom, reaching up to around 2000kN·m at the bottom for load cases LC7 and LC9.

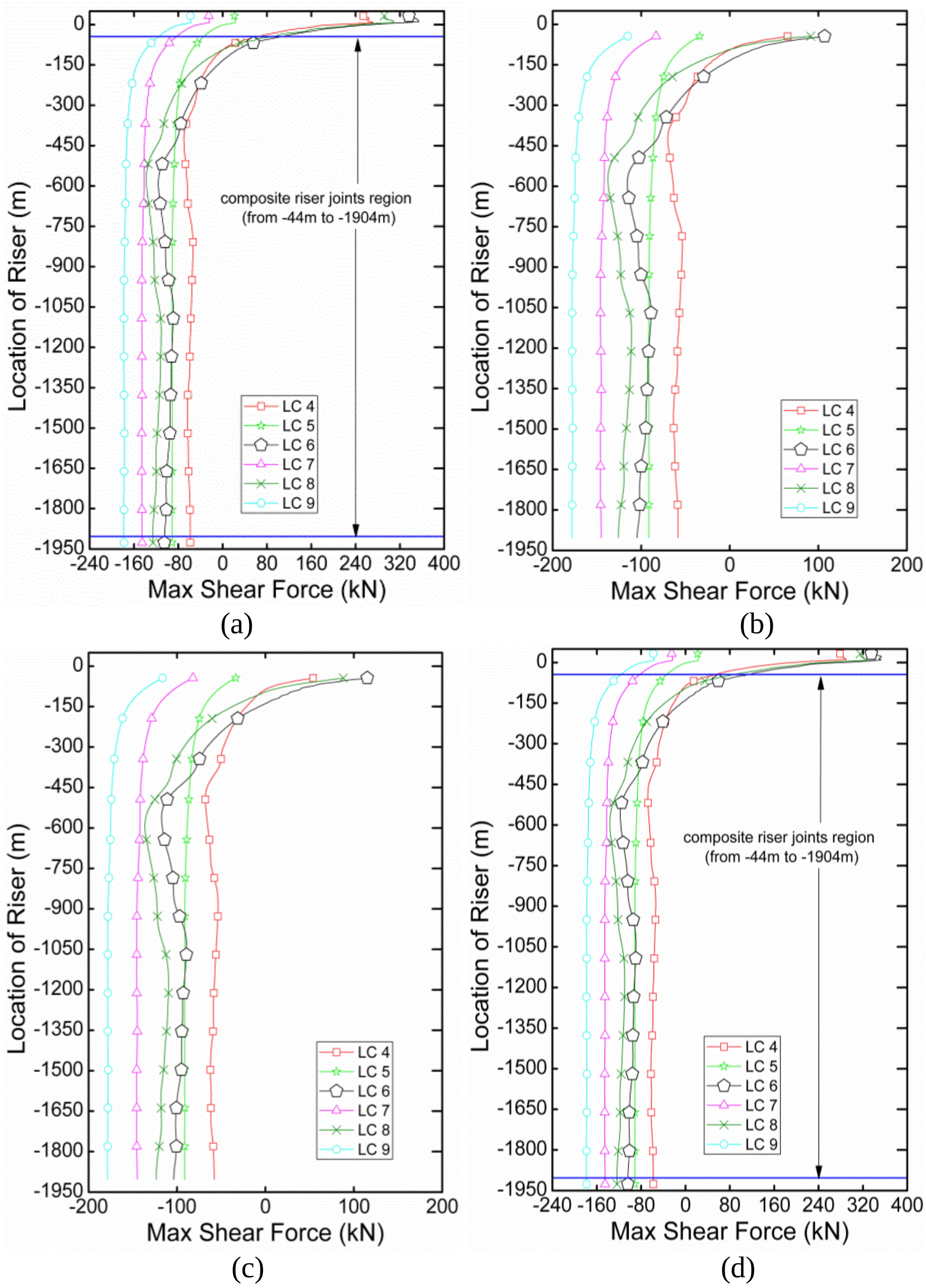

Fig. D.3. Shear forces for different load cases: (a) full-length riser, (b) composite riser region with bending modulus and (c) full-length riser, (d) composite riser region with tension modulus

Fig. D.3 shows the shear force distributions along the entire riser. The maximum shear force (178.5kN) in the composite region occurs under LC9 at the bottom end with tension modulus.

In Figs. D.1-D.3, it can be seen that, in the composite joints region, the tension forces decrease from top to bottom, and the maximum bending moments and shear forces occur at the top or bottom joint under different load cases. Therefore, it can be said that the top and bottom joints are the most critical locations.

The critical locations and force, moment and pressure combinations at these locations are identified, and the magnitudes of the loads at these critical locations are listed in Table D.1. The critical load combinations for the worst cases shown in Table D.1 are taken to be those which are the most severe of those estimated using the tension modulus and those calculated using the bending modulus. From them, the following most critical cases (highlighted in red colour) are selected for structural integrity verification by local stress analysis: LC4_top, LC4_bottom, LC5_bottom, LC6_top, LC6_bottom, LC7_bottom, LC9_top and LC9_bottom.

Table D.1. Worst cases of critical load combinations for AS4/epoxy with titanium liner riser from global analysis

Load Case	Location	Tension (kN)	Internal Pressure (MPa)	External Pressure (MPa)	Shear Force (kN)	Bending Moment (kN·m)
4	Top	3378.1	44.3	0.7	65.3	59.1
	Bottom	2288.4	58.7	19.2	58.4	45.7
5	Top	3313.1	44.3	0.7	43.7	9.9
	Bottom	2250.2	58.7	19.2	91.4	67.0
6	Top	2443.7	1.8	0.7	115.2	50.9
	Bottom	1384.9	35.3	19.2	104.8	51.5
7	Top	2369.9	1.8	0.7	93.8	5.1
	Bottom	1313.5	35.3	19.2	145.2	72.6
8	Top	2214.0	0	0.7	91.4	49.6
	Bottom	346.6	0	19.2	125.8	24.3
9	Top	2152.7	0	0.7	127.0	5.4
	Bottom	301.3	0	19.2	178.5	34.0

D.1.2 Results from Final Structural Verification for AS4/Epoxy Riser with Titanium Liner $[0_3/(\pm 53)_5/90_4]$

Results from the stress analysis of the AS4/epoxy riser with titanium liner for the eight most important load combinations from Table D.1 are presented below for illustration.

(1) FSs for AS4/epoxy with titanium liner $[0_3/(\pm 53)_5/90_4]$ under global load case LC4 at the top of the composite region where, as X_1=1m and the bending moment applied at the top=124.4kN·m, X_2=2.811 m

The FSs obtained under load case LC4_top for the in-plane longitudinal, in-plane transverse and the in-plane shear stresses in all layers are presented in Figs. D.4(a), D.4(b) and D.4(c), respectively, where layer 1 is the innermost composite layer. The minimum FS obtained for the liner is 1.97 and the minimum FSs for the stresses in the fibre direction are 4.60 in the axially reinforced layers (0°) (layer 3), 5.34 in the plies reinforced at ±53° (layer 4) and 6.61 in the circumferentially reinforced layers (90°) (layer 14) (Fig. D.4(a)), for the transverse stresses, 3.61 for the axially reinforced layers (layer 3), 2.09 in the ±53° layers (layer 13) and 1.57 in the 90° layers (layer 17) (Fig. D.4(b)), and, for the shear stresses in all layers, over 10.0 (Fig. D.4(c)). Therefore, the minimum FS under load case LC4_top is 1.57 which is due to the stress in the transverse direction in layer 17 (reinforced in hoop direction) in the composite body.

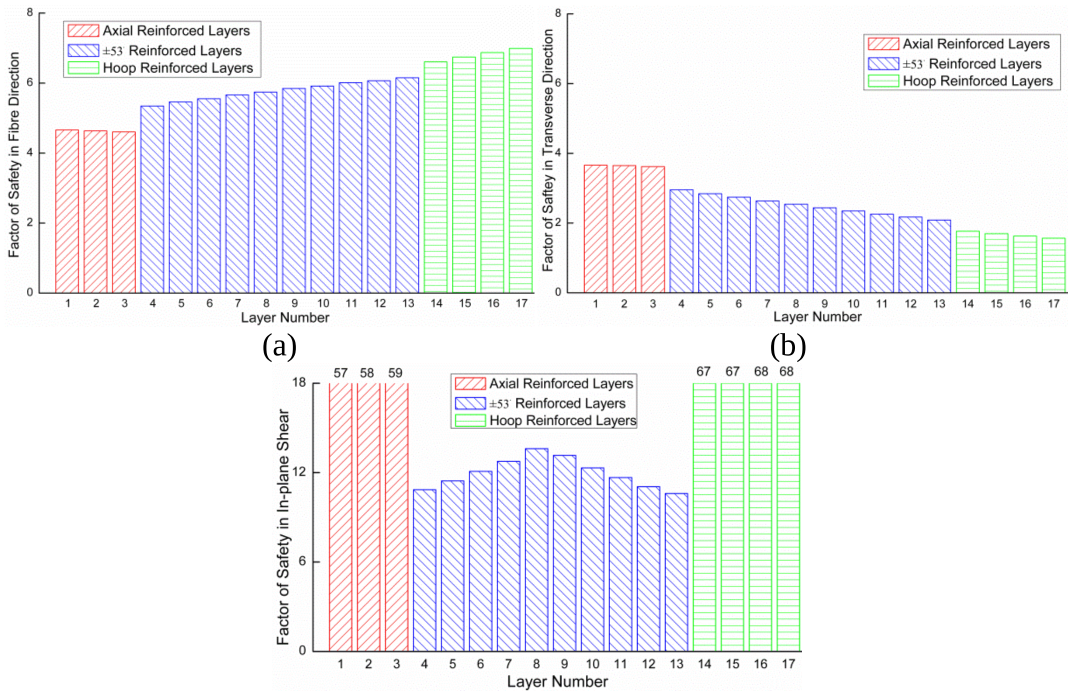

(c)

Fig. D.4. FSs of composite layers with 0°, ±53° and 90° reinforcements under LC4_top for AS4/epoxy with titanium liner in (a) fibre direction, (b) transverse direction and (c) in-plane shear

(2) FSs for the AS4/epoxy with titanium liner $[0_3/(\pm 53)_5/90_4]$ under global load case LC4 at the bottom of the composite region where, as X_1=1m and the bending moment applied at the top=104.1kN·m, X_2=2.566m

The FSs obtained under load case LC4_bottom for the in-plane longitudinal, in-plane transverse and the in-plane shear stresses in all layers are presented in Figs. D.5(a), D.5(b) and D.5(c), respectively. The minimum FS obtained for the liner is 2.29, and the minimum FSs for the stresses in the fibre direction are 6.75 in the axially reinforced layers (0°) (layer 3), 6.50 in the plies reinforced at ±53° (layer 4) and 8.06 in the circumferentially reinforced layers (90°) (layer 14) (Fig. D.5(a)), for the transverse stresses 13.35 for the axially reinforced layers (layer 1), 5.76 in the ±53° layers (layer 13) and 3.48 in the 90° layers (layer 17) (Fig. D.5(b)), and, for the shear stresses in all layers over 9.00 (Fig. D.5(c)). Therefore, the minimum FS under load case LC4_bottom is 2.29, which is due to the Von Mises stress in the liner.

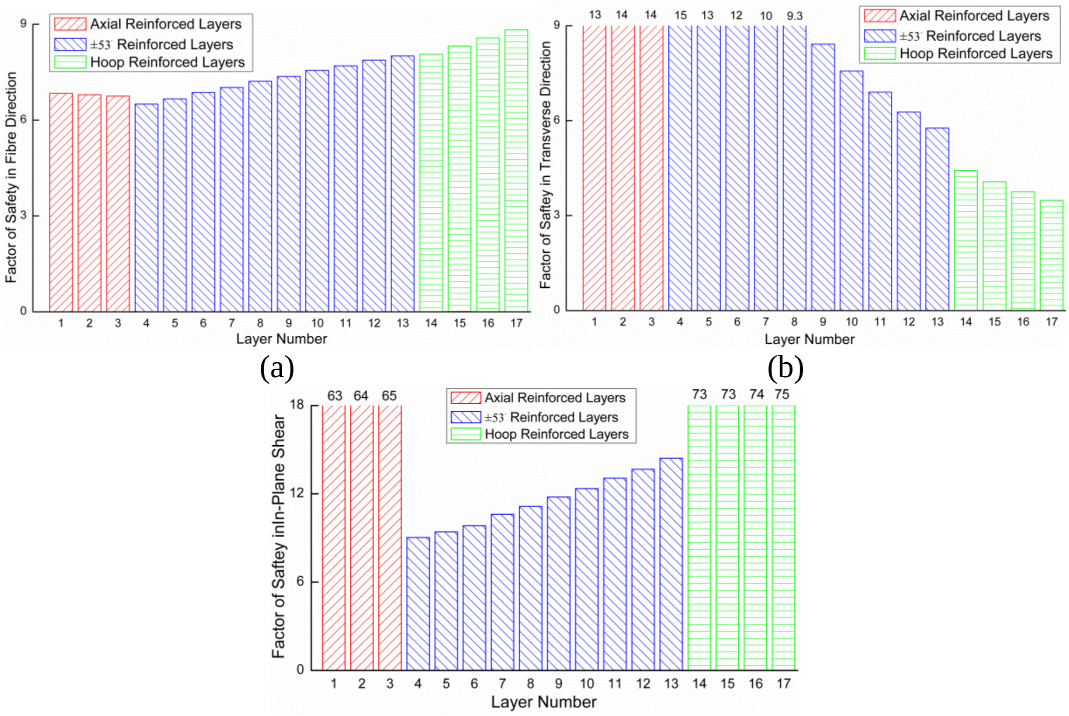

(a) (b) (c)

Fig. D.5. FSs of composite layers with 0°, ±53° and 90° reinforcements under LC4_bottom for AS4/epoxy with titanium liner in (a) fibre direction, (b) transverse direction and (c) in-plane shear

(3) FSs for the AS4/epoxy with titanium liner $[0_3/(\pm 53)_5/90_4]$ under global load case LC5 at the bottom of the composite region where, as X_1=1m and the bending moment applied at the top=158.4kN·m, X_2=2.467 m

The FSs obtained under load case LC5_bottom for the in-plane longitudinal, in-plane transverse and the in-plane shear stresses in all layers are presented in Figs. D.6(a), D.6(b) and D.6(c), respectively. The minimum FS obtained for the liner is 2.22 and the minimum FSs for the stresses in the fibre direction are 5.94 in the axially reinforced layers (0°) (layer 3), 6.26 in the plies reinforced at ±53° (layer 4) and 7.65 in the circumferentially reinforced layers (90°) (layer 14) (Fig. D.6(a)), for the transverse stresses, 12.86 for the axially reinforced layers (layer 1), 4.75 in the ±53° layers (layer 13) and 2.90 in the 90° layers (layer 17) (Fig. D.6(b)) and for the shear stresses,7.20 in layer 4 (Fig. D.6(c)). Therefore, the minimum FS under load case LC5_bottom is 2.22, which is due to the Von Mises stress in the liner.

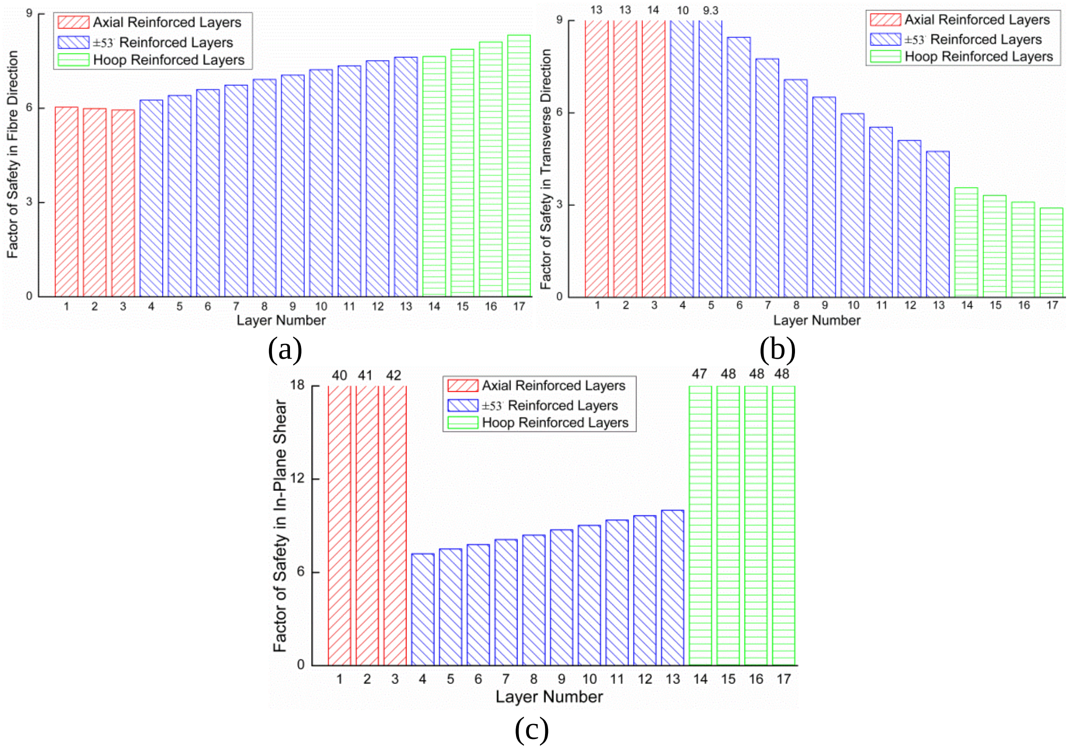

Fig. D.6. FSs of composite layers with 0°, ±53° and 90° reinforcements under LC5_bottom for AS4/epoxy with titanium liner in (a) fibre direction, (b) transverse direction and (c) in-plane shear

(4) FSs for the AS4/epoxy with titanium liner $[0_3/(\pm53)_5/90_4]$ under global load case LC6 at the top of the composite region where, as X_1=1m and the bending moment applied at top=166.1kN·m, X_2=1.884m

The FSs obtained under load case LC6_top for the in-plane longitudinal, in-plane transverse and the in-plane shear stresses in all layers are presented in Figs. D.7(a), D.7(b) and D.7(c), respectively. The minimum FS obtained for the liner is 2.91 and the minimum FSs for the stresses in the fibre direction are 4.37 in the axially reinforced layers (0°) (layer 3), 17.45 in the plies reinforced at ±53° (layer 4) and 13.12 in the circumferentially reinforced layers (90°) (layer 17) (Fig. D.7(a)) and for the transverse stresses, 28.07 for the axially reinforced layers (layer 3), 2.70 in the ±53° layers (layer 13) and 1.78 in the 90° layers (layer 17) (Fig. D.7(b)) and for the shear stresses in all layers, 3.94 in layer 13(Fig. D.7(c)). Therefore, the minimum FS under load case LC6_top is 1.78, which is due to the transverse stresses in layer 17 (reinforced in hoop direction) in the composite body.

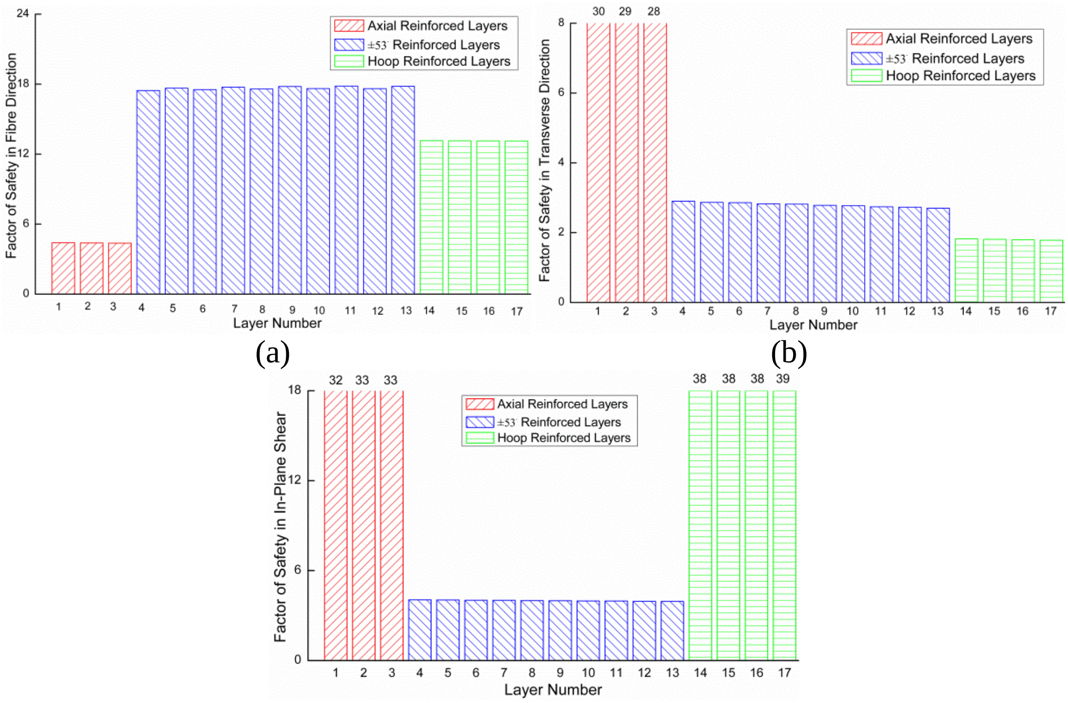

(a) (b) (c)

Fig. D.7. FSs of Composite layers with 0°, ±53° and 90° reinforcements under LC6_top for AS4/epoxy with titanium liner in (a) fibre direction, (b) transverse direction and (c) in-plane shear

(5) FSs for the AS4/epoxy with titanium liner $[0_3/(\pm 53)_5/90_4]$ under global load case LC6 at the bottom of the composite region where, as X_1=1m and the bending moment applied at the top=156.3kN·m, X_2=1.983m

The FSs obtained under load case LC6_bottom for the in-plane longitudinal, in-plane transverse and the in-plane shear stresses in all layers are presented in Figs. D.8(a), D.8(b) and D.8(c), respectively. The minimum FS obtained for the liner is 3.79 and the minimum FSs for the stresses in the fibre direction are 7.26 in the axially reinforced layers (0°) (layer 3), 12.45 in the plies reinforced at ±53° (layer 4) and 27.54 in the circumferentially reinforced layers (90°) (layer 14) (Fig. D.8(a)), for the transverse stresses, 40.19 for the axially reinforced layers (layer 3), 11.10 in the ±53° layers (layer 13) and 4.78 in the 90° layers (layer 17) (Fig. D.8(b)), and for the shear stresses in all layers, 8.38 in layer 13 (Fig. D.8(c)). Therefore, the minimum FS under load case LC6_bottom is 3.79, which is due to the Von Mises stress in liner.

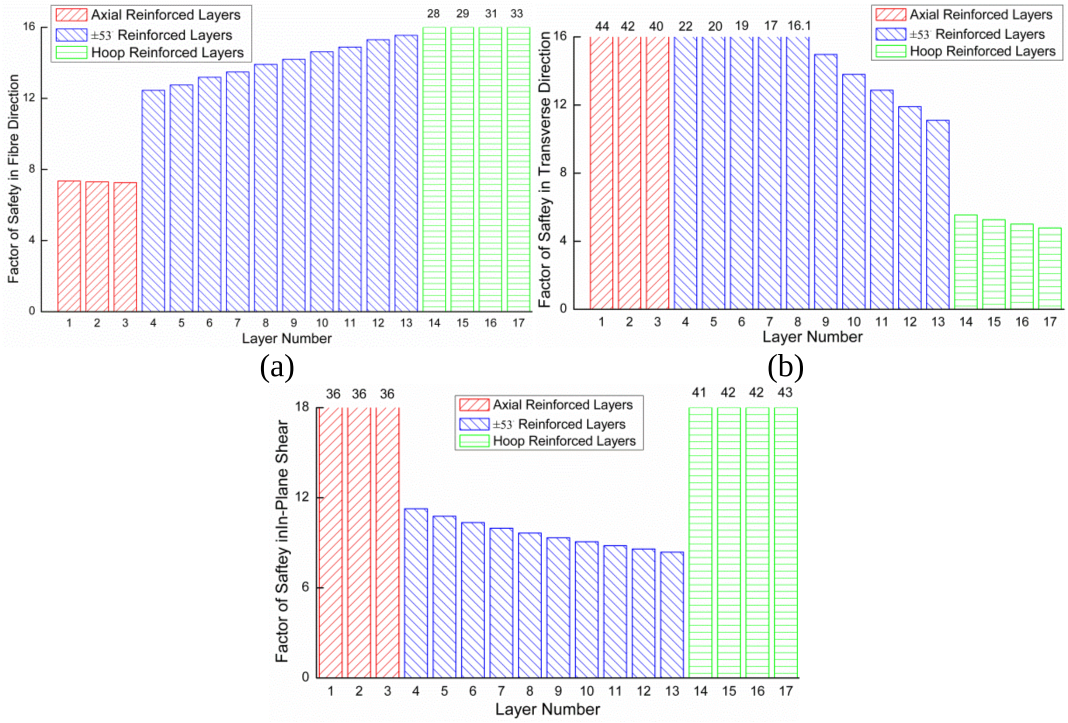

(c)

Fig. D.8. FSs of composite layers with 0°, ±53° and 90° reinforcements under LC6_bottom for AS4/epoxy with titanium liner in (a) fibre direction, (b) transverse direction and (c) in-plane shear

(6) FSs for the AS4/epoxy with titanium liner $[0_3/(\pm53)_5/90_4]$ under global load case LC7 at the bottom of the composite region where, as X_1=1m and the bending moment applied at the top=217.8kN·m, X_2=2.00m

The FSs obtained under load case LC7_bottom for the in-plane longitudinal, in-plane transverse and the in-plane shear stresses in all layers are presented in Figs. D.9(a), D.9(b) and D.9(c), respectively. The minimum FS obtained for the liner is 3.52 and the minimum FSs for the stresses in the fibre direction are 6.44 in the axially reinforced layers (0°) (layer 3), 11.57 in the plies reinforced at ±53° (layer 4) and 22.95 in the circumferentially reinforced layers (90°) (layer 14) (Fig. D.9(a)) and for the transverse stresses, 38.17 for the axially reinforced layers (layer 3), 8.10 in the ±53° layers (layer 13) and 3.84 in the 90° layers (layer 17) (Fig. D.9(b)) and for the shear stresses in all layers, 7.08 in layer 13 (Fig. D.9(c)). Therefore, the minimum FS under load case LC7_bottom is 3.52, which is due to the Von Mises stress in liner.

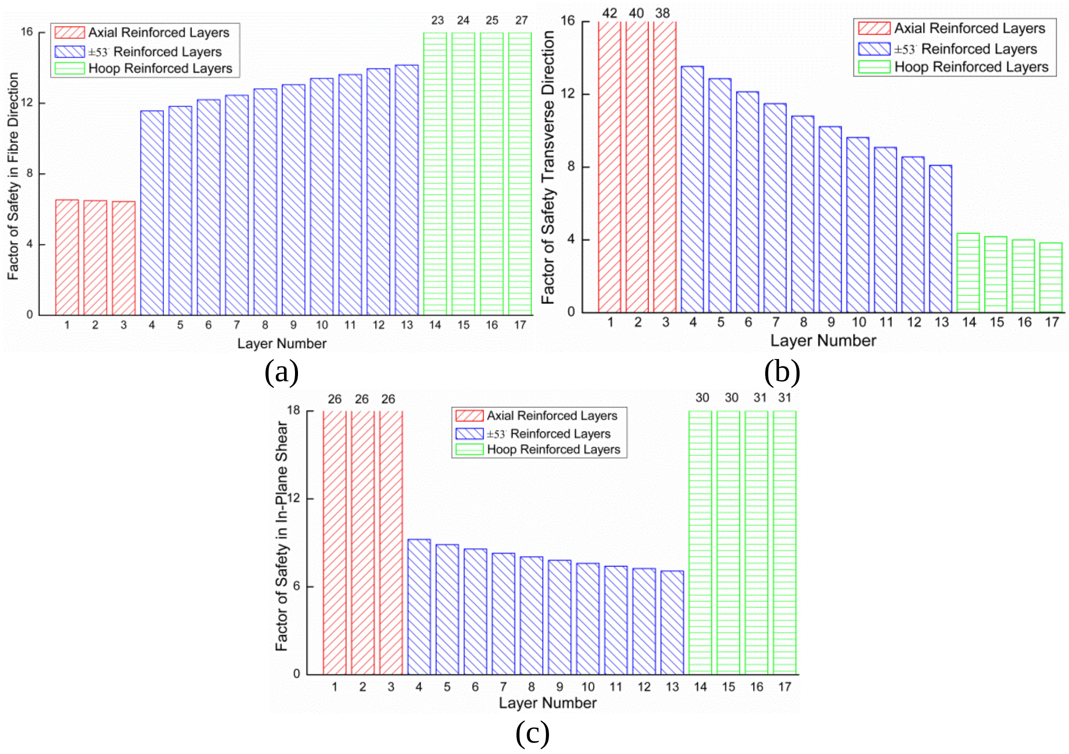

Fig. D.9. FSs of composite layers with 0°, ±53° and 90° reinforcements under LC7_bottom for AS4/epoxy with titanium liner in (a) fibre direction, (b) transverse direction and (c) in-plane shear

(7) FSs for the AS4/epoxy with titanium liner $[0_3/(\pm 53)_5/90_4]$under global load case LC9 at the top of the composite region where, as X_1=1m and the bending moment applied at the top=132.4kN·m, X_2=1.086m

The FSs obtained under load case LC9_top for the in-plane longitudinal, in-plane transverse and the in-plane shear stresses in all layers are presented in Figs. D.10(a), D.10(b) and D.10(c), respectively. The minimum FS obtained for the liner is 4.02 and the minimum FSs for the stresses in the fibre direction are 6.10 in the axially reinforced layers (0°) (layer 3), 21.75 in the plies reinforced at ±53° (layer 4) and 15.97 in the circumferentially reinforced layers (90°) (layer 14) (Fig. D.10(a)), for the transverse stresses, 68.81 for the axially reinforced layers (layer 3), 3.75 in the ±53° layers (layer 13) and 2.62 in the 90° layers (layer 17) (Fig. D.10(b)) and for the shear stresses in all layers, 5.35 in layer 4 (Fig. D.10(c)). Therefore, the minimum FS under load case LC9_top is 2.62, which is due to the transverse stresses in layer 17 (reinforced in hoop direction) in the composite body.

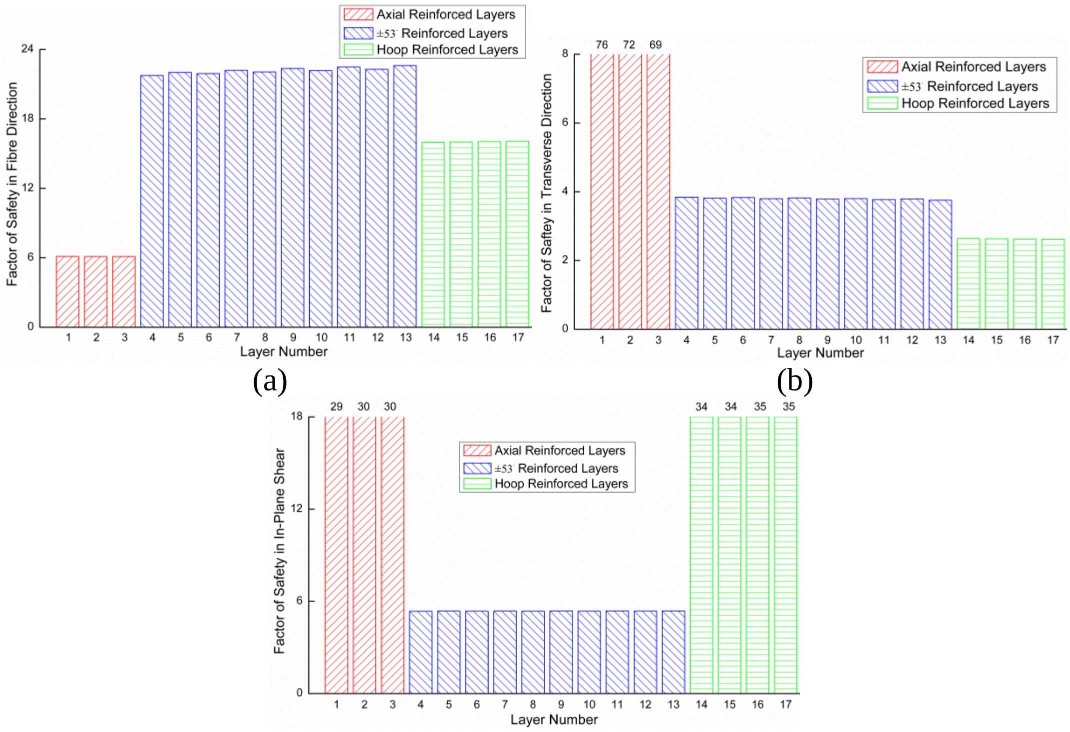

Fig. D.10. FSs of composite layers with 0°, ±53° and 90° reinforcements under LC9_top for AS4/epoxy with titanium liner in (a) fibre direction, (b) transverse direction and (c) in-plane shear

(8) FSs for AS4/epoxy with Titanium liner $[0_3/(\pm53)_5/90_4]$ under global load case LC9 at the bottom of the composite region where, as X_1=1m and the bending moment applied at the top=212.5kN·m, X_2=1.381m

The FSs obtained under load case LC9_bottom for the in-plane longitudinal, in-plane transverse and the in-plane shear stresses in all layers are presented in Figs. D.11(a), D.11(b) and D.11(c), respectively. The minimum FS obtained for the liner is 3.87. The minimum FSs for the stresses in the fibre direction are 8.74 in the axially reinforced layers (0°) (layer 3), 9.27 in the plies reinforced at ±53° (layer 4) and 5.65 in the circumferentially reinforced layers (90°) (layer 14) (Fig. D.11(a)), for the transverse stresses 11.94 for the axially reinforced layers (layer 3), 16.67 in the ±53° layers (layer 13) and 11.79 in the 90° layers (layer 14) (Fig. D.11(b)), and for the shear stresses in all layers, 4.55 in layer 4, (Fig. D.11(c)). Therefore, the minimum FS under load case LC9_bottom is 3.87, which is due to the Von Mises stress in the liner.

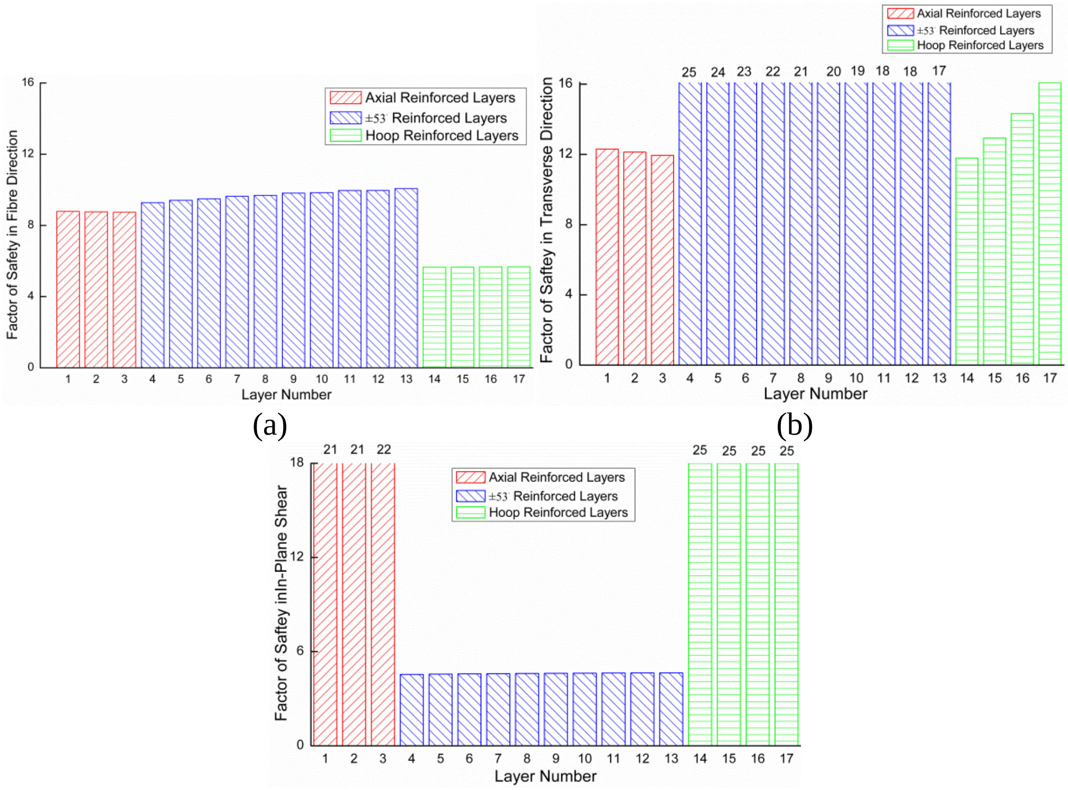

(c)

Fig. D.11. FSs of composite layers with 0°, ±53° and 90° reinforcements under LC9_bottom for AS4/epoxy with titanium liner in (a) fibre direction, (b) transverse direction and (c) in-plane shear

D.2 Global Design Results of AS4/Epoxy with Aluminium Liner $[0_4/(\pm 53.5)_5/90_4]$ Riser

D.2.1 Results from Global Analysis for AS4/Epoxy Riser with Aluminium Liner $[0_4/(\pm 53.5)_5/90_4]$

This section presents the detailed results of the riser with the AS4/epoxy composite body and aluminium liner analysed using its effective 3D properties with pipe elements for the laminate configuration and thickness combinations which provide the least structural weight, as determined by the local analysis performed in *Chapter 5*. The global analysis results for various combinations of tension, bending, shear force and pressure of the different global design load cases are presented. The difference between bending and tension moduli is larger than 5%, hence, both of them are analysed for AS4/epoxy with aluminium liner riser. The results under different global load cases are illustrated below.

The tension force, bending moment and shear force distributions estimated from the global analysis conducted using FE modelling for global load cases LC4 to LC9 are presented in Figs. D.12-D.14, respectively. The blue horizontal lines in these figures indicate the top and bottom of the composite riser section, at depths of -44m and -1904m, respectively. It should be noted that, in designing the composite riser, we are only concerned about the tension, bending moment and shear force magnitudes within this region.

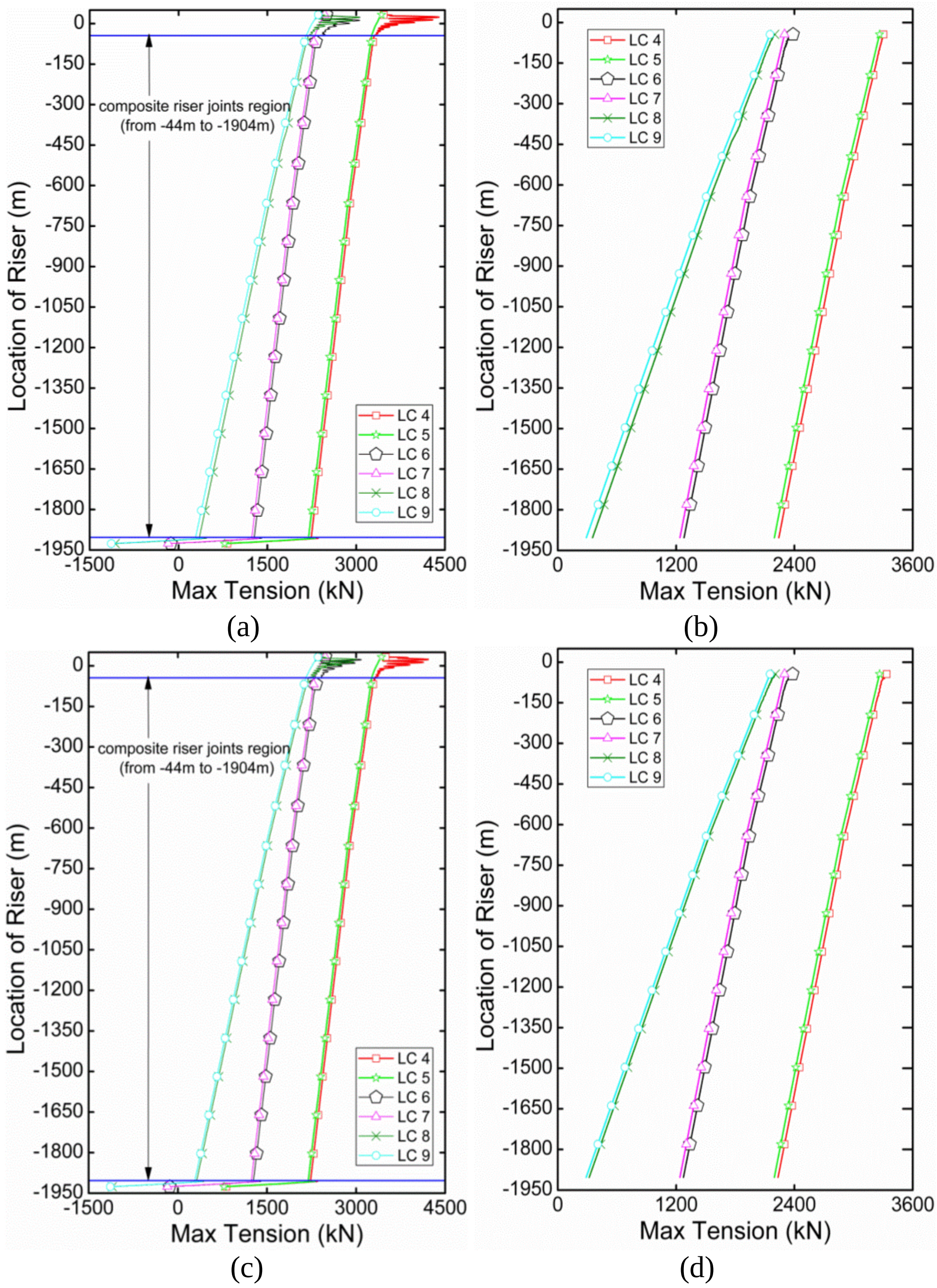

Fig. D.12. Tension forces for different load cases: (a) full-length riser, (b) composite riser region with bending modulus and (c) full-length riser, (d) composite riser region with tension modulus

Fig. D.12 shows the effective tension force distribution along the entire riser. It is clear that the maximum tension force is 3335.7kN in the composite section of the riser which occurs under load case LC4 at the top with tension modulus.

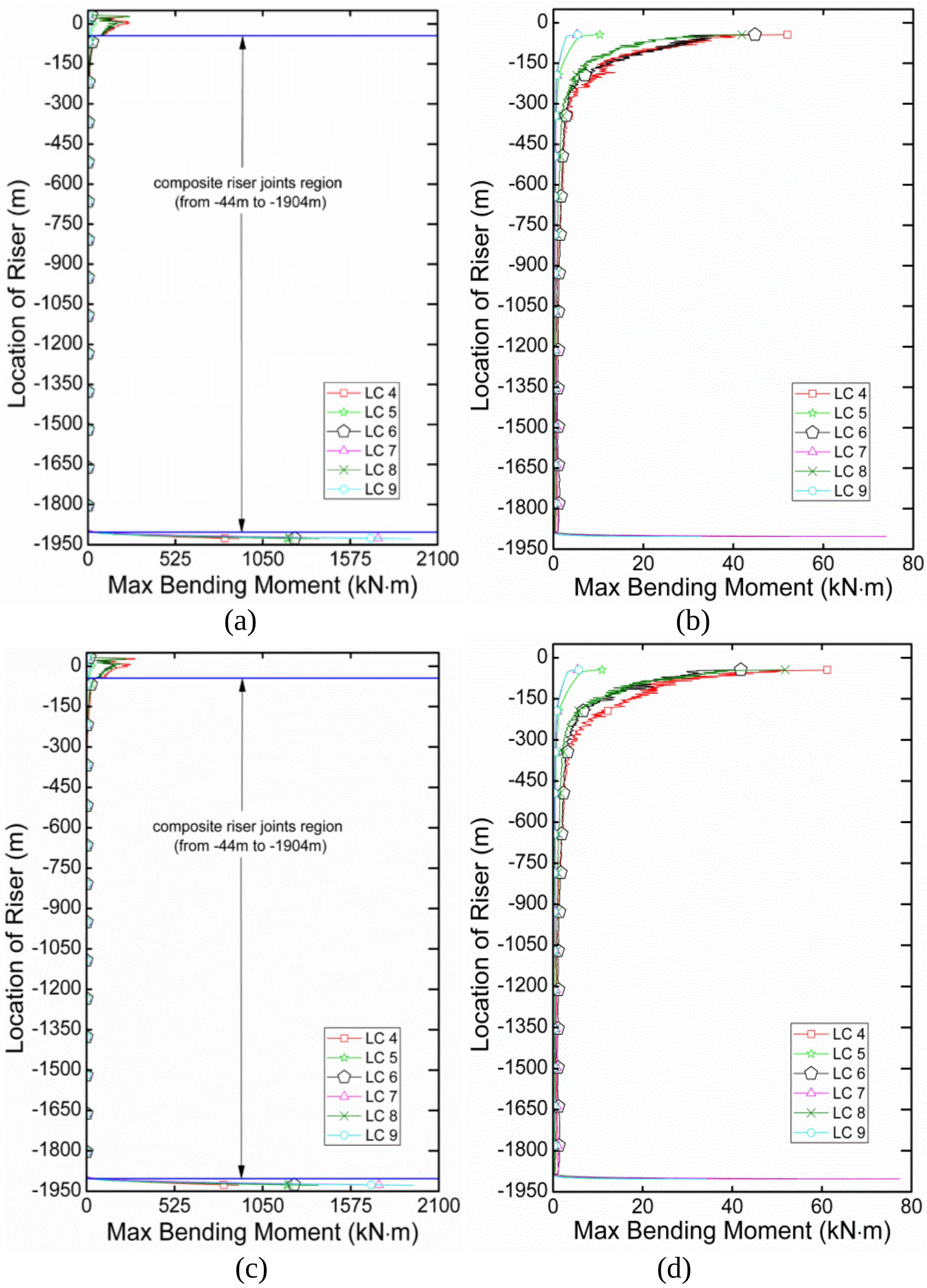

Fig. D.13. Bending moments for different load cases: (a) full-length riser, (b) composite riser region with bending modulus and (c) full-length riser, (d) composite riser region with tension modulus

Fig. D.13 shows the bending moment distribution along the entire riser. The maximum bending moments in the composite section of the riser occur at the top and bottom, with tension modulus, with values of 61.2kN·m under LC4 at the top and

77.3kN·m under LC7 at the bottom. It may be noted that the bending moments are much higher in the metallic stress joints at the bottom, reaching up to around 2000kN·m for load cases LC7 and LC9.

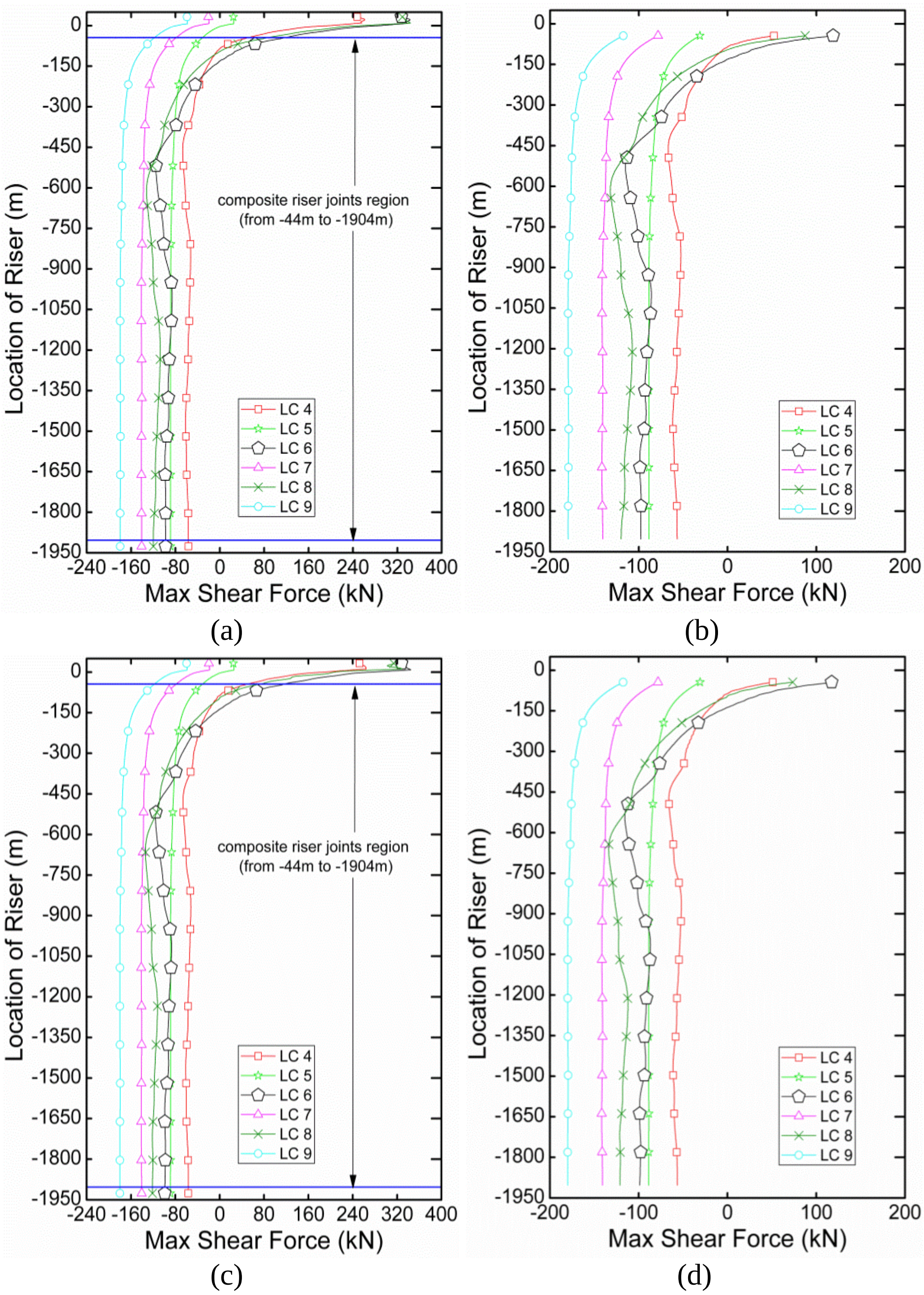

Fig. D.14. Shear forces for different load cases: (a) full-length riser, (b) composite riser region with bending modulus and (c) full-length riser, (d) composite riser region with tension modulus

Fig. D.14 shows the shear force distribution along the entire riser. The maximum shear force (179.9kN) in the composite region occurs under LC9 at the bottom with tension modulus.

In Figs. D.12-D.14, it can be seen that, in the composite joints region, the tension forces decrease from top to bottom, the maximum bending moments and shear forces occur at the top or bottom joint under different load cases. Therefore, it can be said that the top and bottom joints are the most critical locations.

The critical locations and force, moment and pressure combinations at these locations are identified, and the magnitudes of the loads at these critical locations are listed in Table D.2. The critical load combinations for the worst cases shown in Table D.2 are taken to be those which are the most severe of those estimated using the tension modulus and those calculated using the bending modulus. From them, the following most critical cases (highlighted in red colour) are selected for structural integrity verification by local stress analysis: LC4_top, LC4_bottom, LC5_bottom, LC6_top, LC6_bottom, LC7_bottom, LC9_top and LC9_bottom.

Table D.2. Worst cases of critical load combinations for AS4/epoxy with aluminium liner riser from global analysis

Load Case	Location	Tension (kN)	Internal Pressure (MPa)	External Pressure (MPa)	Shear Force (kN)	Bending Moment (kN·m)
4	Top	3335.7	44.3	0.7	52.1	61.2
	Bottom	2251.8	58.7	19.2	56.8	47.4
5	Top	3263.1	44.3	0.7	40.8	10.9
	Bottom	2206.5	58.7	19.2	88.8	69.4
6	Top	2386.3	1.8	0.7	119.0	44.8
	Bottom	1290.5	35.3	19.2	98.8	54.5
7	Top	2299.4	1.8	0.7	88.9	5.5
	Bottom	1249.0	35.3	19.2	140.8	77.3
8	Top	2212.3	0	0.7	87.4	51.8
	Bottom	370.6	0	19.2	121.0	24.2
9	Top	2152.0	0	0.7	128.2	5.7
	Bottom	307.4	0	19.2	179.9	34.2

D.2.2 Results from Final Structural Verification for AS4/Epoxy Riser with Aluminium Liner $[0_4/(\pm 53.5)_5/90_4]$

Results from the stress analysis of the AS4/epoxy riser with titanium liner for the eight most important load combinations from Table D.2 are presented below for illustration.

(1) FSs for the AS4/epoxy with aluminium liner $[0_4/(\pm 53.5)_5/90_4]$ under global load case LC4 at the top of the composite region where, as X_1=1m and the bending moment applied at the top=113.3kN·m, X_2=3.350m

The FSs obtained under load case LC4_top for the in-plane longitudinal, in-plane transverse and the in-plane shear stresses in all layers are presented in Figs.

D.15(a), D.15(b) and D.15(c), respectively, where layer 1 is the innermost composite layer. The minimum FS obtained for the liner is 1.79 and the minimum FSs for the stresses in the fibre direction are 4.82 in the axially reinforced layers (0°) (layer 4), 5.24 in the plies reinforced at ±53.5° (layer 5) and 6.27 in the circumferentially reinforced layers (90°) (layer 15) (Fig. D.15(a)), for the transverse stresses, 3.47 for the axially reinforced layers (layer 4), 2.15 in the ±53.5° layers (layer 14) and 1.62 in the 90° layers (layer 18) (Fig. D.15(b)), and for the shear stresses in all layers, over 9.50 (Fig. D.15(c)). Therefore, the minimum FS under load case LC4_top is 1.62, which is due to the stresses in the transverse direction in layer 18 (reinforced in hoop direction) in the composite body.

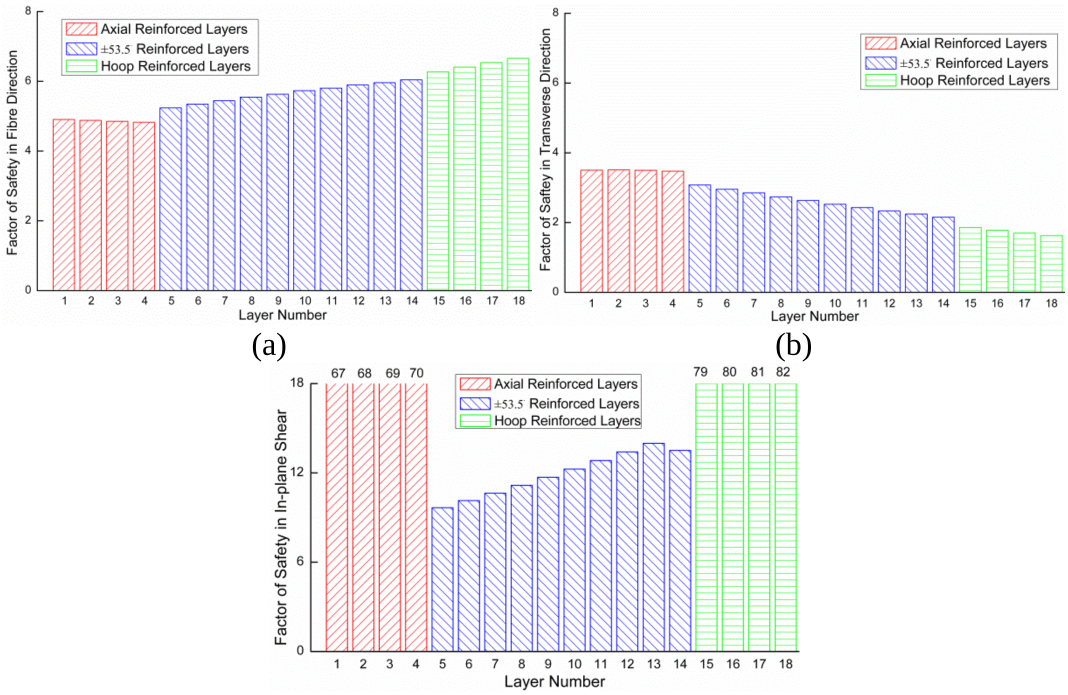

Fig. D.15. FSs of composite layers with 0°, ±53.5° and 90° reinforcements under LC4_top for AS4/epoxy with aluminium liner in (a) fibre direction, (b) transverse direction and (c) in-plane shear

(2) FSs for the AS4/epoxy with aluminium liner $[0_4/(\pm 53.5)_5/90_4]$ under global load case LC4 at the bottom of the composite region where, as X_1=1m and the bending moment applied at the top=104.2kN·m, 2.670m

The FSs obtained under load case LC4_bottom for the in-plane longitudinal, in-plane transverse and the in-plane shear stresses in all layers are presented in Figs. D.16(a), D.16(b) and D.16(c), respectively. The minimum FS obtained for the liner is 2.00, and the minimum FSs for the stresses in the fibre direction are 6.99 in the axially reinforced layers (0°) (layer 4), 6.31 in the plies reinforced at ±53.5° (layer 5) and 7.67

in the circumferentially reinforced layers (90°) (layer 15) (Fig. D.16(a)), for the transverse stresses, 11.44 for the axially reinforced layers (layer 1), 6.04 in the ±53.5° layers (layer 14) and 3.62 in the 90° layers (layer 18) (Fig. D.16(b)) and for the shear stresses in all layers, over 8.50 (Fig. D.16(c)). Therefore, the minimum FS under load case LC4_bottom is 2.00, which is due to the Von Mises stress in the liner.

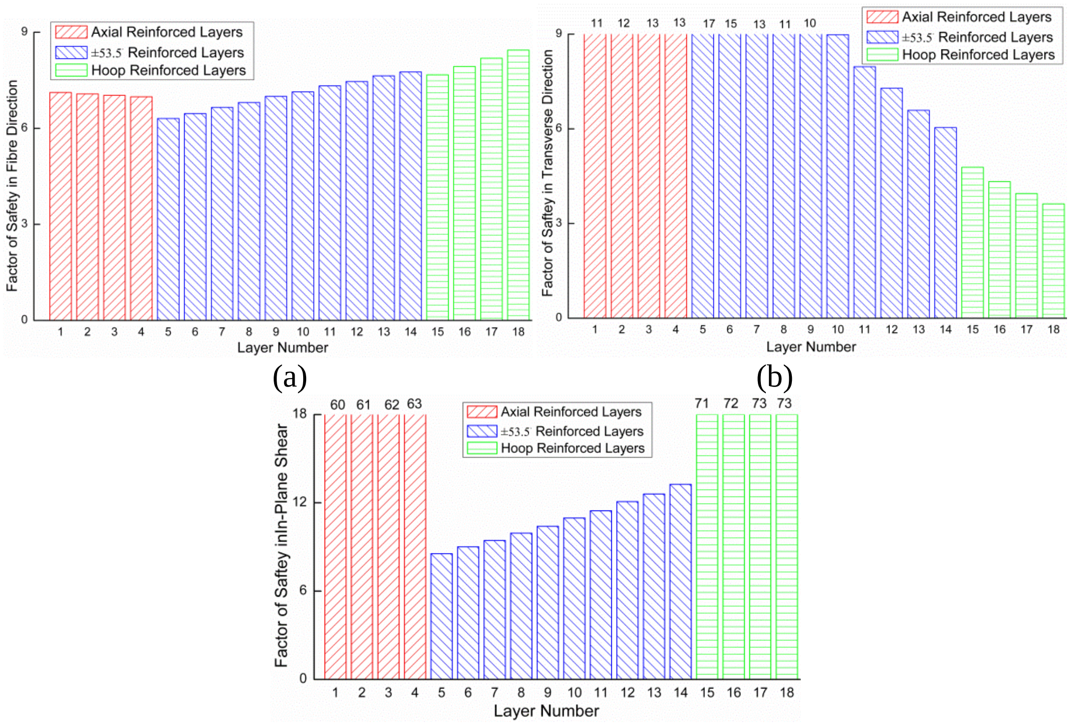

(a) (b)

(c)

Fig. D.16. FSs of composite layers with 0°, ±53.5° and 90° reinforcements under LC4_bottom for AS4/epoxy with aluminium liner in (a) fibre direction, (b) transverse direction, and (c) in-plane shear

(3) FSs for the AS4/epoxy with aluminium liner $[0_4/(\pm53.5)_5/90_4]$ under global load case LC5 at the bottom of the composite region where, as X_1=1m and the bending moment applied at the top=158.2kN·m, X_2=2.564m

The FSs obtained under load case LC5_bottom for the in-plane longitudinal, in-plane transverse and the in-plane shear stresses in all layers are presented in Figs. D.17(a), D.17(b) and D.17(c), respectively. The minimum FS obtained for the liner is 1.95 and the stresses in the fibre direction are 6.18 in the axially reinforced layers (0°) (layer 4), 6.08 in the plies reinforced at ±53.5° (layer 5) and 7.33 in the circumferentially reinforced layers (90°) (layer 15) (Fig. D.17(a)), for the transverse stresses, 11.00 for the axially reinforced layers (layer 1), 4.97 in the ±53.5° layers (layer 14) and 3.03 in the 90° layers (layer 18) (Fig. D.17(b)), and for the shear stresses, 6.95

in layer 5 (Fig. D.17(c)). Therefore, the minimum FS under load case LC5_bottom is 1.95, which is due to the Von Mises stress in the liner.

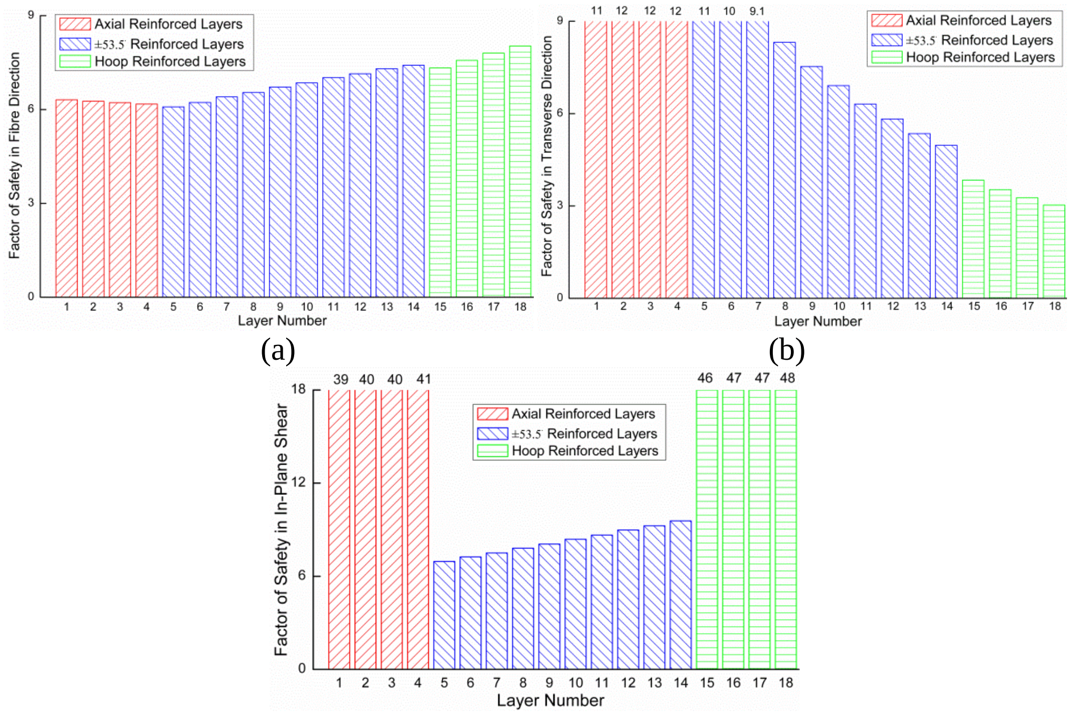

(c)

Fig. D.17. FSs of composite layers with 0°, ±53.5° and 90° reinforcements under LC5_bottom for AS4/epoxy with aluminium liner in (a) fibre direction, (b) transverse direction, and (c) in-plane shear

(4) FSs for the AS4/epoxy with aluminium liner $[0_4/(\pm 53.5)_5/90_4]$ under global load case LC6 at the top of the composite region where, as X_1=1m and the bending moment applied at top=163.8kN·m, X_2=1.753m

The FSs obtained under load case LC6_top for the in-plane longitudinal, in-plane transverse and the in-plane shear stresses in all layers are presented in Figs. D.18(a), D.18(b) and D.18(c), respectively. The minimum FS obtained for the liner is 3.01, and for the stresses in the fibre direction are 4.93 in the axially reinforced layers (0°) (layer 4), 18.18 in the plies reinforced at ±53.5° (layer 5) and 16.26 in the circumferentially reinforced layers (90°) (layer 18) (Fig. D.18(a)), for the transverse stresses, 23.98 for the axially reinforced layers (layer 4), 2.98 in the ±53.5° layers (layer 13) and 2.01 in the 90° layers (layer 18) (see Fig. 6.33(b)) (Fig. D.18(b)), and for the shear stresses in all layers, 4.56 in layer 14 (Fig. D.18(c)). Therefore, the minimum FS under load case LC6_top is 2.01, which is due to the transverse stresses in layer 18 (reinforced in hoop direction) in the composite body.

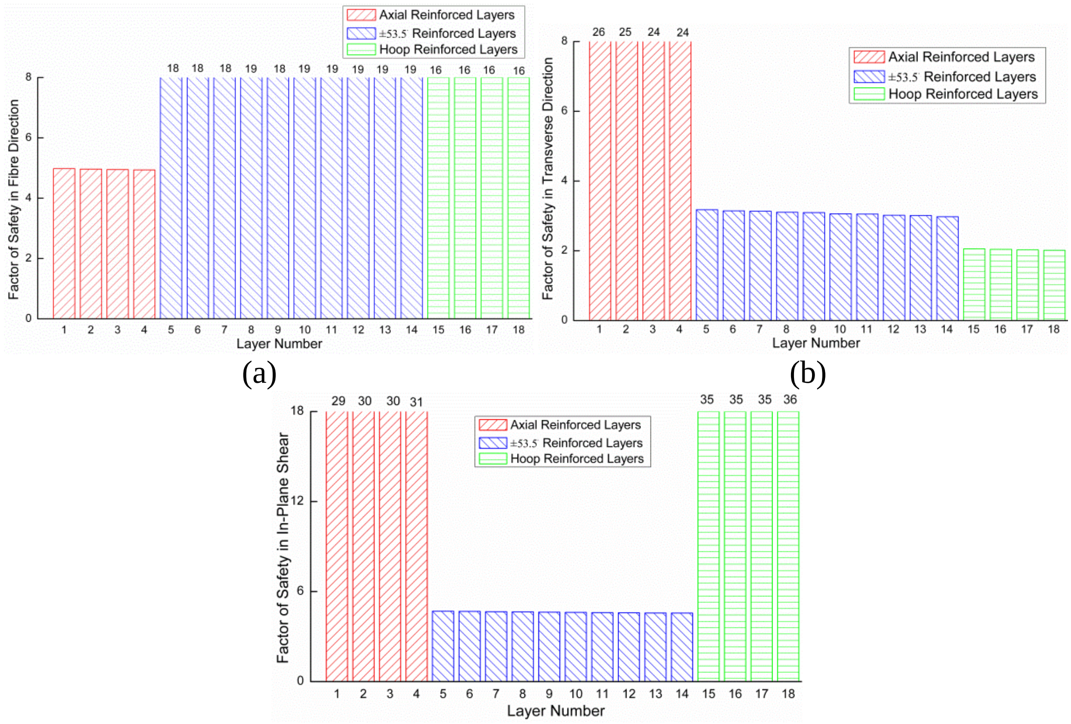

(c)

Fig. D.18. FSs of composite layers with 0°, ±53.5° and 90° reinforcements under LC6_top for AS4/epoxy with aluminium liner in (a) fibre direction, (b) transverse direction and (c) in-plane shear

(5) FSs for the AS4/epoxy with aluminium liner $[0_4/(\pm 53.5)_5/90_4]$ under global load case LC6 at the bottom of the composite region where, as X_1=1m and the bending moment applied at the top=153.3kN·m, X_2=2.104m

The FSs obtained under load case LC6_bottom for the in-plane longitudinal, in-plane transverse and the in-plane shear stresses in all layers are presented in Figs. D.19(a), D.19(b) and D.19(c), respectively. The minimum FS obtained for the liner is 3.49, and for the stresses in the fibre direction are 7.87 in the axially reinforced layers (0°) (layer 4), 12.42 in the plies reinforced at ±53.5° (layer 5) and 24.48 in the circumferentially reinforced layers (90°) (layer 15) (Fig. D.19(a)), for the transverse stresses, 40.39 for the axially reinforced layers (layer 4), 13.10 in the ±53.5° layers (layer 14) and 5.39 in the 90° layers (layer 18) (Fig. D.19(b)), and for the shear stresses, 9.73 in layer 14, (Fig. D.19(c)). Therefore, the minimum FS under load case LC6_bottom is 3.49, which is due to the Von Mises stress in liner.

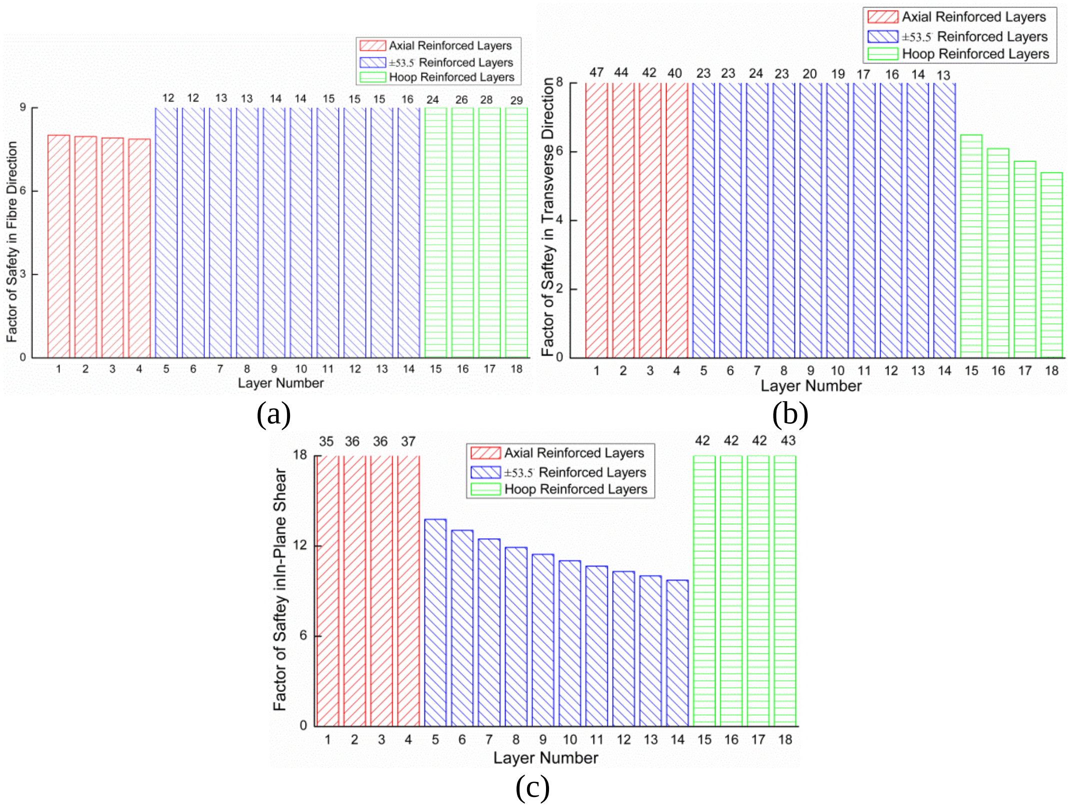

Fig. D.19. FSs of Composite layers with 0°, ±53.5° and 90° reinforcements under LC6_bottom for AS4/epoxy with aluminium liner in (a) fibre direction, (b) transverse direction and (c) in-plane shear

(6) FSs for the AS4/epoxy with aluminium liner $[0_4/(\pm53.5)_5/90_4]$ under global load case LC7 at the bottom of the composite region where, as X_1=1m and the bending moment applied at the top=218.1kN·m, X_2=2.099m

The FSs obtained under load case LC7_bottom for the in-plane longitudinal, in-plane transverse and the in-plane shear stresses in all layers are presented in Figs. D.20(a), D.20(b) and D.20(c), respectively. The minimum FS obtained for the liner is 3.22, and for the stresses in the fibre direction are 6.80 in the axially reinforced layers (0°) (layer 4), 11.42 in the plies reinforced at ±53.5° (layer 5) and 21.28 in the circumferentially reinforced layers (90°) (layer 15) (Fig. D.20(a)), for the transverse stresses, 37.91 for the axially reinforced layers (layer 4), 8.74 in the ±53.5° layers (layer 14) and 4.12 in the 90° layers (layer 18) (Fig. D.20(b)), and for the shear stresses in all layers, 7.88 in layer 14 (Fig. D.20(c)). Therefore, the minimum FS under load case LC7_bottom is 3.22, which is due to the Von Mises stress in liner.

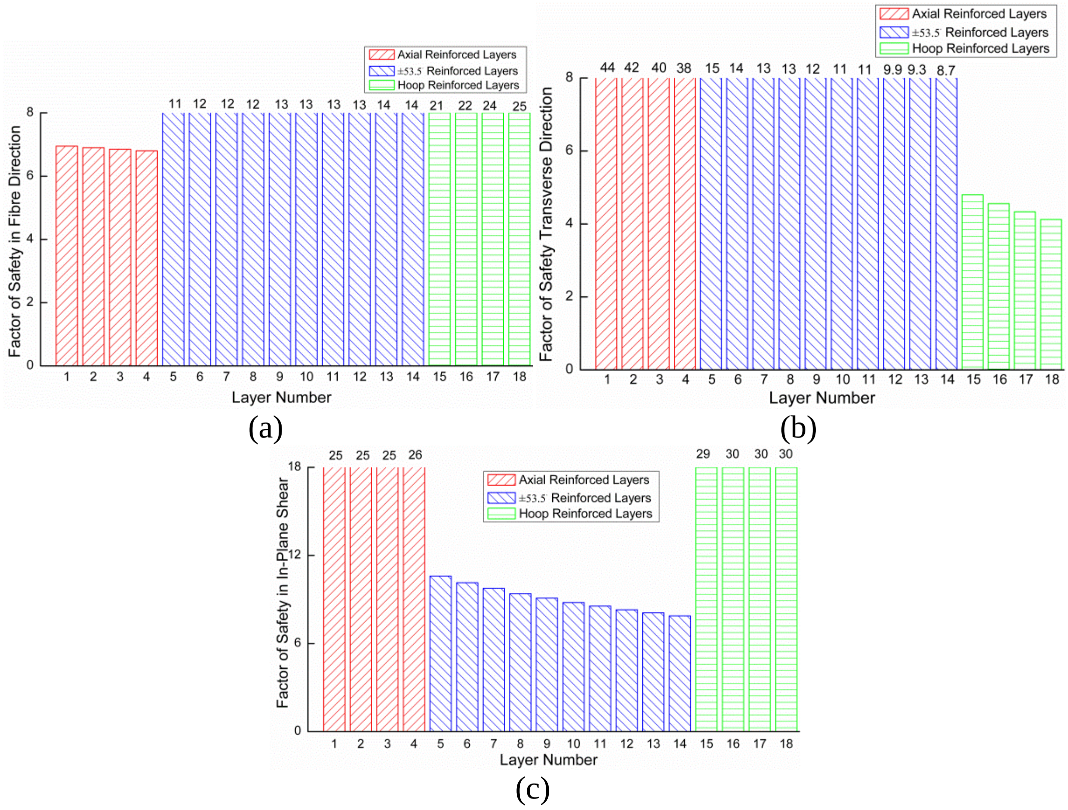

Fig. D.20. FSs of composite layers with 0°, ±53.5° and 90° reinforcements under LC7_bottom for AS4/epoxy with aluminium liner in (a) fibre direction, (b) transverse direction and (c) in-plane shear

(7) FSs for the AS4/epoxy with aluminium liner $[0_4/(\pm 53.5)_5/90_4]$ under global load case LC9 at the top of the composite region where, as X_1=1m and the bending moment applied at the top=133.9kN·m, X_2=1.089m

The FSs obtained under load case LC9_top for the in-plane longitudinal, in-plane transverse and the in-plane shear stresses in all layers are presented in Figs. D.21(a), D.21(b) and D.21(c), respectively. The minimum FS obtained for the liner is 3.94, and the minimum FSs for the stresses in the fibre direction are 6.58 in the axially reinforced layers (0°) (layer 4), 22.09 in the plies reinforced at ±53.5° (layer 5) and 18.35 in the circumferentially reinforced layers (90°) (layer 15) (Fig. D.21(a)), for the transverse stresses, 48.91 for the axially reinforced layers (layer 4), 3.91 in the ±53.5° layers (layer 14) and 2.81 in the 90° layers (layer 18) (Fig. D.21(b)) and for the shear stresses in all layers, 5.68 in layer 10 (Fig. D.21(c)). Therefore, the minimum FS under load case LC9_top is 2.81, which is due to the transverse stresses in layer 18 (reinforced in hoop direction) in the composite body.

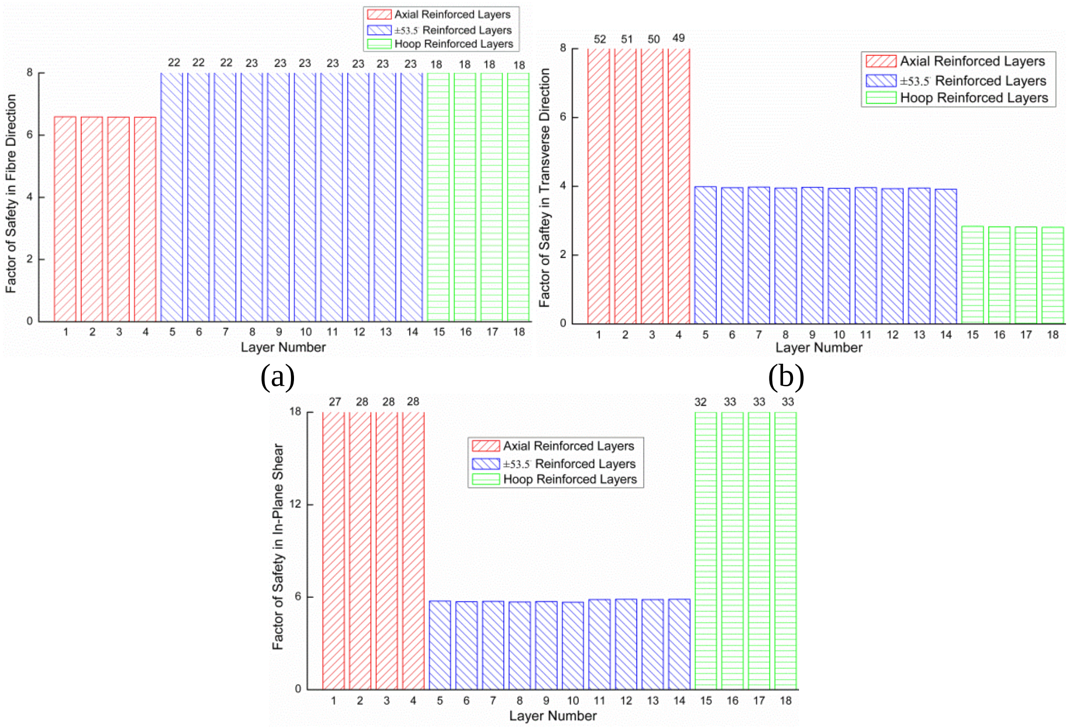

(a) (b) (c)

Fig. D.21. FSs of composite layers with 0°, ±53.5° and 90° reinforcements under LC9_top for AS4/epoxy with aluminium liner in (a) fibre direction, (b) transverse direction and (c) in-plane shear

(8) FSs for AS4/epoxy with aluminium liner $[0_4/(\pm 53.5)_5/90_4]$ under global load case LC9 at the bottom of the composite region where, as X_1=1m and the bending moment applied at the top=214.1kN·m, X_2=1.381m

The FSs obtained under load case LC9_bottom for the in-plane longitudinal, in-plane transverse and the in-plane shear stresses in all layers are presented in Figs. D.22(a), D.22(b) and D.22(c), respectively. The minimum FS obtained for the liner is 3.55, and the minimum FSs for the stresses in the fibre direction are 9.61 in the axially reinforced layers (0°) (layer 4), 8.69 in the plies reinforced at ±53.5° (layer 5) and 5.76 in the circumferentially reinforced layers (90°) (layer 15) (Fig. D.22(a)), for the transverse stresses, 11.91 for the axially reinforced layers (layer 4), 16.33 in the ±53.5° layers (layer 14) and 15.73 in the 90° layers (layer 15) (Fig. D.22(b)), and for the shear stresses in all layers, 4.80 in layer 5 (Fig. D.22(c)). Therefore, the minimum FS under load case LC9_bottom is 3.55, which is due to the Von Mises stress in the liner.

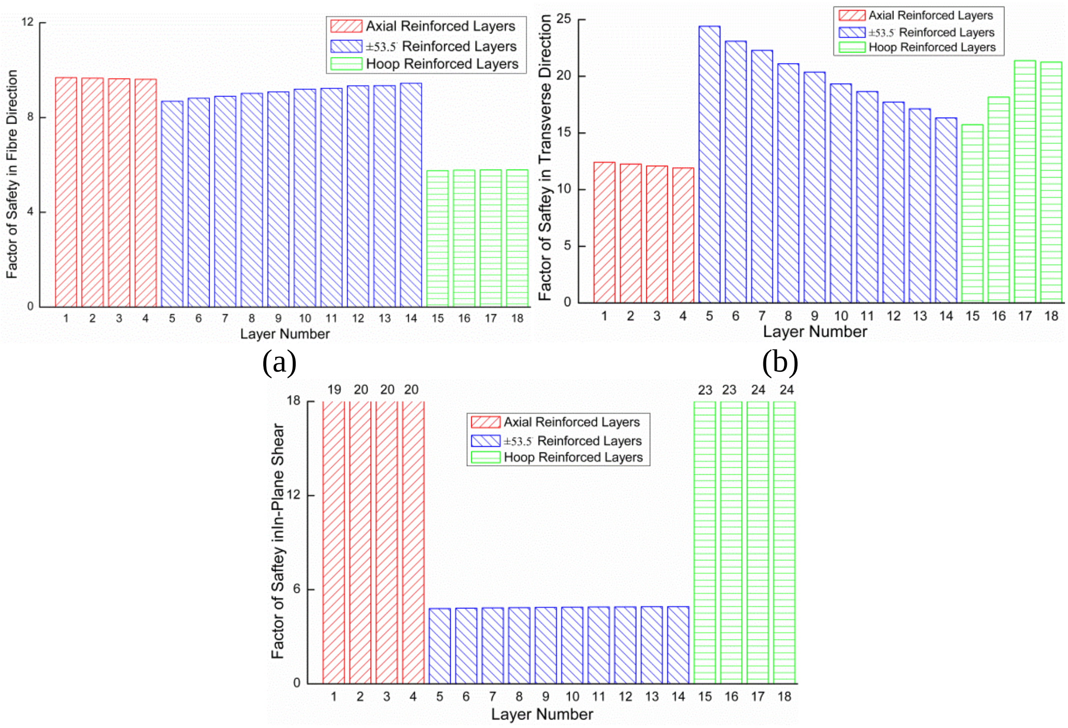

(a) (b)

(c)

Fig. D.22. FSs of composite layers with 0°, ±53.5° and 90° reinforcements under LC9_bottom for AS4/epoxy with aluminium liner in (a) fibre direction, (b) transverse direction and (c) in-plane shear

APPENDIX E

DESIGN OF EXPERIMENT DATABASE

E.1 DOE Database for AS4/PEEK with PEEK liner

Table E.1. DOE database for AS4/PEEK with PEEK liner using orthogonal array

Variables						OA Sampling	Load Capacity					Structural Weight
t_{liner}	t_0	t_θ	t_{90}	θ	n		LC1	LC2(a)	LC2(b)	LC3	LC4	
6	0	0	0	0	1	[0 0 0 0 0]	6.2	560	0	5.3	0.1	6.27
7.5	0.62	1.24	1.86	90	1	[1 1 2 3 4]	45	2700	2700	110	83	38.4
9	1.24	2.5	0.62	67.5	1	[2 2 4 1 3]	105	5100	5500	100	148.8	55.3
10.5	1.86	0.62	2.5	45	1	[3 3 1 4 2]	130	6800	7200	65	45.7	42.44
12	2.5	1.86	1.24	22.5	1	[4 4 3 2 1]	50	19000	21500	35	80.9	59.31
6	0.62	0.62	0.62	22.5	1	[0 1 1 1 1]	25	5400	600	20	6.6	20.36
7.5	1.24	1.86	2.5	0	1	[1 2 3 4 0]	95	19400	21900	60	73	55.01
9	1.86	0	1.24	90	1	[2 3 0 2 4]	40	4900	5700	30	9.6	23.92
10.5	2.5	1.24	0	67.5	1	[3 4 2 0 3]	95	8300	9100	65	35	39.56
12	0	2.5	1.86	45	1	[4 0 4 3 2]	170	5500	5100	55	148.2	61.59
6	1.24	1.24	1.24	45	1	[0 2 2 2 2]	90	5900	6000	45	39.2	35.54
7.5	1.86	2.5	0	22.5	1	[1 3 4 0 1]	15	32300	18800	30	35.9	52.21
9	2.5	0.62	1.86	0	1	[2 4 1 3 0]	70	11900	13600	46	33.1	39.5
10.5	0	1.86	0.62	90	1	[3 0 3 1 4]	25	1400	1300	113	94.2	41.37
12	0.62	0	2.5	67.5	1	[4 1 0 4 3]	40	2300	2400	59	20.8	29.47
6	1.86	1.86	1.86	67.5	1	[0 3 3 3 3]	120	6300	6800	110	141.8	51.8
7.5	2.5	0	0.62	45	1	[1 4 0 1 2]	20	6300	1400	15	7.1	21.35
9	0	1.24	2.5	22.5	1	[2 0 2 4 1]	115	8200	8800	59	41.2	41.42
10.5	0.62	2.5	1.24	0	1	[3 1 4 2 0]	45	23800	28100	38	77.5	58.42
12	1.24	0.62	0	90	1	[4 2 1 0 4]	50	3600	4000	35	12.8	26.65
6	2.5	2.5	2.5	90	1	[0 4 4 4 4]	120	7900	8000	165	298.7	69.74
7.5	0	0.62	1.24	67.5	1	[1 0 1 2 3]	15	800	700	54	17.4	23
9	0.62	1.86	0	45	1	[2 1 3 0 2]	40	6800	4500	45	31.9	38.46
10.5	1.24	0	1.86	22.5	1	[3 2 0 3 1]	55	3600	4000	44	13.8	26.61
12	1.86	1.24	0.62	0	1	[4 3 2 1 0]	25	15800	19700	20	35.7	42.39
6	0.62	1.86	1.24	90	1	[0 1 3 2 4]	50	2800	2800	126	124.9	42.1
7.5	1.24	0	0	67.5	1	[1 2 0 0 3]	0	5400	0	8	1	12.79
9	1.86	1.24	1.86	45	1	[2 3 2 3 2]	130	7900	8300	60	61.5	46.1
10.5	2.5	2.5	0.62	22.5	1	[3 4 4 1 1]	35	23500	11900	27	88.7	63.66
12	0	0.62	2.5	0	1	[4 0 1 4 0]	85	5800	6400	60	28.4	35.9

6	1.24	2.5	1.86	0	1	[0 2 4 3 0]	65	24800	28500	50	87.8	59.15
7.5	1.86	0.62	0.62	90	1	[1 3 1 1 4]	75	5000	5400	50	16.5	27.42
9	2.5	1.86	2.5	67.5	1	[2 4 3 4 3]	145	8300	9000	120	177.3	63.36
10.5	0	0	1.24	45	1	[3 0 0 2 2]	10	500	500	32	5.1	17.88
12	0.62	1.24	0	22.5	1	[4 1 2 0 1]	10	14700	3100	20	11.6	33
6	1.86	0	2.5	22.5	1	[0 3 0 4 1]	80	5000	5400	59	19.6	27.48
7.5	2.5	1.24	1.24	0	1	[1 4 2 2 0]	45	17000	20000	35	41.9	43.23
9	0	2.5	0	90	1	[2 0 4 0 4]	25	1600	1500	131	140.1	45.44
10.5	0.62	0.62	1.86	67.5	1	[3 1 1 3 3]	50	2600	2700	68	33.2	32.95
12	1.24	1.86	0.62	45	1	[4 2 3 1 2]	75	7000	5900	35	64.4	49.18
6	2.5	0.62	0	45	1	[0 4 1 0 2]	15	12100	8400	32	8.5	24.8
7.5	0	1.86	1.86	22.5	1	[1 0 3 3 1]	95	11800	12800	47	51.4	45.05
9	0.62	0	0.62	0	1	[2 1 0 1 0]	20	1800	0	15	3.1	15.32
10.5	1.24	1.24	2.5	90	1	[3 2 2 4 4]	70	4400	4500	120	112.1	49.23
12	1.86	2.5	1.24	67.5	1	[4 3 4 2 3]	130	7100	7600	111	186.6	66.79
6	0	1.24	0.62	67.5	1	[0 0 2 1 3]	25	1000	800	60	34.3	26.48
7.5	0.62	2.5	2.5	45	1	[1 1 4 4 2]	175	7200	7100	75	175.9	62.45
9	1.24	0.62	1.24	22.5	1	[2 2 1 2 1]	50	7300	8200	34	17.2	30.16
10.5	1.86	1.86	0	0	1	[3 3 3 0 0]	10	37300	37100	25	22	46.17
12	2.5	0	1.86	90	1	[4 4 0 3 4]	65	6800	7700	45	22.8	34.01
6	0	0	0	0	2	[0 0 0 0 0]	6.2	560	0	5.3	0.1	6.27
7.5	0.62	1.24	1.86	90	2	[1 1 2 3 4]	50	2900	2900	125	123.9	44.09
9	1.24	2.5	0.62	67.5	2	[2 2 4 1 3]	75	4100	4200	80	48.7	37.65
10.5	1.86	0.62	2.5	45	2	[3 3 1 4 2]	95	6200	6300	135	176.6	60.47
12	2.5	1.86	1.24	22.5	2	[4 4 3 2 1]	70	15800	17300	45	38	53.24
6	0.62	0.62	0.62	22.5	2	[0 1 1 1 1]	25	5600	500	20	3.7	20.36
7.5	1.24	1.86	2.5	0	2	[1 2 3 4 0]	75	26400	30100	50	60.3	61.29
9	1.86	0	1.24	90	2	[2 3 0 2 4]	80	5300	5600	70	33.5	34.74
10.5	2.5	1.24	0	67.5	2	[3 4 2 0 3]	40	6600	7800	30	14.6	28.49
12	0	2.5	1.86	45	2	[4 0 4 3 2]	135	5600	5300	65	111.5	55.28
6	1.24	1.24	1.24	45	2	[0 2 2 2 2]	95	6300	6100	45	35.7	35.54
7.5	1.86	2.5	0	22.5	2	[1 3 4 0 1]	80	5100	5500	60	21.1	29.32
9	2.5	0.62	1.86	0	2	[2 4 1 3 0]	30	23000	28000	20	28.9	29.32
10.5	0	1.86	0.62	90	2	[3 0 3 1 4]	15	1000	900	75	34.1	30.21
12	0.62	0	2.5	67.5	2	[4 1 0 4 3]	85	3900	3600	115	113.5	52.47
6	1.86	1.86	1.86	67.5	2	[0 3 3 3 3]	120	6200	6200	110	140.8	51.8
7.5	2.5	0	0.62	45	2	[1 4 0 1 2]	15	12300	8600	30	10	26.61
9	0	1.24	2.5	22.5	2	[2 0 2 4 1]	70	19300	16600	35	61.2	53.3
10.5	0.62	2.5	1.24	0	2	[3 1 4 2 0]	75	13400	15000	60	32.2	46.3
12	1.24	0.62	0	90	2	[4 2 1 0 4]	20	3400	0	15	7.3	21.36
6	2.5	2.5	2.5	90	2	[0 4 4 4 4]	120	7900	8000	165	298.7	69.74
7.5	0	0.62	1.24	67.5	2	[1 0 1 2 3]	25	1100	700	55	34.6	28.31
9	0.62	1.86	0	45	2	[2 1 3 0 2]	35	2000	2200	45	10.05	22.17
10.5	1.24	0	1.86	22.5	2	[3 2 0 3 1]	10	23500	11400	25	22.1	43.28
12	1.86	1.24	0.62	0	2	[4 3 2 1 0]	40	10400	12100	35	15.9	36.71
6	0.62	1.86	1.24	90	2	[0 1 3 2 4]	45	2600	2600	110	83.2	36.46
7.5	1.24	0	0	67.5	2	[1 2 0 0 3]	0	5400	0	5	1	12.79
9	1.86	1.24	1.86	45	2	[2 3 2 3 2]	120	9600	9400	50	76.1	51.98
10.5	2.5	2.5	0.62	22.5	2	[3 4 4 1 1]	80	11200	12100	60	34.2	45.42
12	0	0.62	2.5	0	2	[4 0 1 4 0]	30	23000	28800	20	39.8	53.47
6	1.24	2.5	1.86	0	2	[0 2 4 3 0]	85	20300	22600	60	47.9	52.92
7.5	1.86	0.62	0.62	90	2	[1 3 1 1 4]	75	5000	5400	50	16.5	27.42
9	2.5	1.86	2.5	67.5	2	[2 4 3 4 3]	155	8500	8400	125	224.2	69.84
10.5	0	0	1.24	45	2	[3 0 0 2 2]	50	3300	700	25	13.5	28.4
12	0.62	1.24	0	22.5	2	[4 1 2 0 1]	30	2000	2200	30	8.2	22.23
6	1.86	0	2.5	22.5	2	[0 3 0 4 1]	15	31900	17900	30	33.7	50.15
7.5	2.5	1.24	1.24	0	2	[1 4 2 2 0]	45	17200	19900	35	20.4	43.23
9	0	2.5	0	90	2	[2 0 4 0 4]	10	700	700	60	16	23.15

10.5	0.62	0.62	1.86	67.5	2	[3 1 1 3 3]	70	3100	2800	80	82.1	44.24
12	1.24	1.86	0.62	45	2	[4 2 3 1 2]	75	5300	5400	50	27.3	37.64
6	2.5	0.62	0	45	2	[0 4 1 0 2]	20	6200	800	15	5.8	19.58
7.5	0	1.86	1.86	22.5	2	[1 0 3 3 1]	80	13800	15400	45	44	45.05
9	0.62	0	0.62	0	2	[2 1 0 1 0]	5	11800	0	10	3.1	20.43
10.5	1.24	1.24	2.5	90	2	[3 2 2 4 4]	80	4900	4900	145	209.7	61.49
12	1.86	2.5	1.24	67.5	2	[4 3 4 2 3]	110	6300	6400	100	104.3	54.28
6	0	1.24	0.62	67.5	2	[0 0 2 1 3]	15	800	600	50	16.9	21.22
7.5	0.62	2.5	2.5	45	2	[1 1 4 4 2]	175	8700	8500	70	179	62.45
9	1.24	0.62	1.24	22.5	2	[2 2 1 2 1]	30	11800	3400	20	14.9	35.66
10.5	1.86	1.86	0	0	2	[3 3 3 0 0]	65	5100	5700	45	16.7	29.31
12	2.5	0	1.86	90	2	[4 4 0 3 4]	110	7400	7800	100	84	51.25
6	0	0	0	0	3	[0 0 0 0 0]	6.2	560	0	5.3	0.1	6.27
7.5	0.62	1.24	1.86	90	3	[1 1 2 3 4]	65	3900	4100	75	58.1	31.93
9	1.24	2.5	0.62	67.5	3	[2 2 4 1 3]	95	7700	8800	70	71.8	41.39
10.5	1.86	0.62	2.5	45	3	[3 3 1 4 2]	165	6400	6300	70	126.2	56.2
12	2.5	1.86	1.24	22.5	3	[4 4 3 2 1]	65	21400	24000	40	110.4	66.79
6	0.62	0.62	0.62	22.5	3	[0 1 1 1 1]	25	5400	600	20	6.8	20.36
7.5	1.24	1.86	2.5	0	3	[1 2 3 4 0]	100	15500	17500	60	54.6	48.09
9	1.86	0	1.24	90	3	[2 3 0 2 4]	25	1500	1400	125	122.2	43.21
10.5	2.5	1.24	0	67.5	3	[3 4 2 0 3]	125	6300	6300	115	116	53.38
12	0	2.5	1.86	45	3	[4 0 4 3 2]	65	6800	7700	45	22.8	34.01
6	1.24	1.24	1.24	45	3	[0 2 2 2 2]	80	6000	6100	45	52.1	35.54
7.5	1.86	2.5	0	22.5	3	[1 3 4 0 1]	15	29300	25000	30	23.4	45.15
9	2.5	0.62	1.86	0	3	[2 4 1 3 0]	65	23700	27200	50	86.2	60.37
10.5	0	1.86	0.62	90	3	[3 0 3 1 4]	20	4900	100	15	7.8	22.2
12	0.62	0	2.5	67.5	3	[4 1 0 4 3]	25	1300	1200	80	46.8	35.9
6	1.86	1.86	1.86	67.5	3	[0 3 3 3 3]	130	6700	7400	110	200.7	51.8
7.5	2.5	0	0.62	45	3	[1 4 0 1 2]	125	4300	3100	30	92.2	47.3
9	0	1.24	2.5	22.5	3	[2 0 2 4 1]	60	3600	3900	60	20	28.48
10.5	0.62	2.5	1.24	0	3	[3 1 4 2 0]	45	11900	14100	35	28.7	37.68
12	1.24	0.62	0	90	3	[4 2 1 0 4]	40	2600	2700	70	29.6	33
6	2.5	2.5	2.5	90	3	[0 4 4 4 4]	135	9000	9200	160	410.6	69.74
7.5	0	0.62	1.24	67.5	3	[1 0 1 2 3]	30	1800	2100	30	4.5	16.98
9	0.62	1.86	0	45	3	[2 1 3 0 2]	15	9900	6400	30	6.1	25.68
10.5	1.24	0	1.86	22.5	3	[3 2 0 3 1]	85	8200	8900	45	34.1	39.47
12	1.86	1.24	0.62	0	3	[4 3 2 1 0]	25	19800	24500	25	49.2	49.18
6	0.62	1.86	1.24	90	3	[0 1 3 2 4]	80	5200	5600	65	51.2	29.16
7.5	1.24	0	0	67.5	3	[1 2 0 0 3]	25	1000	700	60	20.3	24.76
9	1.86	1.24	1.86	45	3	[2 3 2 3 2]	130	7600	7800	60	119.6	52.98
10.5	2.5	2.5	0.62	22.5	3	[3 4 4 1 1]	40	23100	12200	25	93.5	63.66
12	0	0.62	2.5	0	3	[4 0 1 4 0]	40	2300	2400	60	20.8	29.47
6	1.24	2.5	1.86	0	3	[0 2 4 3 0]	70	16900	19400	45	48	45.07
7.5	1.86	0.62	0.62	90	3	[1 3 1 1 4]	50	3000	3000	115	104	40.28
9	2.5	1.86	2.5	67.5	3	[2 4 3 4 3]	145	7800	8400	135	335.2	70.93
10.5	0	0	1.24	45	3	[3 0 0 2 2]	10	500	500	30	5.1	17.88
12	0.62	1.24	0	22.5	3	[4 1 2 0 1]	5	11800	0	15	6.4	26.65
6	1.86	0	2.5	22.5	3	[0 3 0 4 1]	130	11800	12700	60	60.3	47.03
7.5	2.5	1.24	1.24	0	3	[1 4 2 2 0]	45	25000	29400	35	78.3	57.22
9	0	2.5	0	90	3	[2 0 4 0 4]	5	11000	0	10	2.8	19.65
10.5	0.62	0.62	1.86	67.5	3	[3 1 1 3 3]	50	2600	2700	70	41.1	32.95
12	1.24	1.86	0.62	45	3	[4 2 3 1 2]	55	7700	7400	35	49.2	42.39
6	2.5	0.62	0	45	3	[0 4 1 0 2]	50	8300	6000	55	58.1	44.32
7.5	0	1.86	1.86	22.5	3	[1 0 3 3 1]	65	4900	5500	45	13.1	25.64
9	0.62	0	0.62	0	3	[2 1 0 1 0]	20	5300	200	15	7	21.3
10.5	1.24	1.24	2.5	90	3	[3 2 2 4 4]	75	4700	4800	120	150.8	49.23
12	1.86	2.5	1.24	67.5	3	[4 3 4 2 3]	150	8800	9800	100	170.1	59.31
6	0	1.24	0.62	67.5	3	[0 0 2 1 3]	20	3100	0	15	2.55	14.43

7.5	0.62	2.5	2.5	45	3	[1 1 4 4 2]	120	8300	9000	65	67.7	41.44
9	1.24	0.62	1.24	22.5	3	[2 2 1 2 1]	50	9600	10600	35	29.4	36.59
10.5	1.86	1.86	0	0	3	[3 3 3 0 0]	10	37300	37100	25	22	46.17
12	2.5	0	1.86	90	3	[4 4 0 3 4]	35	2200	2000	150	244.2	61.59
6	0	0	0	0	4	[0 0 0 0 0]	6.2	560	0	5.3	0.1	6.27
7.5	0.62	1.24	1.86	90	4	[1 1 2 3 4]	70	5500	6100	65	23.4	31.02
9	1.24	2.5	0.62	67.5	4	[2 2 4 1 3]	65	3300	3400	100	98.6	44.29
10.5	1.86	0.62	2.5	45	4	[3 3 1 4 2]	65	11100	10700	40	62.6	53.16
12	2.5	1.86	1.24	22.5	4	[4 4 3 2 1]	80	20300	22500	50	97.6	67.84
6	0.62	0.62	0.62	22.5	4	[0 1 1 1 1]	25	5400	600	20	4.9	20.36
7.5	1.24	1.86	2.5	0	4	[1 2 3 4 0]	60	17200	19600	45	31.3	47.08
9	1.86	0	1.24	90	4	[2 3 0 2 4]	75	4600	4700	100	73.6	41.3
10.5	2.5	1.24	0	67.5	4	[3 4 2 0 3]	50	2200	2100	100	180.3	55.39
12	0	2.5	1.86	45	4	[4 0 4 3 2]	65	5700	6400	60	21.6	34.97
6	1.24	1.24	1.24	45	4	[0 2 2 2 2]	70	6200	6300	45	36.1	35.54
7.5	1.86	2.5	0	22.5	4	[1 3 4 0 1]	130	11900	12900	60	63.2	49.07
9	2.5	0.62	1.86	0	4	[2 4 1 3 0]	30	27100	33600	25	56.1	58.33
10.5	0	1.86	0.62	90	4	[3 0 3 1 4]	35	2200	2400	45	10	23.95
12	0.62	0	2.5	67.5	4	[4 1 0 4 3]	40	8400	10400	35	11.3	32.17
6	1.86	1.86	1.86	67.5	4	[0 3 3 3 3]	145	7000	7600	110	146.6	51.8
7.5	2.5	0	0.62	45	4	[1 4 0 1 2]	50	8500	6200	55	58.9	46.33
9	0	1.24	2.5	22.5	4	[2 0 2 4 1]	40	6700	8100	30	7.4	26.66
10.5	0.62	2.5	1.24	0	4	[3 1 4 2 0]	70	9000	9900	60	27.8	39.59
12	1.24	0.62	0	90	4	[4 2 1 0 4]	20	1100	1000	85	42.9	33.92
6	2.5	2.5	2.5	90	4	[0 4 4 4 4]	160	9500	9600	165	319.4	69.74
7.5	0	0.62	1.24	67.5	4	[1 0 1 2 3]	20	3300	0	15	1.9	16.13
9	0.62	1.86	0	45	4	[2 1 3 0 2]	50	2000	1800	50	19.8	28.36
10.5	1.24	0	1.86	22.5	4	[3 2 0 3 1]	10	20600	13200	25	13.4	36.65
12	1.86	1.24	0.62	0	4	[4 3 2 1 0]	50	18200	21500	35	48.3	50.17
6	0.62	1.86	1.24	90	4	[0 1 3 2 4]	70	4000	4300	80	34.7	30.06
7.5	1.24	0	0	67.5	4	[1 2 0 0 3]	25	1000	700	60	20.3	24.76
9	1.86	1.24	1.86	45	4	[2 3 2 3 2]	85	9400	9800	50	78.1	51.98
10.5	2.5	2.5	0.62	22.5	4	[3 4 4 1 1]	100	18200	19900	60	106.7	66.82
12	0	0.62	2.5	0	4	[4 0 1 4 0]	20	6800	2500	20	6.4	26.74
6	1.24	2.5	1.86	0	4	[0 2 4 3 0]	80	15500	17300	60	36.9	46.06
7.5	1.86	0.62	0.62	90	4	[1 3 1 1 4]	50	3000	3000	115	96.7	40.28
9	2.5	1.86	2.5	67.5	4	[2 4 3 4 3]	180	9900	10700	125	234	69.84
10.5	0	0	1.24	45	4	[3 0 0 2 2]	0	5600	0	10	1.8	16.18
12	0.62	1.24	0	22.5	4	[4 1 2 0 1]	50	4300	4700	30	14.6	28.45
6	1.86	0	2.5	22.5	4	[0 3 0 4 1]	15	28900	24200	30	21.8	43.15
7.5	2.5	1.24	1.24	0	4	[1 4 2 2 0]	50	25100	29700	35	63.8	57.22
9	0	2.5	0	90	4	[2 0 4 0 4]	10	700	700	60	16	23.15
10.5	0.62	0.62	1.86	67.5	4	[3 1 1 3 3]	50	5600	6300	45	14.5	31.12
12	1.24	1.86	0.62	45	4	[4 2 3 1 2]	85	5100	5000	55	53.32	44.31
6	2.5	0.62	0	45	4	[0 4 1 0 2]	125	4200	3000	30	91.7	45.28
7.5	0	1.86	1.86	22.5	4	[1 0 3 3 1]	50	5200	6000	45	10	25.64
9	0.62	0	0.62	0	4	[2 1 0 1 0]	5	11800	0	10	3.1	20.43
10.5	1.24	1.24	2.5	90	4	[3 2 2 4 4]	110	8000	8600	95	68.3	47.24
12	1.86	2.5	1.24	67.5	4	[4 3 4 2 3]	115	5900	6200	115	172.3	61.39
6	0	1.24	0.62	67.5	4	[0 0 2 1 3]	30	1800	2100	30	3	15.26
7.5	0.62	2.5	2.5	45	4	[1 1 4 4 2]	85	8700	9300	65	38.2	41.44
9	1.24	0.62	1.24	22.5	4	[2 2 1 2 1]	30	11300	3800	20	19.2	35.66
10.5	1.86	1.86	0	0	4	[3 3 3 0 0]	70	16400	18800	45	53.3	49.1
12	2.5	0	1.86	90	4	[4 4 0 3 4]	115	7100	7300	130	146.8	58.52
6	0	0	0	0	5	[0 0 0 0 0]	6.2	560	0	5.3	0.1	6.27
7.5	0.62	1.24	1.86	90	5	[1 1 2 3 4]	70	4200	4200	110	115.4	43.13
9	1.24	2.5	0.62	67.5	5	[2 2 4 1 3]	85	7200	7700	55	58.5	35.75
10.5	1.86	0.62	2.5	45	5	[3 3 1 4 2]	175	8800	8500	60	165.1	62.52

12	2.5	1.86	1.24	22.5	5	[4 4 3 2 1]	95	15200	17000	60	54.5	54.28
6	0.62	0.62	0.62	22.5	5	[0 1 1 1 1]	25	5700	500	20	4.5	20.36
7.5	1.24	1.86	2.5	0	5	[1 2 3 4 0]	55	28100	33700	35	72.4	60.27
9	1.86	0	1.24	90	5	[2 3 0 2 4]	20	1300	1200	110	81.7	37.53
10.5	2.5	1.24	0	67.5	5	[3 4 2 0 3]	60	4000	4400	60	18.8	30.33
12	0	2.5	1.86	45	5	[4 0 4 3 2]	45	15800	13400	70	49.3	51.25
6	1.24	1.24	1.24	45	5	[0 2 2 2 2]	85	6700	6700	45	53.7	35.54
7.5	1.86	2.5	0	22.5	5	[1 3 4 0 1]	55	6900	7900	45	11.8	28.4
9	2.5	0.62	1.86	0	5	[2 4 1 3 0]	90	19400	22200	60	52.8	54.1
10.5	0	1.86	0.62	90	5	[3 0 3 1 4]	50	5000	5700	40	13.8	27.51
12	0.62	0	2.5	67.5	5	[4 1 0 4 3]	50	2100	1600	85	144.7	53.47
6	1.86	1.86	1.86	67.5	5	[0 3 3 3 3]	130	6600	6500	105	204.5	51.8
7.5	2.5	0	0.62	45	5	[1 4 0 1 2]	55	2200	2000	60	30.6	30.23
9	0	1.24	2.5	22.5	5	[2 0 2 4 1]	15	29600	16200	30	33.8	51.31
10.5	0.62	2.5	1.24	0	5	[3 1 4 2 0]	30	17800	22500	20	24.5	43.37
12	1.24	0.62	0	90	5	[4 2 1 0 4]	30	2100	2400	30	6.6	22.23
6	2.5	2.5	2.5	90	5	[0 4 4 4 4]	135	8200	8300	165	415.1	69.74
7.5	0	0.62	1.24	67.5	5	[1 0 1 2 3]	55	2700	2600	65	21.9	27.42
9	0.62	1.86	0	45	5	[2 1 3 0 2]	20	4900	0	15	3.3	20.43
10.5	1.24	0	1.86	22.5	5	[3 2 0 3 1]	60	13900	14800	35	35.1	45.2
12	1.86	1.24	0.62	0	5	[4 3 2 1 0]	55	9400	10900	45	17.9	37.64
6	0.62	1.86	1.24	90	5	[0 1 3 2 4]	85	5200	5300	80	69.7	34.61
7.5	1.24	0	0	67.5	5	[1 2 0 0 3]	5	400	400	30	3.3	14.45
9	1.86	1.24	1.86	45	5	[2 3 2 3 2]	145	8900	9000	60	121.7	52.98
10.5	2.5	2.5	0.62	22.5	5	[3 4 4 1 1]	85	11900	13300	60	37.5	45.42
12	0	0.62	2.5	0	5	[4 0 1 4 0]	10	42300	42000	25	29.2	52.47
6	1.24	2.5	1.86	0	5	[0 2 4 3 0]	50	23400	28100	35	52.7	50.91
7.5	1.86	0.62	0.62	90	5	[1 3 1 1 4]	40	2400	2500	80	44.3	29.21
9	2.5	1.86	2.5	67.5	5	[2 4 3 4 3]	145	7500	7400	135	340.1	70.93
10.5	0	0	1.24	45	5	[3 0 0 2 2]	50	3300	700	25	13.5	28.4
12	0.62	1.24	0	22.5	5	[4 1 2 0 1]	20	3500	0	15	4.5	21.36
6	1.86	0	2.5	22.5	5	[0 3 0 4 1]	95	19000	21400	50	75.3	53.11
7.5	2.5	1.24	1.24	0	5	[1 4 2 2 0]	80	15000	17100	60	38.2	45.18
9	0	2.5	0	90	5	[2 0 4 0 4]	5	11000	0	10	2.8	19.65
10.5	0.62	0.62	1.86	67.5	5	[3 1 1 3 3]	70	3100	2800	80	90.1	44.24
12	1.24	1.86	0.62	45	5	[4 2 3 1 2]	60	7200	7800	40	31.7	36.71
6	2.5	0.62	0	45	5	[0 4 1 0 2]	35	2200	2300	60	15.2	22.2
7.5	0	1.86	1.86	22.5	5	[1 0 3 3 1]	15	25900	13100	25	21.4	42.18
9	0.62	0	0.62	0	5	[2 1 0 1 0]	20	5400	0	15	3.6	21.3
10.5	1.24	1.24	2.5	90	5	[3 2 2 4 4]	80	5000	4900	145	242.2	61.49
12	1.86	2.5	1.24	67.5	5	[4 3 4 2 3]	135	8200	8400	85	144.9	53.24
6	0	1.24	0.62	67.5	5	[0 0 2 1 3]	40	3900	4500	35	6.1	19.5
7.5	0.62	2.5	2.5	45	5	[1 1 4 4 2]	95	13000	9000	40	141	59.35
9	1.24	0.62	1.24	22.5	5	[2 2 1 2 1]	50	10700	12200	35	21.2	36.59
10.5	1.86	1.86	0	0	5	[3 3 3 0 0]	50	5400	6200	45	12	29.31
12	2.5	0	1.86	90	5	[4 4 0 3 4]	30	1900	1800	140	186.5	55.28
6	0	0	0	0	6	[0 0 0 0 0]	6.2	560	0	5.3	0.1	6.27
7.5	0.62	1.24	1.86	90	6	[1 1 2 3 4]	90	5800	6300	85	45.3	36.53
9	1.24	2.5	0.62	67.5	6	[2 2 4 1 3]	90	4100	3700	110	185.9	56.31
10.5	1.86	0.62	2.5	45	6	[3 3 1 4 2]	75	9300	10400	55	30	41.46
12	2.5	1.86	1.24	22.5	6	[4 4 3 2 1]	95	18600	20900	60	70.1	61.39
6	0.62	0.62	0.62	22.5	6	[0 1 1 1 1]	25	5800	500	20	4.1	20.36
7.5	1.24	1.86	2.5	0	6	[1 2 3 4 0]	50	23700	28400	35	52.5	52.98
9	1.86	0	1.24	90	6	[2 3 0 2 4]	45	3700	4200	45	9.7	24.8
10.5	2.5	1.24	0	67.5	6	[3 4 2 0 3]	35	1700	1400	95	96.3	43.4
12	0	2.5	1.86	45	6	[4 0 4 3 2]	60	15400	13000	75	69.3	58.52
6	1.24	1.24	1.24	45	6	[0 2 2 2 2]	70	6900	7100	45	38.4	35.54
7.5	1.86	2.5	0	22.5	6	[1 3 4 0 1]	95	19200	21600	50	74.6	55.21

9	2.5	0.62	1.86	0	6	[2 4 1 3 0]	75	11100	12600	60	28.2	40.47
10.5	0	1.86	0.62	90	6	[3 0 3 1 4]	50	3000	3000	100	72	40.41
12	0.62	0	2.5	67.5	6	[4 1 0 4 3]	20	6800	2500	20	6.4	26.74
6	1.86	1.86	1.86	67.5	6	[0 3 3 3 3]	145	7300	7400	110	148.7	51.8
7.5	2.5	0	0.62	45	6	[1 4 0 1 2]	40	2200	2400	60	15.8	23.99
9	0	1.24	2.5	22.5	6	[2 0 2 4 1]	10	23400	17200	25	14.2	37.62
10.5	0.62	2.5	1.24	0	6	[3 1 4 2 0]	30	26300	32900	25	51.7	57.41
12	1.24	0.62	0	90	6	[4 2 1 0 4]	15	900	800	65	23	28.45
6	2.5	2.5	2.5	90	6	[0 4 4 4 4]	160	9500	9600	165	319.4	69.74
7.5	0	0.62	1.24	67.5	6	[1 0 1 2 3]	35	4200	5000	35	5.4	21.26
9	0.62	1.86	0	45	6	[2 1 3 0 2]	90	4000	1800	25	50.9	39.4
10.5	1.24	0	1.86	22.5	6	[3 2 0 3 1]	35	5200	6200	30	6.9	25.72
12	1.86	1.24	0.62	0	6	[4 3 2 1 0]	65	13400	15700	45	25.6	44.31
6	0.62	1.86	1.24	90	6	[0 1 3 2 4]	80	4600	4700	115	100	41.15
7.5	1.24	0	0	67.5	6	[1 2 0 0 3]	5	400	400	30	3.3	14.45
9	1.86	1.24	1.86	45	6	[2 3 2 3 2]	90	9400	10000	55	56.8	46.1
10.5	2.5	2.5	0.62	22.5	6	[3 4 4 1 1]	105	22100	24700	60	97	66.82
12	0	0.62	2.5	0	6	[4 0 1 4 0]	5	20800	20500	20	9.5	32.17
6	1.24	2.5	1.86	0	6	[0 2 4 3 0]	55	21400	33300	35	73.1	58.13
7.5	1.86	0.62	0.62	90	6	[1 3 1 1 4]	40	2500	2600	80	33.6	29.21
9	2.5	1.86	2.5	67.5	6	[2 4 3 4 3]	165	9800	10000	120	184	63.36
10.5	0	0	1.24	45	6	[3 0 0 2 2]	0	5600	0	10	1.8	16.18
12	0.62	1.24	0	22.5	6	[4 1 2 0 1]	30	8900	1600	20	13.8	33.92
6	1.86	0	2.5	22.5	6	[0 3 0 4 1]	55	6700	7800	45	11.2	26.56
7.5	2.5	1.24	1.24	0	6	[1 4 2 2 0]	80	15000	17100	60	38.2	45.18
9	0	2.5	0	90	6	[2 0 4 0 4]	25	1600	1500	130	140.1	45.44
10.5	0.62	0.62	1.86	67.5	6	[3 1 1 3 3]	55	5800	6300	40	14.5	31.12
12	1.24	1.86	0.62	45	6	[4 2 3 1 2]	85	6900	6700	45	74.1	50.17
6	2.5	0.62	0	45	6	[0 4 1 0 2]	55	2200	2000	60	30.2	28.37
7.5	0	1.86	1.86	22.5	6	[1 0 3 3 1]	15	26000	20400	30	20.1	42.18
9	0.62	0	0.62	0	6	[2 1 0 1 0]	15	1800	0	15	2.2	15.32
10.5	1.24	1.24	2.5	90	6	[3 2 2 4 4]	110	8000	8600	95	68.3	47.24
12	1.86	2.5	1.24	67.5	6	[4 3 4 2 3]	130	6400	6200	125	223.2	67.84
6	0	1.24	0.62	67.5	6	[0 0 2 1 3]	60	2800	2800	65	20.6	25.59
7.5	0.62	2.5	2.5	45	6	[1 1 4 4 2]	85	14300	10200	40	109.3	59.35
9	1.24	0.62	1.24	22.5	6	[2 2 1 2 1]	45	7800	9100	30	10.7	30.16
10.5	1.86	1.86	0	0	6	[3 3 3 0 0]	70	17400	20300	45	35.8	49.1
12	2.5	0	1.86	90	6	[4 4 0 3 4]	65	5700	6400	60	21.6	34.97

Unit and Nomenclature

t_{liner}: thickness of the liner (mm); t_0: thickness of 0° (axial) composite layers (mm); t_θ: thickness of ±θ° (angular) composite layers (mm); t_{90}: thickness of 90° (hoop) composite layers (mm); θ: angle of the ±θ° (angular) composite layers (degrees); and *n*: composite layers stacking sequences (1, 2, 3, 4, 5, 6).

LC1: Burst Case (MPa); LC2(a): Pure Tension Case (kN); LC2(b): Tension with External Pressure Case (kN); LC3: Collapse Case (MPa); LC4: Buckling (MPa).

Structural Weight: kg/m.

E.2 DOE Database for AS4/Epoxy with Titanium liner

Table E.2. DOE database for AS4/epoxy with titanium liner using orthogonal array

Variables						OA Sampling	Load Capacity					Structural Weight
t_{liner}	t_0	t_θ	t_{90}	θ	n		LC1	LC2(a)	LC2(b)	LC3	LC4	
2	1	1	1	45	1	[0 0 0 0 0]	65	4500	4800	65	55.26	29.2
4	1.33	1.66	2	51.7	1	[1 1 2 3 1]	170	6400	6900	125	217.51	53.5
6	1.66	2	1.33	58.3	1	[2 2 3 1 2]	180	7800	8600	145	283.21	63.9
8	2	1.33	1.66	65.0	1	[3 3 1 2 3]	170	9000	10100	165	267.78	65.1
2	1.33	1.33	1.33	51.7	1	[0 1 1 1 1]	110	4950	5300	95	101.32	37.1
4	1	2	1.66	45	1	[1 0 3 2 0]	135	7000	7550	100	224.41	55.1
6	2	1.66	1	65.0	1	[2 3 2 0 3]	155	7900	9000	150	229.89	58.3
8	1.66	1	2	58.3	1	[3 2 0 3 2]	165	8300	9300	150	225.38	60.6
2	1.66	1.66	1.66	65.0	1	[0 2 2 2 3]	110	5200	5700	150	169.45	45.3
4	2	1	1.33	58.3	1	[1 3 0 1 2]	120	6700	7500	115	125.54	42.8
6	1	1.33	2	51.7	1	[2 0 1 3 1]	160	6600	7100	130	205.75	54.8
8	1.33	2	1	45	1	[3 1 3 0 0]	135	9800	10800	105	267.41	68.3
2	2	2	2	58.3	1	[0 3 3 3 2]	150	6300	6900	150	233.73	54.1
4	1.66	1.33	1	65.0	1	[1 2 1 0 3]	120	6000	6700	130	138.02	44.2
6	1.33	1	1.66	45	1	[2 1 0 2 0]	120	7400	8200	110	153.45	49.4
8	1	1.66	1.33	51.7	1	[3 0 2 1 1]	165	7800	8600	125	245.3	63.6
2	1.66	1.33	2	45	1	[0 2 1 3 0]	120	6400	6900	105	131.35	42.4
4	2	2	1	51.7	1	[1 3 3 0 1]	140	7800	8600	110	216.79	55.7
6	1	1.66	1.66	58.3	1	[2 0 2 2 2]	150	6300	6900	145	234.56	57.7
8	1.33	1	1.33	65.0	1	[3 1 0 1 3]	145	7400	8400	145	175.25	55.2
2	2	1	1.66	51.7	1	[0 3 0 2 1]	105	5900	6600	100	97.51	37.1
4	1.66	1.66	1.33	45	1	[1 2 2 1 0]	110	7700	8500	95	182.47	51
6	1.33	2	2	65.0	1	[2 1 3 3 3]	150	7000	7700	185	328.19	66.6
8	1	1.33	1	58.3	1	[3 0 1 0 2]	155	7100	7900	130	183.14	56.7
2	1	2	1.33	65.0	1	[0 0 3 1 3]	95	4100	4400	150	183.28	45.4
4	1.33	1.33	1.66	58.3	1	[1 1 1 2 2]	130	5700	6200	130	160.79	46.6
6	1.66	1	1	51.7	1	[2 2 0 0 1]	105	7400	8300	100	129.36	47
8	2	1.66	2	45	1	[3 3 2 3 0]	165	10800	12100	135	323.98	72.4
2	1.33	1.66	1	58.3	1	[0 1 2 0 2]	120	4700	5000	110	122.73	39.9
4	1	1	2	65.0	1	[1 0 0 3 3]	100	4700	5200	145	131.89	42.3
6	2	1.33	1.33	45	1	[2 3 1 1 0]	115	9100	10200	105	194.02	55.3
8	1.66	2	1.66	51.7	1	[3 2 3 2 1]	200	9500	10500	145	344.26	74
2	1	1	1	45	2	[0 0 0 0 0]	70	4800	4900	65	38.6	29.2
4	1.33	1.66	2	51.7	2	[1 1 2 3 1]	145	7400	7400	120	201.64	56.6
6	1.66	2	1.33	58.3	2	[2 2 3 1 2]	140	7600	8000	150	201.09	57.8
8	2	1.33	1.66	65.0	2	[3 3 1 2 3]	165	9000	9600	170	277.77	68.2
2	1.33	1.33	1.33	51.7	2	[0 1 1 1 1]	95	5300	5300	90	82.87	37.1
4	1	2	1.66	45	2	[1 0 3 2 0]	125	7600	7800	110	146.78	52
6	2	1.66	1	65.0	2	[2 3 2 0 3]	130	7600	8200	145	166.19	52.4
8	1.66	1	2	58.3	2	[3 2 0 3 2]	175	9200	9600	145	275.69	69.8
2	1.66	1.66	1.66	65.0	2	[0 2 2 2 3]	105	5200	5200	150	160.04	45.3
4	2	1	1.33	58.3	2	[1 3 0 1 2]	120	7000	7400	110	127.19	45.6
6	1	1.33	2	51.7	2	[2 0 1 3 1]	155	7800	8000	120	210.18	60.9
8	1.33	2	1	45	2	[3 1 3 0 0]	135	9100	9900	130	153.38	59.2
2	2	2	2	58.3	2	[0 3 3 3 2]	135	6700	6700	145	213.82	54.1
4	1.66	1.33	1	65.0	2	[1 2 1 0 3]	105	5800	6200	125	107.72	41.3
6	1.33	1	1.66	45	2	[2 1 0 2 0]	115	9300	9700	95	141.33	55.3
8	1	1.66	1.33	51.7	2	[3 0 2 1 1]	145	8100	8600	130	177.89	60.6
2	1.66	1.33	2	45	2	[0 2 1 3 0]	115	8200	8300	85	133.76	48.4
4	2	2	1	51.7	2	[1 3 3 0 1]	115	7400	7900	120	124.29	46.7
6	1	1.66	1.66	58.3	2	[2 0 2 2 2]	140	6600	6700	145	205.06	57.7

8	1.33	1	1.33	65.0	2	[3 1 0 1 3]	145	7500	8000	145	186.34	58.1
2	2	1	1.66	51.7	2	[0 3 0 2 1]	115	6900	7100	90	110.91	42.9
4	1.66	1.66	1.33	45	2	[1 2 2 1 0]	110	8100	8600	100	117.19	48
6	1.33	2	2	65.0	2	[2 1 3 3 3]	150	7000	7100	190	307.19	66.6
8	1	1.33	1	58.3	2	[3 0 1 0 2]	135	7100	7500	130	138.54	53.8
2	1	2	1.33	65.0	2	[0 0 3 1 3]	85	3900	3800	145	126.03	39.5
4	1.33	1.33	1.66	58.3	2	[1 1 1 2 2]	125	6000	6100	125	161.84	49.5
6	1.66	1	1	51.7	2	[2 2 0 0 1]	110	7800	8400	100	104.12	47
8	2	1.66	2	45	2	[3 3 2 3 0]	165	12900	13900	125	268.29	75.6
2	1.33	1.66	1	58.3	2	[0 1 2 0 2]	85	4500	4600	110	75.53	34.2
4	1	1	2	65.0	2	[1 0 0 3 3]	120	5100	5000	150	194.4	51.1
6	2	1.33	1.33	45	2	[2 3 1 1 0]	120	10000	10900	105	143.06	55.3
8	1.66	2	1.66	51.7	2	[3 2 3 2 1]	165	10000	10600	145	262.41	70.8
2	1	1	1	45	3	[0 0 0 0 0]	60	4600	4900	65	58.62	29.2
4	1.33	1.66	2	1.7	3	[1 1 2 3 1]	130	7000	7700	125	198.55	50
6	1.66	2	1.33	58.3	3	[2 2 3 1 2]	145	8600	9700	145	247.78	60.3
8	2	1.33	1.66	65.0	3	[3 3 1 2 3]	175	8400	9400	185	351.62	72.4
2	1.33	1.33	1.33	51.7	3	[0 1 1 1 1]	90	5100	5500	95	113.5	37.1
4	1	2	1.66	45	3	[1 0 3 2 0]	100	7800	8700	100	145.16	44.7
6	2	1.66	1	65.0	3	[2 3 2 0 3]	155	7900	9000	165	261.35	61.9
8	1.66	1	2	58.3	3	[3 2 0 3 2]	175	7700	8500	165	304.13	67.7
2	1.66	1.66	1.66	65.0	3	[0 2 2 2 3]	115	5500	6100	155	200.54	45.3
4	2	1	1.33	58.3	3	[1 3 0 1 2]	145	5700	6100	135	224.86	53.1
6	1	1.33	2	51.7	3	[2 0 1 3 1]	130	7000	7800	130	178.89	51.4
8	1.33	2	1	45	3	[3 1 3 0 0]	115	10400	11900	105	198.78	61.1
2	2	2	2	58.3	3	[0 3 3 3 2]	160	6800	7500	150	276.67	54.1
4	1.66	1.33	1	65.0	3	[1 2 1 0 3]	120	5800	6500	145	170.73	47.5
6	1.33	1	1.66	45	3	[2 1 0 2 0]	120	7300	8000	110	184.42	52.8
8	1	1.66	1.33	51.7	3	[3 0 2 1 1]	125	8700	9800	120	178.41	56.7
2	1.66	1.33	2	45	3	[0 2 1 3 0]	115	6400	6900	100	174.09	45.8
4	2	2	1	51.7	3	[1 3 3 0 1]	120	8200	9200	110	219.75	55.7
6	1	1.66	1.66	58.3	3	[2 0 2 2 2]	130	7400	8200	135	172.54	50.9
8	1.33	1	1.33	65.0	3	[3 1 0 1 3]	150	7200	8000	155	206.03	58.6
2	2	1	1.66	51.7	3	[0 3 0 2 1]	130	5200	5400	105	198.88	47.4
4	1.66	1.66	1.33	45	3	[1 2 2 1 0]	105	8000	8800	95	188.48	51
6	1.33	2	2	65.0	3	[2 1 3 3 3]	160	8200	9300	170	260.29	59.3
8	1	1.33	1	58.3	3	[3 0 1 0 2]	120	7700	8700	125	145.33	53.3
2	1	2	1.33	65.0	3	[0 0 3 1 3]	95	5600	6400	120	110.74	35.2
4	1.33	1.33	1.66	58.3	3	[1 1 1 2 2]	125	5900	6400	130	170.99	46.6
6	1.66	1	1	51.7	3	[2 2 0 0 1]	120	6800	7500	105	181.88	53.8
8	2	1.66	2	45	3	[3 3 2 3 0]	165	10900	12100	135	367.38	76.1
2	1.33	1.66	1	58.3	3	[0 1 2 0 2]	90	5300	6000	105	109.65	36.6
4	1	1	2	65.0	3	[1 0 0 3 3]	105	4800	5300	145	141.84	42.3
6	2	1.33	1.33	45	3	[2 3 1 1 0]	125	8900	9800	105	256.76	62.4
8	1.66	2	1.66	51.7	3	[3 2 3 2 1]	160	10200	11400	140	309.19	70.2
2	1	1	1	45	4	[0 0 0 0 0]	55	4700	5100	65	42.95	29.2
4	1.33	1.66	2	51.7	4	[1 1 2 3 1]	100	8000	8800	120	131.72	49.5
6	1.66	2	1.33	58.3	4	[2 2 3 1 2]	140	7500	8200	155	231.01	61.3
8	2	1.33	1.66	65.0	4	[3 3 1 2 3]	160	9300	10400	180	285.45	71.9
2	1.33	1.33	1.33	51.7	4	[0 1 1 1 1]	80	5300	5700	95	83.51	37.1
4	1	2	1.66	45	4	[1 0 3 2 0]	90	7400	8100	110	106.17	45.2
6	2	1.66	1	65.0	4	[2 3 2 0 3]	150	6700	7400	175	265.67	62.9
8	1.66	1	2	58.3	4	[3 2 0 3 2]	135	10000	11300	145	204.03	66.1
2	1.66	1.66	1.66	65.0	4	[0 2 2 2 3]	110	5700	6300	155	150.34	45.3
4	2	1	1.33	58.3	4	[1 3 0 1 2]	120	6500	7100	130	177.86	52.6
6	1	1.33	2	51.7	4	[2 0 1 3 1]	95	8600	9700	115	107.62	50.4
8	1.33	2	1	45	4	[3 1 3 0 0]	130	8800	9700	130	209.45	62.6
2	2	2	2	58.3	4	[0 3 3 3 2]	125	7200	7800	150	209.12	54.1

4	1.66	1.33	1	65.0	4	[1 2 1 0 3]	115	5300	5800	150	158.63	48
6	1.33	1	1.66	45	4	[2 1 0 2 0]	90	9000	10100	95	120.75	51.8
8	1	1.66	1.33	51.7	4	[3 0 2 1 1]	115	8300	9200	130	149.92	57.1
2	1.66	1.33	2	45	4	[0 2 1 3 0]	80	8100	8900	90	111.5	44.8
4	2	2	1	51.7	4	[1 3 3 0 1]	130	6600	7000	125	231.84	57.2
6	1	1.66	1.66	58.3	4	[2 0 2 2 2]	105	7600	8400	135	123.77	50.9
8	1.33	1	1.33	65.0	4	[3 1 0 1 3]	125	7900	9000	150	159.27	58.1
2	2	1	1.66	51.7	4	[0 3 0 2 1]	95	6700	7200	95	136.55	46.4
4	1.66	1.66	1.33	45	4	[1 2 2 1 0]	100	7800	8500	105	161.3	51.5
6	1.33	2	2	65.0	4	[2 1 3 3 3]	135	8400	9400	170	190.98	59.3
8	1	1.33	1	58.3	4	[3 0 1 0 2]	110	7200	8000	130	131.71	53.8
2	1	2	1.33	65.0	4	[0 0 3 1 3]	90	4600	5000	135	87.47	36.2
4	1.33	1.33	1.66	58.3	4	[1 1 1 2 2]	100	6700	7400	125	117.12	46.1
6	1.66	1	1	51.7	4	[2 2 0 0 1]	110	7100	7700	110	158.69	53.8
8	2	1.66	2	45	4	[3 3 2 3 0]	140	12300	13700	130	286.73	75.6
2	1.33	1.66	1	58.3	4	[0 1 2 0 2]	90	4300	4500	120	101.24	37.6
4	1	1	2	65.0	4	[1 0 0 3 3]	85	6800	7800	120	72.76	40.9
6	2	1.33	1.33	45	4	[2 3 1 1 0]	115	9400	10300	105	219.49	62.4
8	1.66	2	1.66	51.7	4	[3 2 3 2 1]	145	10000	11000	150	266.17	70.8
2	1	1	1	45	5	[0 0 0 0 0]	60	5000	5200	65	44.68	29.2
4	1.33	1.66	2	51.7	5	[1 1 2 3 1]	85	11800	8700	65	171.26	56.1
6	1.66	2	1.33	58.3	5	[2 2 3 1 2]	95	14400	11600	85	153.88	57.3
8	2	1.33	1.66	65.0	5	[3 3 1 2 3]	165	8100	8400	185	308.26	69.2
2	1.33	1.33	1.33	51.7	5	[0 1 1 1 1]	100	5500	5700	90	101.27	37.1
4	1	2	1.66	45	5	[1 0 3 2 0]	95	10000	10600	85	142.68	50.5
6	2	1.66	1	65.0	5	[2 3 2 0 3]	135	7300	7700	155	181.51	52.9
8	1.66	1	2	58.3	5	[3 2 0 3 2]	175	8300	8500	160	301.74	70.8
2	1.66	1.66	1.66	65.0	5	[0 2 2 2 3]	110	5400	5500	150	199.7	45.3
4	2	1	1.33	58.3	5	[1 3 0 1 2]	120	5500	5600	135	159.74	47.1
6	1	1.33	2	51.7	5	[2 0 1 3 1]	150	8700	9000	110	211.86	60.4
8	1.33	2	1	45	5	[3 1 3 0 0]	115	11000	12400	110	130.59	58.2
2	2	2	2	58.3	5	[0 3 3 3 2]	145	7100	7100	145	269.03	54.1
4	1.66	1.33	1	65.0	5	[1 2 1 0 3]	105	5400	5700	135	125.69	41.8
6	1.33	1	1.66	45	5	[2 1 0 2 0]	125	9000	9500	100	149.7	55.7
8	1	1.66	1.33	51.7	5	[3 0 2 1 1]	130	9800	10600	115	166.93	59.6
2	1.66	1.33	2	45	5	[0 2 1 3 0]	120	8100	8400	95	168.27	48.9
4	2	2	1	51.7	5	[1 3 3 0 1]	120	7800	8400	120	133.85	46.7
6	1	1.66	1.66	58.3	5	[2 0 2 2 2]	150	8000	8400	125	201.35	56.7
8	1.33	1	1.33	65.0	5	[3 1 0 1 3]	145	7100	7400	155	197.62	58.6
2	2	1	1.66	51.7	5	[0 3 0 2 1]	120	5500	5400	115	158.32	44.4
4	1.66	1.66	1.33	45	5	[1 2 2 1 0]	110	8600	9300	100	125.98	48
6	1.33	2	2	65.0	5	[2 1 3 3 3]	165	8400	8600	170	308.6	65.5
8	1	1.33	1	58.3	5	[3 0 1 0 2]	125	7900	8600	120	132.58	53.3
2	1	2	1.33	65.0	5	[0 0 3 1 3]	105	5700	5900	115	128.23	38.1
4	1.33	1.33	1.66	58.3	5	[1 1 1 2 2]	130	6300	6400	125	178.73	49.5
6	1.66	1	1	51.7	5	[2 2 0 0 1]	120	6800	7200	115	112.41	48
8	2	1.66	2	45	5	[3 3 2 3 0]	175	13000	14100	135	280.09	76.1
2	1.33	1.66	1	58.3	5	[0 1 2 0 2]	95	5300	5500	100	89.94	33.8
4	1	1	2	65.0	5	[1 0 0 3 3]	120	5200	5100	150	207.39	51.1
6	2	1.33	1.33	45	5	[2 3 1 1 0]	135	9200	9900	120	153.44	56.3
8	1.66	2	1.66	51.7	5	[3 2 3 2 1]	170	11200	12200	140	261.74	70.2
2	1	1	1	45	6	[0 0 0 0 0]	55	5100	5400	65	32.6	29.2
4	1.33	1.66	2	51.7	6	[1 1 2 3 1]	105	9000	9700	110	130.09	52.5
6	1.66	2	1.33	58.3	6	[2 2 3 1 2]	145	8200	8400	155	232.11	64.5
8	2	1.33	1.66	65	6	[3 3 1 2 3]	145	8900	9400	180	206.64	65.6
2	1.33	1.33	1.33	51.7	6	[0 1 1 1 1]	80	5700	5900	90	73.03	37.1
4	1	2	1.66	45	6	[1 0 3 2 0]	95	10300	10700	90	131.7	54.1
6	2	1.66	1	65	6	[2 3 2 0 3]	140	6600	6700	180	217.61	59.8

8	1.66	1	2	58.3	6	[3 2 0 3 2]	120	9700	10600	145	134.13	60.1
2	1.66	1.66	1.66	65	6	[0 2 2 2 3]	110	5800	5900	150	145.65	45.3
4	2	1	1.33	58.3	6	[1 3 0 1 2]	100	6000	6300	130	95.48	43.7
6	1	1.33	2	51.7	6	[2 0 1 3 1]	100	9600	10500	105	103.66	53.3
8	1.33	2	1	45	6	[3 1 3 0 0]	130	11300	11900	115	191.43	38.8
2	2	2	2	58.3	6	[0 3 3 3 2]	125	7600	7800	150	200.4	54.1
4	1.66	1.33	1	65	6	[1 2 1 0 3]	110	5200	5300	145	124.3	45.1
6	1.33	1	1.66	45	6	[2 1 0 2 0]	90	9100	10200	100	73.48	48.9
8	1	1.66	1.33	51.7	6	[3 0 2 1 1]	120	9700	10500	120	159.85	63.1
2	1.66	1.33	2	45	6	[0 2 1 3 0]	80	8400	9200	95	79.45	41.9
4	2	2	1	51.7	6	[1 3 3 0 1]	130	7300	7500	130	196.91	57.2
6	1	1.66	1.66	58.3	6	[2 0 2 2 2]	120	8400	8800	130	150.53	56.7
8	1.33	1	1.33	65	6	[3 1 0 1 3]	115	7700	8300	145	123.06	55.2
2	2	1	1.66	51.7	6	[0 3 0 2 1]	85	6200	6500	110	70.43	37.6
4	1.66	1.66	1.33	45	6	[1 2 2 1 0]	100	8800	9500	105	121.85	51.5
6	1.33	2	2	65	6	[2 1 3 3 3]	150	8900	9300	175	235.01	65.5
8	1	1.33	1	58.3	6	[3 0 1 0 2]	120	7700	8100	130	133.52	56.7
2	1	2	1.33	65	6	[0 0 3 1 3]	110	5100	5100	145	151.06	45
4	1.33	1.33	1.66	58.3	6	[1 1 1 2 2]	100	7000	7300	120	103.52	46.1
6	1.66	1	1	51.7	6	[2 2 0 0 1]	100	6900	7400	115	91.2	48
8	2	1.66	2	45	6	[3 3 2 3 0]	140	13200	14700	135	196.16	72.4
2	1.33	1.66	1	58.3	6	[0 1 2 0 2]	95	4700	4600	115	113.55	40.4
4	1	1	2	65	6	[1 0 0 3 3]	85	6900	7400	115	67.43	40.9
6	2	1.33	1.33	45	6	[2 3 1 1 0]	115	9300	10200	120	125.62	56.3
8	1.66	2	1.66	51.7	6	[3 2 3 2 1]	150	11400	12200	145	244.64	74

Unit and Nomenclature

t_{liner}: thickness of the liner (mm); t_0: thickness of 0° (axial) composite layers (mm); t_θ: thickness of ±θ° (angular) composite layers (mm); t_{90}: thickness of 90° (hoop) composite layers (mm); θ: angle of the ±θ° (angular) composite layers (degrees); and *n*: composite layers stacking sequences (1, 2, 3, 4, 5, 6).

LC1: Burst Case (MPa); LC2(a): Pure Tension Case (kN); LC2(b): Tension with External Pressure Case (kN); LC3: Collapse Case (MPa); LC4: Buckling (MPa).

Structural Weight: kg/m.

E.3 DOE Database for AS4/Epoxy with Aluminium liner

Table E.3. DOE database for AS4/epoxy with aluminium liner using orthogonal array

Variables						OA Sampling	Load Capacity					Structural Weight
t_{liner}	t_0	t_θ	t_{90}	θ	*n*		LC1	LC2(a)	LC2(b)	LC3	LC4	
2	1	1	1	45	1	[0 0 0 0 0]	60	4700	5000	60	48.4	27.9
4	1.33	1.66	2	51.7	1	[1 1 2 3 1]	160	6500	7000	120	192.69	50.3
6	1.66	2	1.33	58.3	1	[2 2 3 1 2]	165	7700	8500	135	253.29	58.6
8	2	1.33	1.66	65.0	1	[3 3 1 2 3]	145	8700	9800	150	240.84	57.5
2	1.33	1.33	1.33	51.7	1	[0 1 1 1 1]	100	5400	5800	90	91.15	36.4
4	1	2	1.66	45	1	[1 0 3 2 0]	120	6900	7200	90	196.6	51.4
6	2	1.66	1	65.0	1	[2 3 2 0 3]	140	8000	9100	140	207.77	53.4
8	1.66	1	2	58.3	1	[3 2 0 3 2]	140	7800	8700	130	200.24	52.4
2	1.66	1.66	1.66	65.0	1	[0 2 2 2 3]	110	5800	6400	150	156.71	45.2
4	2	1	1.33	58.3	1	[1 3 0 1 2]	105	7100	8100	105	114.99	40.4
6	1	1.33	2	51.7	1	[2 0 1 3 1]	140	6100	6600	120	177.78	48.4
8	1.33	2	1	45	1	[3 1 3 0 0]	105	9100	9600	90	238.45	59.6
2	2	2	2	58.3	1	[0 3 3 3 2]	160	7200	7900	145	217.51	54.6
4	1.66	1.33	1	65.0	1	[1 2 1 0 3]	115	6200	7100	120	124.13	41.3
6	1.33	1	1.66	45	1	[2 1 0 2 0]	100	7100	7800	95	135.1	43.4
8	1	1.66	1.33	51.7	1	[3 0 2 1 1]	140	6900	7400	105	213.04	54.4
2	1.66	1.33	2	45	1	[0 2 1 3 0]	110	7000	7700	100	118.53	42.3
4	2	2	1	51.7	1	[1 3 3 0 1]	120	8400	9100	100	197.05	53.5
6	1	1.66	1.66	58.3	1	[2 0 2 2 2]	130	5800	6300	130	204.26	51.3
8	1.33	1	1.33	65.0	1	[3 1 0 1 3]	115	6700	7600	125	153.54	46.5
2	2	1	1.66	51.7	1	[0 3 0 2 1]	95	6800	7600	95	90.1	37.4
4	1.66	1.66	1.33	45	1	[1 2 2 1 0]	95	8100	8800	90	163.28	48.2
6	1.33	2	2	65.0	1	[2 1 3 3 3]	130	6600	7300	175	292.05	60.7
8	1	1.33	1	58.3	1	[3 0 1 0 2]	125	6200	6700	110	158.06	47.4
2	1	2	1.33	65.0	1	[0 0 3 1 3]	95	4300	4600	150	168.97	44.3
4	1.33	1.33	1.66	58.3	1	[1 1 1 2 2]	120	5700	6300	120	142.28	43.3
6	1.66	1	1	51.7	1	[2 2 0 0 1]	85	7300	8100	85	117.77	41.5
8	2	1.66	2	45	1	[3 3 2 3 0]	135	10600	11800	120	293.53	64.8
2	1.33	1.66	1	58.3	1	[0 1 2 0 2]	120	5100	5500	105	111.67	39.3
4	1	1	2	65.0	1	[1 0 0 3 3]	90	4500	5000	135	115.38	38.5
6	2	1.33	1.33	45	1	[2 3 1 1 0]	90	9300	10300	90	177.45	50.3
8	1.66	2	1.66	51.7	1	[3 2 3 2 1]	170	9000	9900	125	307.87	65.9
2	1	1	1	45	2	[0 0 0 0 0]	60	5100	5200	60	35.39	27.9
4	1.33	1.66	2	51.7	2	[1 1 2 3 1]	130	7500	7400	110	183.53	53.4
6	1.66	2	1.33	58.3	2	[2 2 3 1 2]	125	7600	7900	135	180.52	52.4
8	2	1.33	1.66	65.0	2	[3 3 1 2 3]	140	8800	9400	150	250.25	60.6
2	1.33	1.33	1.33	51.7	2	[0 1 1 1 1]	95	5800	5800	85	76.64	36.4
4	1	2	1.66	45	2	[1 0 3 2 0]	110	7500	7500	100	132.28	48.3
6	2	1.66	1	65.0	2	[2 3 2 0 3]	115	7800	8400	130	151.6	47.4
8	1.66	1	2	58.3	2	[3 2 0 3 2]	150	8700	9000	125	246.66	61.7
2	1.66	1.66	1.66	65.0	2	[0 2 2 2 3]	105	5900	6000	145	149.35	45.2
4	2	1	1.33	58.3	2	[1 3 0 1 2]	110	7600	8000	100	117.52	43.3
6	1	1.33	2	51.7	2	[2 0 1 3 1]	135	7200	7000	105	186.59	54.5
8	1.33	2	1	45	2	[3 1 3 0 0]	105	8400	8900	110	135.71	50.5
2	2	2	2	58.3	2	[0 3 3 3 2]	135	7600	7700	140	201.52	54.6
4	1.66	1.33	1	65.0	2	[1 2 1 0 3]	100	6100	6600	115	97.82	38.4
6	1.33	1	1.66	45	2	[2 1 0 2 0]	95	8900	8900	80	127.72	49.3
8	1	1.66	1.33	51.7	2	[3 0 2 1 1]	120	7200	7400	110	154.64	51.4
2	1.66	1.33	2	45	2	[0 2 1 3 0]	105	9000	9100	80	125.54	48.3
4	2	2	1	51.7	2	[1 3 3 0 1]	105	8000	8500	110	114.81	44.4
6	1	1.66	1.66	58.3	2	[2 0 2 2 2]	120	6100	6100	130	180.56	51.3
8	1.33	1	1.33	65.0	2	[3 1 0 1 3]	115	6800	7200	125	163.51	49.4

2	2	1	1.66	51.7	2	[0 3 0 2 1]	105	7900	8100	85	104.37	43.3
4	1.66	1.66	1.33	45	2	[1 2 2 1 0]	100	8500	8800	90	107.49	45.2
6	1.33	2	2	65.0	2	[2 1 3 3 3]	125	6700	6800	175	275.03	60.7
8	1	1.33	1	58.3	2	[3 0 1 0 2]	105	6200	6500	110	119.88	44.5
2	1	2	1.33	65.0	2	[0 0 3 1 3]	80	4100	4100	140	116.37	38.4
4	1.33	1.33	1.66	58.3	2	[1 1 1 2 2]	115	6100	6200	115	145.85	46.2
6	1.66	1	1	51.7	2	[2 2 0 0 1]	85	7700	8100	85	96.17	41.5
8	2	1.66	2	45	2	[3 3 2 3 0]	135	12700	13100	110	245.45	68.1
2	1.33	1.66	1	58.3	2	[0 1 2 0 2]	85	4900	5100	105	69.5	33.5
4	1	1	2	65.0	2	[1 0 0 3 3]	105	5000	4900	140	174.22	47.4
6	2	1.33	1.33	45	2	[2 3 1 1 0]	100	10200	10700	90	133.26	50.3
8	1.66	2	1.66	51.7	2	[3 2 3 2 1]	140	9500	9900	130	235	62.7
2	1	1	1	45	3	[0 0 0 0 0]	55	4800	5200	65	55.32	27.9
4	1.33	1.66	2	1.7	3	[1 1 2 3 1]	120	7400	8100	120	190.95	47.3
6	1.66	2	1.33	58.3	3	[2 2 3 1 2]	125	8800	10000	130	236.76	55.4
8	2	1.33	1.66	65.0	3	[3 3 1 2 3]	145	7800	8700	170	319.15	63.8
2	1.33	1.33	1.33	51.7	3	[0 1 1 1 1]	85	5600	6100	95	112.7	36.4
4	1	2	1.66	45	3	[1 0 3 2 0]	85	8300	9400	95	140.91	42.3
6	2	1.66	1	65.0	3	[2 3 2 0 3]	135	7900	9100	155	243.48	56.5
8	1.66	1	2	58.3	3	[3 2 0 3 2]	145	6800	7500	145	270.71	58.5
2	1.66	1.66	1.66	65.0	3	[0 2 2 2 3]	120	6200	7100	150	207.43	45.2
4	2	1	1.33	58.3	3	[1 3 0 1 2]	130	5600	6000	130	209.2	49.4
6	1	1.33	2	51.7	3	[2 0 1 3 1]	110	6800	7500	115	163.64	45.4
8	1.33	2	1	45	3	[3 1 3 0 0]	90	10300	11400	90	186.81	53.5
2	2	2	2	58.3	3	[0 3 3 3 2]	160	7800	8700	150	286.07	54.6
4	1.66	1.33	1	65.0	3	[1 2 1 0 3]	115	5900	6800	135	162.37	44.2
6	1.33	1	1.66	45	3	[2 1 0 2 0]	100	6900	7400	100	163.42	46.3
8	1	1.66	1.33	51.7	3	[3 0 2 1 1]	95	8300	9300	105	164.98	48.4
2	1.66	1.33	2	45	3	[0 2 1 3 0]	110	6900	7500	100	167.9	45.2
4	2	2	1	51.7	3	[1 3 3 0 1]	105	8900	9900	105	212.83	53.5
6	1	1.66	1.66	58.3	3	[2 0 2 2 2]	110	7300	8300	120	163.72	45.3
8	1.33	1	1.33	65.0	3	[3 1 0 1 3]	120	6200	7000	140	181.37	49.4
2	2	1	1.66	51.7	3	[0 3 0 2 1]	120	5500	5800	105	191.82	46.3
4	1.66	1.66	1.33	45	3	[1 2 2 1 0]	90	8400	9200	90	177.96	48.2
6	1.33	2	2	65.0	3	[2 1 3 3 3]	145	8400	9600	155	252.97	54.4
8	1	1.33	1	58.3	3	[3 0 1 0 2]	95	7000	7900	105	131.1	44.5
2	1	2	1.33	65.0	3	[0 0 3 1 3]	90	6500	7600	115	120.98	35.5
4	1.33	1.33	1.66	58.3	3	[1 1 1 2 2]	115	6000	6600	125	163.38	43.3
6	1.66	1	1	51.7	3	[2 2 0 0 1]	100	6400	6800	95	162.24	47.3
8	2	1.66	2	45	3	[3 3 2 3 0]	140	10600	11600	120	337	68.1
2	1.33	1.66	1	58.3	3	[0 1 2 0 2]	85	6100	6900	100	113.42	36.4
4	1	1	2	65.0	3	[1 0 0 3 3]	90	4700	5200	135	133.99	38.5
6	2	1.33	1.33	45	3	[2 3 1 1 0]	105	8700	9400	95	233.75	56.5
8	1.66	2	1.66	51.7	3	[3 2 3 2 1]	130	10100	11300	125	288.71	62.7
2	1	1	1	45	4	[0 0 0 0 0]	50	5100	5400	60	36.29	27.9
4	1.33	1.66	2	51.7	4	[1 1 2 3 1]	90	8700	9600	110	114.37	47.3
6	1.66	2	1.33	58.3	4	[2 2 3 1 2]	120	7400	8100	145	198.19	55.4
8	2	1.33	1.66	65.0	4	[3 3 1 2 3]	135	8900	10100	165	244.16	63.8
2	1.33	1.33	1.33	51.7	4	[0 1 1 1 1]	75	5900	6400	90	74.42	36.4
4	1	2	1.66	45	4	[1 0 3 2 0]	80	7800	8600	100	88.86	42.3
6	2	1.66	1	65.0	4	[2 3 2 0 3]	125	6300	6900	165	230.91	56.5
8	1.66	1	2	58.3	4	[3 2 0 3 2]	110	9900	11100	125	173.08	58.5
2	1.66	1.66	1.66	65.0	4	[0 2 2 2 3]	105	6500	7200	150	141.38	45.2
4	2	1	1.33	58.3	4	[1 3 0 1 2]	105	6700	7300	125	156.98	49.4
6	1	1.33	2	51.7	4	[2 0 1 3 1]	80	8900	9900	100	90.8	45.4
8	1.33	2	1	45	4	[3 1 3 0 0]	100	8000	8600	110	172.57	53.5
2	2	2	2	58.3	4	[0 3 3 3 2]	120	8300	9100	150	197.46	54.6
4	1.66	1.33	1	65.0	4	[1 2 1 0 3]	100	5200	5700	145	139.26	44.2

6	1.33	1	1.66	45	4	[2 1 0 2 0]	75	9100	9900	80	101.74	46.3
8	1	1.66	1.33	51.7	4	[3 0 2 1 1]	90	7700	8500	110	122.63	48.4
2	1.66	1.33	2	45	4	[0 2 1 3 0]	75	9300	10200	85	100.31	45.2
4	2	2	1	51.7	4	[1 3 3 0 1]	115	6600	7000	120	203.04	53.5
6	1	1.66	1.66	58.3	4	[2 0 2 2 2]	90	7600	8500	120	103.6	45.3
8	1.33	1	1.33	65.0	4	[3 1 0 1 3]	100	7300	8200	130	131.31	49.4
2	2	1	1.66	51.7	4	[0 3 0 2 1]	85	7600	8200	100	125.46	46.3
4	1.66	1.66	1.33	45	4	[1 2 2 1 0]	85	8000	8600	100	137.16	48.2
6	1.33	2	2	65.0	4	[2 1 3 3 3]	115	8700	9800	155	165.08	54.4
8	1	1.33	1	58.3	4	[3 0 1 0 2]	90	6300	7000	110	106.81	44.5
2	1	2	1.33	65.0	4	[0 0 3 1 3]	85	5100	5600	130	80.29	35.5
4	1.33	1.33	1.66	58.3	4	[1 1 1 2 2]	90	7100	7900	115	101.82	43.3
6	1.66	1	1	51.7	4	[2 2 0 0 1]	90	6700	7000	95	133.27	47.3
8	2	1.66	2	45	4	[3 3 2 3 0]	110	12400	13500	115	245.83	68.1
2	1.33	1.66	1	58.3	4	[0 1 2 0 2]	85	4600	4900	115	91.5	36.4
4	1	1	2	65.0	4	[1 0 0 3 3]	75	7400	8500	110	64.11	38.5
6	2	1.33	1.33	45	4	[2 3 1 1 0]	95	9300	9900	95	186.99	56.5
8	1.66	2	1.66	51.7	4	[3 2 3 2 1]	120	9700	10600	135	225.06	62.7
2	1	1	1	45	5	[0 0 0 0 0]	55	5300	5500	60	46.31	27.9
4	1.33	1.66	2	51.7	5	[1 1 2 3 1]	135	8800	8900	105	213.99	53.4
6	1.66	2	1.33	58.3	5	[2 2 3 1 2]	135	8900	9500	125	205.77	52.4
8	2	1.33	1.66	65.0	5	[3 3 1 2 3]	135	7500	7700	165	284.89	60.6
2	1.33	1.33	1.33	51.7	5	[0 1 1 1 1]	95	6100	6200	85	106.18	36.4
4	1	2	1.66	45	5	[1 0 3 2 0]	80	10800	11300	75	146.79	48.3
6	2	1.66	1	65.0	5	[2 3 2 0 3]	120	7200	7700	140	176.7	47.4
8	1.66	1	2	58.3	5	[3 2 0 3 2]	145	7400	7500	140	274.1	61.7
2	1.66	1.66	1.66	65.0	5	[0 2 2 2 3]	115	6100	6300	145	209.71	45.2
4	2	1	1.33	58.3	5	[1 3 0 1 2]	105	5400	5500	125	154.37	43.3
6	1	1.33	2	51.7	5	[2 0 1 3 1]	125	8400	8300	95	199.78	54.5
8	1.33	2	1	45	5	[3 1 3 0 0]	90	10800	11800	90	127.08	50.5
2	2	2	2	58.3	5	[0 3 3 3 2]	150	8100	8300	140	285.1	54.6
4	1.66	1.33	1	65.0	5	[1 2 1 0 3]	95	5500	5800	120	124.87	38.4
6	1.33	1	1.66	45	5	[2 1 0 2 0]	100	8500	8500	85	139.8	49.3
8	1	1.66	1.33	51.7	5	[3 0 2 1 1]	105	9300	9700	95	158.3	51.4
2	1.66	1.33	2	45	5	[0 2 1 3 0]	115	8800	9000	90	173.76	48.3
4	2	2	1	51.7	5	[1 3 3 0 1]	105	8500	9200	110	139.59	44.4
6	1	1.66	1.66	58.3	5	[2 0 2 2 2]	135	8000	8200	110	193.12	51.3
8	1.33	1	1.33	65.0	5	[3 1 0 1 3]	115	6200	6400	135	176.98	49.4
2	2	1	1.66	51.7	5	[0 3 0 2 1]	115	5800	5800	110	160.76	43.3
4	1.66	1.66	1.33	45	5	[1 2 2 1 0]	95	9100	9600	90	128.42	45.2
6	1.33	2	2	65.0	5	[2 1 3 3 3]	155	8600	8900	155	299.93	60.7
8	1	1.33	1	58.3	5	[3 0 1 0 2]	100	7200	7600	100	122.56	44.5
2	1	2	1.33	65.0	5	[0 0 3 1 3]	110	6600	6900	110	138.39	38.4
4	1.33	1.33	1.66	58.3	5	[1 1 1 2 2]	125	6400	6500	115	175.14	46.2
6	1.66	1	1	51.7	5	[2 2 0 0 1]	100	6300	6500	100	103.91	41.5
8	2	1.66	2	45	5	[3 3 2 3 0]	145	12600	13100	115	265.61	68.1
2	1.33	1.66	1	58.3	5	[0 1 2 0 2]	85	6000	6400	95	98.05	33.5
4	1	1	2	65.0	5	[1 0 0 3 3]	110	5100	5000	140	195.87	47.4
6	2	1.33	1.33	45	5	[2 3 1 1 0]	115	8900	9400	105	146.01	50.3
8	1.66	2	1.66	51.7	5	[3 2 3 2 1]	140	11100	11700	120	252.05	62.7
2	1	1	1	45	6	[0 0 0 0 0]	50	5500	5700	60	30.91	27.9
4	1.33	1.66	2	51.7	6	[1 1 2 3 1]	95	9900	10400	105	121.46	50.3
6	1.66	2	1.33	58.3	6	[2 2 3 1 2]	125	8000	8300	140	206.21	58.6
8	2	1.33	1.66	65	6	[3 3 1 2 3]	120	8600	9100	160	175.86	57.5
2	1.33	1.33	1.33	51.7	6	[0 1 1 1 1]	75	6300	6600	90	69.92	36.4
4	1	2	1.66	45	6	[1 0 3 2 0]	80	10800	11300	80	122.79	51.4
6	2	1.66	1	65	6	[2 3 2 0 3]	120	6200	6300	165	190.3	53.4
8	1.66	1	2	58.3	6	[3 2 0 3 2]	100	9700	10600	125	114.49	52.4

2	1.66	1.66	1.66	65	6	[0 2 2 2 3]	105	6600	6900	145	140.02	45.2
4	2	1	1.33	58.3	6	[1 3 0 1 2]	90	6200	6600	120	85.29	40.4
6	1	1.33	2	51.7	6	[2 0 1 3 1]	85	9900	10600	95	92.83	48.4
8	1.33	2	1	45	6	[3 1 3 0 0]	105	10400	10400	95	166.38	59.6
2	2	2	2	58.3	6	[0 3 3 3 2]	120	8800	9200	145	195.93	54.6
4	1.66	1.33	1	65	6	[1 2 1 0 3]	95	5100	5200	135	110.44	41.3
6	1.33	1	1.66	45	6	[2 1 0 2 0]	75	9100	9900	85	65.38	43.4
8	1	1.66	1.33	51.7	6	[3 0 2 1 1]	100	9100	9300	100	136.93	54.4
2	1.66	1.33	2	45	6	[0 2 1 3 0]	75	9600	10500	90	79.84	42.3
4	2	2	1	51.7	6	[1 3 3 0 1]	115	7300	7400	120	181.03	53.5
6	1	1.66	1.66	58.3	6	[2 0 2 2 2]	100	8500	8800	115	132.01	51.3
8	1.33	1	1.33	65	6	[3 1 0 1 3]	95	7100	7700	125	101.5	46.5
2	2	1	1.66	51.7	6	[0 3 0 2 1]	80	7000	7500	105	68.5	37.4
4	1.66	1.66	1.33	45	6	[1 2 2 1 0]	90	9100	9600	95	112.56	48.2
6	1.33	2	2	65	6	[2 1 3 3 3]	130	9300	9800	160	209.86	60.7
8	1	1.33	1	58.3	6	[3 0 1 0 2]	95	6800	7000	110	110.94	47.4
2	1	2	1.33	65	6	[0 0 3 1 3]	105	5700	5800	140	143.7	44.3
4	1.33	1.33	1.66	58.3	6	[1 1 1 2 2]	90	7400	7900	110	93.96	43.3
6	1.66	1	1	51.7	6	[2 2 0 0 1]	85	6400	6700	100	77.53	41.5
8	2	1.66	2	45	6	[3 3 2 3 0]	115	13200	14300	120	174.24	64.8
2	1.33	1.66	1	58.3	6	[0 1 2 0 2]	90	5000	5000	110	107.24	39.3
4	1	1	2	65	6	[1 0 0 3 3]	80	7500	8200	105	61.23	38.5
6	2	1.33	1.33	45	6	[2 3 1 1 0]	95	9100	9700	110	110.81	50.3
8	1.66	2	1.66	51.7	6	[3 2 3 2 1]	125	11100	11600	125	214.8	65.9

Unit and Nomenclature

t_{liner}: thickness of the liner (mm); t_0: thickness of 0° (axial) composite layers (mm); t_θ: thickness of ±θ° (angular) composite layers (mm); t_{90}: thickness of 90° (hoop) composite layers (mm); θ: angle of the ±θ° (angular) composite layers (degrees); and *n*: composite layers stacking sequences (1, 2, 3, 4, 5, 6).

LC1: Burst Case (MPa); LC2(a): Pure Tension Case (kN); LC2(b): Tension with External Pressure Case (kN); LC3: Collapse Case (MPa); LC4: Buckling (MPa).

Structural Weight: kg/m.

APPENDIX F

SAEA OPTIMISATION FOR AS4/EPOXY WITH TITANIUM AND ALUMINIUM LINERS

F.1 Critical Load Combinations for AS4/PEEK with PEEK Liner with Optimised Geometry from Global Analysis

Table F.1. Critical load combinations and locations for AS4/PEEK with PEEK Liner with optimised geometry from global analysis

Load Case	Location	Tension (kN)	Internal Pressure (MPa)	External Pressure (MPa)	Shear Force (kN)	Bending Moment (kN·m)
4	Top	3156.0	44.3	0.7	43.4	50.9
	Bottom	2202.3	58.7	19.2	50.4	40.1
5	Top	3117.5	44.3	0.7	30.9	9.5
	Bottom	2162.4	58.7	19.2	78.3	59.0
6	Top	2294.9	1.8	0.7	107.8	44.9
	Bottom	1306.7	35.3	19.2	95.6	44.6
7	Top	2219.1	1.8	0.7	85.5	4.3
	Bottom	1273.2	35.3	19.2	136.9	62.8
8	Top	2070.8	0	0.7	77.6	38.1
	Bottom	324.1	0	19.2	115.8	20.0
9	Top	2033.0	0	0.7	120.8	4.6
	Bottom	289.3	0	19.2	171.8	28.2

F.2 Optimisation Results for AS4/Epoxy Composite Body with Titanium Liner

The geometry of the composite riser is optimised following the optimisation chain given in Section 7.2.5 in *Chapter 7* for the AS4/epoxy composite body with titanium liner. The results obtained by SAEA after verification of its optimised geometry are detailed below for illustration.

F.2.1 Iteration Cycles of Optimisation

As shown in the optimisation chain in Fig. 7.2, in the first cycle of optimisation, the initial DOE database (for the AS4/epoxy with titanium liner riser consisting of the design variables, load capacities and structural weight listed in Table E.2 in *Appendix E*) is employed. The progressive result for the objective function value (structural weight) using the initial DOE database in the first SAEA optimisation cycle is plotted in Fig. F.1. This optimisation, performed for up to 200 generations based on the initial DOE database, provides a reduction in structural weight from 66.5kg/m to 43.7kg/m (the true value is 45.1kg/m). It may be noted that this optimisation result approaches its asymptotic value within about 70 generations.

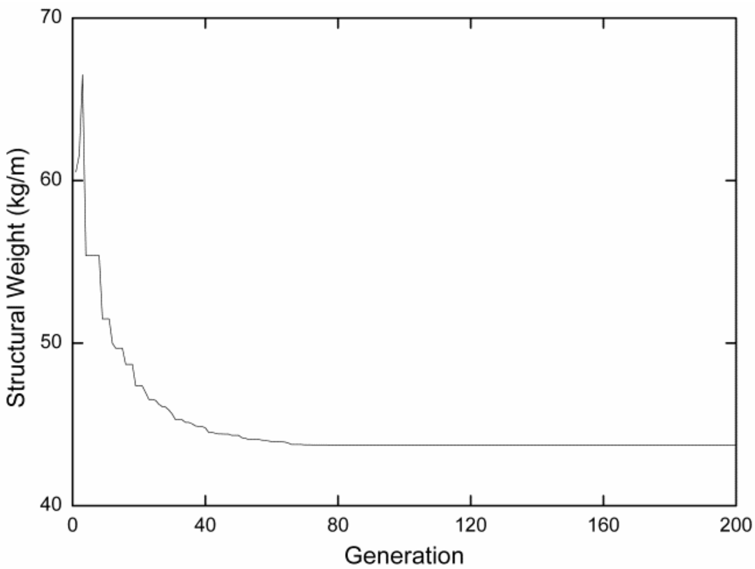

Fig. F.1. Progress of optimisation in the first cycle

The ‘optimised’ structural weight of 45.1kg/m obtained from the first optimisation cycle fails in the verification step. Therefore, it is obvious that more iterative cycles are needed to generate a more accurate ‘optimised’ geometry. In the iterative optimisation process, the ranges of the variables, training database and constraint functions are modified after each cycle to converge towards the final geometry. It is found that the predicted load capacities are somewhat larger than their true values while the predicted minimum structural weight is correct. Although the errors in load capacities predicted by the surrogate models in the optimisation are quite small, they can cause many predicted 'feasible' points to violate the constraint functions in the verification using the FEA simulation. A detailed analysis shows that, for the AS4/epoxy with titanium liner riser, the constraint of load cases 1 (burst), is quite sensitive to the design.

The true structural weights obtained after every optimum design cycle are plotted against the cycle numbers in Fig. F.2, where the dashed-dotted green line represents the structural weight obtained by the manually tailored design developed in *Chapter 5* (45.71kg/m). The blocks in the figure show the true structural weights after each optimisation cycle and a cross inside any of them indicates that the 'optimised' geometry in the given cycle number satisfies all the constraint requirements (local load cases 1-4), as determined from the results using the FEA simulation.

In Fig. F.2, it is evident that, after six or seven cycles, the optimised structural weight asymptotes to the value of the minimum weight from the manually tailored design but that a fully feasible optimised geometry which satisfies all the constraints and provides less structural weight than that of the manually tailored design is obtained only in the twelfth cycle, after which the optimised structural weight is 45.46kg/m.

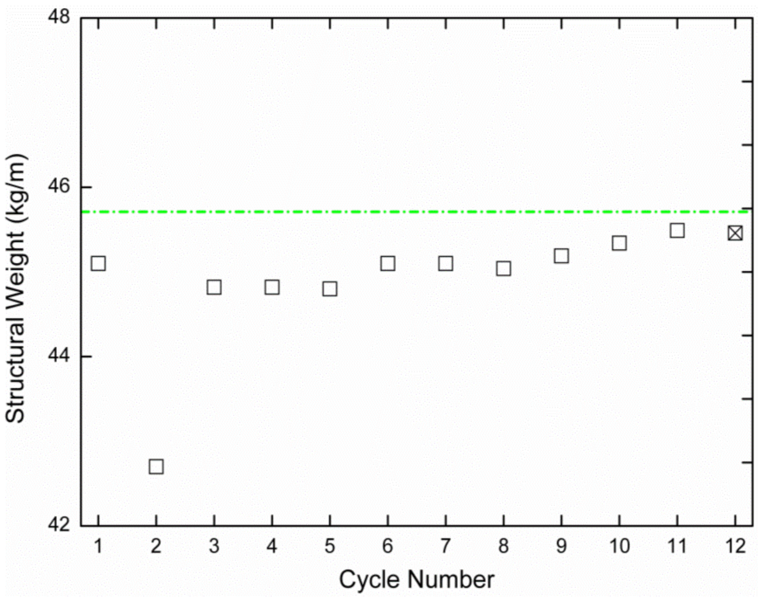

Fig. F.2. True structural weight results for every optimisation design cycle

The final values obtained after the 12th cycle for the six design parameters, t_{liner}, t_0, t_θ, t_{90}, $\pm\theta^o$ and n, are 2.00mm, 1.77mm, 1.61mm, 1.73mm, 53.4^o and 1, respectively, for the AS4/epoxy with titanium liner riser. This optimised geometry providing the least weight is verified by the FEA simulation during the optimisation process.

The values of the design variables of the optimum design (SAEA) of the AS4/epoxy with titanium liner are plotted in Fig. F.3 for comparison with those of the conventional and tailored designs using the iterative approach of manual inspection and selection. It should be noted that, for the conventional design, as there is no off-axis angle of reinforcement, θ, there is no t_θ and no stacking sequence variable, *n*. In this figure, the values of the design variables in the Y axis are normalised with the values shown at the top of the figure in order to facilitate the display of all the values in the same graph. It can be seen that the thicknesses of the axial, hoop and off-axis layers from the tailored designs using the manual approach and mathematical optimisation (SAEA) yield different results, while the thicknesses of liner are the same as are the stacking sequences. The optimum angles of the off-axis layers are also different, being 53.0^o for the manually tailored design and 53.4^o for the SAEA tailored design. However, the overall thicknesses of the configurations of both tailored designs are quite close, being 30.50mm and 30.33mm, respectively as are the structural weights, being 45.71kg/m and 45.46kg/m, respectively.

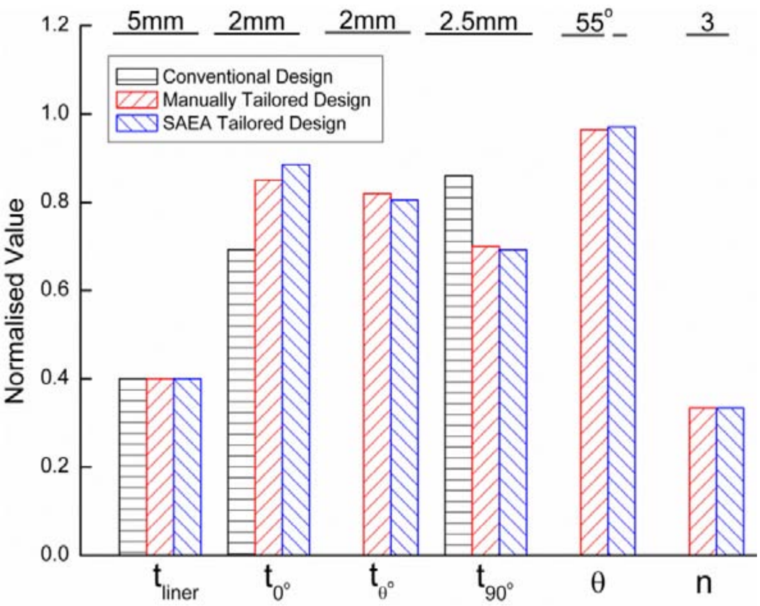

Fig. F.3. Design variables obtained for three designs

F.2.2 Verification under Local Load Cases

The local load capacities of the optimum geometry using SAEA for the AS4/epoxy with titanium liner are presented in Fig. F.4, normalised with respect to the magnitudes of the corresponding load requirements, and the normalised load capacities of the manually optimised geometry (manually tailored design). It can be seen that, although there are some differences in the load capacities provided by the two tailored design approaches, their structural weights are very close. The green dashed line with the ordinate value of 1.0 represents the normalised load requirement for each case.

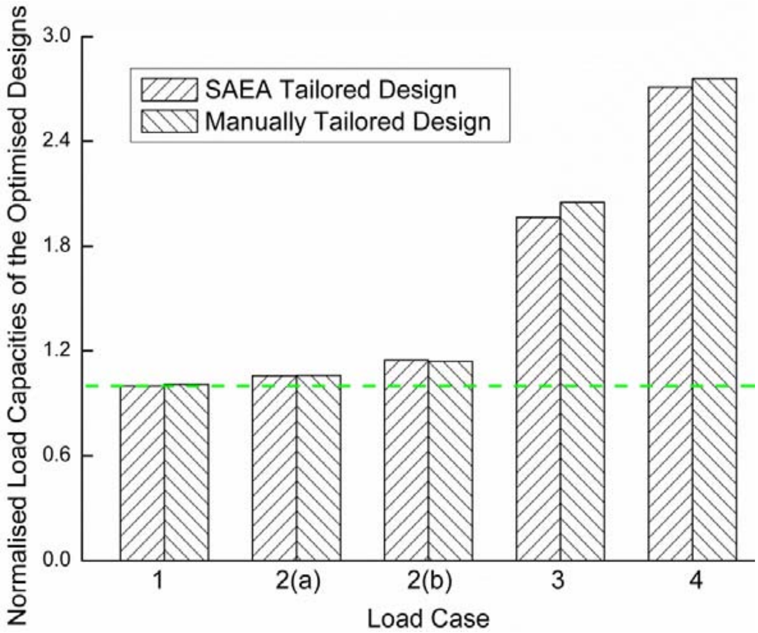

Fig. F.4. Comparison of load capacities of tailored designs

F.2.3 Verification under Global Load Cases

As the optimisation process using SAEA is based on local load constraints, the performance of the optimum geometry for global load cases has to be verified. Both the global design procedure for all the material combinations selected, and the global design load cases used for the global FE analysis are the same as those in *Chapter 6*. The effective 3D composite tubular properties employed in the global FE analysis are listed in Table F.2 using the same calculation process as in *Chapter 6*.

Table F.2. Effective 3D properties of composite tubular used in global analysis

Name	$\rho_{effective}$ (kg/m^3)	$E_{x\_tension}$ (GPa)	$E_{x\_bending}$ (GPa)	E_y (GPa)	E_z (GPa)	G_{xy} (GPa)	G_{xz} (GPa)	G_{yz} (GPa)	ν_{xy}	ν_{xz}	ν_{yz}
AS4/epoxy-Ti liner [0/±53.4/90]	1701.9	41.22	37.18	66.68	12.02	22.54	4.09	4.34	0.27	0.346	0.277

Conducting a global analysis of the entire riser using pipe elements (Pipe288) as in *Chapter 6*, the critical locations and the force, moment and pressure combinations at these locations are identified. The magnitudes of the loads at the critical locations are listed in Table F.3.

Table F.3. Critical load combinations and locations for AS4/epoxy with titanium liner with optimised geometry from global analysis

Load Case	Location	Tension (kN)	Internal Pressure (MPa)	External Pressure (MPa)	Shear Force (kN)	Bending Moment (kN·m)
4	Top	3373.5	44.3	0.7	50.7	57.7
	Bottom	2295.1	58.7	19.2	60.6	45.8
5	Top	3313.3	44.3	0.7	44.2	10.0
	Bottom	2254.8	58.7	19.2	91.6	67.1
6	Top	2447.2	1.8	0.7	114.9	54.0
	Bottom	1366.1	35.3	19.2	102.8	51.7
7	Top	2370.1	1.8	0.7	94.2	5.2
	Bottom	1318.0	35.3	19.2	145.2	72.8
8	Top	2223.7	0	0.7	80.1	54.2
	Bottom	356.2	0	19.2	120.0	24.0
9	Top	2162.8	0	0.7	128.1	5.4
	Bottom	315.6	0	19.2	179.3	33.9

In the final stage, a local analysis of the identified critical sections with the corresponding load combinations is conducted again using layered solid elements, as in *Chapter 6*. The minimum FSs in the titanium liner and various layers of the composite body of the AS4/epoxy riser with the geometry optimised using the optimisation technique SAEA are given in Table F.4.

Table F.4. Minimum FSs for liner and composite layers of the AS4/epoxy with titanium liner with SAEA optimised geometry

Material Combination	Liner		Composite Layers-Fibre Direction			Composite Layers-Transverse Direction			Composite Layers–In-Plane Shear		
	FS	LC	FS	Layer	LC	FS	Layer	LC	FS	Layer	LC
AS4-Titanium [0/±53.4/90]	1.97	LC4-T	4.34	3	LC6-T	1.58	17	LC4-T	3.95	13	LC6-T

Minimum FS required: 1.53 for composite layers, 1.74 for PEEK liner and 1.68 for metallic liners [72]

The results presented in Table F.4 show that the composite tubular geometry optimised for minimum weight in the local design stage using SAEA is able to successfully withstand the global loads providing their FSs are just above the values required by the standards [72].

F.3 Optimisation Results for AS4/Epoxy Composite Body with Aluminium Liner

The geometry of the composite riser is optimised following the optimisation chain given in Section 7.2.5 in *Chapter 7* for the AS4/epoxy composite body with aluminium liner. The results obtained by SAEA after verification of its optimised geometry are detailed below for illustration.

F.3.1 Iteration Cycles of Optimisation

As shown in the optimisation chain in Fig. 7.2, in the first cycle of optimisation, the initial DOE database (for the AS4/epoxy with aluminium liner riser consisting of the design variables, load capacities and structural weight listed in Table E.3 in *Appendix E*) is employed. The progressive result for the objective function value (structural weight) using the initial DOE database in the first SAEA optimisation cycle is plotted in Fig. F.5. This optimisation, performed for up to 200 generations based on the initial DOE database, provides a reduction in structural weight from 57.6kg/m to 48.4kg/m (the true value is 47.9kg/m). It may be noted that this optimisation result approaches its asymptotic value within about 40 generations.

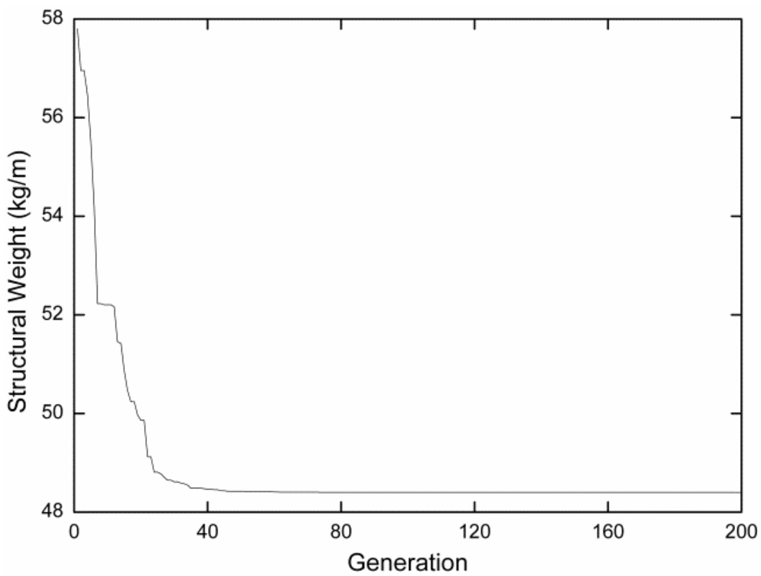

Fig. F.5. Progress of optimisation in the first cycle

Although the 'optimised' structural weight of 47.9kg/m obtained from the first optimisation cycle is about 6% higher than the minimum weight of 45.35kg/m obtained from the manually tailored design in *Chapter 5*, it is still lower than the minimum weight from the conventional design of 60.93kg/m. Therefore, it is obvious that more iterative cycles are needed to generate a more accurate 'optimised' geometry. In the iterative optimisation process, the ranges of the variables, training database and constraint functions are modified after each cycle to converge towards the final geometry. It is found that the predicted load capacities are somewhat larger than their true values while the predicted minimum structural weight is correct. Although the errors in load capacities predicted by the surrogate models in the optimisation are quite small, they can cause many predicted 'feasible' points to violate the constraint functions in the verification using the FEA simulation. A detailed analysis shows that, for the AS4/epoxy with aluminium liner riser, the constraint of load cases 1 (burst) is quite sensitive to the design.

The true structural weights obtained after every optimum design cycle are plotted against the cycle numbers in Fig. F.6, where the dashed-dotted green line represents the structural weight obtained by the manually tailored design developed in *Chapter 5* (45.35kg/m). The blocks in the figure show the true structural weights after each optimisation cycle and a cross inside any of them indicates that the 'optimised' geometry in the given cycle number satisfies all the constraint requirements (local load cases 1-4), as determined from the results using the FEA simulation.

In Fig. F.6, it is evident that, after three or four cycles, the optimised structural weight asymptotes to the value of the minimum weight from the manually tailored design but that a fully feasible optimised geometry which satisfies all the constraints and provides less structural weight than that of the manually tailored design is obtained only in the eighth cycle, after which the optimised structural weight is 45.20kg/m.

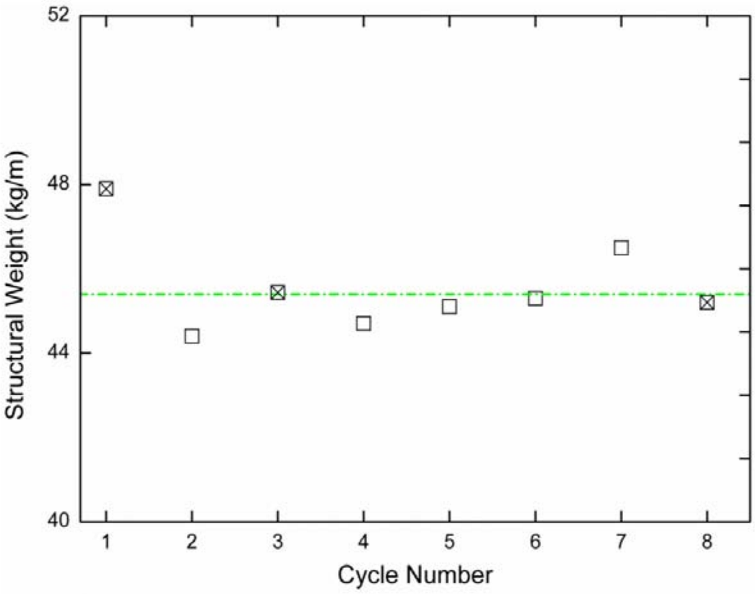

Fig. F.6. True structural weight results for every optimisation design cycle

The final values obtained after the 8th cycle for the six design parameters, t_{liner}, t_0, t_θ, t_{90}, $\pm\theta^o$ and n, are 6.0mm, 1.62mm, 1.57mm, 1.93mm, 53.4^o and 1, respectively, for the AS4/epoxy with aluminium liner riser. This optimised geometry providing the least weight is verified by the FEA simulation during the optimisation process.

The values of the design variables of the optimum design (SAEA) of the AS4/epoxy with aluminium liner are plotted in Fig. F.7 for comparison with those of the conventional and tailored designs using the iterative approach of manual inspection and selection. It should be noted that, for the conventional design, as there is no off-axis angle of reinforcement, θ, there is no t_θ and no stacking sequence variable, *n*. In this figure, the values of the design variables in the Y axis are normalised with the values shown at the top of the figure in order to facilitate the display of all the values in the same graph. It can be seen that the thicknesses of the hoop and off-axis layers from the tailored designs using the manual approach and mathematical optimisation (SAEA) yield different results, while the thicknesses of the axial layers and liner are the same as are the stacking sequences. The optimum angles of the off-axis layers are also different, being 53.5^o for the manually tailored design and 53.4^o for the SAEA tailored design. However, the overall thicknesses of the configurations of both tailored designs are quite close, being 32.00mm and 31.90mm, respectively as are the structural weights, being 45.35kg/m and 45.20kg/m, respectively.

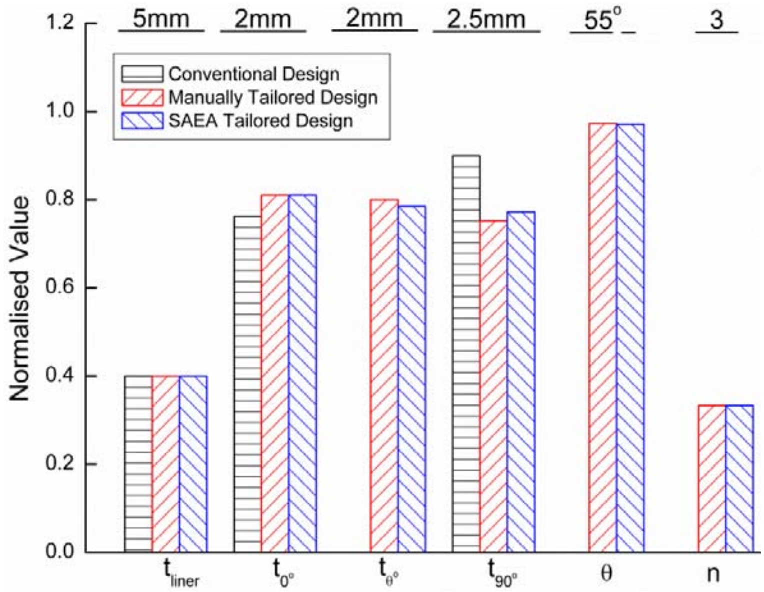

Fig. F.7. Design variables obtained for three designs

F.3.2 Verification under Local Load Cases

The local load capacities of the optimum geometry using SAEA for the AS4/epoxy with aluminium liner are presented in Fig. F.8, normalised with respect to the magnitudes of the corresponding load requirements, and the normalised load capacities of the manually optimised geometry (manually tailored design). It can be seen that, although there are some differences in the load capacities provided by the two tailored design approaches, their structural weights are very close. The green dashed line with the ordinate value of 1.0 represents the normalised load requirement for each case.

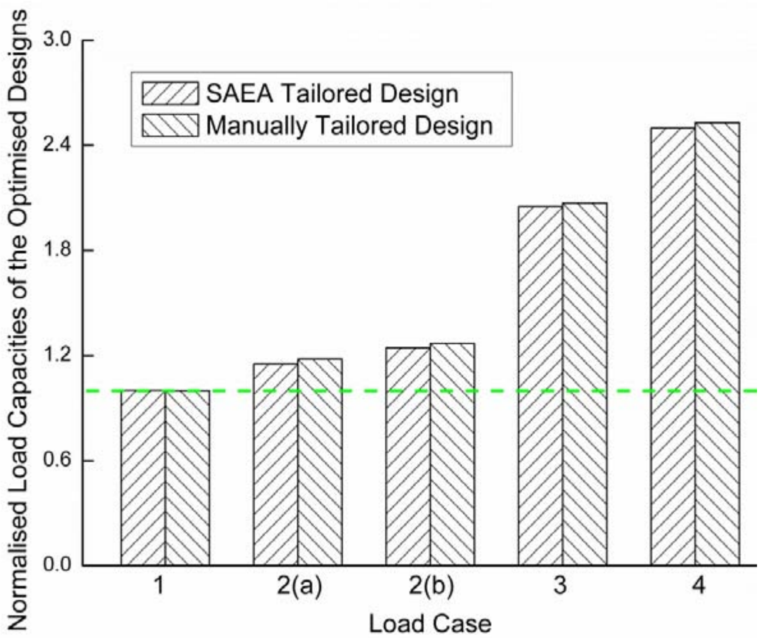

Fig. F.8. Comparison of load capacities of tailored designs

F.3.3 Verification under Global Load Cases

As the optimisation process using SAEA is based on local load constraints, the performance of the optimum geometry for global load cases has to be verified. Both the global design procedure for all the material combinations selected, and the global design load cases used for the global FE analysis are the same as those in *Chapter 6*. The effective 3D composite tubular properties employed in the global FE analysis are listed in Table F.5 using the same calculation process as in *Chapter 6*.

Table F.5. Effective 3D properties of composite tube used in global analysis

Name	$\rho_{effective}$ (kg/m^3)	$E_{x\_tension}$ (GPa)	$E_{x\_bending}$ (GPa)	E_y (GPa)	E_z (GPa)	G_{xy} (GPa)	G_{xz} (GPa)	G_{yz} (GPa)	ν_{xy}	ν_{xz}	ν_{yz}
AS4/epoxy-Al liner [0/±53.4/90]	1600.1	41.58	37.47	64.61	11.92	20.37	4.08	4.29	0.25	0.351	0.295

Conducting a global analysis of the entire riser using pipe elements (Pipe288), as in *Chapter 6*, the critical locations and the force, moment and pressure combinations at these locations are identified. The magnitudes of the loads at the critical locations are listed in Table F.6.

Table F.6. Critical load combinations and locations for AS4/epoxy with aluminium liner with optimised geometry from global analysis

Load Case	Location	Tension (kN)	Internal Pressure (MPa)	External Pressure (MPa)	Shear Force (kN)	Bending Moment (kN·m)
4	Top	3327.0	44.3	0.7	55.5	63.3
	Bottom	2254.5	58.7	19.2	57.9	47.3
5	Top	3263.1	44.3	0.7	41.3	10.9
	Bottom	2209.2	58.7	19.2	88.8	69.3
6	Top	2364.8	1.8	0.7	110.5	52.9
	Bottom	1297.0	35.3	19.2	99.9	54.6
7	Top	2299.5	1.8	0.7	90.1	5.5
	Bottom	1251.8	35.3	19.2	141.0	77.2
8	Top	2218.6	0	0.7	87.7	57.5
	Bottom	363.2	0	19.2	124.5	24.2
9	Top	2152.2	0	0.7	129.0	5.7
	Bottom	311.1	0	19.2	179.7	34.2

In the final stage a local analysis of the identified critical sections with the corresponding load combinations is conducted once again using layered solid elements as in *Chapter 6*. The minimum factors of safety in the aluminium liner and the various layers of the composite body of the AS4/epoxy riser with the geometry optimised using the optimisation technique SAEA are given in Table F.7.

Table F.7. Minimum FSs for liner and composite layers of AS4/epoxy with aluminium liner with SAEA optimised geometry

Material Combination	Liner		Composite Layers-Fibre Direction			Composite Layers-Transverse Direction			Composite Layers–In-Plane Shear		
	FS	LC	FS	Layer	LC	FS	Layer	LC	FS	Layer	LC
AS4-Aluminiun [0/±53.4/90]	1.78	LC4-T	4.75	4	LC4-T	1.60	18	LC4-T	4.34	14	LC8-T

Minimum FS required: 1.53 for composite layers, 1.74 for PEEK liner and 1.68 for metallic liners [72]

The results presented in Table F.7 show that the composite tubular geometry optimised for minimum weight in the local design stage using SAEA is able to successfully withstand the global loads providing their FSs are just above the values required by the standards [72].